Overview of Ocean Color EDR Team Activities

Menghua Wang
& VIIRS Ocean Color EDR Team

VIIRS Ocean Color Breakout Session
August 27, 2015

VIIRS Ocean Color EDR & Cal/Val Teams Members

EDR	Name	Organization	Funding Agency	Task
Lead	**Menghua Wang (OC EDR & Cal/Val Lead),** L. Jiang, X. Liu, W. Shi, S. Son, L. Tan, X. Wang, J. Sun, K. Mikelsons, V. Lance, **M. Ondrusek,** E. Stengel	NOAA/NESDIS/ STAR	JPSS/NJO	Leads – Ocean Color EDR Team & Cal/Val Team OC products, algorithms, SDR, EDR, Cal/Val, vicarious cal., refinements, data processing, algorithm improvements, software updates, data validations and analyses
Ocean Color	**Robert Arnone** Sherwin Ladner, Ryan Vandermeulen Adam Lawson, Paul Martinolich, Jen Bowers	U. Southern MS NRL QinetiQ Corp. SDSU	JPSS/NJO	Satellite data evaluation, in situ data Look Up Tables – SDR-EDR impacts, vicarious calibration Satellite matchup tool (SAVANT) – Golden Regions Cruise participation and support WAVE_CIS (AERONET-OC site) operation
	Carol Johnson	NIST	JPSS/NJO	Traceability, AERONET-OC Uncertainty
	Curt Davis, Nicholas Tufillaro	OSU	JPSS/NJO	Ocean color validation, Cruise data matchup West Coast
	Burt Jones, Matthew Ragan	USC	JPSS/NJO	Eureka (AERONET-OC Site)
	Sam Ahmed, Alex Gilerson	CUNY	JPSS/NJO	LISCO (AERONET-OC Site) Cruise data and matchup
	Chuanmin Hu	USF	JPSS/NJO	NOAA data continuity, cruise participation/support
	Ken Voss & MOBY team	RSMAS –Miami	JPSS/NJO	Marine Optical Buoy (MOBY)
	Zhongping Lee, Jianwei Wei	UMB	JPSS/NJO	Ocean color IOP data validation and evaluation Ocean color optics matchup, cruise participation

Working with: NOAA **CoastWatch**, VIIRS **SDR team**, DPA/DPE, Raytheon, NOAA OC Working Group, NOAA Coral Reef Watch, NOAA various line-office reps, NASA OBPG, NOAA OCPOP, etc.

Collaborators: D. Antoine (BOUSSOLE), B. Holben (NASA-GSFC), G. Zibordi (JRC-Italy), R. Frouin (for PAR), and others.

VIIRS Spectral Bands for Ocean Color

VIIRS on Suomi NPP

has Ocean and SWIR spectral bands similar to **MODIS**

VIIRS†		MODIS		SeaWiFS
Ocean Bands (nm)	Other Bands (nm)	Ocean Bands (nm)	Other Bands (nm)	Ocean Band (nm)
410 (M1)	640 (I1)	412	645	412
443 (M2)	865 (I2)	443	859	443
486 (M3)	1610 (I3)	488	469	490
Ñ		531	555	510
551 (M4)	*SWIR Bands*	551	*SWIR Bands*	555
671 (M5)	1238 (M8)	667	1240	670
745 (M6)	1610 (M10)	748	1640	765
862 (M7)	2250 (M11)	869	2130	865

†VIIRS nominal center wavelength

Spatial resolution for VIIRS M-band: 750 m, I-band: 375 m

Summary of VIIRS Ocean Color EDR Products

- **Inputs**:
  - VIIRS M1-M7 and the **SWIR** M8, M10, and M11 bands SDR data
  - Terrain-corrected geo-location file
  - Ancillary meteorology and ozone data
- **Operational (Standard) Products** (8):
  - Normalized water-leaving radiance (nL_w's) at VIIRS visible bands M1-M5
  - Chlorophyll-a (Chl-a) concentration
  - Diffuse attenuation coefficient for the downwelling spectral irradiance at the wavelength of 490 nm, K_d(490) (New)
  - Diffuse attenuation coefficient of the downwelling photosynthetically available radiation (PAR), K_d(PAR) (New)
  - Level-2 quality flags
- **Experimental Products:**
  - Inherent Optical Properties (IOP-a, IOP-a_{ph}, IOP-a_{dg}, IOP-b_b, IOP-b_{bp}) at VIIRS M2 or other visible bands (M1-M5) from the Quasi-Analytical Algorithm (QAA) (Lee et al., 2002)
  - Photosynthetically Available Radiation (PAR) (R. Frouin)
  - Chlorophyll-a from ocean color index (OCI) method (Hu et al., 2012)
  - Others from users requests

➢ Data quality of ocean color EDR are extremely sensitive to the SDR quality. It requires **~0.1%** data accuracy (degradation, band-to-band accuracy…)!

Multi-Sensor Level-1 to Level-2 (MSL12) Ocean Color Data Processing

- Multi-Sensor Level-1 to Level-2 (MSL12)
  - ✓ MSL12 was developed for the purpose of using a consistent and common data processing system to produce ocean color products from multiple satellite ocean color sensors (Wang, 1999; Wang and Franz, 2000; Wang et al., 2002), i.e., it is **measurement-based** ocean color data processing system.
  - ✓ It has been used for producing ocean color products from various satellite ocean color sensors, e.g., SeaWiFS, MOS, OCTS, POLDER, MODIS, GOCI, etc.
  - ✓ **MSL12 is the official VIIRS ocean color data processing system.**
- NOAA-MSL12 Ocean Color Data Processing
  - ✓ NOAA-MSL12 is based on SeaDAS version 4.6.
  - ✓ Some significant improvements: (1) the SWIR-based data processing, (2) **Rayleigh** (new) and aerosol LUTs, (3) algorithms for detecting absorbing aerosols and turbid waters, (4) ice detection algorithm, (5) improved straylight/cloud shadow algorithm, & others.
  - ✓ In 2014, some new algorithms (BMW–new NIR reflectance correction, Destriping, K_d(PAR), etc.)
- NOAA-MSL12 for VIIRS (and others) Ocean Color Data Processing
  - ✓ Routine ocean color data processing (daily, 8-day, monthly) since VIIRS launch.
  - ✓ Coastal turbid and inland waters from other approaches, e.g., the **SWIR approach**, results in the US east coastal, China's east coastal, Lake Taihu, Lake Okeechobee, Aral Sea, etc.
  - ✓ Capability for multi-sensor ocean color data processing, e.g., MODIS-Aqua, VIIRS, GOCI, and will also add J1, OLCI/Stentinel-3, and SGLI/GCOM-C data processing capability.

New Rayleigh Lookup Tables

- Developed **Hyperspectral** Rayleigh Lookup Tables (LUTs)
  - ✓ Developed new Rayleigh lookup tables including polarization effects for the entire solar reflective spectrum (335-2555 nm) for satellite ocean color remote sensing.
  - ✓ The new Rayleigh LUTs cover solar-zenith angles of 0-88 Deg., sensor-zenith angles of 0-84 Deg., all azimuth angles, and wind speeds of 0-30 m/s.
  - ✓ The same Rayleigh LUTs can be applied to any satellite sensors (multi-spectral and hyperspectral).
  - ✓ The same LUTs can be applied for **High Altitude Lakes**.
  - ✓ The LUTs can be used to account for the effect of sensor spectral response function.
  - ✓ **Consistent Rayleigh radiance computations for all satellite sensors.**
- New Rayleigh LUTs for Ocean Color Data Processing (MSL12)
  - ✓ VIIRS **detector-based** exact Rayleigh radiance computations.
  - ✓ Exact Rayleigh radiance computation with atmospheric pressure variation.
  - ✓ More accurately account for the effect of VIIRS sensor spectral response function, particularly for large solar-zenith angles.
  - ✓ More accurate Rayleigh radiance computations and improved ocean color products.
  - ✓ The same Rayleigh LUTs for J1, J2, J3, J4, ……., as well as for satellite sensors from Sentinel-3, GCOM-C, etc.

Developed new NIR ocean reflectance correction algorithm: BMW (*Bailey* (2010), *MUMM* (2000), and *Wang* (2012))

The BMW Algorithm for Ocean Color Data Processing

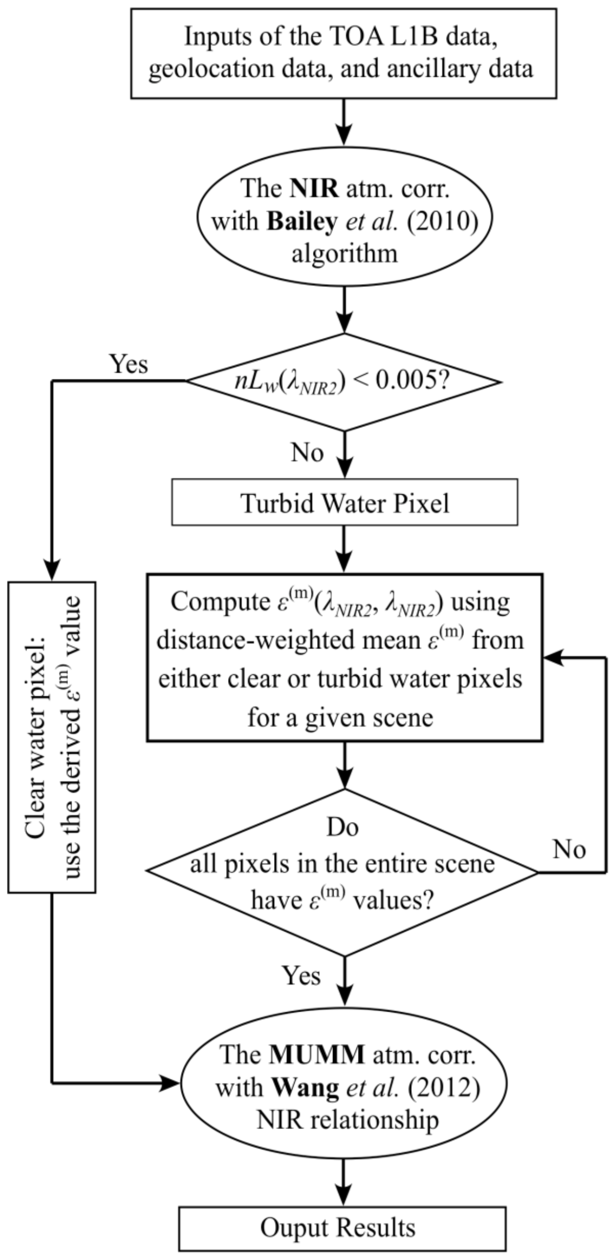

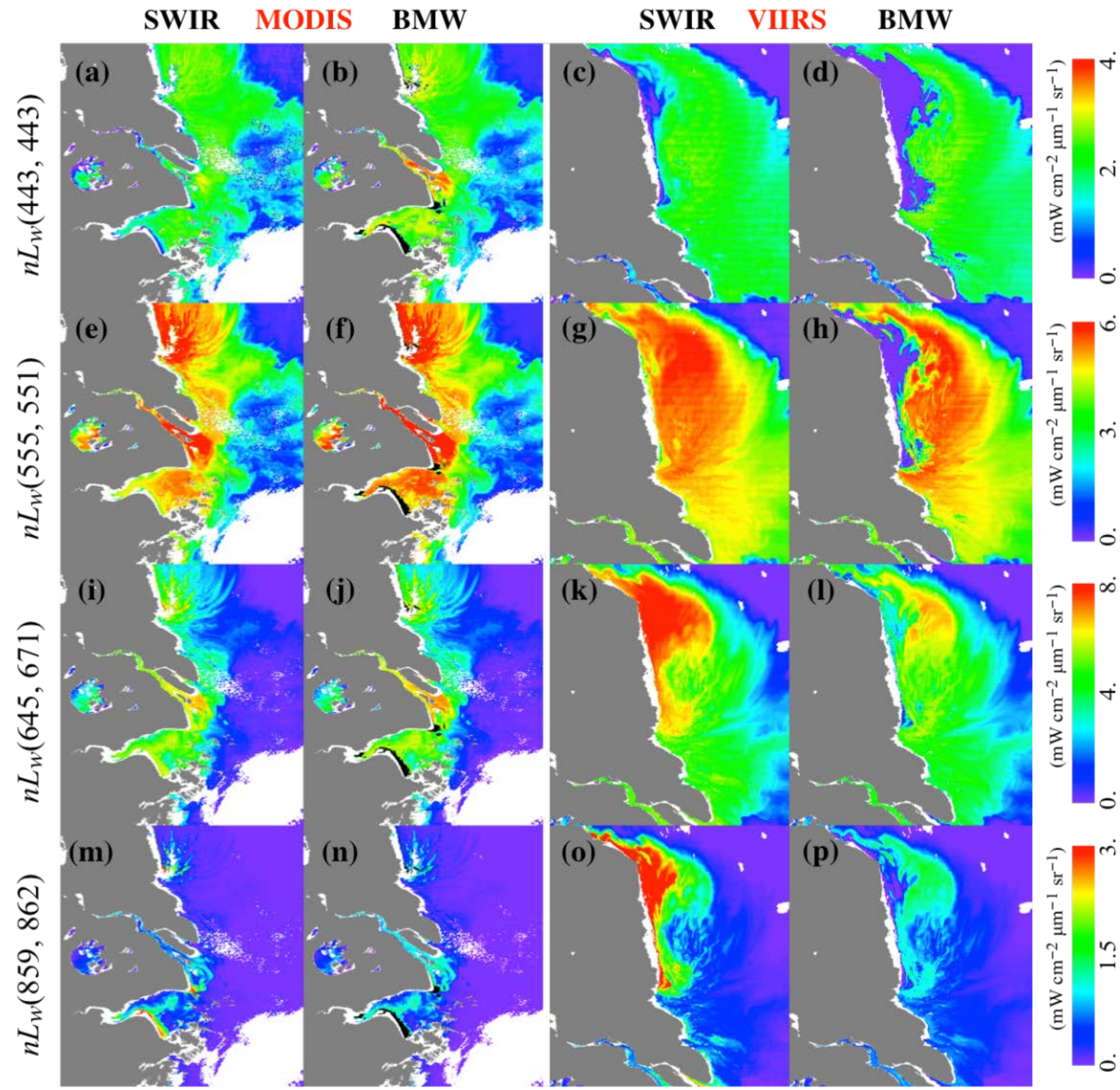

Comparisons of MODIS and VIIRS-derived $nL_w(\lambda)$ images at four selected bands.

Jiang, L. and M. Wang, "Improved near-infrared ocean reflectance correction algorithm for satellite ocean color data processing," *Opt. Express*, **22**, 21,657–21,678, 2014. http://dx.doi.org/10.1364/OE.22.021657

Destriping of VIIRS Ocean Color Products
(Examples)

$nL_w(412)$

$K_d(490)$

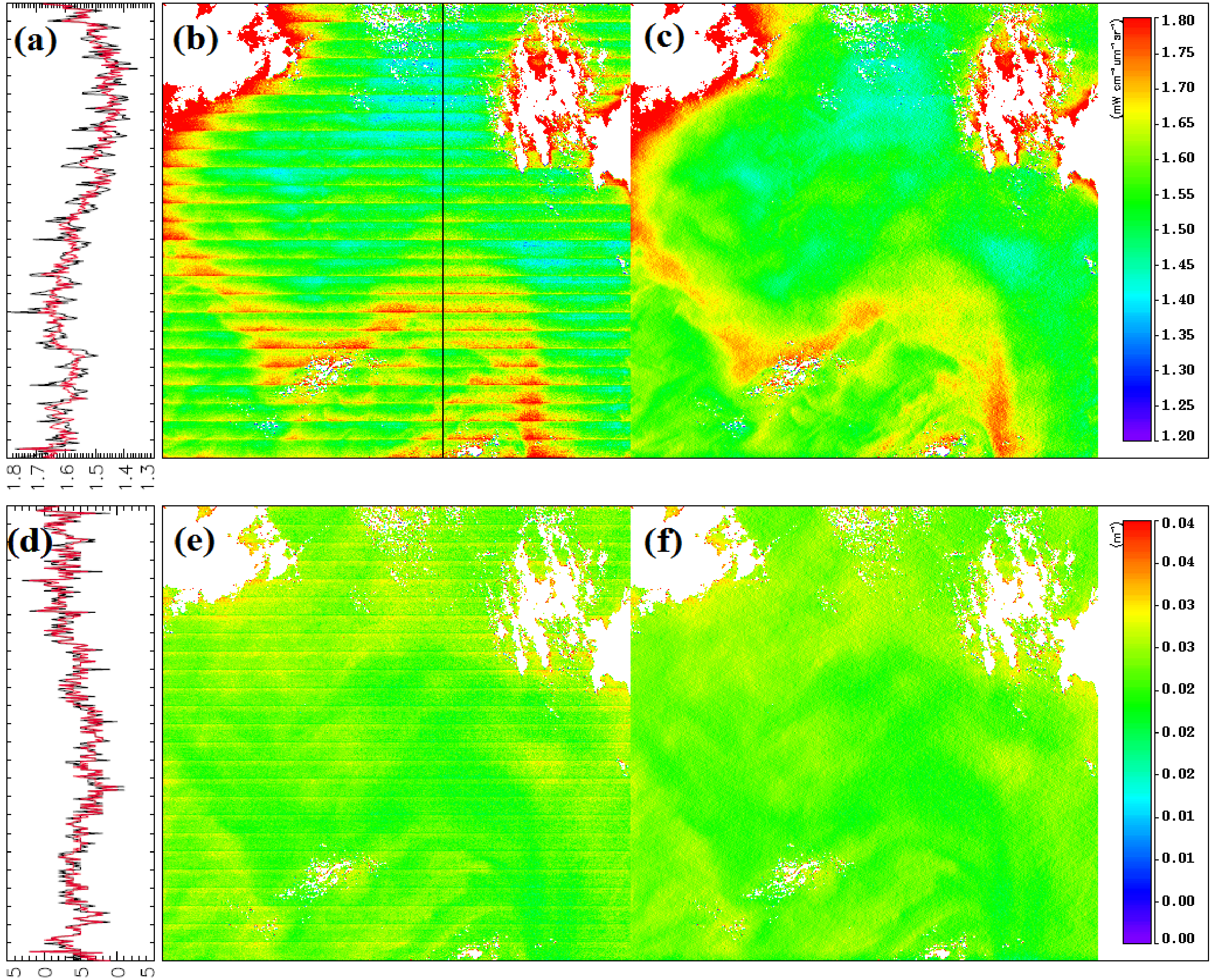

Mikelsons, K., M. Wang, L. Jiang, and M. Bouali, "Destriping algorithm for improved satellite-derived ocean color product imagery," *Opt. Express*, **22**, 28058-28070, 2014. http://dx.doi.org/10.1364/OE.22.028058

Polarization Correction (1)

Case Study: 04/14/2014 00:43 UTC

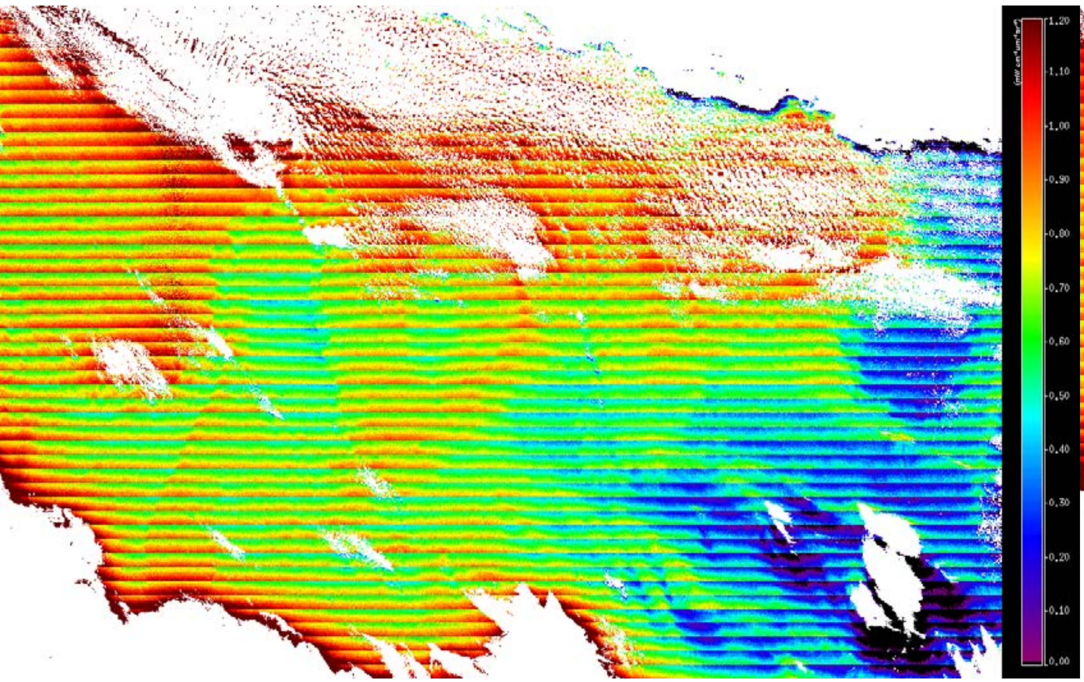

nL_w(412) without polarization correction

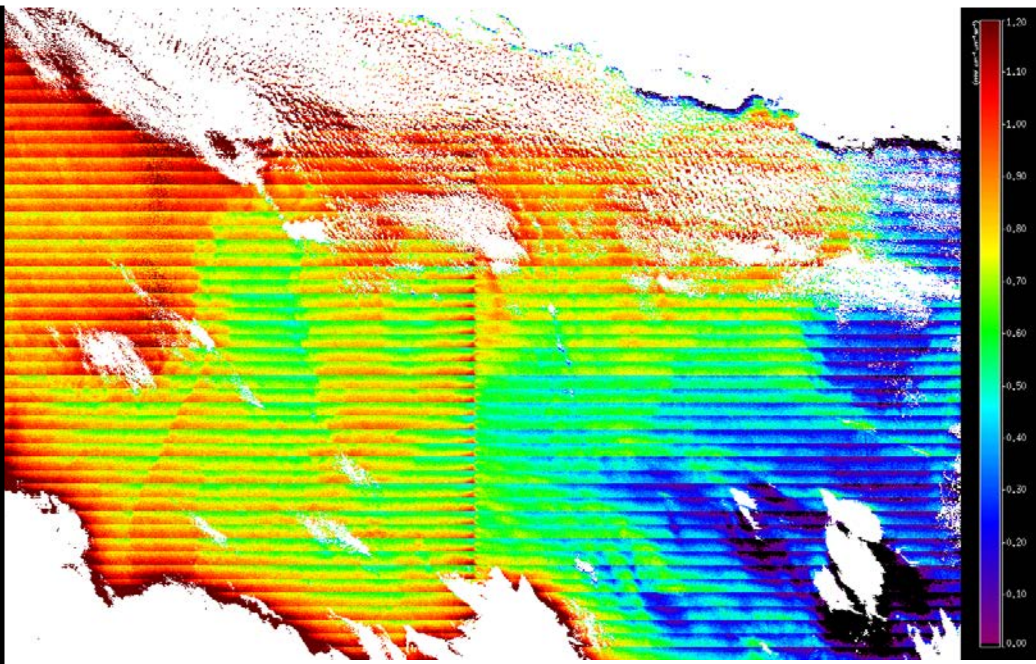

nL_w(412) with **old** polarization correction

VIIRS Granule at 55^{o}S and 155^{o}W in South Pacific Ocean

Polarization Correction (2)

Case Study: 04/14/2014 00:43 UTC

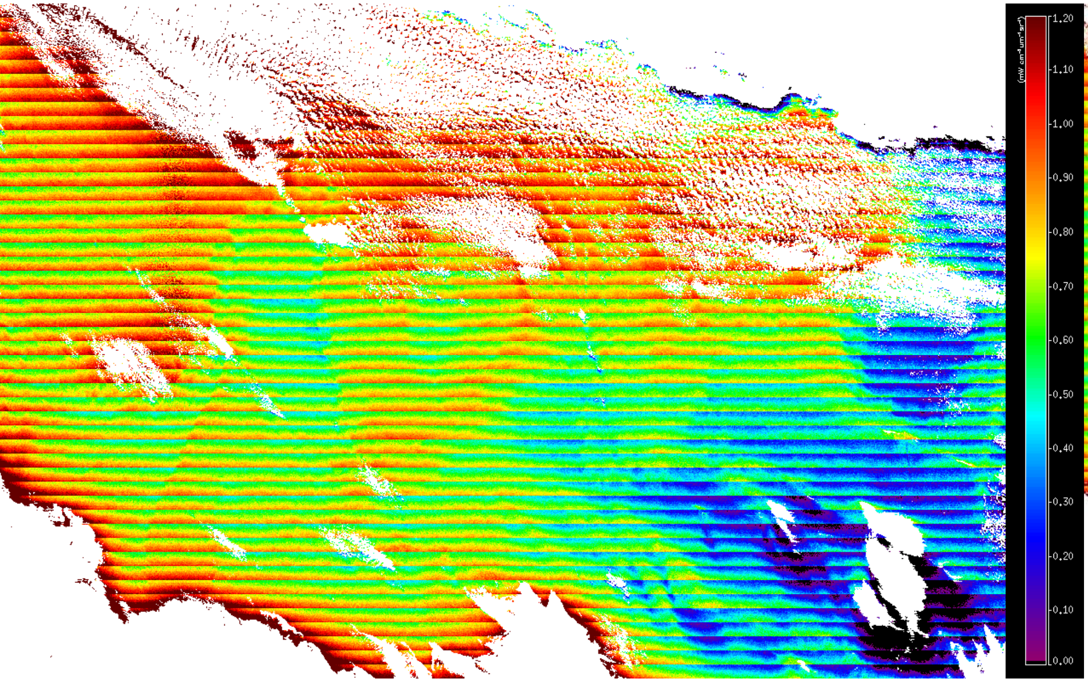

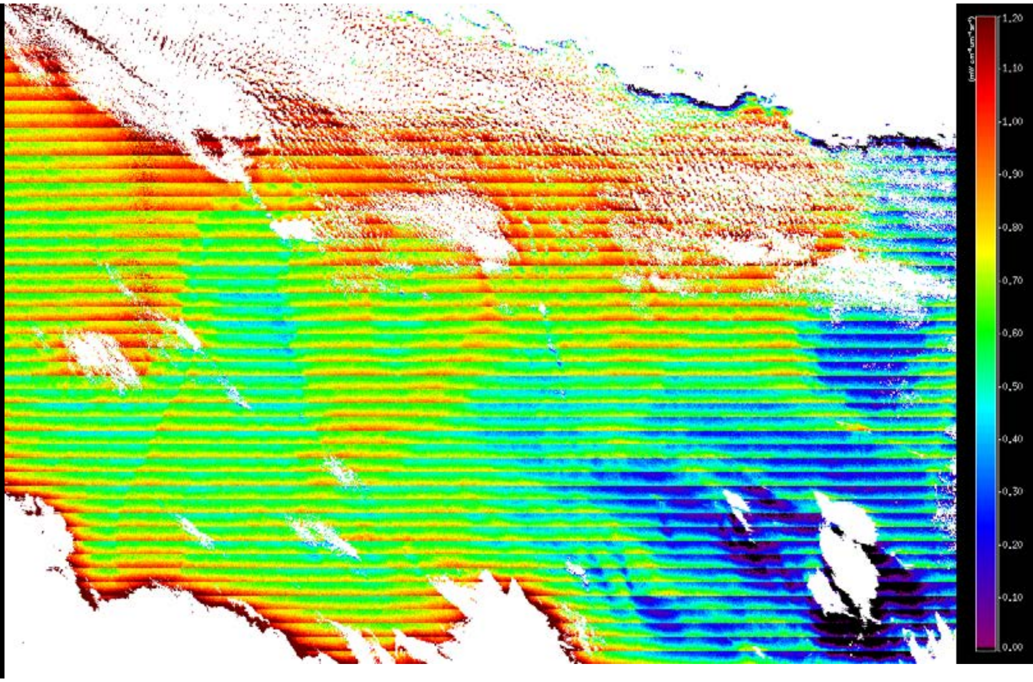

$nL_w(412)$ without polarization correction

$nL_w(412)$ with **new** polarization correction

VIIRS Granule at 55^{o}S and 155^{o}W in South Pacific Ocean

Stray Light & Cloud Shadow Effects (Implemented in MSL12)

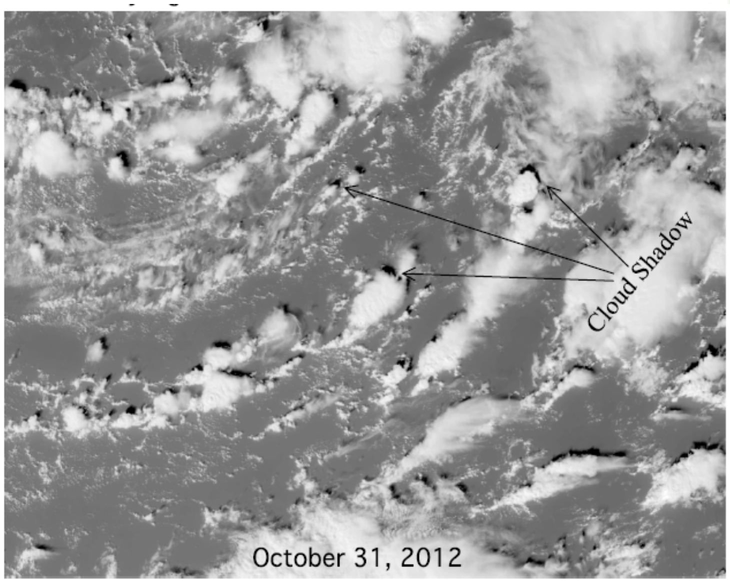

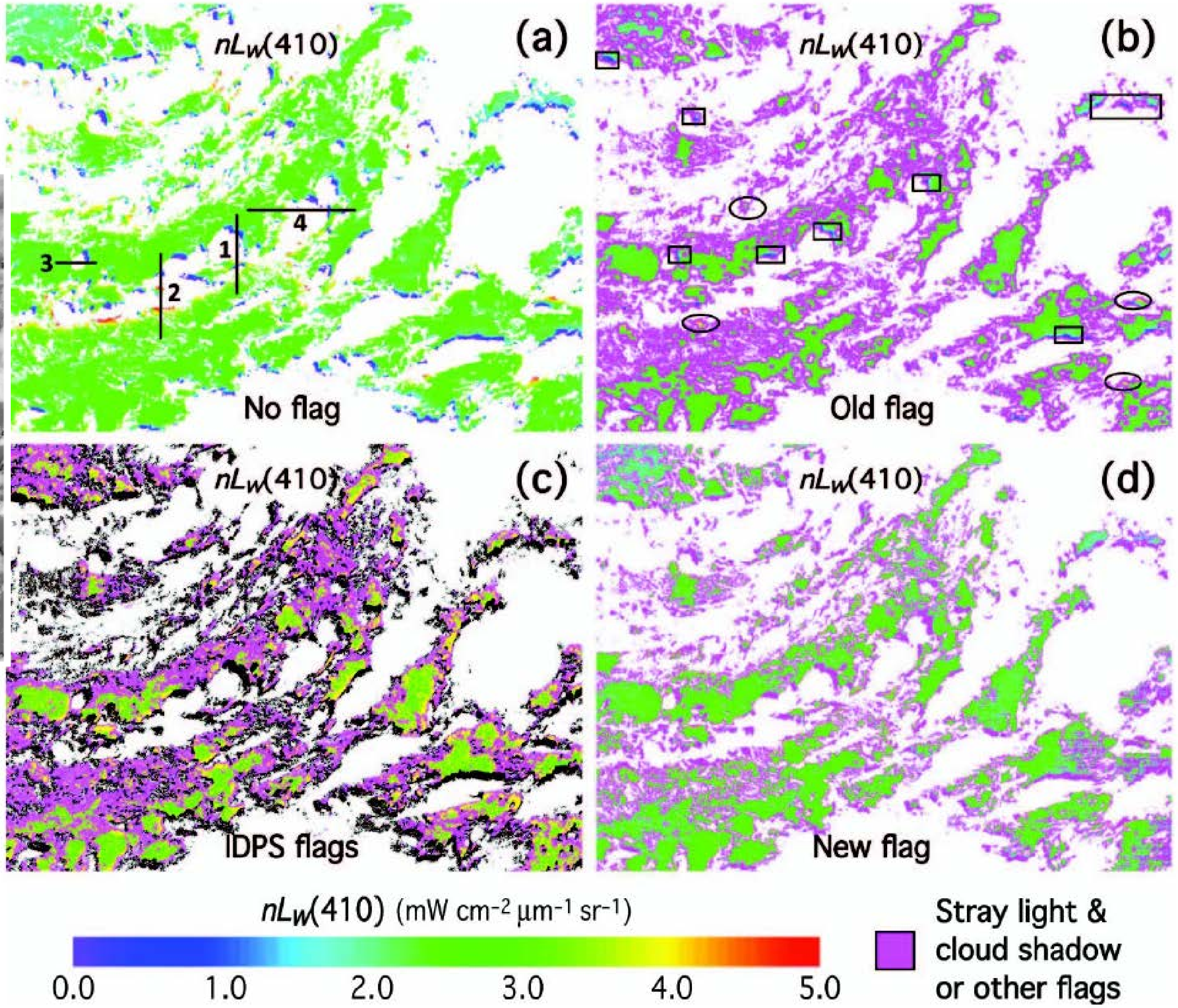

Jiang, L. and M. Wang, "Identification of pixels with stray light and cloud shadow contaminations in the satellite ocean color data processing," *Appl. Opt.*, **52**, 6757–6770, 2013. http://dx.doi.org/10.1364/AO.52.006757

End-to-End Ocean Color Data Processing

- NOAA Ocean Color Team has been developing/building the capability for the **End-to-End** satellite ocean color data processing including:
  - Level-0 (or Raw Data Records (RDR)) to Level-1B (or Sensor Data Records (SDR)).
  - Level-1B (SDR) to ocean color Level-2 (Environmental Data Records (EDR).
  - Level-2 to global Level-3 (routine daily, 8-day, monthly, and climatology data/images).
  - Validation of satellite ocean color products (in situ data and data analysis capability).
- Support of in situ data collections for VIIRS Cal/Val activities, e.g., **MOBY**, **AERONET-OC** sites, **NOAA dedicated cruise**, etc.
- On-orbit instrument calibration (solar and **lunar**) for ocean color data processing (Cal effort is needed to meet ocean color requirement):
  - J. Sun and M. Wang, "Radiometric calibration of the VIIRS reflective solar bands with robust characterizations and hybrid calibration coefficients," *Appl. Opt.* (Submitted).
  - J. Sun and M. Wang, "On-orbit calibration of Visible Infrared Imaging Radiometer Suite reflective solar bands and its challengers using a solar diffuser," *Appl. Opt.*, **54**, 7210-7223, 2015.
  - J. Sun and M. Wang, "On-orbit characterization of the VIIRS solar diffuser and solar diffuser screen," *Appl. Opt.*, **54**, 236-252, 2015.
  - J. Sun and M. Wang, "Visible Infrared Imaging Radiometer Suite solar diffuser calibration and its challenges using solar diffuser stability monitor," *Appl. Opt.*, **53**, 8571-8584, 2014.
- RDR (Level-0) to SDR (Level-1B) data processing (needed for quick data reprocessing):
  - Sun, J., M. Wang, L. Tan, and L. Jiang, "An efficient approach for VIIRS RDR to SDR data processing," *IEEE Geosci. Remote Sens. Lett.*, **11**, 2037–2041, 2014.
  - L. Tan, M. Wang, J. Sun, and L. Jiang, "VIIRS RDR to SDR Data Processing for Ocean Color EDR," *Proc. SPIE* 9261, *Ocean Remote Sensing and Monitoring from Space*, October 13-16, 2014.

Two Data Streams for VIIRS Ocean Color EDR

To meet requirements from **All** users (operational, research, modeling, etc.), we plan to produce VIIRS ocean color products in two data streams:

- **Near-Real-Time (NRT) Ocean Color Data Processing (**12-24 hours**):**
  - Quick turn around with ~12-24 hours latency (operational)
  - Using standard IDPS SDR data
  - Ancillary data using the Global Forecast System (GFS) model
  - Data may not be completed due to various issues (SDR missing, computer, etc.)
  - Data will be processed in NOAA CoastWatch and OSPO
- **Science Quality Ocean Color Data Processing (**One-two weeks delay**):**
  - About one-two weeks delay
  - Reprocessed mission-long ocean color data and continue-forward data stream
  - Using improved SDR (based on IDPS SDR data)
  - Science quality (assimilated) NCEP ancillary data
  - Complete global coverage
  - May expand to more experimental products & test with improved algorithms
  - Ocean color EDR will be reprocessed (mission-long) about every two-three years (or as needed, e.g., short-term data reprocessing, error fixing, etc.)
  - Data will be processed in NOAA/STAR and transferred to CoastWatch for distributions

VIIRS Climatology Chlorophyll-a Image
(April 2012 to October 2014)

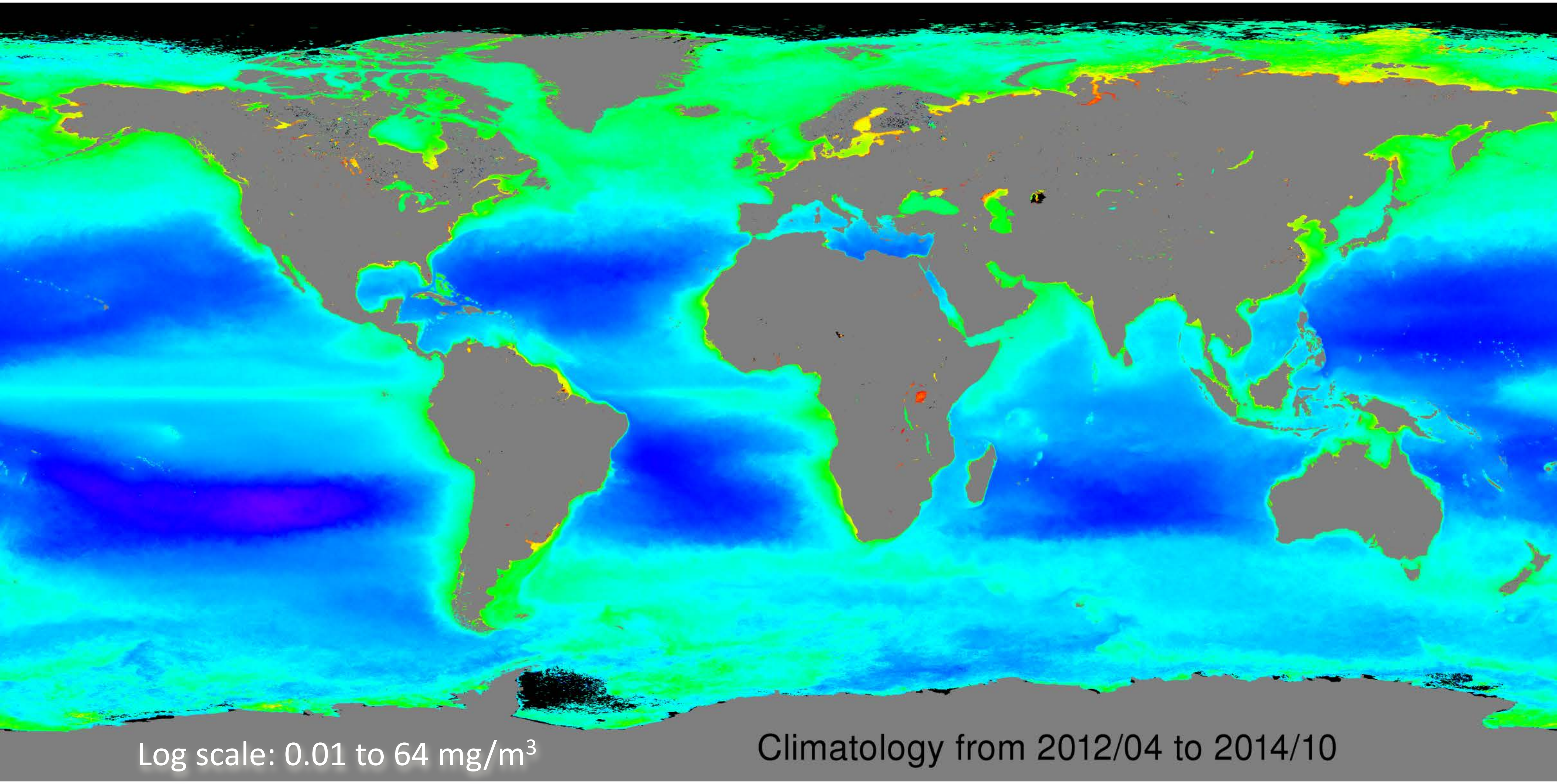

Generated using MSL12 for VIIRS ocean color data processing

Wang, M., X. Liu, L. Tan, L. Jiang, S. Son, W. Shi, K. Rausch, and K. Voss, "Impacts of VIIRS SDR performance on ocean color products," *J. Geophys. Res. Atmos.*, **118**, 10,347–10,360, 2013. http://dx.doi.org/10.1002/jgrd.50793

VIIRS Climatology $K_d(490)$ Image
(March 2012 to February 2015)

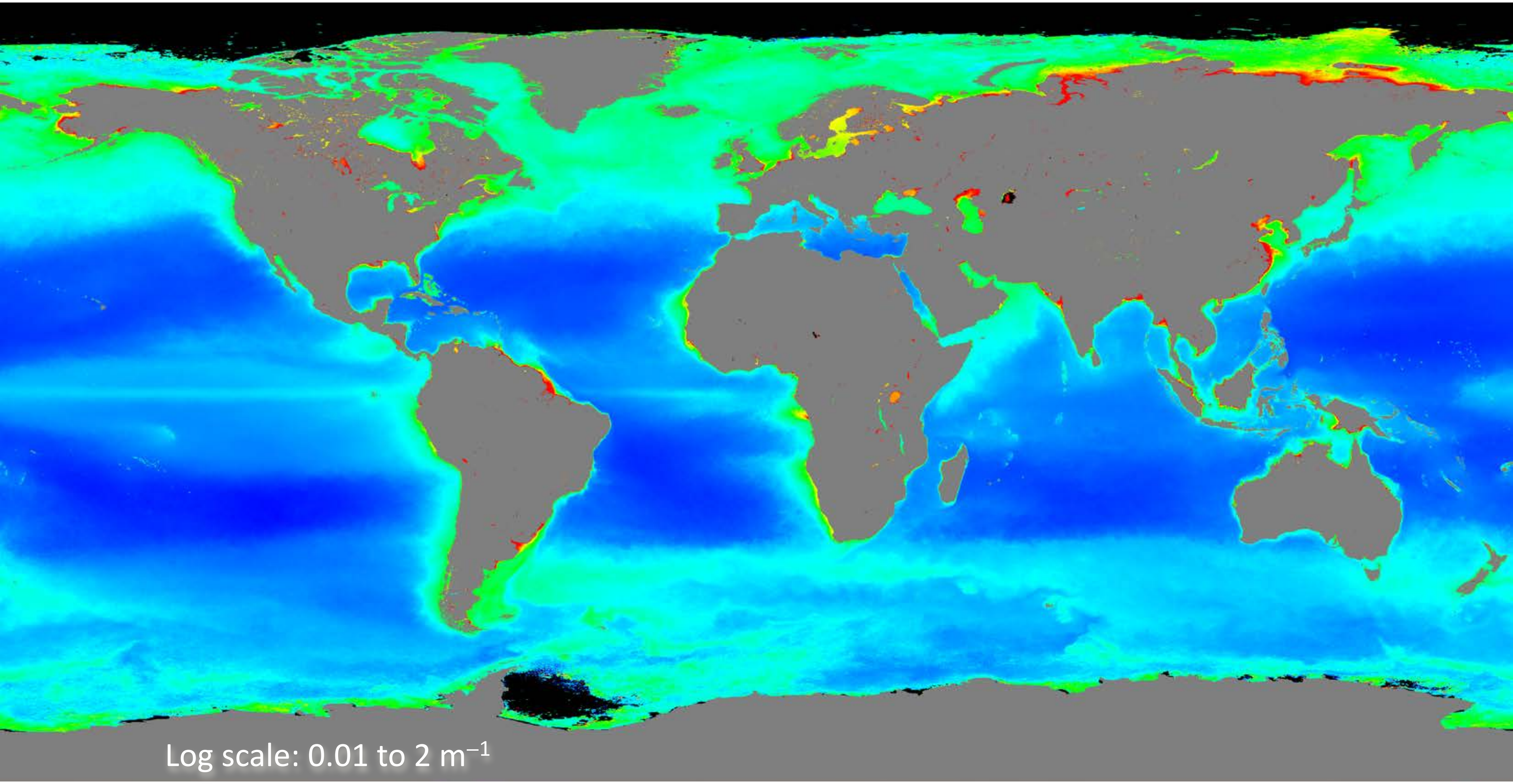

Generated using MSL12 for VIIRS ocean color data processing

Wang, M., S. Son, and L. W. Harding Jr., "Retrieval of diffuse attenuation coefficient in the Chesapeake Bay and turbid ocean regions for satellite ocean color applications," *J. Geophys. Res.*, **114**, C10011, 2009. http://dx.doi.org/10.1002/2009JC005286

VIIRS Climatology K_d(PAR) Image
(March 2012 to February 2015)

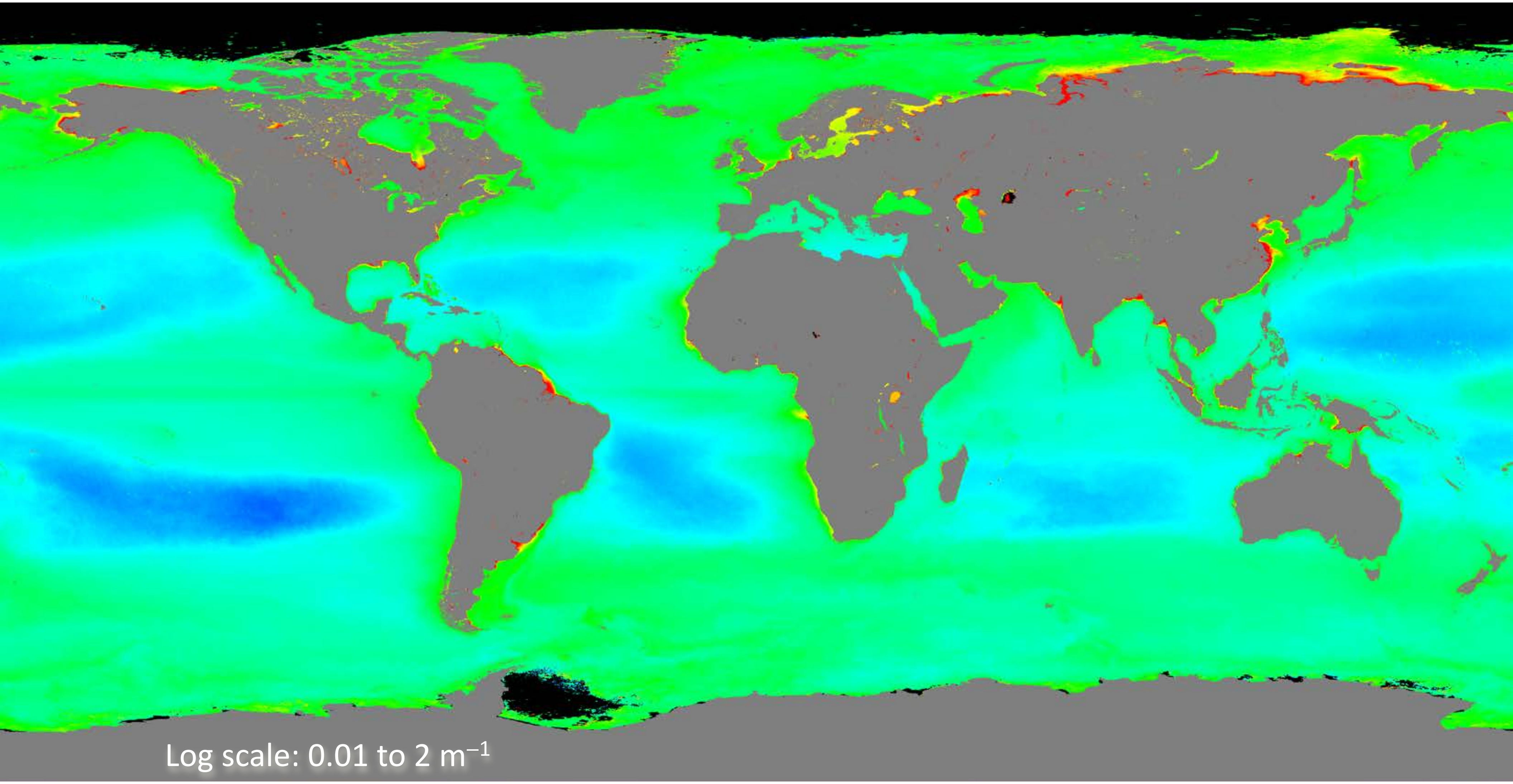

Generated using MSL12 for VIIRS ocean color data processing

Son, S. and M. Wang, "Diffuse attenuation coefficient of the photosynthetically available radiation Kd(PAR) for global open ocean and coastal waters," *Remote Sens. Environ.*, **159**, 250–258, 2015. http://dx.doi.org/10.1016/j.rse.2014.12.011

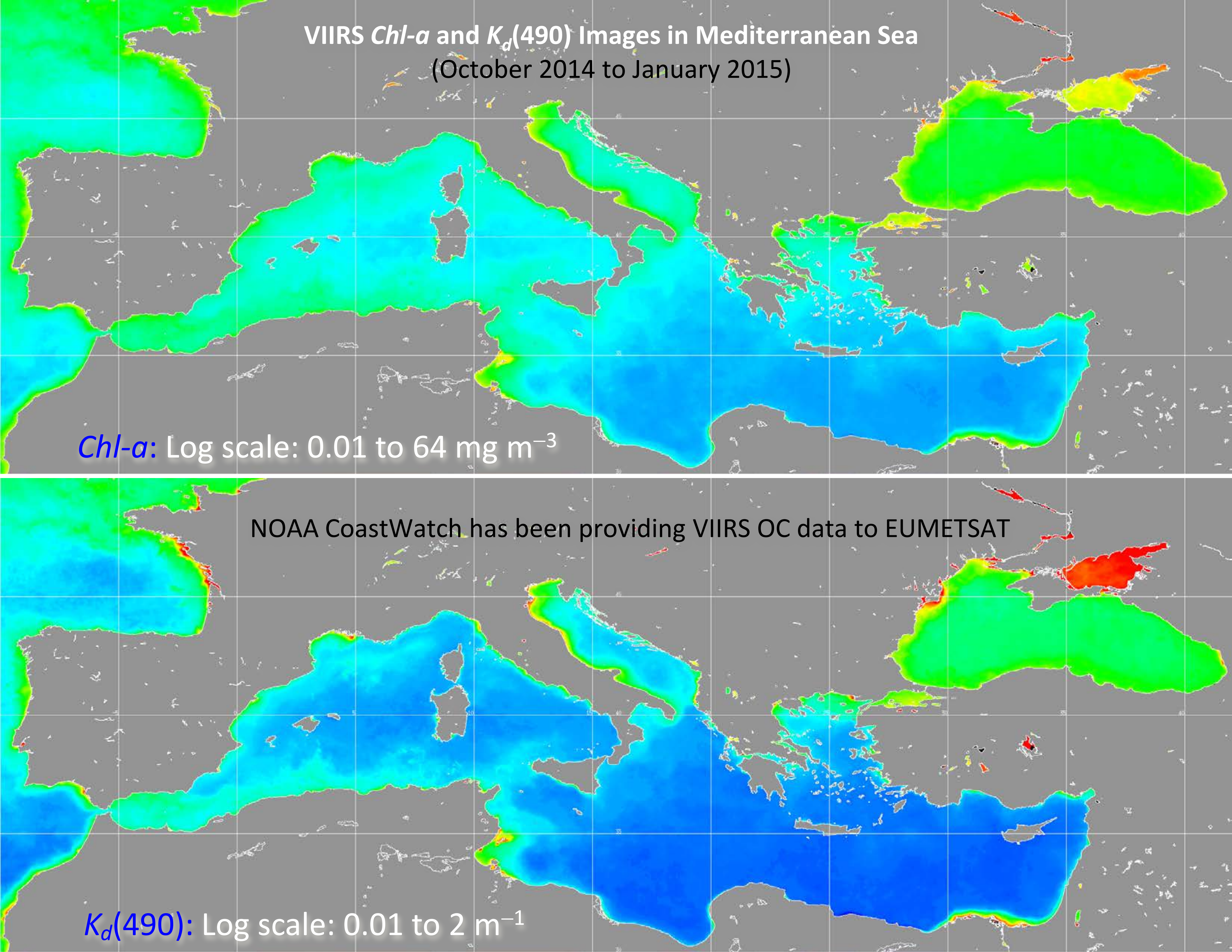

VIIRS *Chl-a* and K_d(490) Images in Mediterranean Sea
(October 2014 to January 2015)
Chl-a: Log scale: 0.01 to 64 mg m^{-3}
NOAA CoastWatch has been providing VIIRS OC data to EUMETSAT
K_d(490): Log scale: 0.01 to 2 m^{-1}

Global Oligotrophic Water OC Product Time Series

OC-SDR: Generated by the OC Team with OC calibration approach
IDPS-SDR: From operational IDPS-generated SDR

Reprocessed both mission-long SDR data using the **same new MSL12**

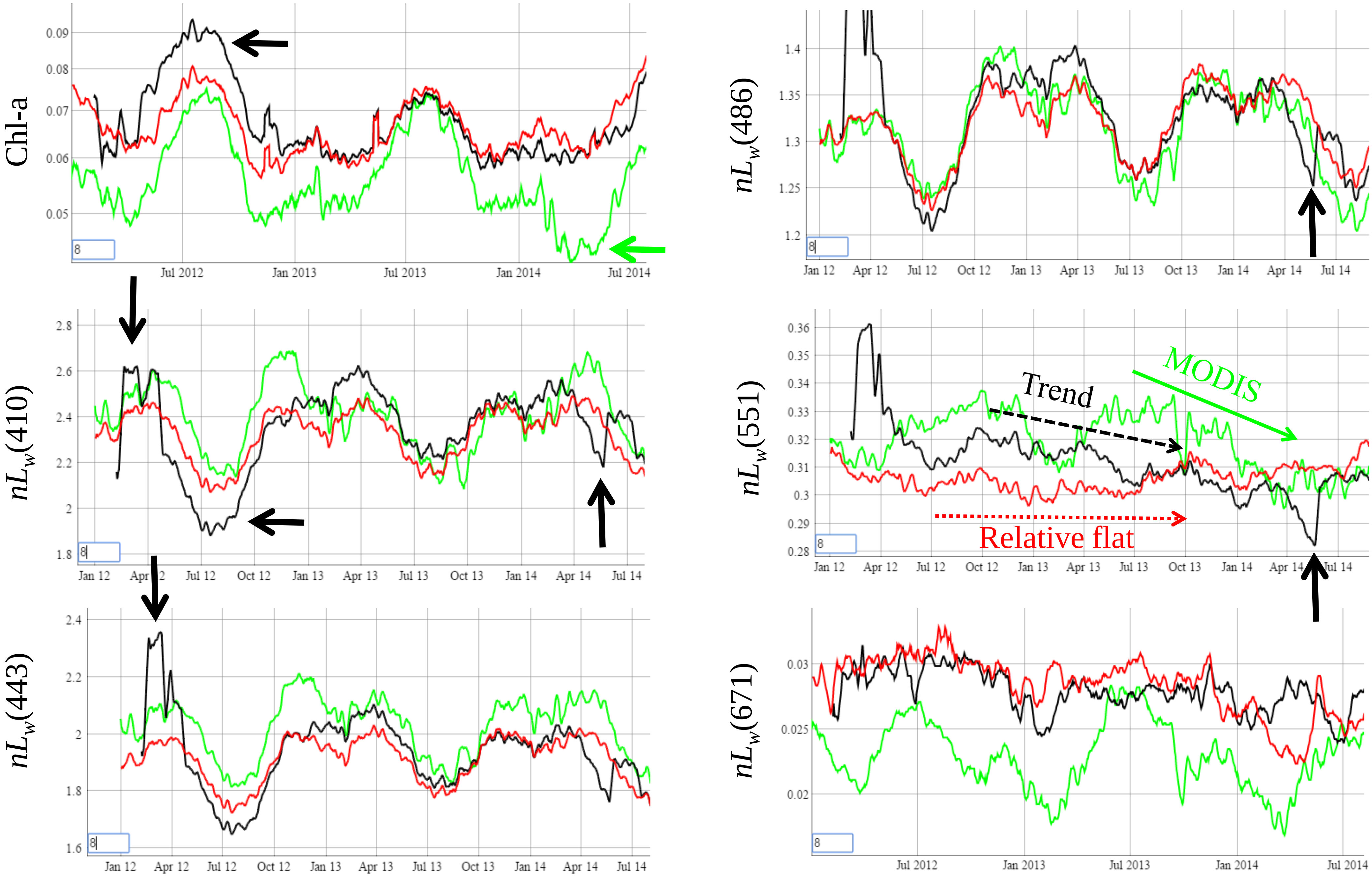

Red: VIIRS **OC-SDR** Black: VIIRS **IDPS-SDR** Green: MODIS-Aqua (NASA)

Global Deep Water (> 1km depth) OC Product Time Series

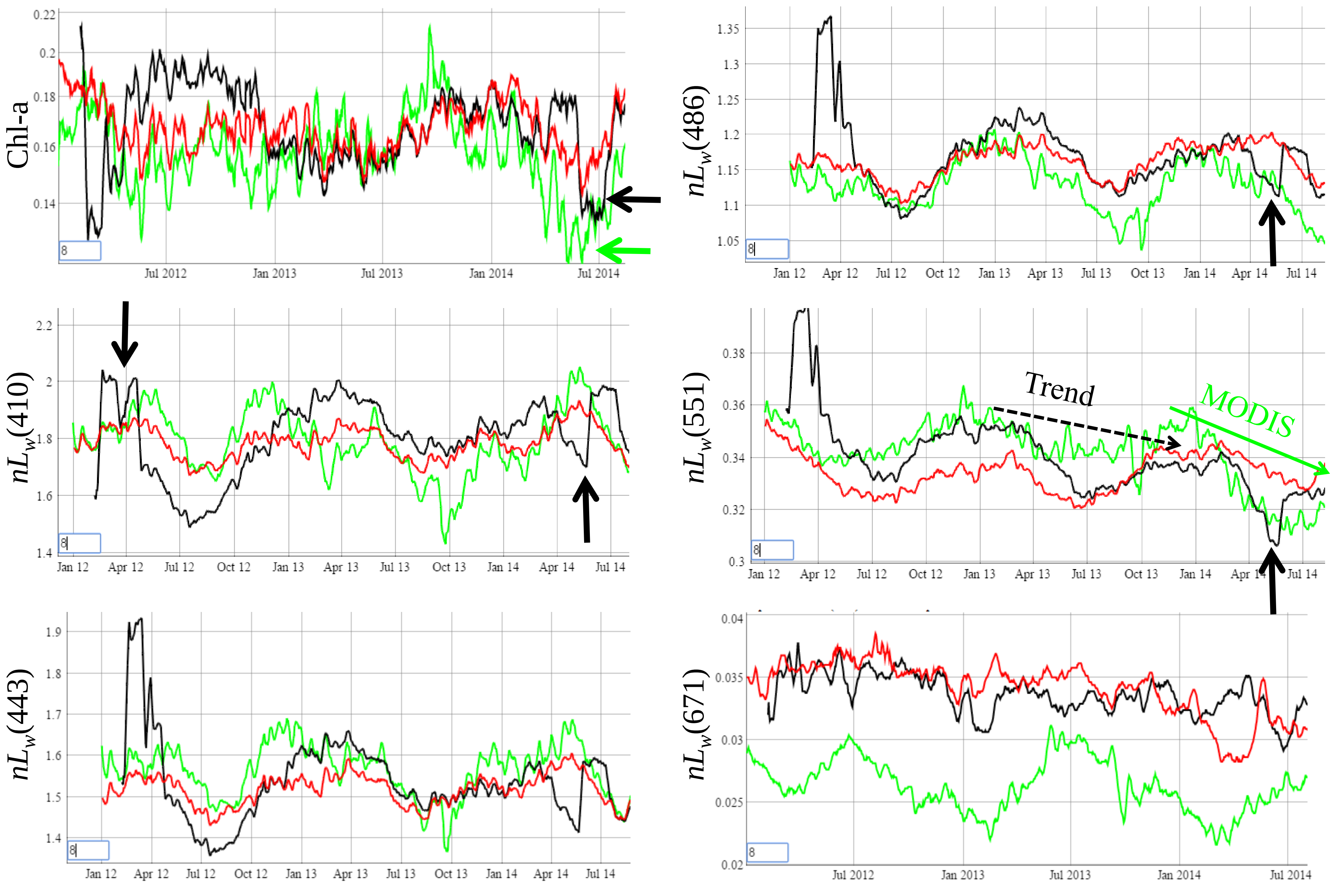

Red: VIIRS **OC-SDR** Black: VIIRS **IDPS-SDR** Green: MODIS-Aqua (NASA)

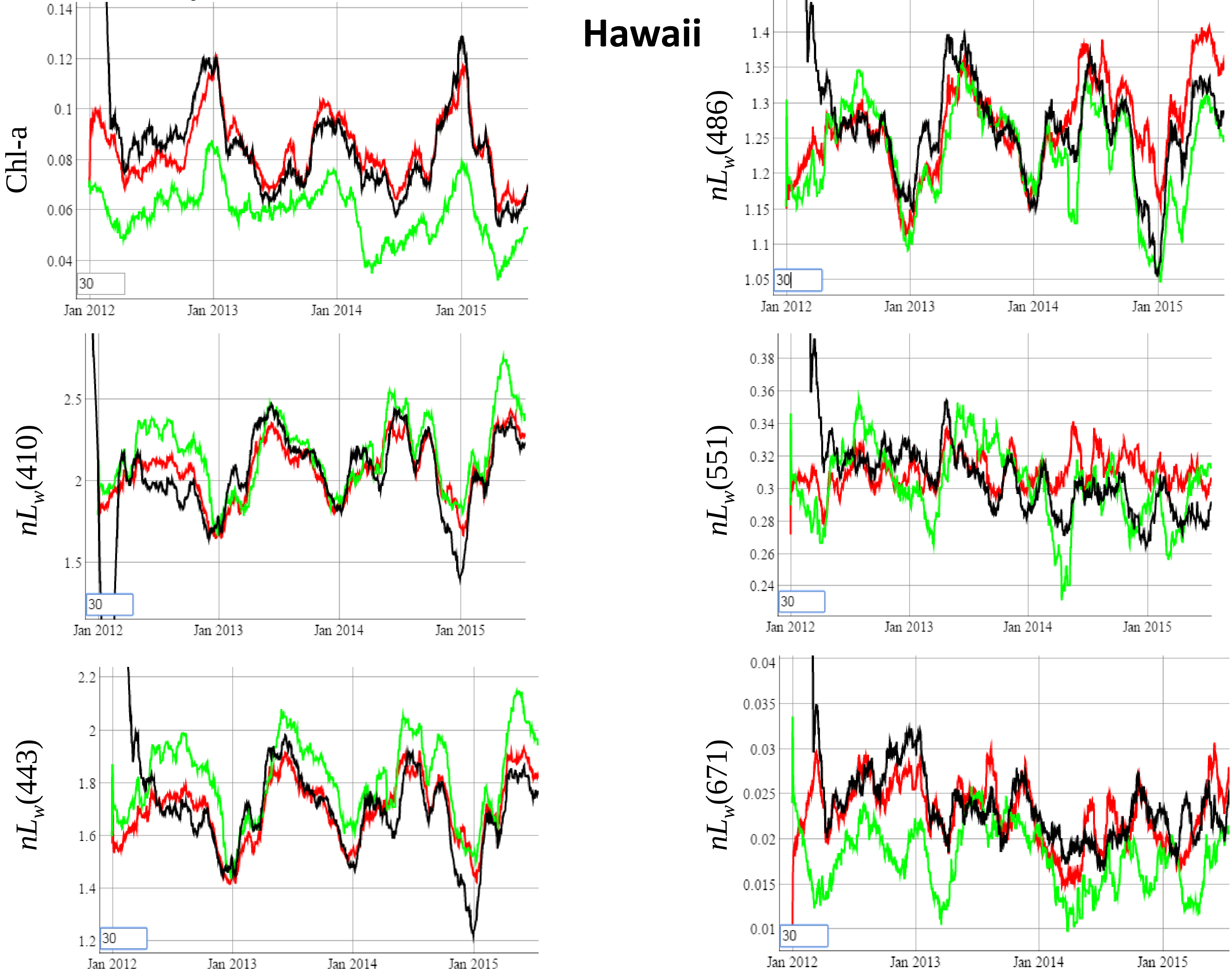

Red: VIIRS **OC-SDR** Black: VIIRS **IDPS-SDR** Green: MODIS-Aqua (NASA)

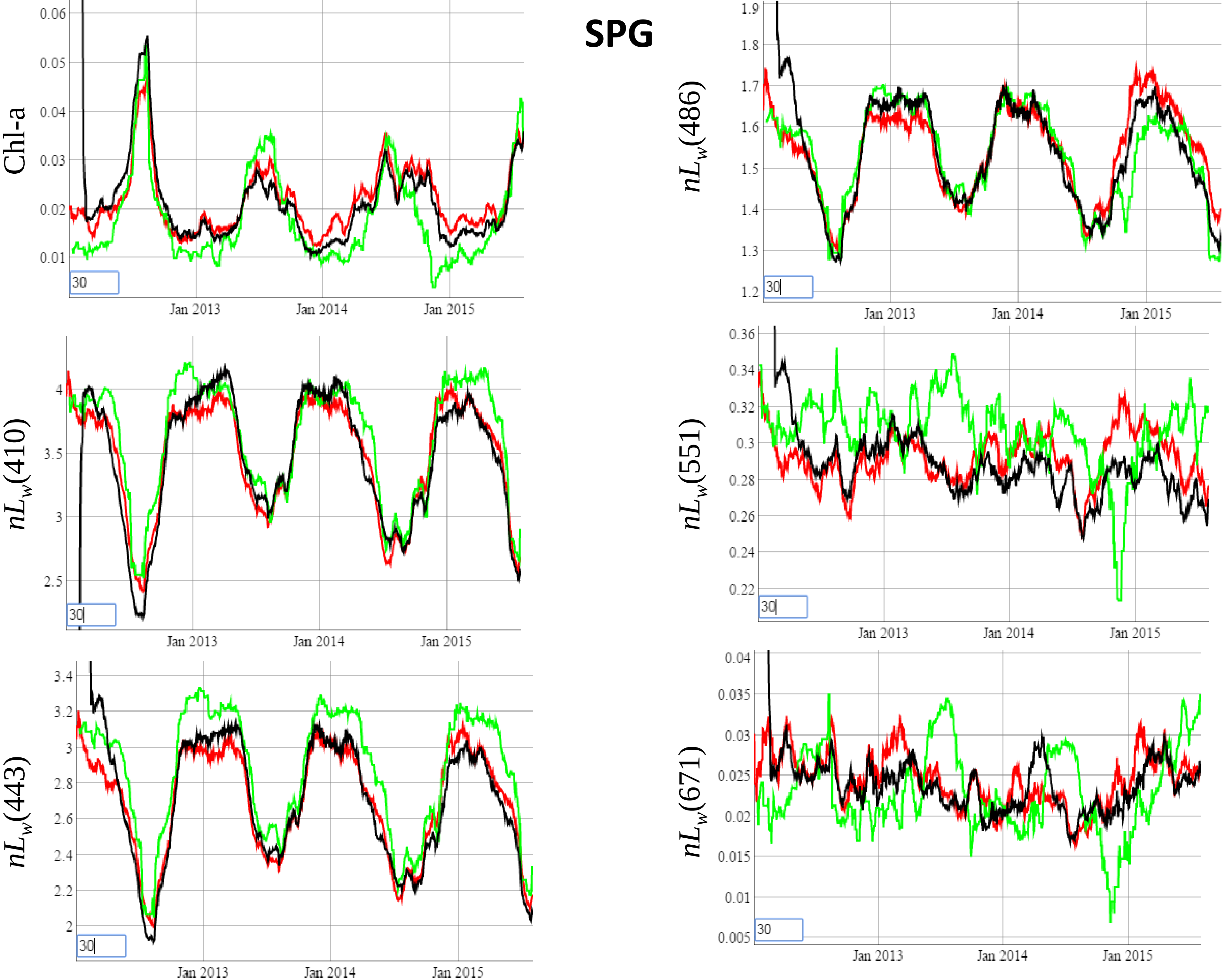

Red: VIIRS **OC-SDR** Black: VIIRS **IDPS-SDR** Green: MODIS-Aqua (NASA)

VIIRS Ocean Color EDR Monitoring Sites

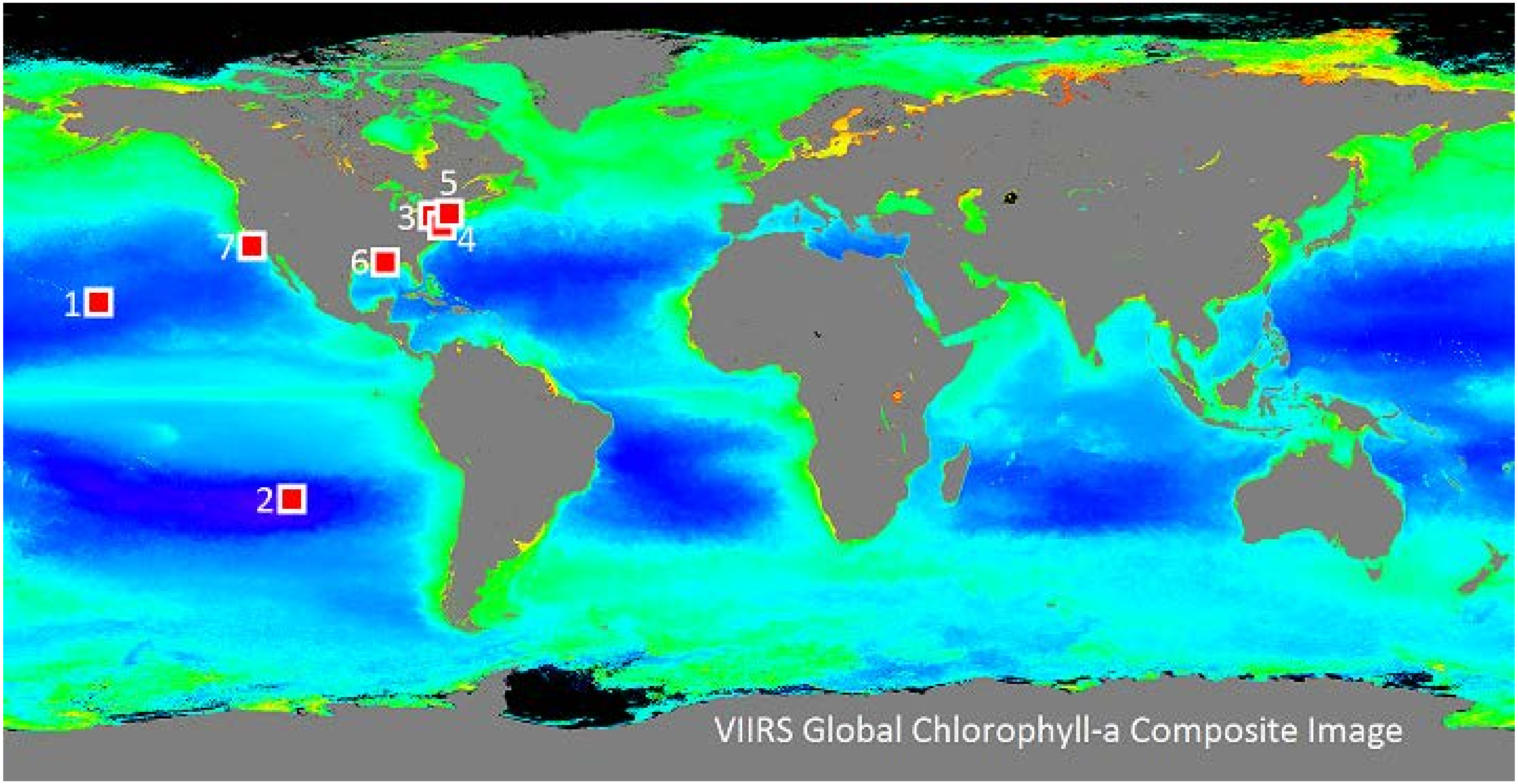

1. **MOBY Site**; 2. South Pacific Gyre; 3. Chesapeake Bay; 4. US East Coast; 5. **AERONET-OC CSI Site**; 6. **AERONET-OC LISCO Site**; 7. **AERONET-OC USC Site**.

Website:
http://www.star.nesdis.noaa.gov/sod/mecb/color/

Matchup comparison
of
MOBY In Situ
(with **VIIRS MSL12**)

We thank MOBY team (PI: Ken Voss) for in situ MOBY radiance data.

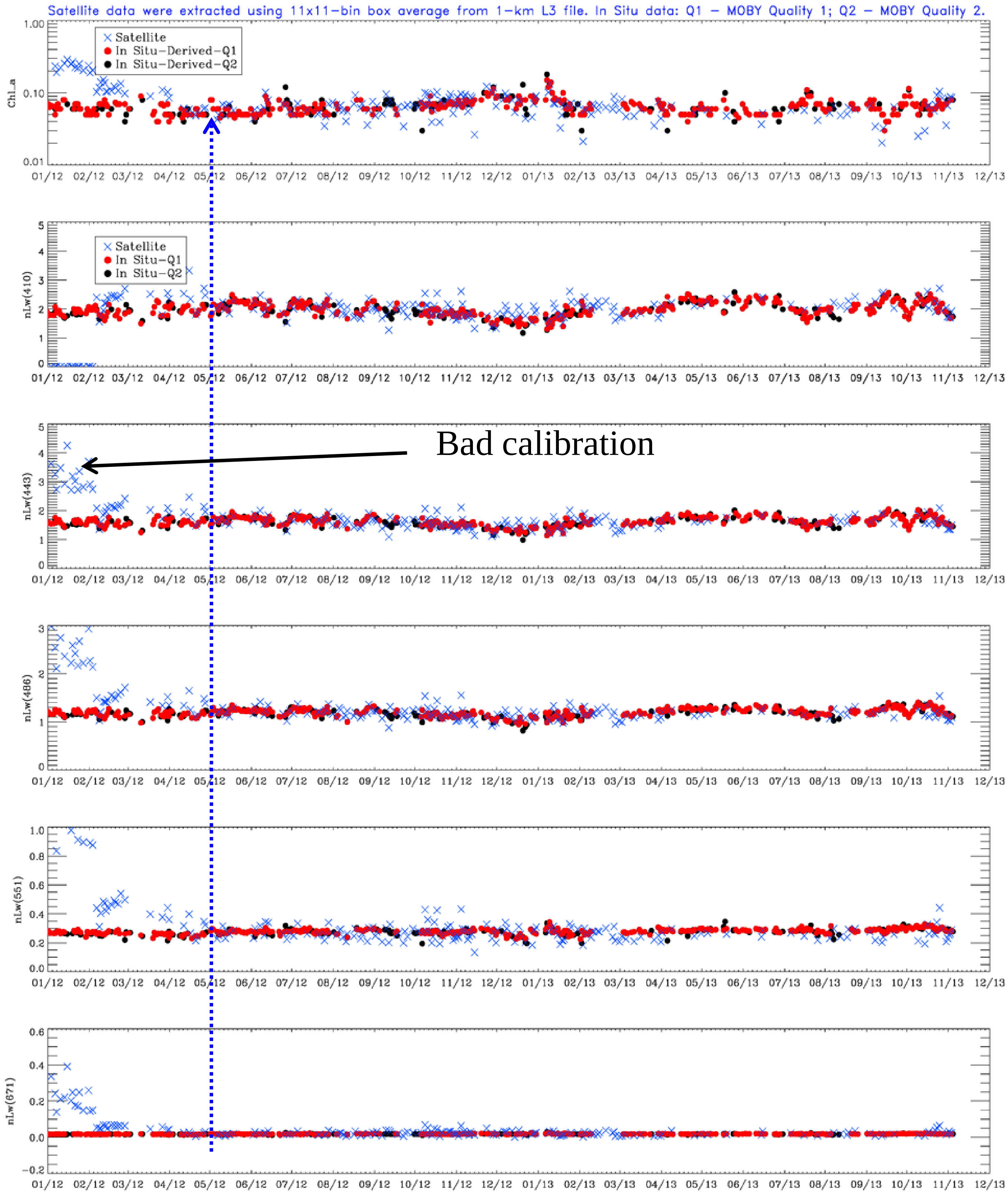

MOBY

Comparison of NOAA VIIRS ocean color products with **Marine Optical Buoy** (**MOBY)** in situ data.

Note:
Vicarious calibration gains applied since **May 2012**.

Vicarious gains were derived using **MOBY** in situ data.

MOBY in situ optics data have been providing critical data set in support of VIIRS calibration and validation activities, including VIIRS Level-1B (SDR) data monitoring for sensor on-orbit calibration.

MOBY Matchup
with
VIIRS Current Data Processing

MOBY

(2012-01-01 ~ **2014-05-31**)
Q1+Q2, ±3hr

Use IDPS-SDR with Old MSL12

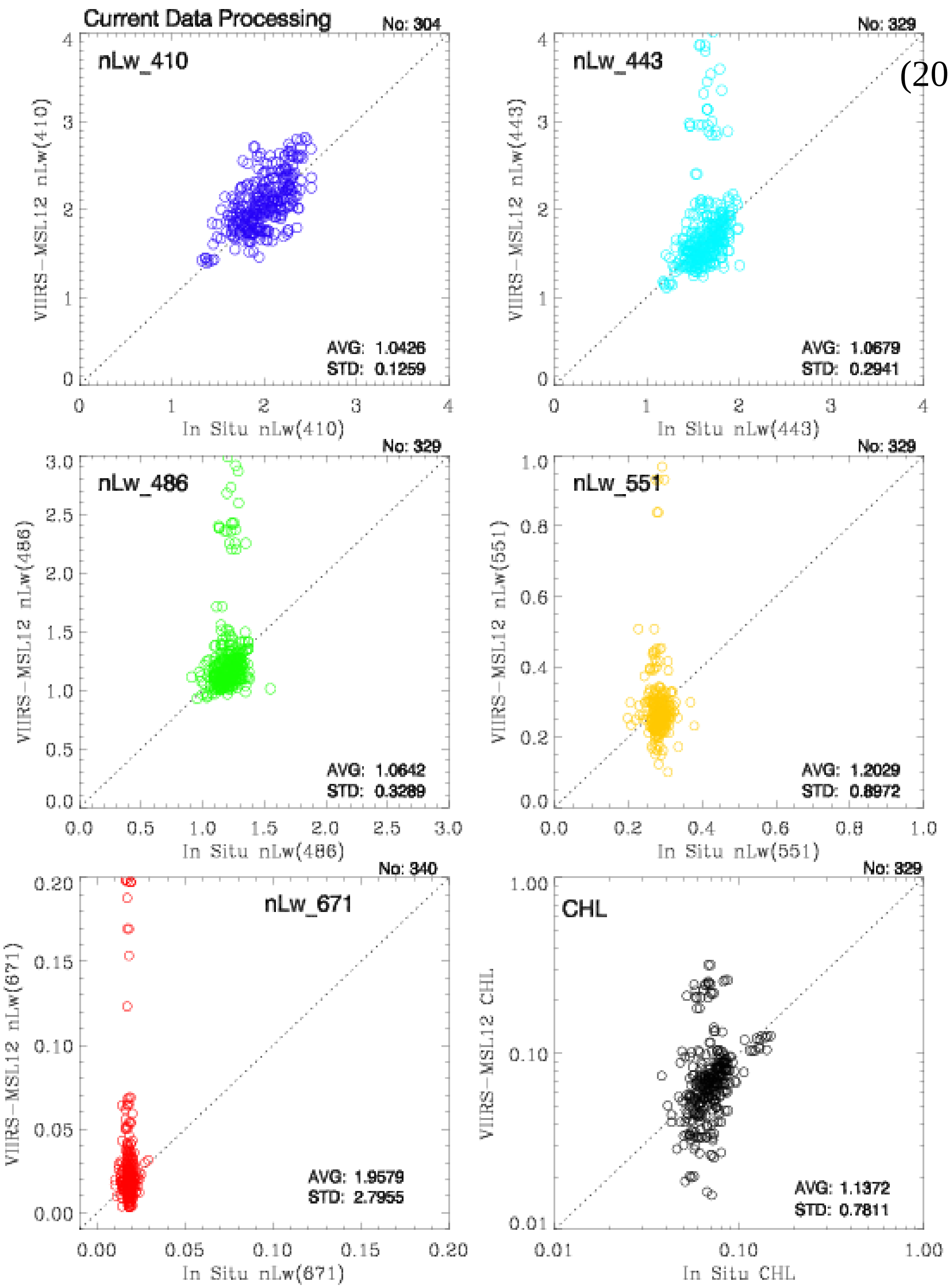

MOBY Matchup
with
VIIRS New EDR Processing (BMW-hdf)

MOBY

(2012-01-01 ~ **2014-05-31**)

Q1+Q2, ±3hr

Use IDPS-SDR with New MSL12

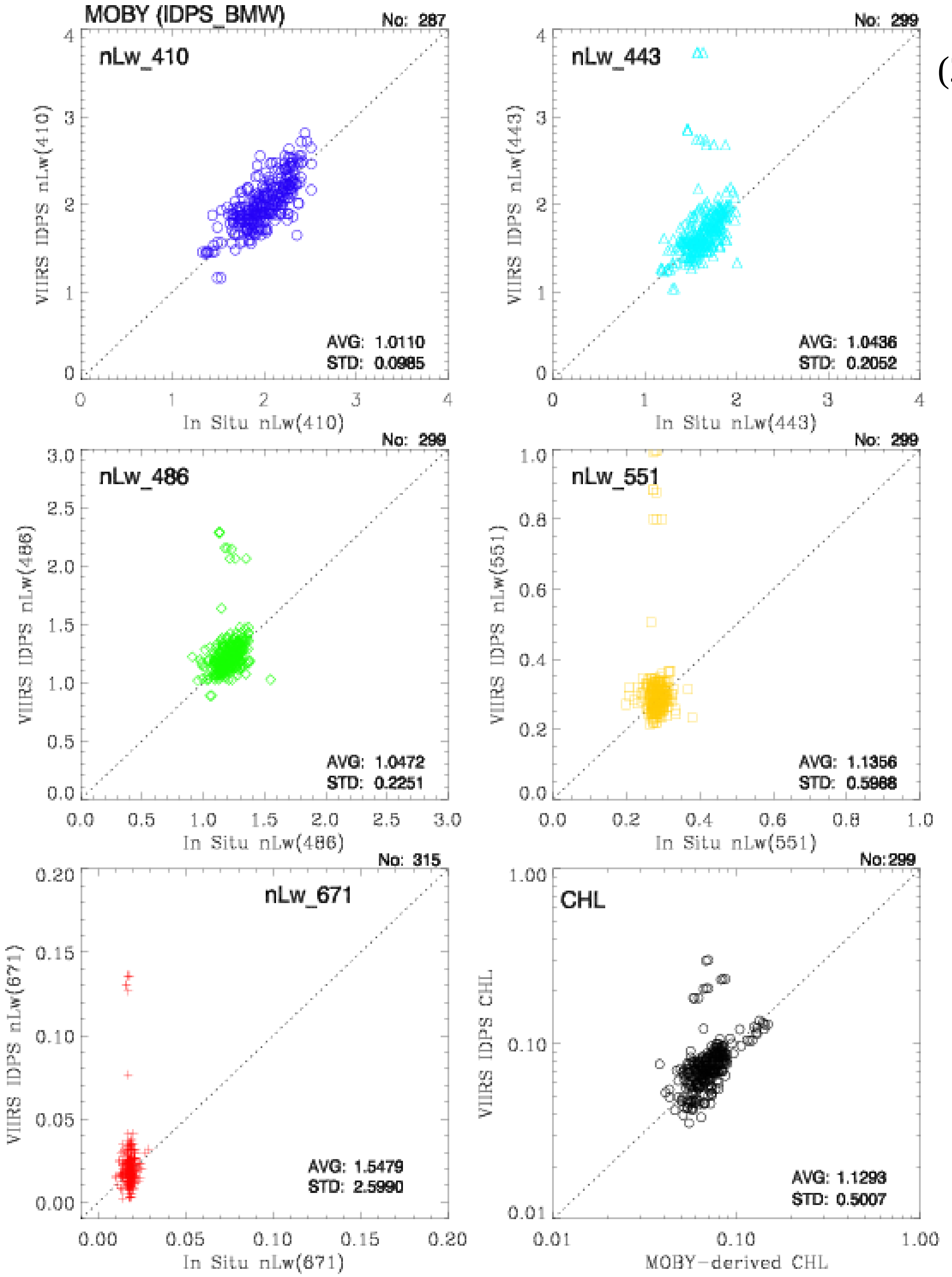

MOBY Matchup

with

VIIRS OC-SDR/EDR Processing (BMW-netCDF4)

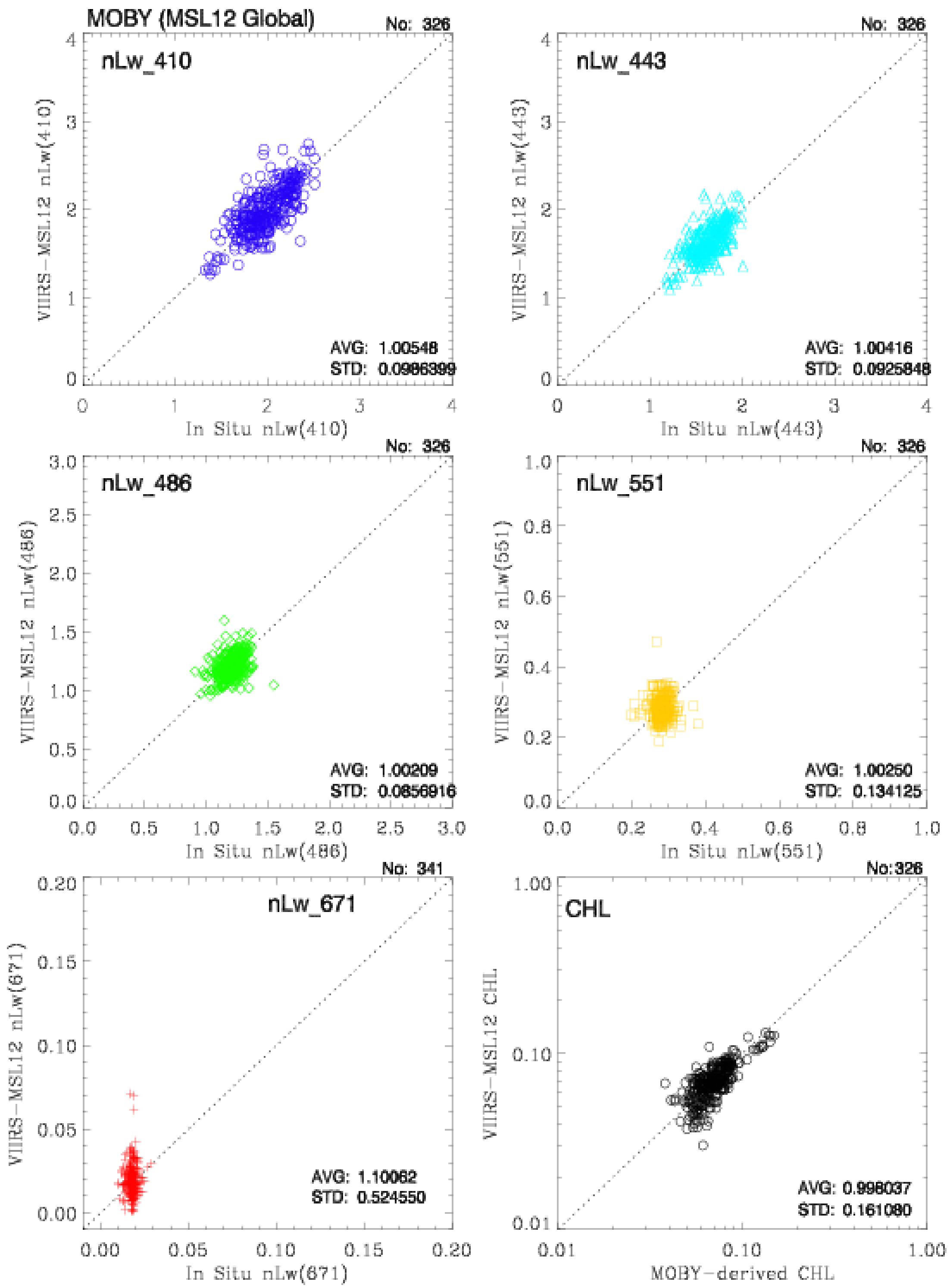

MOBY

(2012-01-01 ~ **2014-05-31**)

Q1+Q2, ±3hr

Use OC-SDR with New MSL12

MOBY

Statistics of VIIRS MSL12 vs. In-Situ (MOBY)

	Current Data Processing (2012-01-01 ~ **2014-05-31**)				New EDR Processing (BMW-hdf) (2012-01-01 ~ **2014-05-31**)				OC-SDR/EDR Processing (BMW-netCDF4) (2012-01-01 ~ **2014-05-31**)			
	AVG	**MED**	**STD**	**No**	**AVG**	**MED**	**STD**	**No**	**AVG**	**MED**	**STD**	**No**
$nL_w(410)$	**1.0426**	1.0329	0.126	304	**1.0110**	1.0065	0.099	287	**1.0055**	1.0002	0.099	326
$nL_w(443)$	**1.0679**	0.9904	0.294	329	**1.0436**	1.0107	0.210	299	**1.0042**	1.0009	0.093	326
$nL_w(486)$	**1.0642**	0.9743	0.329	329	**1.0472**	1.0071	0.225	299	**1.0021**	0.9992	0.086	326
$nL_w(551)$	**1.2029**	0.9225	0.897	329	**1.1376**	1.0077	0.600	299	**1.0025**	0.9947	0.134	326
$nL_w(671)$	**1.9579**	1.1263	2.796	340	**1.5479**	1.1000	2.599	315	**1.1006**	1.0588	0.525	341
Chl-a	**1.1372**	0.9488	0.781	329	**1.1293**	1.0333	0.501	299	**0.9980**	0.9852	0.161	326
$K_d(490)$	**1.0867**	0.9846	0.435	329	**1.0698**	1.0214	0.281	299	**0.9769**	0.9769	0.101	506

All Same Data

MOBY

Statistics of VIIRS MSL12 vs. In-Situ (MOBY)

	Current Data Processing (2012-02-28 ~ 2014-05-31)				New EDR Processing (BMW_hdf) (2012-02-28 ~ 2014-05-31)				OC-SDR/EDR Processing (BMW_nc4) (2012-02-28 ~ 2014-05-31)			
	AVG	**MED**	**STD**	**No**	**AVG**	**MED**	**STD**	**No**	**AVG**	**MED**	**STD**	**No**
$nL_w(410)$	**1.0351**	1.0173	0.123	282	**1.0180**	1.0085	0.108	282	**1.0003**	0.9961	0.101	282
$nL_w(443)$	**0.9817**	0.9672	0.114	282	**1.0149**	1.0066	0.107	282	**1.0025**	0.9982	0.096	282
$nL_w(486)$	**0.9671**	0.9557	0.102	282	**1.0140**	1.0024	0.098	282	**1.0038**	0.9994	0.089	282
$nL_w(551)$	**0.9311**	0.9069	0.198	282	**1.0353**	1.0012	0.164	282	**1.0004**	0.9898	0.140	282
$nL_w(671)$	**1.2011**	1.0889	0.596	281	**1.1558**	1.1222	0.525	281	**1.1241**	1.1111	0.530	281
Chl-a	**0.8956**	0.9034	0.279	282	**1.0439**	1.0298	0.204	282	**0.9966**	0.9875	0.165	282

"same STRAYLIGHT_FLAG (from OC-SDR/EDR processing) applied.."
& "same Geolocation information (since 2012-02-28)**"**

Matchup comparison
of
Aeronet-OC In Situ

(with **VIIRS MSL12**)

AERONET-OC data were obtained at:
http://aeronet.gsfc.nasa.gov/new_web/ocean_color.html
We thank AERONET-OC PIs for contributing useful ocean color radiance data.

Zibordi et al., “AERONET-OC: A network for the validation of the ocean color primary products,” *J. Atmos. Oceanic Technol.*, **26**, 1634–1651, 2009. http://dx.doi.org/10.1175/2009JTECHO654.1

Aeronet-OC CSI
with
VIIRS New EDR Processing
(BMW-hdf)

Use IDPS-SDR with New MSL12

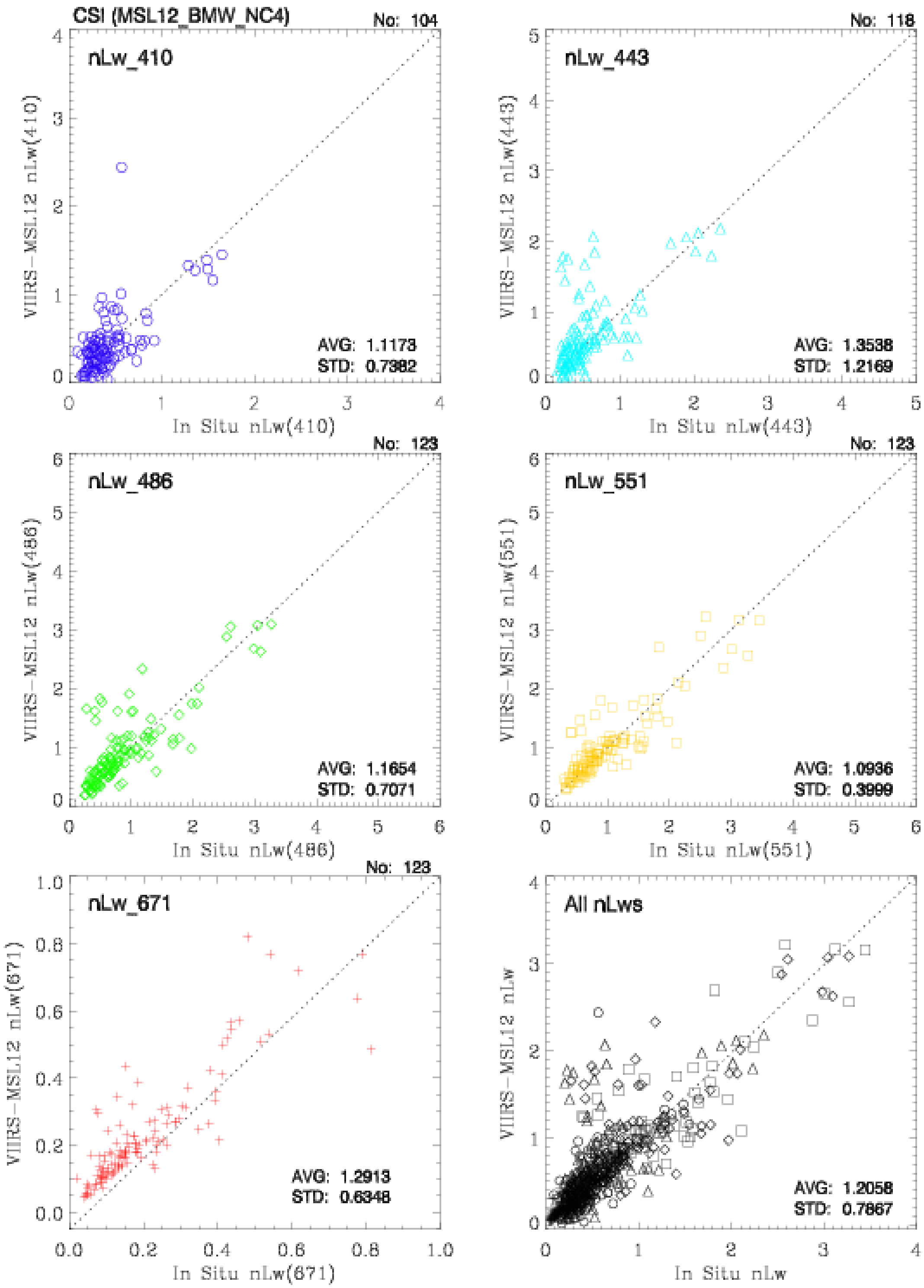

CSI

(2012-01-01 ~ 2014-05-31)

Aeronet-OC CSI

with

VIIRS OC-SDR/EDR Processing

(BMW-netCDF4)

Use OC-SDR with New MSL12

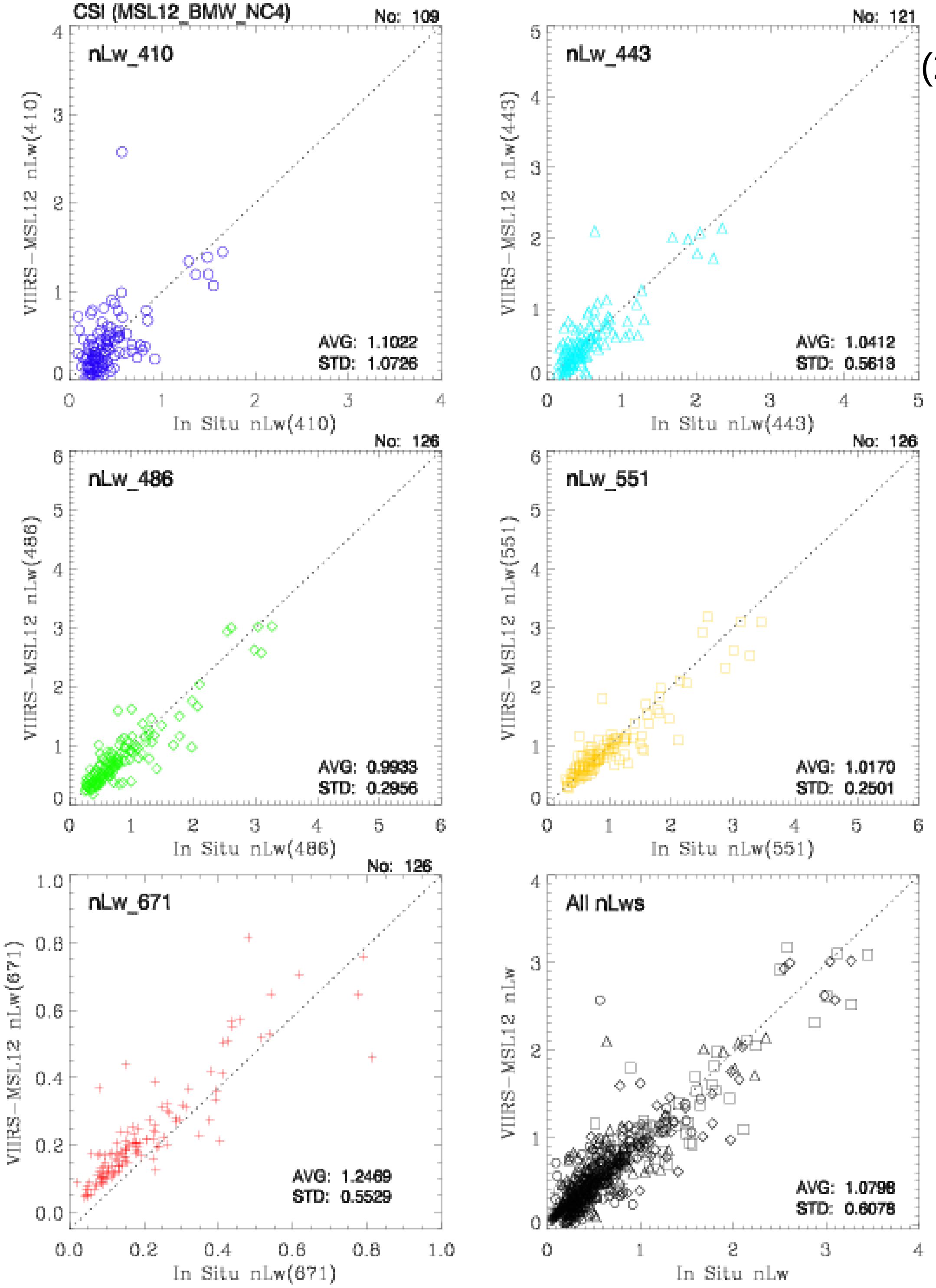

CSI

(2012-01-01 ~ 2014-05-31)

CSI

Statistics of VIIRS MSL12 vs. Aeronet-OC

	Current Data Processing (2012-01-01 ~ **2014-12-31**)				New EDR Processing (BMW-hdf) (2012-01-01 ~ **2014-05-31**)				OC-SDR/EDR Processing (BMW-netCDF4) (2012-01-01 ~ **2014-05-31**)			
	AVG	**MED**	**STD**	**No**	**AVG**	**MED**	**STD**	**No**	**AVG**	**MED**	**STD**	**No**
$nL_w(410)$	**1.6340**	1.2724	1.361	126	**1.1173**	0.9357	0.738	104	**1.1022**	0.8894	1.073	109
$nL_w(443)$	**1.6317**	1.0883	1.679	142	**1.3538**	0.9909	1.217	118	**1.0412**	0.9471	0.561	121
$nL_w(486)$	**1.4266**	1.0330	1.328	148	**1.1654**	1.0037	0.707	123	**0.9933**	0.9416	0.296	126
$nL_w(551)$	**1.1939**	0.9796	0.675	149	**1.0936**	1.0115	0.400	123	**1.0170**	0.9790	0.250	126
$nL_w(671)$	**1.5453**	1.1529	1.133	149	**1.2913**	1.1520	0.645	123	**1.2469**	1.1514	0.553	126
nL_w_All	**1.4802**	1.0773	1.278	714	**1.2058**	1.0241	0.787	591	**1.0798**	0.9831	0.608	608

All Same Data

CSI

Statistics of VIIRS MSL12 vs. Aeronet-OC

	Current Data Processing (2012-01-01 ~ **2014-05-31**)				New EDR Processing (BMW-hdf) (2012-01-01 ~ **2014-05-31**)				OC-SDR/EDR Processing (BMW-netCDF4) (2012-01-01 ~ **2014-05-31**)			
	AVG	**MED**	**STD**	**No**	**AVG**	**MED**	**STD**	**No**	**AVG**	**MED**	**STD**	**No**
$nL_w(410)$	**1.4653**	1.2082	0.925	94	**1.1958**	0.9449	0.792	94	**1.0124**	0.8979	0.747	94
$nL_w(443)$	**1.5460**	1.0108	1.874	110	**1.5347**	1.0089	1.602	110	**1.0839**	0.9533	0.562	110
$nL_w(486)$	**1.1970**	0.9556	0.910	116	**1.2287**	1.0438	0.762	116	**1.0120**	0.9444	0.294	116
$nL_w(551)$	**1.1044**	0.9523	0.497	116	**1.1368**	1.0239	0.422	116	**1.0299**	0.9838	0.250	116
$nL_w(671)$	**1.3809**	1.1529	0.771	116	**1.3635**	1.1767	0.713	116	**1.2646**	1.1591	0.565	116
nL_w_All	**1.3314**	1.0393	1.104	552	**1.2931**	1.0451	0.948	552	**1.0832**	0.9951	0.514	552

"same STRAYLIGHT_FLAG (from OC-SDR/EDR processing) applied.."

Aeronet-OC USC

with

VIIRS OC-SDR/EDR Processing

(BMW-netCDF4)

USC

(2012-01-01 ~ 2014-05-31)

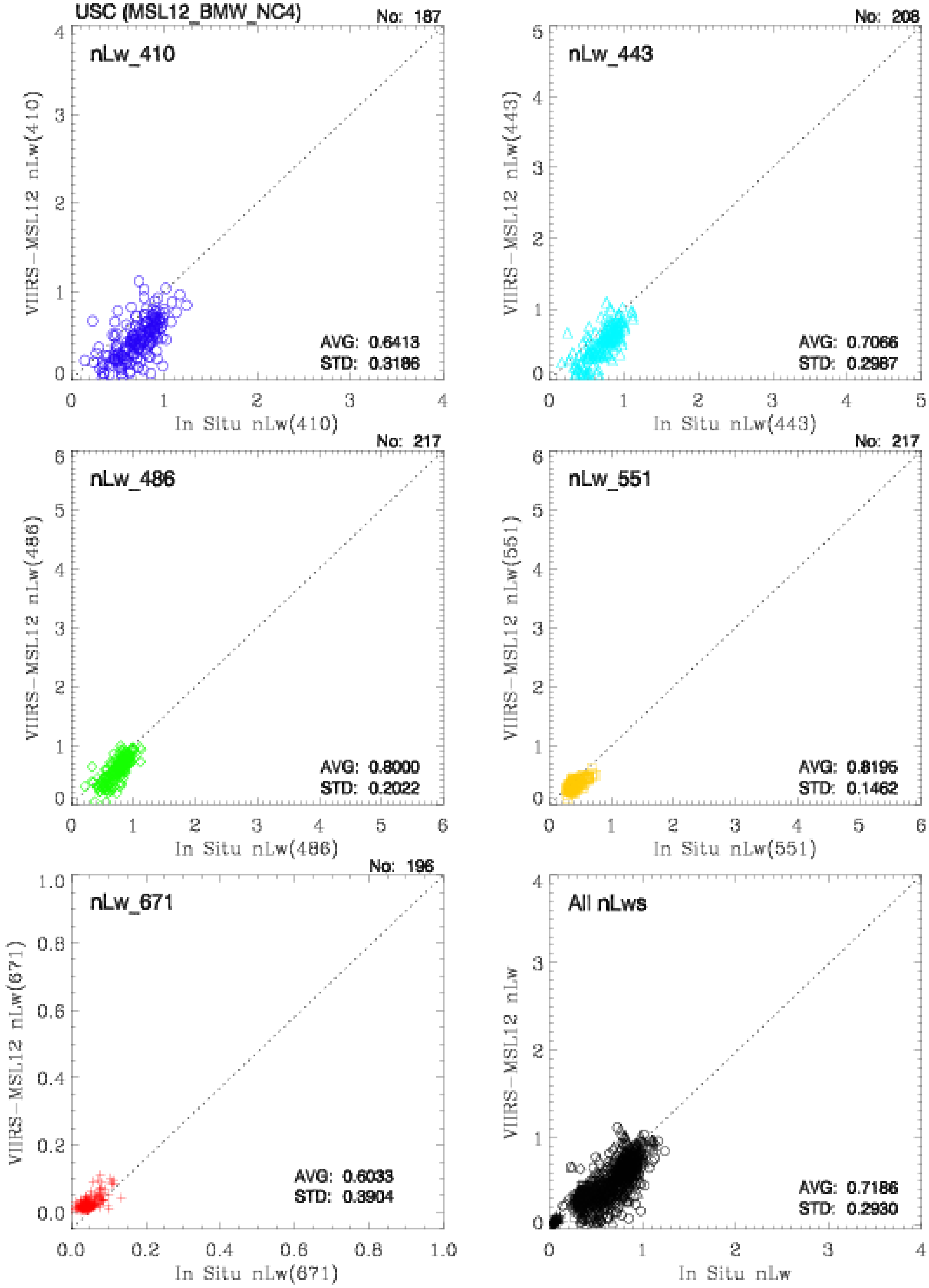

Use OC-SDR with New MSL12

USC

Statistics of VIIRS MSL12 vs. Aeronet-OC

	Current Data Processing (2012-01-01 ~ **2014-12-31**)				New EDR Processing (BMW-hdf) (2012-01-01 ~ **2014-05-31**)				OC-SDR/EDR Processing (BMW-netCDF4) (2012-01-01 ~ **2014-05-31**)			
	AVG	**MED**	**STD**	**No**	**AVG**	**MED**	**STD**	**No**	**AVG**	**MED**	**STD**	**No**
$nL_w(410)$	**0.8442**	0.7756	0.668	171	**0.6619**	0.6484	0.322	197	**0.6413**	0.6264	0.319	187
$nL_w(443)$	**0.8200**	0.7413	0.645	172	**0.7681**	0.7489	0.293	208	**0.7066**	0.7213	0.299	208
$nL_w(486)$	**0.8532**	0.8018	0.556	174	**0.8366**	0.8346	0.194	214	**0.8000**	0.8106	0.202	217
$nL_w(551)$	**0.8026**	0.7759	0.179	173	**0.8597**	0.8476	0.153	214	**0.8195**	0.8083	0.146	217
$nL_w(671)$	**0.6621**	0.5354	0.772	153	**0.6243**	0.5642	0.387	190	**0.6033**	0.5275	0.390	196
nL_w_All	**0.800**	0.7563	0.597	843	**0.7544**	0.7665	0.294	1023	**0.7186**	0.7384	0.293	1025

Conclusions/Path Forward (1)

- With improved SDR (calibration) and EDR (processing algorithms), **VIIRS ocean color products are now comparable to or better than those from MODIS-Aqua.**
- We have completed mission-long OC data reprocessing using IDPS-SDR with new MSL12.
- We have started VIIRS mission-long science quality ocean color data **reprocessing** (including **SDR** and **EDR**), and will finish that in **late 2015**, & the data stream will go forward. **Two data streams will be produced: near-real-time and science quality ocean color data.**
- Calibration from both solar and lunar is necessary. We need lunar model data!
- VIIRS ocean color products have been improved after the implementation of some important updates, new algorithms, and with vicarious calibrations.
- In general, VIIRS **normalize water-leaving radiance** spectra show reasonable agreements with in situ measurements at MOBY, AERONET-OC sites, and various other ocean regions.
- The new NIR ocean reflectance correction algorithm (BMW) improves ocean color data over coastal and inland waters. The destriping algorithm significantly improves VIIRS-derived ocean color imageries.
- New **K_d(PAR)** product has been developed and routinely produced to meet users requirements.
- NOAA dedicated Cal/Val cruise in Nov. 2014, and plan to have it in late 2015. The report for the 2014 Cal/Val cruise has been completed.
- There will be many applications using VIIRS ocean color products.
- We have developed VIIRS instrument calibration capability, and with new calibration LUTs, VIIRS ocean color products are significantly improved.
- Our evaluation results show that VIIRS-SNPP is capable of providing high-quality global ocean color products in support of science research and operational applications.
- We have been actively working with other current and future ocean color sensors, e.g., MODIS-Aqua, Korean GOCI, EUMETSAT for Sentinel-3 (launch late 2015), JAXA GCOM-C (launch early 2017), and **VIIRS on J1** (launch 2017).

Conclusions/Path Forward (2)

- Complete VIIRS mission-long ocean color data reprocessing (science quality, i.e., improved SDR, algorithms, and science quality ancillary data).
- VIIRS reprocessed data stream will go forward (about one-two weeks delay). VIIRS science quality data will be distributed through CoastWatch and other means (e.g., NODC effort).
- Cal/Val team will finish the 2014 VIIRS dedicated cruise report and in situ data analyses (e.g., improve in situ data quality).
- More in situ data are needed for validation and improvement of VIIRS ocean color products.
- In situ data quality (instrument calibration, measurement protocols, data processing methodology, etc.)
- Dedicated VIIRS ocean color Cal/Val cruise in December 2015, and establishing annual Cal/Val cruises.
- Continue work on sensor on-orbit calibration (solar and lunar), algorithms improvements, etc.
- We have been working on J1 instrument. Need more efforts for J1 VIIRS pre-launch data analyses as J1 close to launch (access to J1 sensor data).
- Algorithms improvements for both open oceans and coastal/inland waters. In particular, significant efforts are needed for coastal/inland waters.

Questions?

Aeronet-OC LISCO

with

VIIRS OC-SDR/EDR Processing

(BMW-netCDF4)

LISCO

(2012-01-01 ~ 2014-05-31)

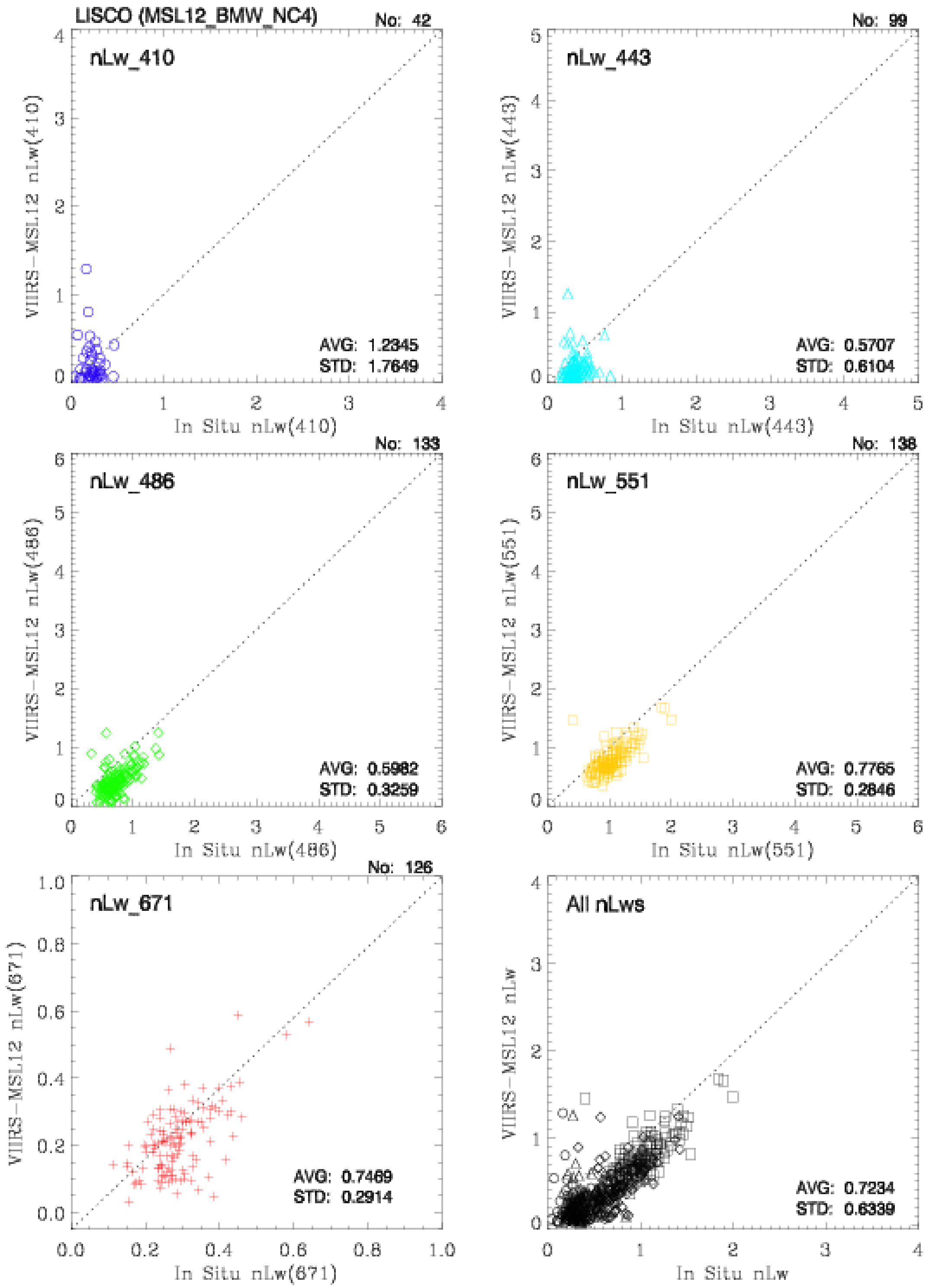

Use OC-SDR with New MSL12

LISCO

Statistics of VIIRS MSL12 vs. Aeronet-OC

	Current Data Processing (2012-01-01 ~ **2014-12-31**)				New EDR Processing (BMW-hdf) (2012-01-01 ~ **2014-05-31**)				OC-SDR/EDR Processing (BMW-netCDF4) (2012-01-01 ~ **2014-05-31**)			
	AVG	**MED**	**STD**	**No**	**AVG**	**MED**	**STD**	**No**	**AVG**	**MED**	**STD**	**No**
$nL_w(410)$	**1.8557**	1.0733	1.885	51	**1.3582**	0.7842	1.689	40	**1.2345**	0.5524	1.765	42
$nL_w(443)$	**1.3563**	0.7418	1.506	73	**1.0520**	0.5899	1.258	100	**0.5707**	0.4082	0.610	99
$nL_w(486)$	**0.8040**	0.5911	0.598	99	**0.7524**	0.6112	0.552	134	**0.5982**	0.5679	0.326	133
$nL_w(551)$	**0.8465**	0.7841	0.307	100	**0.8491**	0.7632	0.349	140	**0.7765**	0.7425	0.285	138
$nL_w(671)$	**0.8315**	0.7698	0.432	97	**0.8072**	0.7591	0.404	130	**0.7469**	0.7606	0.291	126
nL_{w}_All	**1.0442**	0.7418	1.046	420	**0.8900**	0.7167	0.816	544	**0.7234**	0.6618	0.634	538

SNPP VIIRS SDR Calibration for Improvement of Ocean Color Products

Junqiang Sun[1,2] and Menghua Wang[1]

[1]NOAA/NESDIS Center for Satellite Applications and Research
E/RA3, 5830 University Research Ct., College Park, MD 20740, USA
[2]Global Science and Technology, 7855 Walker Drive, Maryland, USA

8/27/2015 9:00-9:15 AM

Key Points

- **Ocean color products are highly sensitive to details in processing algorithms and calibration.**
- VIIRS RSB uncertainty specification is 2%; For ocean color EDR products, the ocean bands (M1-M7) are required to be calibrated with an uncertainty of ~0.1-0.3%.
- Solar diffuser (SD) degrades non-uniformly, resulting in long-term bias in calibration results, especially for short wavelength bands
- A hybrid approach properly combining the SD and lunar calibration coefficients restores the accuracy of the calibration coefficients from the non-uniformity issue and other various effects:
  - Lunar calibration provides long-term baseline
  - SD calibration provides smoothness and frequency
- **Every component must itself be accurately characterized!**
  - SDSM calibration/SD calibration; Lunar calibration; Hybrid approach
- Challenges and potential issues

Solar Illumination and Sweet Spot

Illumination of SD and SDSM Aperture

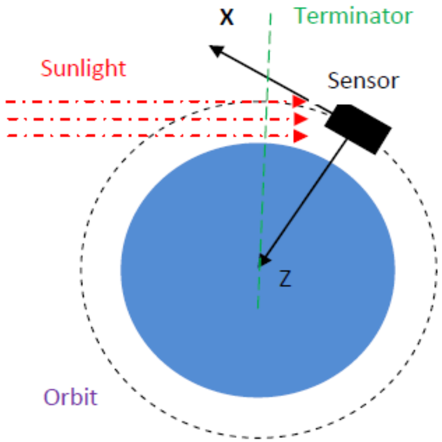

Solar angles

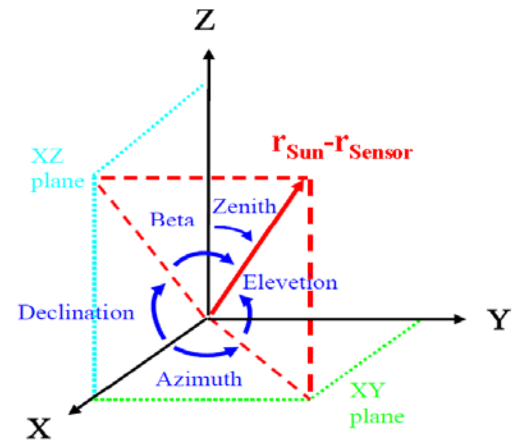

SDSM response

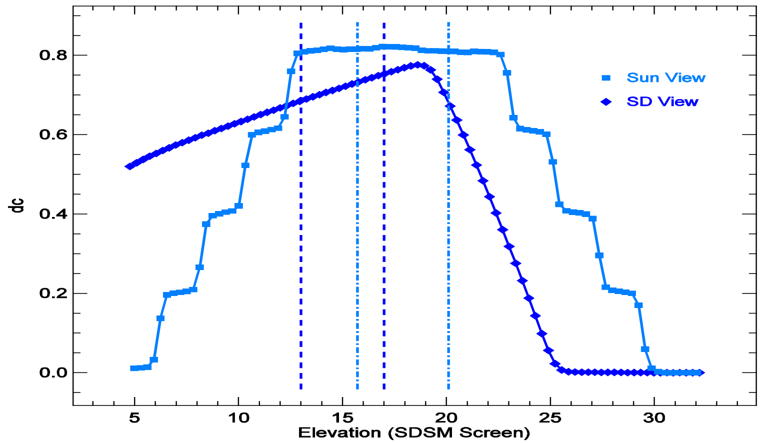

Band M1 Detector 1 response

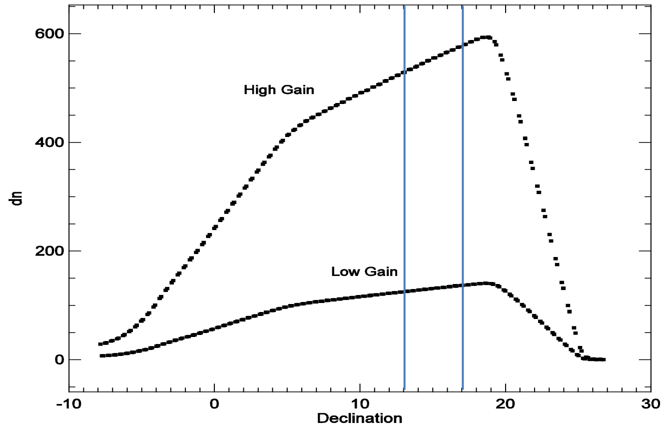

Good selections stabilizes results, reduce noise – Different from ATBD

Prelaunch BRFs of the SD and the VFs of SD and SDSM Screens

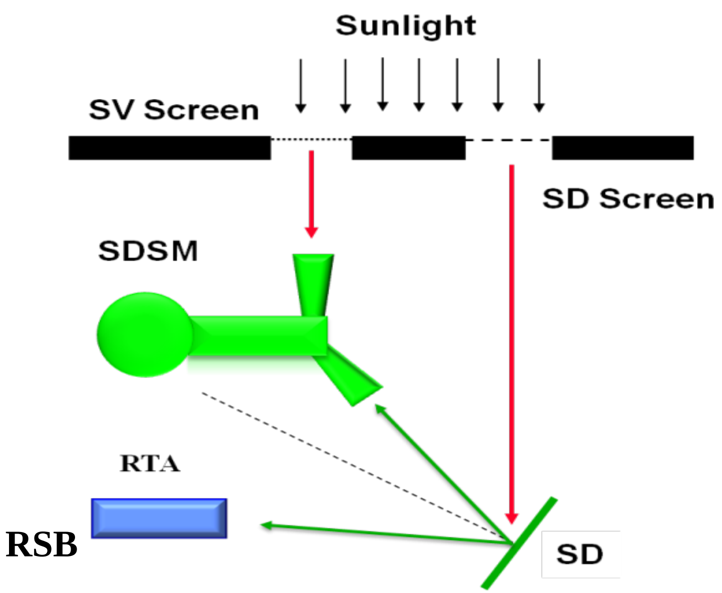

The author carefully made yaw planning in 2012 with NASA colleagues for on-orbit validation of BRDF and VF.

We have carefully re-derived BRFs and VFs from the yaw measurements (removes seasonal variation artifacts and noises)

*J. Sun and X. Xiong, "Solar and lunar observation planning for Earth-observing sensor", Proc. SPIE, **8176**, 817610, (2011).*

- SD and SDSM sun view screens:
  - Prevent RSB and SDSM saturation
  - Vignetting functions (VFs)
  - VFs measured prelaunch and validated by yaw measurements
- SD bidirectional reflectance factors (BRFs)
  - BRFs measured prelaunch and validated by yaw measurements
  - SD on-orbit degradation is tracked by the SDSM measurements at 8 wavelength from 412 nm to 935 nm

J. Sun and M. Wang, "On-orbit characterization of the VIIRS solar diffuser and solar diffuser screen," Appl. Opt., 54, 236 -252(2015).

SDSM Calibration Algorithm

- SDSM is a ratio radiometer, which views SD, Sun, and an internal dark scene successively in three-scan cycles.

- SD BRF for SDSM view direction

$$BRF_{SD,SDSM}(\lambda) = \rho_{SD,SDSM}(\lambda) H(\lambda)$$

  - $\rho_{SD,SDSM}(\lambda)$: Prelaunch BRF for SDSM view direction
  - $H(\lambda)$ is solar diffuser degradation since launch

- SD degradation, H factors, for SDSM view direction at the wavelength of the SDSM detector D

$$H(\lambda_D) = \left\langle \frac{dc_{SD,D}}{\rho_{SD,SDSM}(\lambda_D)\tau_{SDS}\cos(\theta_{SD})} \right\rangle_{Scan} \Bigg/ \left\langle \frac{dc_{SV,D}}{\tau_{SVS}} \right\rangle_{Scan}$$

- ***Improvements***
  - *Carefully re-derived the VFs and BRFs from yaw measurements*
  - ***Ratio of the averages (different from ATBD!)***
  - *Sweet spots selection*

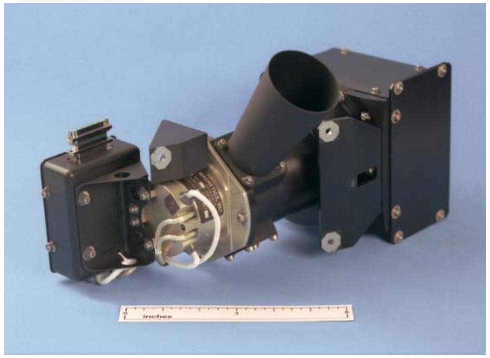

SDSM operations: Every orbit first few months, then once per day for about two years, and once per two days since May, 2014.

J. Sun and M. Wang, “Visible infrared image radiometer suite solar diffuser calibration and its challenges using solar diffuser stability monitor,” Appl. Opt., 53, 8571-8584 (2014).

SDSM Calibration Results

Sun view response trending

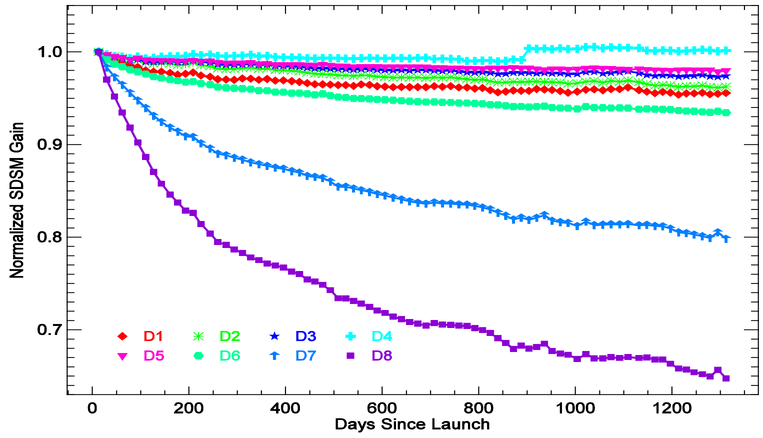

SD view response trending

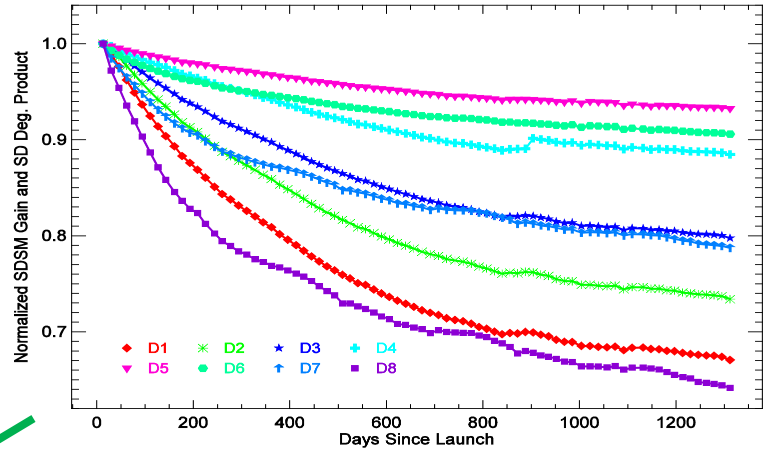

SD degradation

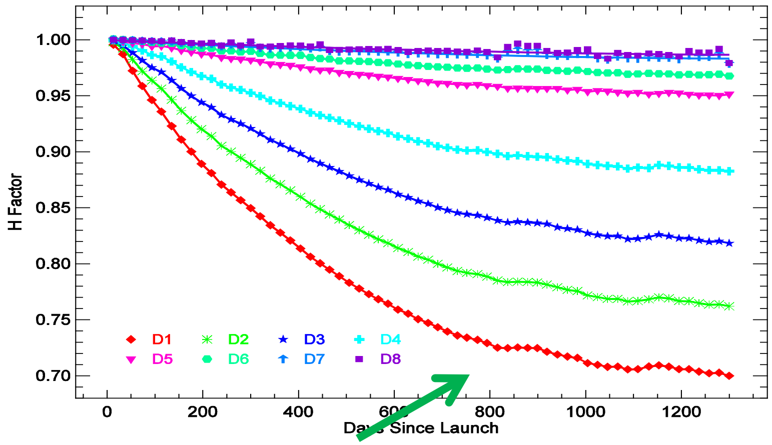

SD degradation

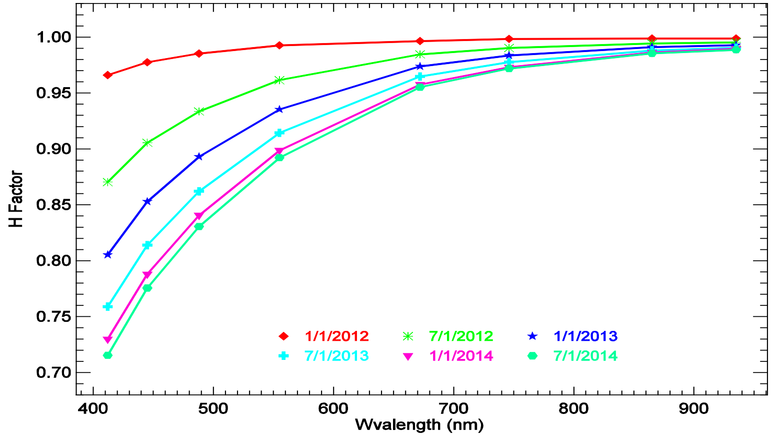

Unexpected but real degradation (Nov., 2014)

SDSM can accurately track the SD degradation for SDSM direction

SD Calibration Algorithm

- SD is made of Spectralon®, near Lambertian property
- Solar radinace reflected by the SD

$$L_{SD}(\lambda) = I_{Sun}(\lambda) \cdot \tau_{SDS} \cdot \cos(\theta_{SD}) \cdot \rho_{SD,RTA}(\lambda) \cdot h(\lambda) / d_{VS}^2$$

  - $\rho_{RSD,RTA}(\lambda)$: Prelaunch BRF for RTA view direction
  - $h(\lambda)$: SD degradation for SDSM view direction is used as the SD degradation for the RTA direction

SD Calibration: Every orbit

- RSB calibration coefficients, F factors

$$F(B,D,M,G,t) = \frac{RVS_{B,SD} \cdot \int RSR_B(\lambda,t) \cdot L_{SD}(\lambda) \cdot d\lambda}{\sum_i c_i(B,D,M,G) \cdot dn^i \cdot \int RSR_B(\lambda,t) \cdot d\lambda}$$

  - *B*, *D*, *M*, *G*: Band, Detector, HAM side, and gain status

- ***Improvements***
  - *Carefully rederived the VFs and BRFs from yaw measurements*
  - ***Improved H factors***
  - *Sweet spot selection*
  - ***Time-dependent RSR***

J. Sun and M. Wang, "On-orbit calibration of Visible Infrared Imaging Radiometer Suite reflective solar bands and its challenges using a solar," Appl. Opt., 54, 7210-7223 (2015).

SD Calibration Results

Band M1 HAM 1 HG F-factors

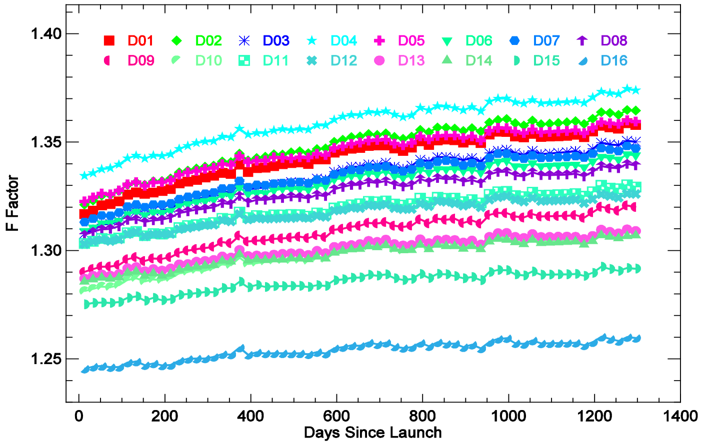

Band Averaged HAM1 HG F-factors

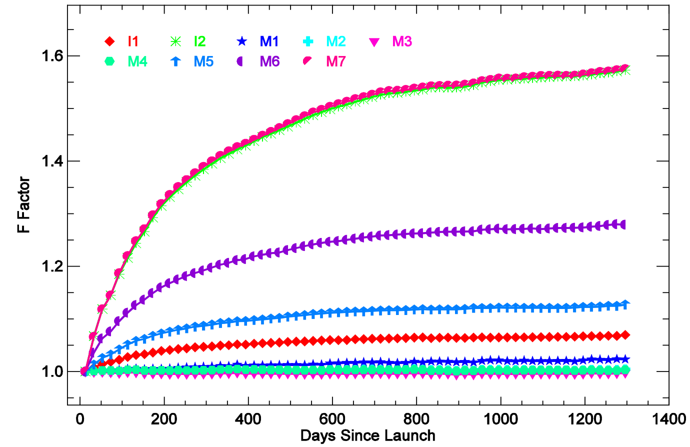

HG = High Gain
LG = Low Gain

Time-dependent RSR

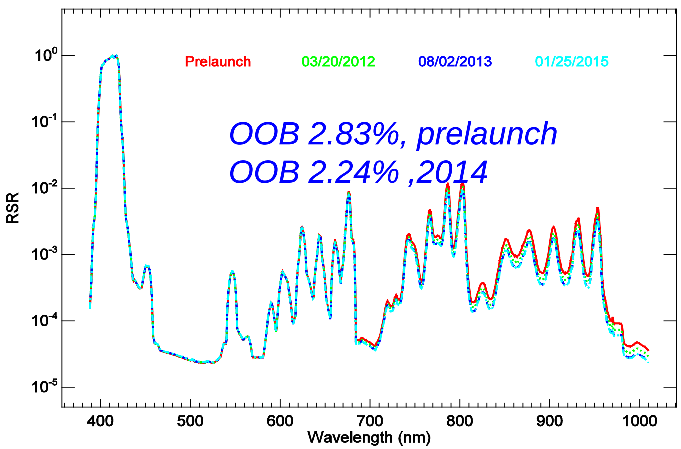

Impact of RSR on F-factors

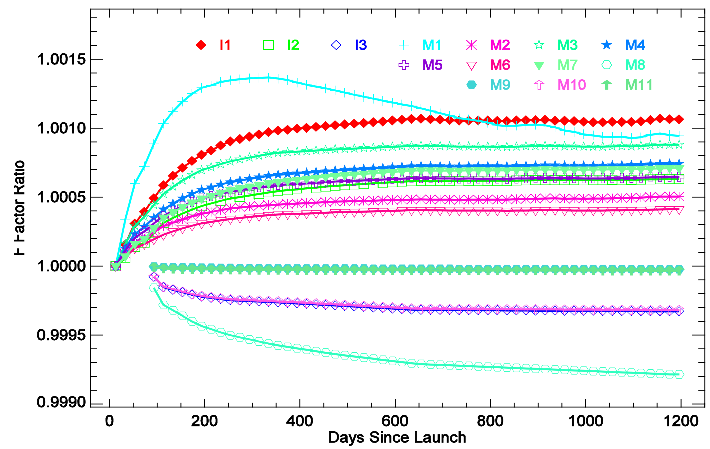

SD can accurately track the RSB gain change as long as SD degradation for the RTA view can be approximated as that for the SDSM view.

Lunar Calibration Algorithm

- Moon is very stable in its reflectance

- RSB calibration coefficients , F factors, from lunar observations

$$F(B,M)=\frac{g(B)N_{t,M}}{\sum_{D,S,N}L_{pl}(B,D,S,N)\delta(M,M_N)},$$

  – *g(B)*: View geometric effect correction (ROLO lunar model and extra correction)

SNPP VIIRS is scheduled to view the Moon approximately monthly (about nine months every year)

- *Advantages*
  - *Lunar surface reflectance has no observable degradation*
  - *Can be used for inter-comparison*

J. Sun, X. Xiong, and J. Butler, "NPP VIIRS on-orbit calibration and characterization using the moon", Proc. SPIE, 8510,85101I, (2012).
X. Xiong, J. Sun, J. Fulbright, Z. Wang, and J. Butler, "Lunar Calibration and Performance for S-NPP VIIRS reflective Solar Bands", IEEE Trans. Geosci. Remote Sens., accepted.

Lunar Planning and Calibration Results

Roll maneuver

Required roll maneuver

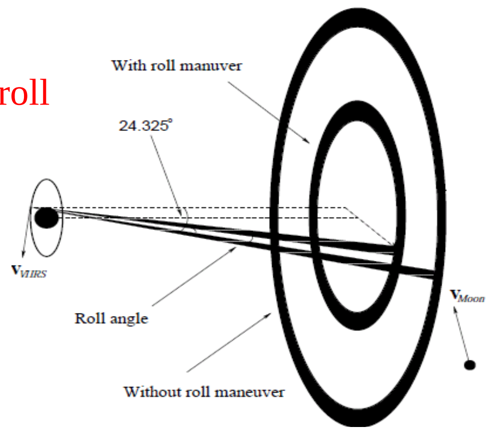

Lunar image (M6 in April, 2012)

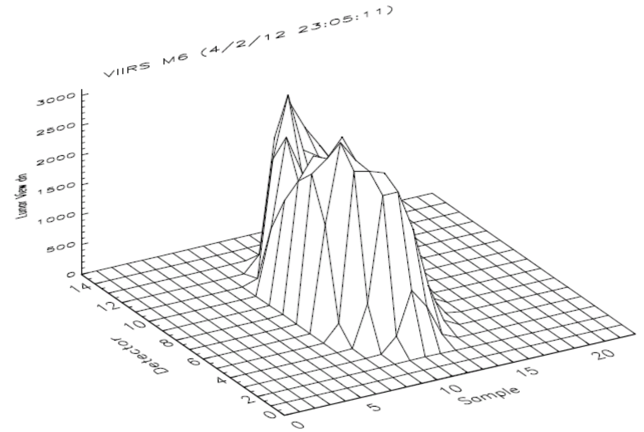

Lunar and SD F Factors

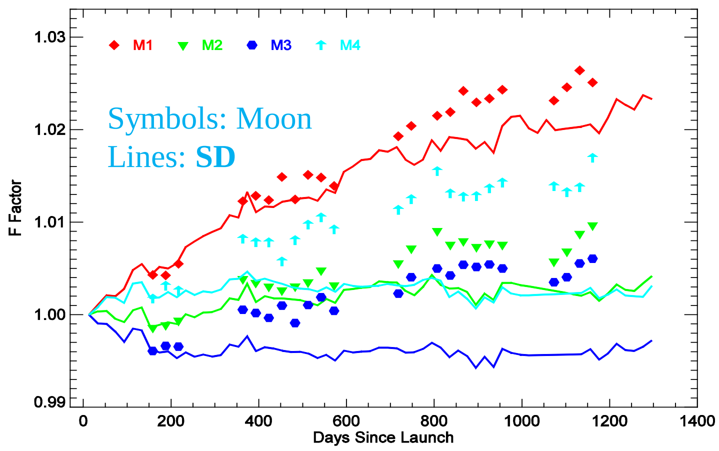

- View geometry dependence
- ***Planning is important starting point – made lunar planning tool and planned lunar observations in early mission***
- However, the phase angle range change from [-56°, -55°] to [-50.5°, 51.5°]
- Size of the moon
- Oversampling effect
- Scans seeing full lunar image

*J. Sun and X. Xiong, "Solar and lunar observation planning for Earth-observing sensor", Proc. SPIE, **8176**, 817610, (2011).*

Hybrid Approach

- SD Calibration
  - SD degrades non-uniformly, resulting long-term drifts
  - Results are stable and smooth
  - Observation in every orbit
- Lunar Calibration
  - No degradation issue
  - Infrequent and no observation in three months every year
- Hybrid Approach

$$\mathcal{F}(B,D,M,G)=R(B,t)\cdot F(B,D,M,G)$$

$$R(B,t)=\left\langle f(B,M,t)\right\rangle_{M} / \left\langle F(B,D,M,0,t)\right\rangle_{D,t-15<t_i<t+15,M}$$

F-Factors Ratios are fitted to quadratic polynomials of time

- **Lunar calibration provides long-term baseline**
- **SD calibration provides smoothness and frequency**

J. Sun and M. Wang, "Radiometric Calibration of the VIIRS Reflective Solar Bands with Robust Characterizations and Hybrid Calibration Coefficients," submitted to Applied Optics.

Hybrid Calibration Coefficients

Calibration coefficients Ratios

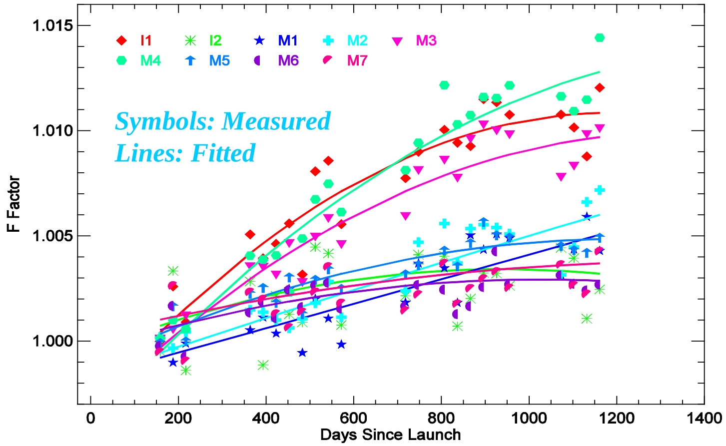

Calibration Coefficients (M1)

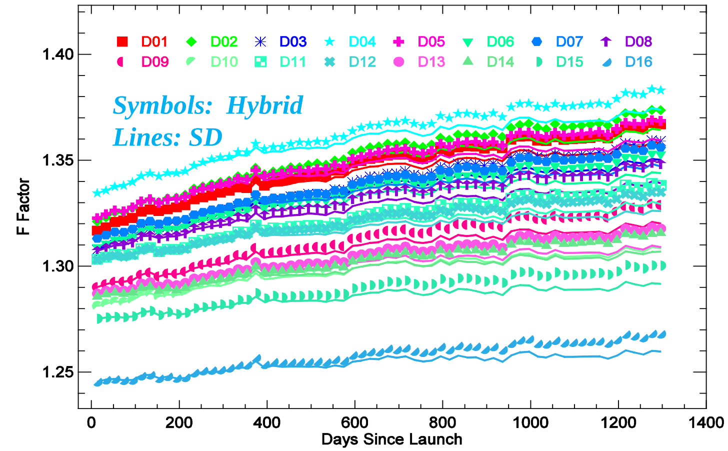

Calibration Coefficients (M4)

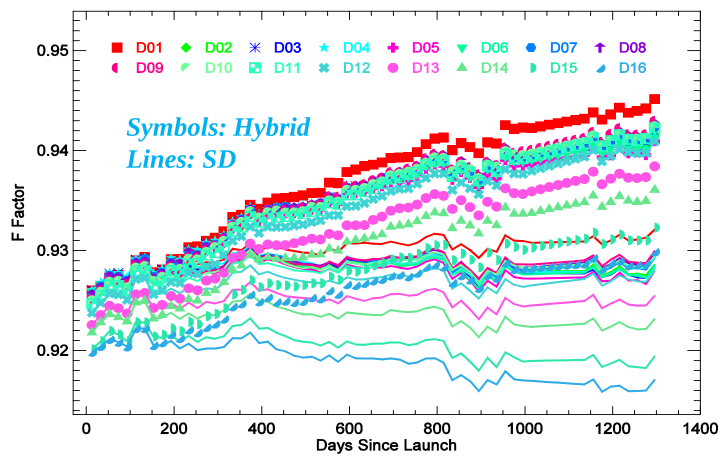

Calibration Coefficients

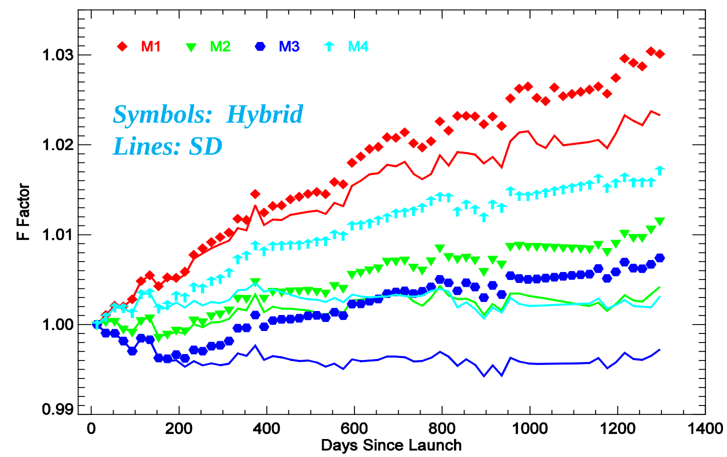

Improvements in Ocean Color Products

- VIIRS data were reprocessed using **MSL12** with SDR generated with updated hybrid calibration coefficients.
- NOAA ocean color products produced with the hybrid calibration coefficients have met validated maturity in March 2015.
- **Hybrid results agree with MOBY in situ!**

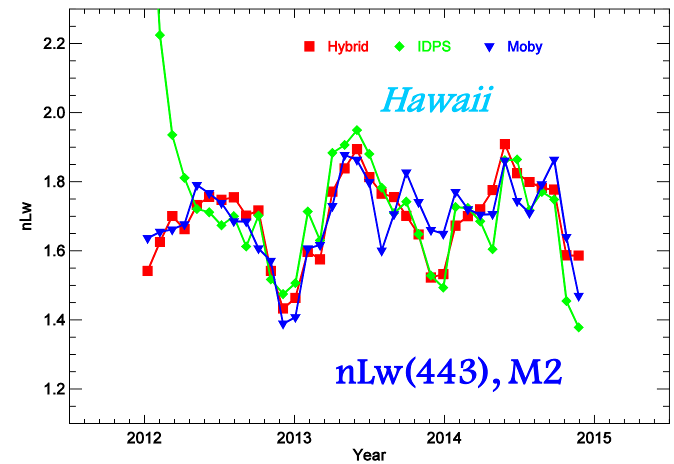

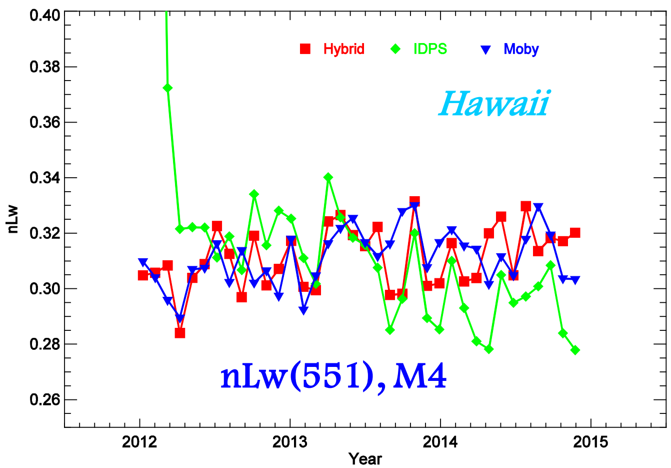

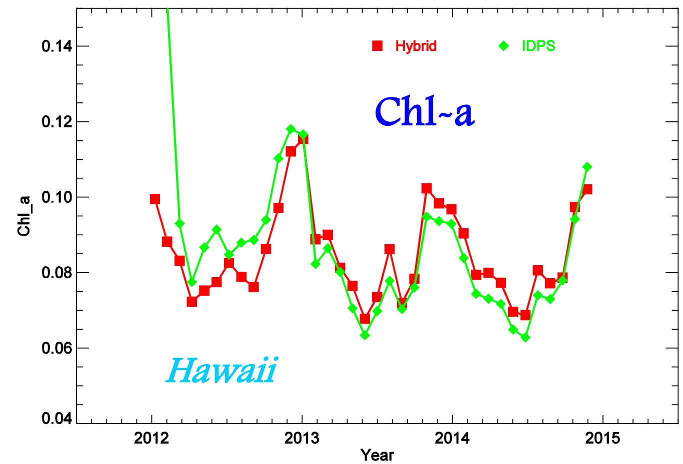

Green: VIIRS IDPS; Red: VIIRS Hybrid; Blue: Moby in Situ

- *J. Sun and M. Wang, "VIIRS Reflective Solar Bands On-Orbit Calibration and Performance: A Three-Year Update," Proc. SPIE, 9264, 92640L (2014).*
- *M. Wang, et al, "Evaluation of VIIRS ocean color products," Proc. SPIE 9261, 92610E (2014).*

Some Other Challenges

- SD degrades abnormally

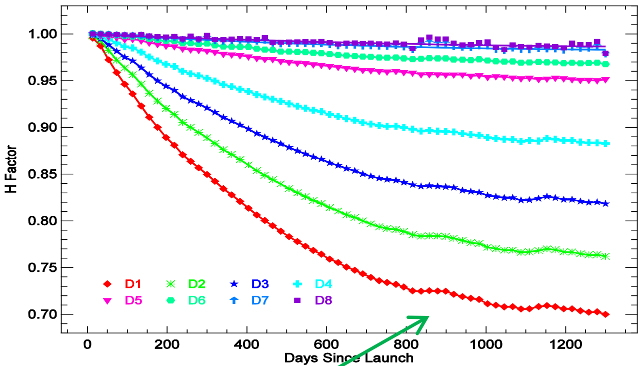

Unexpected but real degradation (Nov., 2014)

- S-NPP orbit drift

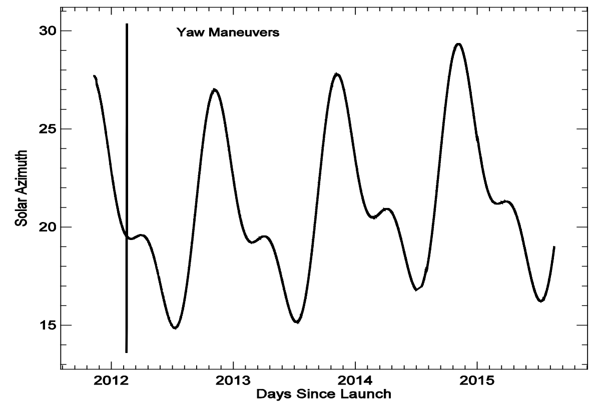

Azimuth angle in instrument coordinate system

- RVS may change on-orbit
  - Aqua and Terra MODIS RVS have changed more than 20% and 40%, respectively, at small AOI.

- *J. Sun, X. Xiong, A. Angal, H. Chen, A. Wu, and X. Geng, "Time dependent response versus scan angle for MODIS reflective solar bands," IEEE Trans. Geosci. Remote Sens., 52, 3159-3174 (2014).*
- *J. Sun and X. Xiong, "TMODIS polarization sensitiivity analysis", IEEE Trans. Geosci. Remote Sens., 45, 2875-2885 (2007).*

- Polarization sensitivity may change on-orbit

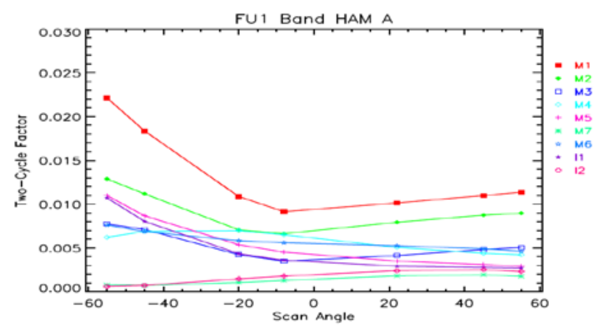

  - Terra MODIS polarization sensitivity changed dramatically on-orbit

Summary

- Robust characterizations of essential calibration components have been completed
- A hybrid approach combining the SD and lunar calibration coefficients, along with robust inputs, achieves the highest accuracy up to date
- Hybrid calibration approach, using both solar and lunar calibrations, has significantly improved VIIRS ocean color products
- "Solar diffuser degradation uniformity condition" will be a key issue for all instruments such as VIIRS J1, VIIRS J2, etc, that use SD/SDSM for reflective solar bands calibration - Lunar calibration is necessary as a solution.
- There will be more challenge issues/problems when the instrument begins to age. Thus, more effort for instrument on-orbit calibration will be needed.

Backup

Non-Uniformity of the SD Degradation

Non-uniformity of SD degradation

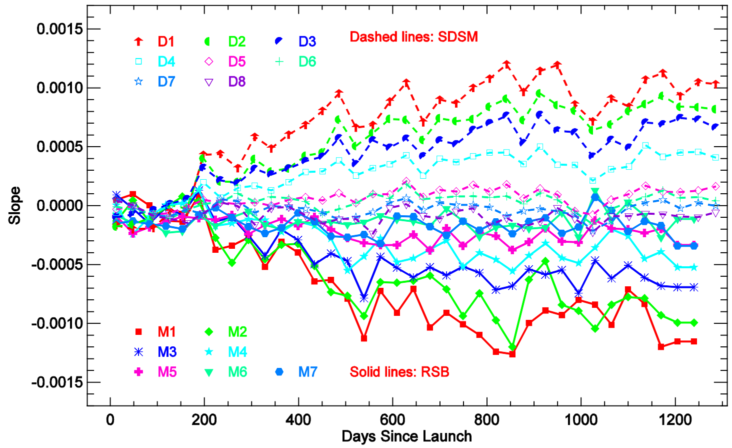

Slopes of H-factors and F-factors in each individual event with respect to solar declination

SDSM and RTA views

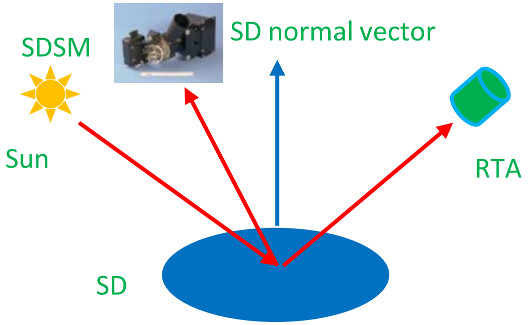

- SD degrades non-uniformly with respect to the incident angle for SDSM view direction
- SD degrades non-uniformly with respect to the incident angle for rotating telescope assembly (RTA, RSB) view direction
- According to *optical reciprocity*, then SD also degrades non-uniformly with respect to the outgoing direction
- The different signs of the variation slopes of the H-Factors and F-Factors with respect to incident direction confirm that SD degrades non-uniformly with respect to outgoing direction

- *0.1% per degree; 1% per 10 degrees for 412 nm (D1 and M1)*
- *Angle between SDSM view direction and RTA view direction is larger than 100 degree?*
- ***SD calibration is not accurate enough for ocean color data processing***

VIIRS RSB Specification

Table 1. Specification for SNPP VIIRS RSBs and SDSM detectors.

VIIRS Band	CW* (nm)	Band Gain	Detectors	Resolution*	SDSD Detector	CW* (nm)
M1	410	DG	16	742m x 776m	D1	412
M2	443	DG	16	742m x 776m	D2	450
M3	486	DG	16	742m x 776m	D3	488
M4	551	DG	16	742m x 776m	D4	555
I1	640	SG	32	371m x 387m	NA	NA
M5	671	DG	16	742m x 776m	D5	672
M6	745	SG	16	742m x 776m	D6	746
M7	862	DG	16	742m x 776m	D7	865
I2	862	SG	32	371m x 387m	D7	865
NA	NA	N	16		D8	935
M8	1238	SG	16	742m x 776m	NA	NA
M9	1378	SG	16	742m x 776m	NA	NA
M10	1610	SG	16	742m x 776m	NA	NA
I3	1610	SG	32	371m x 387m	NA	NA
M11	2250	SG	16	742m x 776m	NA	NA

*CW: Center Wavelength; DG: Dual Gain; SG: Singla Gain; Resolution: Track x Scan at Nadir after aggregation

Statistical Evaluation of VIIRS Ocean Color Data Retrievals

Karlis Mikelsons, Lide Jiang, Menghua Wang
STAR VIIRS Ocean Color Team

STAR JPSS
2015 Annual Science Team Meeting
August 27, 2015

Methodology

- Analyze SNPP-VIIRS ocean color data granules from two regions, from time period 2012 - 2014, processed with the most recent MSL12 (BMW algorithm)
- Exclude all nL_w data flagged as land, clouds, high sun-glint, and atmospheric correction failure, as well as all masked or out-of range nL_w data
- Subtract lat-lon binned and time averaged nL_w over 31 days (day-15…day+15) from nL_w data in each granule: $\Delta nL_w = nL_w$ – time_averaged(binned(nL_w))
- Collect statistics in VIIRS bands M1-M5 for ΔnL_w (410, 443, 486, 551, 671 nm) dependence on solar-zenith angle, sensor-zenith angle, glint coefficient, wind speed, atmospheric pressure, and other retrieval and auxiliary parameters
- Also collect number of data points dependence on retrieval parameters
- Plot ΔnL_w *vs.* retrieval parameters and look for deviations from average and other artifacts

Region 1: North Atlantic

region of study: 50-62.5N, 15-40W box

binned nL_w: **(0.5°lat × 1°lon ≈ 50 × 50km)**

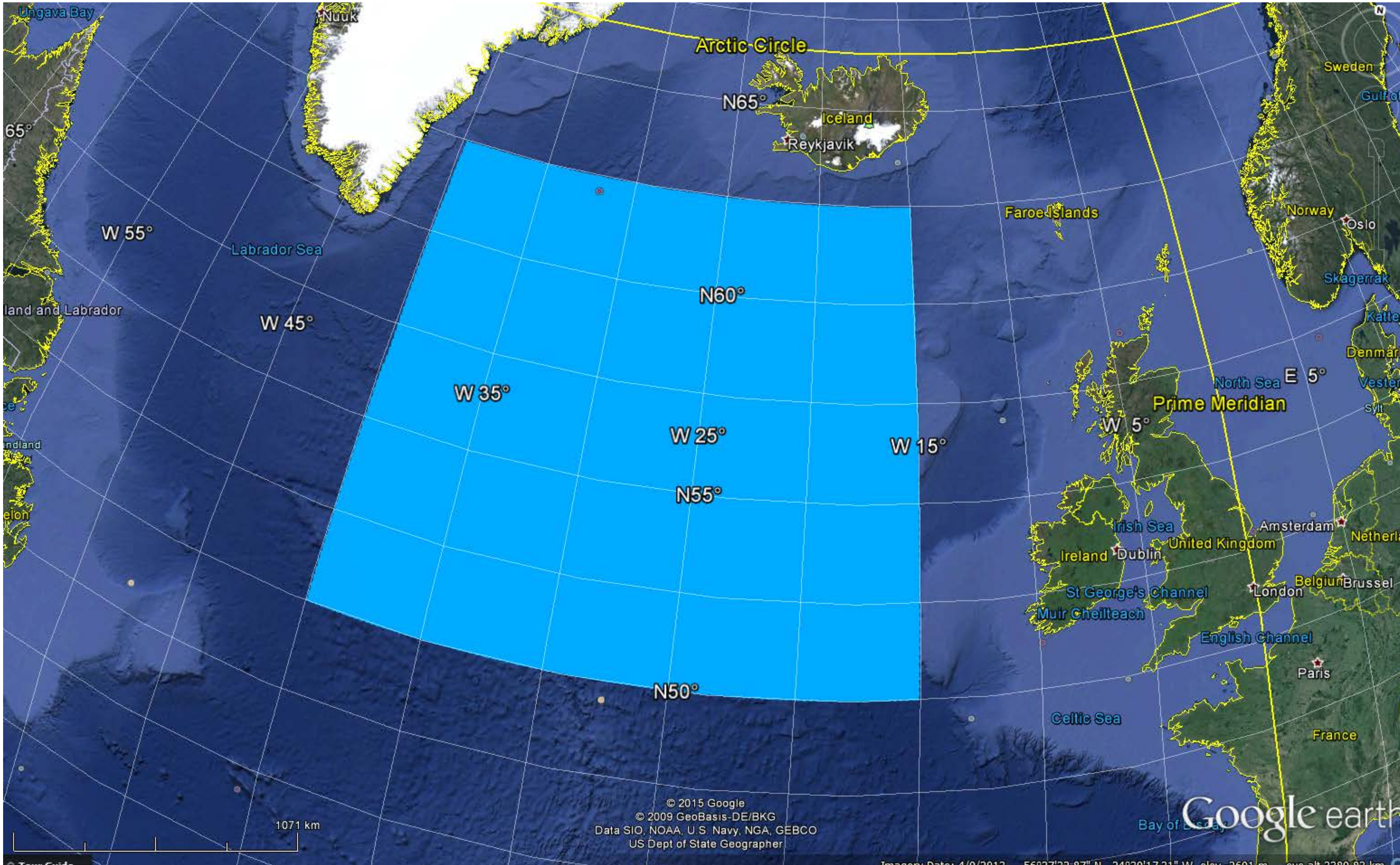

Region 2: South Pacific

region of study: 10-60S, 90-140W box

binned nL_w: **(0.5°lat × 0.5°lon)**

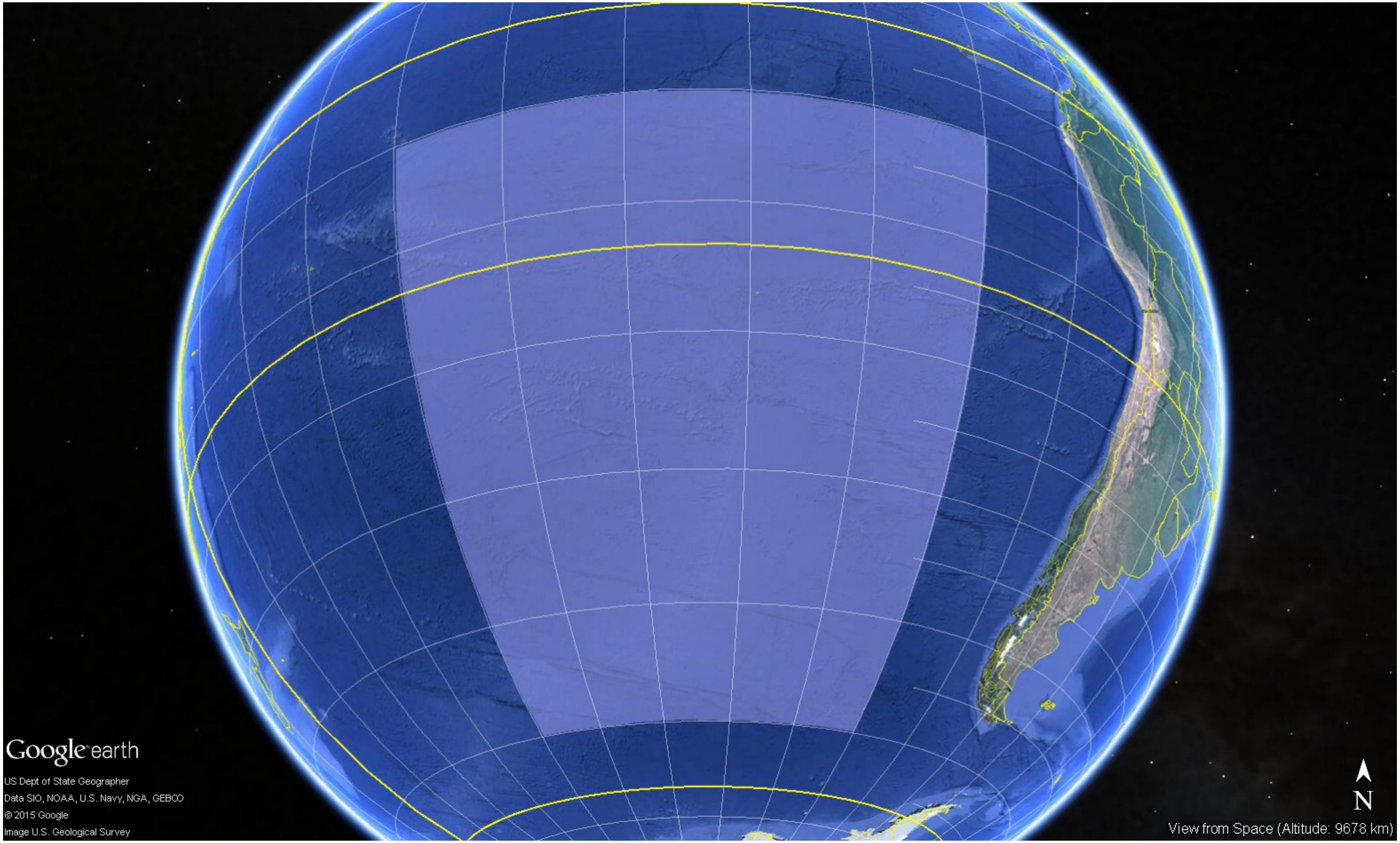

nL_w dependence on sensor-zenith angle

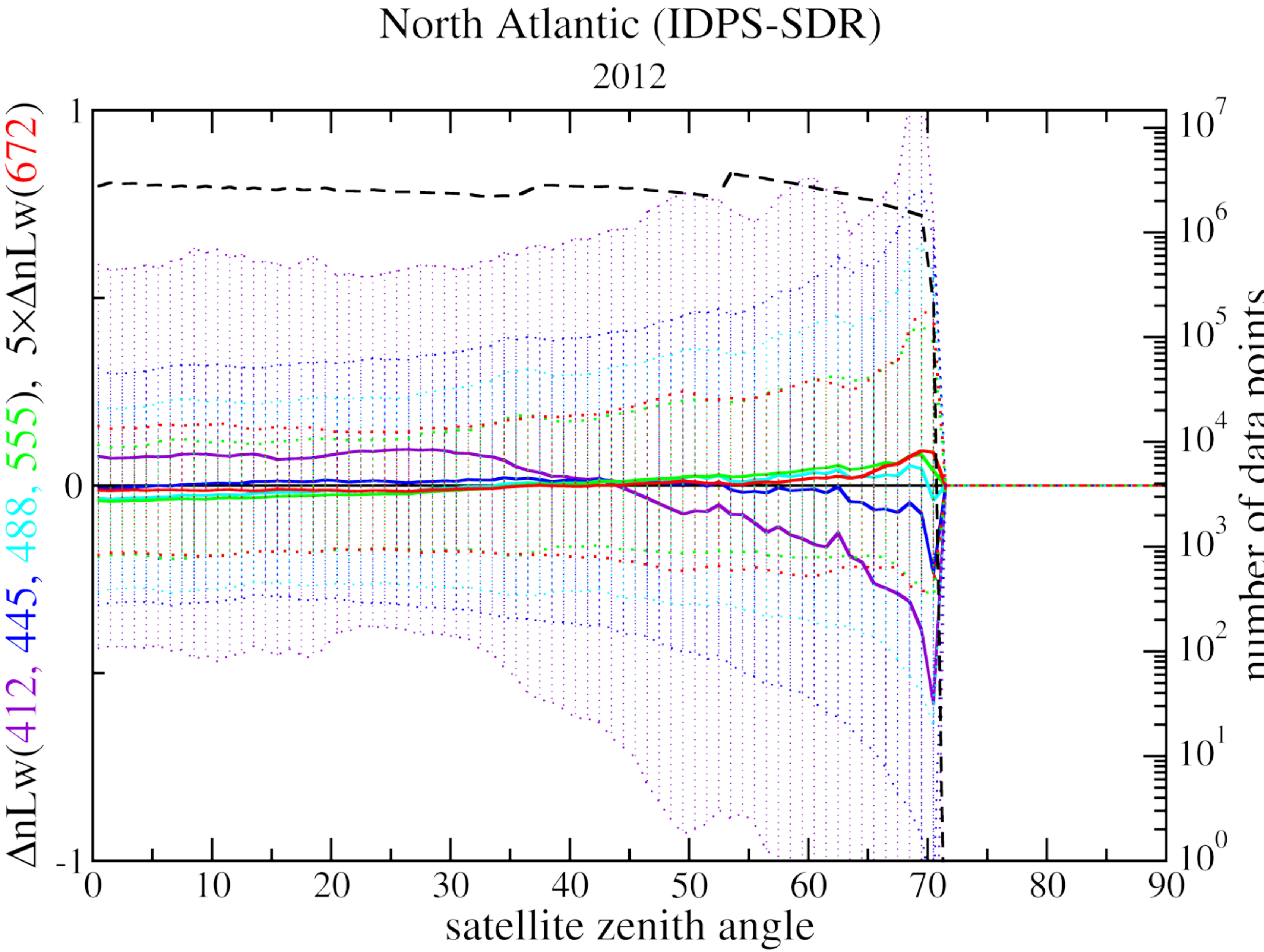
North Atlantic (IDPS-SDR)
2012
ΔnLw(412, 445, 488, 555), 5×ΔnLw(672)
number of data points
satellite zenith angle
1
0
-1
0
10
20
30
40
50
60
70
80
90
10^7
10^6
10^5
10^4
10^3
10^2
10^1
10^0

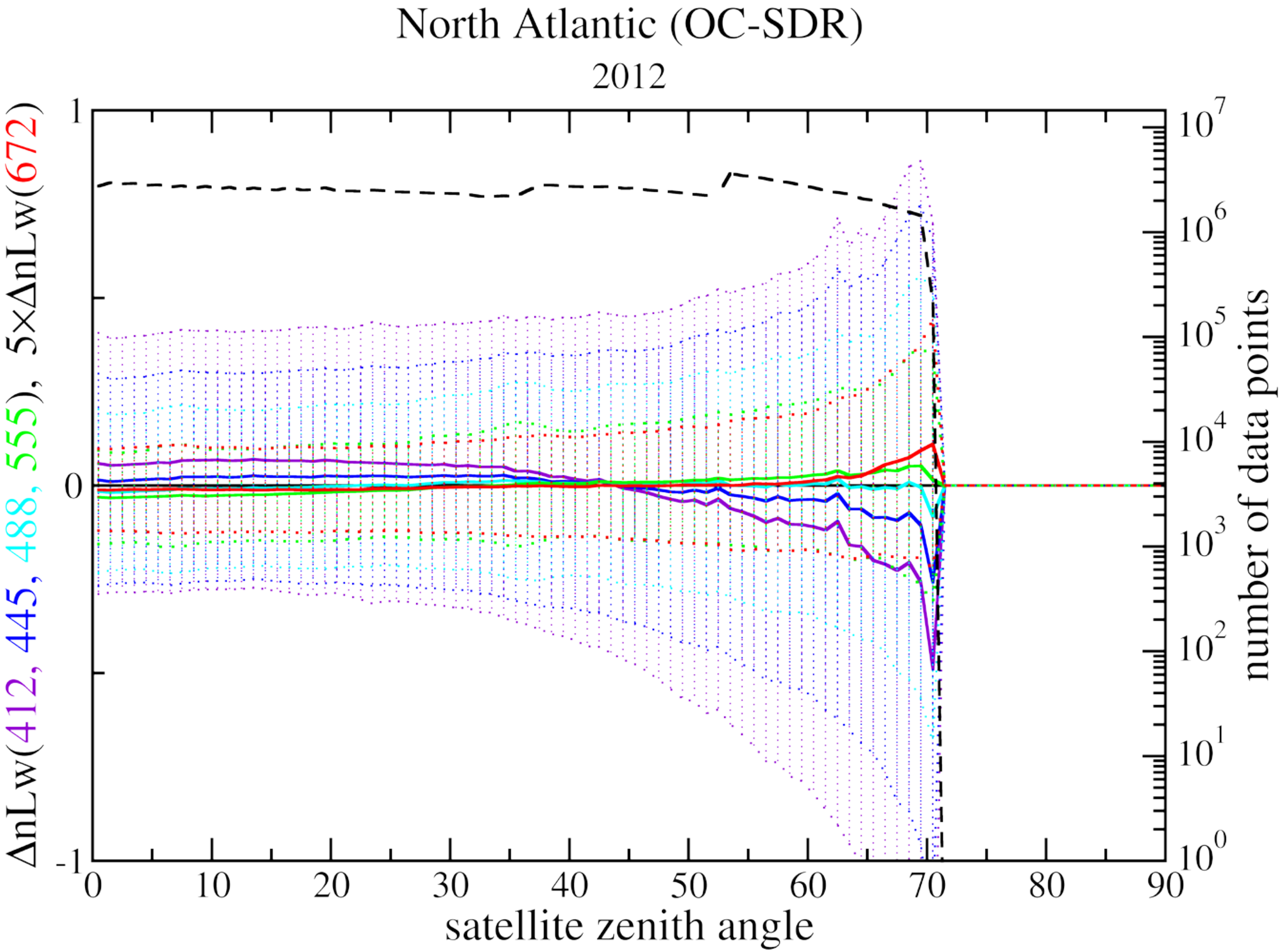
North Atlantic (OC-SDR)
2012
ΔnLw(412, 445, 488, 555), 5×ΔnLw(672)
number of data points
satellite zenith angle
1
0
-1
0
10
20
30
40
50
60
70
80
90
10^7
10^6
10^5
10^4
10^3
10^2
10^1
10^0

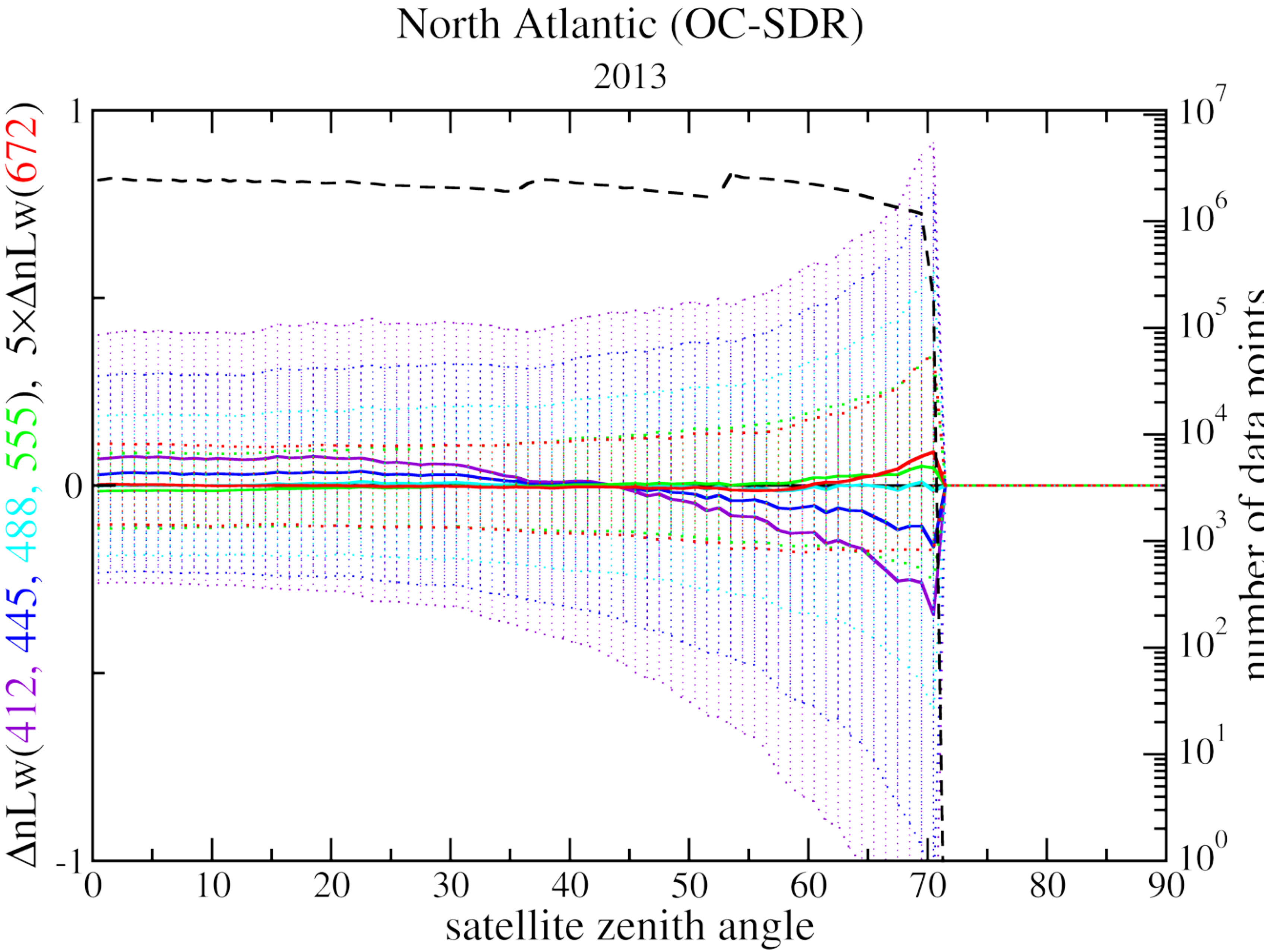

North Atlantic (OC-SDR)
2013
ΔnLw(412, 445, 488, 555), 5×ΔnLw(672)
number of data points
satellite zenith angle
1
0
-1
0
10
20
30
40
50
60
70
80
90
10^0
10^1
10^2
10^3
10^4
10^5
10^6
10^7

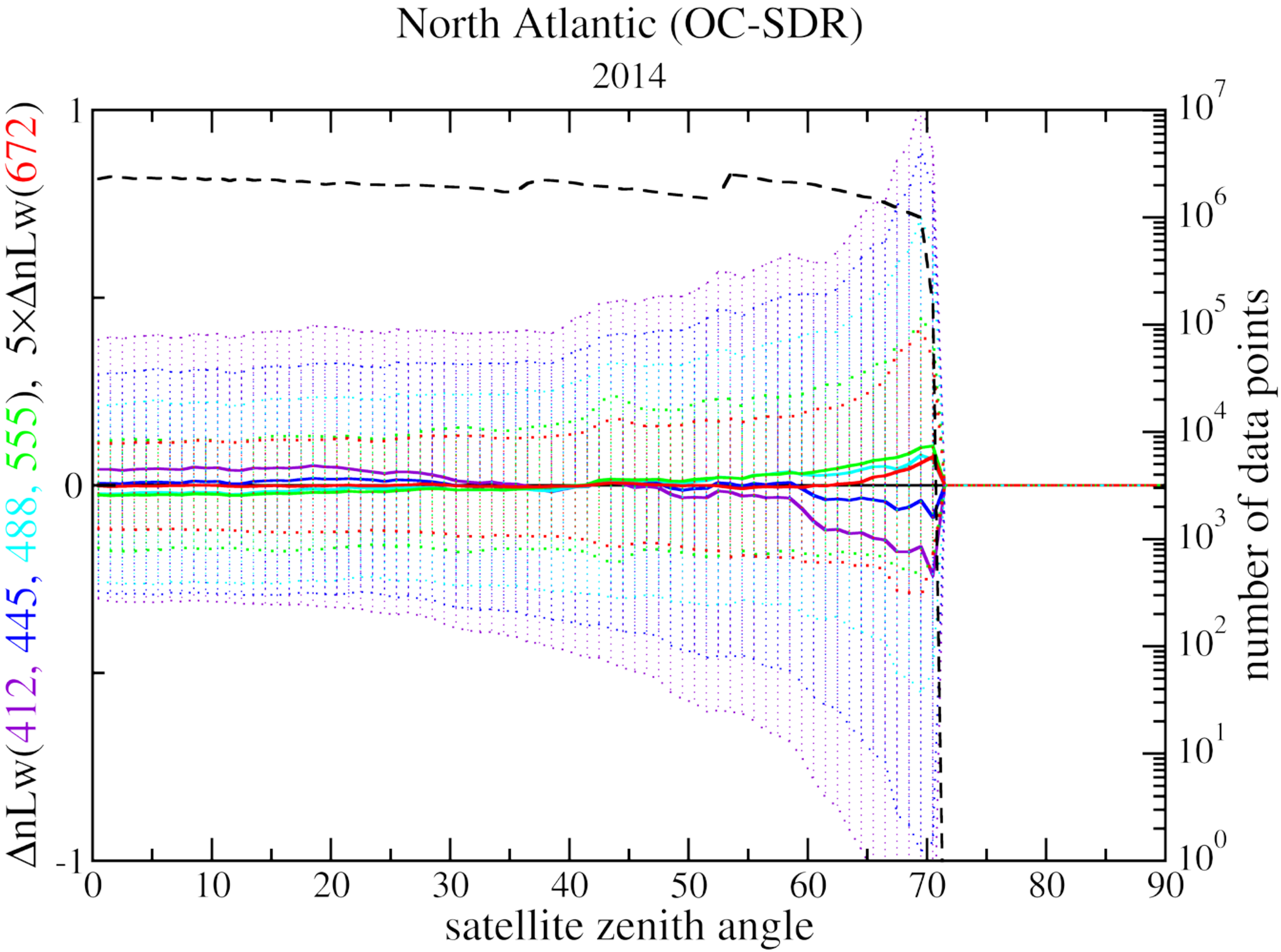
North Atlantic (OC-SDR)
2014
ΔnLw(412, 445, 488, 555), 5×ΔnLw(672)
number of data points
satellite zenith angle
1
0
-1
0
10
20
30
40
50
60
70
80
90
10^7
10^6
10^5
10^4
10^3
10^2
10^1
10^0

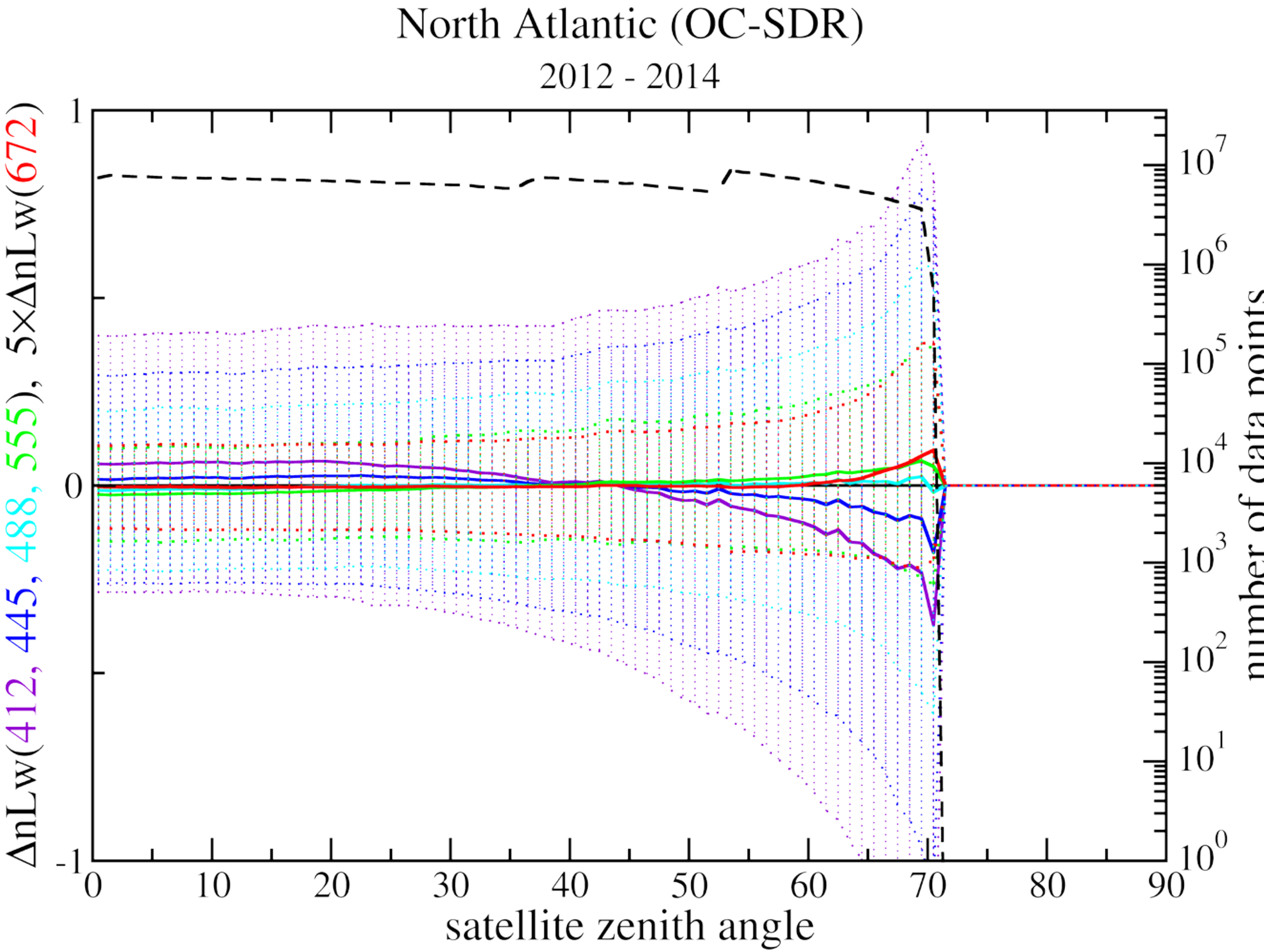

North Atlantic (OC-SDR)
2012 - 2014
ΔnLw(412, 445, 488, 555), 5×ΔnLw(672)
number of data points
satellite zenith angle
1
0
-1
0
10
20
30
40
50
60
70
80
90
10^0
10^1
10^2
10^3
10^4
10^5
10^6
10^7

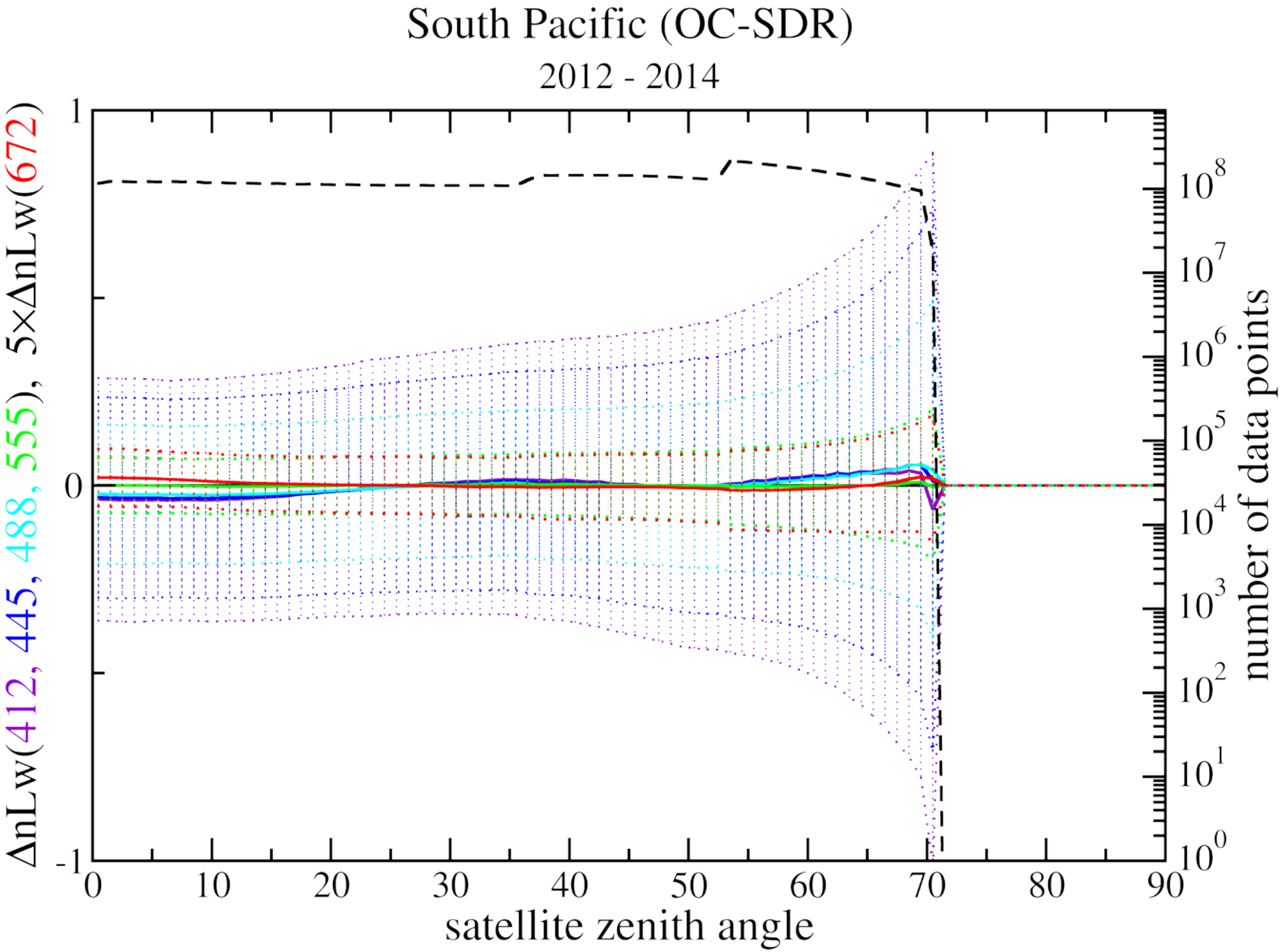

South Pacific (OC-SDR)
2012 - 2014
ΔnLw(412, 445, 488, 555), 5×ΔnLw(672)
number of data points
satellite zenith angle
1
0
-1
0
10
20
30
40
50
60
70
80
90
10^0
10^1
10^2
10^3
10^4
10^5
10^6
10^7
10^8

nL_w dependence on solar-zenith angle

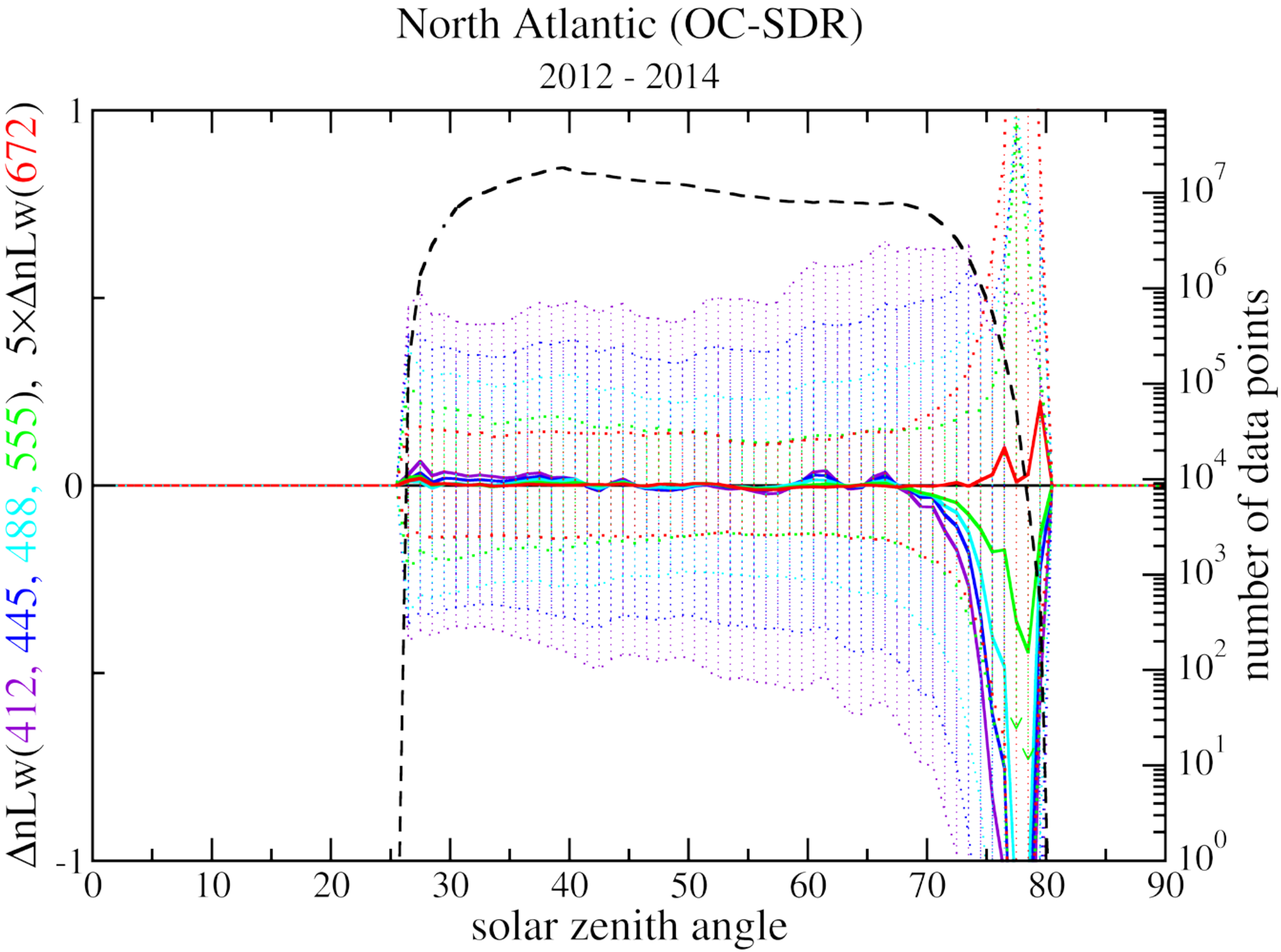
North Atlantic (OC-SDR)
2012 - 2014
ΔnLw(412, 445, 488, 555), 5×ΔnLw(672)
number of data points
solar zenith angle
1
0
-1
0
10
20
30
40
50
60
70
80
90
10^0
10^1
10^2
10^3
10^4
10^5
10^6
10^7

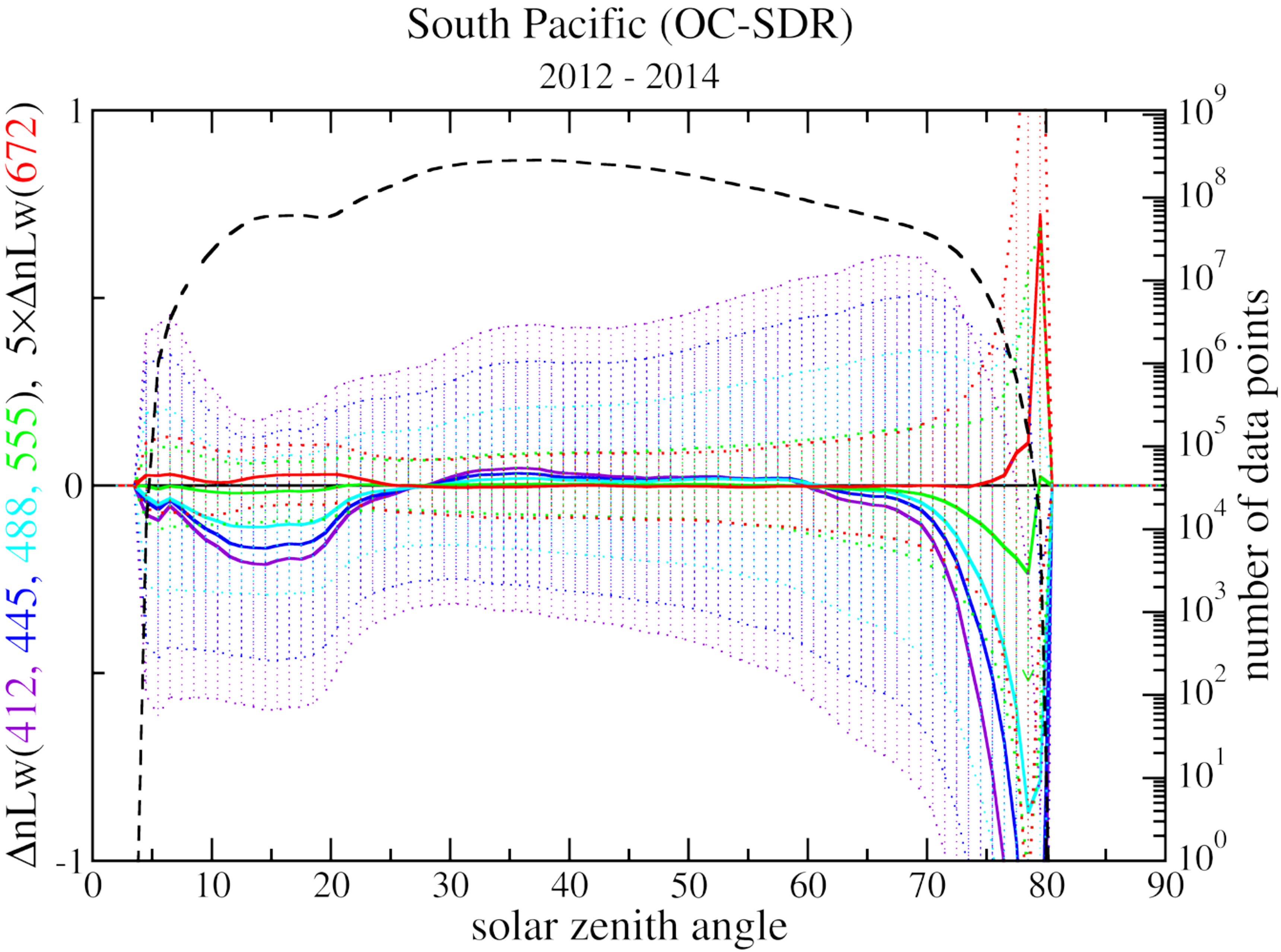

South Pacific (OC-SDR)
2012 - 2014
ΔnLw(412, 445, 488, 555), 5×ΔnLw(672)
number of data points
solar zenith angle
1
0
-1
0
10
20
30
40
50
60
70
80
90
10^9
10^8
10^7
10^6
10^5
10^4
10^3
10^2
10^1
10^0

nL_w dependence on pixel number along the scan

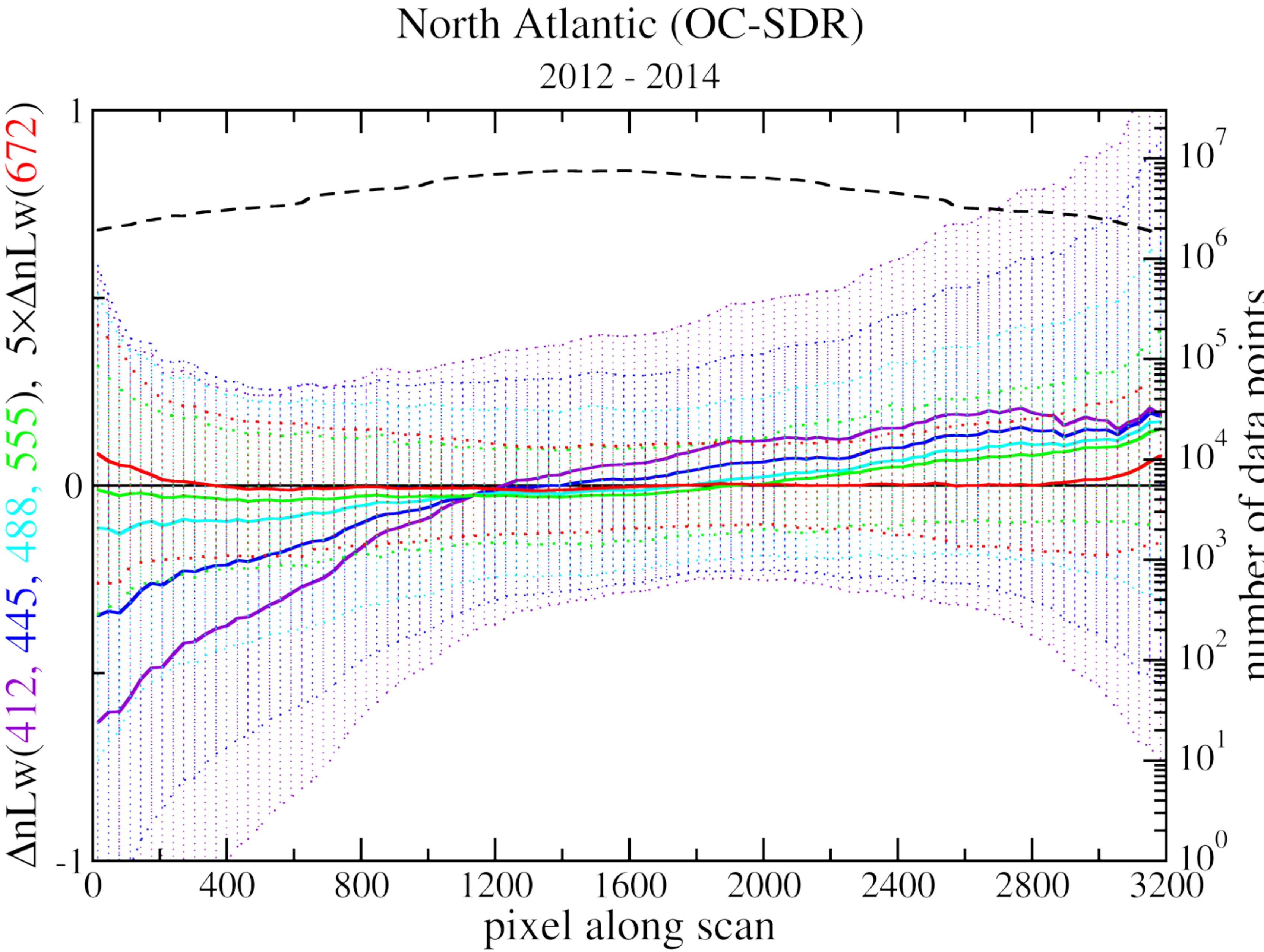
North Atlantic (OC-SDR)
2012 - 2014
ΔnLw(412, 445, 488, 555), 5×ΔnLw(672)
number of data points
pixel along scan
1
0
-1
0
400
800
1200
1600
2000
2400
2800
3200
10^0
10^1
10^2
10^3
10^4
10^5
10^6
10^7

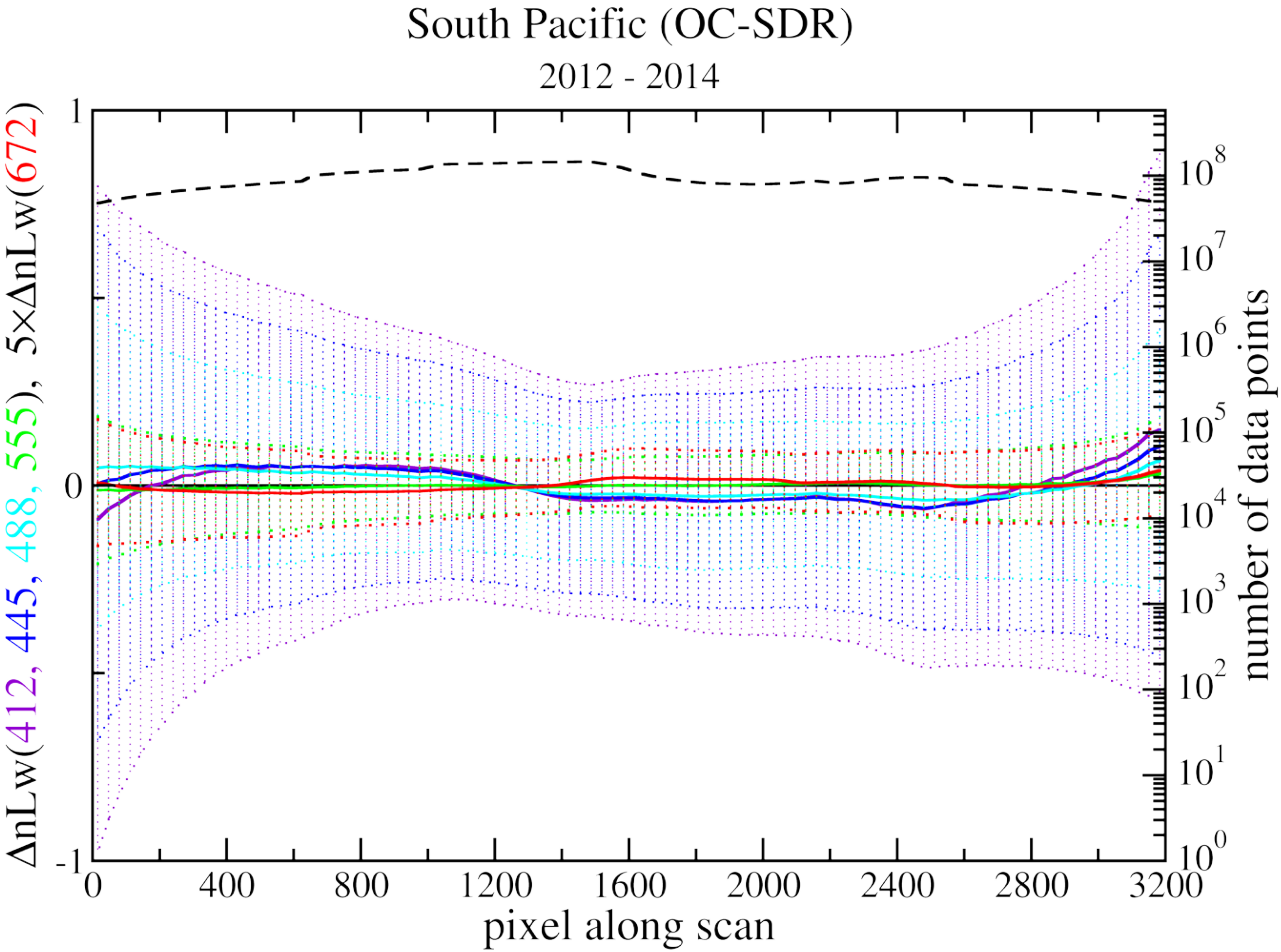
South Pacific (OC-SDR)
2012 - 2014
ΔnLw(412, 445, 488, 555), 5×ΔnLw(672)
number of data points
pixel along scan
1
0
-1
0
400
800
1200
1600
2000
2400
2800
3200
10^0
10^1
10^2
10^3
10^4
10^5
10^6
10^7
10^8

nL_w dependence on detector number

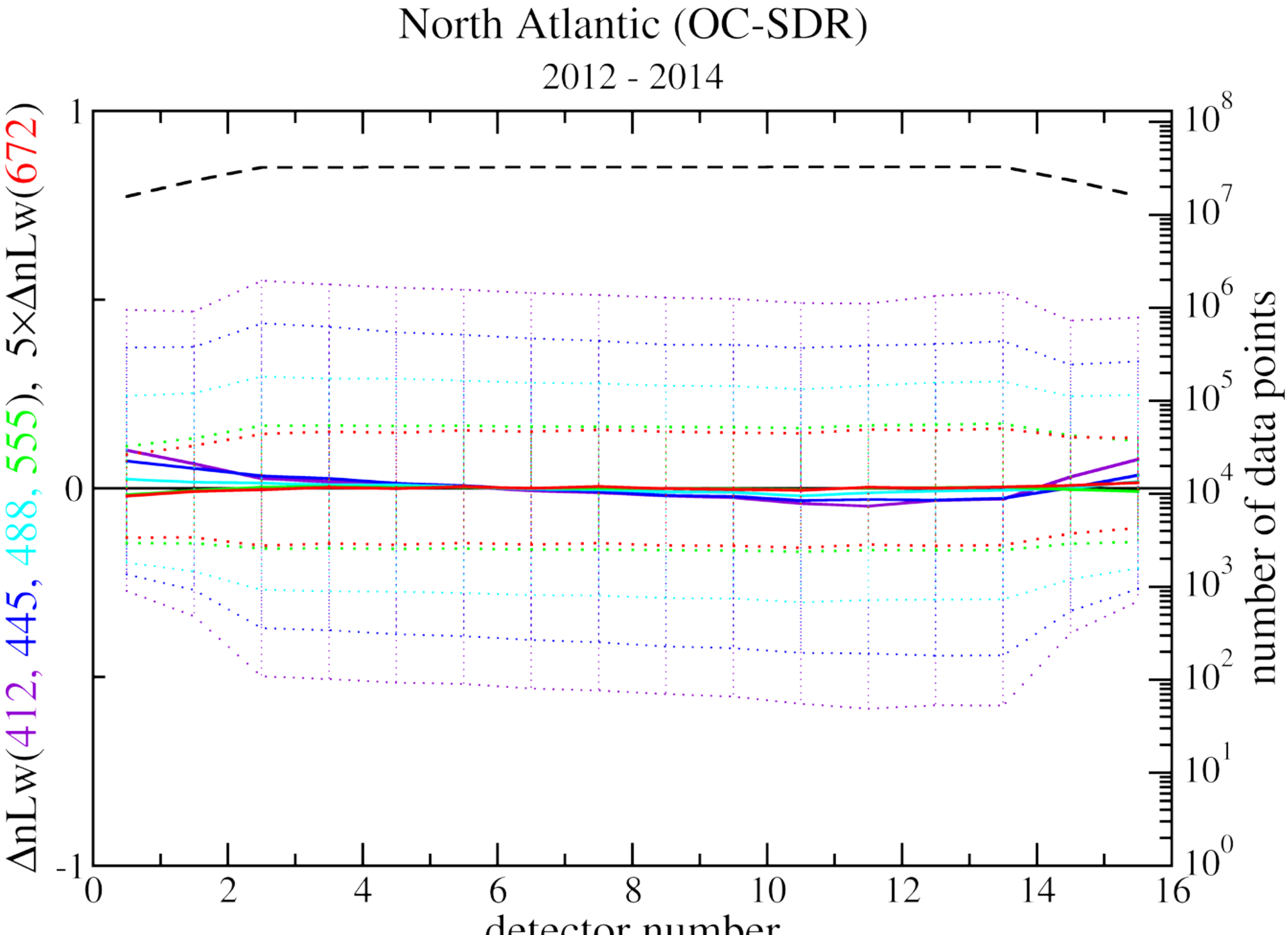
North Atlantic (OC-SDR)
2012 - 2014
ΔnLw(412, 445, 488, 555), 5×ΔnLw(672)
number of data points
detector number
1
0
-1
0
2
4
6
8
10
12
14
16
10^8
10^7
10^6
10^5
10^4
10^3
10^2
10^1
10^0

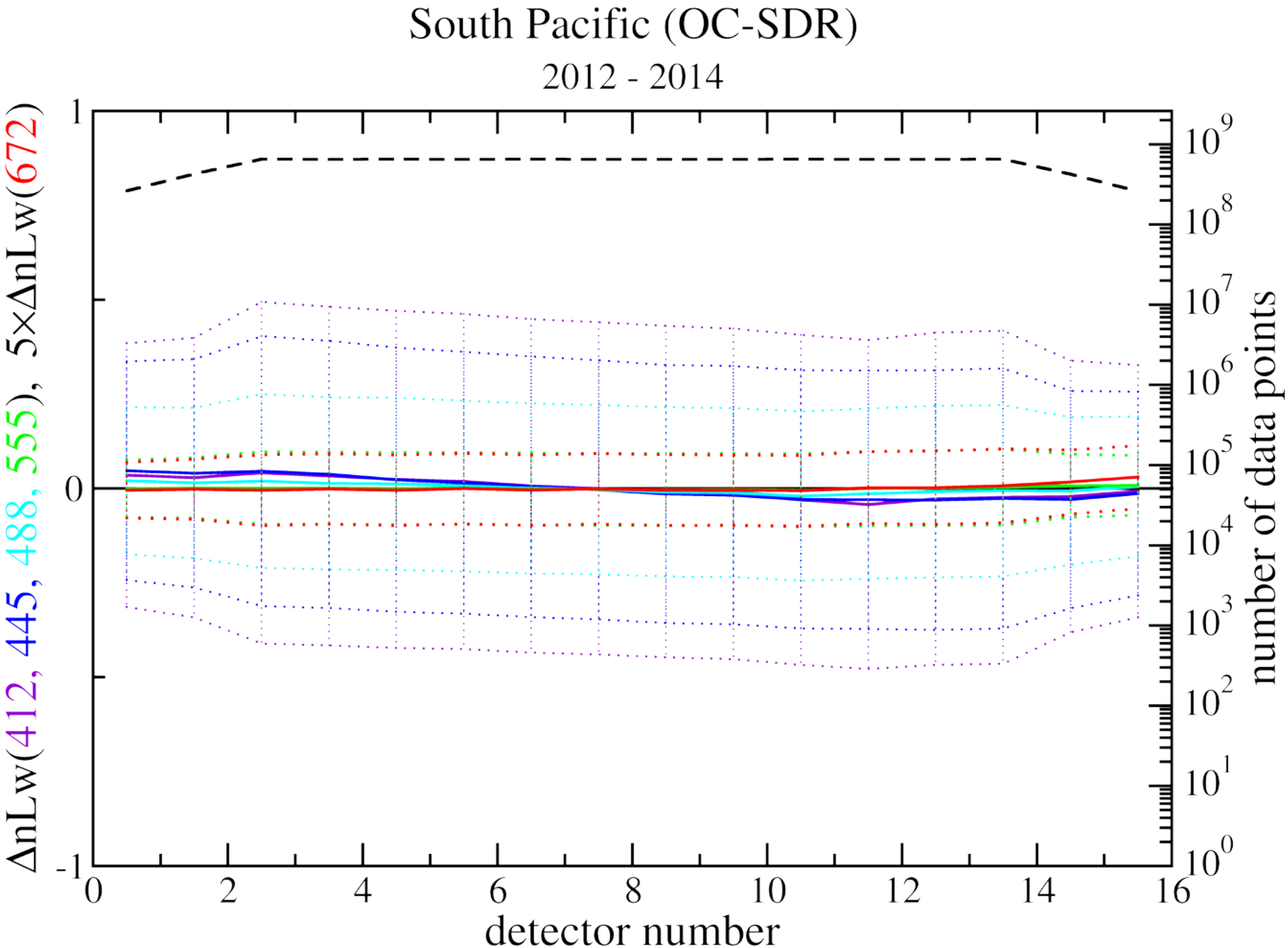
South Pacific (OC-SDR)
2012 - 2014
ΔnLw(412, 445, 488, 555), 5×ΔnLw(672)
number of data points
detector number
1
0
-1
0
2
4
6
8
10
12
14
16
10^9
10^8
10^7
10^6
10^5
10^4
10^3
10^2
10^1
10^0

nL_w dependence on sun glint coefficient

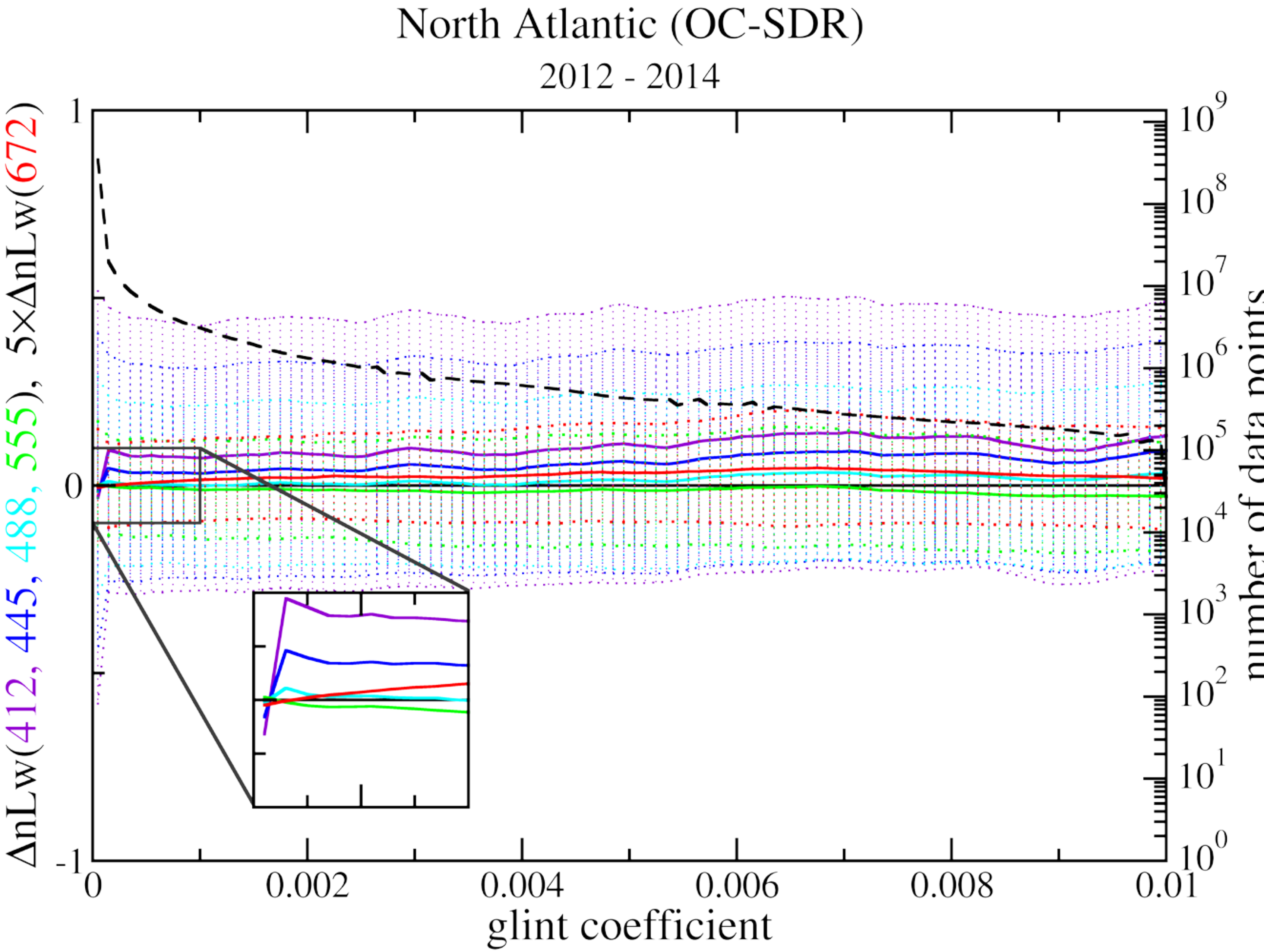
North Atlantic (OC-SDR)
2012 - 2014
ΔnLw(412, 445, 488, 555), 5×ΔnLw(672)
number of data points
glint coefficient
1
0
-1
0
0.002
0.004
0.006
0.008
0.01
10^9
10^8
10^7
10^6
10^5
10^4
10^3
10^2
10^1
10^0

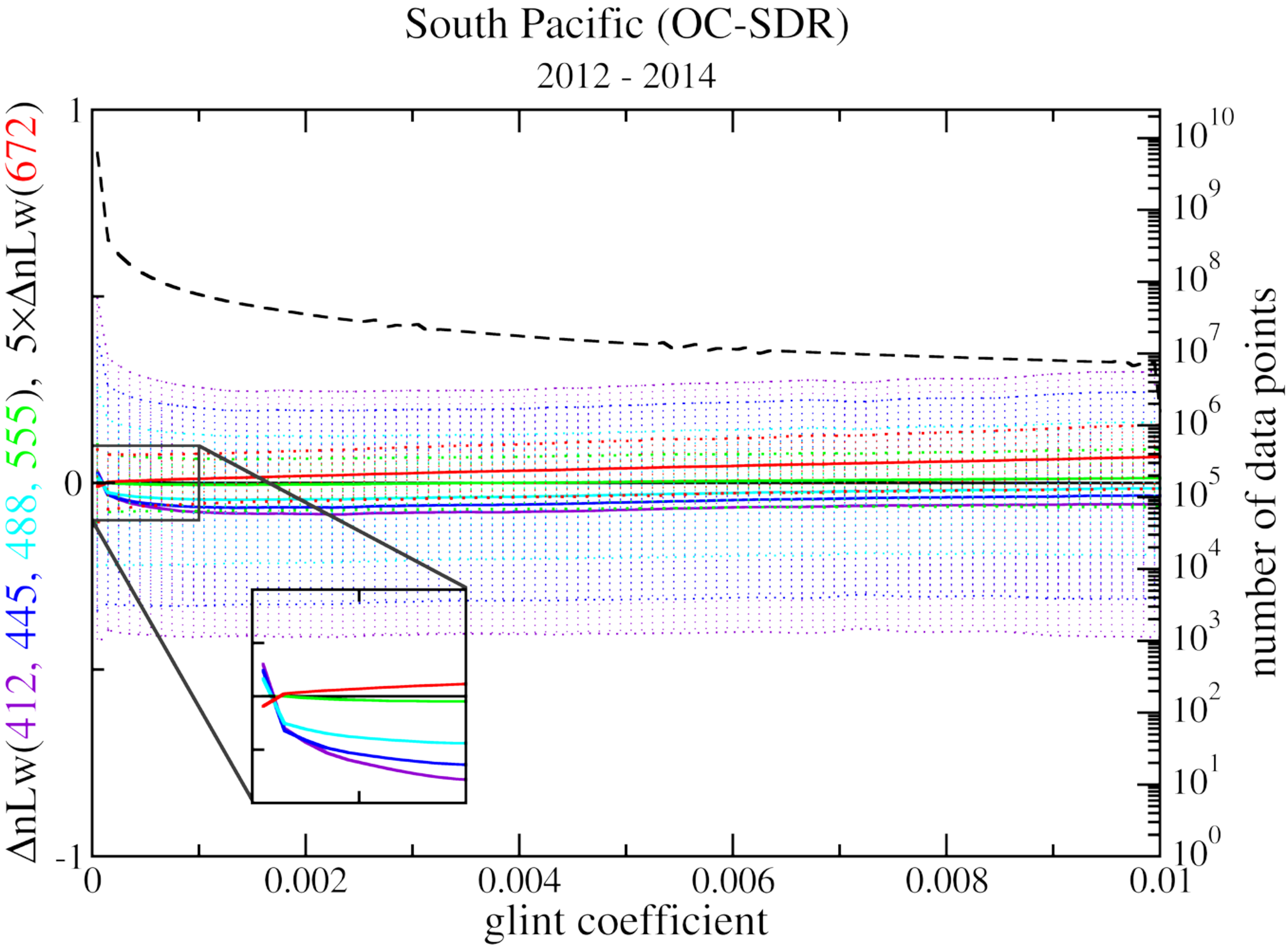
South Pacific (OC-SDR)
2012 - 2014
ΔnLw(412, 445, 488, 555), 5×ΔnLw(672)
1
0
-1
0
0.002
0.004
0.006
0.008
0.01
glint coefficient
10^{10}
10^{9}
10^{8}
10^{7}
10^{6}
10^{5}
10^{4}
10^{3}
10^{2}
10^{1}
10^{0}
number of data points

nL_w dependence on atmospheric pressure

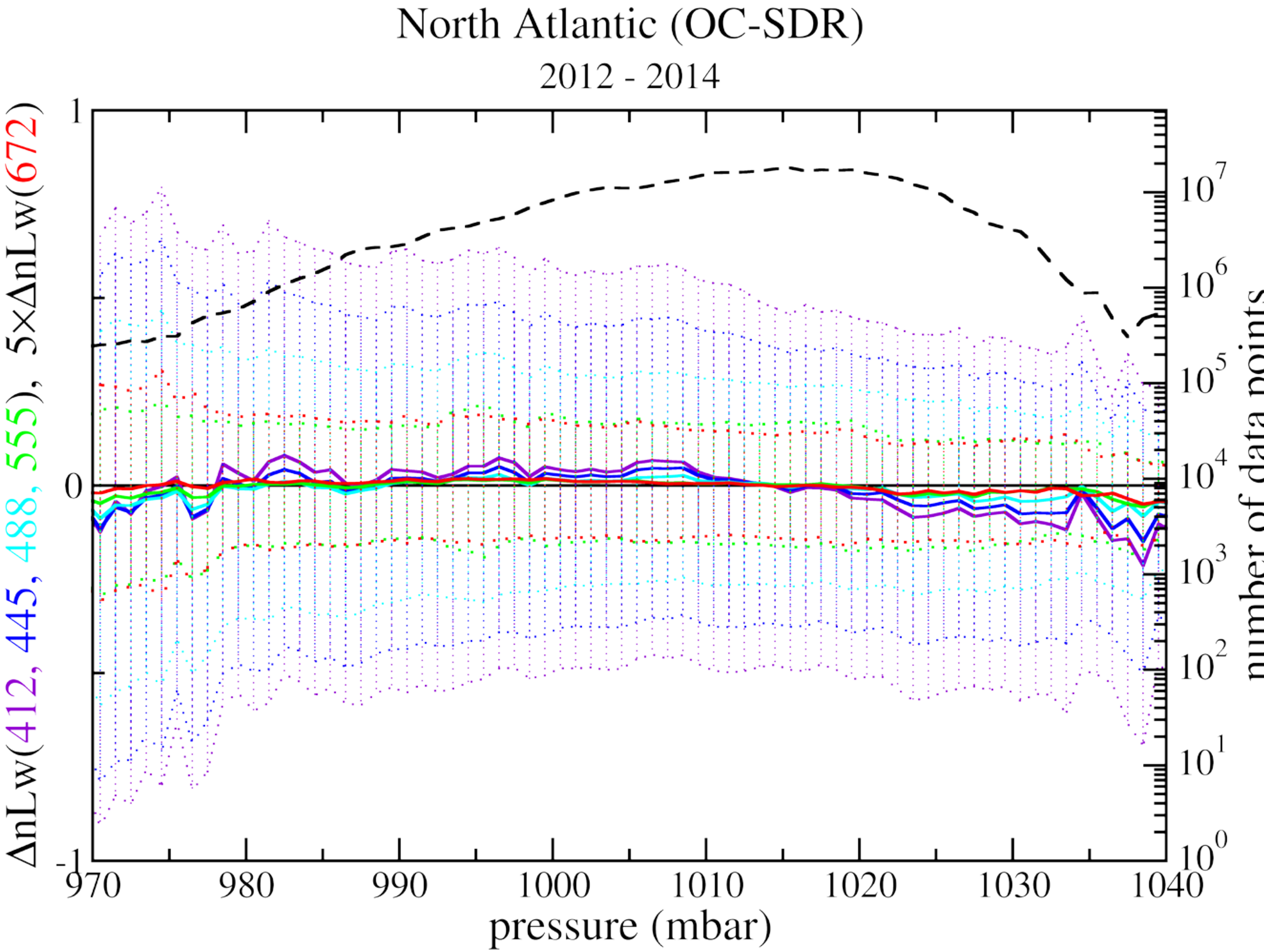
North Atlantic (OC-SDR)
2012 - 2014
ΔnLw(412, 445, 488, 555), 5×ΔnLw(672)
number of data points
pressure (mbar)
1
0
-1
970
980
990
1000
1010
1020
1030
1040
10^0
10^1
10^2
10^3
10^4
10^5
10^6
10^7

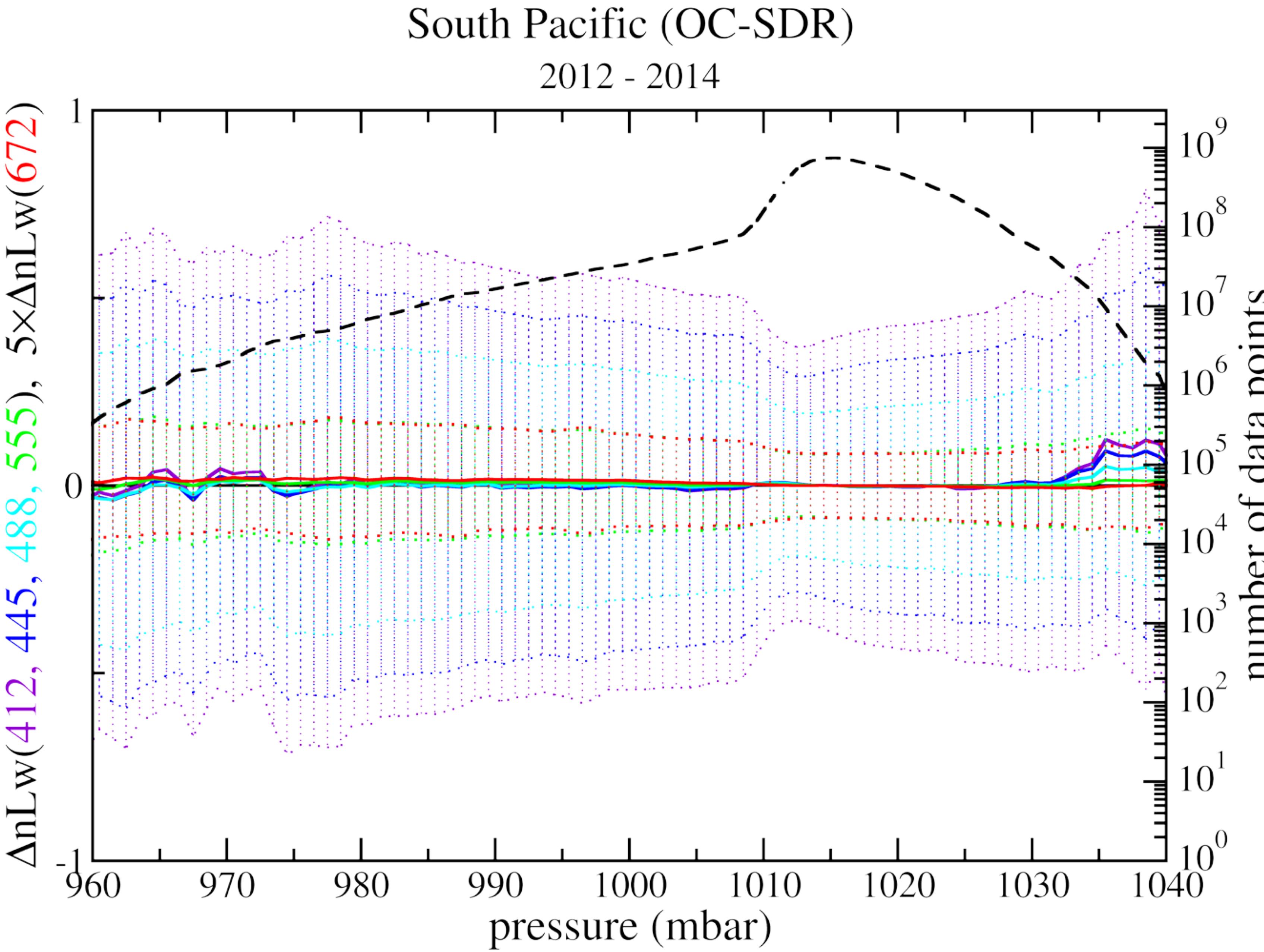
South Pacific (OC-SDR)
2012 - 2014
ΔnLw(412, 445, 488, 555), 5×ΔnLw(672)
number of data points
pressure (mbar)
1
0
-1
960
970
980
990
1000
1010
1020
1030
1040
10^0
10^1
10^2
10^3
10^4
10^5
10^6
10^7
10^8
10^9

nL_w dependence on wind speed

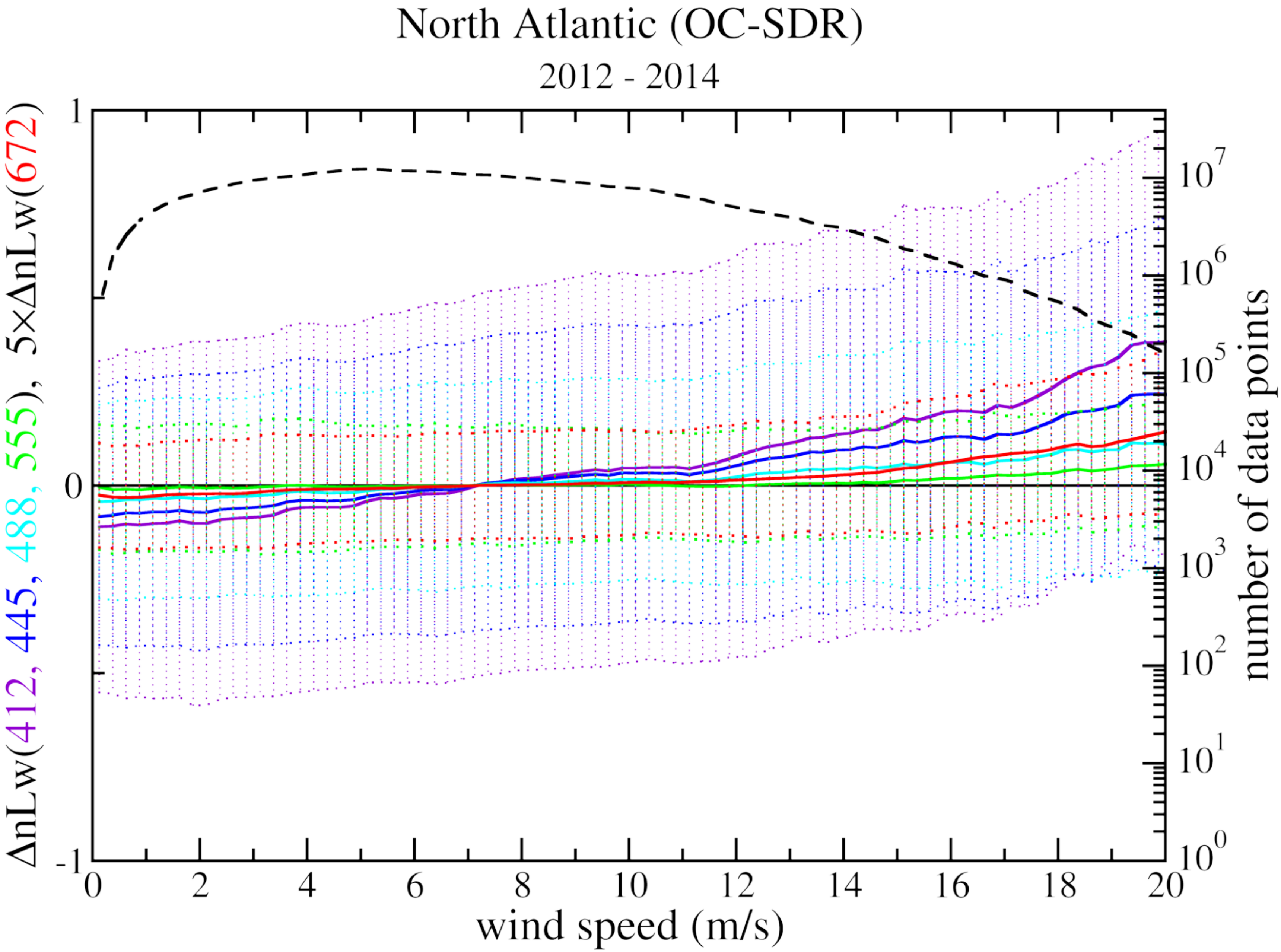

North Atlantic (OC-SDR)
2012 - 2014
ΔnLw(412, 445, 488, 555), 5×ΔnLw(672)
number of data points
wind speed (m/s)
1
0
-1
0
2
4
6
8
10
12
14
16
18
20
10^0
10^1
10^2
10^3
10^4
10^5
10^6
10^7

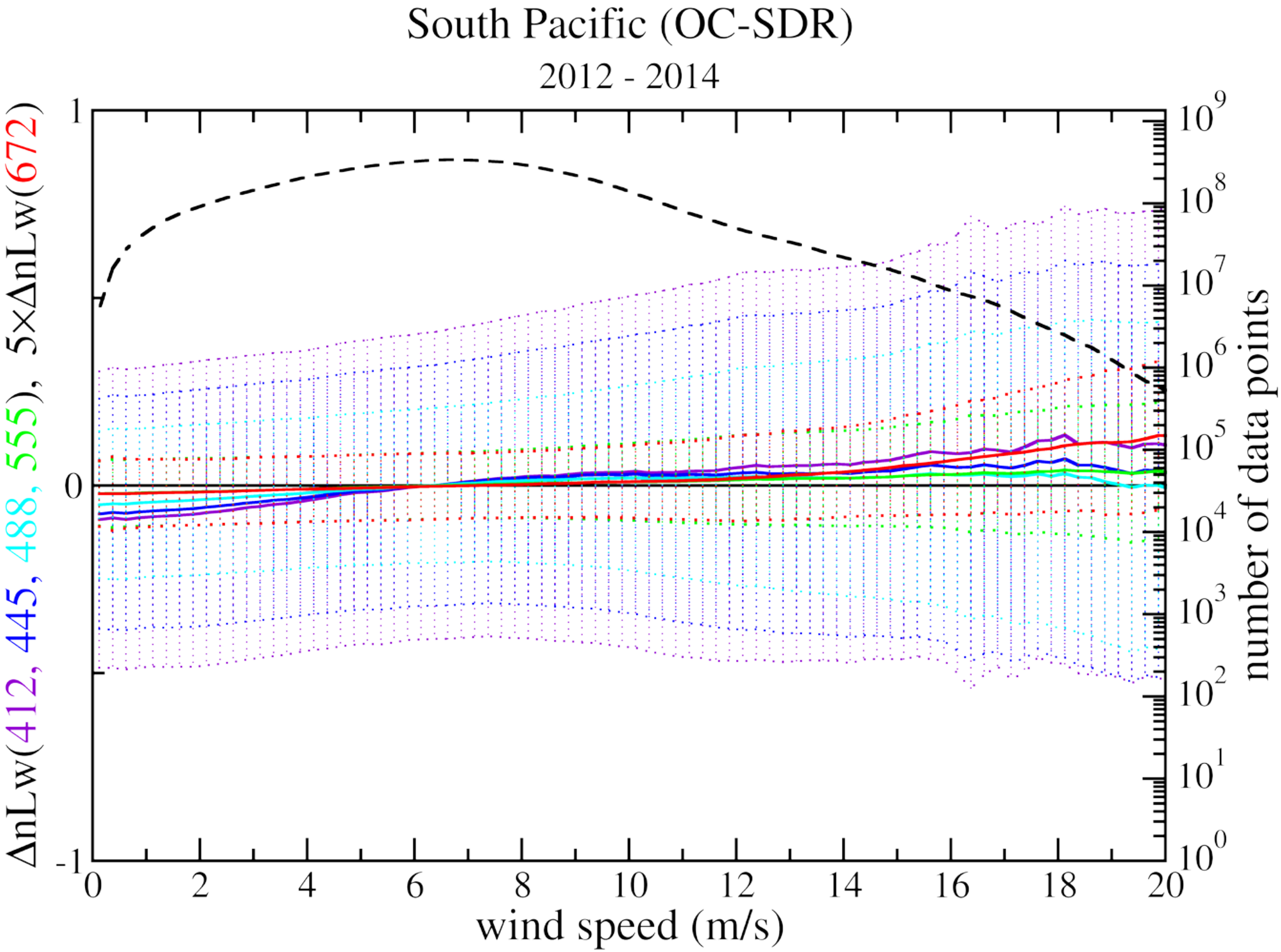
South Pacific (OC-SDR)
2012 - 2014
ΔnLw(412, 445, 488, 555), 5×ΔnLw(672)
number of data points
wind speed (m/s)
1
0
-1
0
2
4
6
8
10
12
14
16
18
20
10^9
10^8
10^7
10^6
10^5
10^4
10^3
10^2
10^1
10^0

nL_w dependence on water vapor concentration

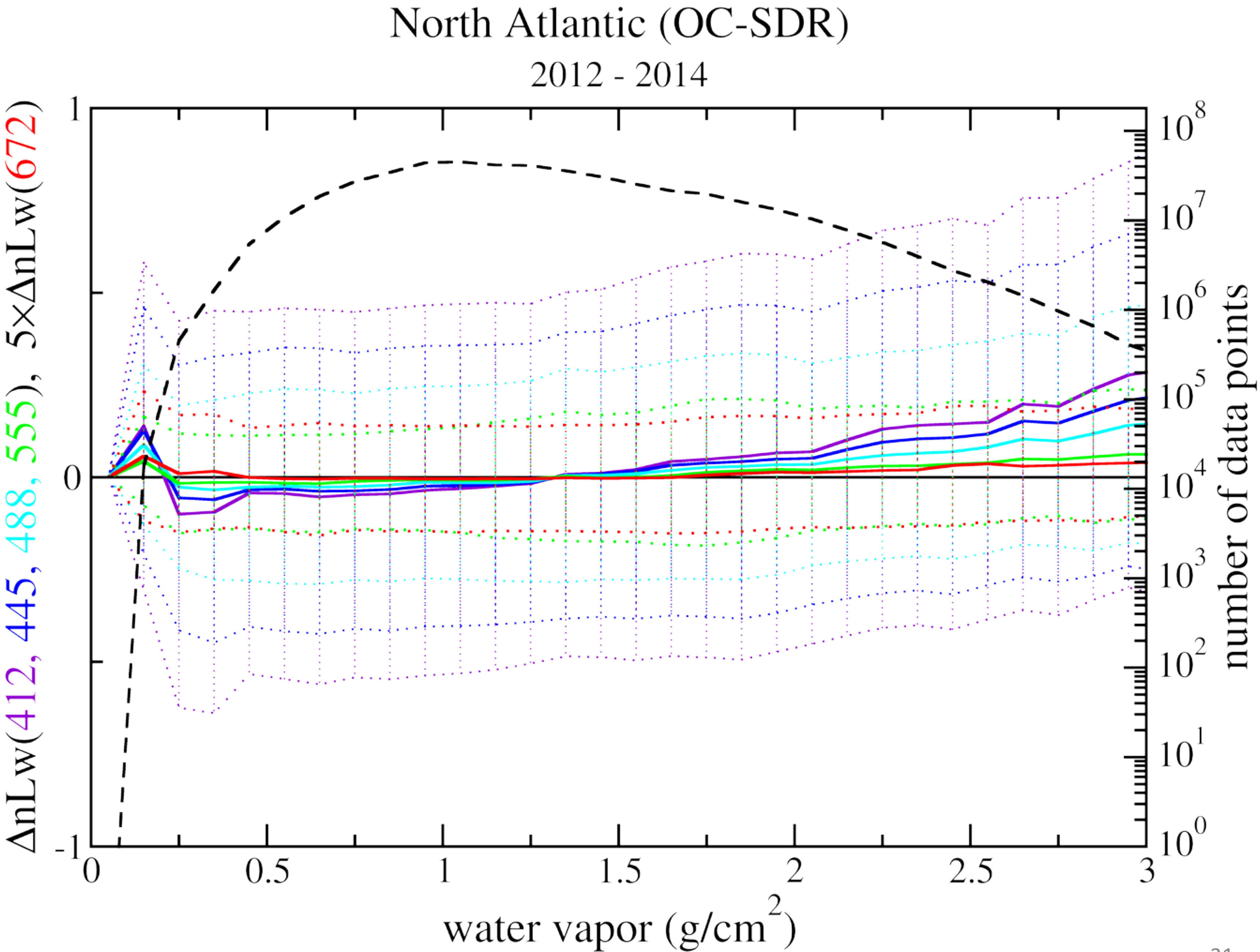

North Atlantic (OC-SDR)
2012 - 2014
ΔnLw(412, 445, 488, 555), 5×ΔnLw(672)
number of data points
water vapor (g/cm^2)
1
0
-1
0
0.5
1
1.5
2
2.5
3
10^8
10^7
10^6
10^5
10^4
10^3
10^2
10^1
10^0

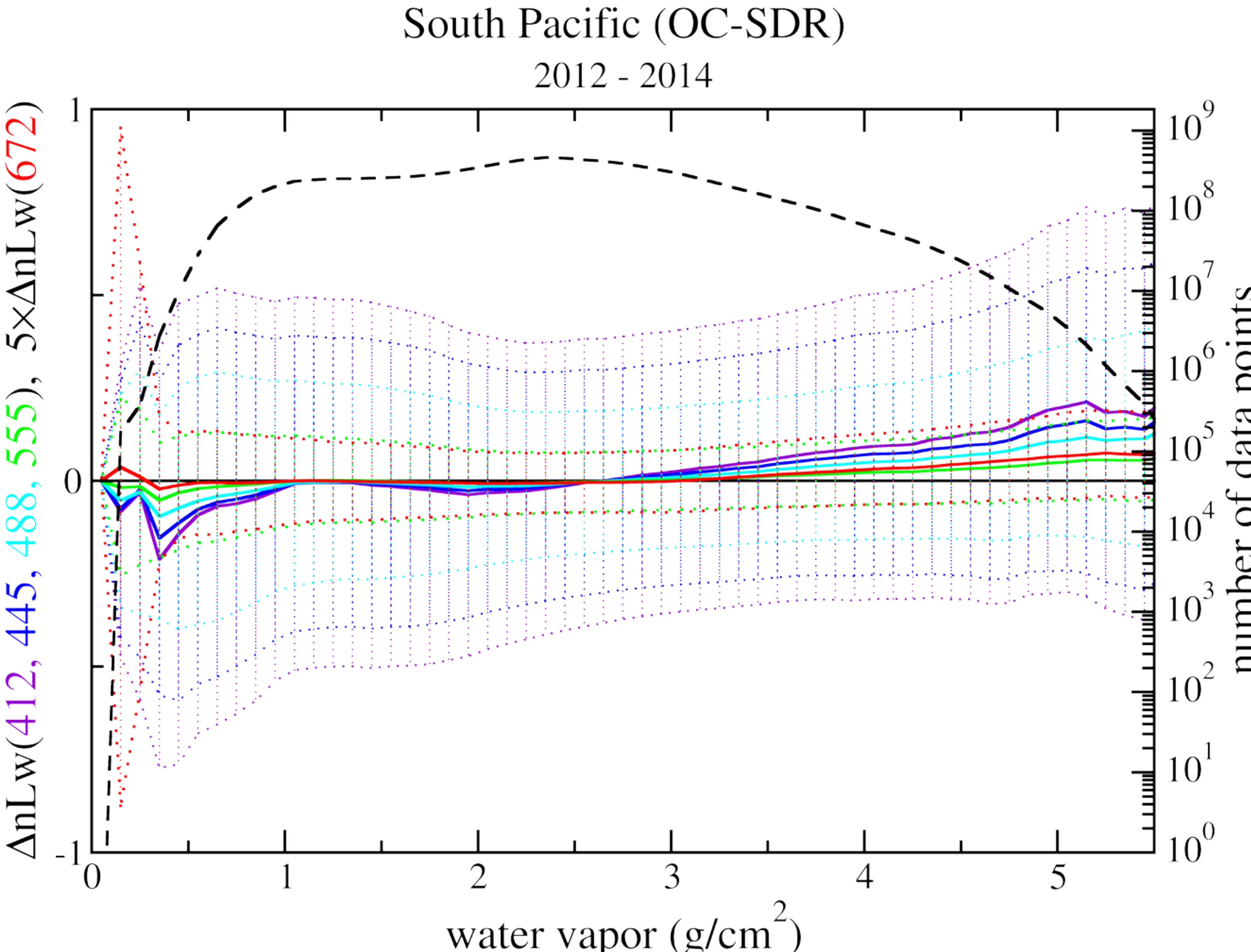
South Pacific (OC-SDR)
2012 - 2014
ΔnLw(412, 445, 488, 555), 5×ΔnLw(672)
number of data points
water vapor (g/cm^2)
1
0
-1
0
1
2
3
4
5
10^0
10^1
10^2
10^3
10^4
10^5
10^6
10^7
10^8
10^9

nL_w dependence on ozone concentration

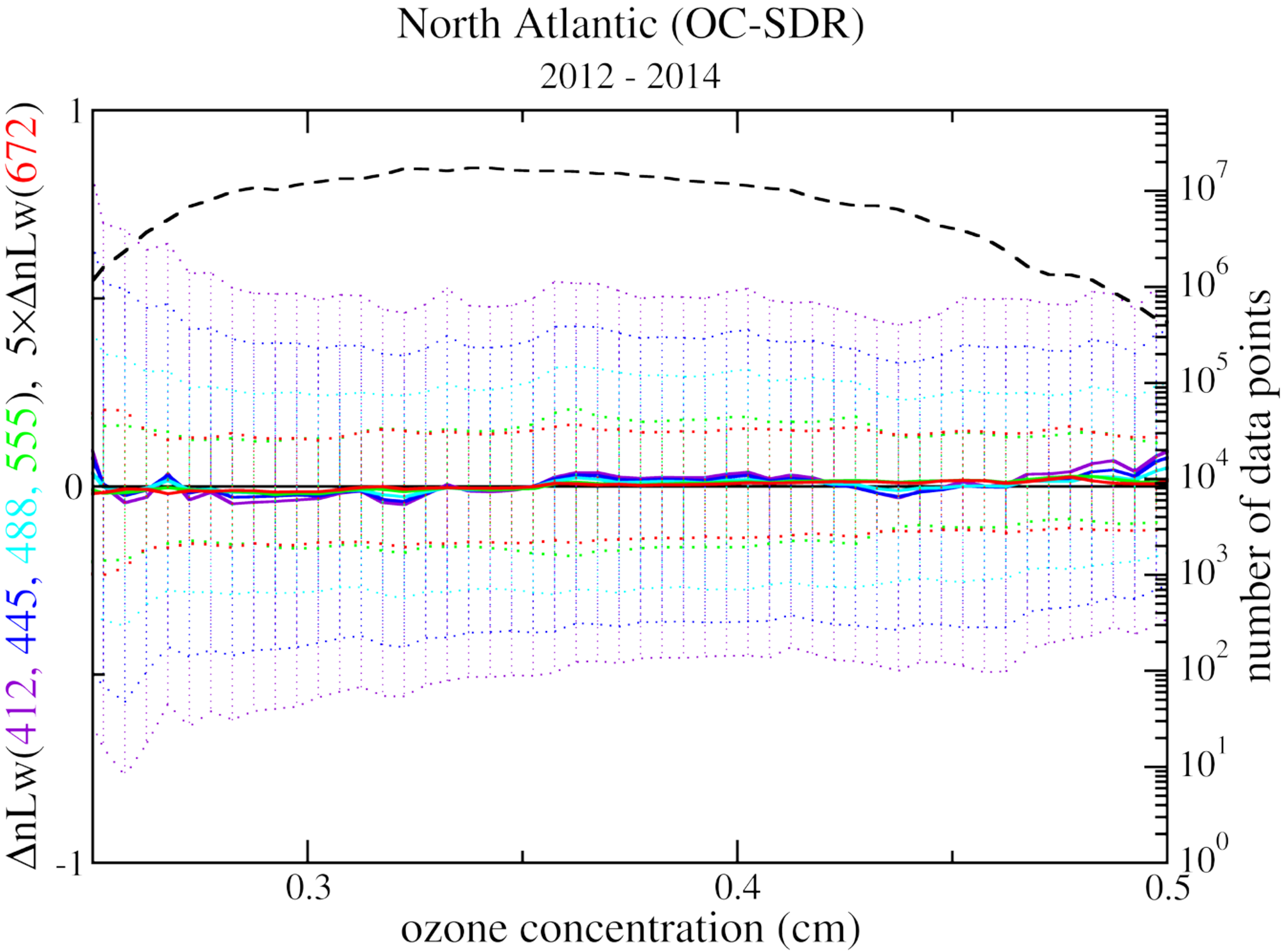
North Atlantic (OC-SDR)
2012 - 2014
ΔnLw(412, 445, 488, 555), 5×ΔnLw(672)
number of data points
ozone concentration (cm)
1
0
-1
0.3
0.4
0.5
10^7
10^6
10^5
10^4
10^3
10^2
10^1
10^0

South Pacific (OC-SDR)

2012 - 2014

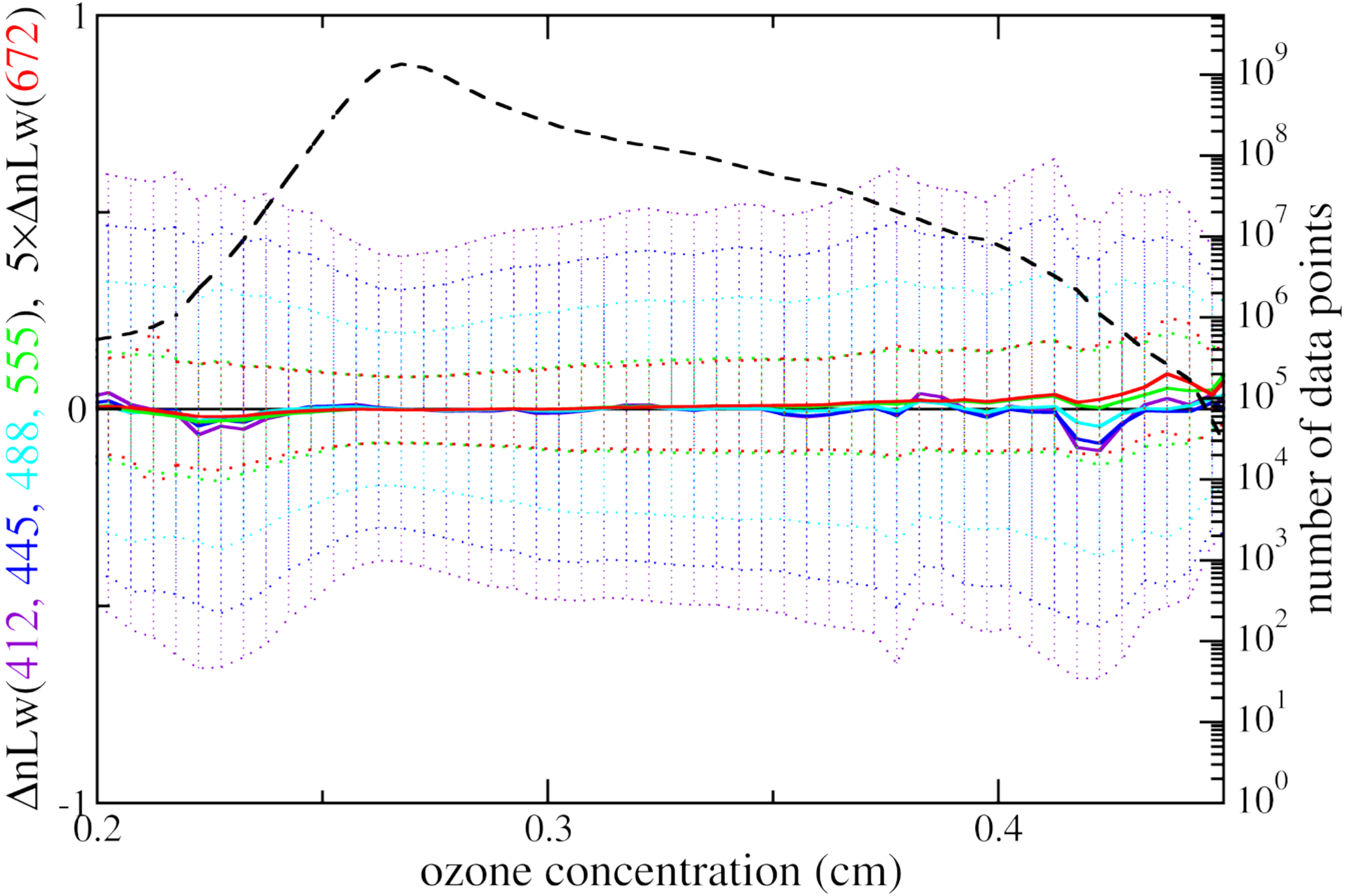

Summary

1. Better calibration in OC-SDR significantly improves retrieval consistency for 2012
2. Statistical dependence of nL_w on most retrieval parameters is nearly flat, signifying consistency of the new MSL12 ocean color data processing system in various conditions
3. In all cases, no significant year-to-year changes in statistics were observed
4. Good nL_w retrievals for satellite zenith angle up to 50° (North Atlantic) and nearly 70° (South Pacific)
5. nL_w underestimated for solar zenith angles > ~67° in both regions
6. Significantly decreased nL_w for low values of solar zenith angle (<25°) in South Pacific (likely due to seasonal effects/variations in the region)
7. Noticeable dependence on pixel along the scan in North Atlantic
8. Slightly increased nL_w with higher wind speed (whitecaps?) and higher water vapor concentration

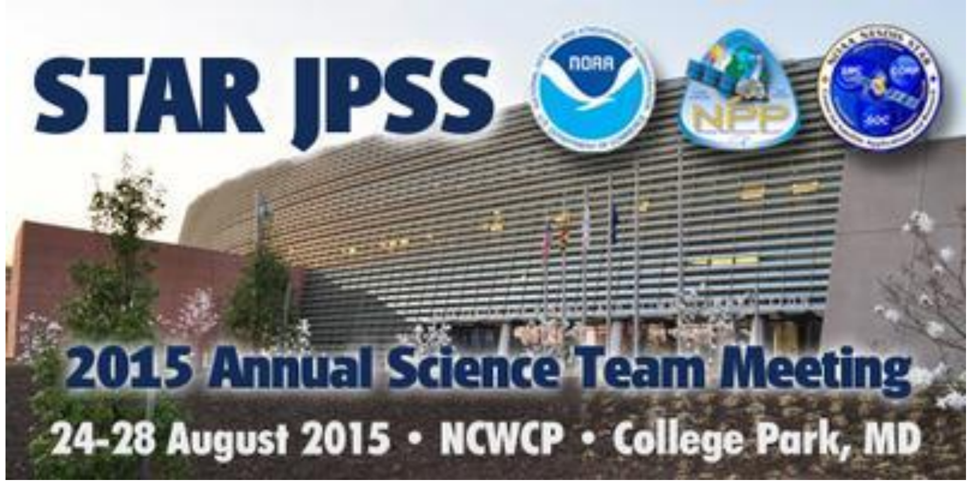

VIIRS Ocean Color Breakout
Thursday, 27 August 2015

Overview of VIIRS Cal/Val Nov. 2014 Cruise & Cruise Objectives

Michael Ondrusek

Dedicated VIIRS Cal/Val Cruise
NOAA Ship Nancy Foster
11-20 November 2014

International, Interagency and Academic Collaborations:

US Agencies

- **NOAA**/NESDIS/STAR (NOAA)
- Naval Research Laboratory, Stennis Space Center (**NRL**)
- NASA/Goddard Space Flight Center (**NASA**)
- National Institute of Standards and Technology (**NIST**)

European Union

- Joint Research Center of the European Commission (**JRC**)

Universities

- City University of New York, Long Island; CREST
- Lamont-Doherty Earth Observatory, Columbia University
- University of Massachusetts, Boston
- University of Miami
- University of South Florida
- University of Southern Mississippi

Principal investigators (PIs)

PI Name (Last, First)	Participating Institutions	Research Group Abbreviation
Ondrusek, Michael*	NOAA/NESDIS Center for Science, Technology and Research	NOAA/STAR
Ahmed, Sam	City College of New York	CCNY
Arnone, Robert	University of Southern Mississippi (USM) and Naval Research Center (NRL)	Stennis
Freeman, Scott	NASA Goddard Space Flight Center	NASA/GSFC
Gilerson, Alex	City College of New York	CCNY
Goes, Joaquim	Lamont-Doherty Earth Observatory at Columbia University	LDEO
Hu, Chuanmin	University of South Florida	USF
Johnson, B. Carol	National Institute of Standards and Technology	NIST
Lee, ZhongPing	University of Massachusetts, Boston	UMB
Neeley, Aimee	NASA Goddard Space Flight Center	NASA/GSFC
Voss, Kenneth	University of Miami	U. Miami
Zibordi, Giuseppe	Joint Research Centre of the European Commission	JRC

List of science party personnel aboard the *Nancy Foster*

Name (Last, First)	Title	Research Group/Home Institution*
Arnone, Robert	Research Professor	Stennis/USM
Freeman, Scott	Staff Research Scientist	NASA/GSFC
Goes, Joaquim	Research Professor	LDEO
el Habashi, Ahmed	PhD Student	CCNY
Ibrahim, Amir	PhD Student	CCNY
Kovach, Charles	Researcher	USF
Lin, Junfang	Postdoctoral Researcher	UMB
Neeley, Aimee	Staff Research Scientist	NASA/GSFC
Ondrusek, Michael	Chief Scientist	NOAA/STAR
Goode, Wesley	Researcher	Stennis/NRL
Stengel, Eric	Researcher	NOAA/STAR
Talone, Marco	Researcher	JRC
Vandermeulen, Ryan	Remote Sensing Analyst	Stennis/USM
Wei, Jianwei	Postdoctoral Researcher	UMB
Zibordi, Giuseppe	Researcher	JRC

Science Objectives for the Cruise

Goals

1) Validation of VIIRS JPSS Satellite Ocean Color products

- **Occupied 23 Stations over 10 Days, 9 station matchups with VIIRS**
- **Conducted pre- and post-cruise inter-cals**
- **Water-Leaving Radiance** - HyperPro, MicroPro, HyperTSRB, C-OPS, GER, SBA, TRIOS, HyperSAS, ASD Handheld 2
- **Aerosol Optical Depth** - Microtops
- **Bi-directional radiance distribution** - NURADS
- **Chlorophyll** - HPLC, Fluorometric, (in situ and extracted)
- **Absorption** - ACS, AC9, Spectrophotometric
- **Backscatter** - BB9, BB7, BB3, ECO Puck
- **Phytoplankton Physiology -** Flowcam, FIRe, Alf
- **Carbon** - POC and DOC water analysis; plus CDOM
- **Total Suspended Matter** - Gravimetric

Science Objectives for the Cruise

Goals (cont.)

2) Characterization of differences among the in situ ocean color measurements

a) replicate observations from multiple identical (same model) instruments deployed in parallel;
b) observations of the same in situ parameters but using different types of instruments;
c) different deployment protocols for sample collection;
d) different post-processing methods for the in situ data; and
e) spatial and temporal variability of the ocean waters.

characterization of differences among the in situ ocean color measurements

Science Objectives for the Cruise

Goals (cont.)

3) Optical characterization of ocean variability (i.e. coastal, near-shore, cross-shelf, eddies, fronts, filaments, blue

-Can water mass characterization of the representing different bio-physical processes be defined using VIIRS bio-optical products in the a dynamic system such as the Gulf Stream?

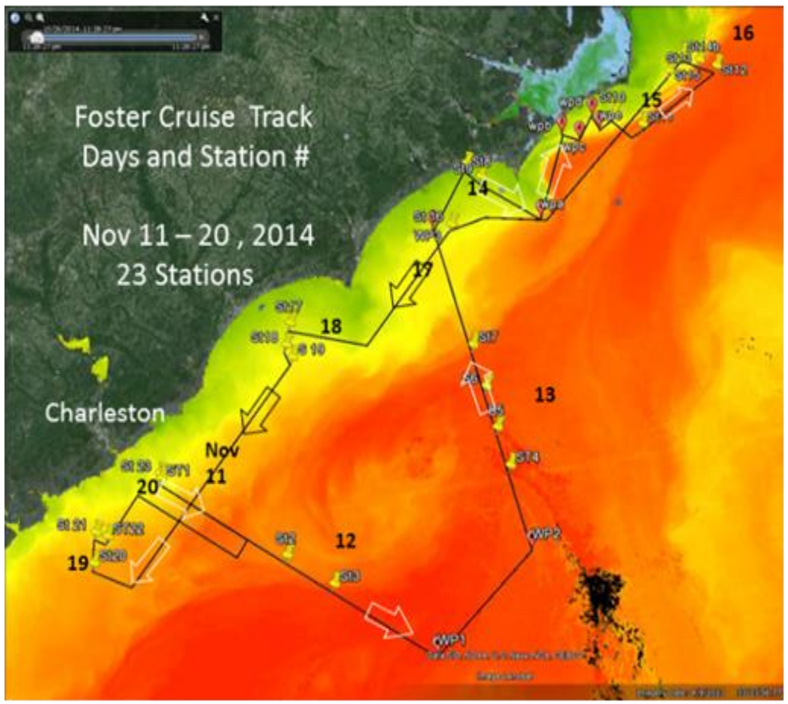

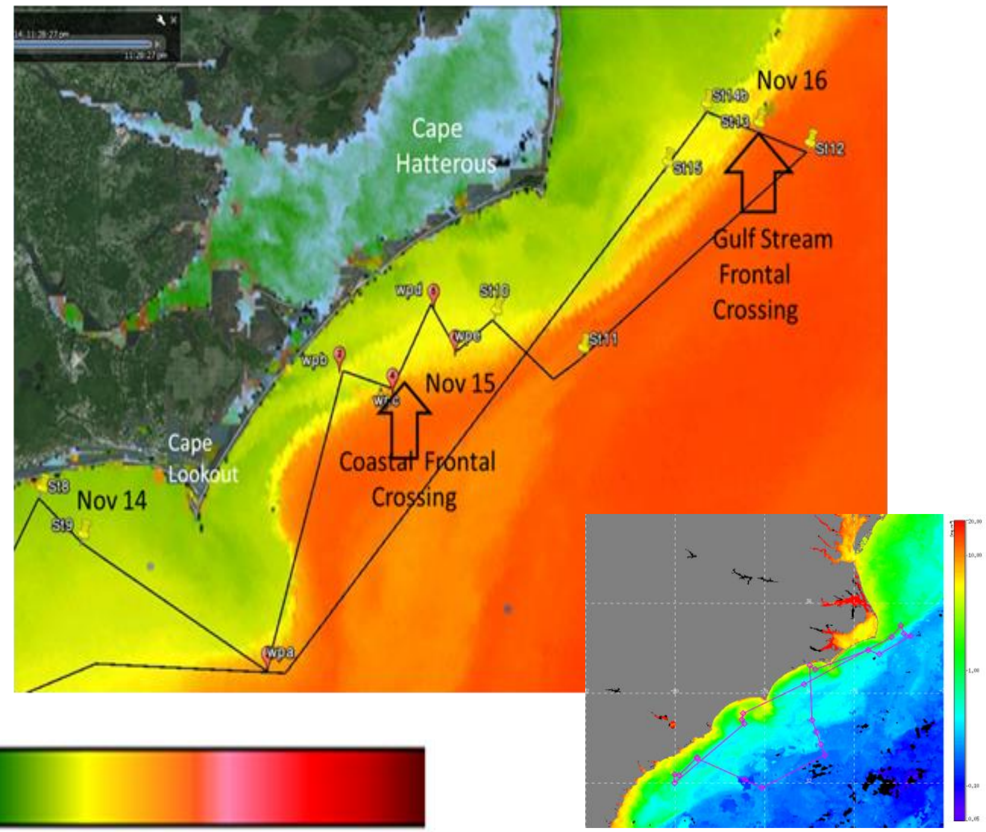

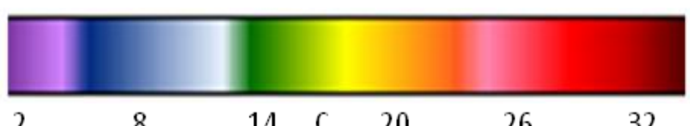

2015 STAR JPSS Annual Science Team Meeting,
College Park, Maryland
August 24-28, 2015

Evaluation of VIIRS ocean color products and development of enhanced ocean products and applications

Robert Arnone[1], Ryan. Vandermuelen[1], Sherwin. Ladner[2]

Stennis - Cal val Team
Annual Summary

- Maintain WavCis – Aeronet Site
- Cal Val Cruises

Ocean Weather
Real-time monitoring

THE UNIVERSITY OF SOUTHERN MISSISSIPPI

Overview - Annual Highlights – Details in Posters

Stennis
Cal Val Team

1) **Ocean Color product stability using VIIRS orbital overlaps to track monthly trends**
2) **VIIRS validation of Gulf Stream water masses Foster Cruise**
3) **Characterizing the diurnal changes in coastal bio-optical properties in coastal waters**
4) **Temporal Assessment of the Calibration and Accuracy of VIIRS Radiometric (SDR) and Ocean Color Products (EDR) at MOBY and WavCIS**
5) **Using the VIIRS I 1-band to enhance bio-optical monitoring of coastal waters**
6) **Applications of VIIRS ocean color for real time adaptive sampling**

1) Ocean Color product stability using VIIRS orbital overlaps to track monthly trends

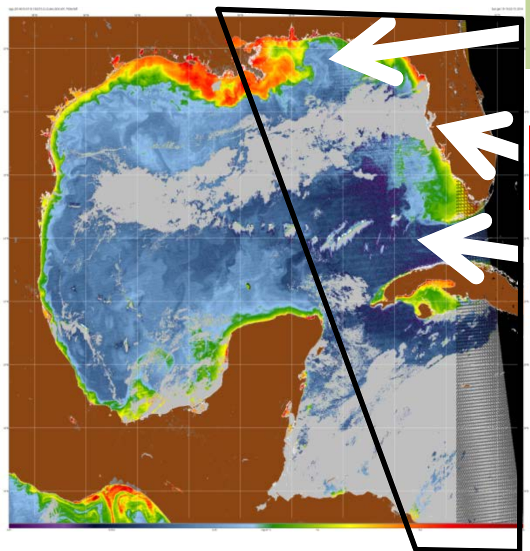

Right Side of NADIR

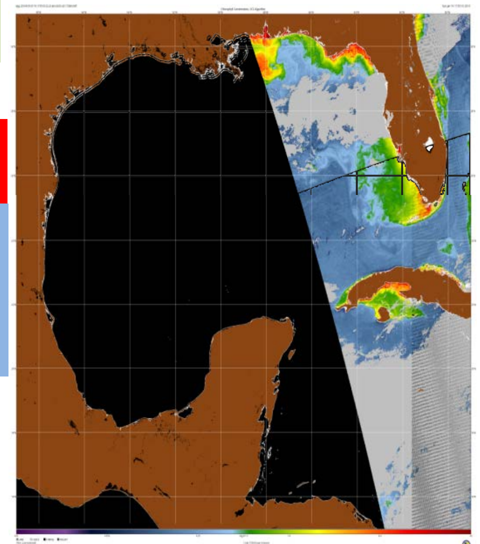

Left side of NADIR

VIIRS 100 minute Overlap

Track the differences in products to test VIIRS Stability

Approach evaluates complete VIIRS sensor cal val process. " SDR cal, atm corr, Product"

How do the differences in the color products within 100 minute change with season?

Example of Open ocean waters ROI

T175147 GMT

T193215

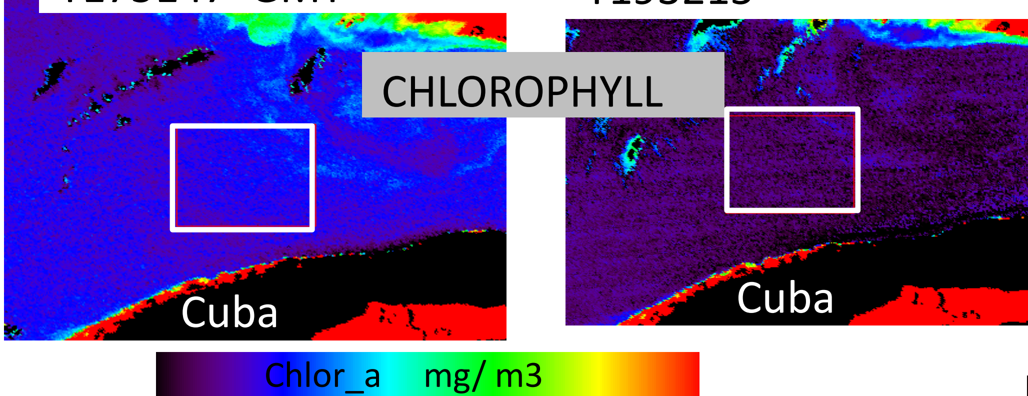

Chlor_a difference mg/ m

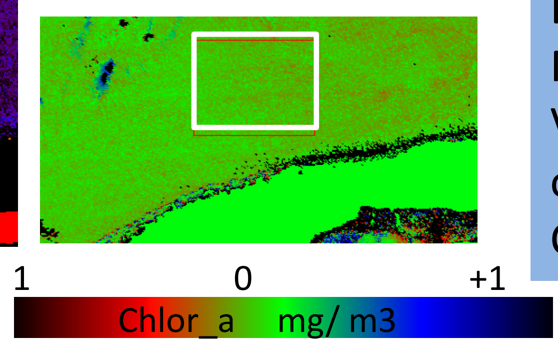

VIIRS Product Difference Mean and Variance of the M CHANNELS

1) Ocean Color product stability using VIIRS orbital overlaps to track monthly trends

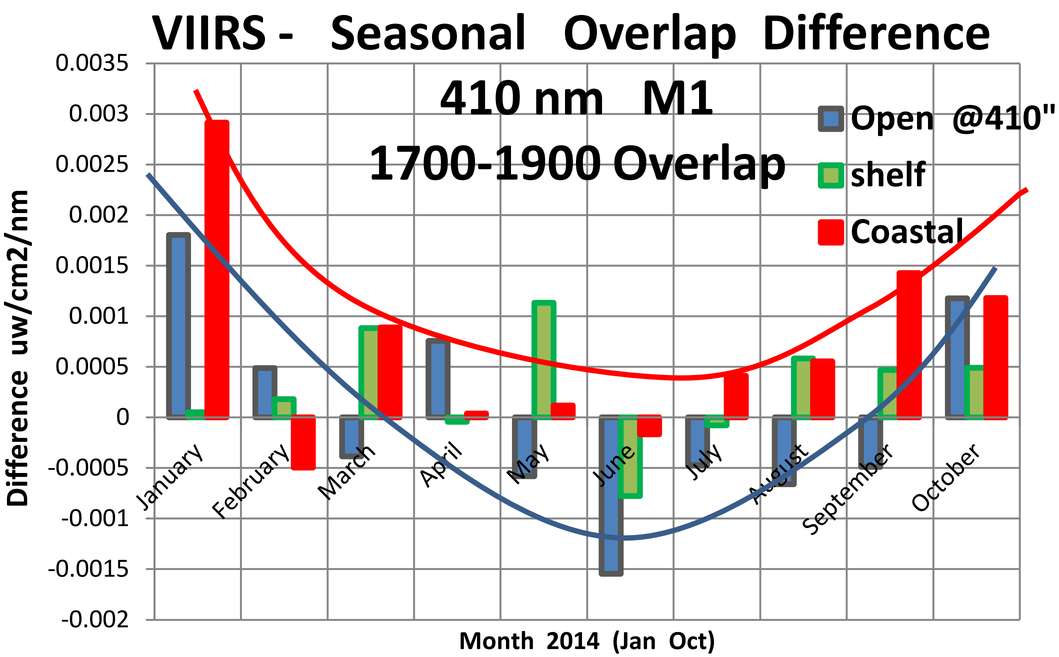

First orbit minus Second orbit .

Which orbit has higher reflectance ?

Changes in winter to Summer
- Solar Angle

Largest in M1 Minimal in M5

- Strongest in Open ocean water !
- Similar trend in Coastal waters

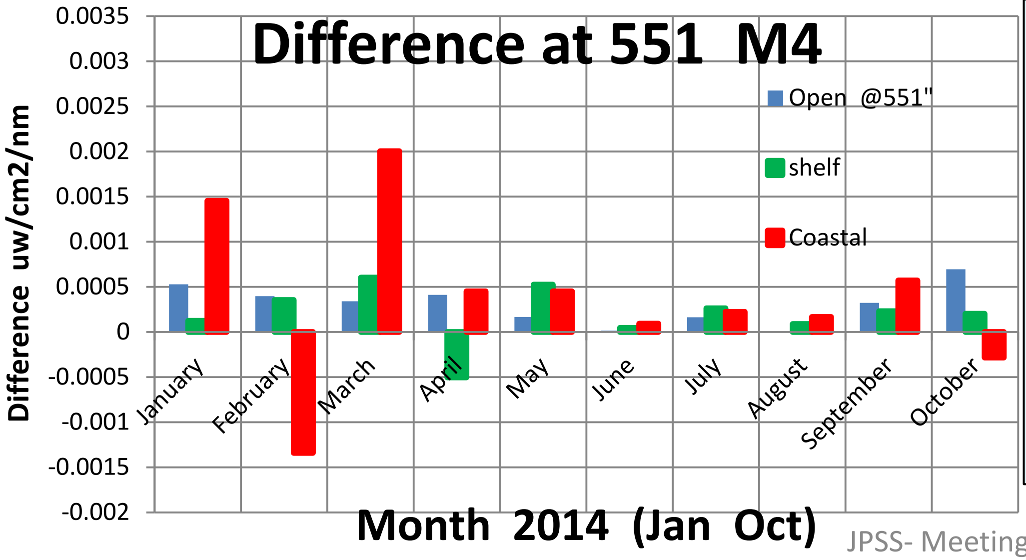

Summary:

1. Overlap nLw differences provides very sensitive ability to track the trends in both the Sensor response and processing.
- Dependent on diurnal changes ! Next ..

2. Enables internal consistency within the sensor across the orbital swath.
3. Can be applied on a global basis.

2) VIIRS validation of Gulf Stream water masses Foster Cruise

Characterized multiple instruments for Spectral radiance .. Above and in water etc.

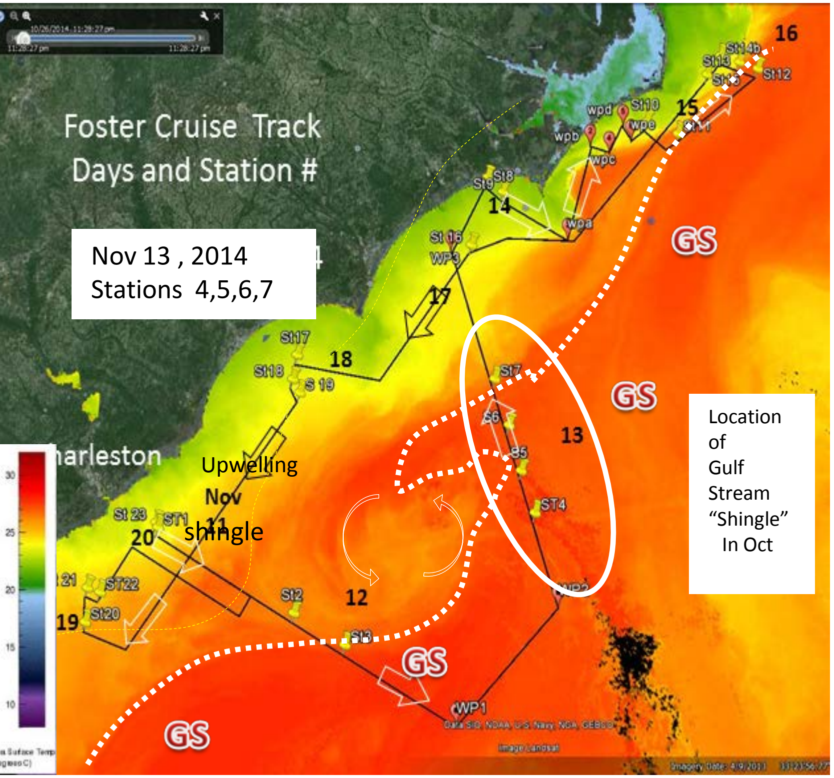

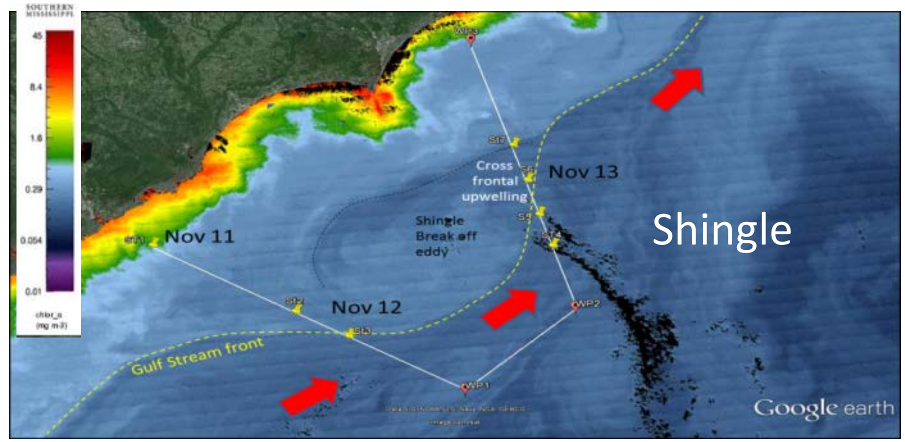

VIIRS – Validation crossing
Dynamics Gulf Stream Fronts . -
1) Shingle
2) Cape Hatteras.
3) Charleston
Upwelling - Bio-optical response.

Characterized the Spatial Variability At each station - Station 18

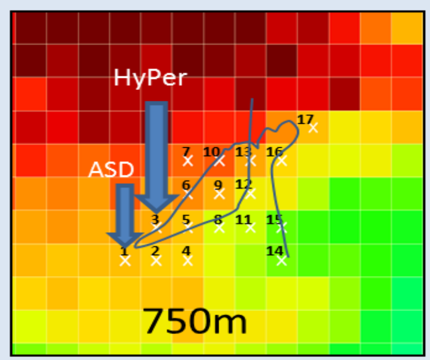

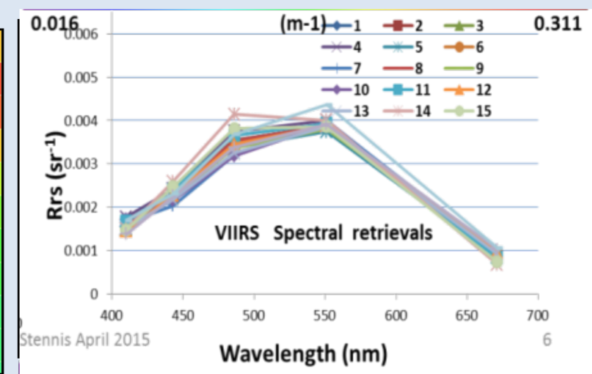

Calibration - Matchup requires Defining the VIIRS pixel variability

2) VIIRS validation of Gulf Stream water masses Foster Cruise

VIIRS Ocean color Validation Along track across front

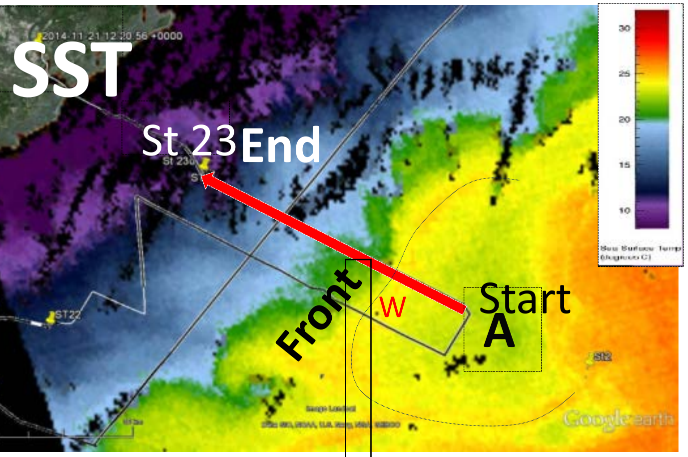

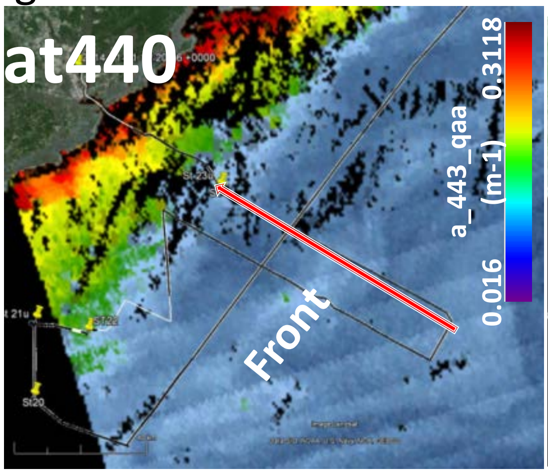

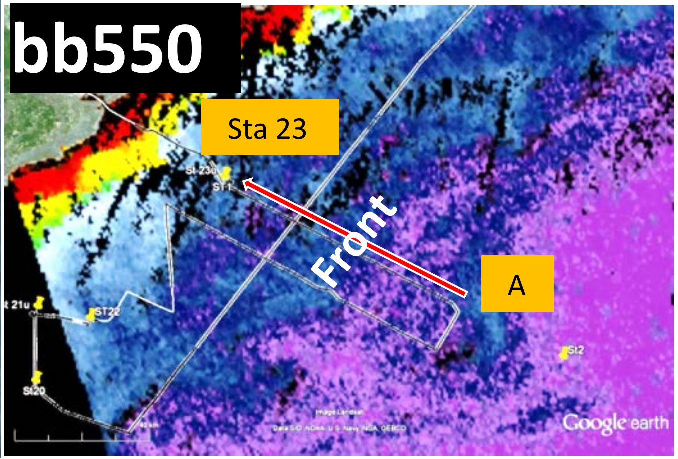

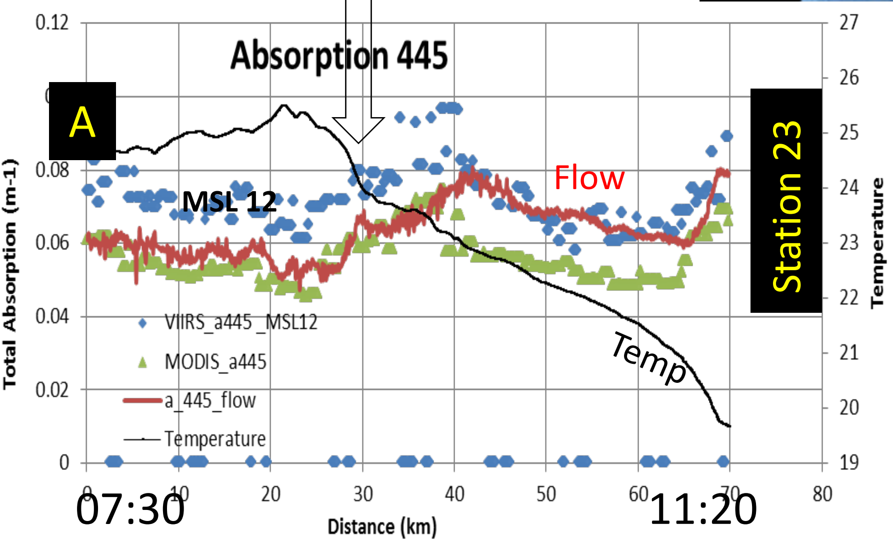

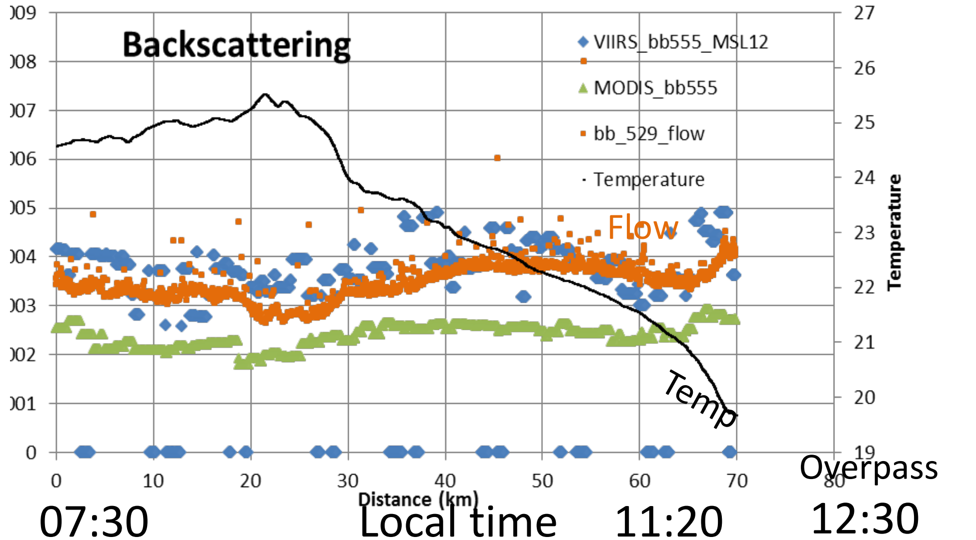

Summary -- see poster !!

1. Unique data sets for instrument protocols
2. OC Spatial variability on Station
3. OC response to ocean processes !
4. Agreement of VIIRS and Flowthrough optics
5. New Questions to address → accuracy of instruments vs temporal and spatial variability.
6. Bio-optical Water Mass classification -

3) Characterizing the diurnal changes in bio-optical properties in coastal waters

How fast can Ocean Color change in ~ 100 minutes?

VIIRS nLw validated
The diurnal changes !
Poster includes MOBY

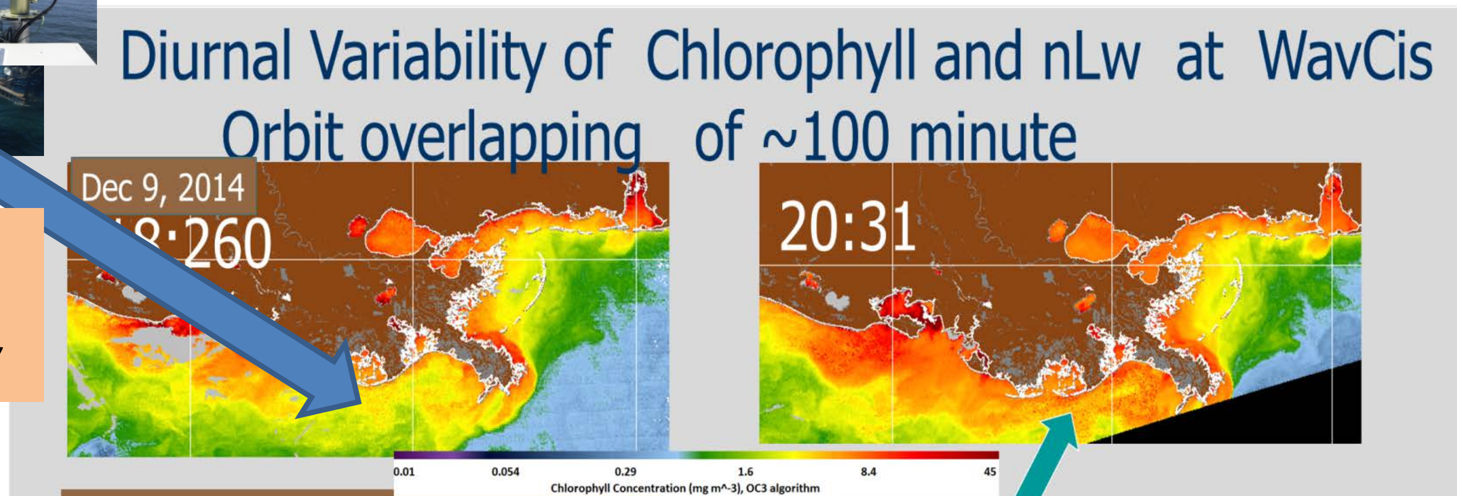

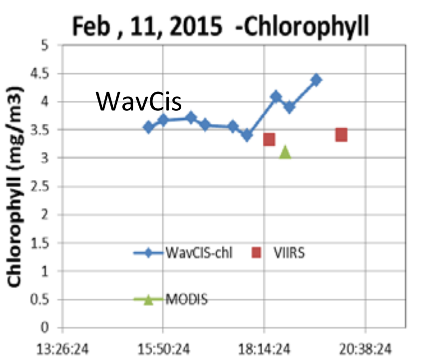

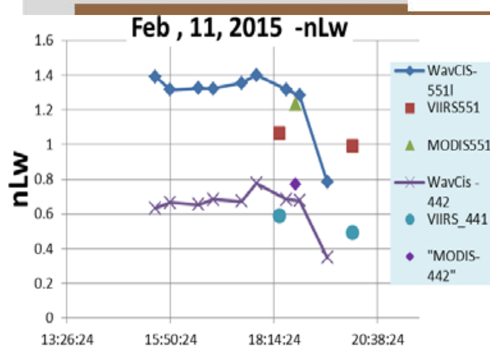

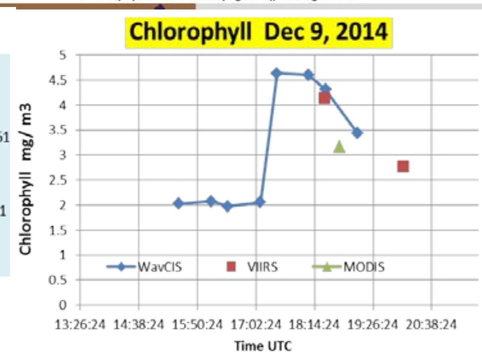

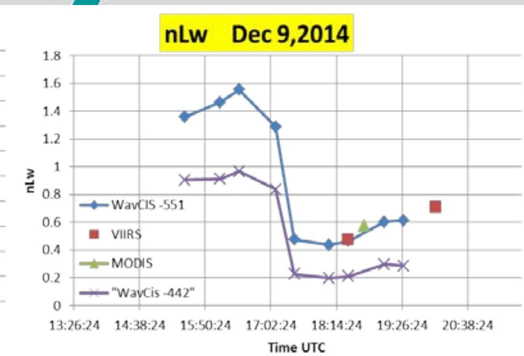

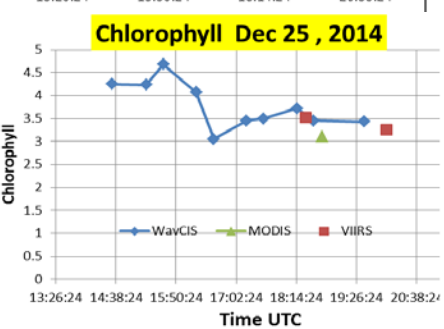

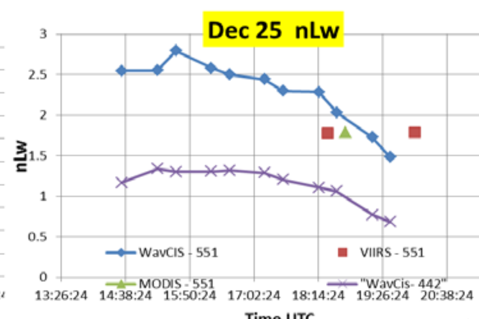

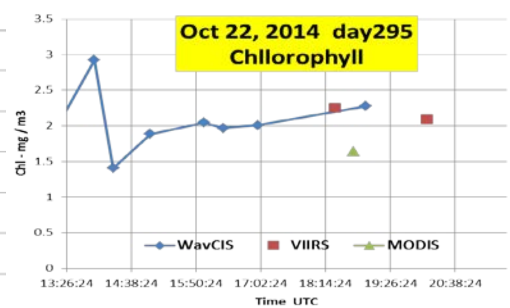

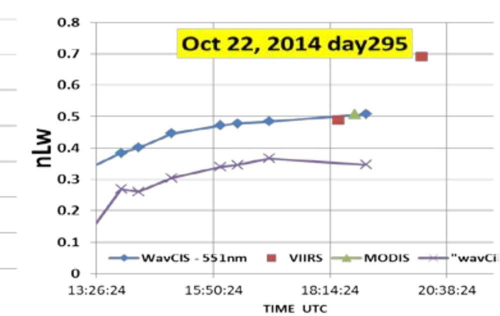

3) Characterizing the diurnal changes in bio-optical properties in coastal waters

Summary;

1. **VIIRS – Overlap products was able to capture hourly changes in ocean color !!**
2. **Calibration and validation in coastal areas requires short time for matchup !**
3. **New product capability from VIIRS ! See poster !**

Diurnal Changes identifies new ocean processes product . Bloom occurring!

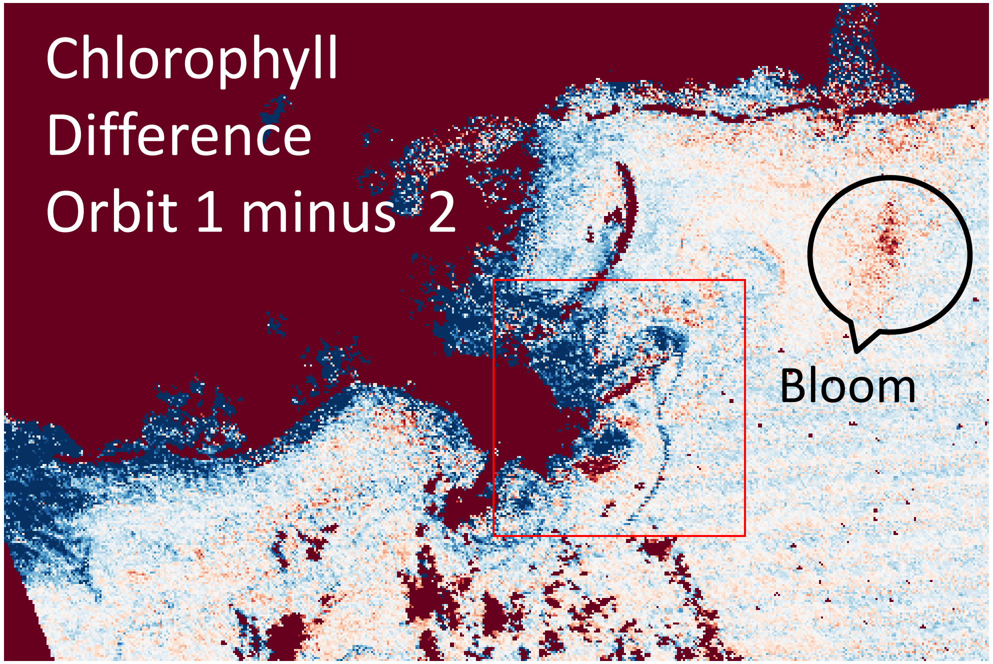

Second Pass Greater

-1 (mg/m3) +1

Bloom Decay

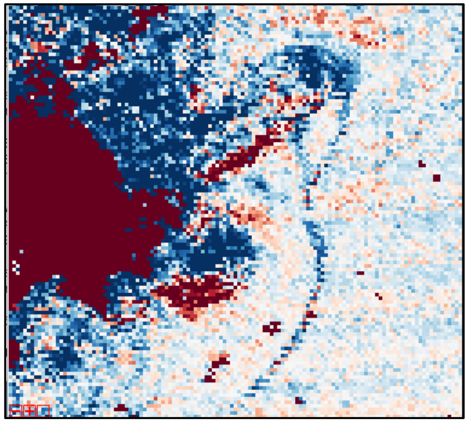

Frontal Movement

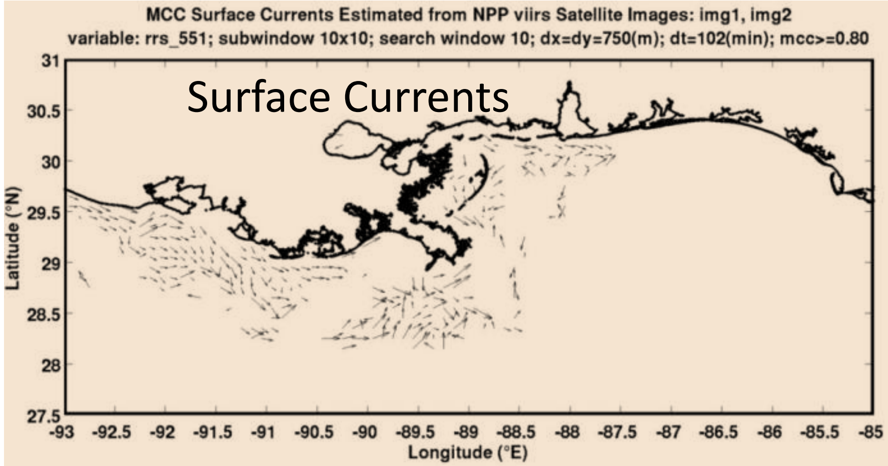

Yang, H.; Arnone, R.; Jolliff, J.; Estimating Advective near – surface currents from ocean color satellite images. Remote Sensing of Environment Volume 158, 1 March 2015, Pages 1–14

4) Temporal Assessment of the Calibration and Accuracy of VIIRS Radiometric (SDR) and Ocean Color Products (EDR) at MOBY and WavCIS (Aeronet-OC)

SDR (Real time) Gains Trend @ MOBY

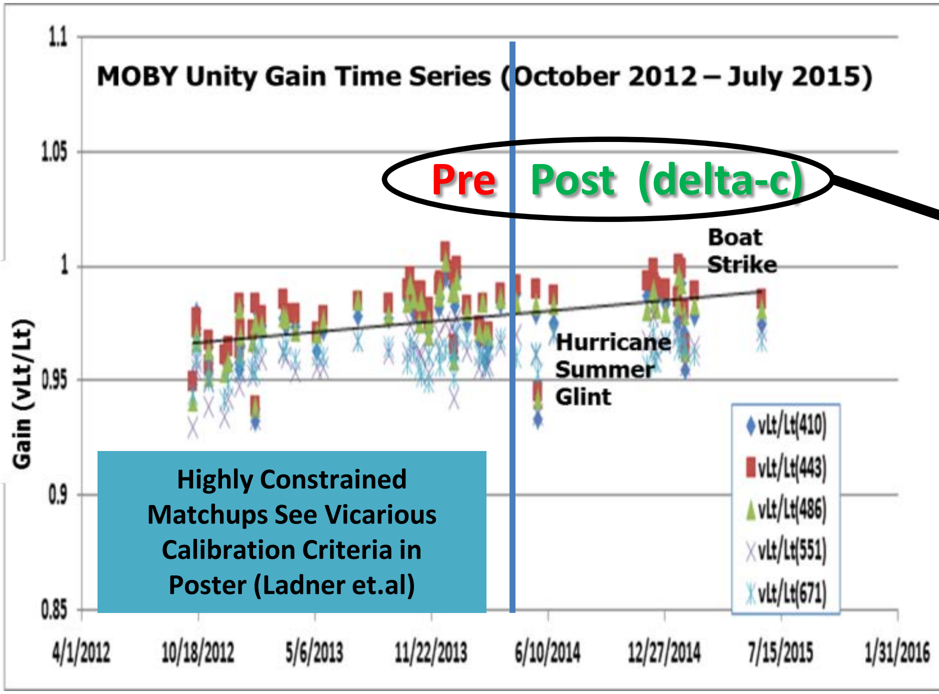

Effect of SDR Calibration Change May 2014 (Delta-c) on Vicarious Calibration Gain Sets

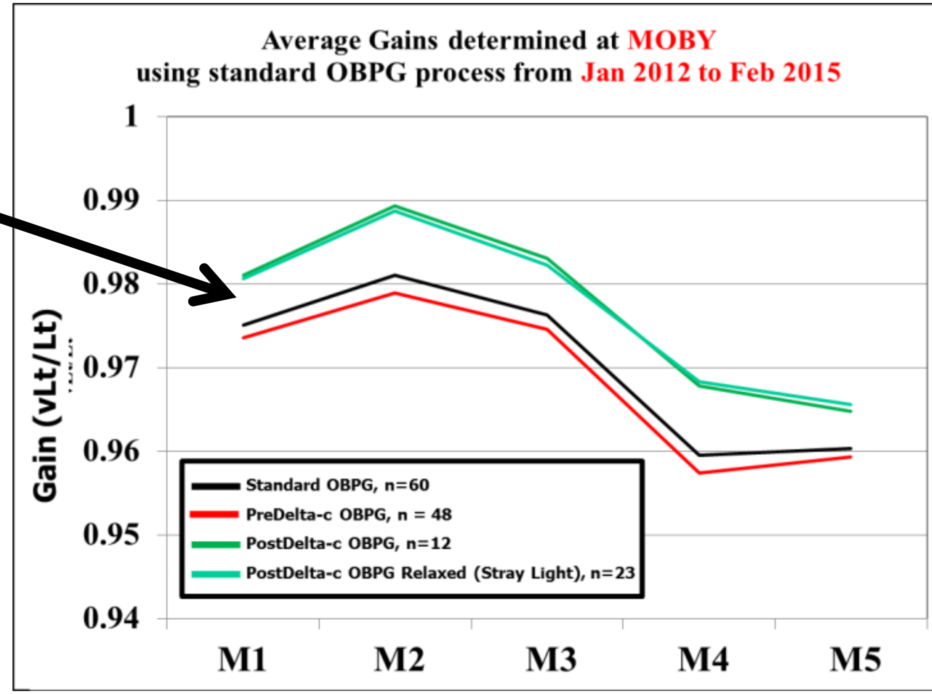

Trend (unity gains) shows:
- NOAA real-time SDR improvement over time (not stabilized).
- Need continuous vicarious calibration for operations.

- A pre and post delta-c (May 2014) calibration change exist.
- Needs further evaluation w/ more matchups highly constrained matchups.
- Evaluation at green water AERONET site (WavCIS) underway.

4) Temporal Assessment of the Calibration and Accuracy of VIIRS Radiometric (SDR) and Ocean Color Products (EDR) at MOBY and WavCIS (Aeronet-OC

MOBY and WavCIS Time Series Analysis and SDR Calibration Effect (Delta-c May 2014)

(See poster for more results including post delta-c green water analysis at WavCIS, cruise matchups, etc.)

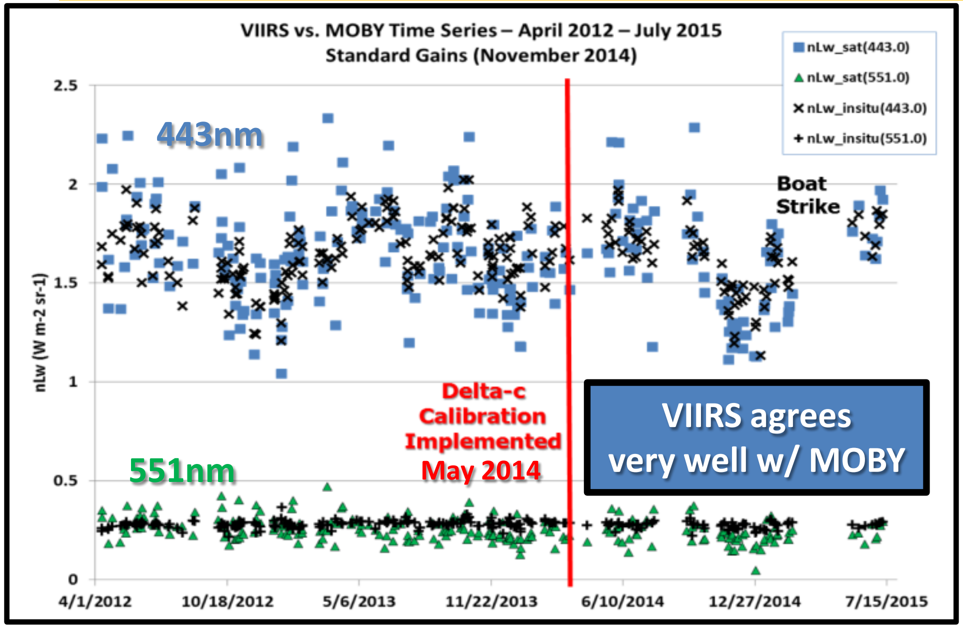

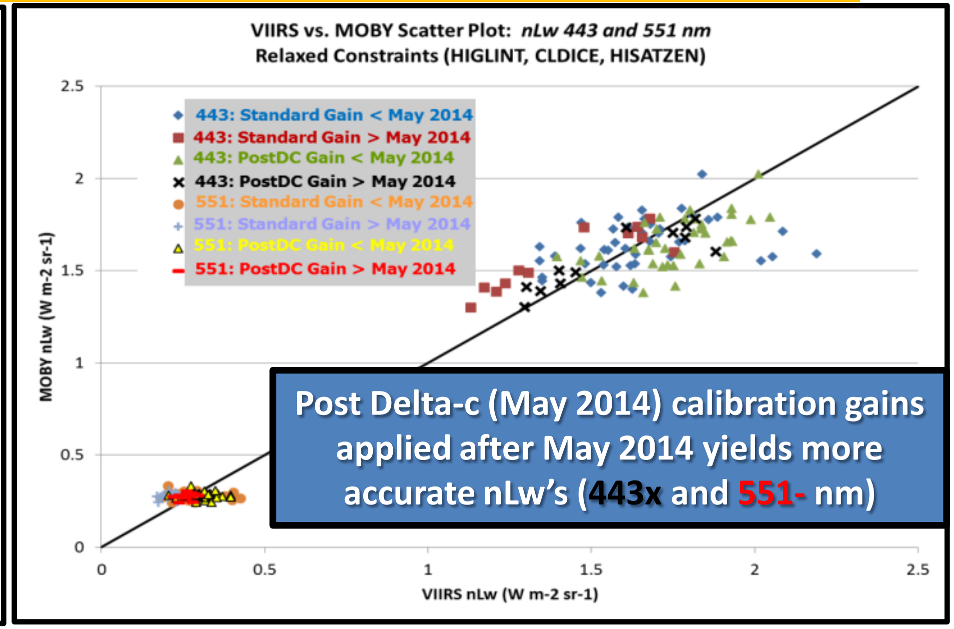

VIIRS Chlorophyll June 7, 2015 – Post Delta-c Calibration Effect

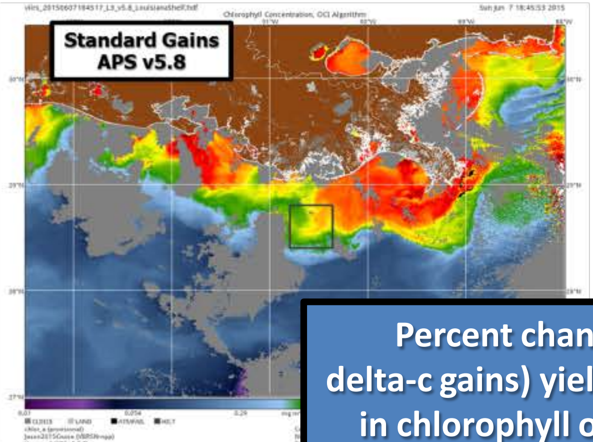

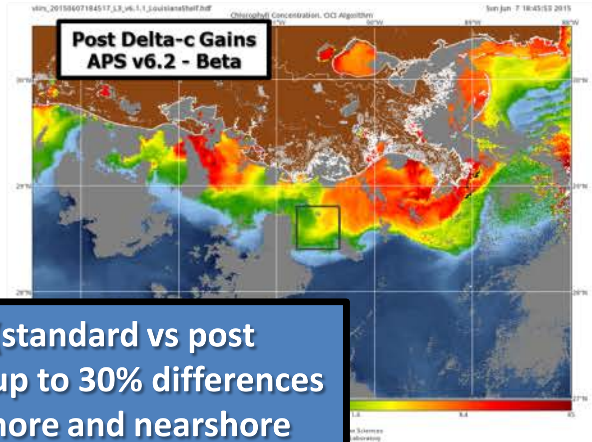

Percent change (standard vs post delta-c gains) yields up to 30% differences in chlorophyll offshore and nearshore

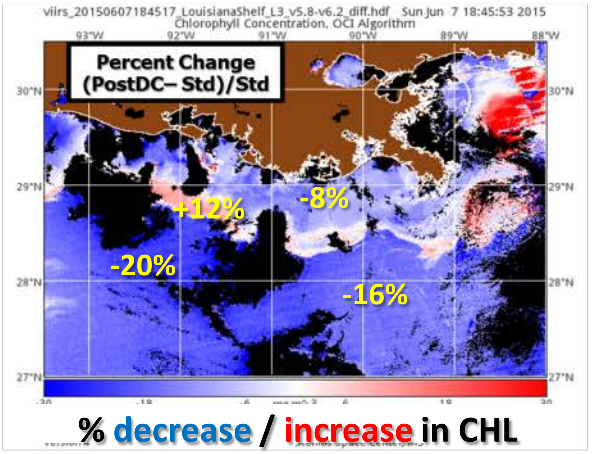

5) Using the VIIRS I 1-band to enhance bio-optical monitoring of coastal waters

New VIIRs Ocean Color Product for Coastal Applications - See Poster

Spatially improved ocean color products are obtained by combining the 750-m M(λ) bands with the 375-m I1-band

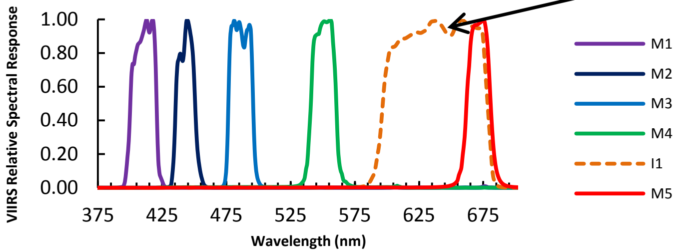

Algorithm based on covariance of each M(λ) band with I1-band

For each pixel and λ, the sharpening is weighted as a direct function of M(λ) covariance with the high resolution (I-1) band in a 5x5 subarray. Maps of "sharpening confidence" are created

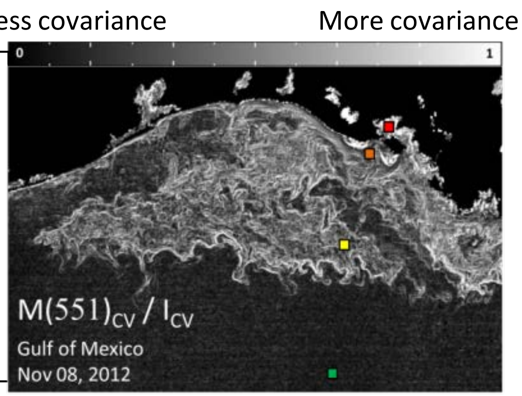

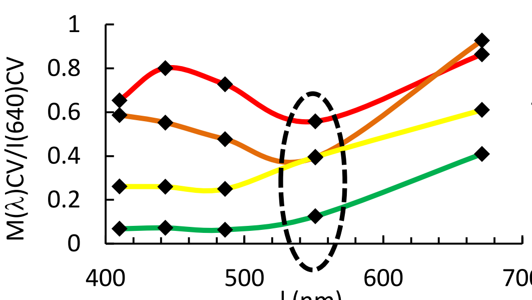

MORE COVARIANCE
=
MORE SHARPENING

Sharpened Normalized Water Leaving Radiance Spectrum

nLw_410 : 375-m

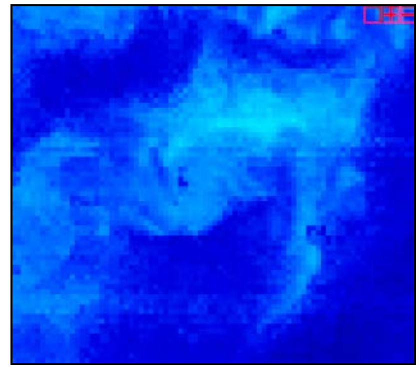

nLw_410 : 750-m

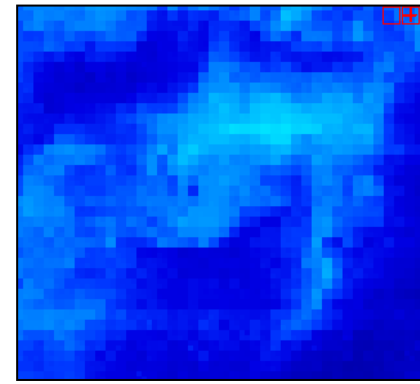

44 coastal matchups show that sharpened nLw have improved R-values, RMSE, and NMB!

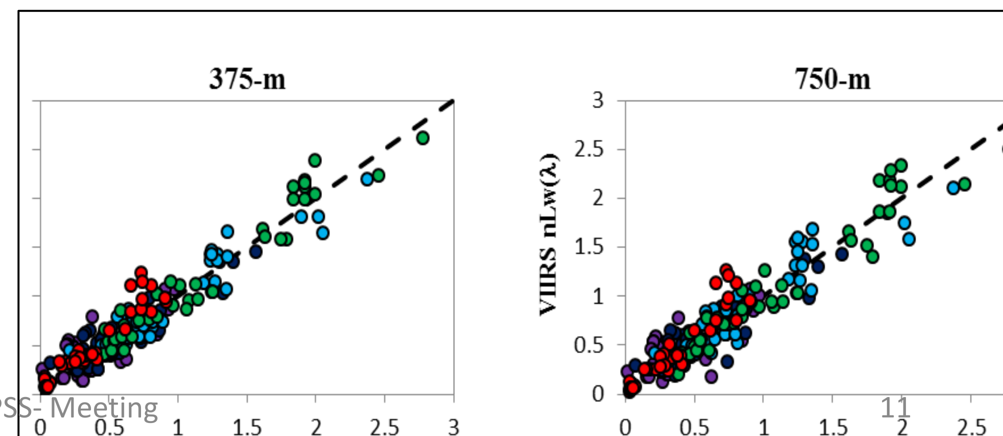

5) Using the VIIRS I 1-band to enhance bio-optical monitoring of coastal waters

Gulf of Mexico, 05/14/13

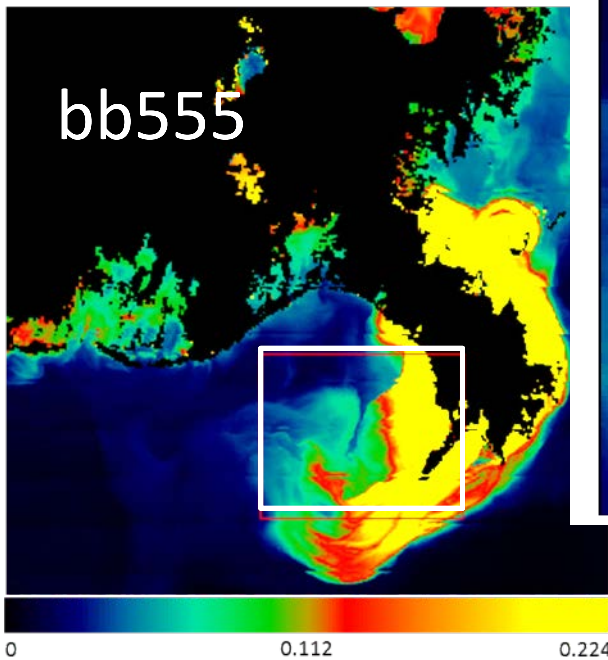

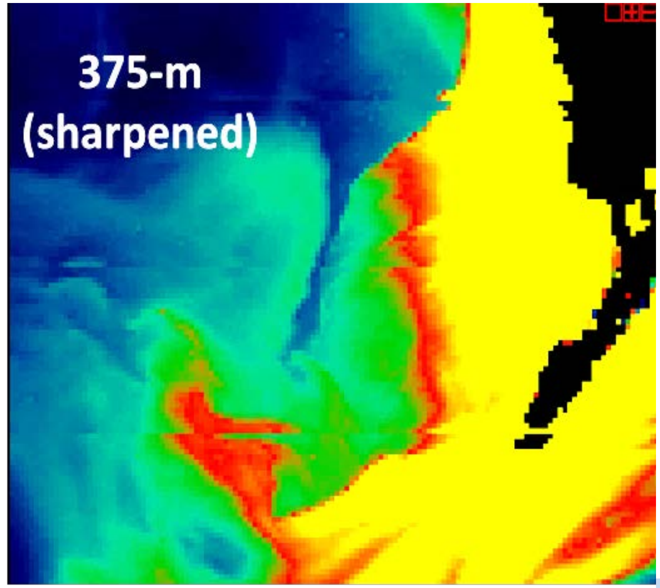

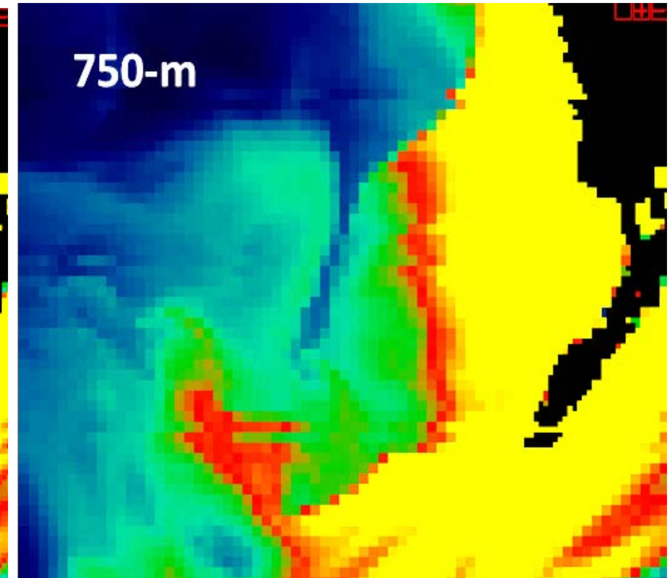

***Sharpened* (375) nLw M bands are linked into processing to produce high resolution Ocean Color Products**

375-m products (QAA, chlorophyll) match up better with in situ than 750-m

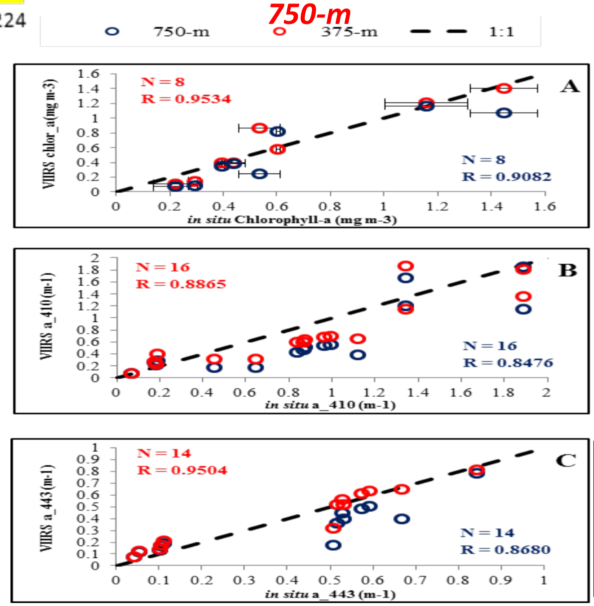

Summary

1. **New product and coastal applications for VIIRS sensor in ocean color.**
2. **Enhance resolutions for VIIRS ocean color can be achieved by combining the I bands with the M bands**
3. **New VIIRS Coastal ocean product derived at 375m for coastal waters !**
4. **Spatial Covariance used to spectrally weight Band sharpening**
5. **Results are confirmed in coastal waters and demonstrate improved VIIRS validation.**

Validation

New VIIRS use of I BANDS

Vandermeulen, R. A., Arnone, R., Ladner, S., & Martinolich, P. (2015). Enhanced satellite remote sensing of coastal waters using spatially improved bio-optical products from SNPP–VIIRS. *Remote Sensing of Environment*, *165*, 53-63.

6) Applications of VIIRS ocean color for real time adaptive sampling

Using Circulation Models and VIIRS Ocean Color to direct sampling locations in Fronts, River Plumes, and validating Ocean Models

--See Poster

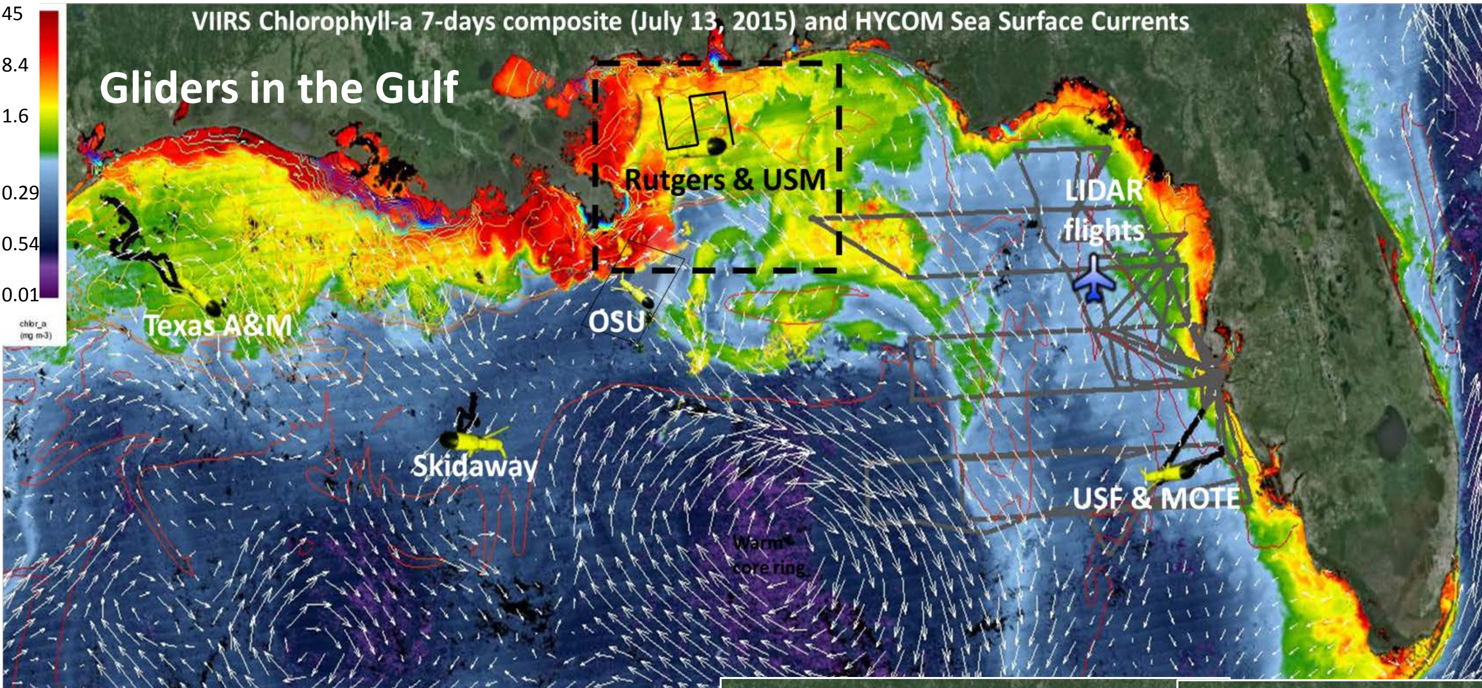

Real time Animated VIIRS Color and models to validate coastal plumes.

Enabled Glider Deployments Adaptive Sampling.

Define Model Uncertainty

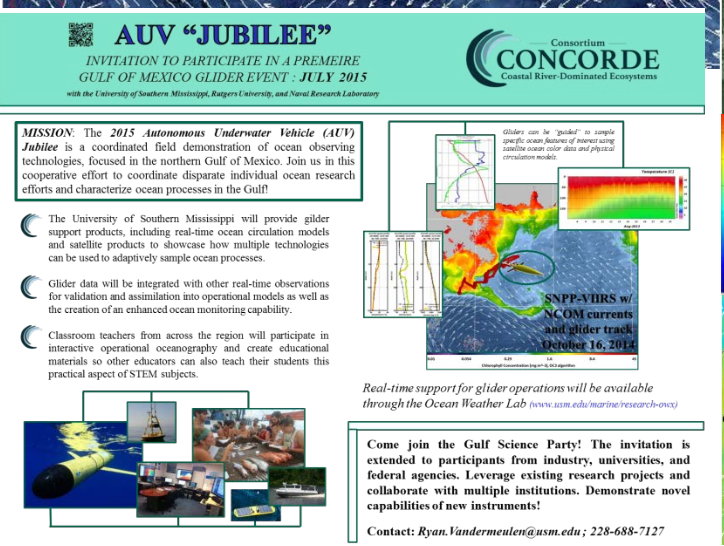

AUV "JUBILEE"

*INVITATION TO PARTICIPATE IN A PREMEIRE GULF OF MEXICO GLIDER EVENT : **JULY 2015***

with the University of Southern Mississippi, Rutgers University, and Naval Research Laboratory

Consortium CONCORDE Coastal River-Dominated Ecosystems

MISSION: The ***2015 Autonomous Underwater Vehicle (AUV) Jubilee*** is a coordinated field demonstration of ocean observing technologies, focused in the northern Gulf of Mexico. Join us in this cooperative effort to coordinate disparate individual ocean research efforts and characterize ocean processes in the Gulf!

- The University of Southern Mississippi will provide gilder support products, including real-time ocean circulation models and satellite products to showcase how multiple technologies can be used to adaptively sample ocean processes.
- Glider data will be integrated with other real-time observations for validation and assimilation into operational models as well as the creation of an enhanced ocean monitoring capability.
- Classroom teachers from across the region will participate in interactive operational oceanography and create educational materials so other educators can also teach their students this practical aspect of STEM subjects.

Gliders can be "guided" to sample specific ocean features of interest using satellite ocean color data and physical circulation models.

SNPP-VIIRS w/ NCOM currents and glider track October 16, 2014

Real-time support for glider operations will be available through the Ocean Weather Lab (www.usm.edu/marine/research-owx)

Come join the Gulf Science Party! The invitation is extended to participants from industry, universities, and federal agencies. Leverage existing research projects and collaborate with multiple institutions. Demonstrate novel capabilities of new instruments!

Contact: ***Ryan.Vandermeulen@usm.edu ; 228-688-7127***

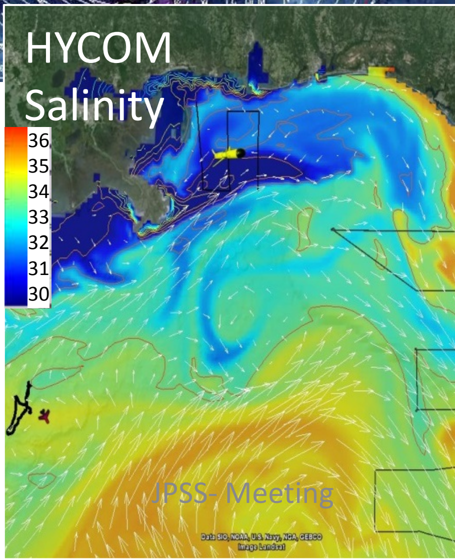

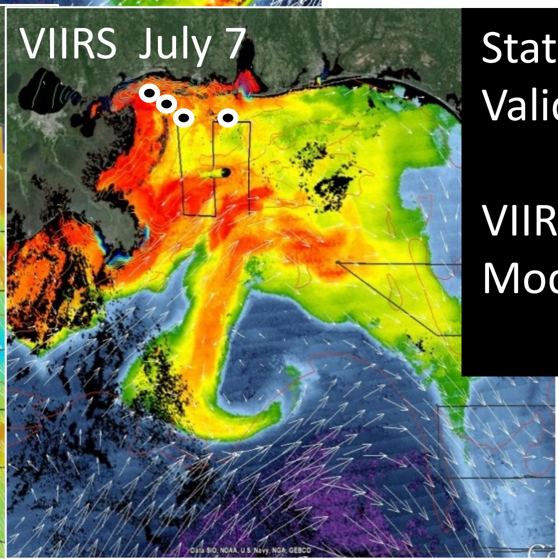

Stations for Validation of

VIIRS

Models

6) Applications of VIIRS ocean color for real time adaptive sampling

Management Decisions for

Near Real-time Adaptive Sampling

STEP1: Gather data into google Earth

VIIRS Ocean Data
Chlorophyll-a, backscattering, absorption, euphotic depth, sea surface temperature

Physical circulation models
SST, currents, salinity, mixed layer depth, sea surface height

Ancillary data
Real-time data from buoys or moorings, weather data, meteorological models (wind data)

How to optimally apply VIIRS data for sampling ! "Plume"

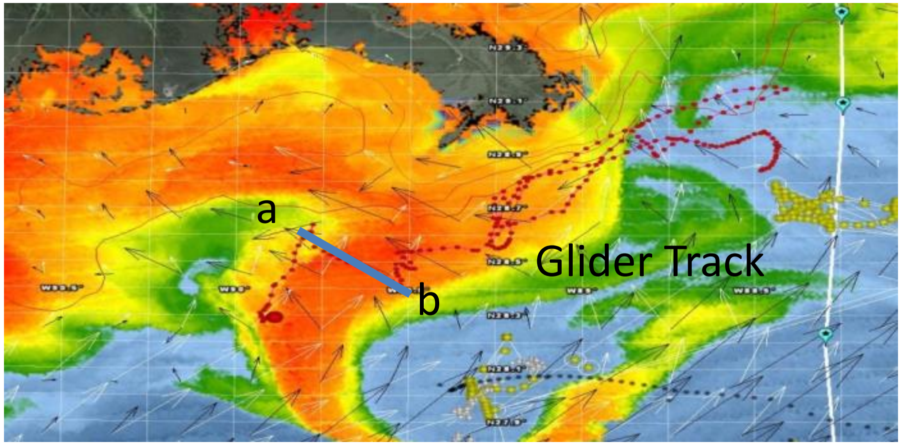

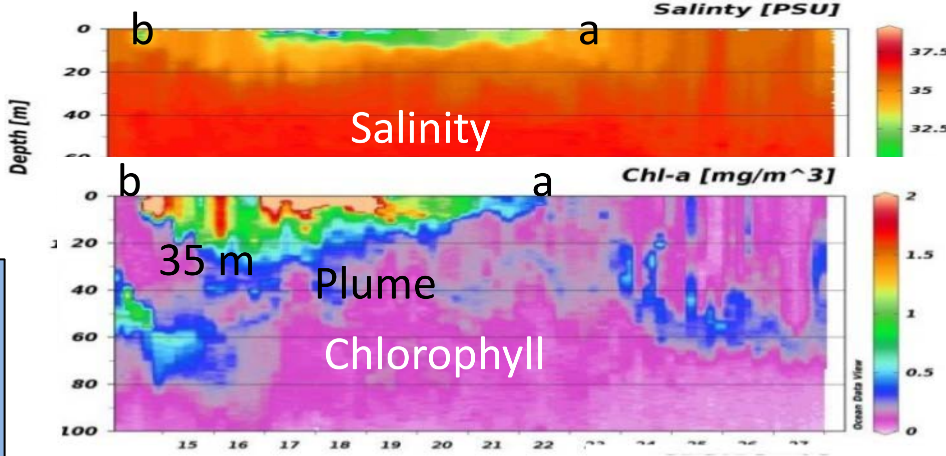

Poster details 4 Steps on how VIIRS is used In steps for adaptive sampling!

Summary:
1. Fusing Satellite color and SST with circulation models defines uncertainty.
2. VIIRS Color data used for Model Validation
3. Glider deployment is dependent on density Requires accurate location of Plumes!
4. Adaptive sampling used to optimize samples for VIIRS validation

VIIRS ocean color provides a critical component in defining River Plumes ecosystems!
AUV Jubilee activities in Gulf

Evaluation of VIIRS ocean color products
and development of enhanced ocean products and applications

Stennis Cal Val Team

Summary:

See 6 Posters for details .

1. **VIIRS Orbital Overlaps – tracks the trends are stable**
   - **Validated the diurnal response – 100 minutes of VIIRS color**
   - **Spatial and temporal response of ocean color is required for cal val procedures.**
2. **Foster Cruises validated VIIRS ocean color transects**
3. **VIIRS cal val :**
   - **VIIRS real-time SDR improving over time @ MOBY**
   - **VIIRS/insitu matchups indicate high quality operational OC products.**
   - **Cal/val @ MOBY indicates a pre and post delta-c (May 2014) calibration change.**
4. **VIIRS new products:**
   - **Enhanced spatial resolution - I and M band Sharpening**
   - **Diurnal changes in Color -- Blooms and Currents**
   - **Tested the cal val protocols.**
5. **VIIRS color Applications for Adaptive sampling and models validation**
6. **WavCIS Platform – maintained and updated with calibrated Seaprism Aug. 2015 !**

Plans:
Cruises - a) Cal Val Foster Gulf Stream, b) Gulf of Mexico Cruise – Plumes
Monitor Diurnal Changes.
Maintain - Operational WavCIS – Aeronet

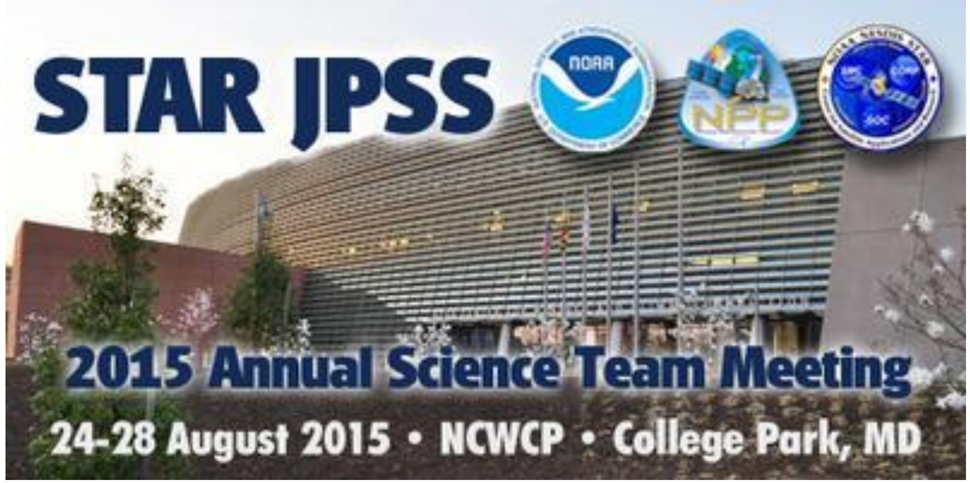

VIIRS Ocean Color Breakout
Thursday, 27 August 2015

Comparisons of Optical Validation Measurements from the November 2014 VIIRS Cal/Val Cruise

Michael Ondrusek, Bob Arnone, Zhongping Lee, Giuseppe Zibordi, Eric Stengel, Ryan Vandermeulen, Sherwin Ladner, Scott Freeman, Wesley Goode, Chuanmin Hu, David English, Charles Kovach, Jianwei Wei, Junfang Lin, Marco Talone, Alex Gilerson, Sam Ahmed, Amir Ibrahim, Ahmed El-Habashi, Robert Foster

Instruments used to measure Remote Sensing Reflectance

Profilers

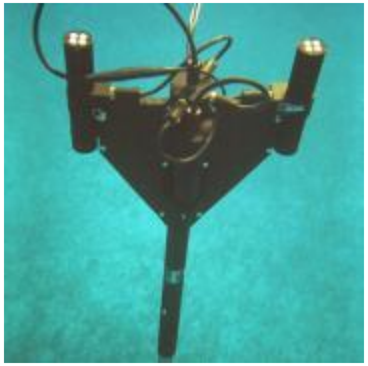

HyperPro (Satlantic) – free-falling hyperspectral optical profiler. 10 nm bands sampled every 3 nm. Radiance FOV 8.5 degrees. Calibrated from 350 to 800 nm.

MicroPro (Satlantic) - free-falling multispectral optical profiler. Seven spectral bands with 10 nm bandwidth centered at nominal wavelengths of 412 nm, 443 nm, 490 nm, 510 nm, 555 nm, 665 nm, and 683 nm. 18 degree FOV.

C-OPS (Biospherical Instruments, Inc.) – compact multispectral optical profiling system. a spectral range from 300 nm to 900 nm, with 19 wavebands wavelengths each: 305 nm, 320 nm, 340 nm, 380 nm, 395 nm, 412 nm, 443 nm, 465 nm, 490 nm, 510 nm, 532 nm, 555 nm, 565 nm, 625 nm, 665 nm, 683 nm, 710 nm, 780 nm, and 875 nm.

Instruments used to measure Remote Sensing Reflectance

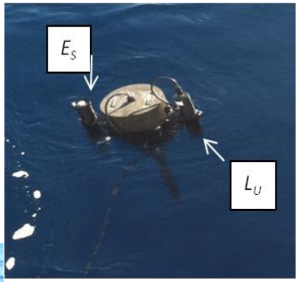

Surface

HyperTSRB (Satlantic) – Same instrument as hyperpro but collared to float at surface.

SBA (Satlantic) – Sky- Blocking Apparatus (SBA) radiometer package composed of one HyperOCR radiance sensor and one irradiance sensor. directly measures the water-leaving radiance Lw while blocking out sky-light (Lee et al., 2013).

Above-water

ASD Analytical Spectral Device (PANalytical) – Handheld 2 above-water spectrometer. Spectral range of 325 to 1075 nm. Spectral Resolution <3.0 nm, FOV 10 degrees. 2nd asd has 7 degrees FOV.

GER (Spectra Vista Corporation) – The GER 1500, Field Portable hand-held Spectroradiometer. Wavelengths from 350 nm to 1050 nm at 3 nm resolution with 4° nominal field of view (FOV).

HyperSAS (Satlantic) – Autonomous above-water OCR's with narrow FOV of 3 degrees. Also set up to measure polarization

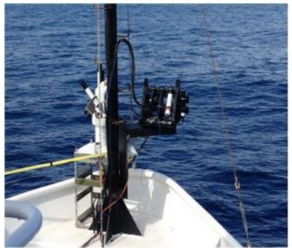
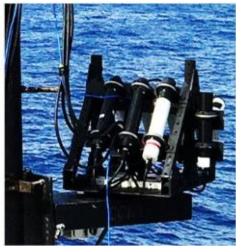

Pre- and Post-cruise inter-calibration of Satlantic irradiance Ed sensors used in Nov. 2014 Cal/Val cruise

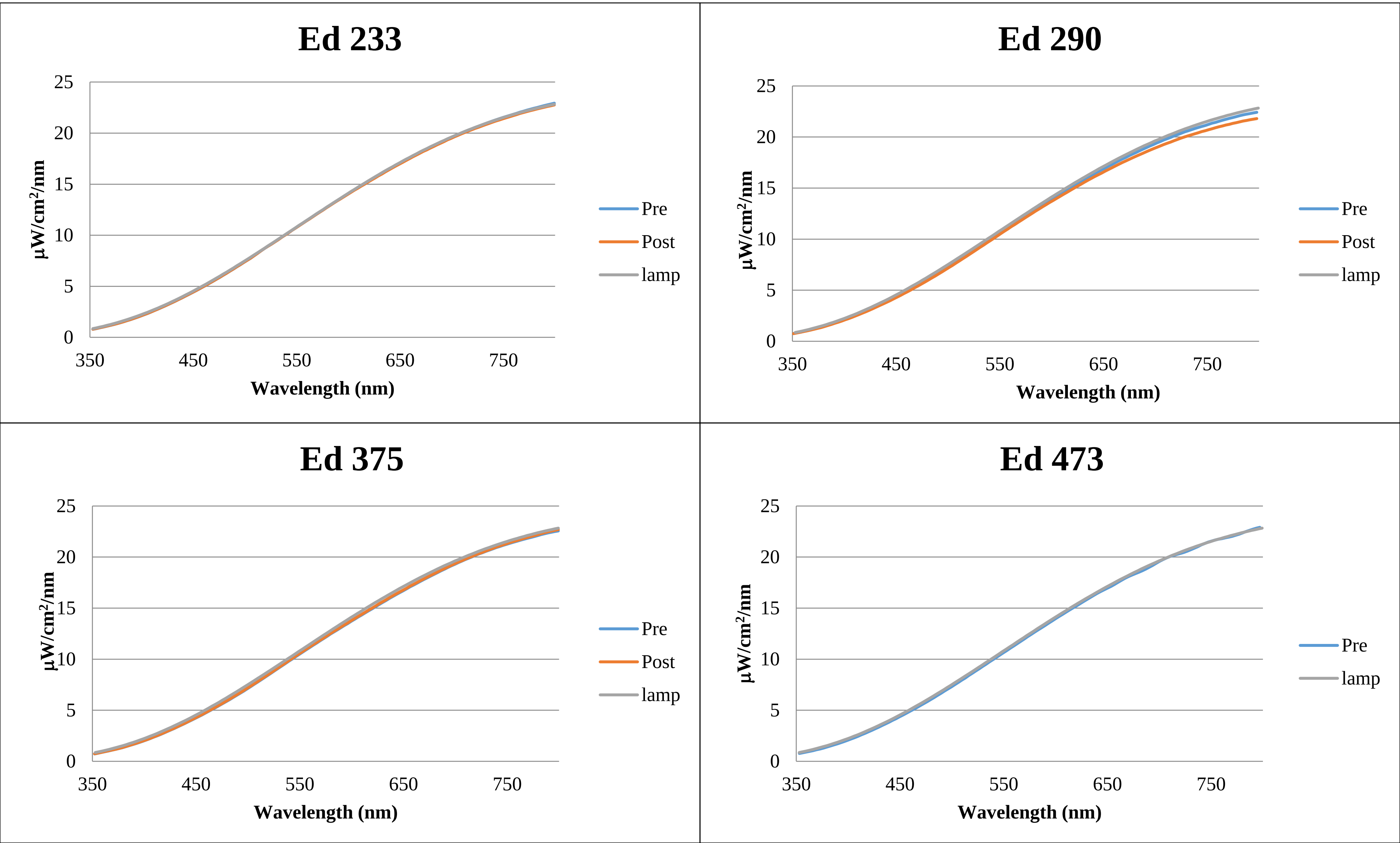

Pre- and Post-cruise inter-calibration of Satlantic radiance Lu sensors used in Nov. 2014 Cal/Val cruise

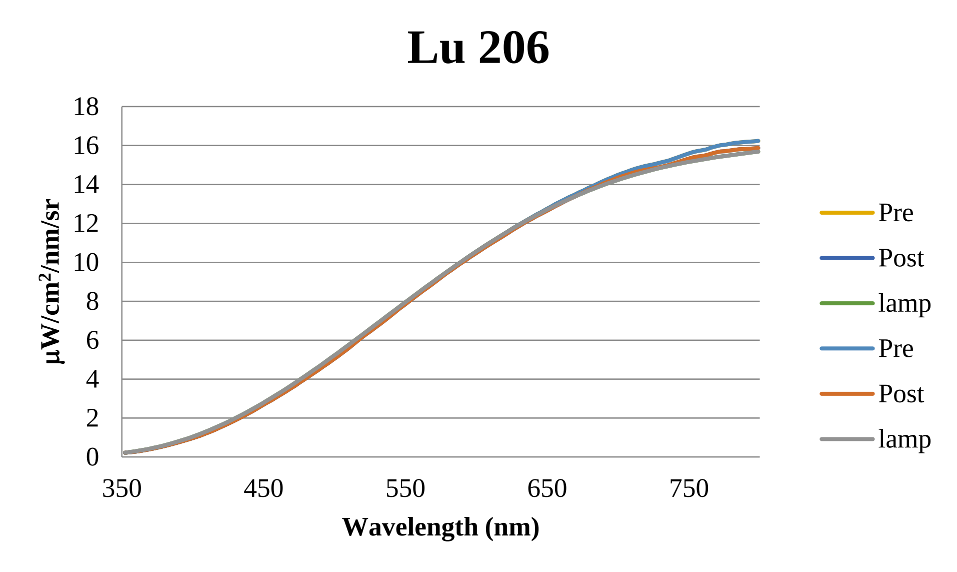

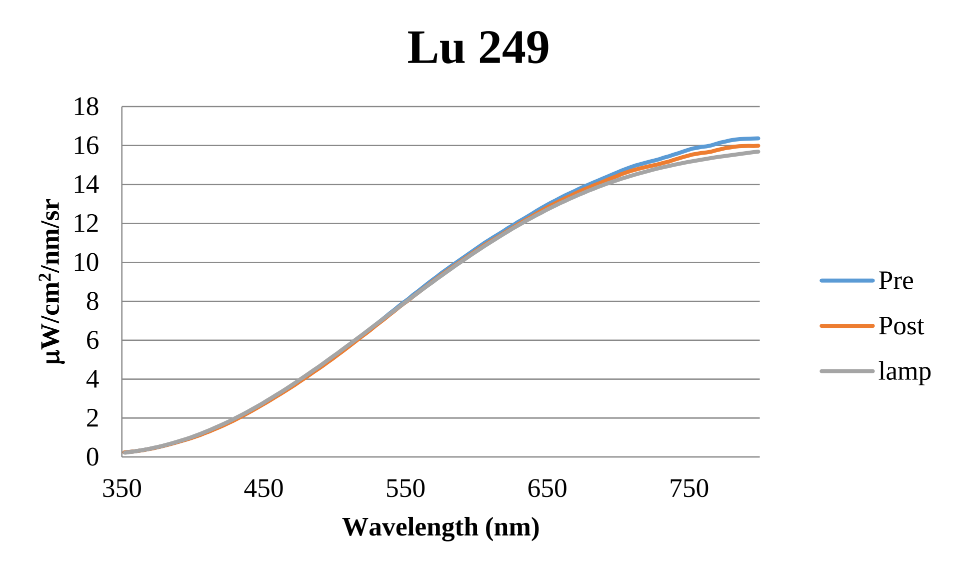

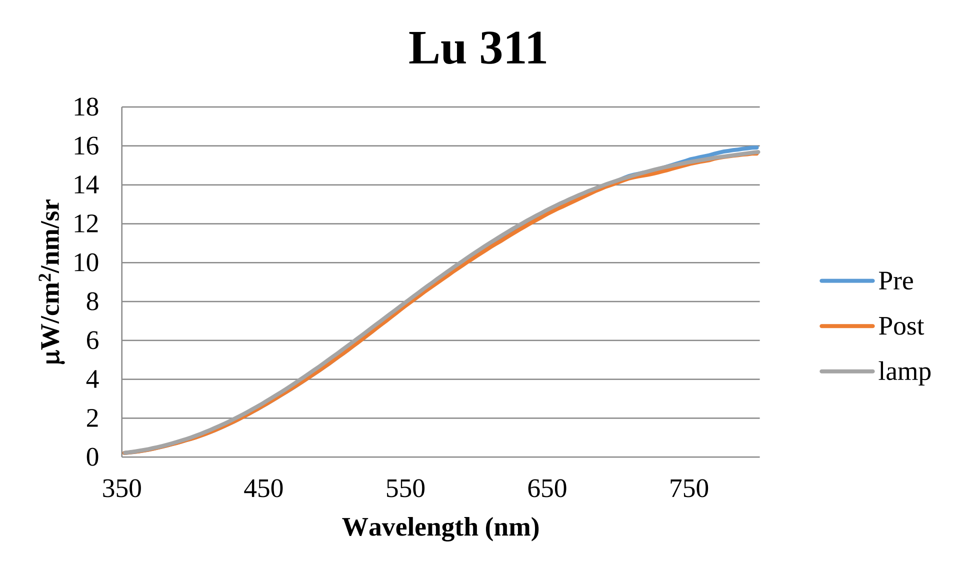

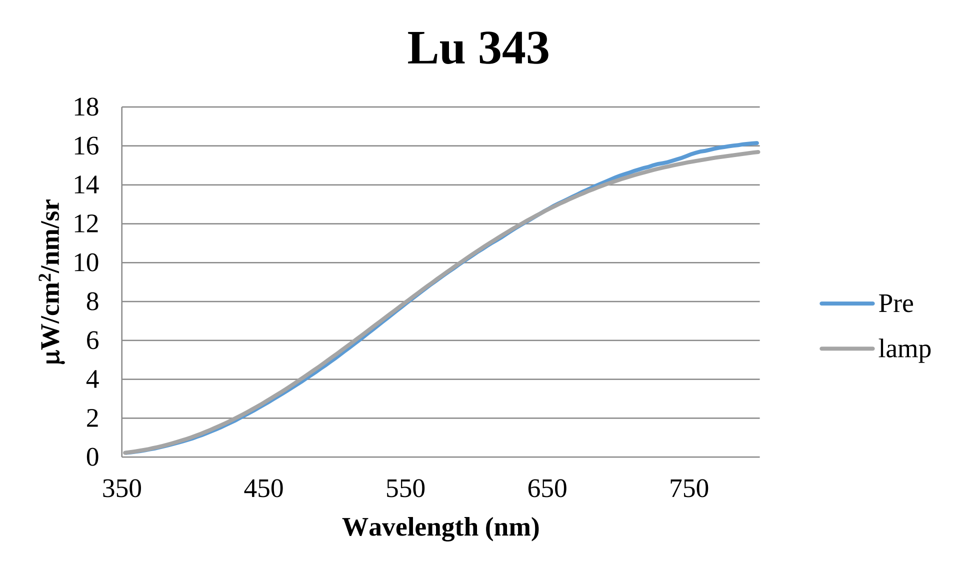

Pre- and Post-cruise inter-calibration of Satlantic irradiance Es sensors used in Nov. 2014 Cal/Val cruise

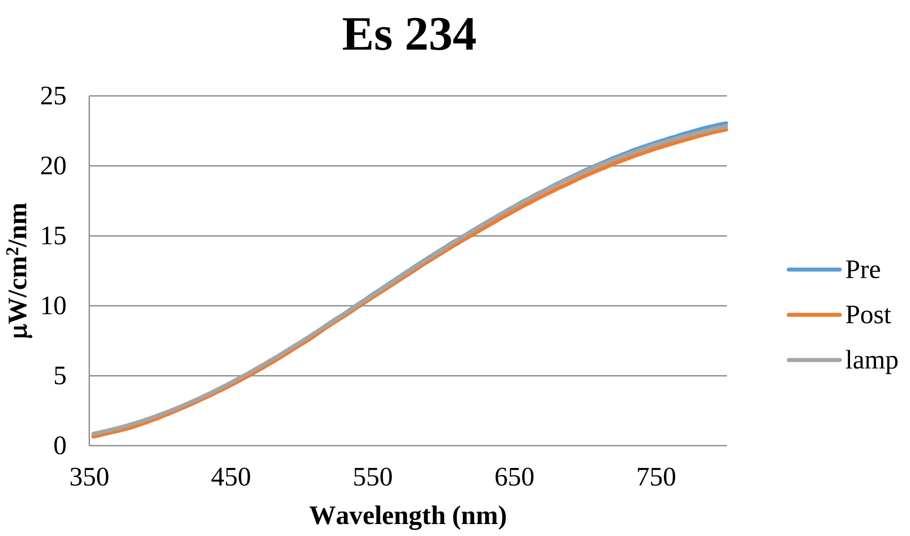

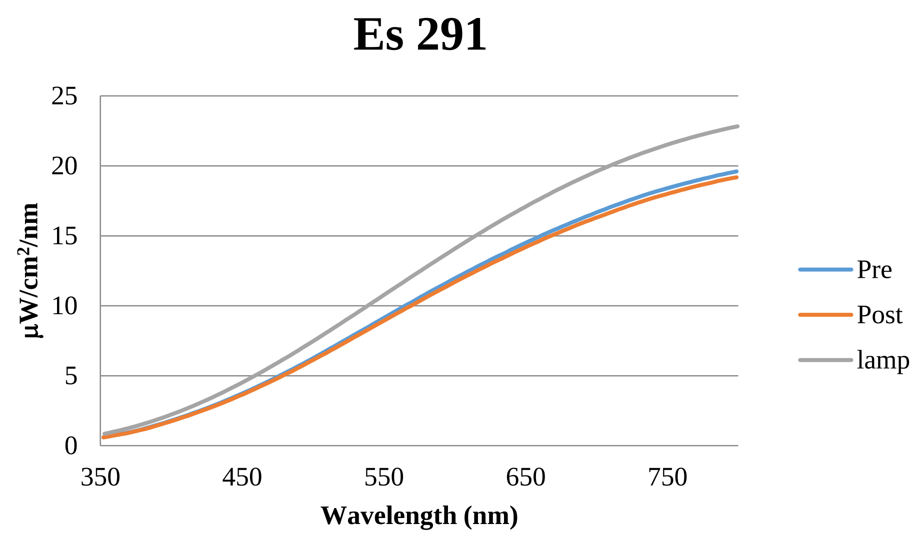

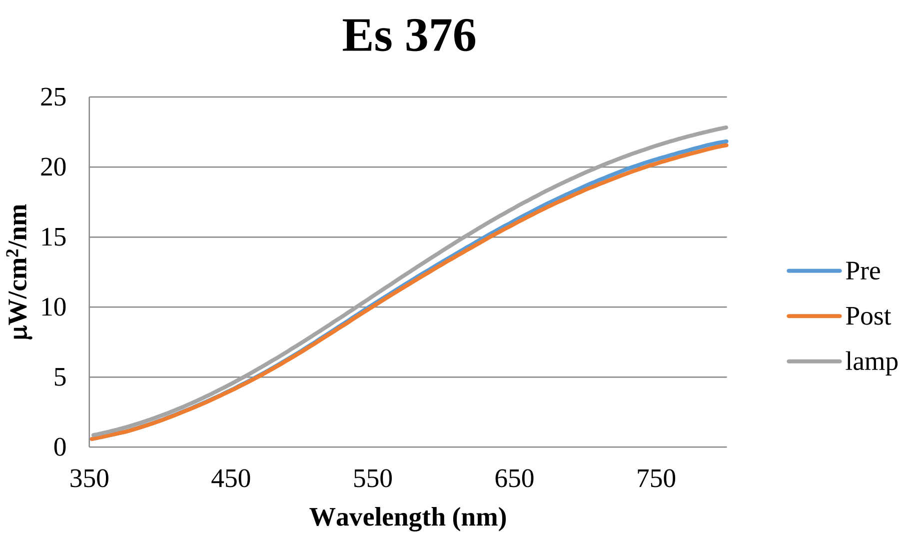

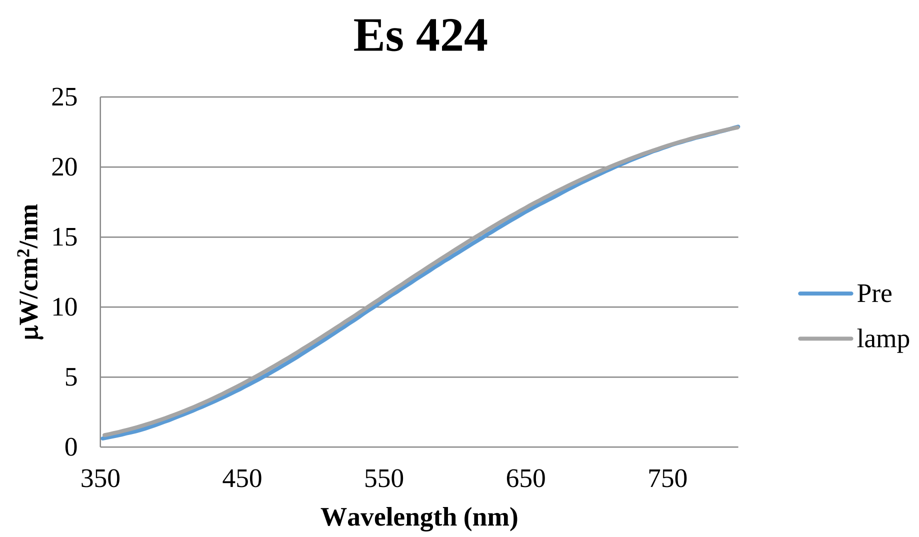

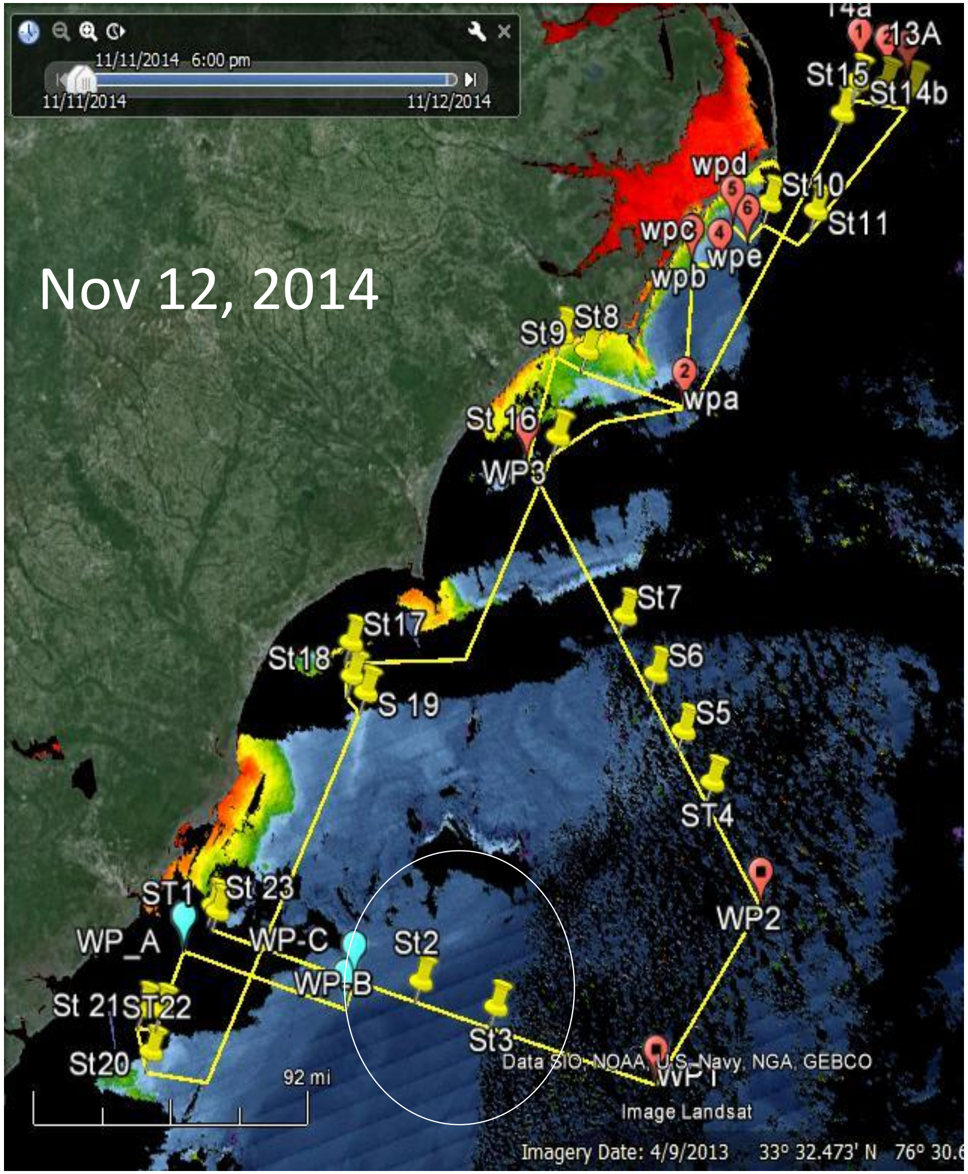

November 12, 2014 Blue water validations

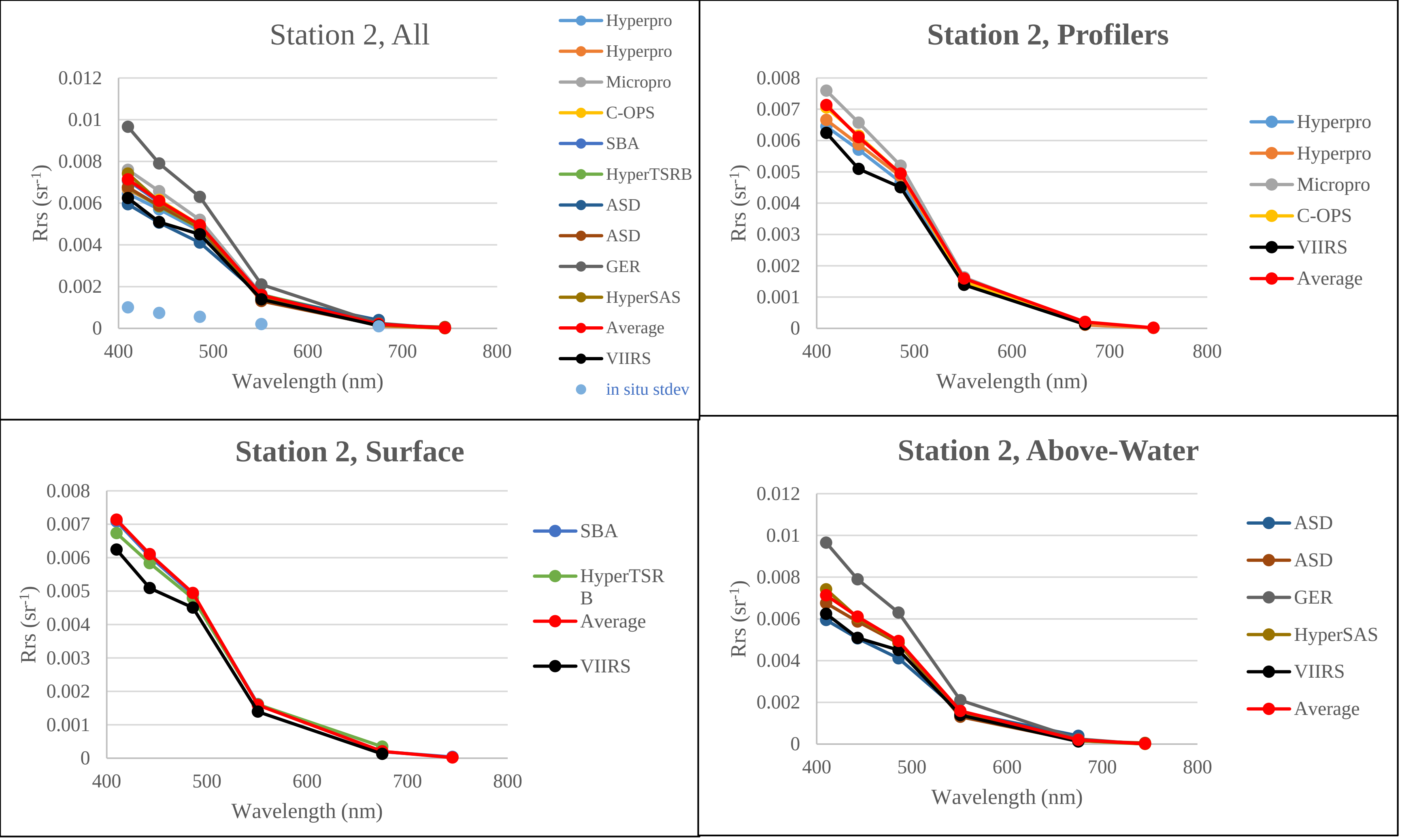

Date (Nov): **18th**
Description: **offshore shelf, Just west of Stream**
Above-Water time: **1000**
Surface time: **1030**
Profile time: **1200**
Depth (m): **103**
Cloud cover (%): **15**
Wind speed (kts): **10**
Seas (ft.): **2-4**
Chl (mg/m3) **0.24**

Percent difference relative to Average										
Band	Hyperpro	Hyperpro	Micropro	C-OPS	SBA	HyperTSRB	ASD	ASD	GER	HyperSAS
410	-9.61	-6.69	6.44	-1.10	-0.75	-5.62	-16.68	-5.30	35.33	3.97
443	-6.59	-3.81	7.61	0.79	-1.17	-4.45	-17.09	-3.84	29.34	-0.77
486	-5.51	-1.63	5.16	-0.06	-0.94	-3.20	-16.89	-2.25	27.39	-2.07
551	-5.49	-0.98	2.40	-6.91	1.65	1.02	-2.82	-17.83	32.30	-3.34
675	-38.69	-45.58	-25.35	-32.09	-2.83	69.76	94.66	-24.12	21.40	-17.18

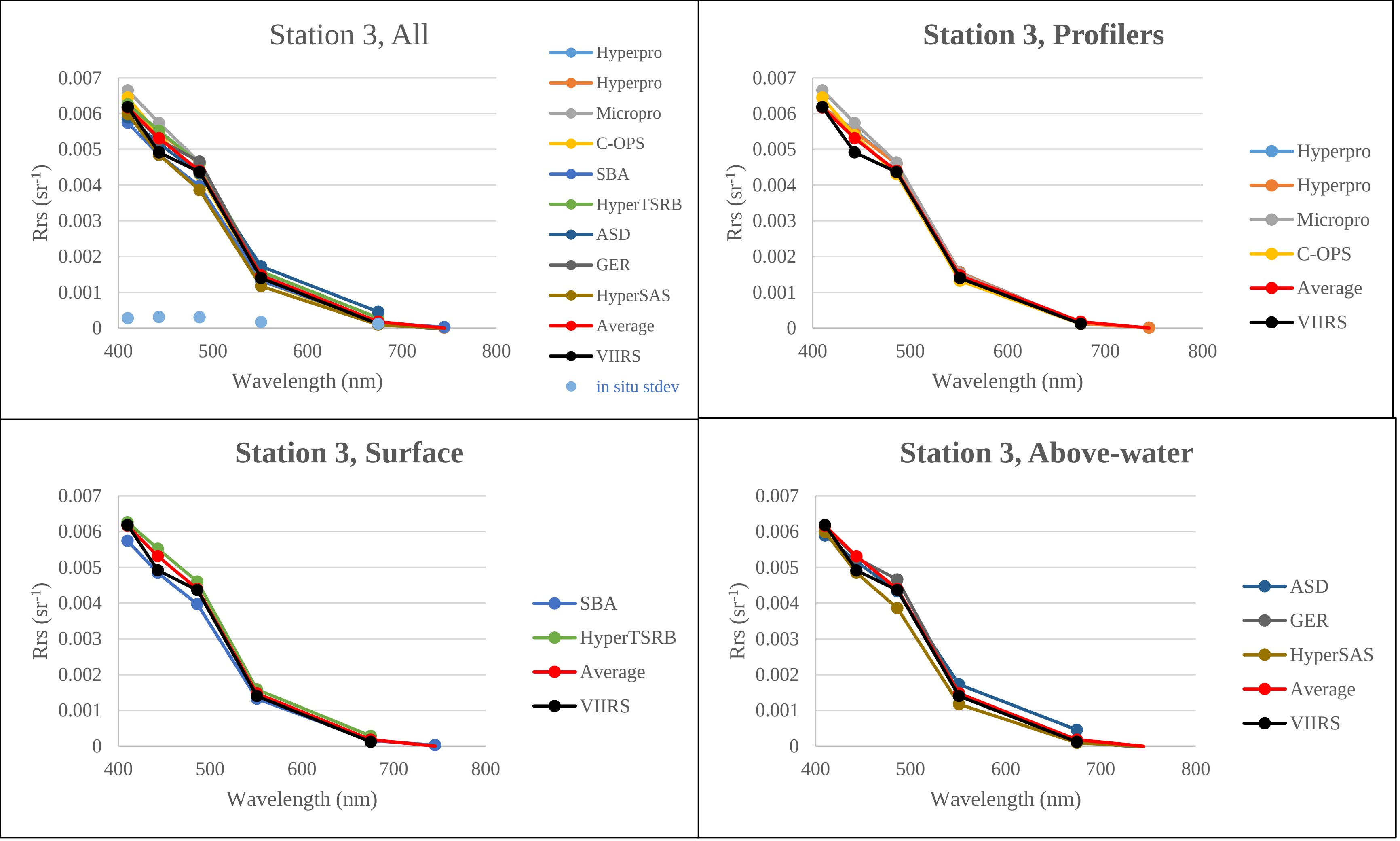

Date: 12
Description: Offshore,East of stream front
Above-Water time: 1435
Surface time: 1530
Profile time: 1445
Depth: 120
Cloud cover: 10
Wind speed: 10
Seas (ft.): 1-3
Chl (mg/m3) 0.23

Percent difference relative to Average										
Band	Hyperpro	Hyperpro	Micropro	C-OPS	SBA	HyperTSRB	ASD	ASD	GER	HyperSAS
410	0.40	0.26	7.82	4.56	-6.92	1.52	-4.51		-0.21	-2.92
443	4.09	3.37	8.08	1.52	-8.77	3.99	-2.76		-0.82	-8.70
486	4.53	4.57	5.44	-1.96	-9.64	4.70	-1.49		6.05	-12.20
551	6.12	5.54	3.47	-10.07	-10.05	7.51	17.27		0.69	-20.47
675	-23.07	-30.03	-24.94	-36.06	-13.55	57.23	152.43		-33.31	-48.69

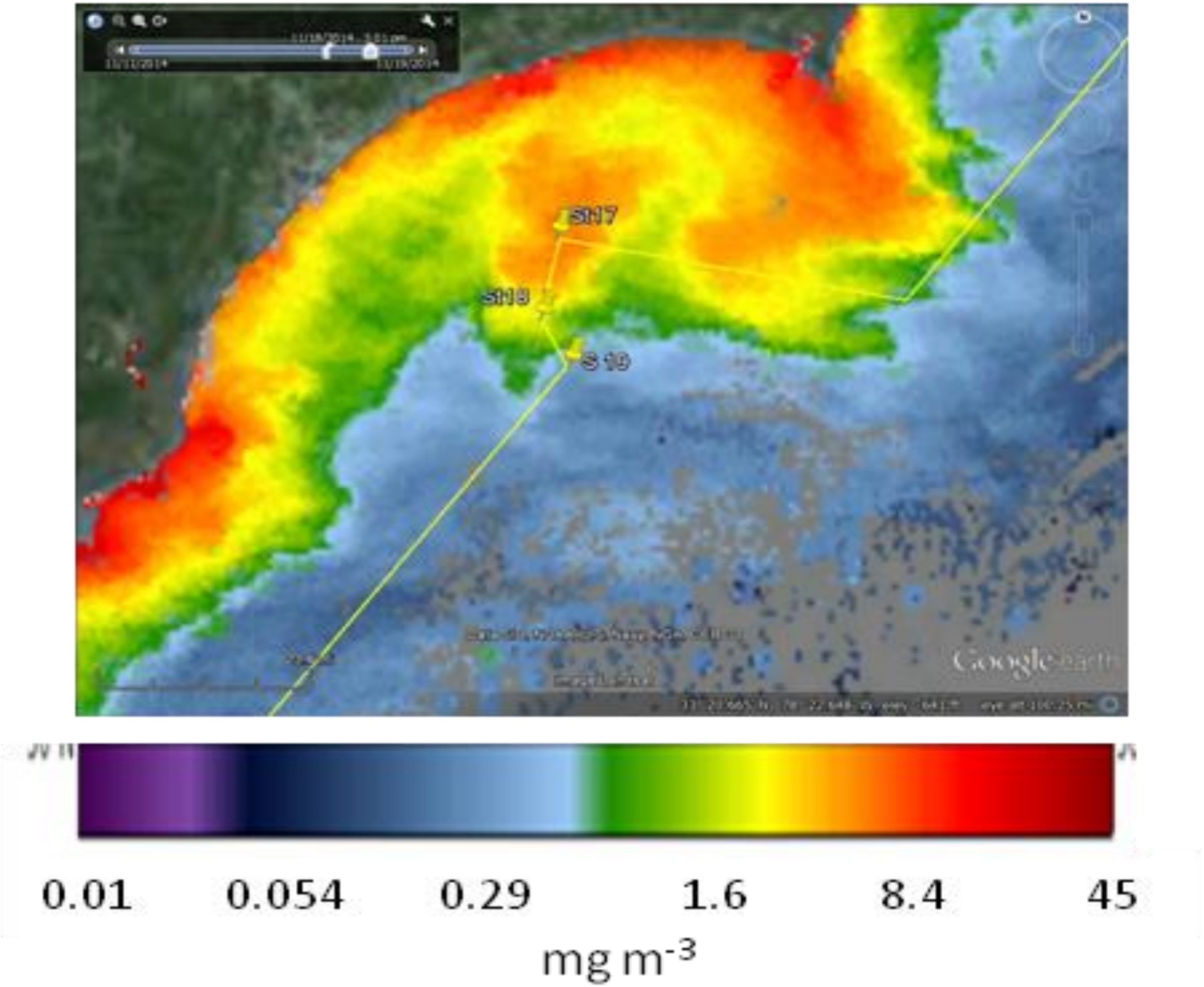

Locations of stations and track from 18 November with the VIIRS-NRL chlorophyll imagery

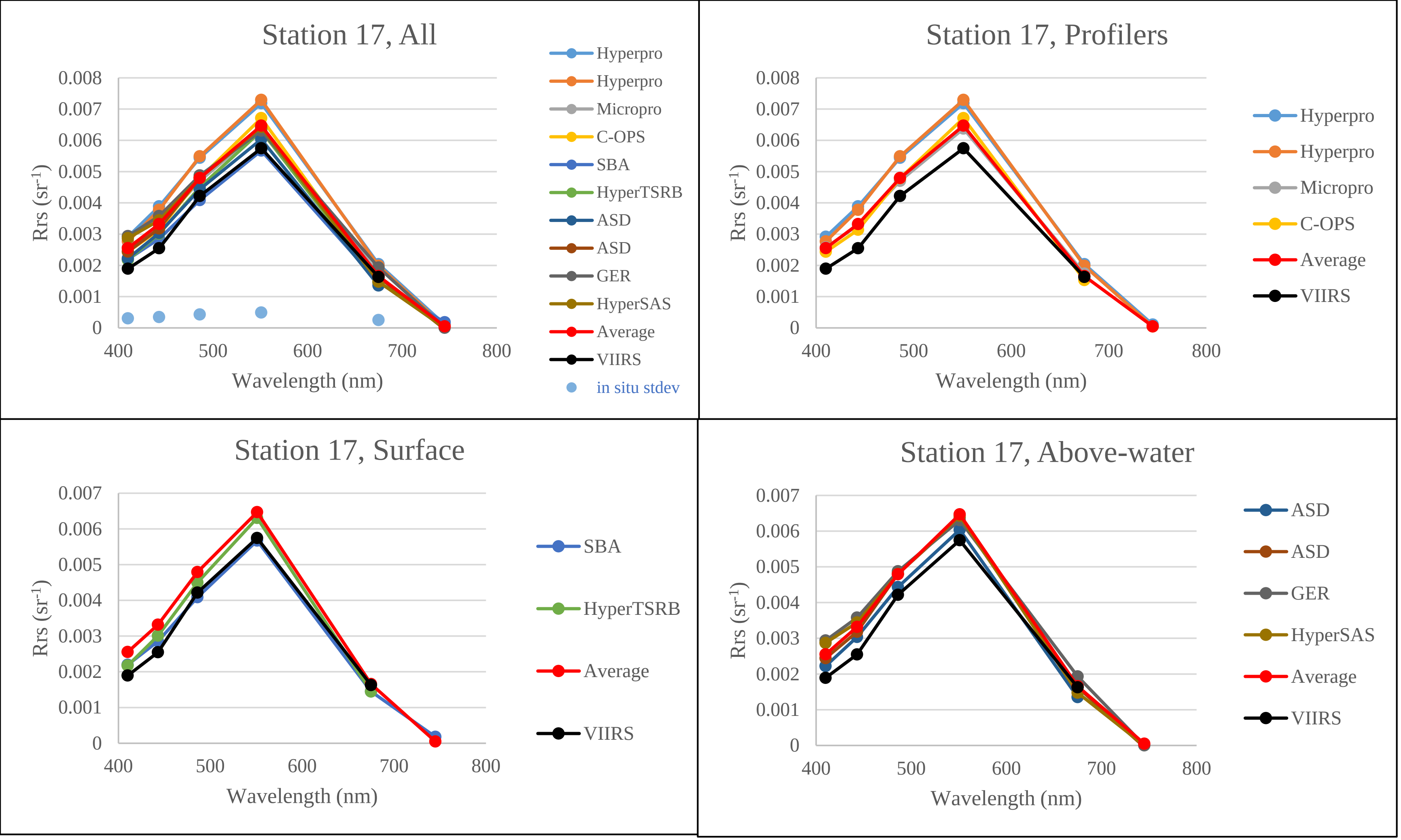

Date: 18
Description: Coastal, in bloom
Above-Water time: 1047
Surface time: 920
Profile time: 1005
Depth: 18
Cloud cover: 5
Wind speed: 18.5
Seas (ft.): 2-4
Chl (mg/m3) 6-8

Percent difference relative to Average

Band	Hyperpro	Hyperpro	Micropro	C-OPS	SBA	HyperTSRB	ASD	ASD	GER	HyperSAS
410	14.13	8.40	0.78	-4.57	-14.01	-14.85	-12.99	-4.38	15.07	12.41
443	17.17	13.77	-1.02	-5.42	-14.02	-9.26	-8.56	-4.15	7.79	3.70
486	13.49	14.58	-1.84	-0.04	-14.76	-6.10	-7.47	0.22	1.77	0.15
551	11.08	12.78	-1.47	3.71	-12.34	-2.52	-6.67	-1.46	-2.49	-0.63
675	23.04	19.76	4.70	-7.82	-12.48	-12.74	-18.37	-1.55	16.48	-11.03

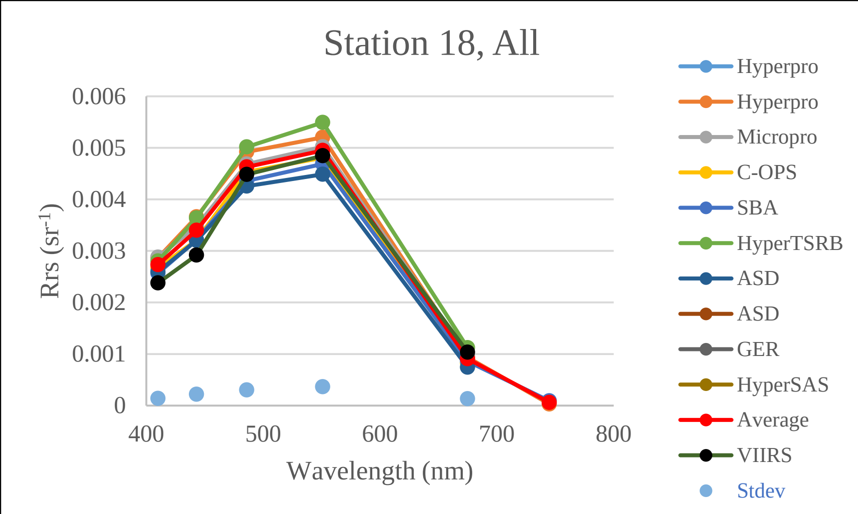

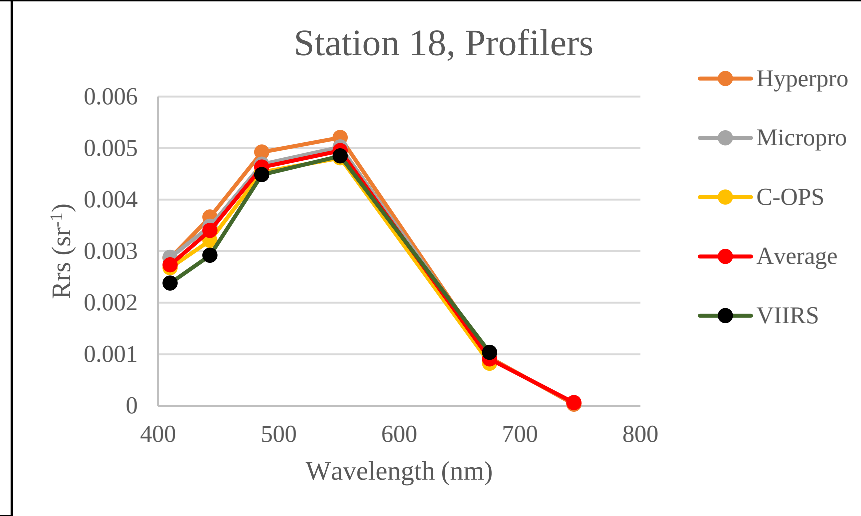

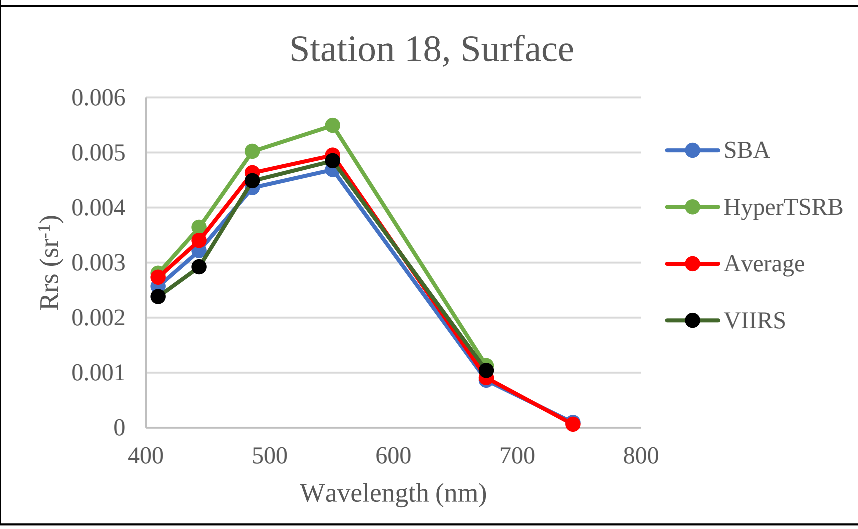

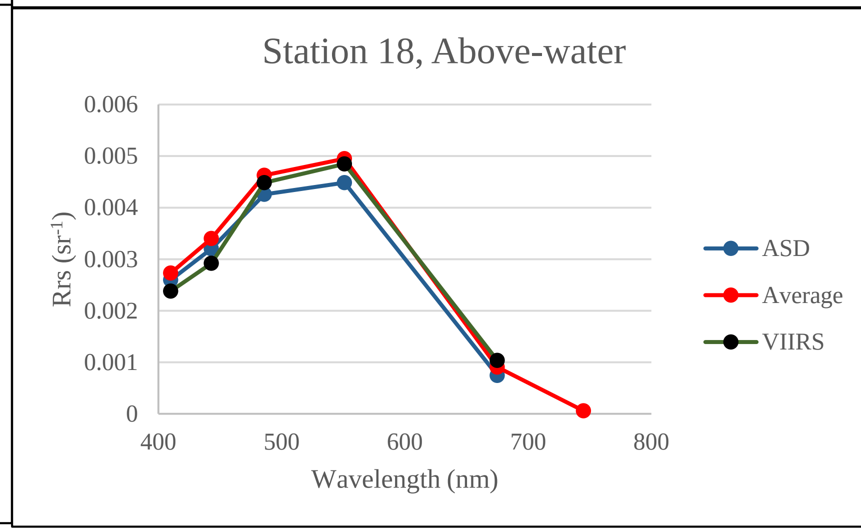

Date: 18
Description: Coastal, in bloom near front
Above-Water time: 1315
Surface time: 1240
Profile time: 1328
Depth: 22
Cloud cover: 5
Wind speed: 15
Seas (ft.): 2-4
Chl (mg/m3) 2.2

Percent difference relative to Average										
Band	Hyperpro	Hyperpro	Micropro	C-OPS	SBA	HyperTSRB	ASD	ASD	GER	HyperSAS
410		4.96	5.37	-2.01	-6.03	2.61	-4.91			
443		7.62	2.38	-5.68	-5.49	6.97	-5.80			
486		6.30	1.23	-2.09	-5.83	8.42	-8.02			
551		5.12	1.41	-2.85	-5.27	10.96	-9.37			
675		3.27	5.11	-9.01	-5.24	23.80	-17.92			

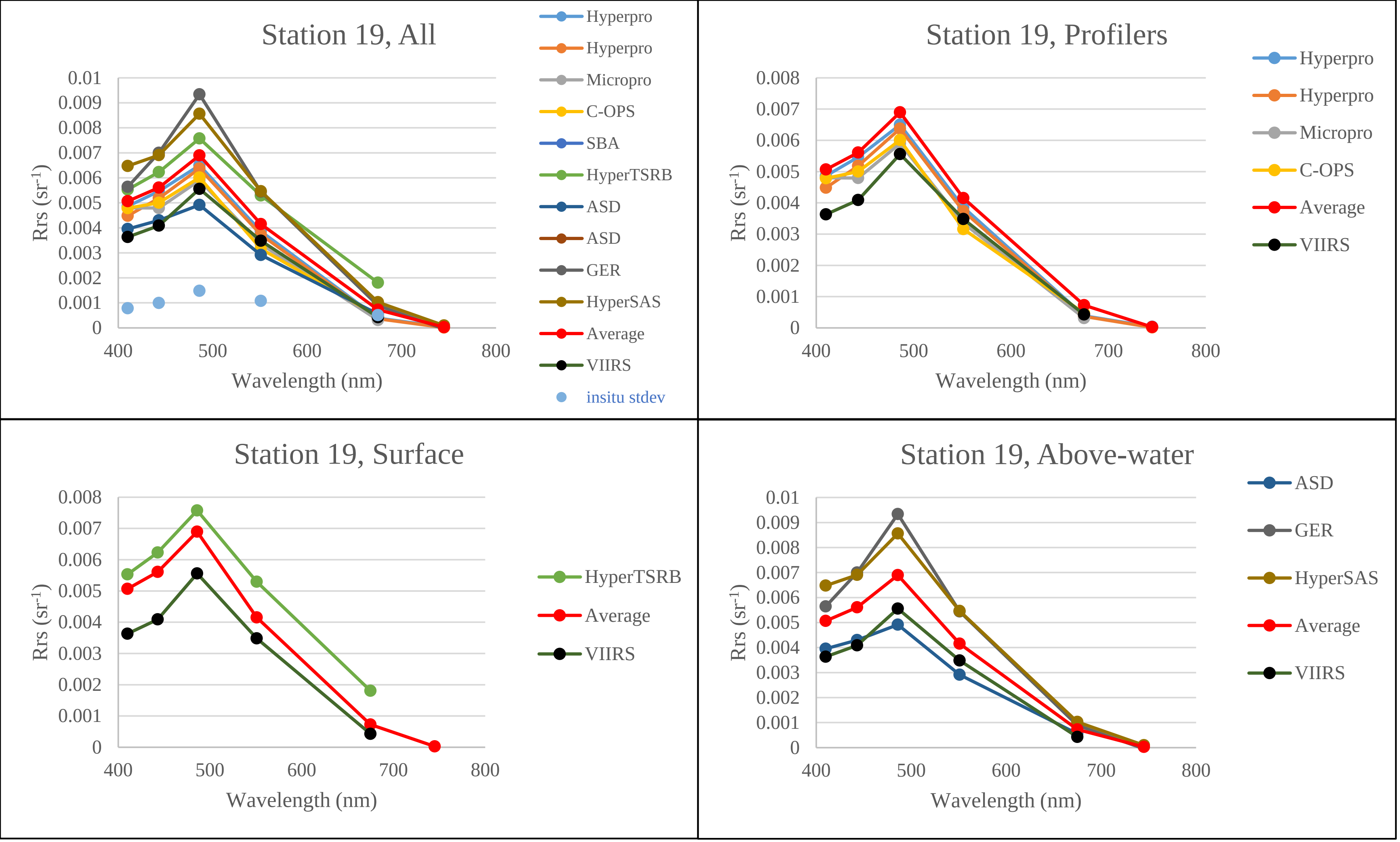

Date: 18
Description: Coastal, Clear side of front
Above-Water time: 1610
Surface time: 1645
Profile time: 1600
Depth: 26
Cloud cover: 35
Wind speed: 10
Seas (ft.): 2-3
Chl (mg/m3) 0.59

Percent difference relative to Average										
Band	Hyperpro	Hyperpro	Micropro	C-OPS	SBA	HyperTSRB	ASD	ASD	GER	HyperSAS
410	-3.99	-11.54	-5.21	-5.55		9.11	-21.97		11.35	27.78
443	-2.60	-7.59	-14.54	-10.85		11.02	-23.35		24.76	23.14
486	-5.77	-7.58	-14.49	-12.85		9.82	-28.70		35.40	24.17
551	-7.03	-10.21	-19.23	-23.88		27.48	-29.82		31.05	31.63
675	-46.65	-49.78	-57.18	-35.52		148.52	-23.56		22.70	41.48

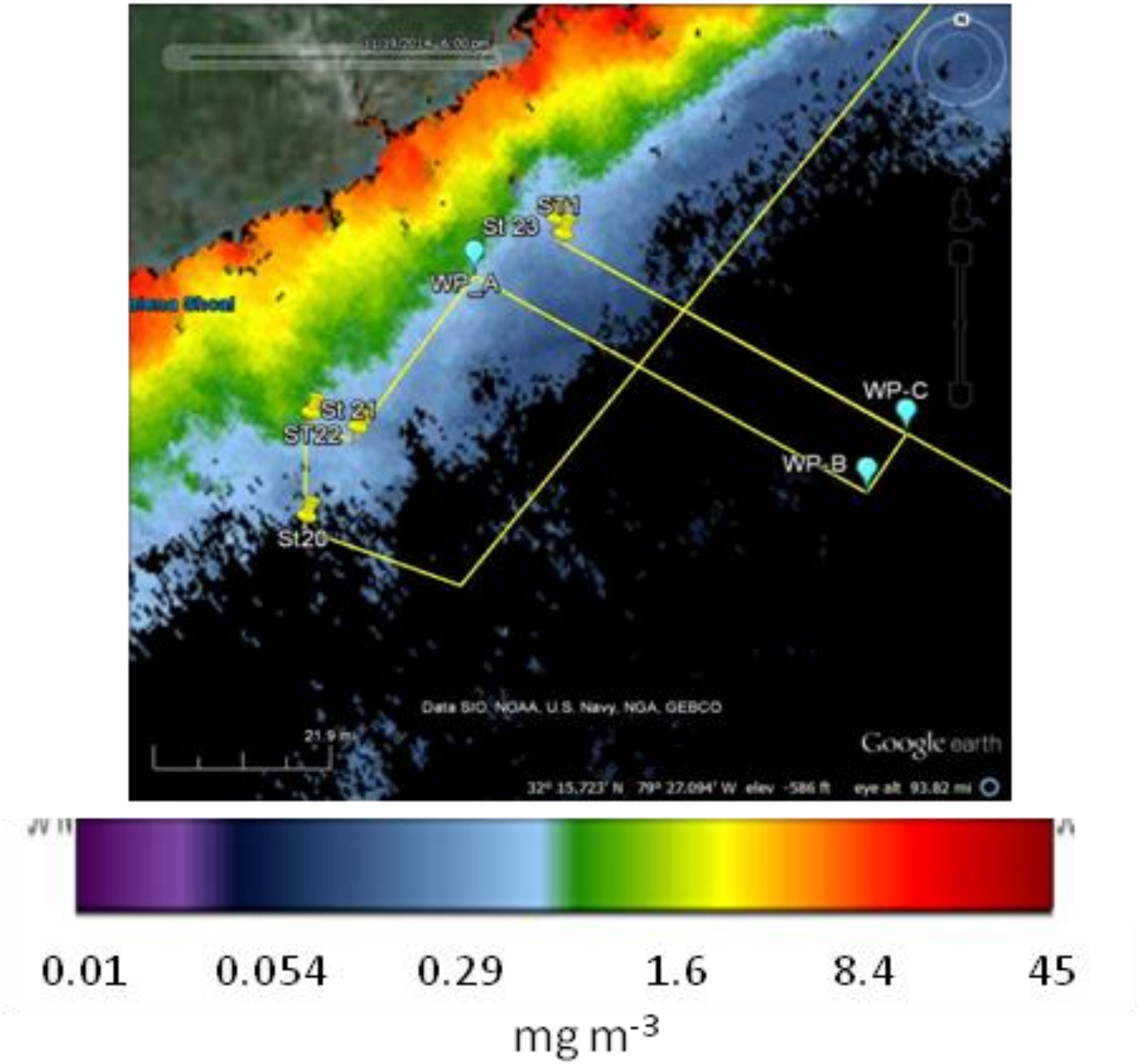

Locations of Stations 20, 21 and 22 on 19 November showing the transect of the shelf fronts with respect to chlorophyll image.

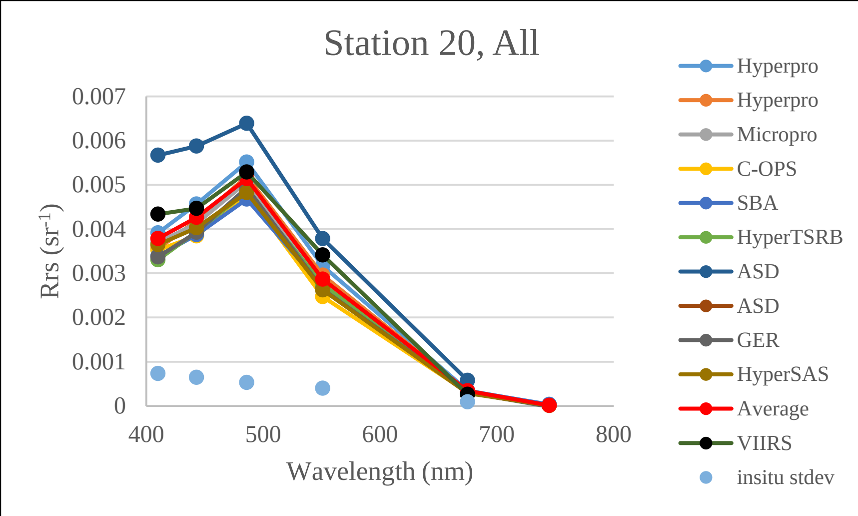

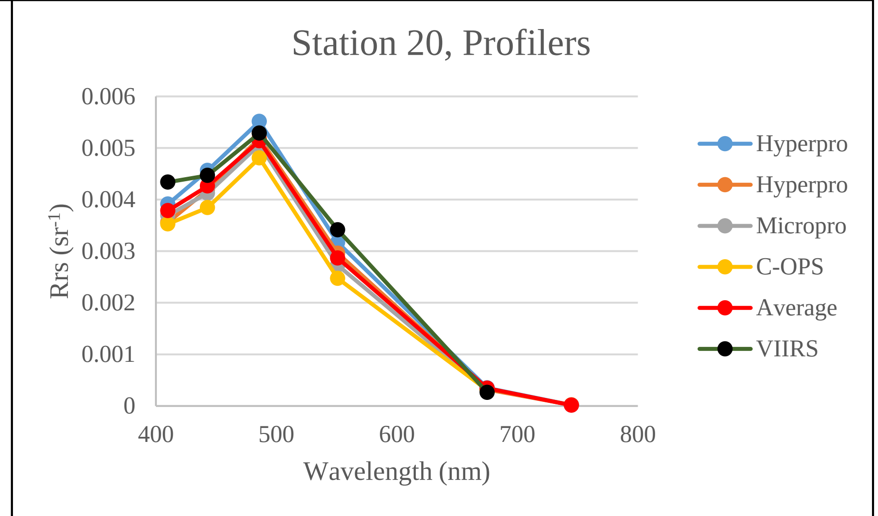

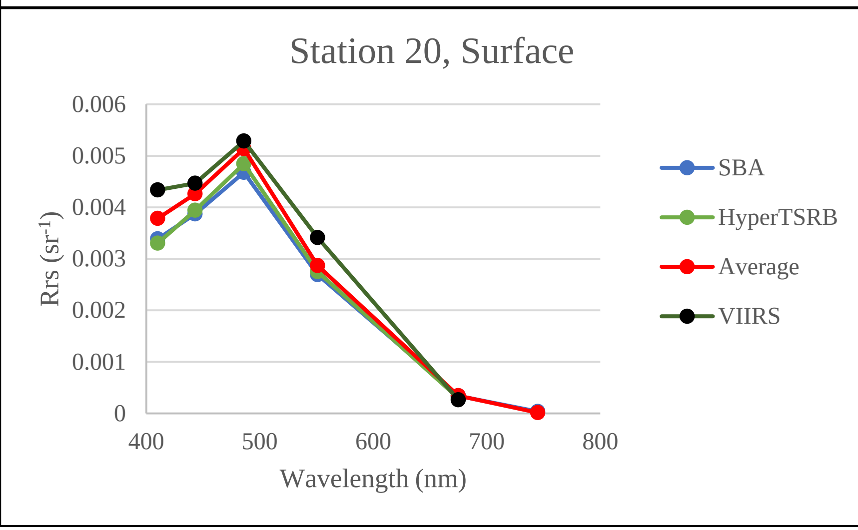

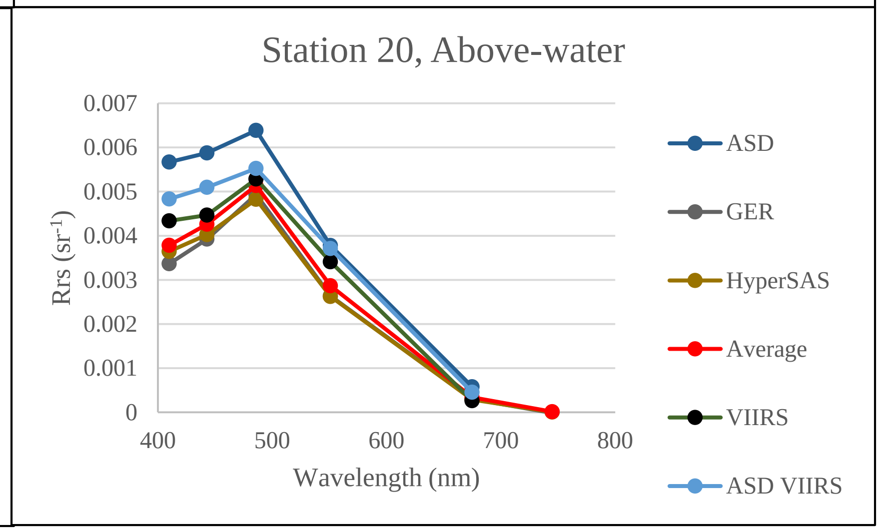

Date: 19
Description: South of Charleston, shelf
Above-Water time: 1026
Surface time: 930
Profile time: 1008
Depth: 24
Cloud cover: 40
Wind speed: 10.5
Seas (ft.): 1-2
Chl (mg/m3) 0.54

Percent difference relative to Average										
Band	Hyperpro	Hyperpro	Micropro	C-OPS	SBA	HyperTSRB	ASD	ASD	GER	HyperSAS
410	3.38	-6.01	-2.38	-6.83	-10.49	-12.74	49.75		-11.04	-3.65
443	7.09	-1.70	-3.25	-9.83	-9.16	-7.53	37.85		-7.92	-5.55
486	7.29	1.02	-1.44	-6.47	-8.97	-5.70	24.32		-3.98	-6.07
551	10.46	3.15	-4.95	-13.83	-6.08	-4.04	31.84		-8.03	-8.51
675	2.41	-7.16	-12.94	-10.93	-0.91	-13.52	69.38		-10.70	-15.63

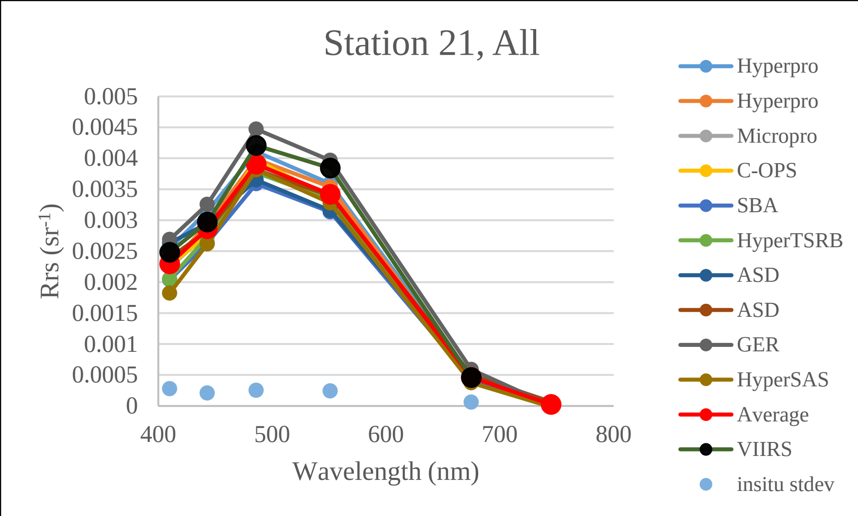

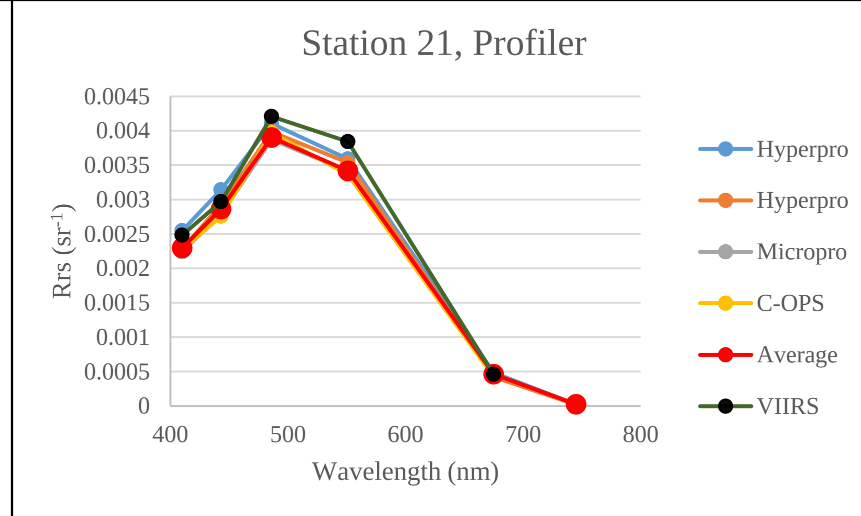

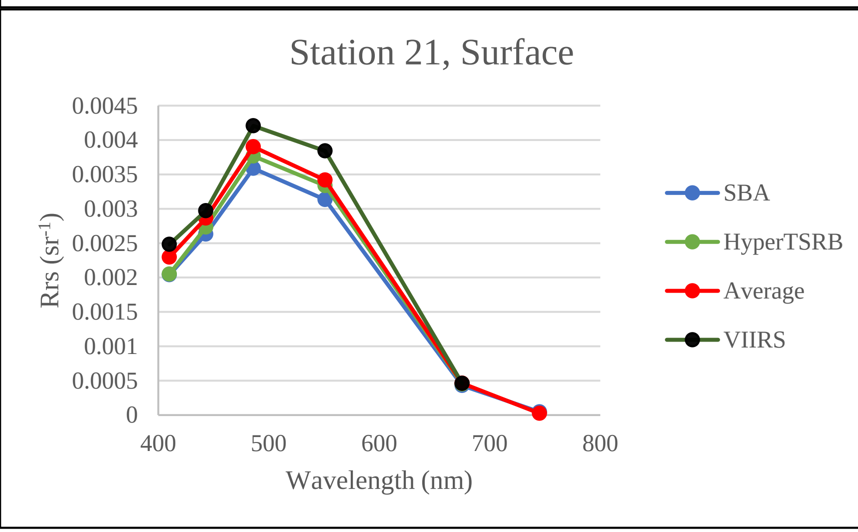

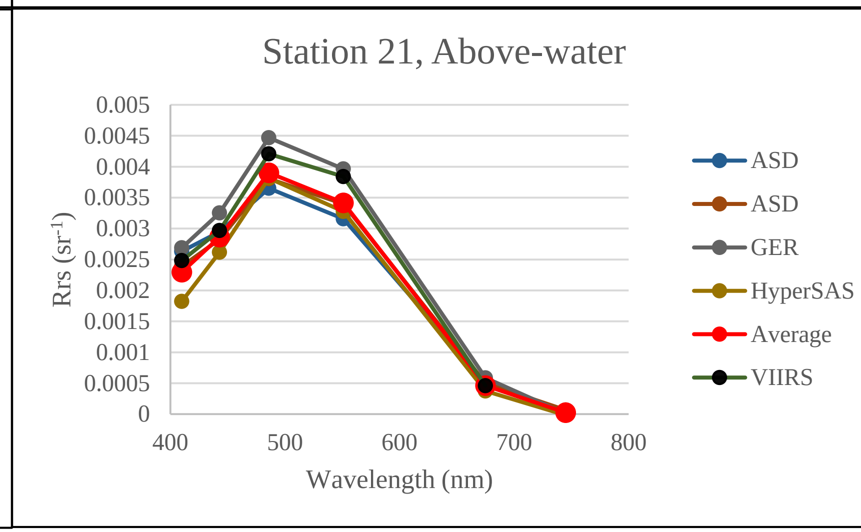

Date: 19
Description: South of Charleston, shelf
Above-Water time: 1301
Surface time: 1255
Profile time: 1305
Depth: 18
Cloud cover: 0
Wind speed: 9
Seas (ft.): 1
Chl (mg/m3) 0.95

Percent difference relative to Average

Band	Hyperpro	Hyperpro	Micropro	C-OPS	SBA	HyperTSRB	ASD	ASD	GER	HyperSAS
410	10.91	-0.61	-2.46	-1.17	-11.17	-10.75	14.65	4.11	17.13	-20.65
443	9.77	2.22	-2.57	-3.66	-8.10	-4.51	3.03	-1.28	13.68	-8.59
486	5.18	2.06	-0.78	1.72	-8.08	-3.50	-6.45	-2.44	14.54	-2.25
551	5.07	3.49	-0.02	-1.59	-8.33	-2.39	-7.61	-0.57	16.03	-4.08
675	4.44	-9.16	-3.87	-7.84	-7.19	-2.63	10.07	7.90	27.23	-18.93

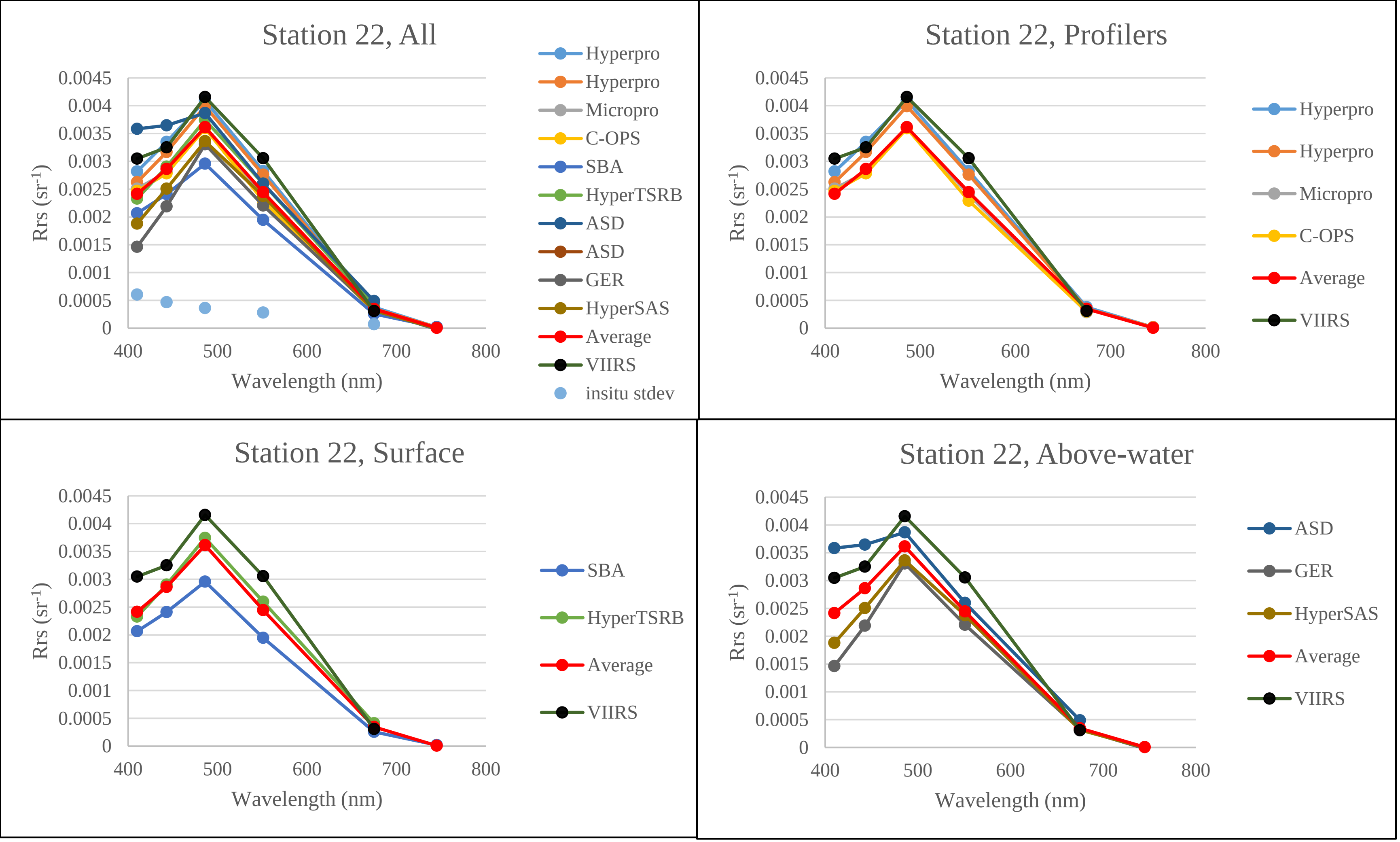

Date: 19
Description: South of Charleston, shelf
Above-Water time: 1520
Surface time: 1555
Profile time: 1520
Depth: 26
Cloud cover: 0
Wind speed: 4
Seas (ft.): 1
Chl (mg/m3) 0.62

Percent difference relative to Average										
Band	Hyperpro	Hyperpro	Micropro	C-OPS	SBA	HyperTSRB	ASD	ASD	GER	HyperSAS
410	16.63	8.63	3.86	2.14	-14.47	-3.60	48.41		-39.39	-22.21
443	17.01	10.65	-1.96	-2.82	-15.82	1.48	27.39		-23.51	-12.41
486	13.18	10.43	-0.02	-0.58	-18.20	3.63	7.04		-8.50	-6.98
551	15.55	12.83	-1.66	-6.25	-20.38	6.17	6.28		-9.81	-2.73
675	9.16	1.46	-16.96	-13.56	-25.67	18.79	41.11		-5.57	-8.75

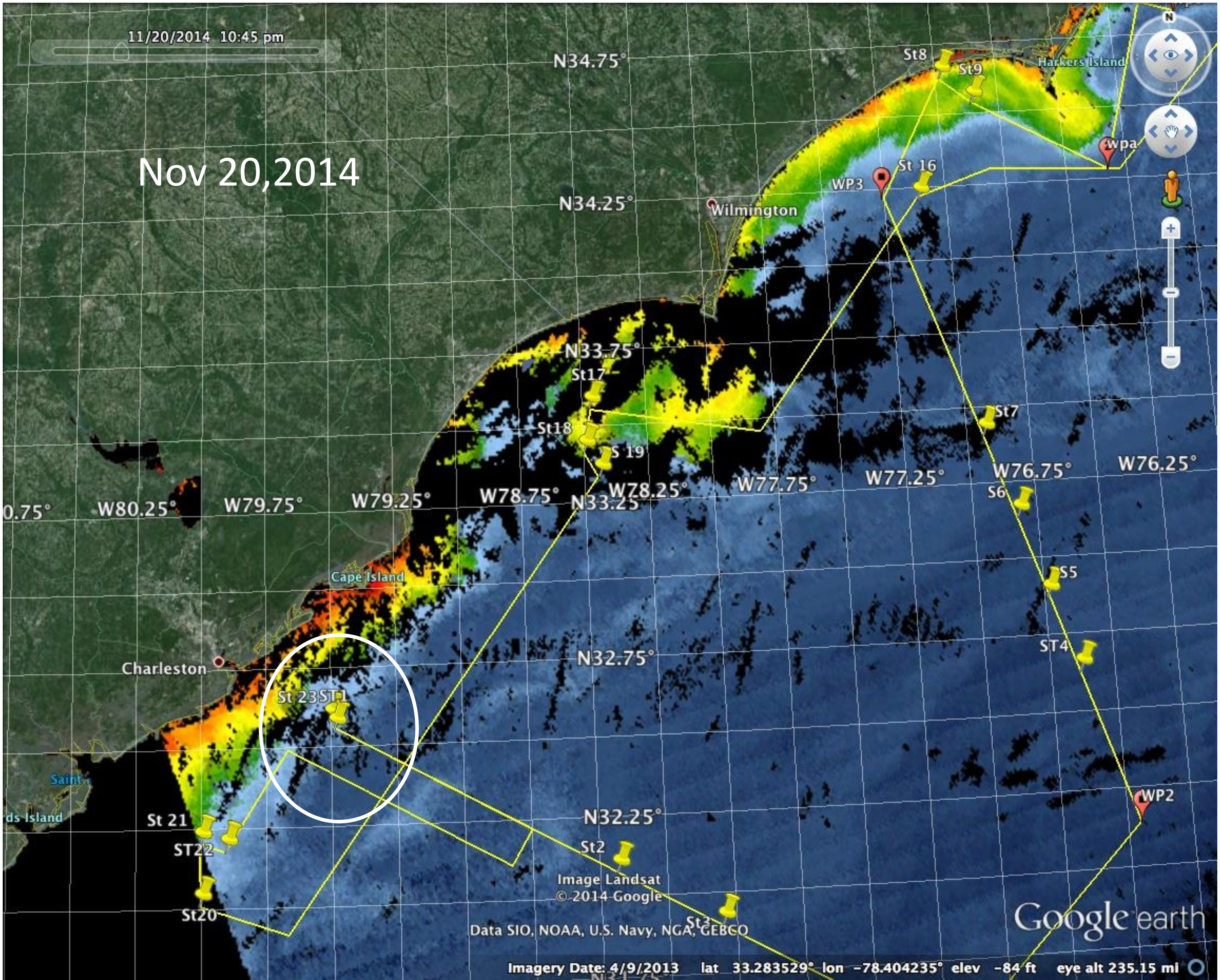
11/20/2014 10:45 pm
Nov 20,2014
N34.75°
N34.25°
N33.75°
N33.25°
N32.75°
N32.25°
0.75°
W80.25°
W79.75°
W79.25°
W78.75°
W78.25°
W77.75°
W77.25°
W76.75°
W76.25°
Wilmington
Harkers Island
Cape Island
Charleston
Saint
ds Island
St8
St9
wpa
WP3
St 16
St17
St18
S 19
St7
S6
S5
ST4
WP2
St 23
ST1
St 21
ST22
St20
St2
St3
Image Landsat
© 2014 Google
Data SIO, NOAA, U.S. Navy, NGA, GEBCO
Google earth
Imagery Date: 4/9/2013 lat 33.283529° lon -78.404235° elev -84 ft eye alt 235.15 mi

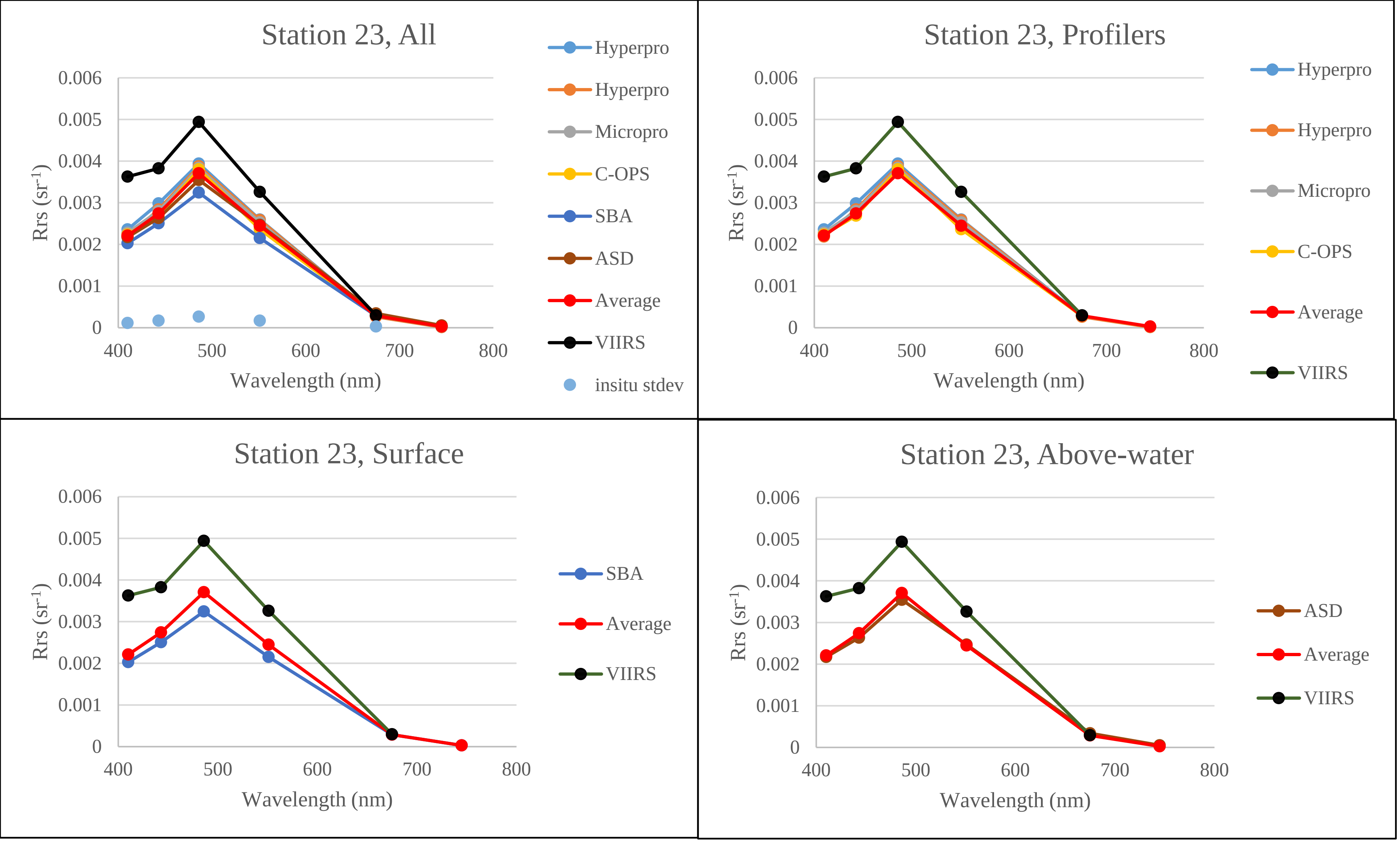

Date: 20
Description: **Charleston Sea Buoy**
Above-Water time:950
Surface time: 825
Profile time: 900
Depth: 19
Cloud cover: 0
Wind speed: 16
Seas (ft.): 1-2
Chl (mg/m3) 0.5

Percent difference relative to Average										
Band	Hyperpro	Hyperpro	Micropro	C-OPS	SBA	HyperTSRB	ASD	ASD	GER	HyperSAS
410	6.76	-1.13	3.17	1.14	-8.24			-1.70		
443	8.81	3.53	2.16	-1.90	-8.66			-3.94		
486	6.25	4.50	3.43	2.64	-12.45			-4.37		
551	6.02	5.56	3.27	-3.54	-12.16			0.84		
675	-4.10	-8.97	-2.75	-2.20	-0.70			18.72		

Instrument Percent difference relative to average of all instruments

Band	Hyperpro	Hyperpro	Micropro	C-OPS	SBA	HyperTSRB	ASD	ASD	GER	HyperSAS
410	4.83	-0.41	1.93	-1.49	-9.01	-4.29	6.47	-1.82	4.04	-0.75
443	6.84	3.12	-0.35	-4.21	-8.90	-0.28	1.34	-3.30	6.19	-1.31
486	4.83	3.81	-0.37	-2.19	-9.86	1.01	-4.71	-2.21	10.38	-0.75
551	5.22	4.14	-1.86	-7.24	-9.12	5.52	-0.11	-4.75	8.53	-1.16
675	-9.18	-14.02	-14.91	-17.22	-8.57	36.15	38.47	0.24	5.46	-11.25
All	2.51	-0.67	-3.11	-6.47	-9.09	7.62	8.29	-2.37	6.92	-3.04

MSL12 VIIRS Percent difference relative to in situ (with Sta 23)

Band	Hyperpro	Hyperpro	Micropro	C-OPS	SBA	HyperTSRB	ASD	ASD	GER	HyperSAS	Average
410	0.82	4.34	1.76	5.01	18.87	1.57	-8.17	10.18	3.33	3.85	**3.75**
443	-7.99	-5.81	-2.57	1.19	10.21	-7.42	-8.53	4.25	-8.44	-3.90	**-3.01**
486	-2.51	-2.01	1.93	3.71	16.39	-2.84	3.67	7.71	-8.83	0.35	**1.65**
551	0.07	0.49	6.81	13.31	19.27	-2.89	2.89	10.40	-2.82	5.52	**4.72**
675	-8.22	1.01	1.54	2.05	-2.53	-28.45	-25.91	-10.19	-22.89	-4.94	**-14.87**
All	-3.57	-0.40	1.89	5.05	12.44	-8.01	-7.21	4.47	-7.93	0.18	**-1.55**

MSL12 VIIRS Percent difference relative to in situ without (Sta. 23)

Band	Hyperpro	Hyperpro	Micropro	C-OPS	SBA	HyperTSRB	ASD	ASD	GER	HyperSAS	Average
410	-6.73	-3.36	-5.39	-2.15	10.31	1.57	-8.17	-8.73	3.33	3.85	**-3.79**
443	-13.15	-10.87	-7.45	-3.93	4.15	-7.42	-8.53	-9.38	-8.44	-3.90	**-8.31**
486	-6.49	-5.70	-1.44	0.45	11.28	-2.84	3.67	-2.83	-8.83	0.35	**-2.30**
551	-3.58	-2.71	4.05	10.21	14.65	-2.89	2.89	3.18	-2.82	5.52	**1.17**
675	-10.37	-0.44	1.06	1.70	-3.34	-28.45	-25.91	-9.02	-22.89	-4.94	**-17.04**
All	-8.07	-4.62	-1.83	1.26	7.41	-8.01	-7.21	-5.36	-7.93	0.18	**-6.05**

MSL12 VIIRS 5x5 avg vs avg of all Rrs measurements

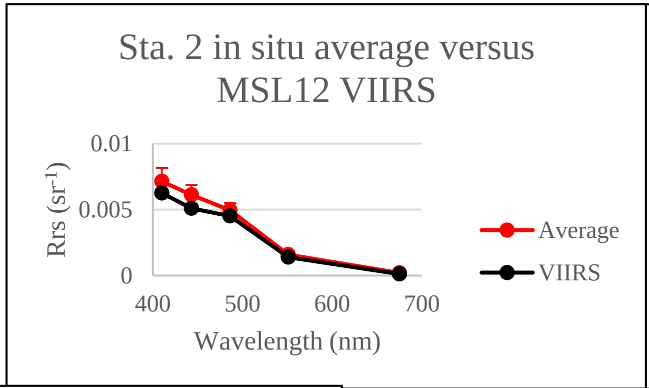

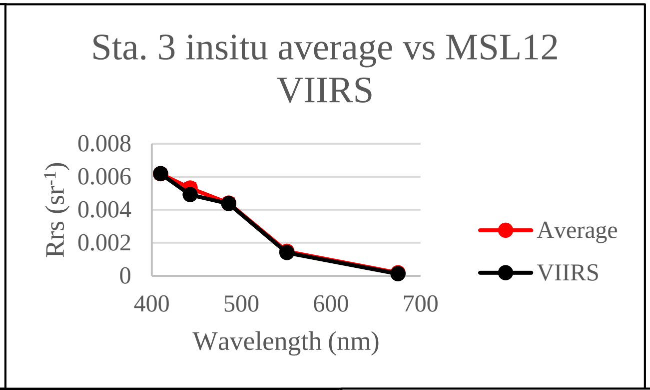

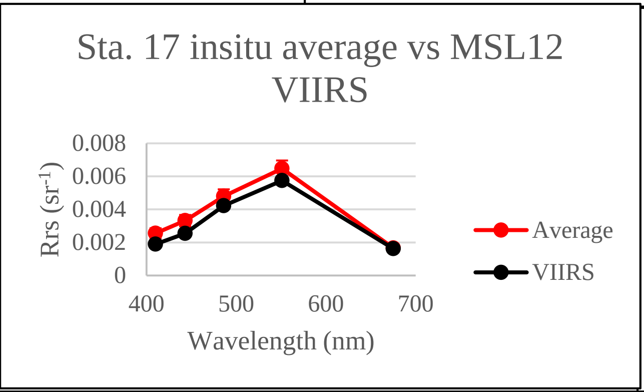

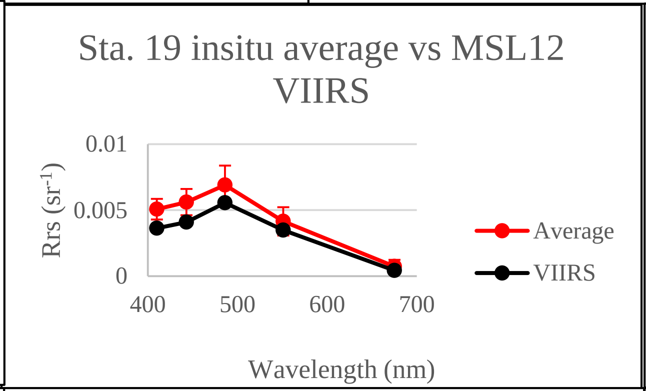

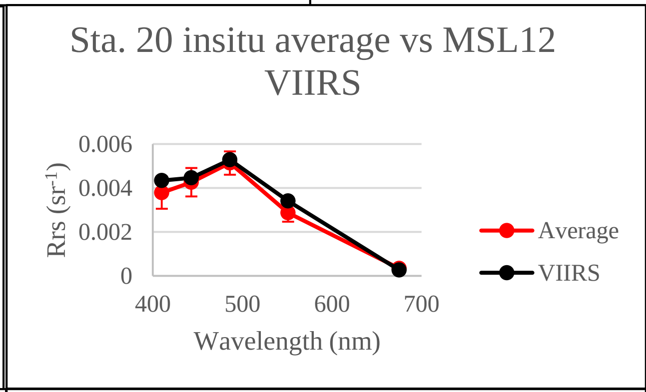

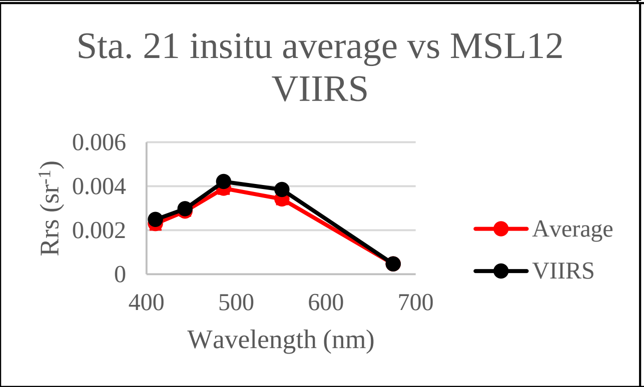

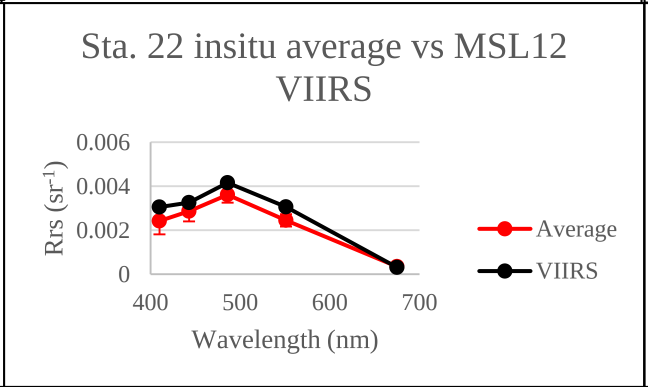

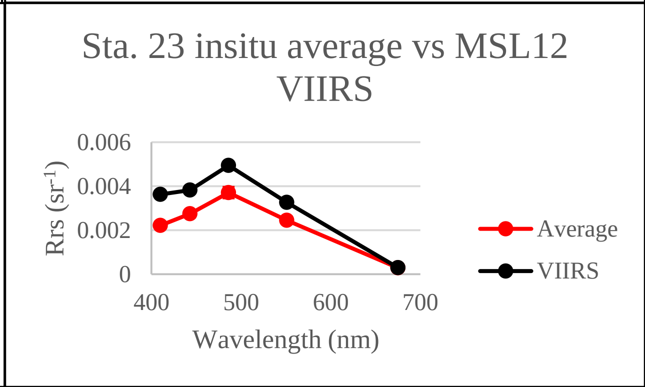

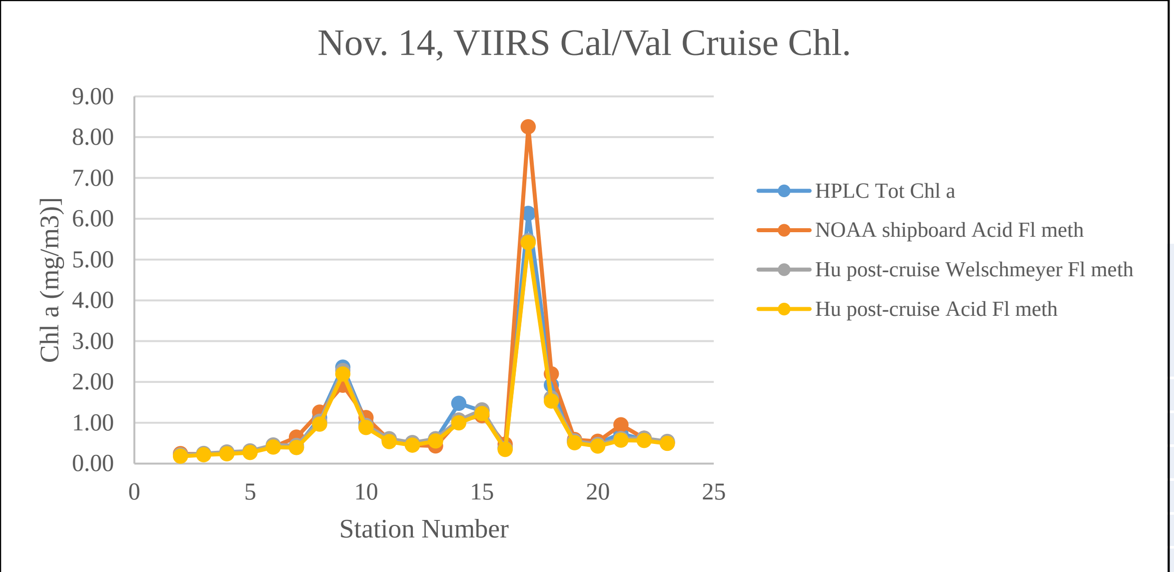

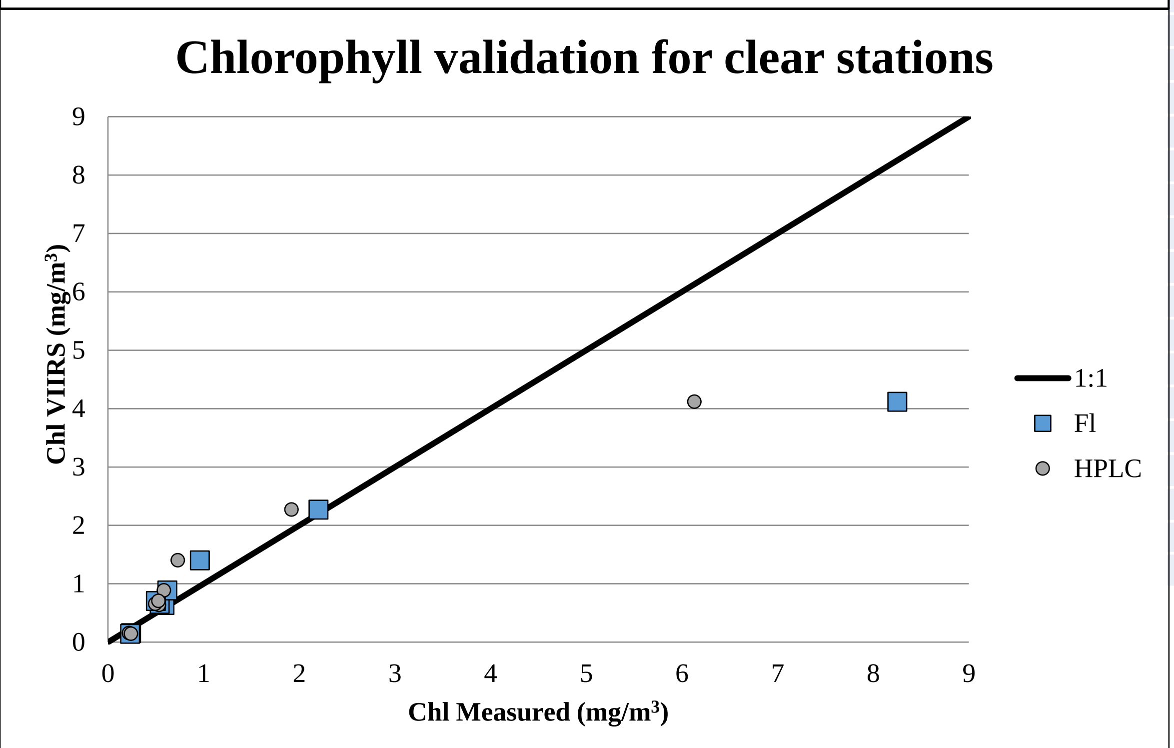

Station	HPLC Tot Chl a	NOAA shipboard Acid Fl meth	Hu post-cruise Welschmeyer Fl meth	Hu post-cruise Acid Fl meth
1	0.77	0.77	0.82	0.78
2	0.22	0.24	0.21	0.18
3	0.24	0.23	0.25	0.22
4	0.25	0.27	0.28	0.24
5	0.28	0.29	0.31	0.27
6	0.41	0.41	0.45	0.40
7	0.39	0.65	0.44	0.39
8	1.12	1.26	1.03	0.96
9	2.36	1.92	2.28	2.19
10	0.99	1.12	0.93	0.88
11	0.59	0.57	0.60	0.54
12	0.48	0.45	0.51	0.45
13	0.59	0.43	0.61	0.55
14	1.47	1.06	1.06	0.99
15	1.29	1.17	1.31	1.22
16	0.39	0.47	0.37	0.34
17	6.13	8.25	5.46	5.42
18	1.92	2.20	1.61	1.53
19	0.53	0.59	0.55	0.51
20	0.50	0.54	0.47	0.43
21	0.73	0.95	0.61	0.57
22	0.59	0.62	0.62	0.56
23	0.53	0.50	0.54	0.49

Conclusions:

Consistency between 10 independent measurements of water leaving radiance is within 10%.

Differences between in situ measurements is most likely dominated by variability in water masses

VIIRS matchups to in-water validation measurements are promising.

CCNY VIIRS validations at the Long Island Sound Coastal Observatory (LISCO) and on cruises, algorithm development

Sam Ahmed, Alex Gilerson

The City College of New York

Scientists: Matteo Ottaviani, Amir Ibrahim (now at GSFC)
Students: Robert Foster, Ahmed El-Habashi, Carlos Carrizo, Eder Herrera, Anna McGilloway

Outline

- Validation on the LISCO site
- Validation on SABOR and VIIRS cruises
- VIIRS algorithms development
- Radiative transfer vicarious calibration/validation
- Sky glint correction in polarization mode

Validation from Long Island Sound Coastal Observatory (LISCO)

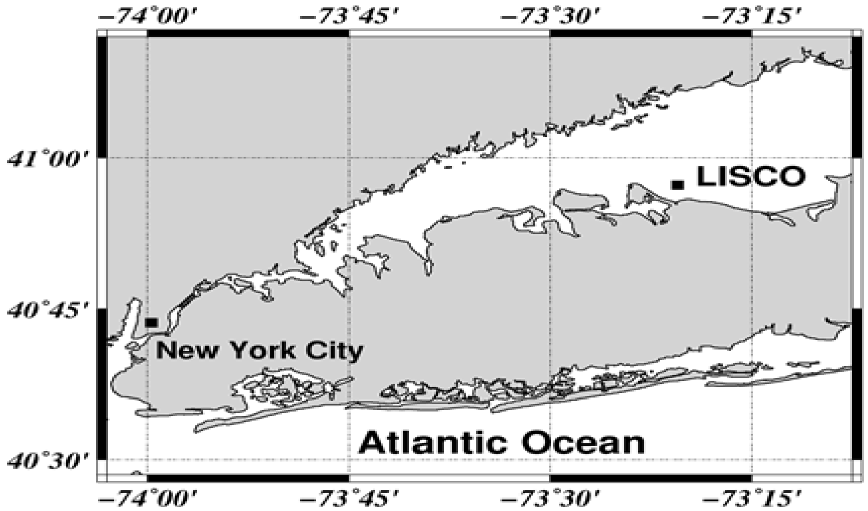

Mult-spectral SeaPRISM instrument. Transmits data to NASA AERONET every hour.

HyperSAS-POL with polarimetric sensors. Transmits data to CCNY server every hour.

Time series and Match-up Comparison

(June 14 2014- January 15 2015) **(June 10 2015- August 21 2015)**

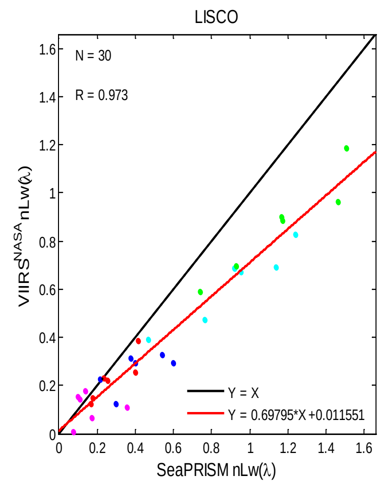

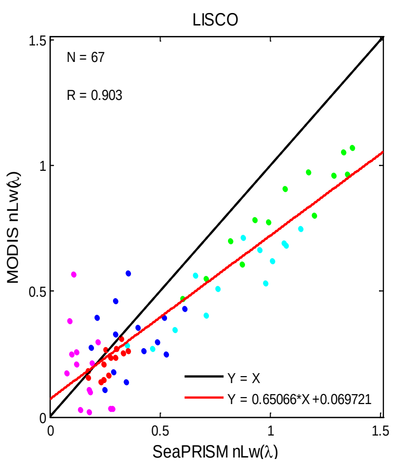

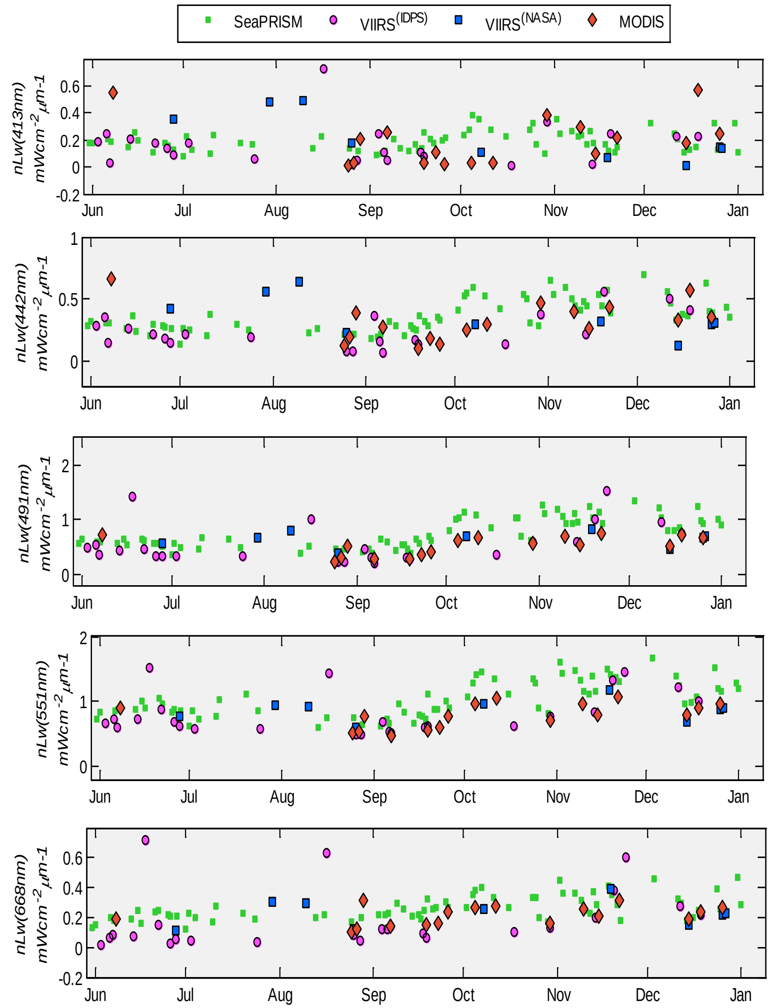

No Stray light flag

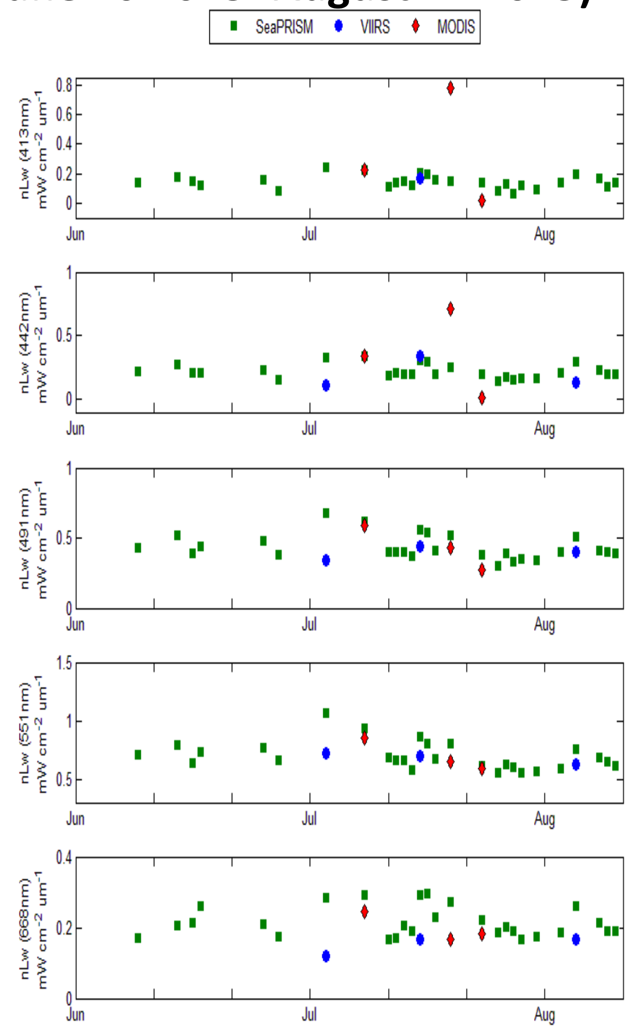

No Stray light and modglint flags

Match-up plots show fairly high correlation for 491, 551, and 668nm for all sensors. Much lower correlation is observed for violet (413nm) and blue (442nm), which is independent of the processing scheme or the sensor.

Ship-Airborne Bio-Optical Research (SABOR)
NASA Cruise July 17- August 7, 2014

R/V Endeavor owned by NSF operated by University of Rhode Island, 185 feet, crew -12, scientists -15

NASA GISS, NASA Langley CCNY, U. of Maine, Oregon State University, Sequoia Scientific, WET Labs

CCNY team: A. Gilerson, PhD students R. Foster, C. Carrizo

Rhode Island – Bermuda – Norfolk, VA - Rhode Island

Research Scanning Polarimeter (RSP) and lidar were installed on the aircraft

Included satellite validation component

NOAA VIIRS Cal/Val Cruise, November 2014

R/V Nancy Foster

CCNY team: PhD students A. Ibrahim, A. El-Habashi

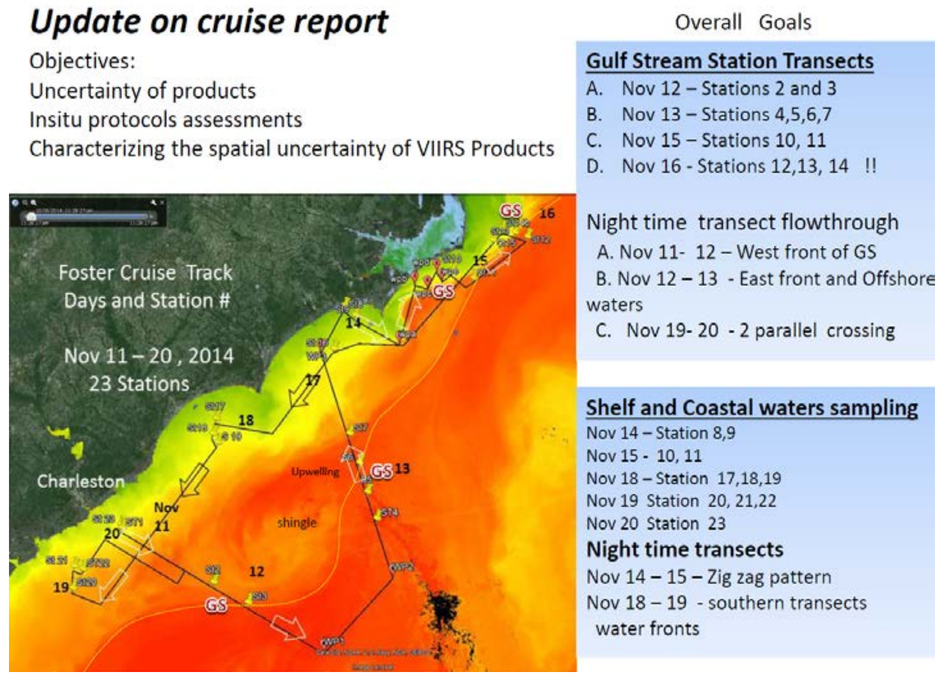

From R. Arnone, 02/12/15

Participants: NOAA/NESDIS, NASA – Goddard, NRL, U. Southern Mississippi, U. of Massachusetts, U. of South Florida, CCNY, Columbia U., JRC (Italy)

HyperSAS-POL, Handheld spectroradiometers

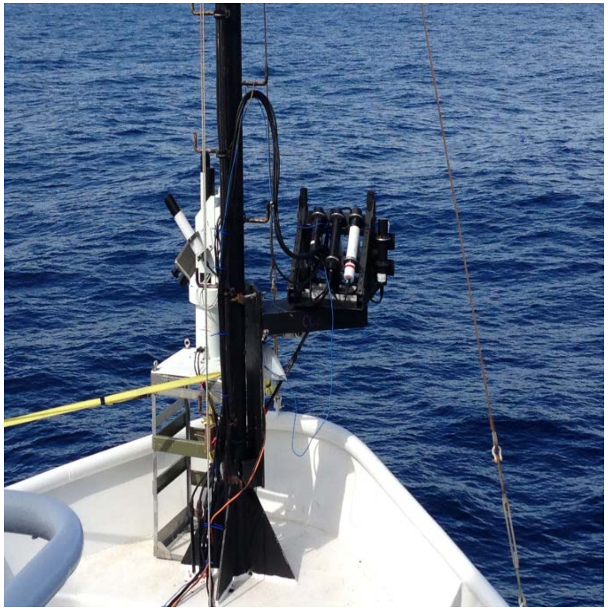

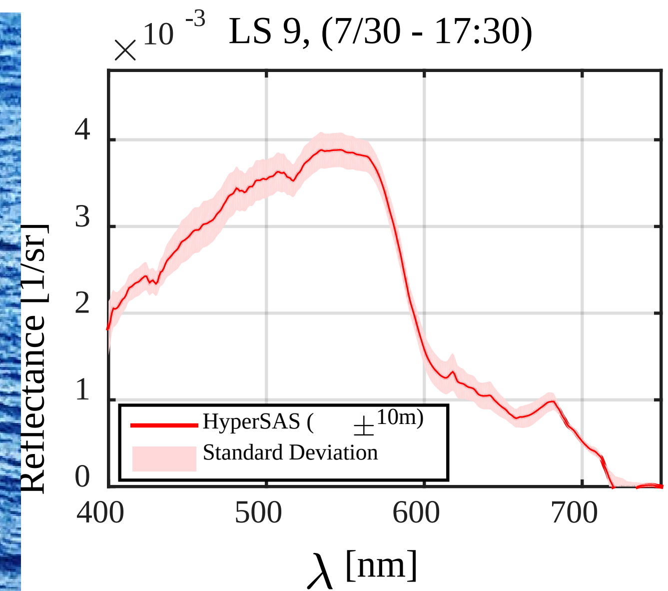

HyperSAS had 2 radiometers in unpolarized mode and 4 with polarization sensitivity

GER-1500

ASD Handheld2

HyperSAS integration time was 2000ms for water and 128-250 ms for sky measurements, 6-4000ms for ASD and 160 ms for GER

Remote Sensing Reflectance comparison between GER, HyperSAS, HyperPRO, MODIS and VIIRS on July 26th and on July 31st (SABOR cruise)

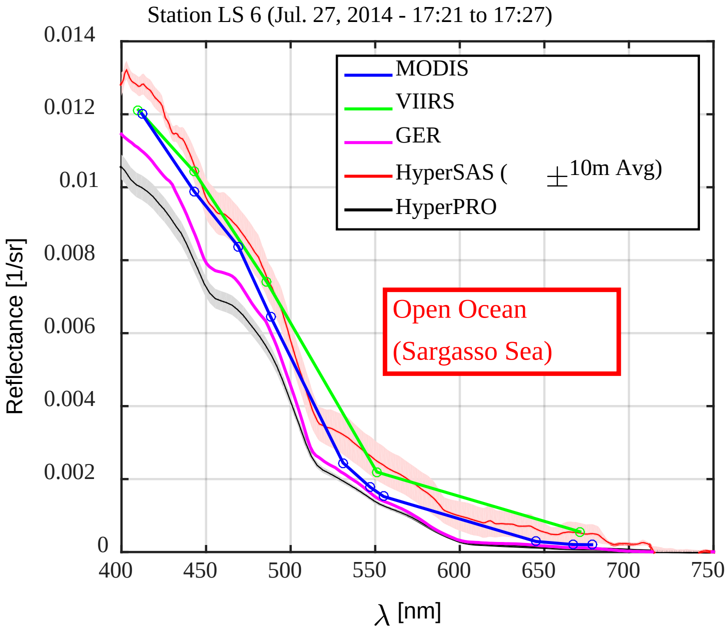

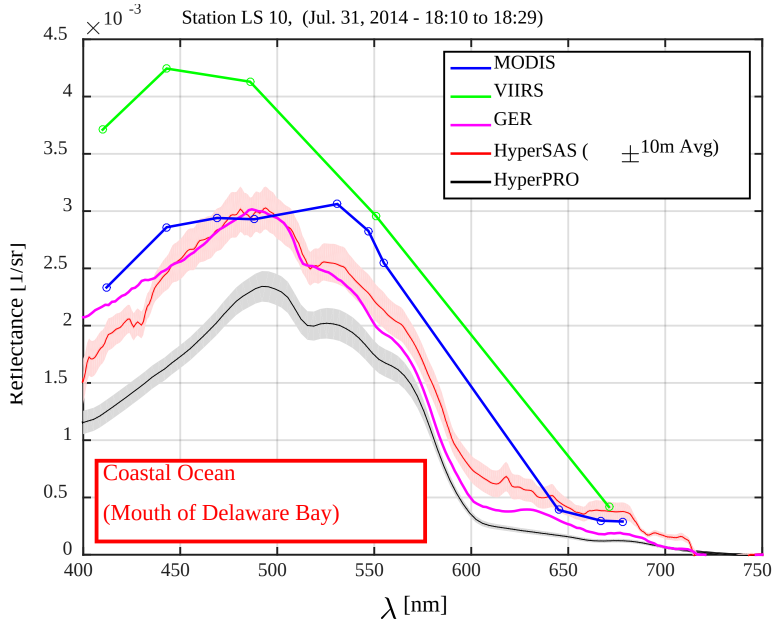

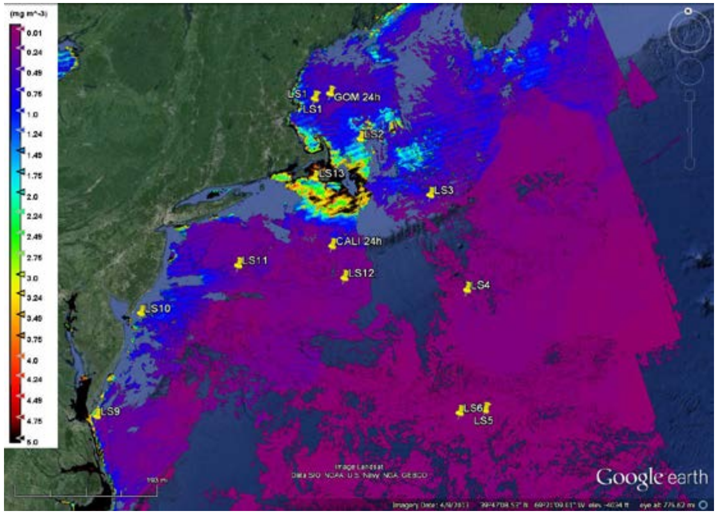

VIIRS and MODIS

- Grid size: 3x3
- Pixels flagged: 0%
- Flags not checked: high and moderate sun glint contamination and stray light contamination.

Several other instruments from other groups (above and below water) were deployed, comparison is in progress

Spectral Remote Sensing Reflectance comparison between GER, HyperSAS, HyperPRO, MODIS and VIIRS (VIIRS cruise)

November 12, 2014

Blue water

Station 03

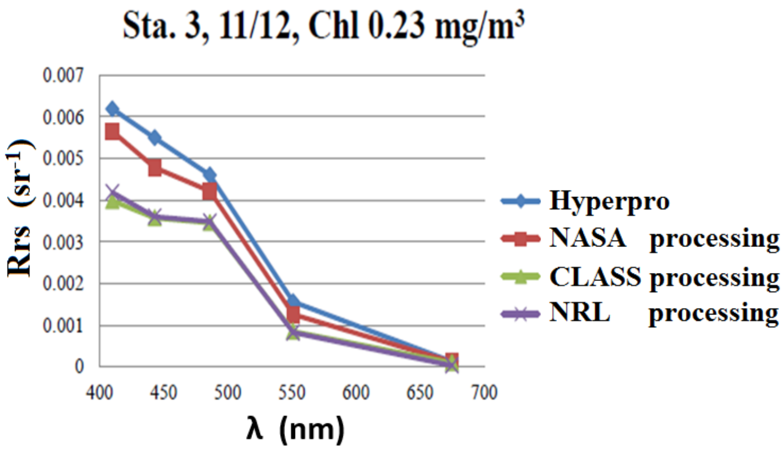

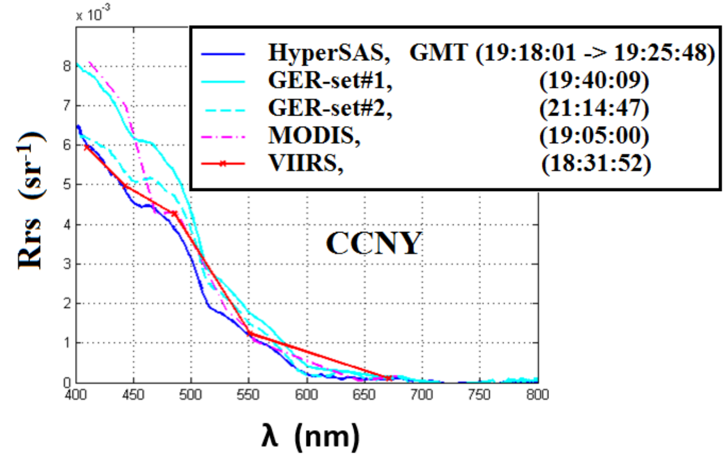

November 20, 2014

Blue water
Turbid water on the way into port

Station 23

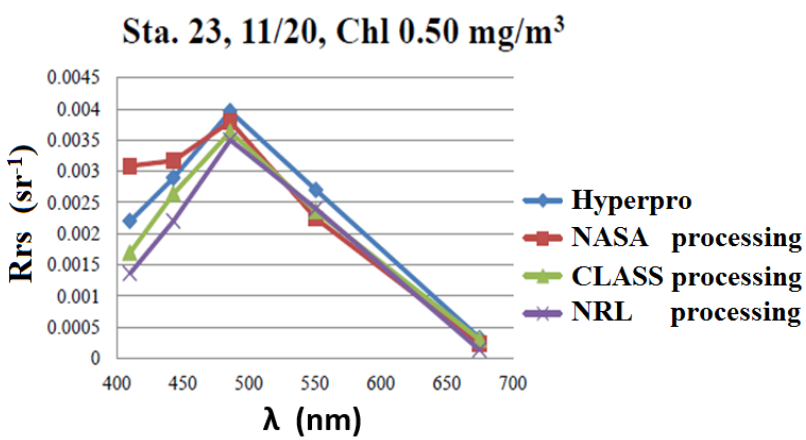

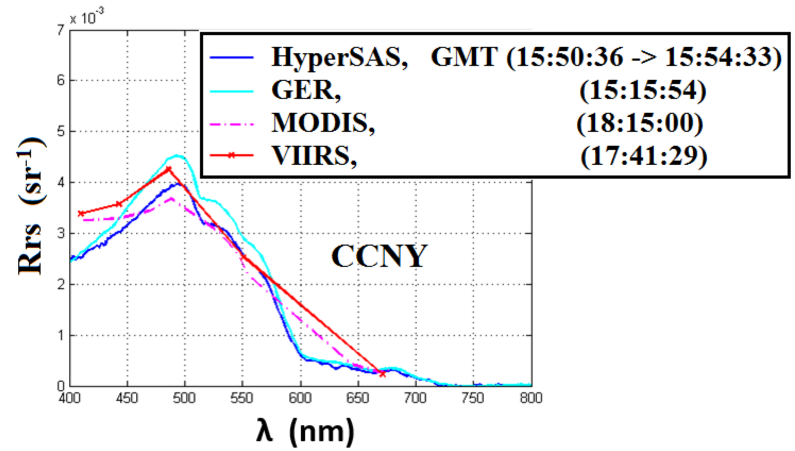

From M. Ondrusek Dec 18, 2014

Algorithm Developments-Neural Network (NN) algorithm for VIIRS KB Harmful Algal Bloom (HABS) retrievals in WFS

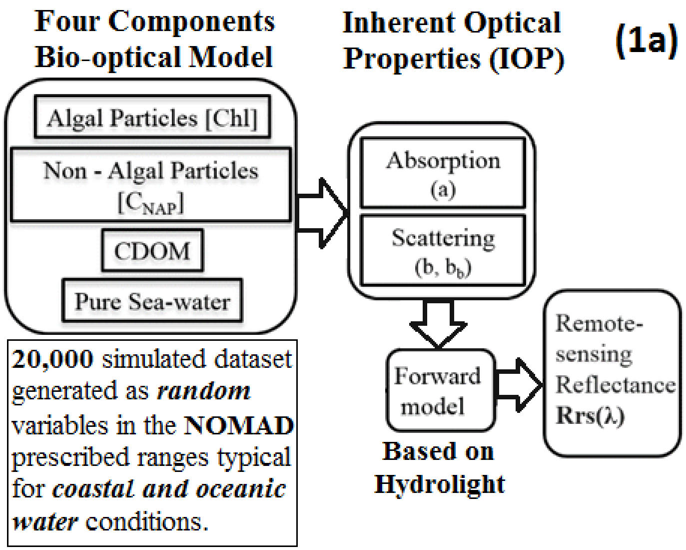

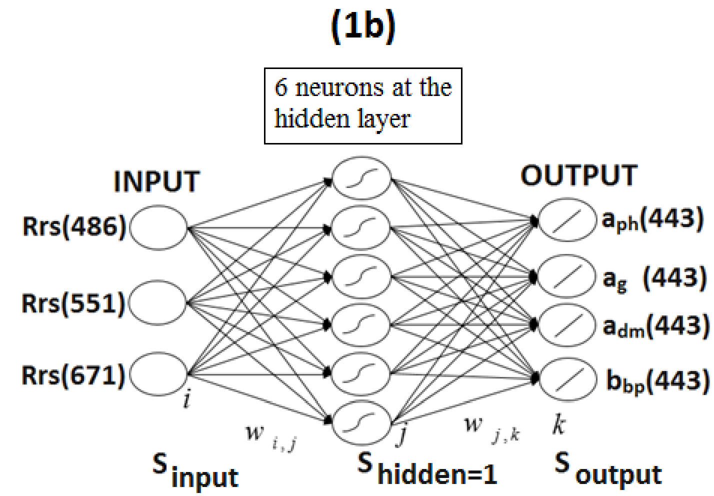

Fig. 1a Shows the Bio-Optical model and the Radiative Transfer simulations. of 20000 random IOP data sets within NOMAD **prescribed ranges and resulting related Rrs values generated by Hydrologht**

Fig. 1b Architecture of NNVIIRS, one-hidden layer multilayer perceptron (MLP) with 6 neurons at the hidden layer, trained with 10,000 set of Rrs and related IOPs
NN trained on 10,000 data sets to model relationship of Rrs values to IOPs at 443 nm

NN KB HABS retrieval comparisons site 1 on 9/2/2014-major HAB occurence

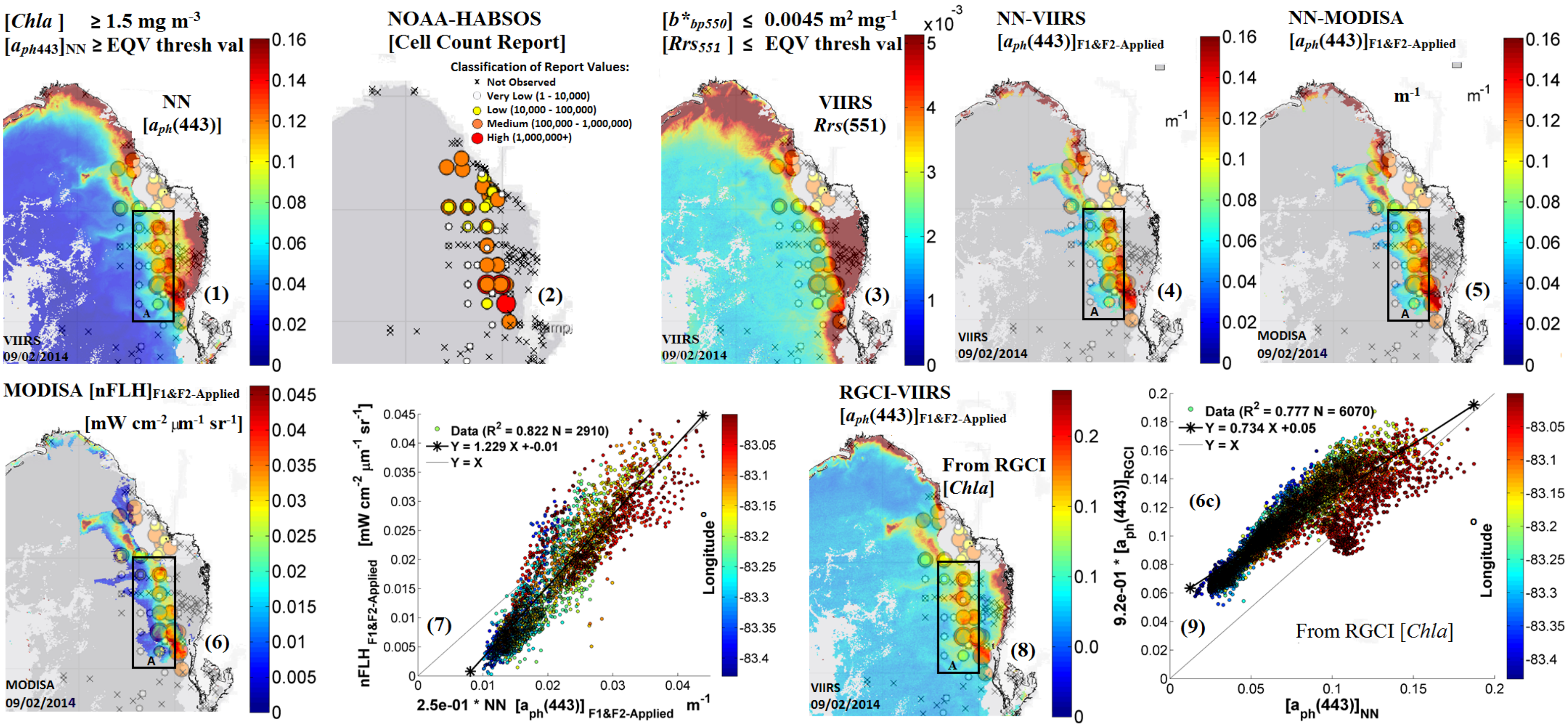

NN KB HABS retrieval comparisons site 2 on 9/16/2014 much nearer coast

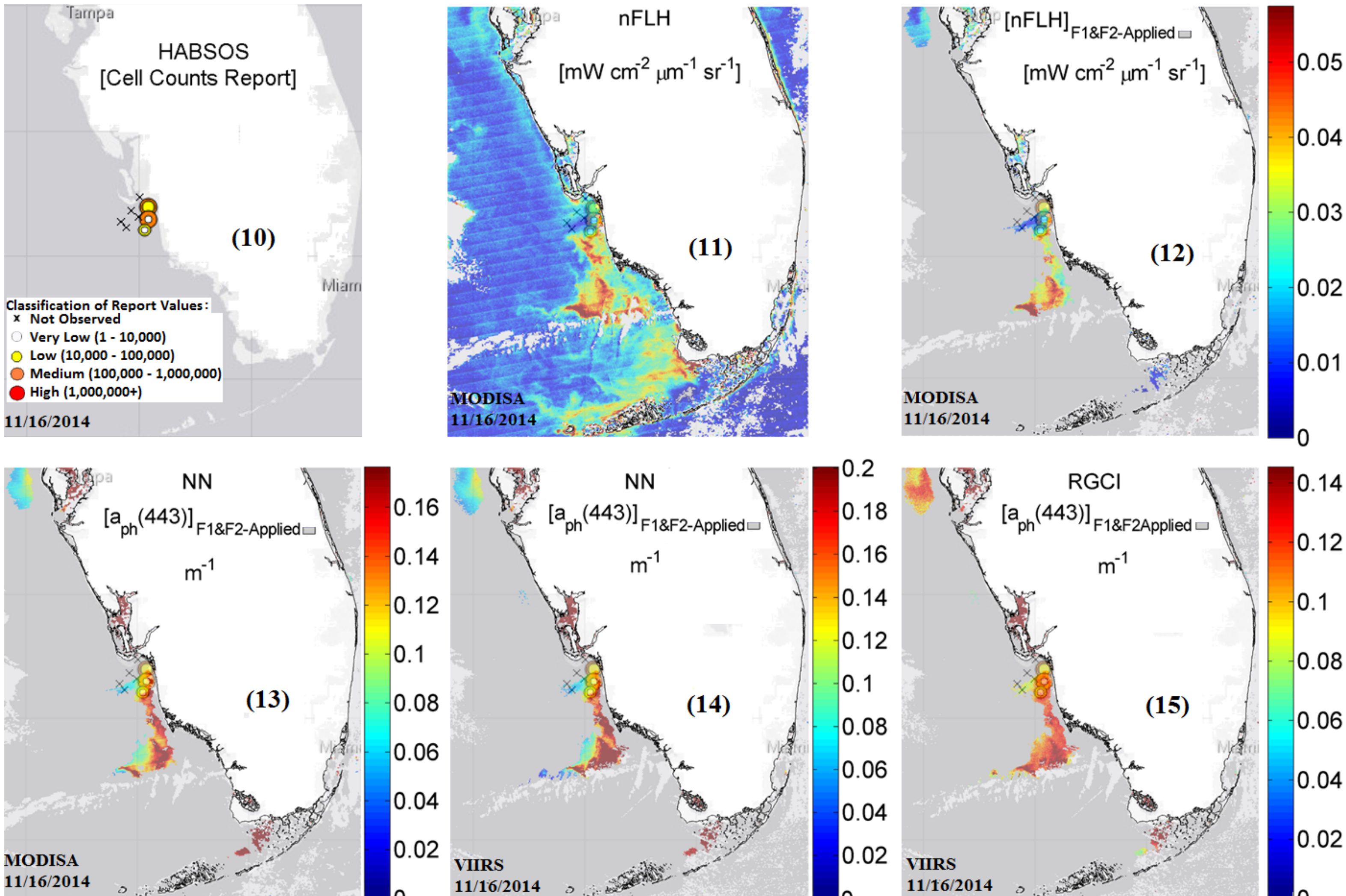

Development of Algorithms for Retrieval of Chlorophyll-a in the Chesapeake Bay and other Coastal Waters Based on JPSS-VIIRS Bands

Evaluation on the field data, Chesapeake Bay, 2013

OC3V

[Chl] =(35.75*(Rrs708/Rrs665) - 19.30).^1.124
Gilerson et al 2010 very high data consistency;
no 708nm band on VIIRS

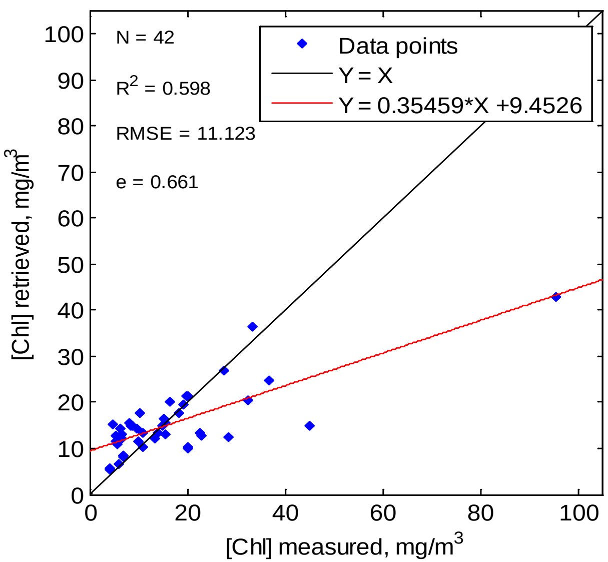

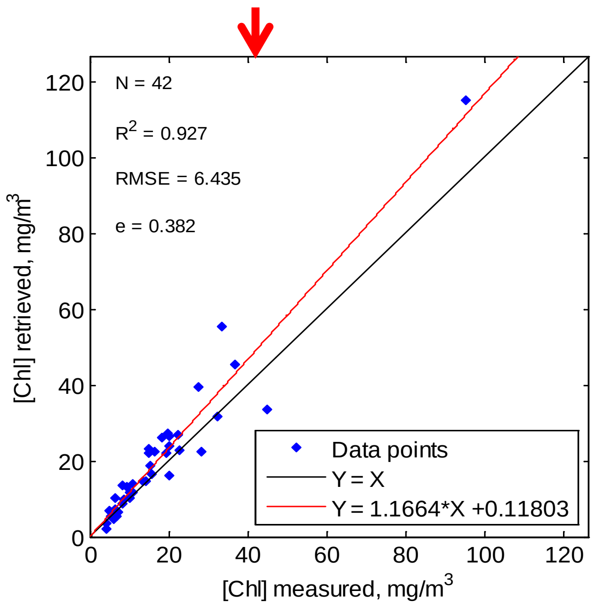

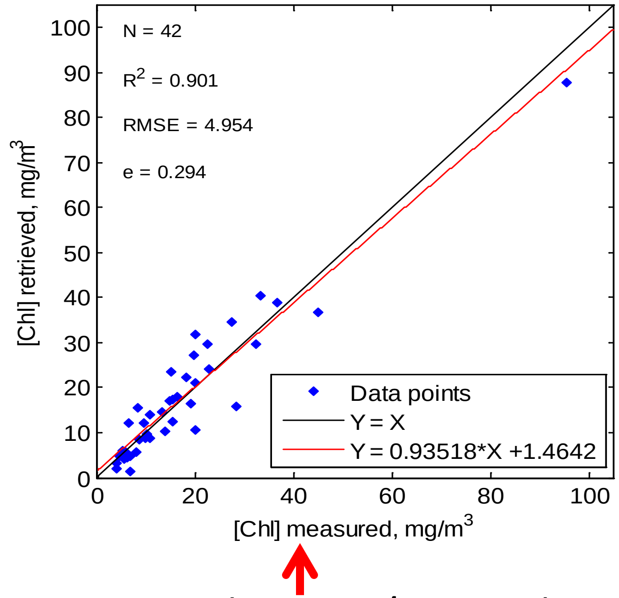

Algorithms which include 745nm band

chl1 = 10^(a1 + a2*Rrs488/Rrs550 + a3*Rrs671/Rrs745)

Similar results chl2 = ((2.459*(t1*Rrs745/Rrs671) - 0.439 + t2)/(0.022))^1.124

Performance of the algorithms based on the satellite data

Evaluation on the satellite data VIIRS 2012-15, strict filtering, matchups with the in situ data of the Chesapeake Bay Program

OC3V

chl1 = 10^(a1 + a2*Rrs488/Rrs550 + a3*Rrs671/Rrs745)

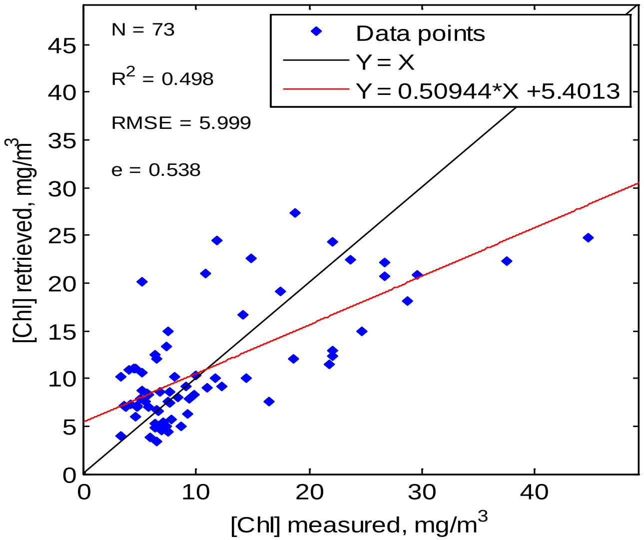

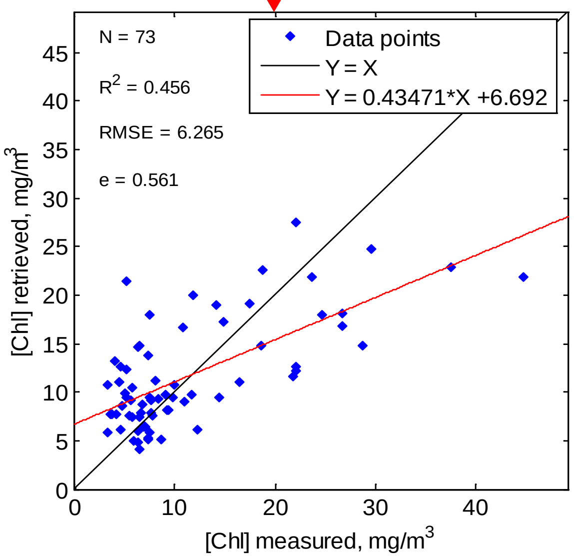

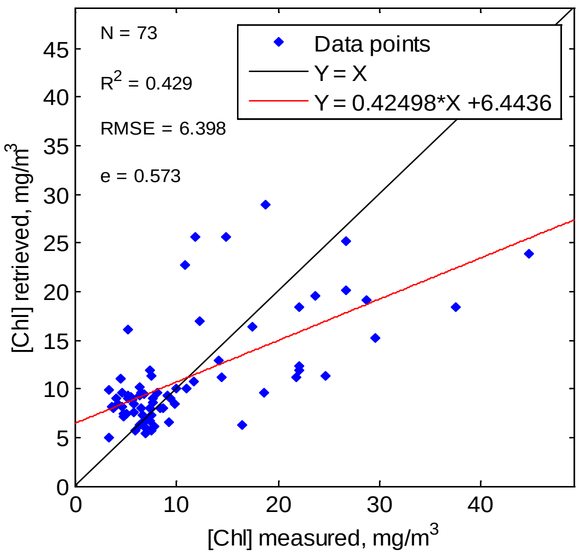

chl2 = ((2.459*(t1*Rrs745/Rrs671) - 0.439 + t2)/(0.022))^1.124

- Relatively good performance of OC3V on VIIRS in comparison with MODIS probably due to the better VIIRS spatial resolution.
- Algorithms based on 745nm band show performance similar to OC3V. That means that statistics of retrieval is determined by the spatial and temporal characteristics of matchups

A Radiometric Approach for Calibration of Current and Future Ocean Color Satellite Sensors using AERONET-OC data

- To demonstrate a Radiative Transfer (RT) based radiometric vicarious calibration methodology for current and future satellite OC sensors.

- We envision our methodology as being capable of carrying out OC sensor validation of SDR independently of the atmospheric correction process.

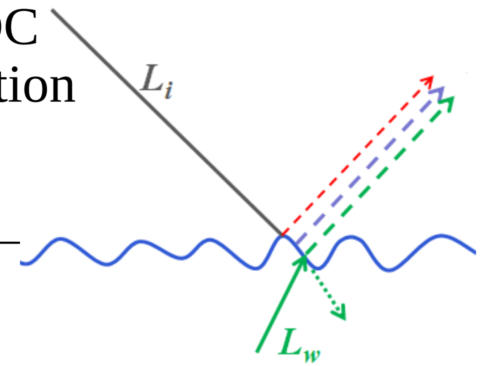

TOA – Ocean - TOA

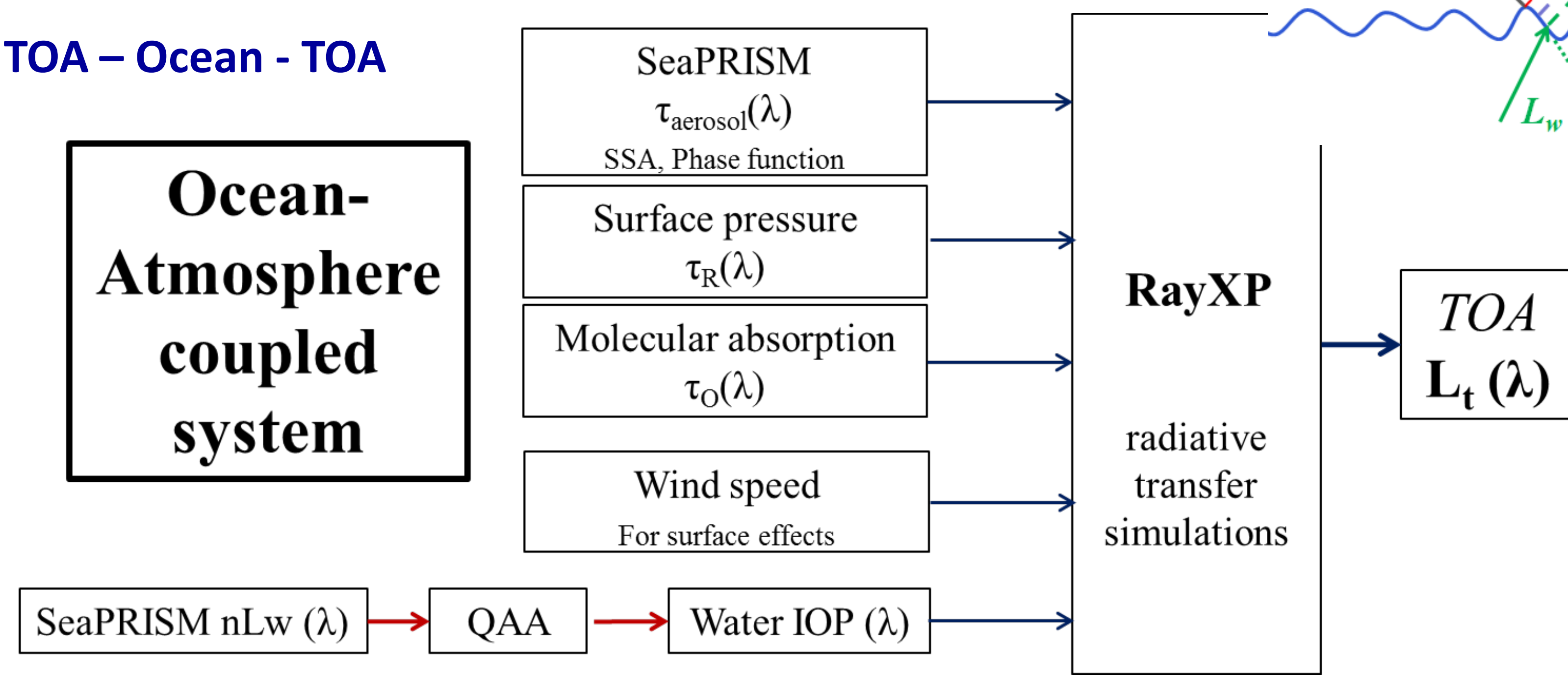

Optics Express, 2014

RT-satellite matchups and estimated gain factors

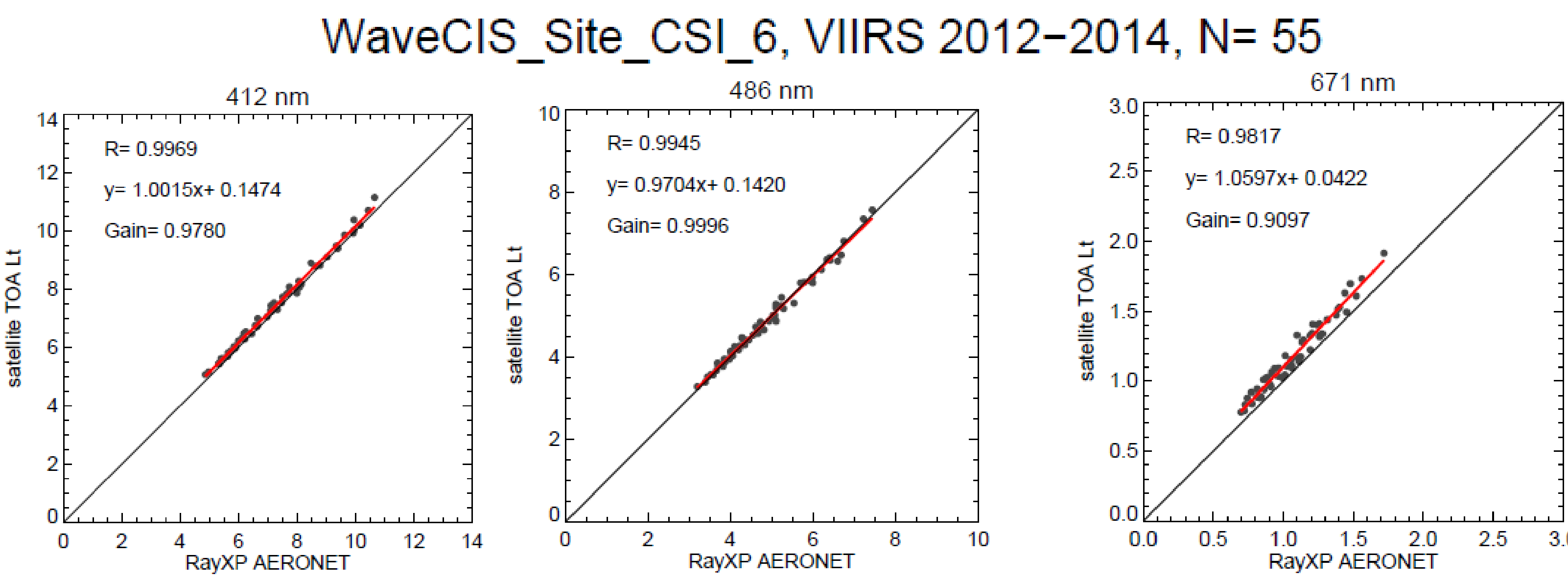

Estimated gain factors based on WaveCIS, Venise and USC

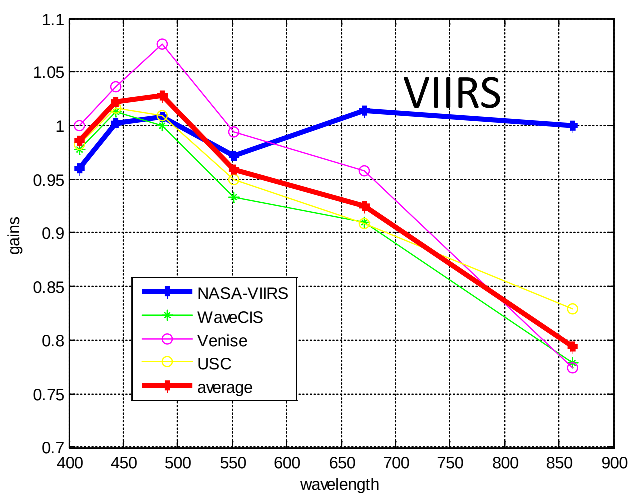

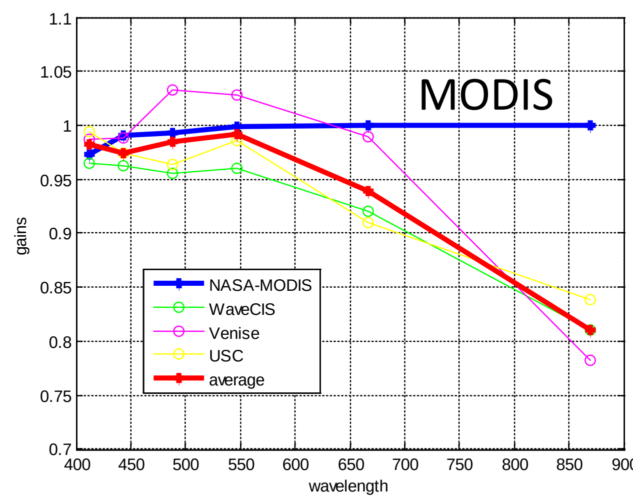

Scalar Sky Glint Correction Methods

For scalar reflectance:

$$\overline{Rrs} = (\bar{L}_t - \rho \cdot \bar{L}_s)/\bar{E}_d$$

ρ estimates how much incident light is reflected from the surface.

$$\rho = f\left(\begin{matrix}\theta_s, \phi_s, \theta_v, \phi_v, n(\lambda), \Omega \\ windspeed, sky\ illumi\end{matrix}\right.$$

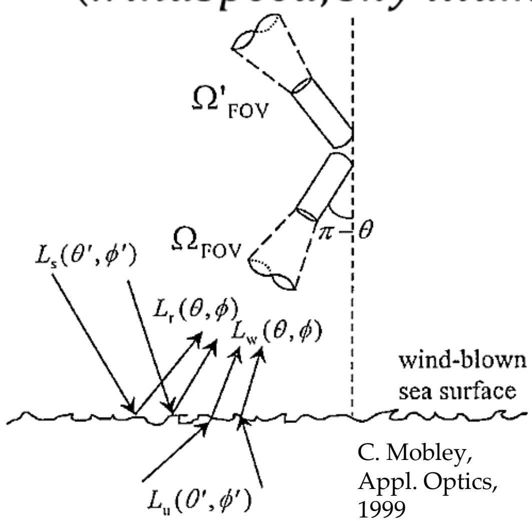

C. Mobley, Appl. Optics, 1999

How do we estimate polarized Remote Sensing Reflectance?

How much polarized light is reflected from a sea surface?

D

Stokes Vector Rotation

$$\bar{R}_s(\theta) = \begin{bmatrix} 1 & 0 & 0 & 0 \\ 0 & \cos(2\theta) & -\sin(2\theta) & 0 \\ 0 & \sin(2\theta) & \cos(2\theta) & 0 \\ 0 & 0 & 0 & 1 \end{bmatrix}$$

polarized ρ

$$\bar{S}_{Refl} = [\bar{R}_s(\beta)\cdot\bar{F}\cdot\bar{R}_s(\alpha)]\cdot\bar{S}_{sky}$$

Fresnel matrix for facet.

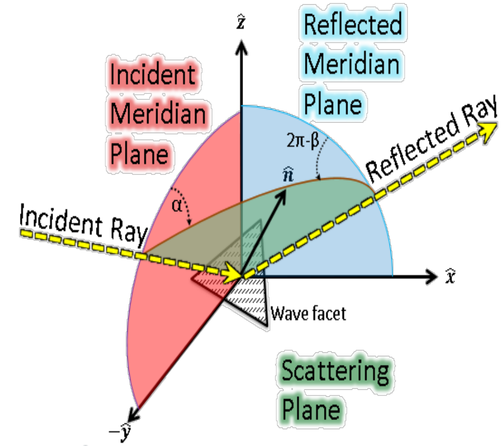

Effective Fresnel Matrices (ρ) For Glint Correction

vs. Detector Zenith, 440 nm, 40° Solar Zenith, 90° relative azimuth

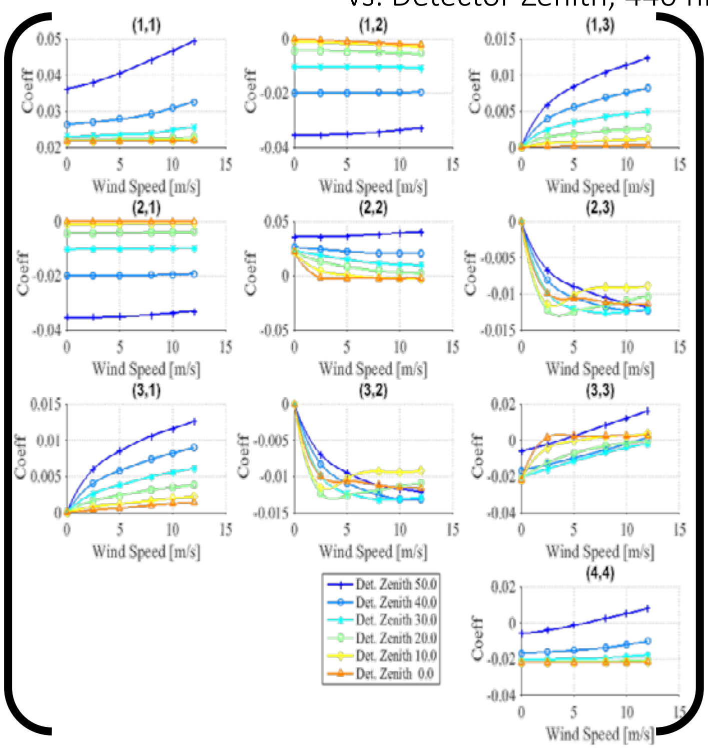

Reflection of light from surface

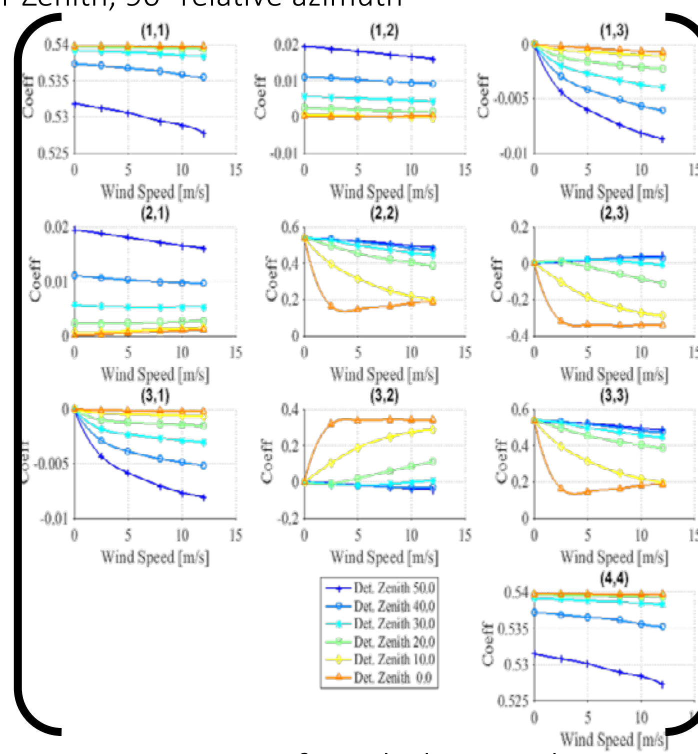

Transmission from below to above

Comparison with Underwater Polarimeter

16:37 UTC, July 30th, 2014.
80 *km* South-East of Norfolk, VA.

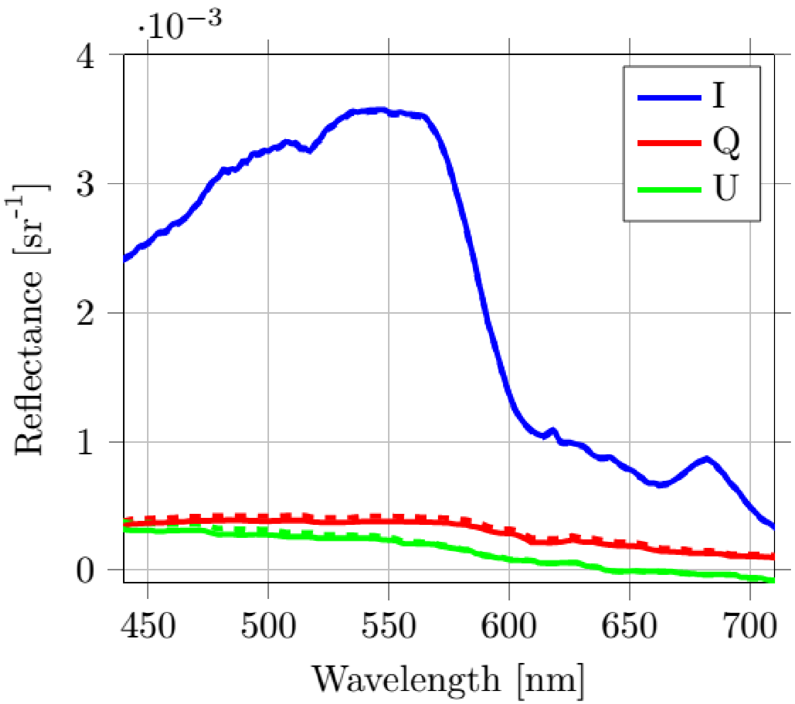

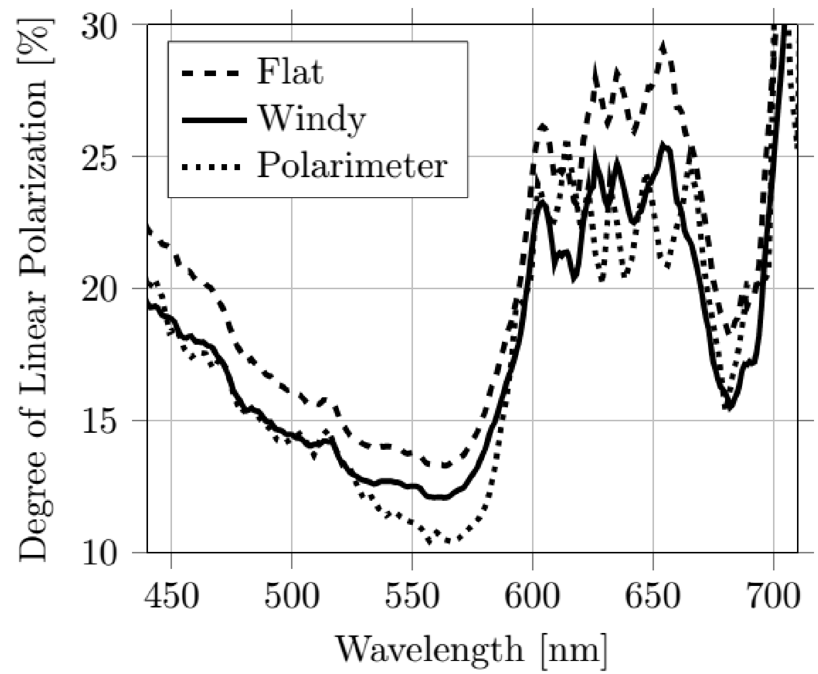

Evaluation of VIIRS performance over coastal waters and its capacity to detect dark water and harmful algal blooms

Chuanmin Hu, Lin Qi, Jennifer Cannizzaro, David English, Brian Barnes, and Alina A Corcoran

Univ. South Florida, huc@usf.edu

NOAA JPSS/VIIRS Team Meeting, August 24 – 28, 2015

Objectives

- Evaluate/Validate VIIRS ocean color data products
- Demonstrate VIIRS capacity in studying coastal oceans (water quality, harmful algal blooms, oil spills)
- Share data and results with community to advance science and mission planning

How?

- Field measurements following community-accepted protocols
- Satellite data analysis and comparison with field measurements
- Communication with science team and the community
- Technical reports and publications

Field Measurements

Conducted by USF Optical Oceanography Lab in collaboration with other groups.

All measurements have filter-pads absorptions and CDOM absorptions. Most measurements also have scattering and reflectance IOPs. Some have taxonomy and profiling data.

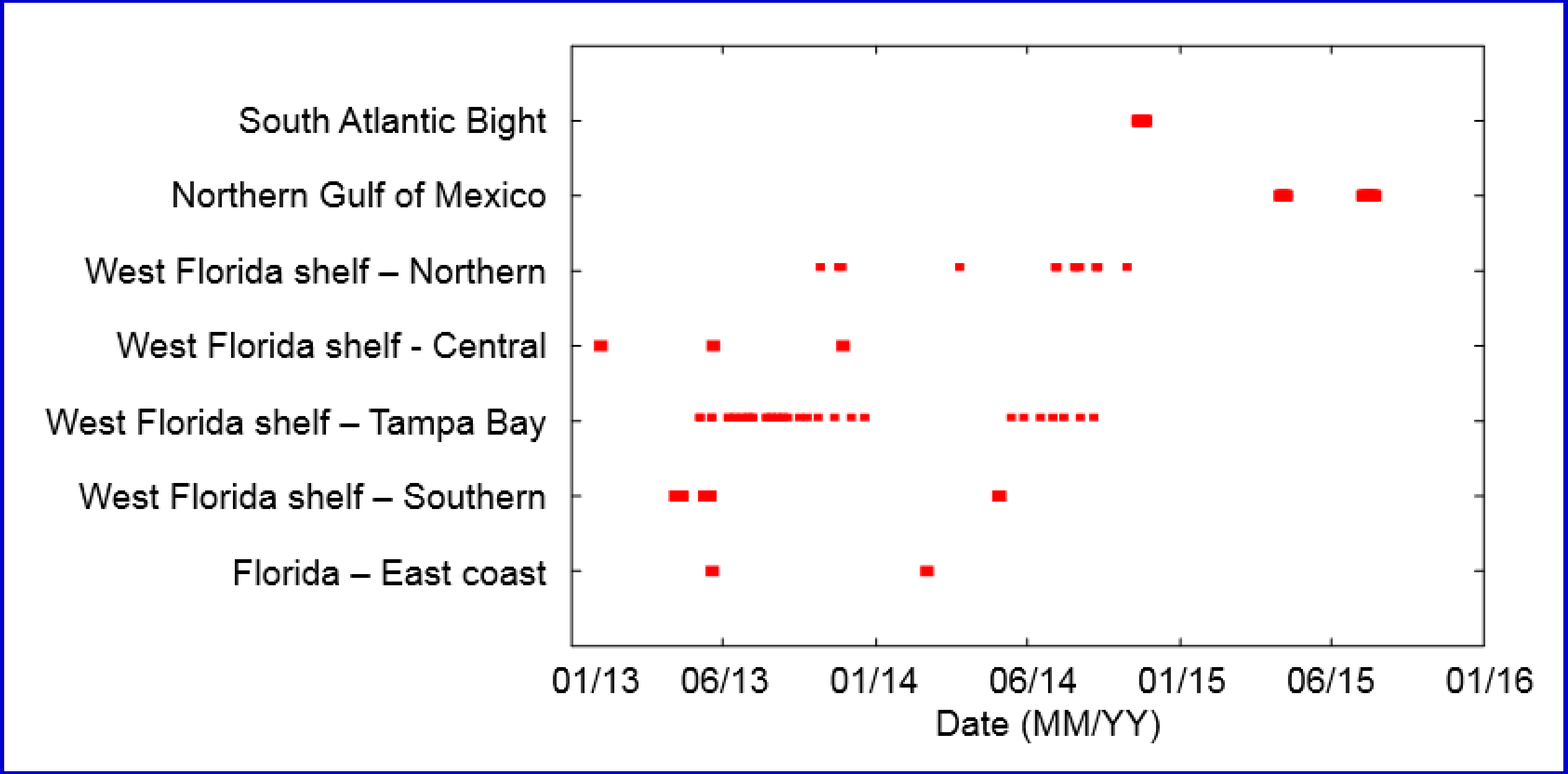

Field Measurements

An example from the DEEPEND02 cruise (Aug 8 – 22, 2015)

MODIS 5-day composite ending Aug 12, overlaid with cruise stations and glider track to Aug 12

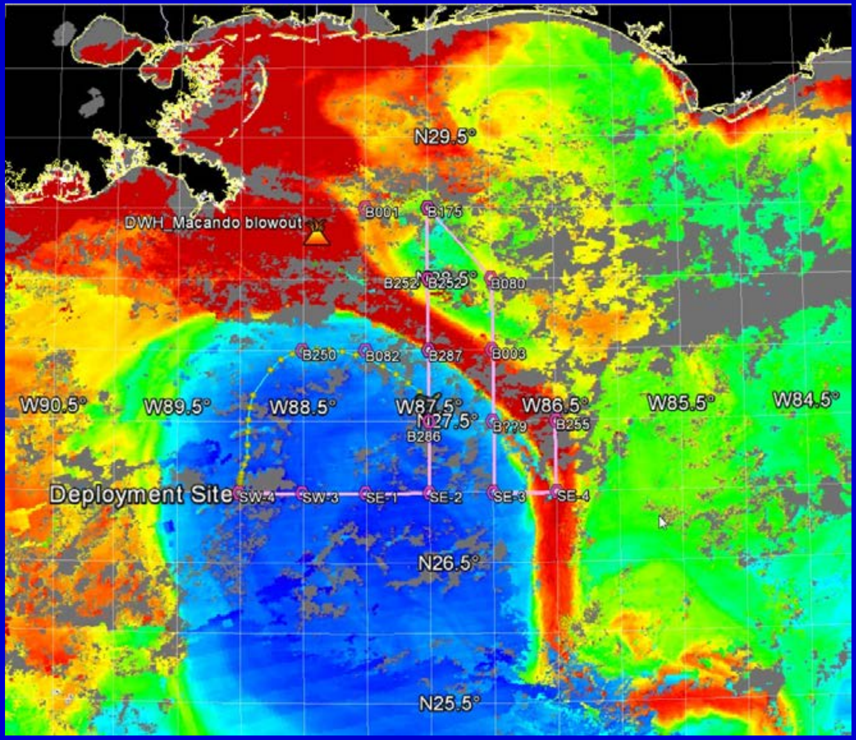

MODIS 3-day composite showing glider track up to Aug 18

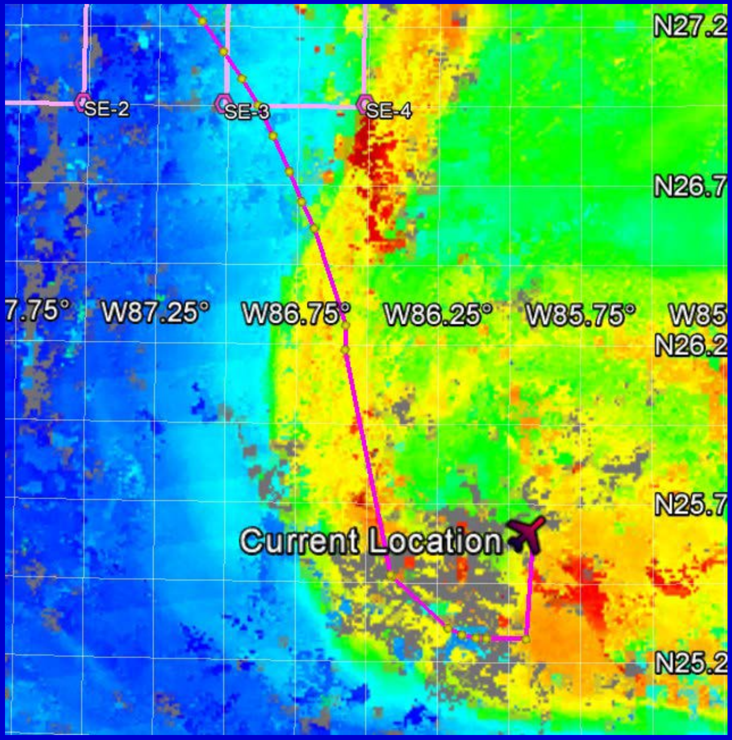

Field Measurements

Protocols follow community standards to assure high quality

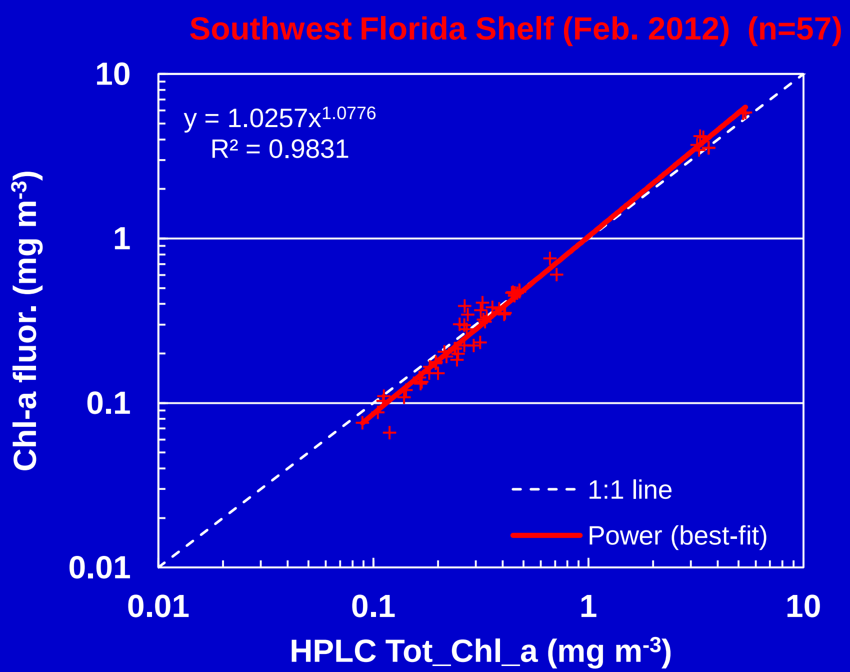

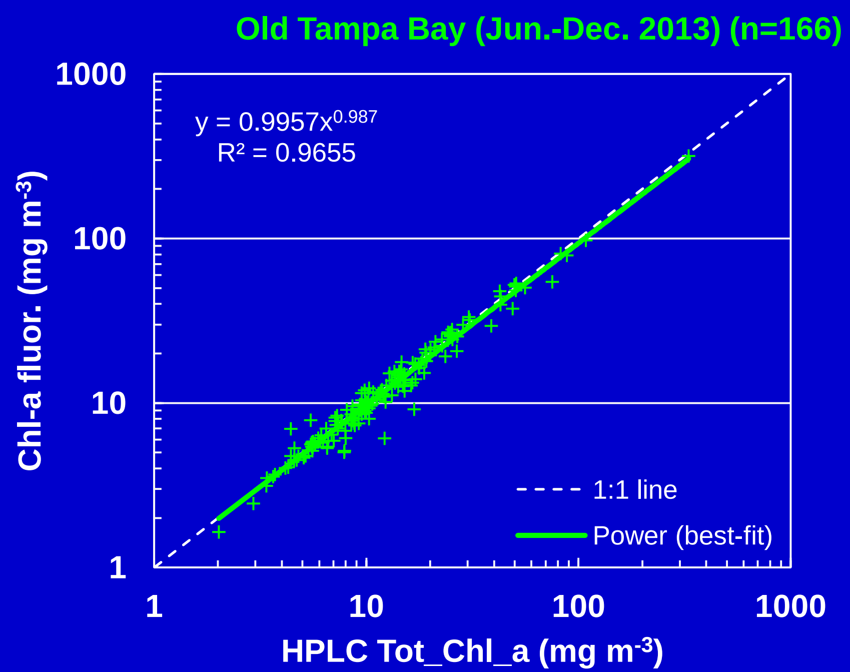

VIIRS data processing

Three data sources

- IDPS processing – during early stage of validation
- NOAA/NESDIS MSL12 processing – limited availability
- NASA/GSFC L2GEN processing – for cross-sensor comparison

VIIRS data product evaluation

Evaluation during initial phase (IDPS processing)

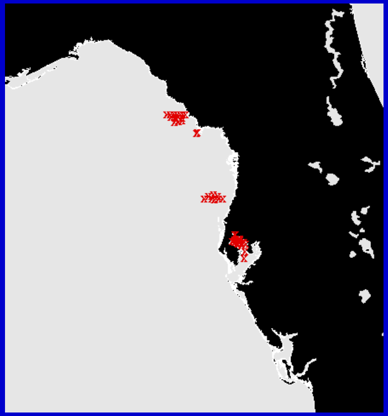

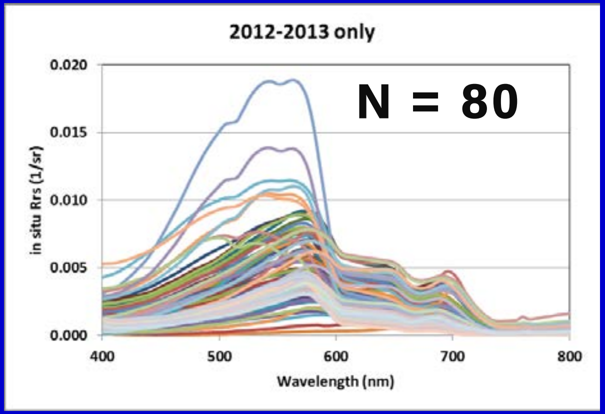

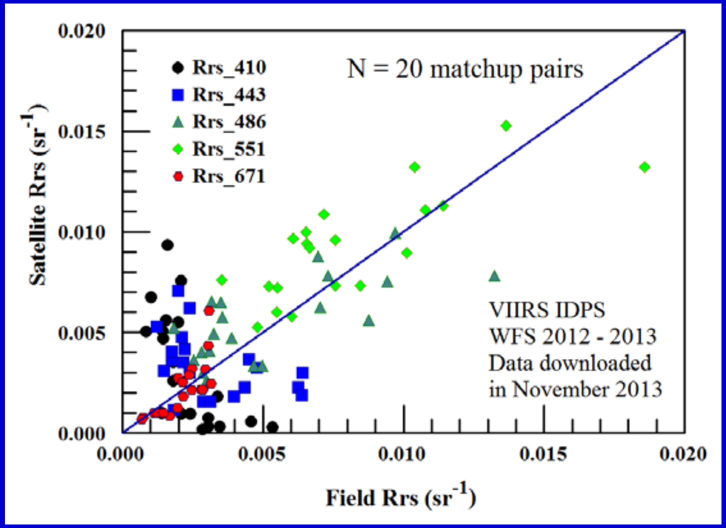

QF Flags not applied

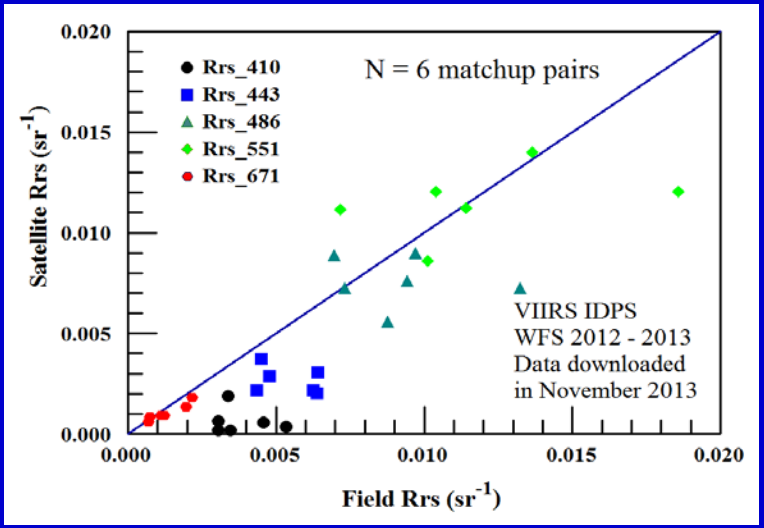

QF Flags applied

VIIRS over dark water and HABs

Demonstration of difficiency and temporal solution

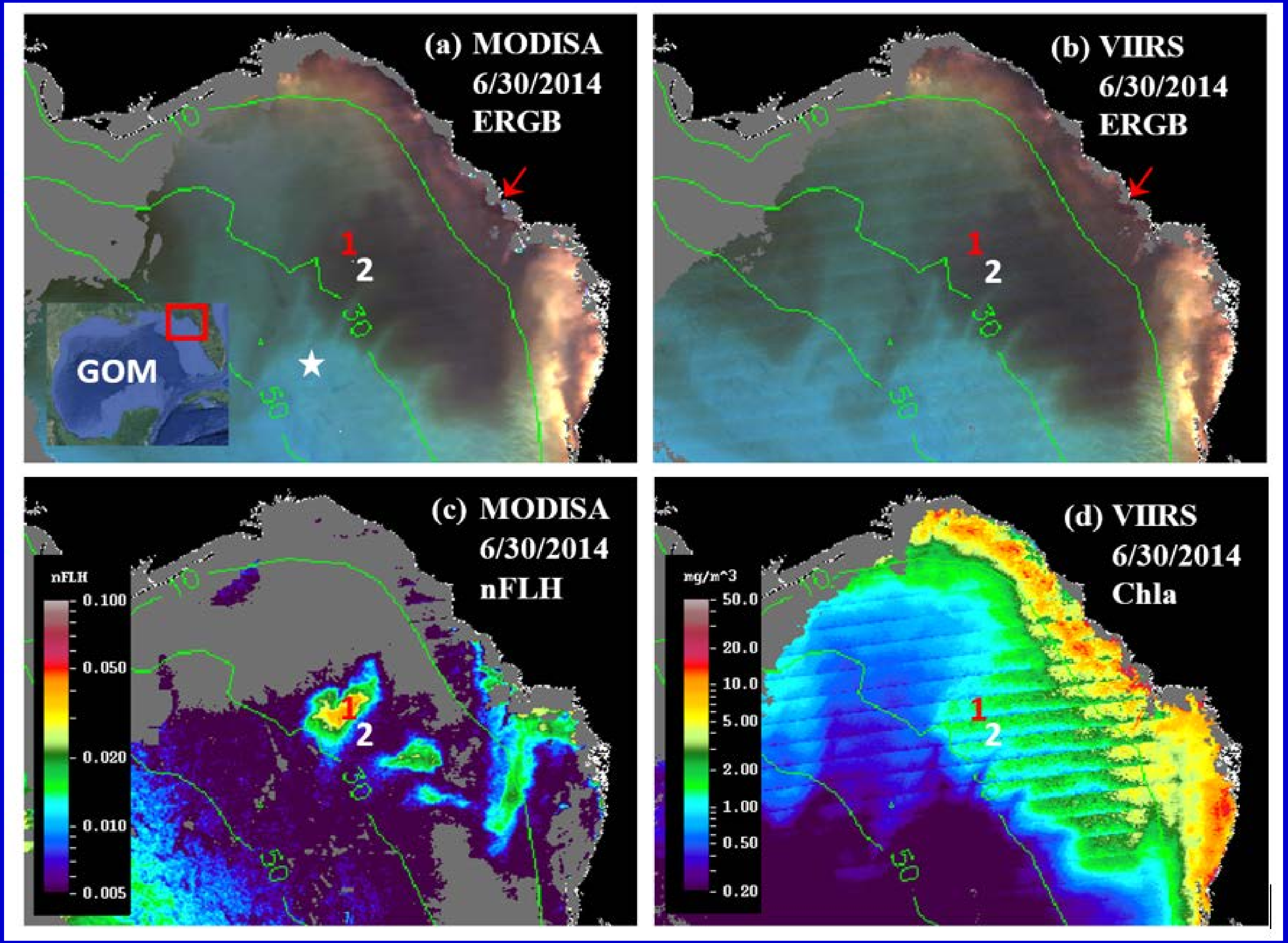

VIIRS over dark water and HABs

Most pixels agree will between MODIS and VIIRS, for all bands

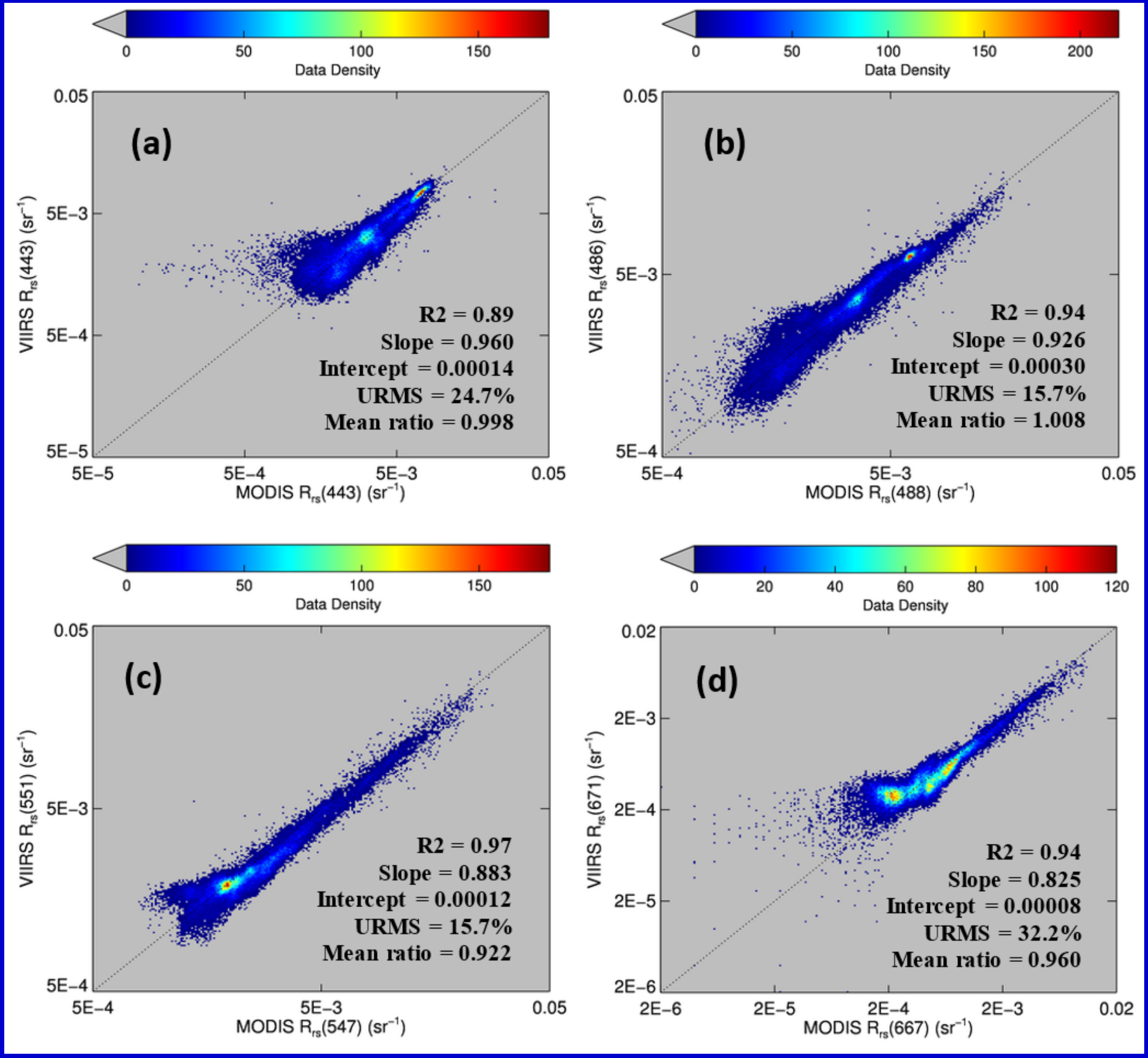

VIIRS over dark water and HABs

However, bloom patterns can only be revealed by MODIS FLH (Hu et al., 2015)

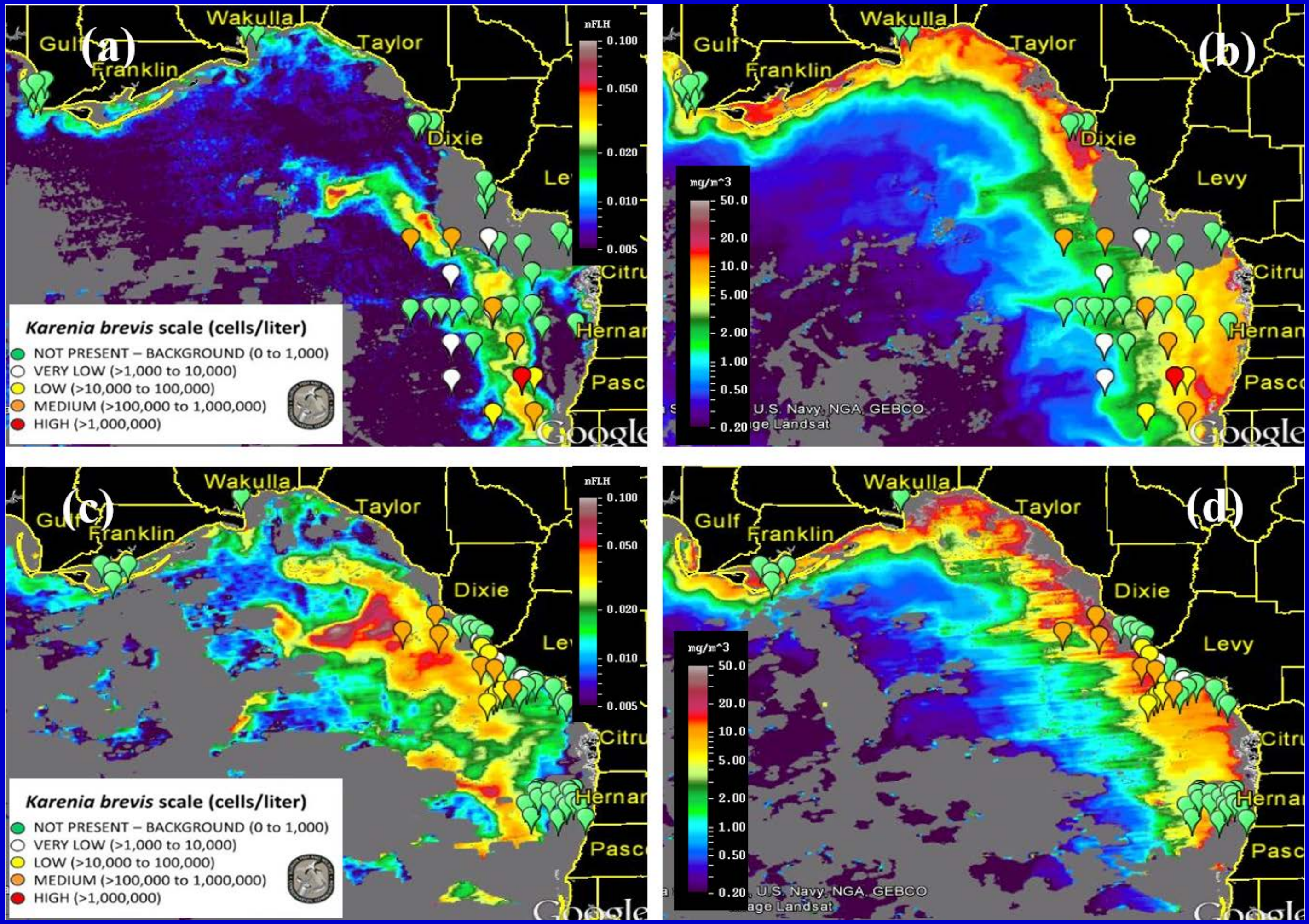

FWC has been using MODIS FLH to track HABs in near real-time for years

VIIRS over dark water and HABs

A Red-Green-Chlorophyll-Index (RGCI) performs better than OC3

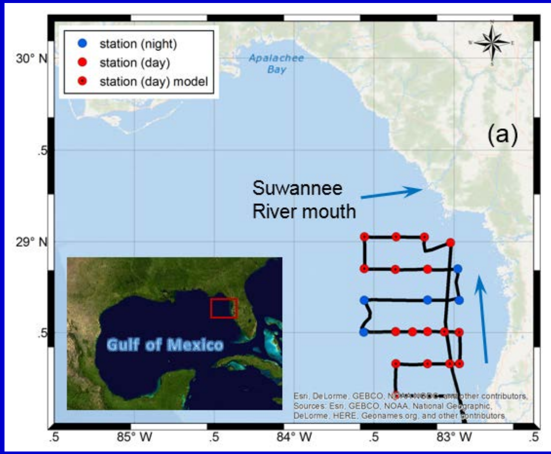

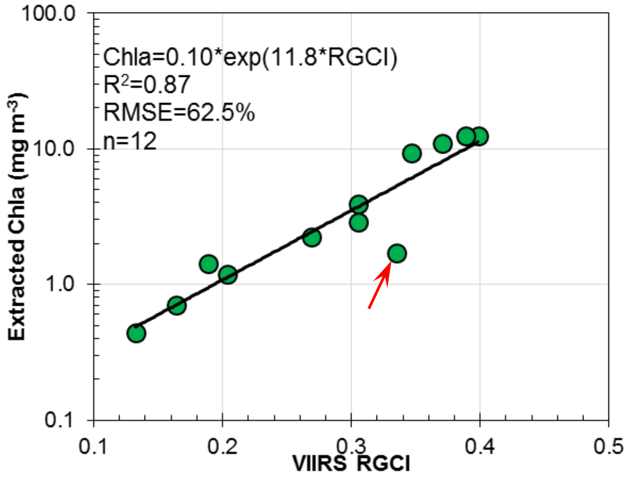

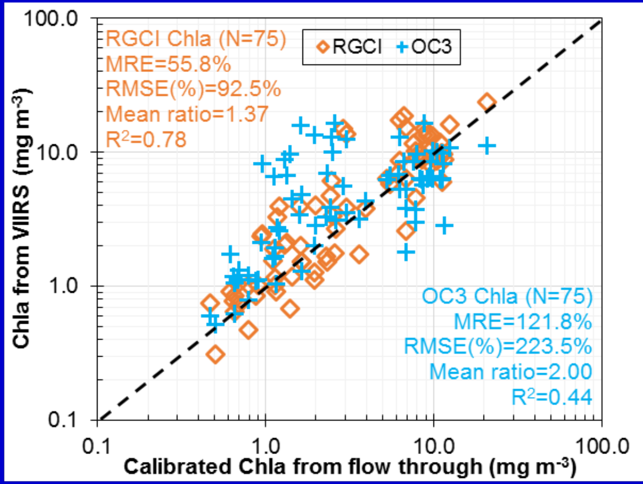

VIIRS over dark water and HABs

VIIRS RGCI reveals similar patterns as MODIS FLH (Qi et al., in press)

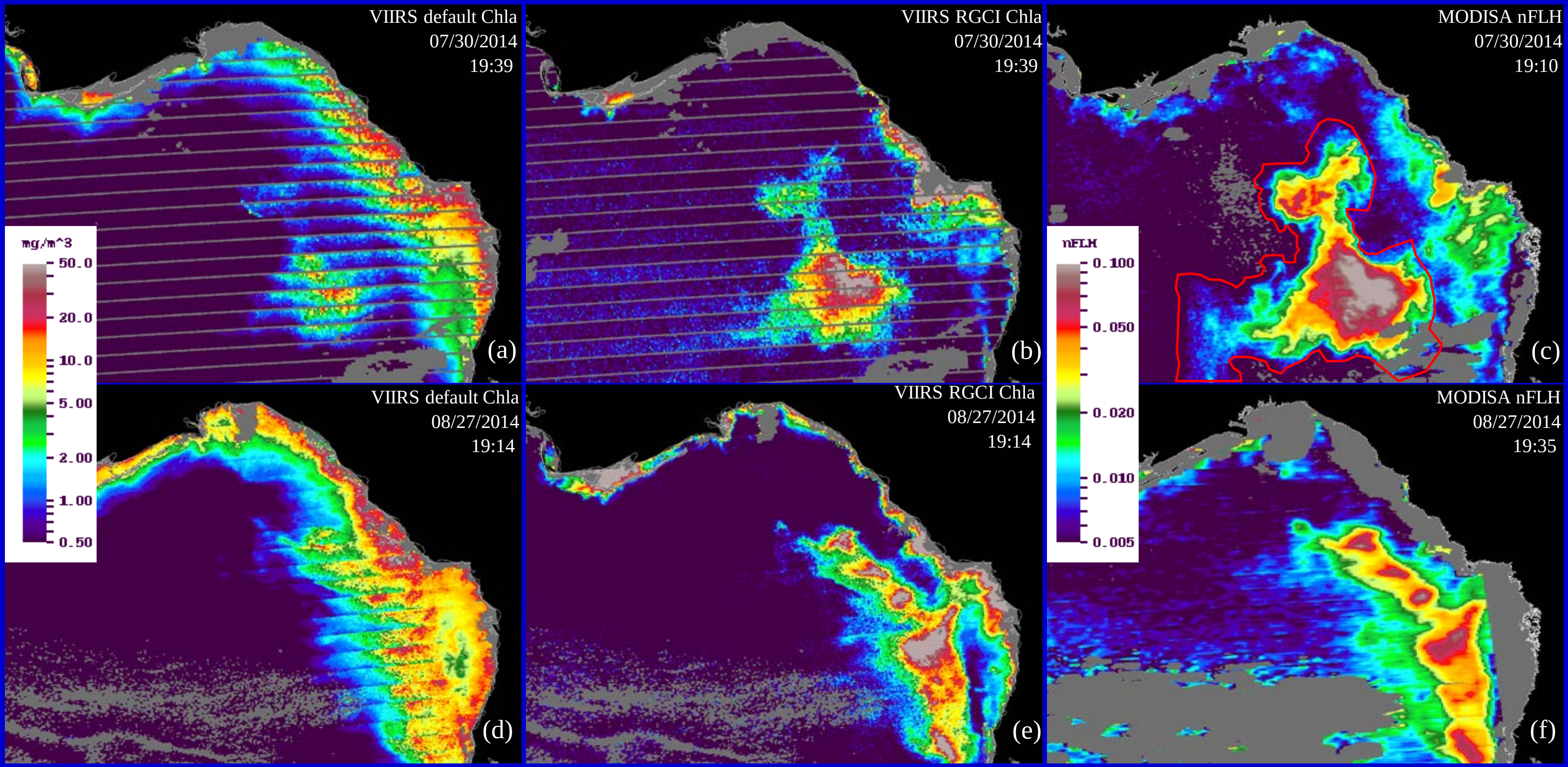

VIIRS over dark water and HABs

Why? CDOM dominates light absorption in the blue so blue bands cannot be used. VIIRS red band (662 – 682 nm) encompasses the MODIS red band (662 – 672) and FLH band (672 – 682).

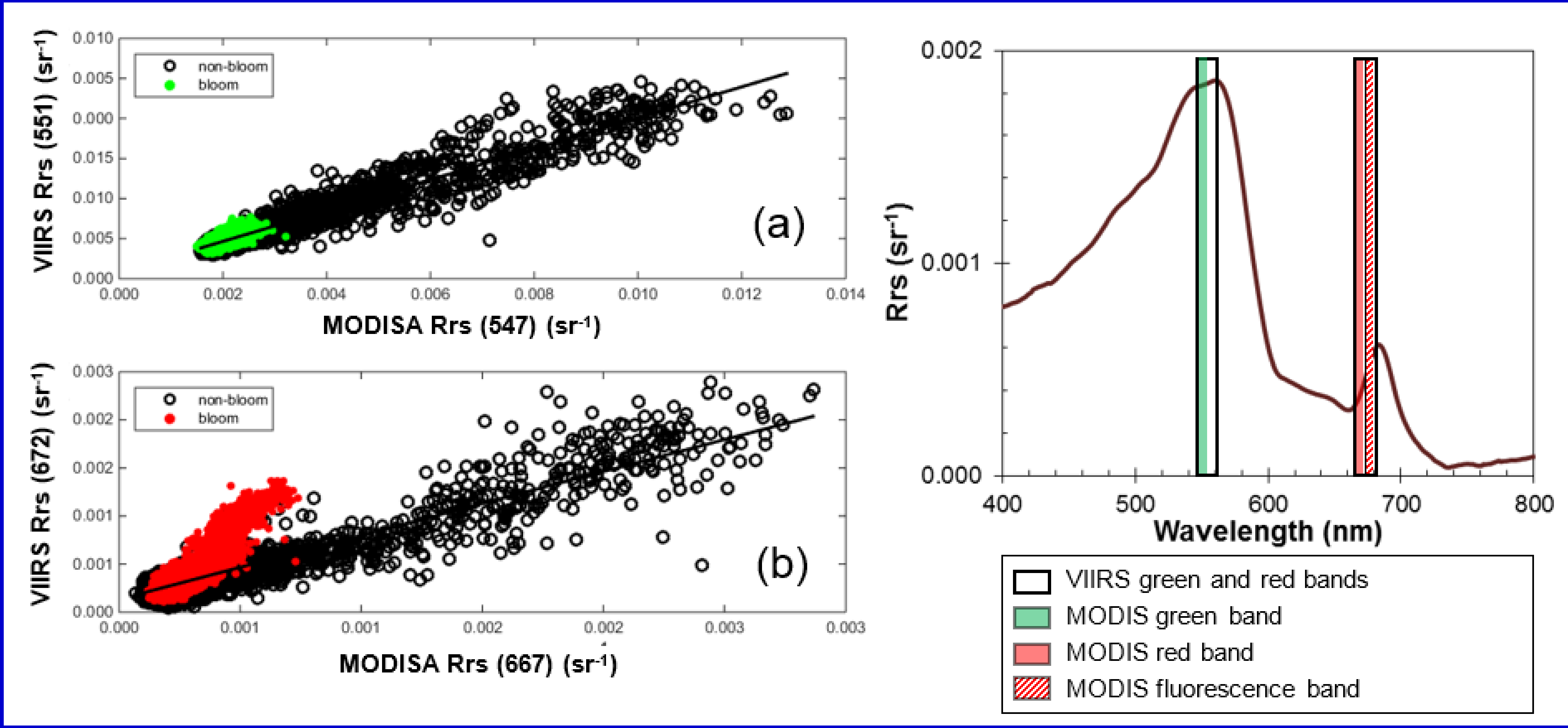

RGCI for other coastal regions?

Test over the South Atlantic Bight using NOAA/VIIRS Nov 2014 cruise data

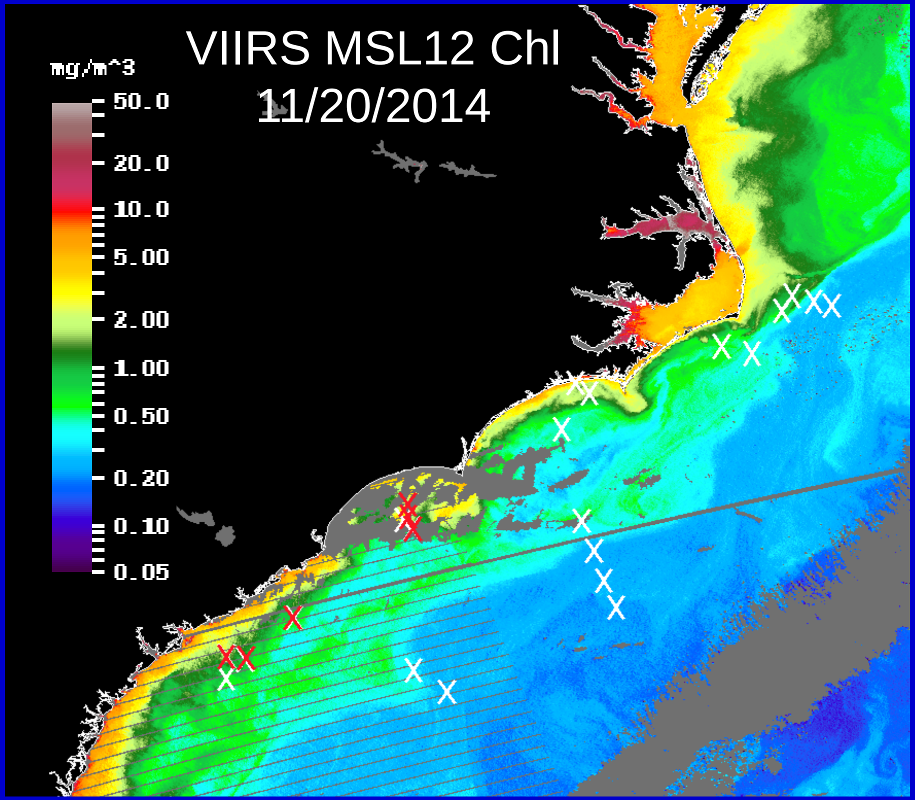

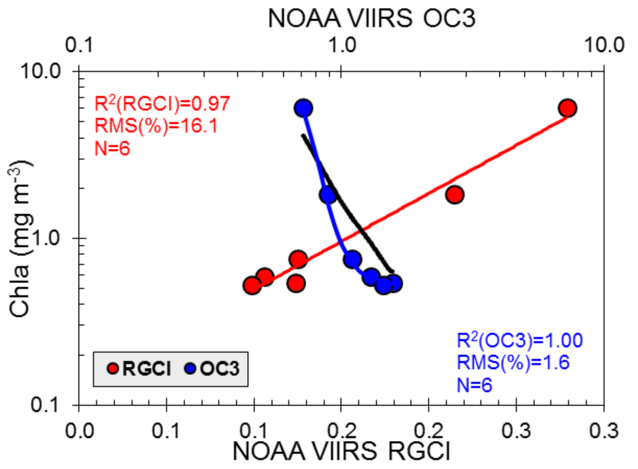

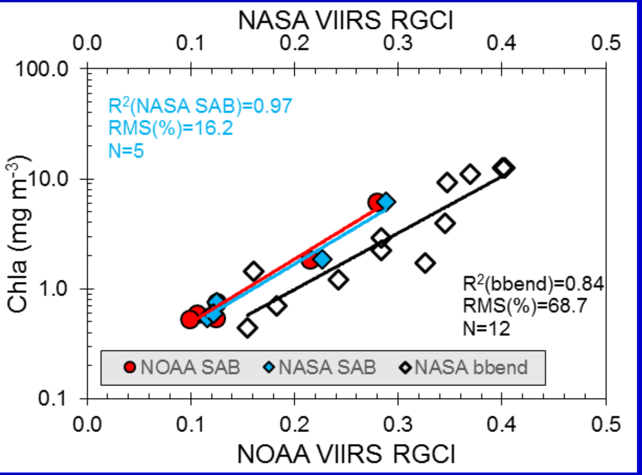

23 stations in total, each with about 3 depths measured. Only 6 found same day (+- 12 hours) VIIRS data.

RGCI for other coastal regions?

Test over the South Atlantic Bight using NOAA/VIIRS Nov 2014 cruise data

RGCI is not applicable in very low (< 0.2) or very high (> 10) chl waters

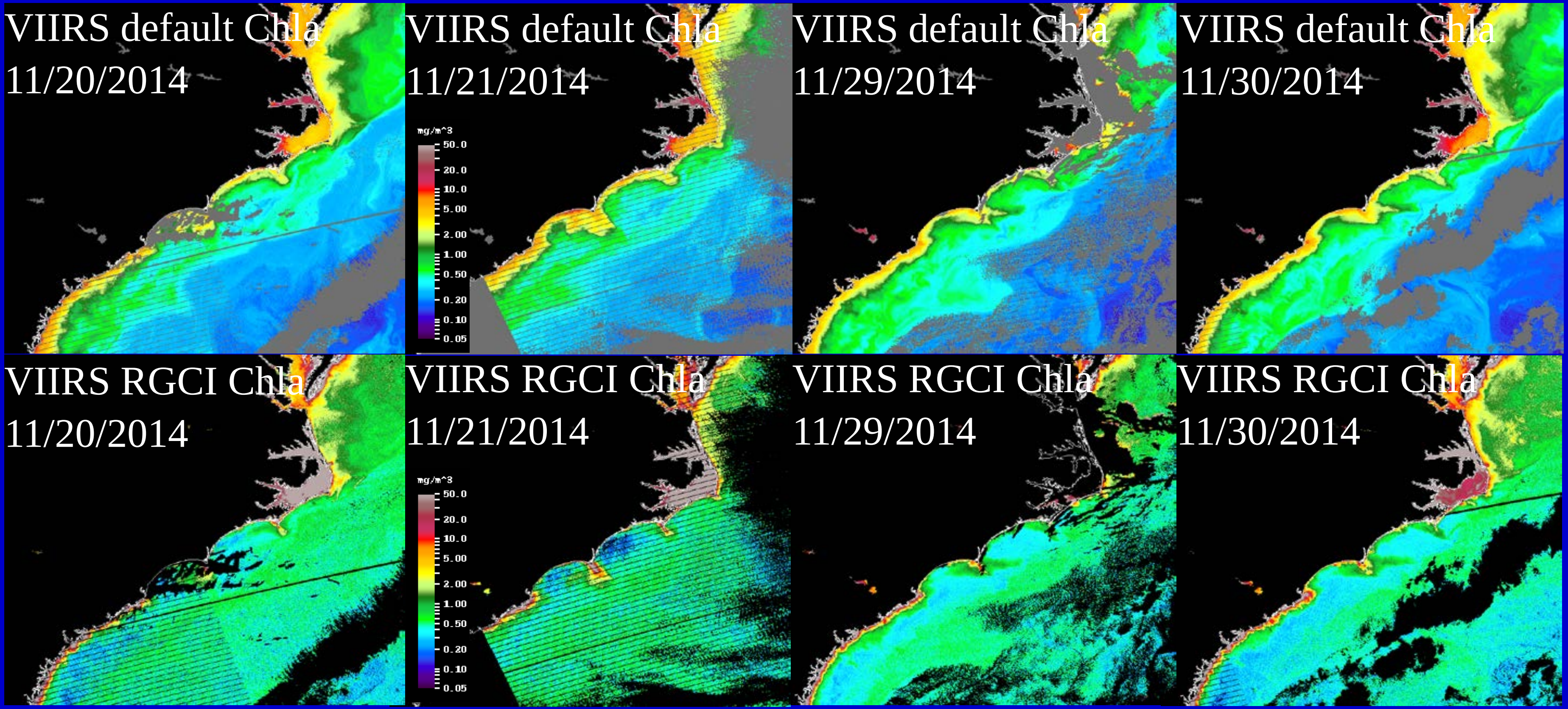

These results were derived from NOAA MSL12 processing

Cross-sensor comparison

SeaWiFS, MODIS, VIIRS products as a function of viewing angle, Gulf of Mexico

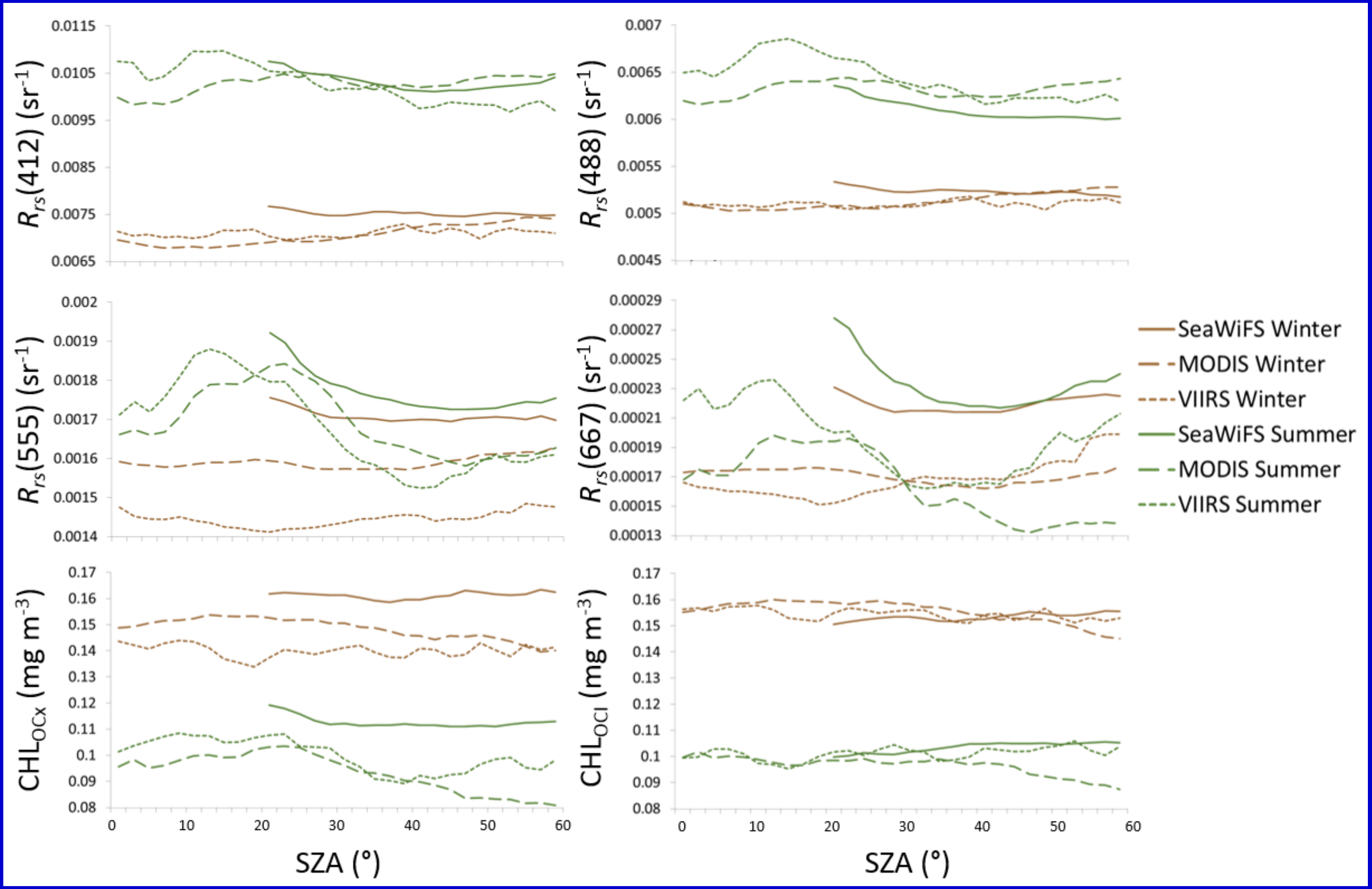

From Barnes and Hu (submitted, also see poster)

Summary

- Collected, processed, and shared field data through several dedicated cruises and cruises of opportunity
- Evaluated of VIIRS data from different processings (IDPS, NASA GSFC, NOAA MSL12)
- Demonstrated VIIRS capacity in detecting and monitoring dark water and HAB events

Publications

Hu, C., B. B. Barnes, L. Qi, et al. (2015). A harmful algal bloom of Karenia brevis in the northeastern Gulf of Mexico as revealed by MODIS and VIIRS: A comparison. Sensors, 15:2873-2887, doi:10.3390/s150202873.

Qi, L., C. Hu, J. Cannizzaro (in press). VIIRS observations of a Karenia brevis bloom in the Northeastern Gulf of Mexico in the absence of a fluorescence band. IEEE GRSL.

Barnes, B. B., and C. Hu (submitted). Dependence of satellite ocean color data products on viewing angles: A comparison between SeaWiFS, MODIS, and VIIRS. RSE.

Barnes, B. B., and C. Hu (2015). Cross-sensor continuity of satellite-derived water clarity in the Gulf of Mexico: Insights into temporal aliasing and implications for long-term water clarity assessment. IEEE Trans. Geosci. & Remote Sens., 53:1761-1772.

What’s Next?

- Continue field and laboratory experiments to support VIIRS cal/val and science applications
  - Finish processing data from past cruises
  - Participate in new cruises
- Continue evaluation of VIIRS products, especially from MSL12 processing
  - Use data collected by the Cal/Val team
  - Extend to data collected by other groups
- Improve algorithms and data products to have better absolute accuracy and relative consistency
  - Biooptical properties
  - Blooms and other image features
- Publish results in journal articles and promote VIIRS II

Backup slide: relax to 12-day matchup instead of 1-day matchup for SAB cruise

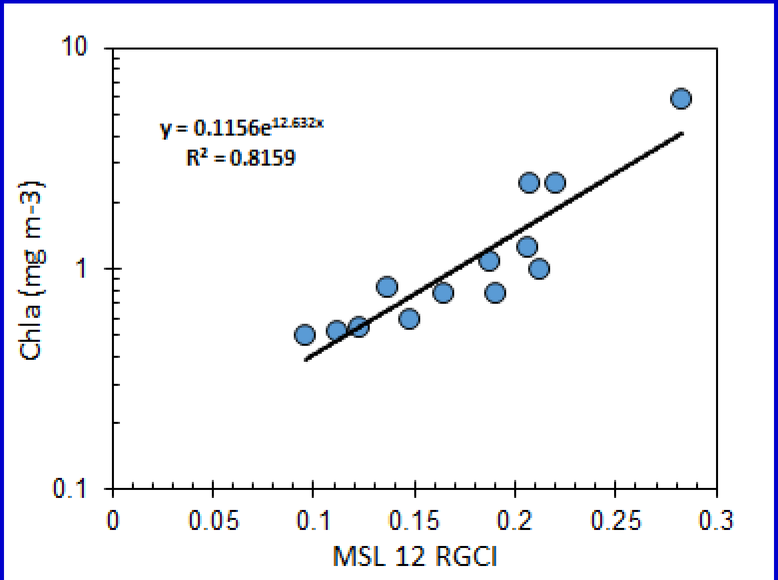

Towards consistent VIIRS AOP and IOP products

ZhongPing Lee, JunFang Lin, JianWei Wei, Lin Qi

University of Massachusetts Boston

UMB activities:

1. Evaluation of VIIRS Rrs products

1a. Compare VIIRS Rrs with climatological Rrs of gyre waters

1b. Compare VIIRS Rrs with in situ measurements

1c. Compare VIIRS Rrs with concurrent MODIS Rrs

1d. Compare Rrs from fixed platform

2. Measurement and processing of in situ IOPs

2a. Participate NOAA Cal/Val cruise

2b. Scattering correction of the ac-s system

3. Application of in situ measurements

Hyperspectral absorption coefficient of “pure” seawater derived from in situ Rrs

1a. Compare VIIRS Rrs with climatological Rrs of gyre waters

Band characteristics

	VIIRS		MODISA	
	CW [nm]	Bandwidth [nm]	CW [nm]	Bandwidth [nm]
M1	410	20	412	15
M2	443	15	442	10
M3	486	19	488	10
M4	551	19	547	10

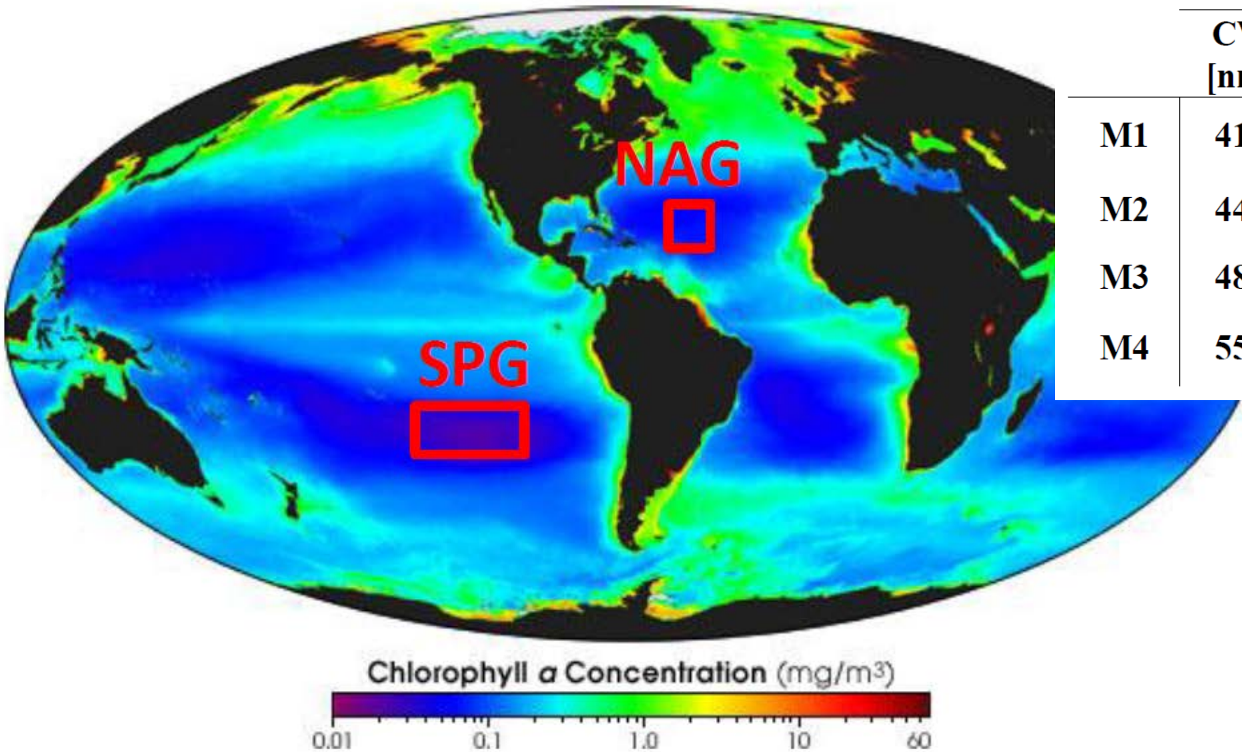

Location: South Pacific Gyre (SPG) and North Atlantic Gyre (NAG)

Data: VIIRS (from CLASS), 5/2013-2/2014
MODIS_Aqua (from OBPG; daily-climatology)
all are area average

South Pacific Gyre (SPG)

Ocean color comparisons between CoastWatch <1-year data and MODIS Aqua 10-year climatology

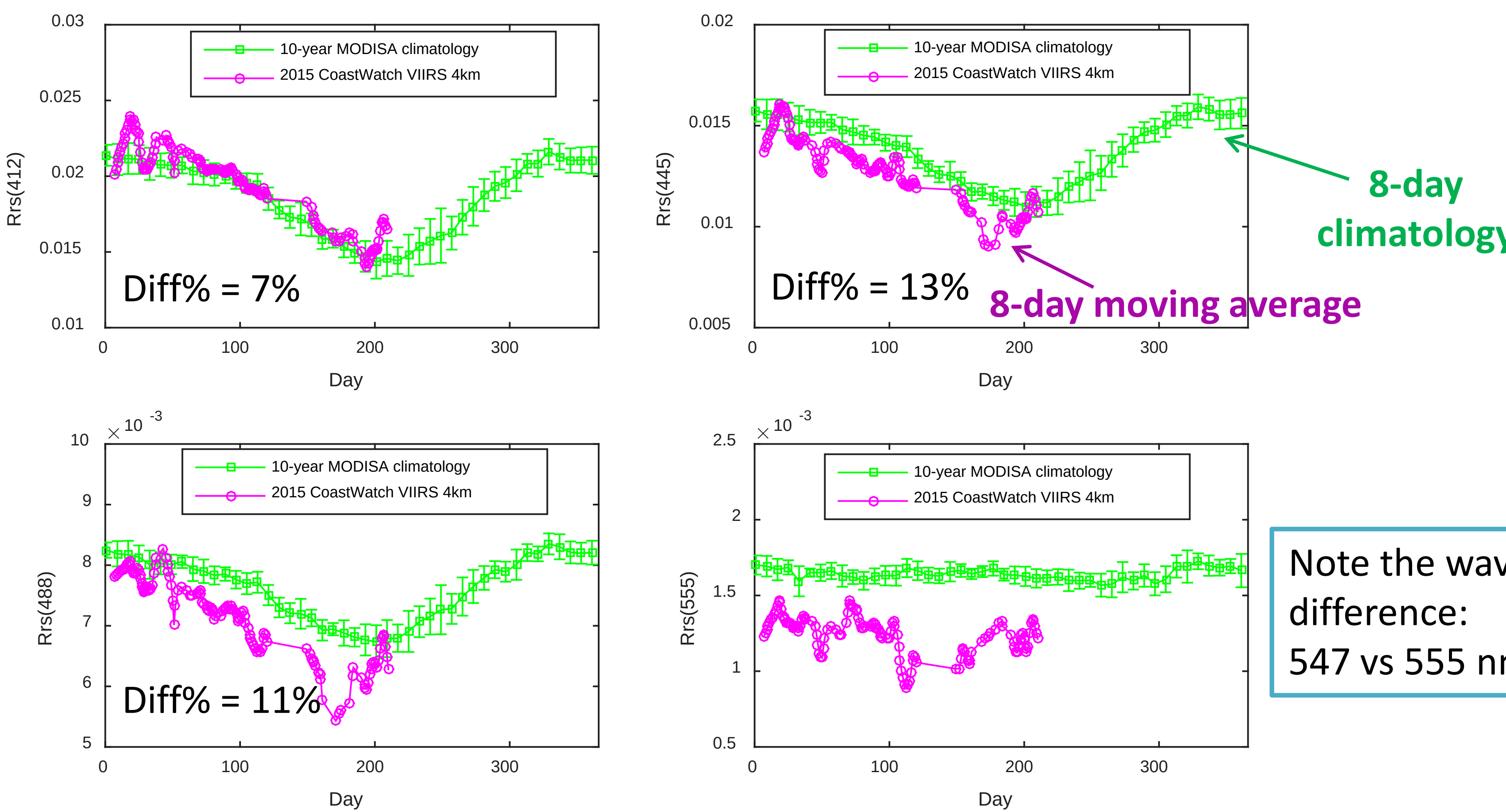

Note the wave
difference:
547 vs 555 nm

North Atlantic Gyre (NAG)

Ocean color comparisons between CoastWatch <1-year data and MODIS Aqua 10-year climatology

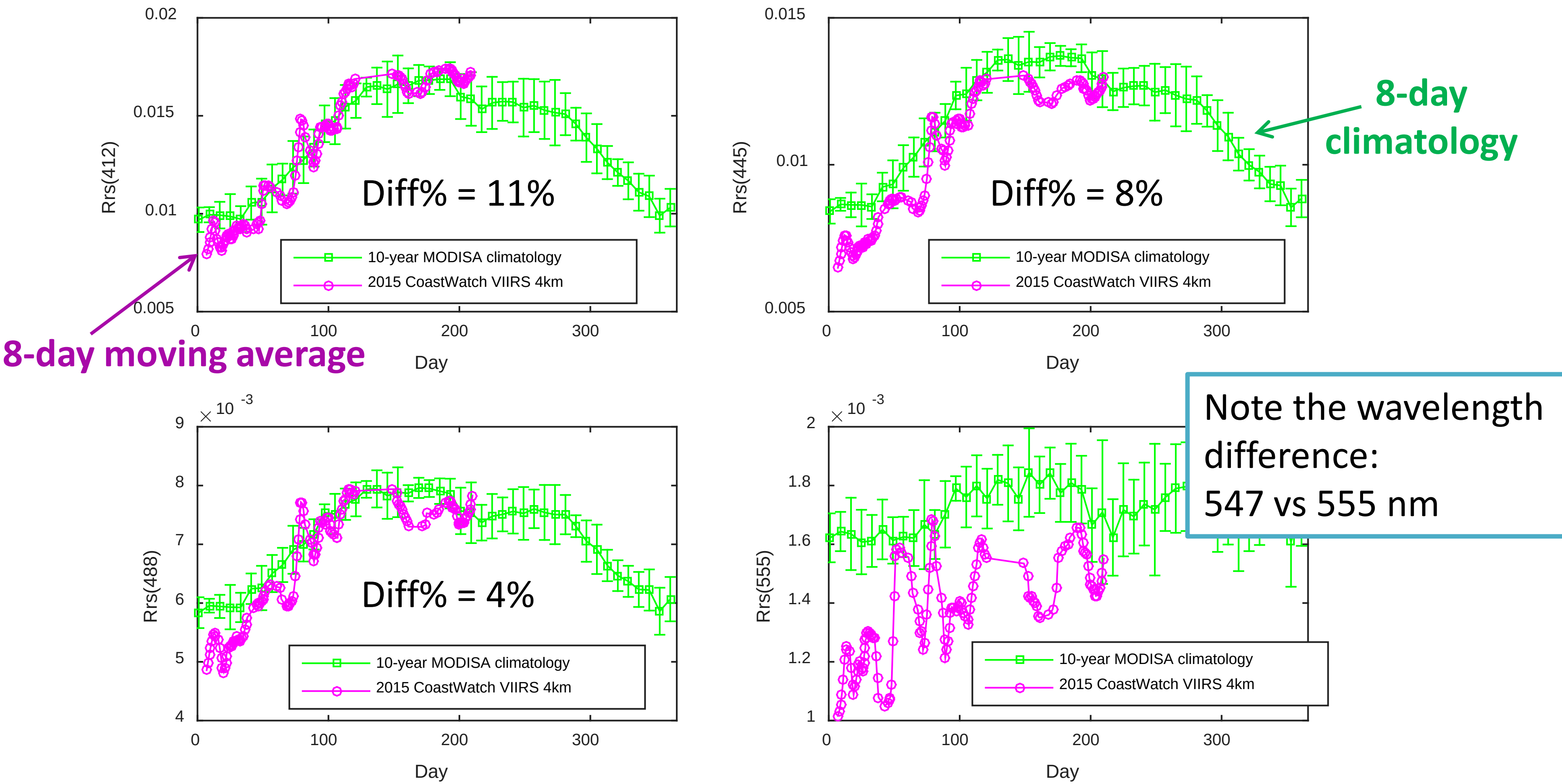

CoastWatch VIIRS Rrs at subtropic gyres are generally consistent with MODIS-A climatology; but occasionally display unexpected values.

1b. Compare VIIRS Rrs with in situ measurements

SBA-VIIRS Data Comparison

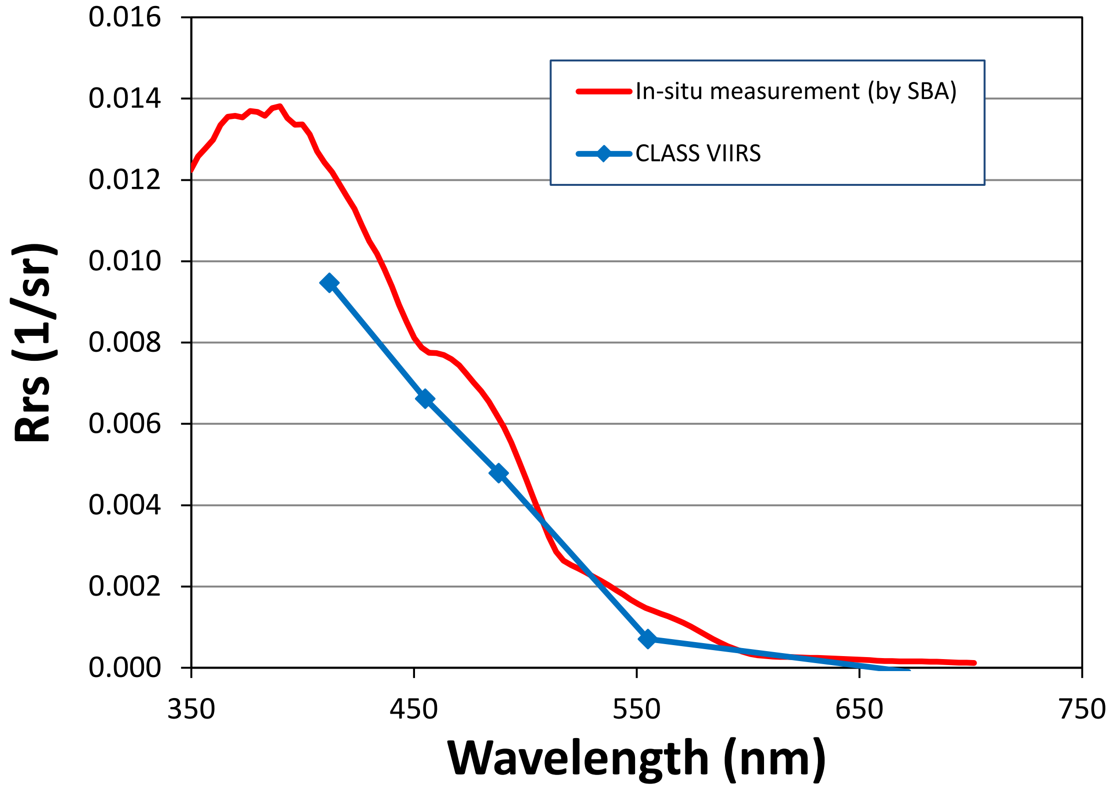

VIIRS data was averaged over 9 pixels.

Caribbean Sea (Puerto Rico) Experiments
Dec-13-2014

20141213, VIIRS overpass at 17:00pm
Clear sky; 1.5 m waves;
Time difference: **~1 hrs**

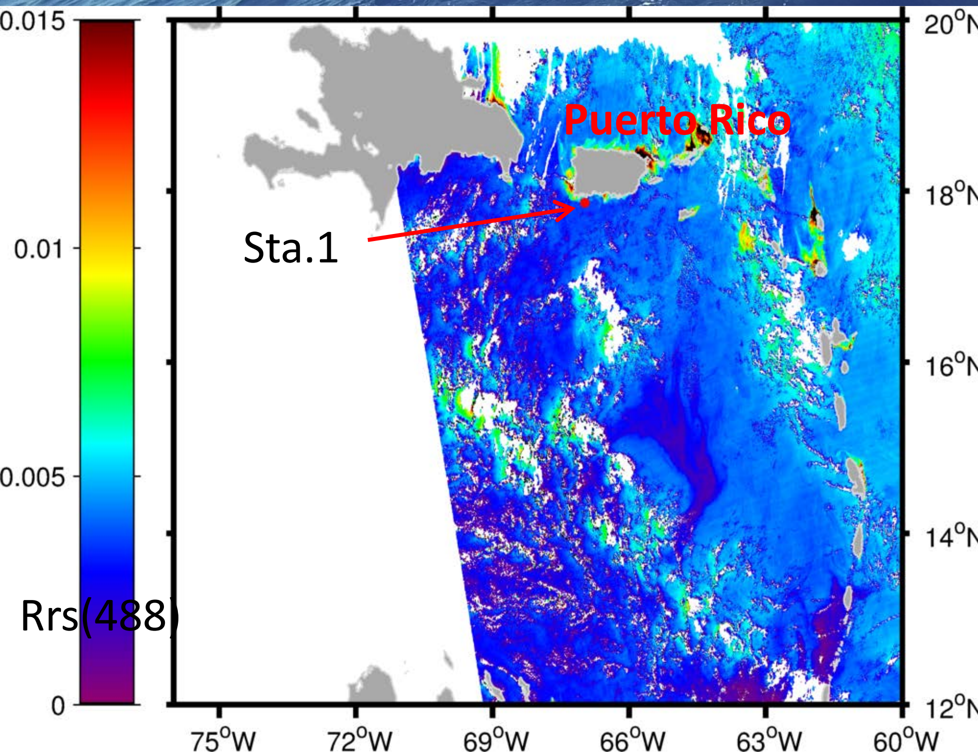

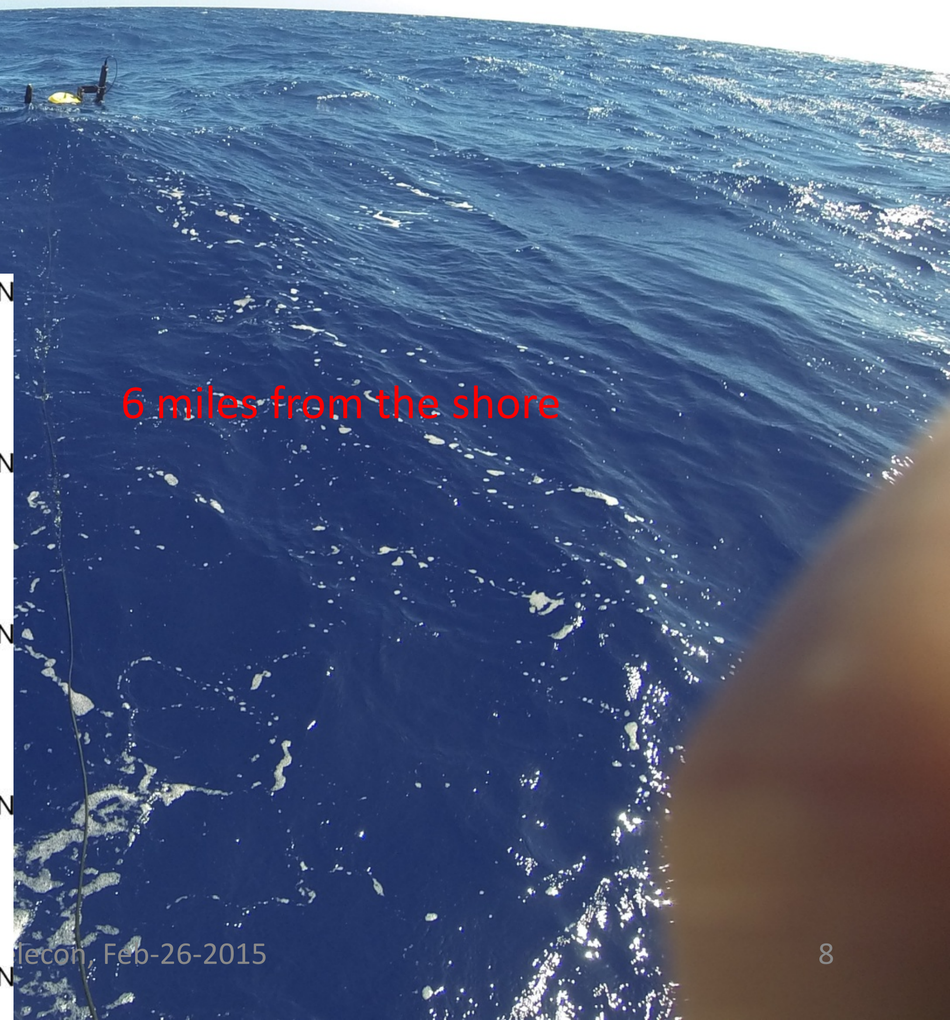

Comparison of in-situ Rrs, CLASS VIIRS and CoastWatch VIIRS products

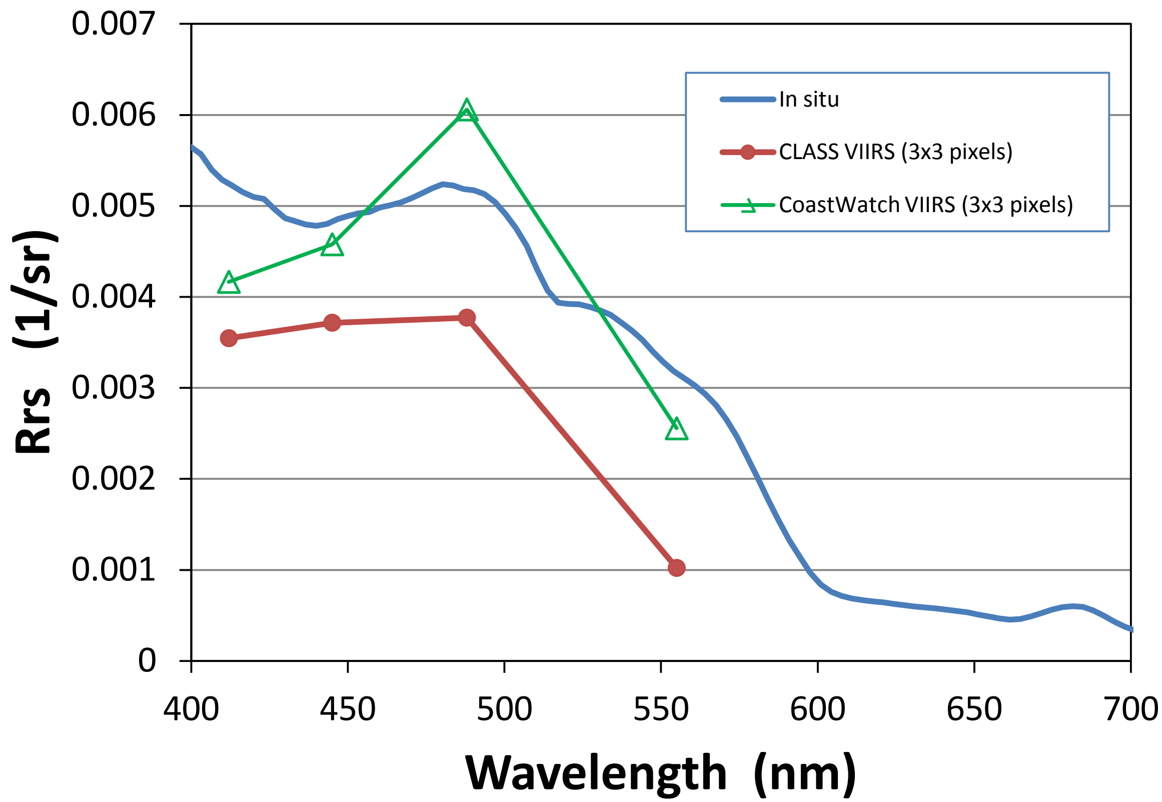

CoastWatch VIIRS products show much better results in this region.

CLASS VIIRS Ocean Color EDR

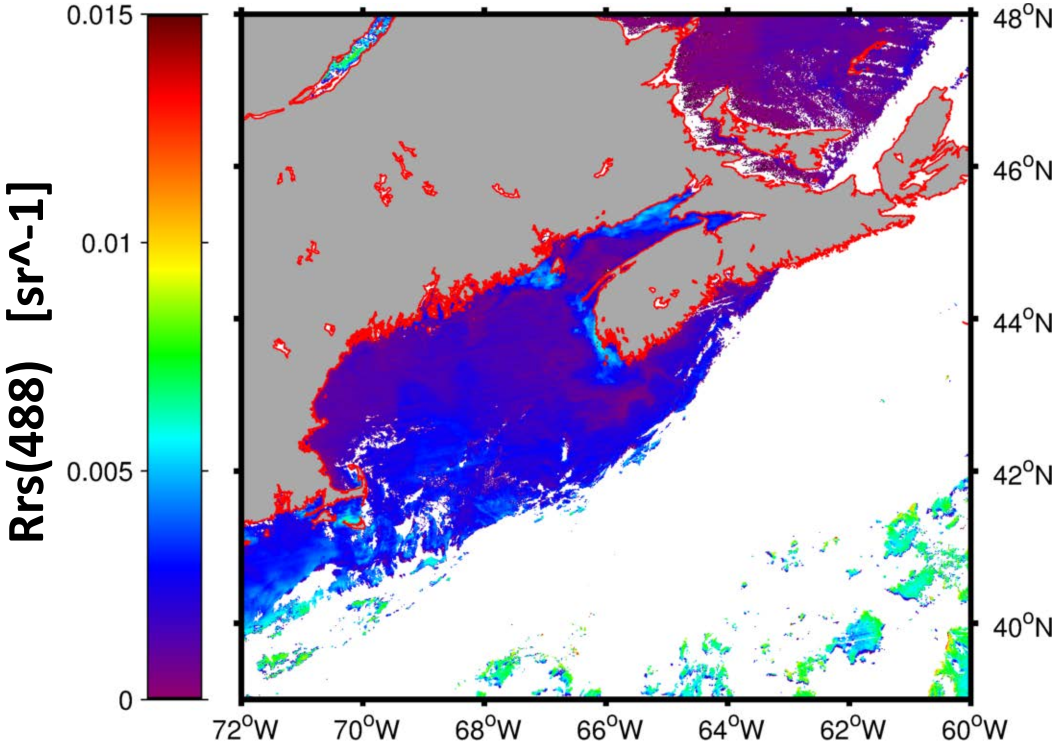

The VIIRS ocean color EDR data is used as is, without further quality control. (Considering ATMWARN flag, all data in Massachusetts Bay can be questionable)

Rrs spectra comparison

STA1

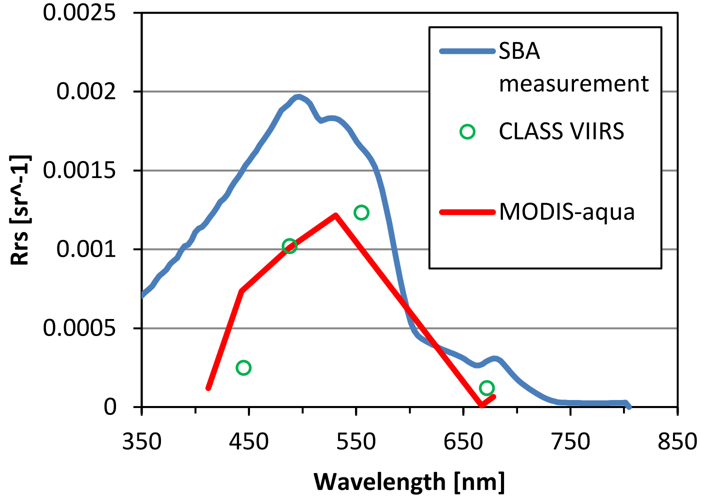

STA2

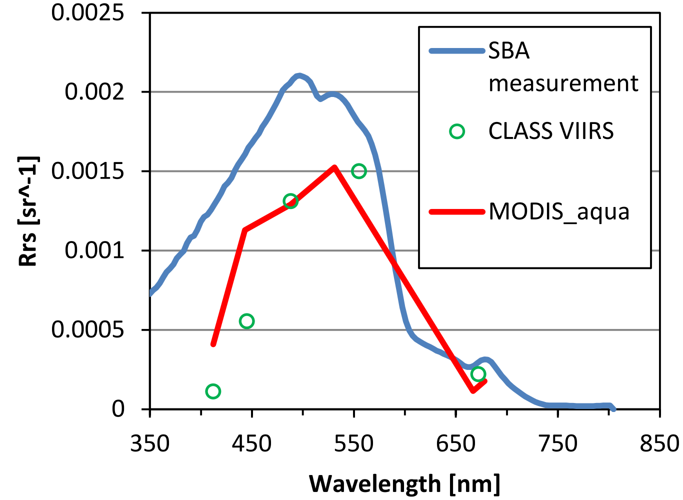

STA3

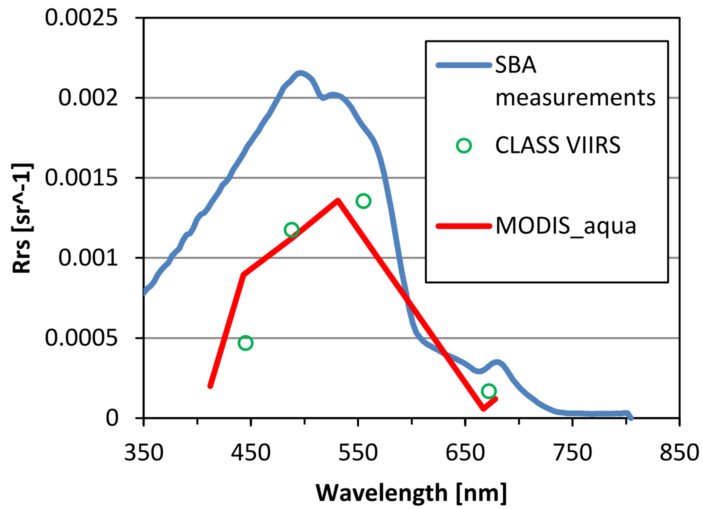

STA4

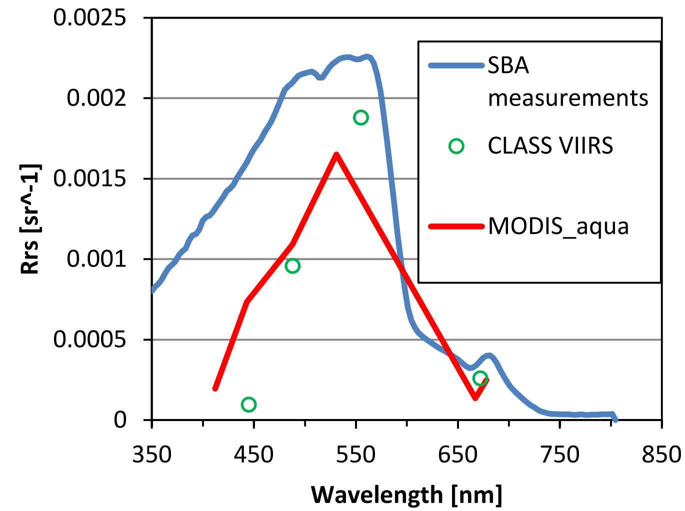

CLASS VIIRS products VS in situ measurements

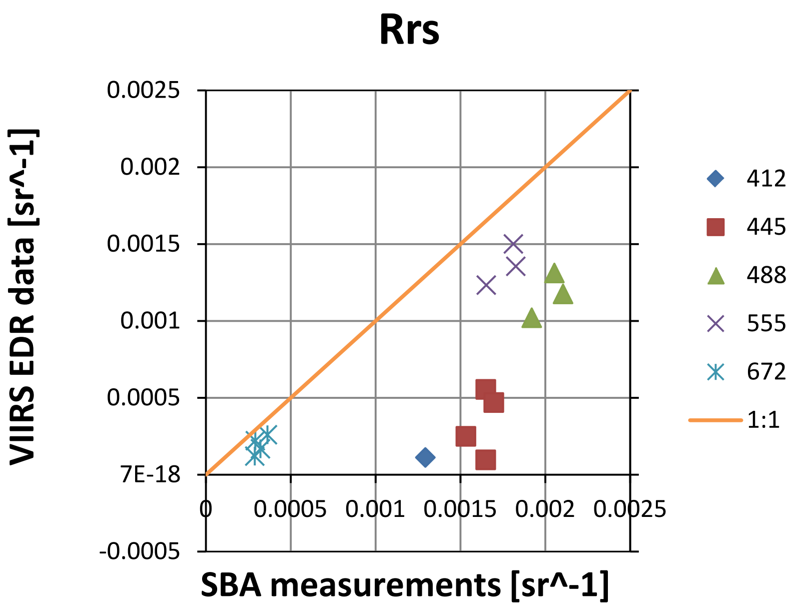

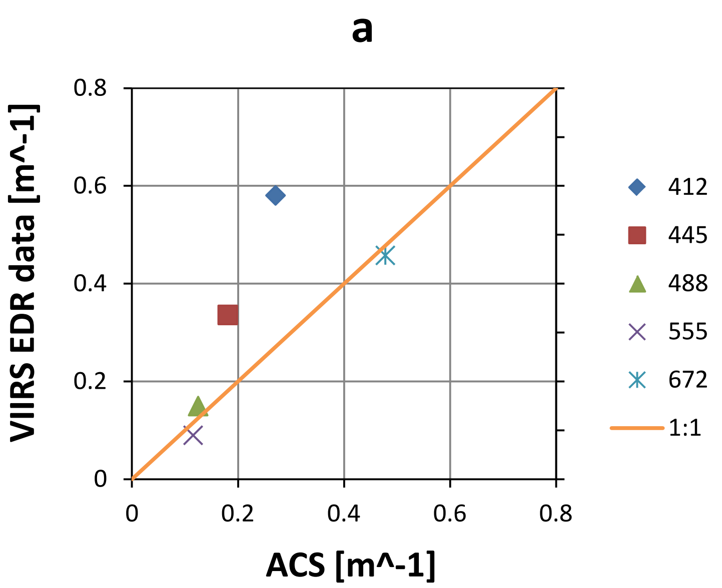

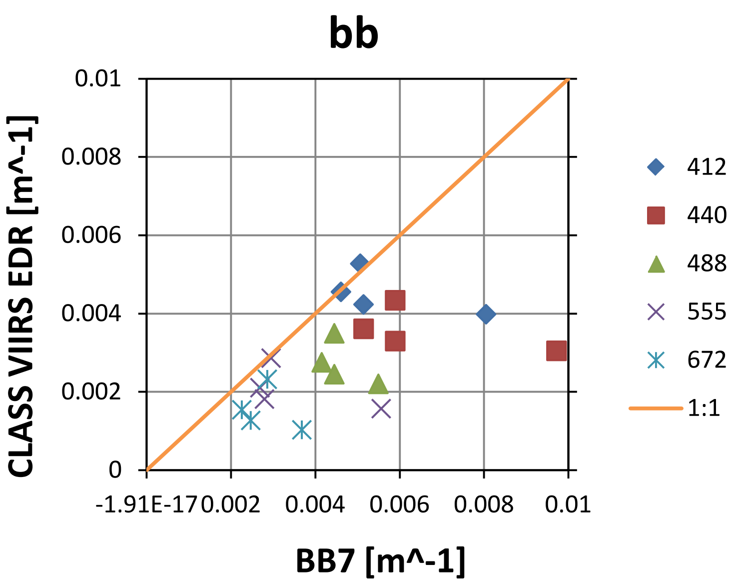

1c. Compare VIIRS Rrs with concurrent MODIS Rrs

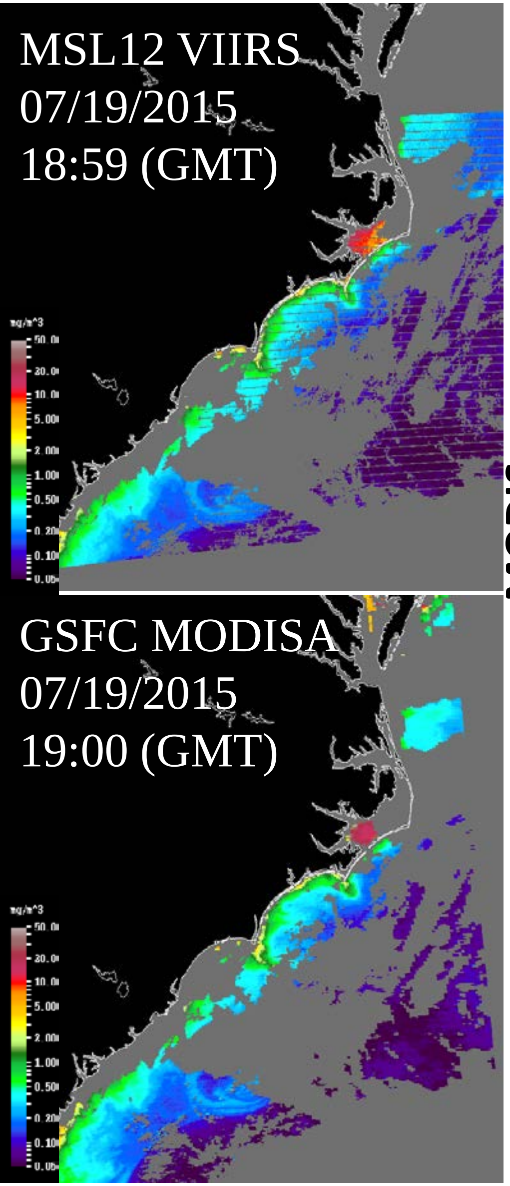

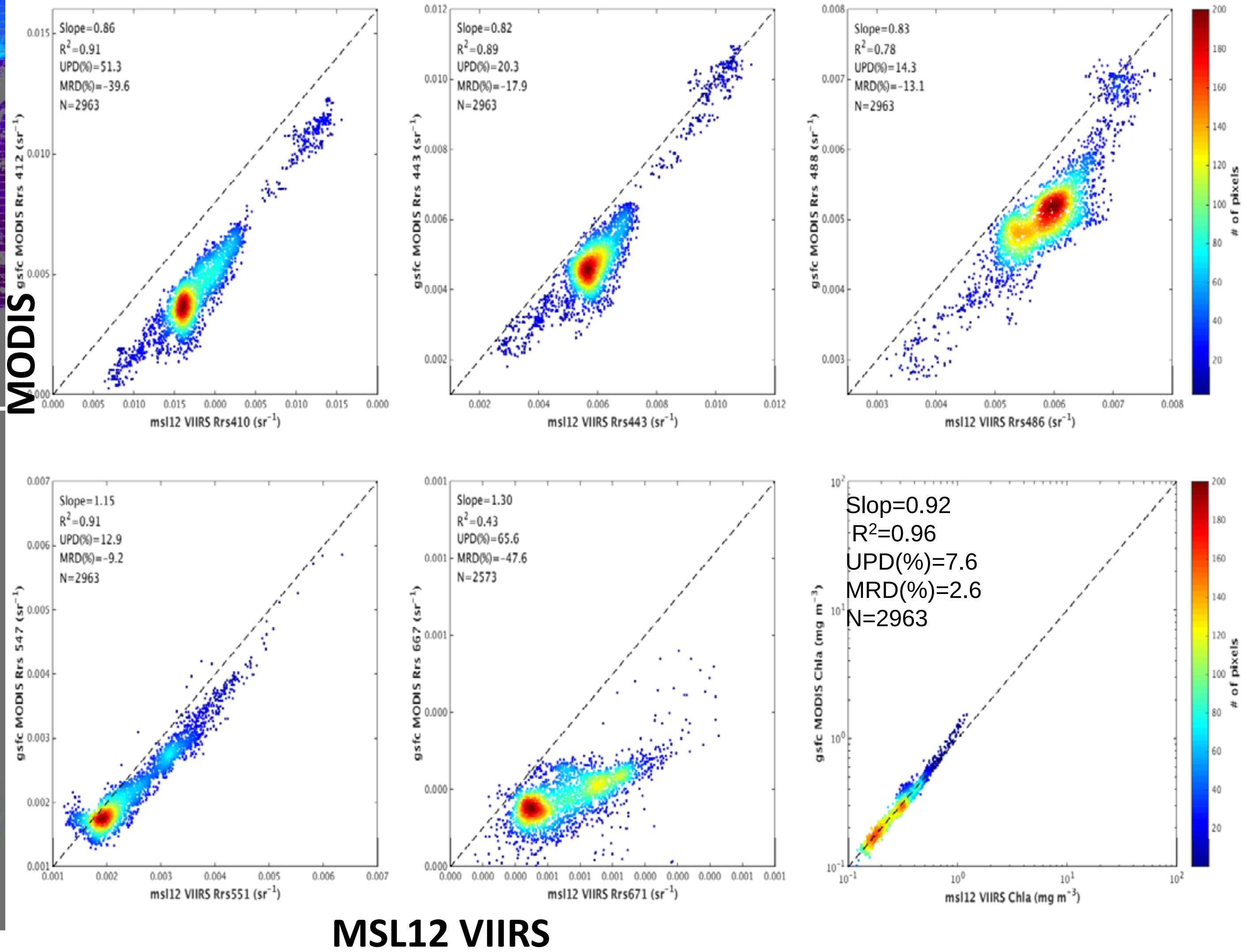

1c. Compare VIIRS Rrs with concurrent MODIS Rrs

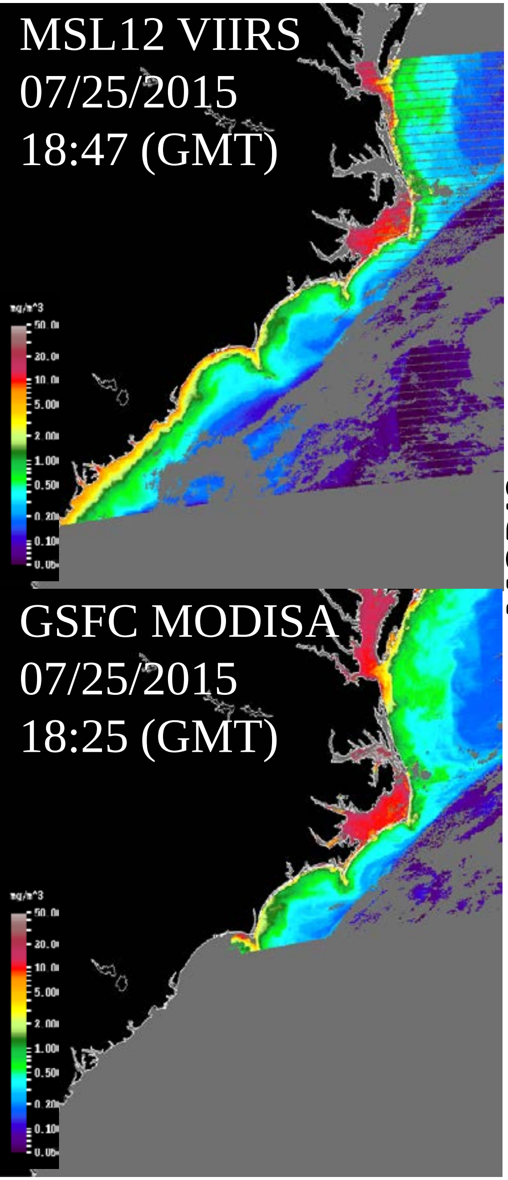

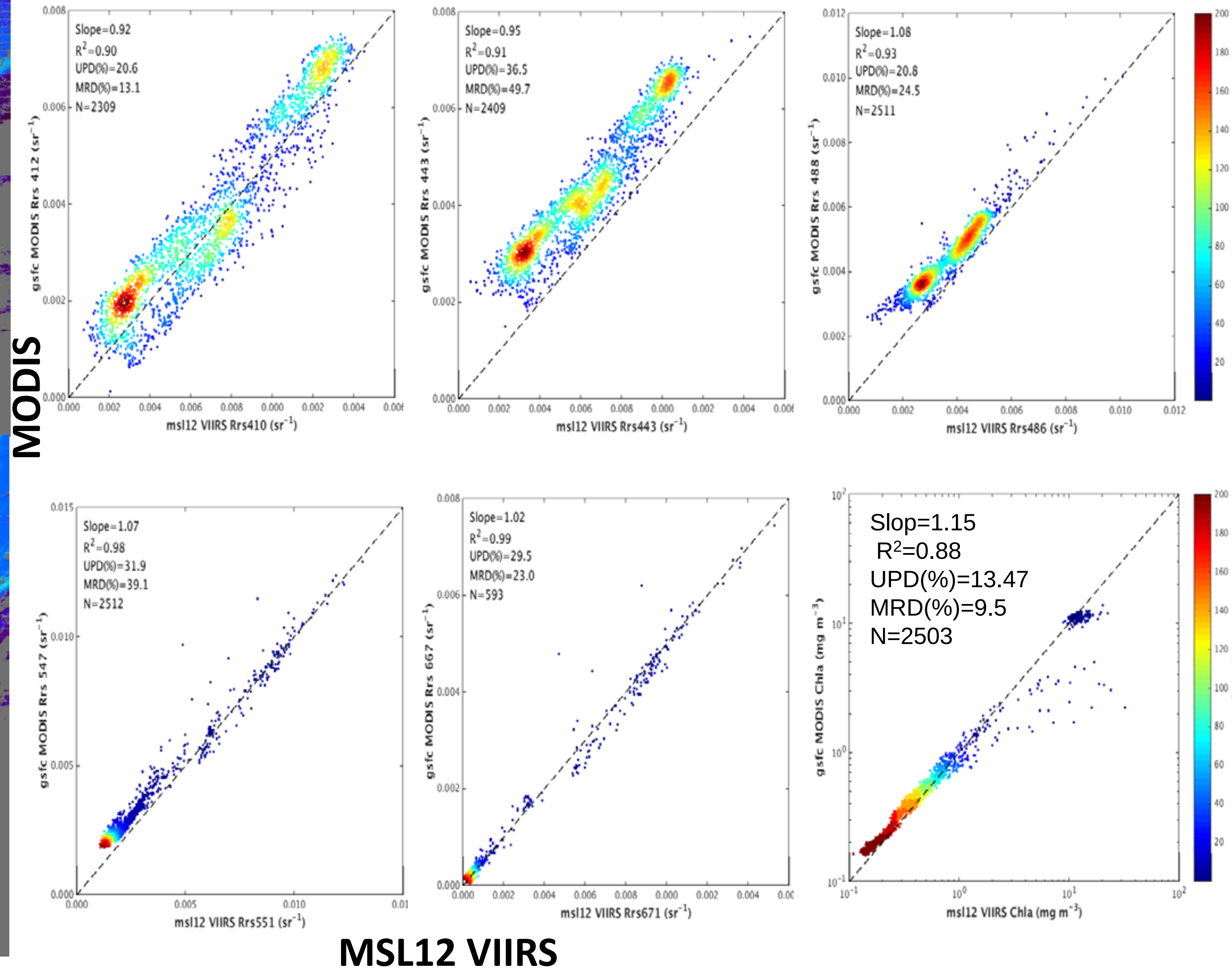

1d. Compare Rrs from fixed platform

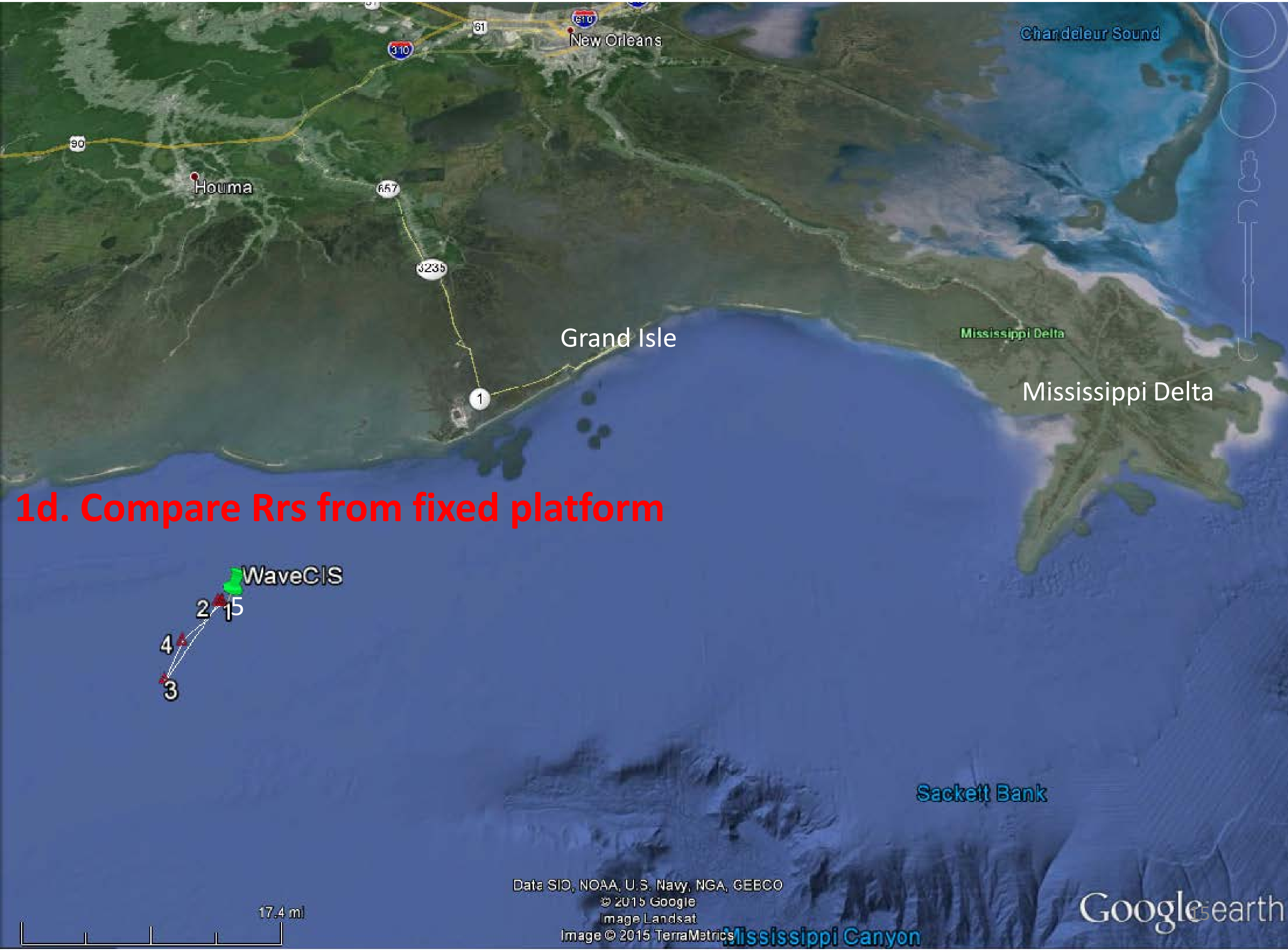

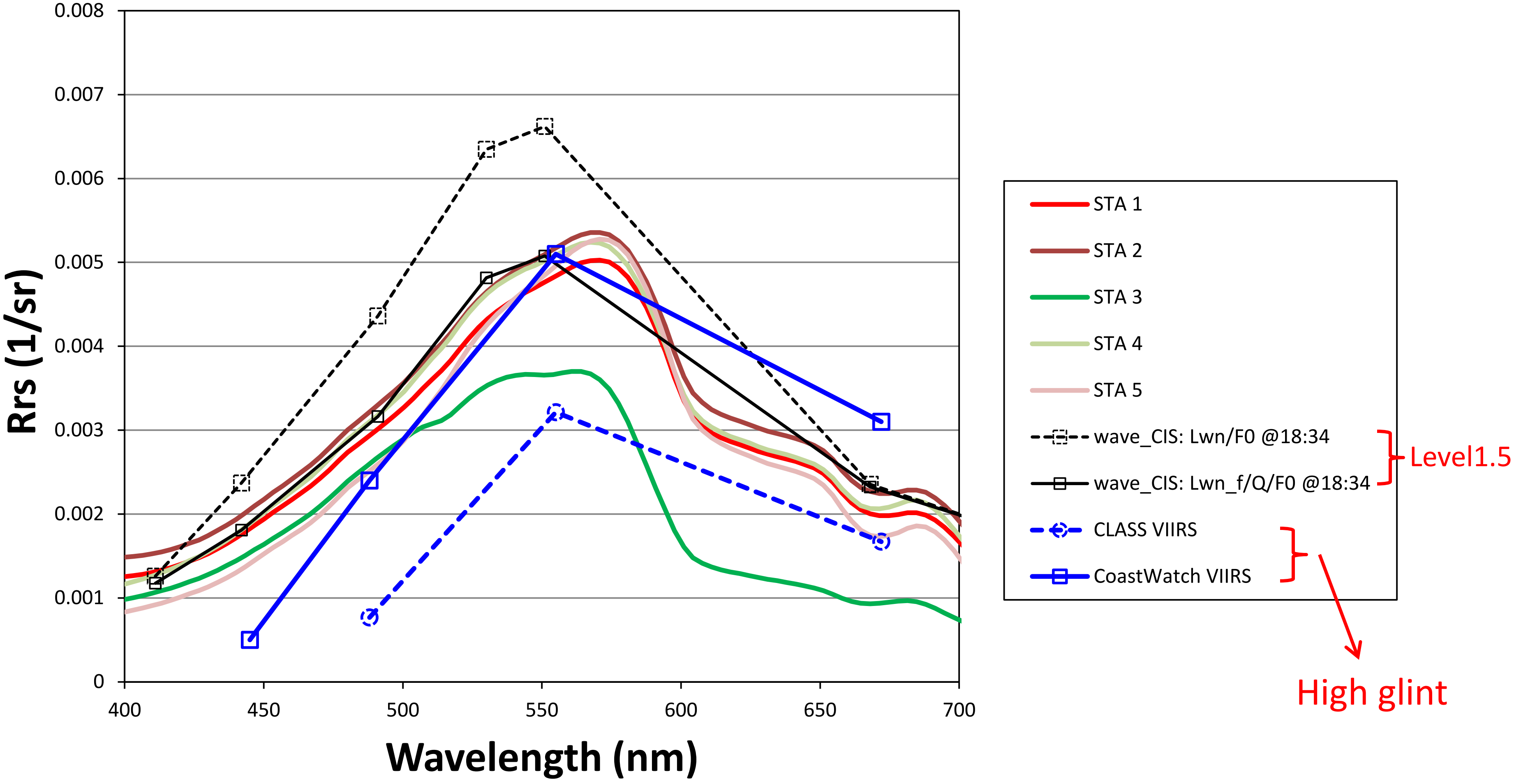

0.008
0.007
0.006
0.005
0.004
0.003
0.002
0.001
0
Rrs (1/sr)
400
450
500
550
600
650
700
Wavelength (nm)
STA 1
STA 2
STA 3
STA 4
STA 5
wave_CIS: Lwn/F0 @18:34
wave_CIS: Lwn_f/Q/F0 @18:34
CLASS VIIRS
CoastWatch VIIRS
Level1.5
High glint

2a. Participate NOAA Cal/Val cruise

VIRRS Cruise (11/11/2014 - 11/20/2014)

VIRRS	Days	ACSs	BB9	SBA	Spectral Evolution (SR1900)
N	10	21	21	21	11

ECOA Cruise Leg1 (6/17/2015 - 7/3/2015)

ECOA	Days	ACS	HS6	Hyper-Pro	ASD	Micro-TOP
N	17	26	26	20	25	25

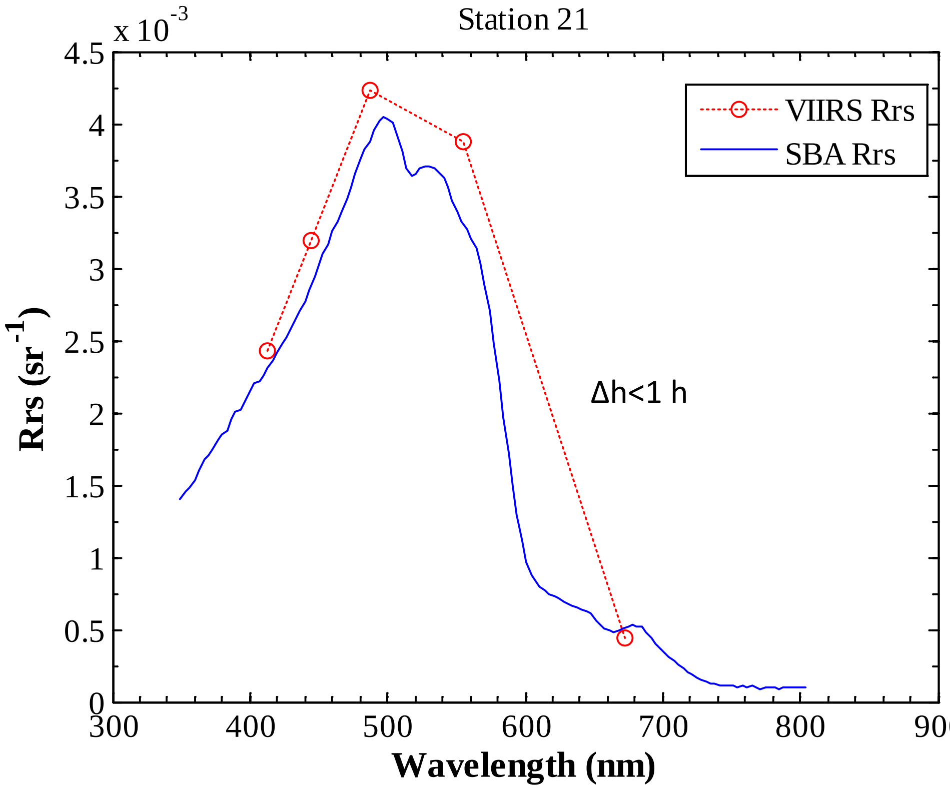
Station 21
x 10^-3
Rrs (sr^-1)
Wavelength (nm)
VIIRS Rrs
SBA Rrs
Δh<1 h

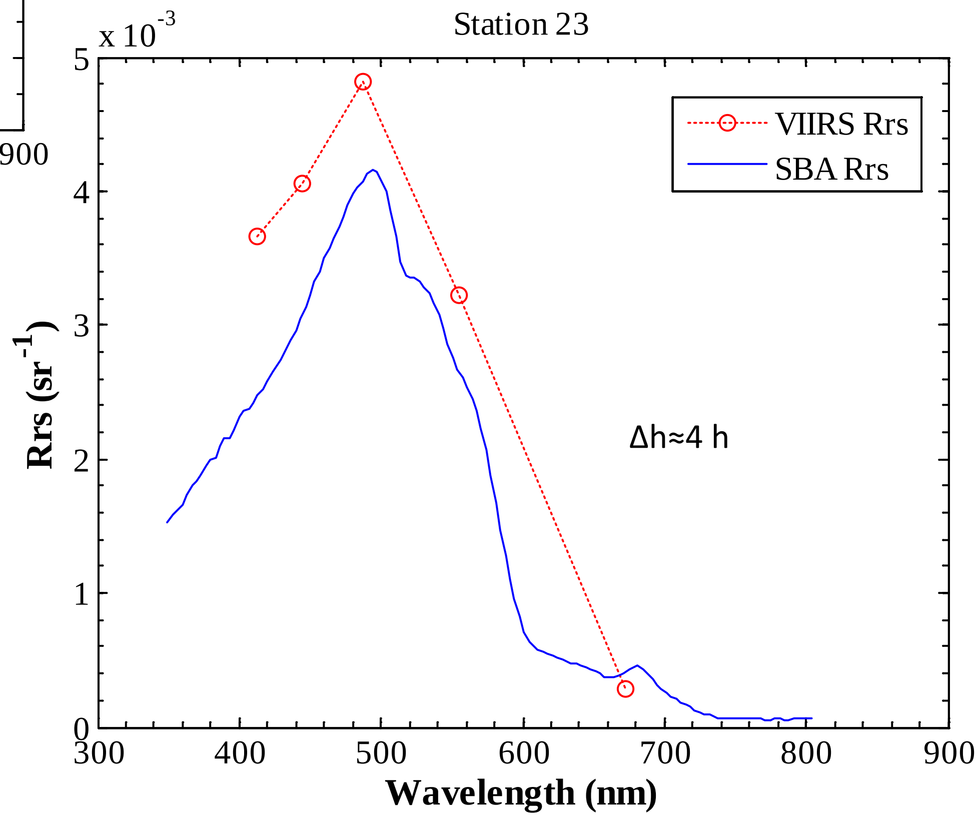
Station 23
x 10^-3
Rrs (sr^-1)
Wavelength (nm)
VIIRS Rrs
SBA Rrs
Δh≈4 h

2b. Scattering correction of the ac-s system

Proportional Scattering Correction

$$a(\lambda) = a(\lambda) - \varepsilon \cdot [c(\lambda) - a(\lambda)], \quad \boxed{\varepsilon = 0.18}$$

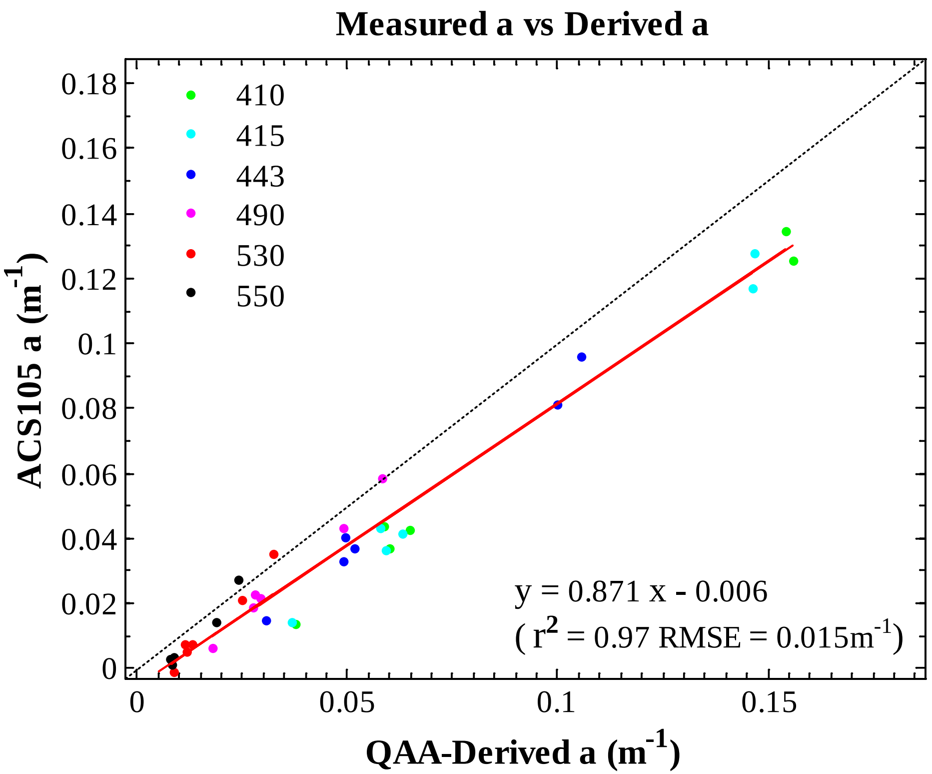

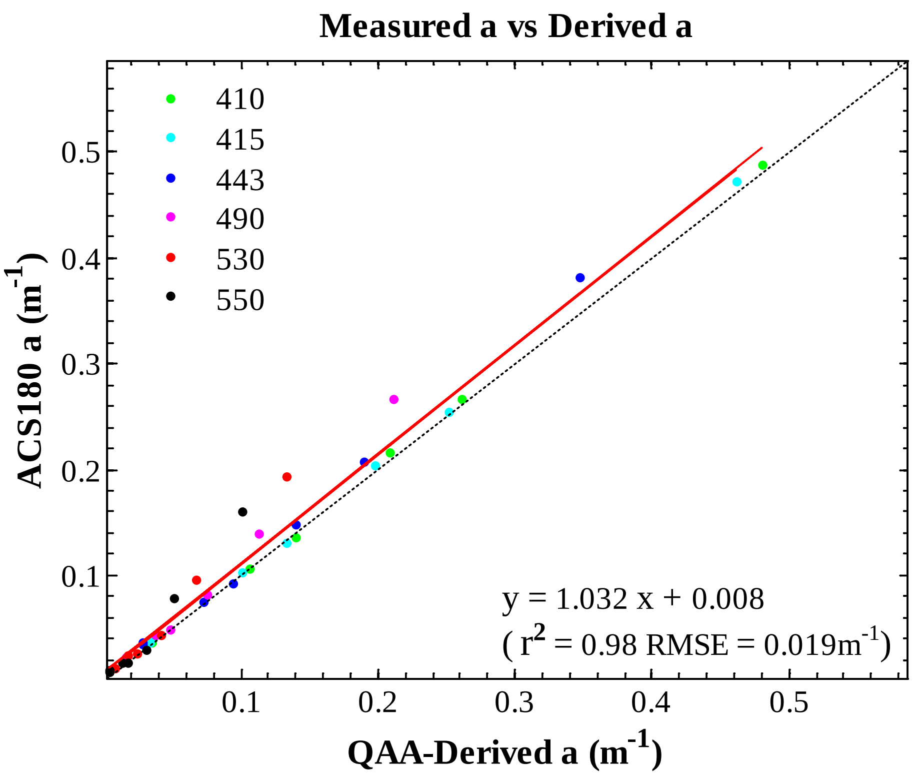

A value of ~0.18 has been suggested for ε when sediments dominate the scattering (Kirk ,1993).

3. Application of in situ measurements

Hyperspectral absorption coefficient of “pure” seawater derived from in situ Rrs

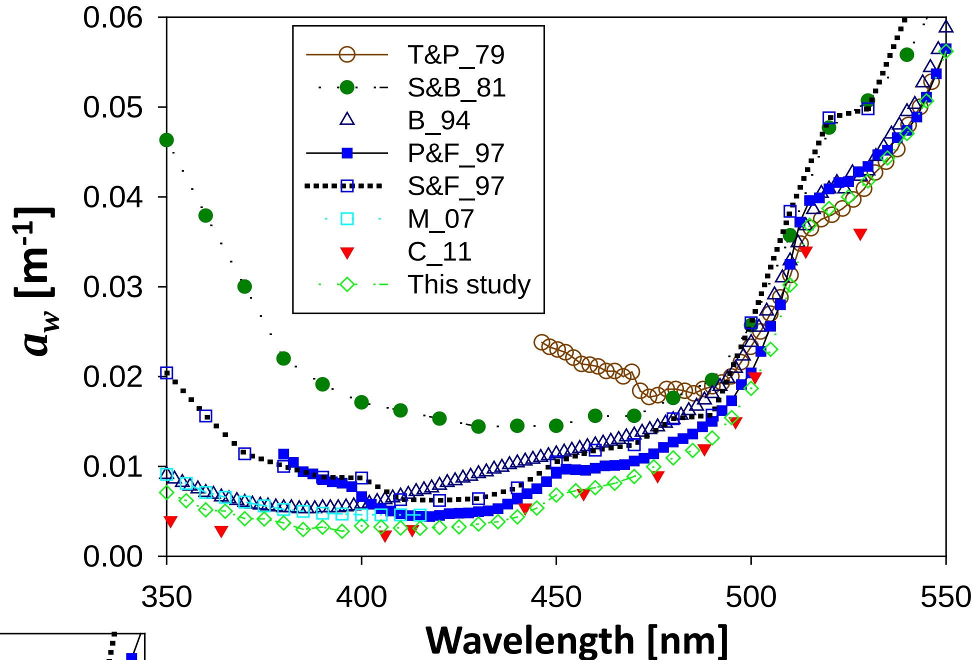

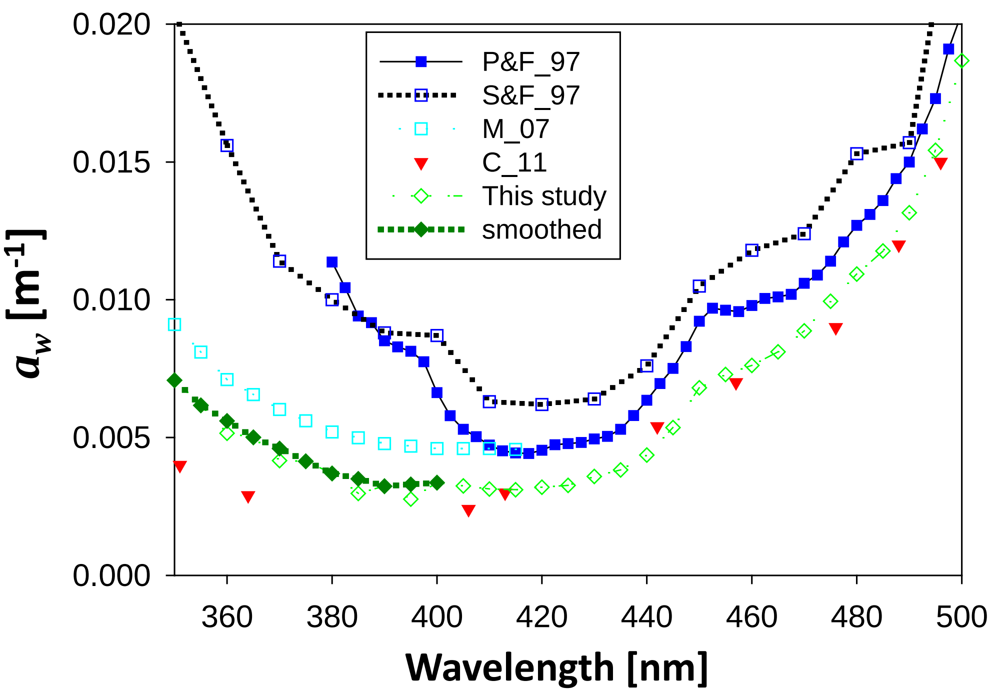

(Lee, Wei, Voss, Lewis, Bricaud, Huot, 2014, “ Hyperspectral absorption coefficient of "pure" seawater in the 350-550 nm range inverted from remote-sensing reflectance,” Appl. Opt., Vol .54, 546-558).

Plan of FY15

Continue …

1a. Compare VIIRS Rrs with climatological Rrs of gyre waters

1b. Compare VIIRS Rrs with concurrent MODIS Rrs

1c. Compare VIIRS Rrs with in situ measurements
(Puerto Rico, Mass Bay, other opportunities)

2a. Participate NOAA Cal/Val cruise to collect AOP/IOP

Acknowledgements:

NOAA/STAR

Thank you!

" Present Status of MOBY and MOBY-Refresh"

UNIVERSITY OF MIAMI

Kenneth Voss, Physics Dept., Univ of Miami

Collaborators: Carol Johnson (NIST), Mark Yarbrough (and others at MLML), Art Gleason (UM), Yong Sung Kim and Paul DiGiacomo (NOAA/NESDIS/STAR)

8/15, STAR JPSS 2015 annual meeting, College Park, Md.

The current MOBY site is off of Lanai, Hawaii.

Tent constructed on UHMC site

Ships available

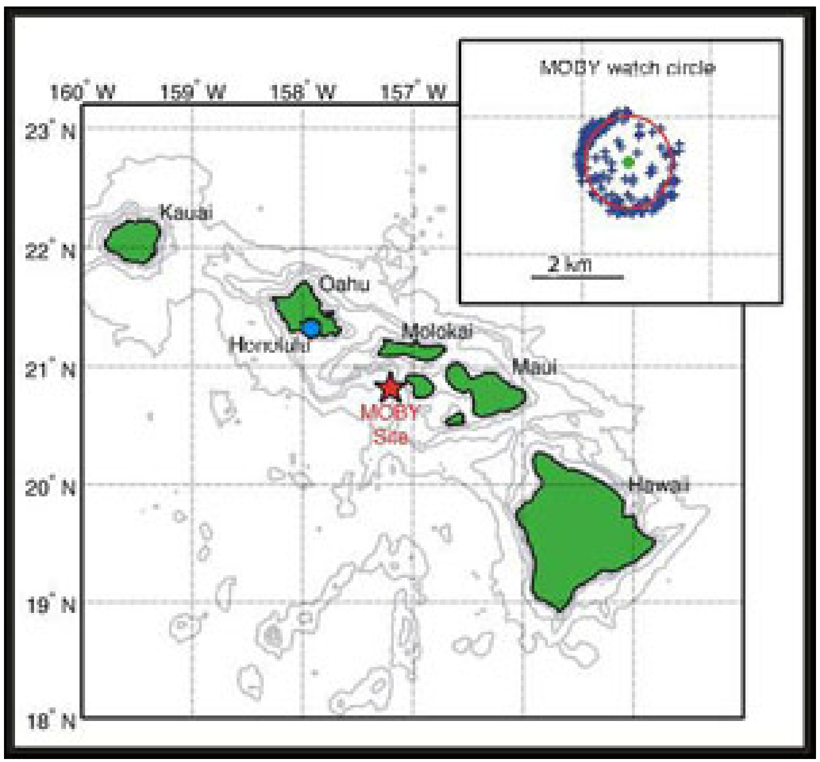

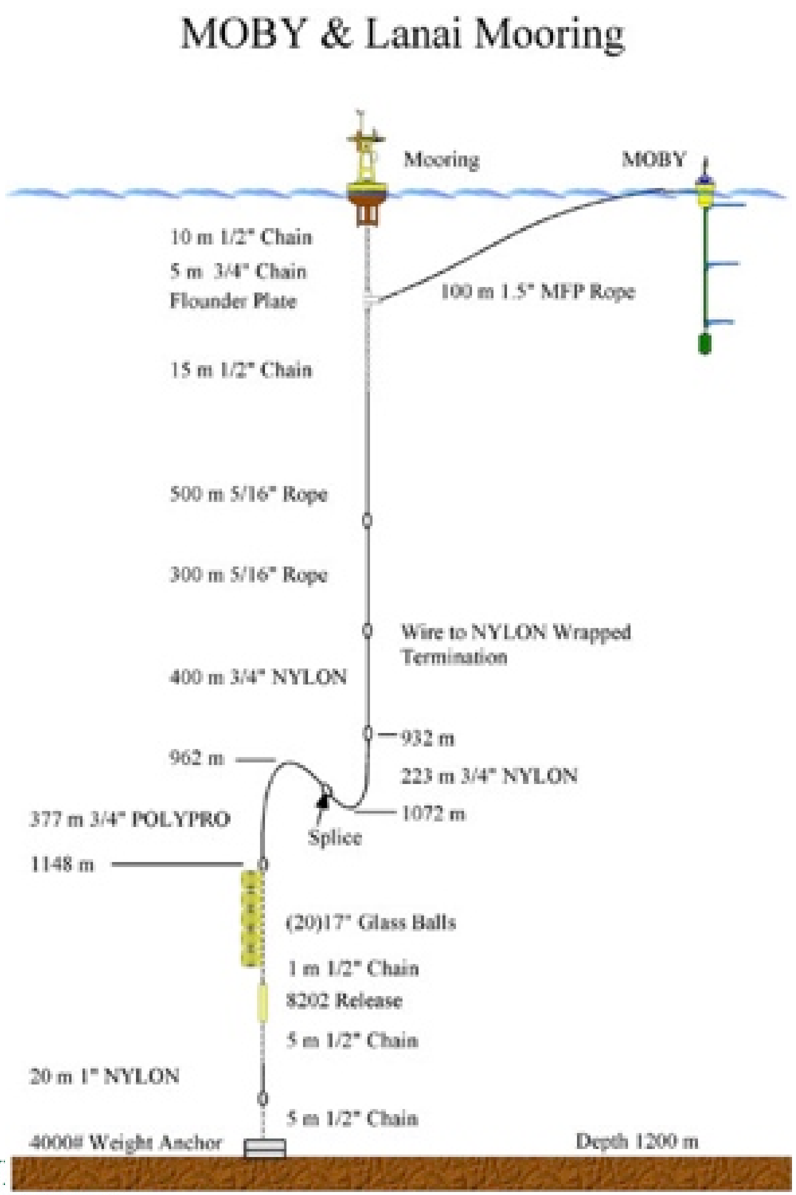

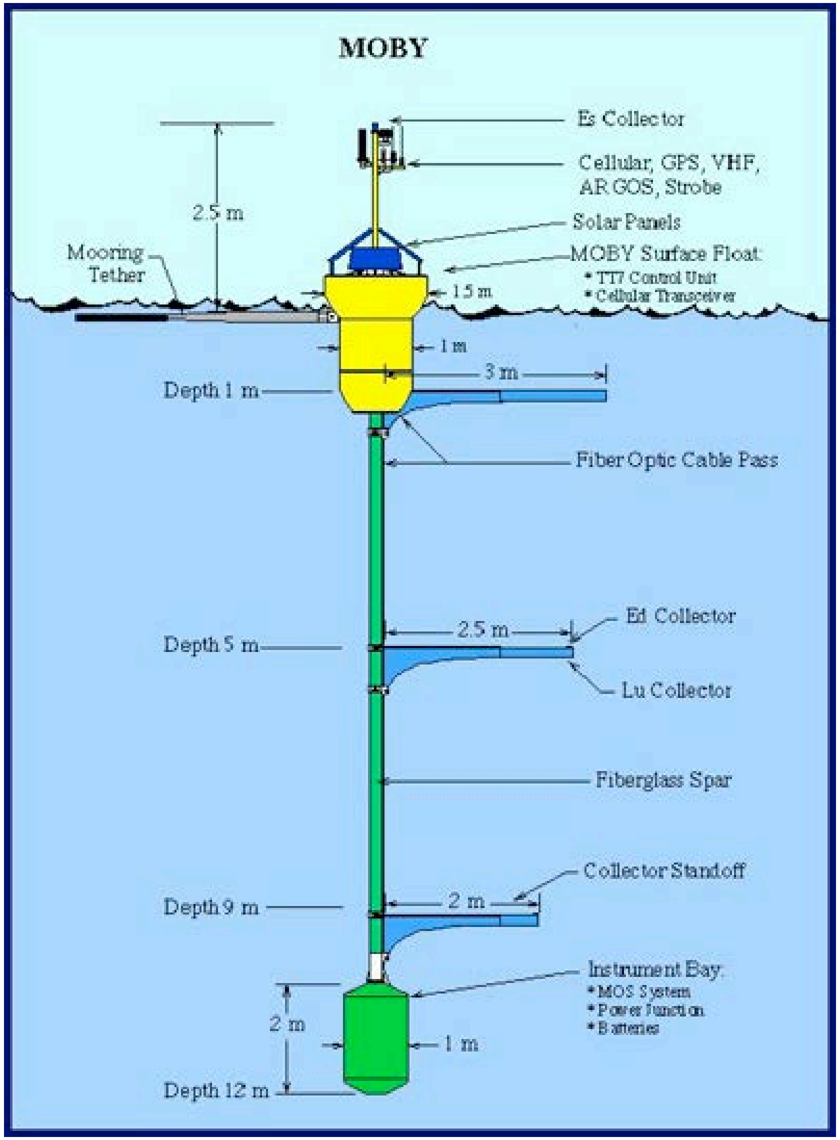

UNIVERSITY OF MIAMI

Currently have a 17 yr + time series

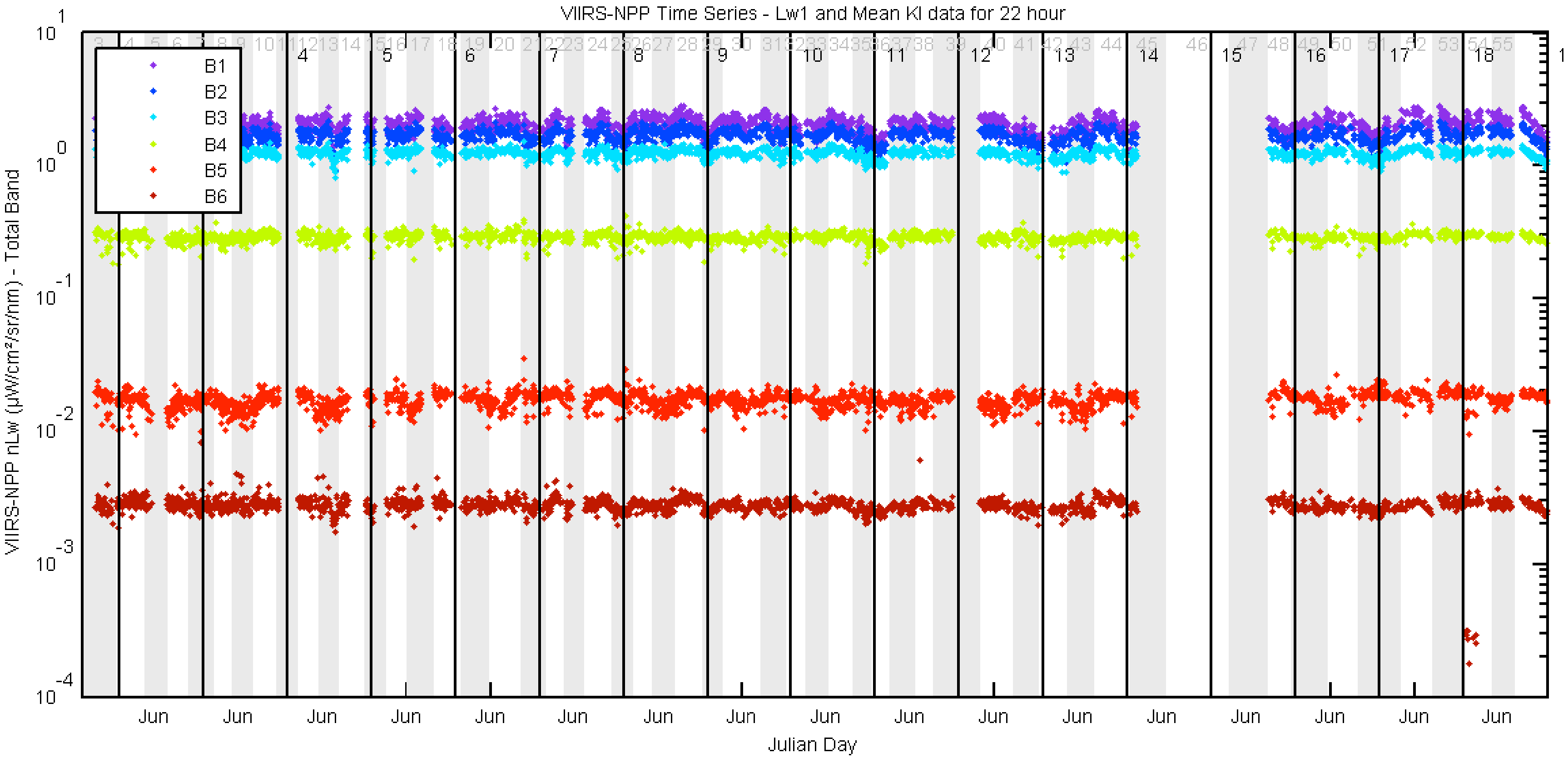

Primary ocean color vicarious calibration site for VIIRS.

Current status

- Next deployment will be in mid September.
- Currently an issue with top battery in MOBY dating back to mid August.
- Trying to get out to fix, but there are currently 3 hurricanes in the vicinity of the Hawaiian islands (they are up to the letter "I" out there)…so going out to fix the instrument has been an issue. Maybe fixed yesterday (Wednesday).

Instruments are getting old, so we are now in the middle of a “refresh” of the optical system and onboard control system.

Changes include upgraded and new control computers and new optical system.

In-line Volume Phase Holographic grating

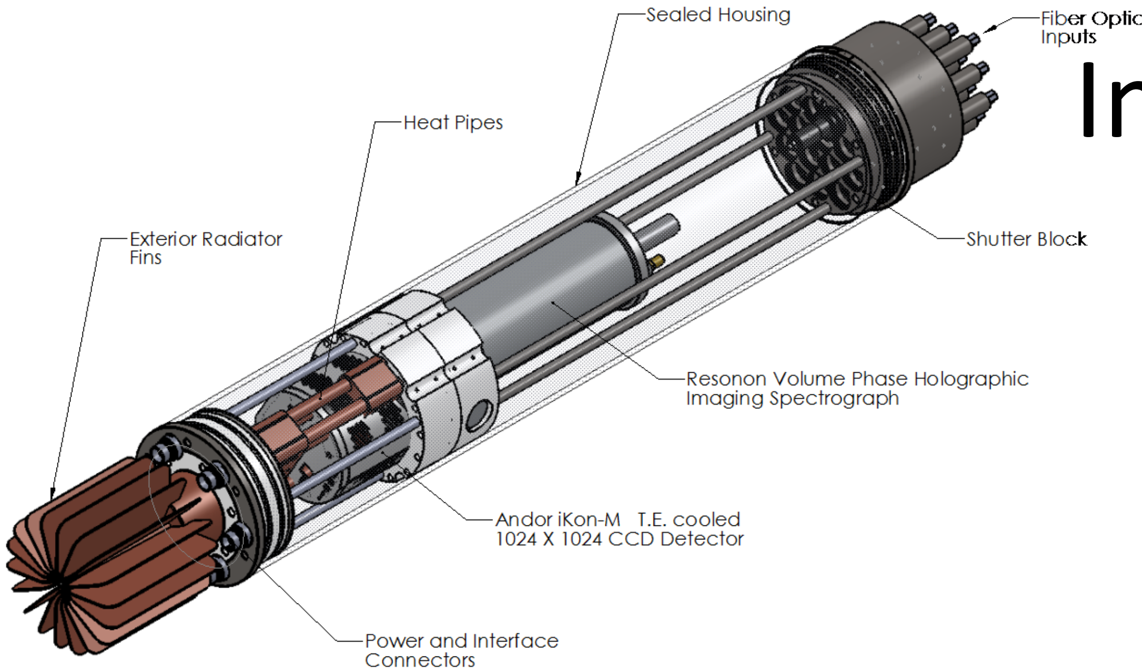

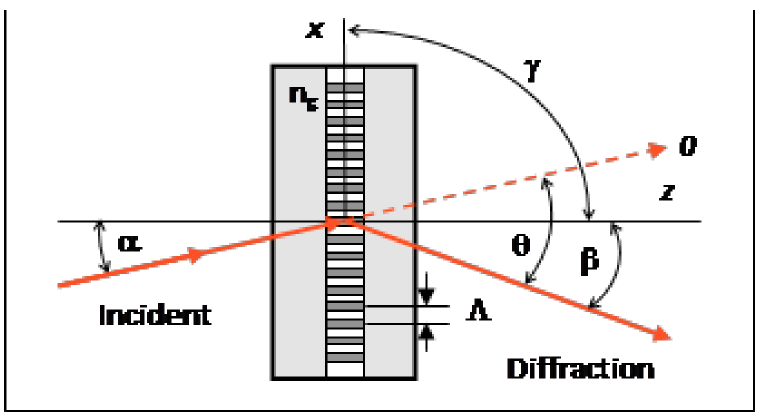

From http://www.bayspec.com/technical-support/definitions/vpg/

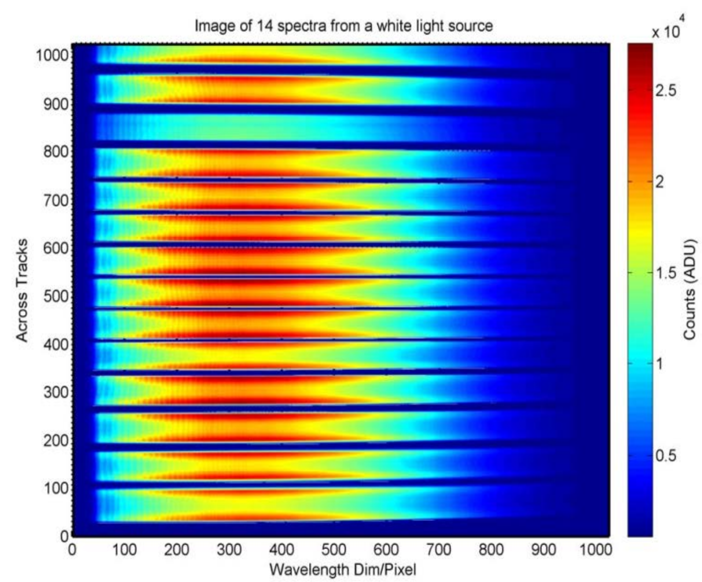

Currently testing Blue spectrometer and components of new system

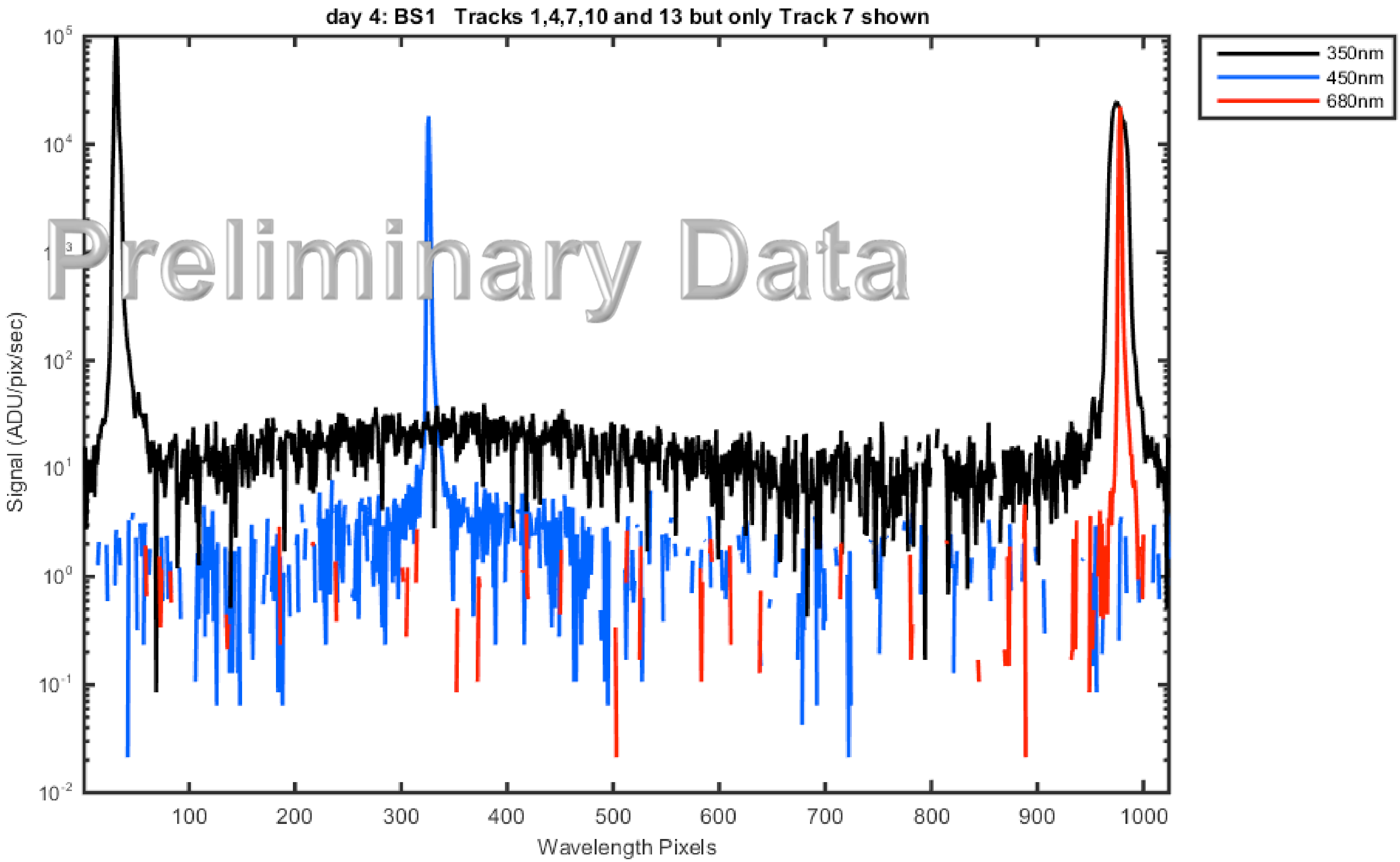

Wavelength calibration…approximately 0.3 nm/pixel

Currently testing Blue spectrometer and components of new system

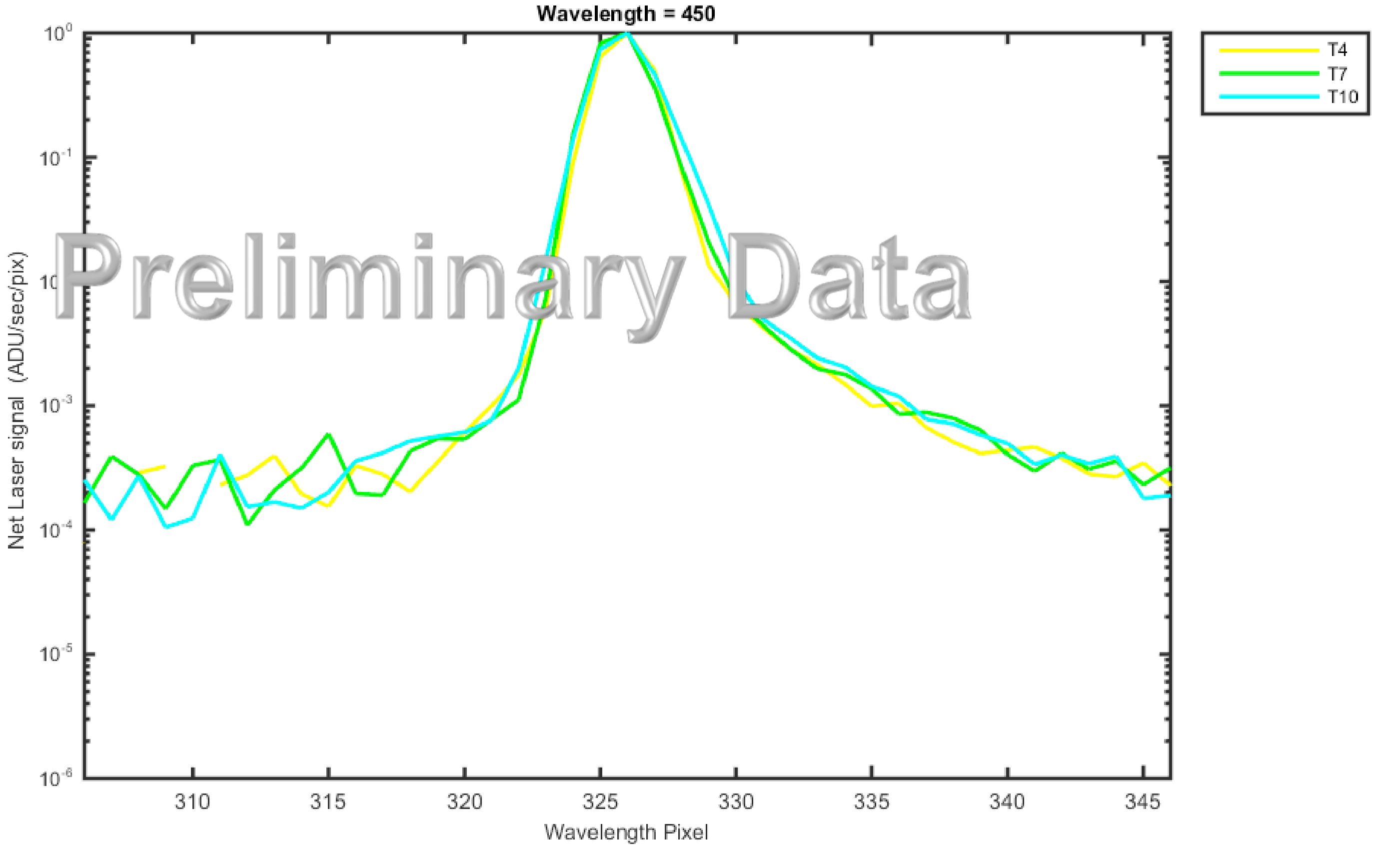

Zoom in on the 450 nm data, shows good stray light characteristics, and a Full Width at Half Maximum of approx. 1 nm.

UNIVERSITY OF MIAMI

Preliminary results from the blue spectrometer prototype

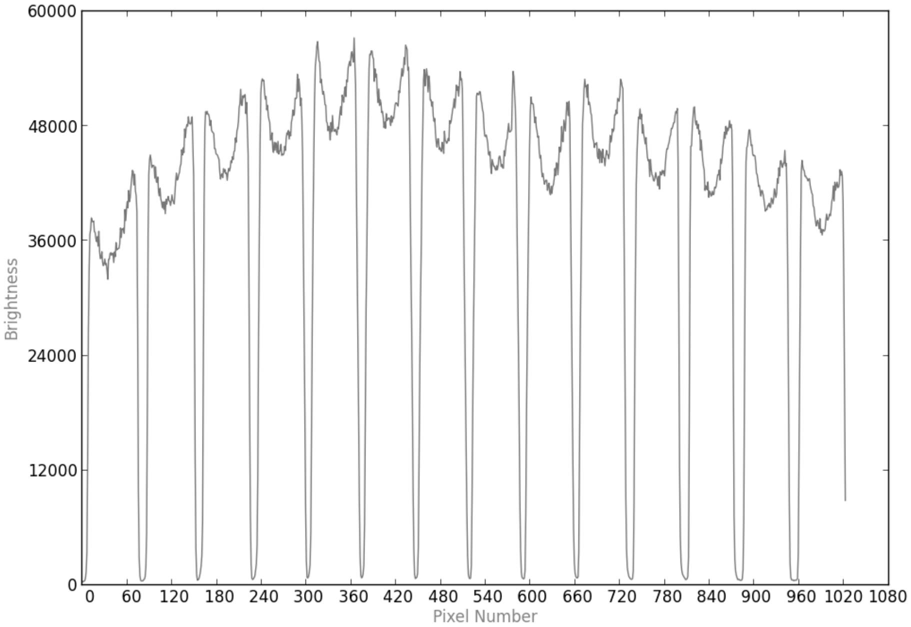

White light illumination

Showing spatial resolution

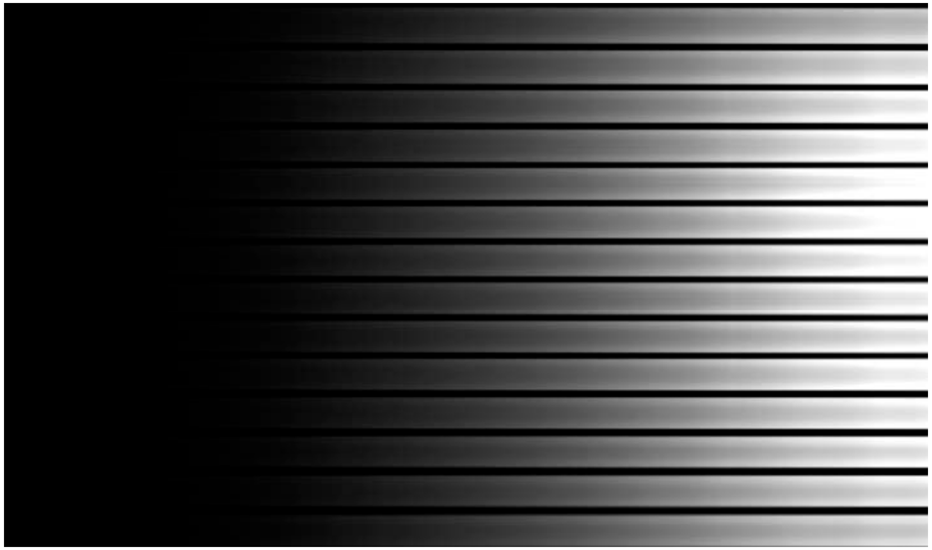

We will be doing spectral resolution, stray light analysis on the system in Hawaii.

Some data showing more detail on cross track imaging

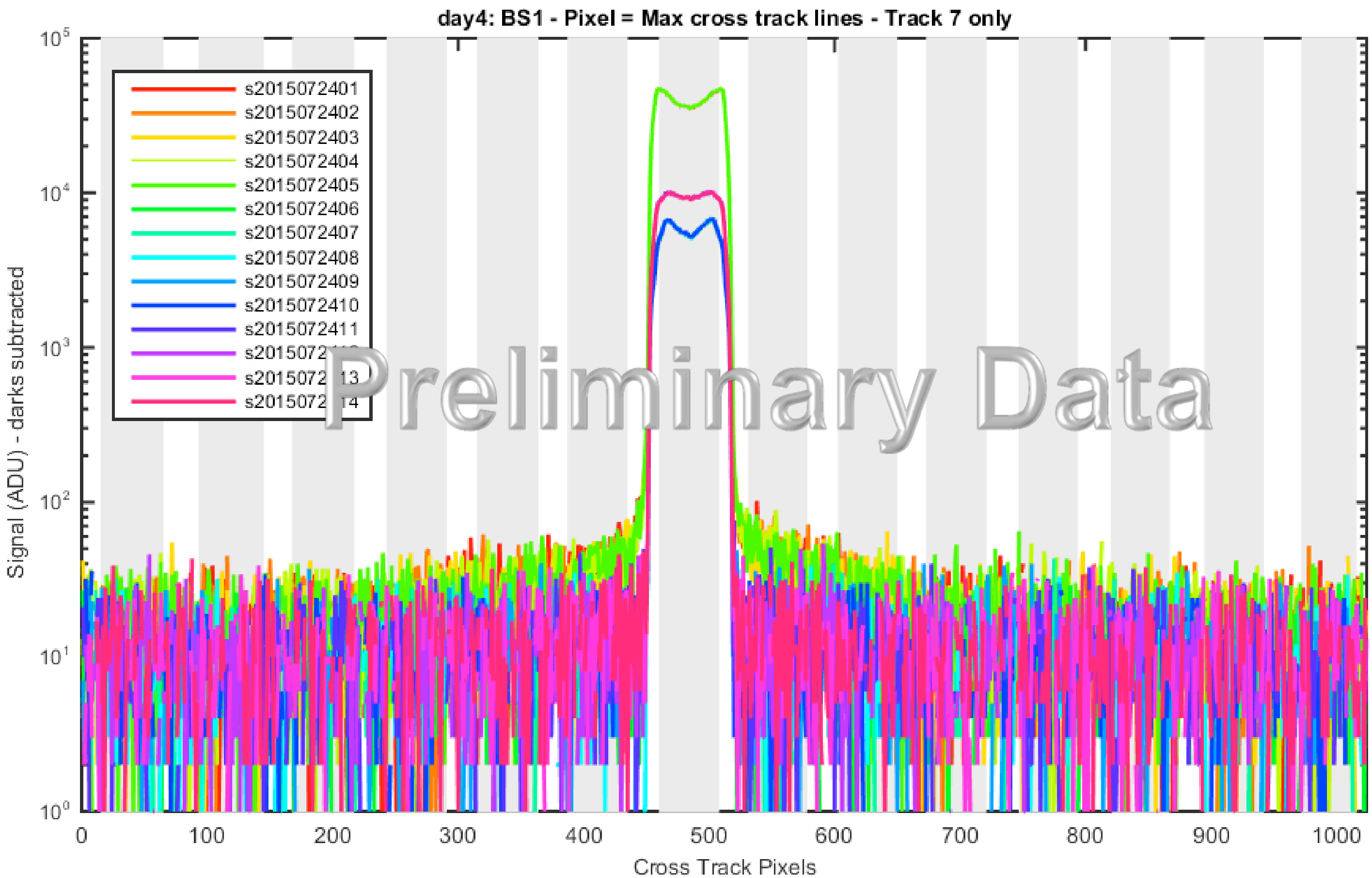

Testing new components to be used in new system, such as a fiber optic splitter instead of dichroic beam splitter:

Splitting ratio could be effected by how the light is put into the fiber at the collector, We tested by varying the incident angle of light on the cosine collector (worse case), no change in ratio….tests also help us learn more about the spectrometer systems operating parameters as we go along.

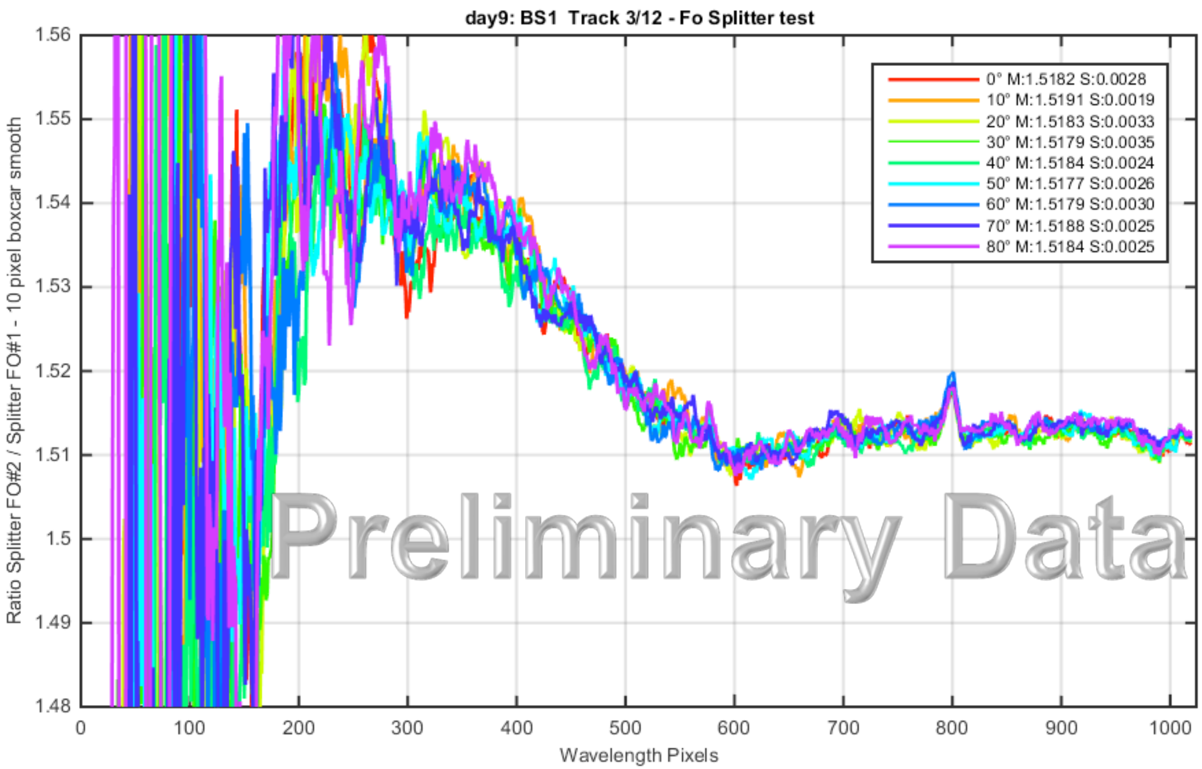

In the process we are cleaning up other issues we find with MOBY: slight polarization sensitivity

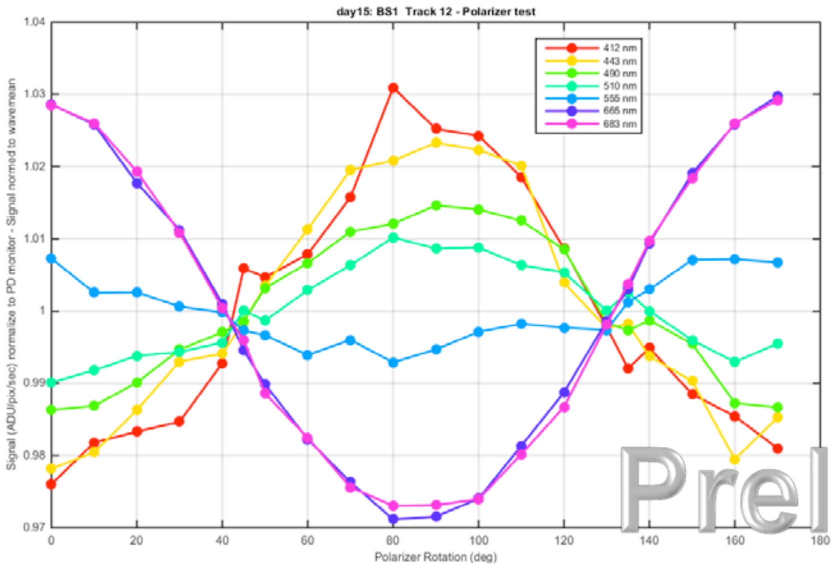

Before, +-3% (effectively 1.0% in field)

NOTE: SCALE CHANGE, LEFT +-4%
Bottom +-0.8%

Preliminary Data

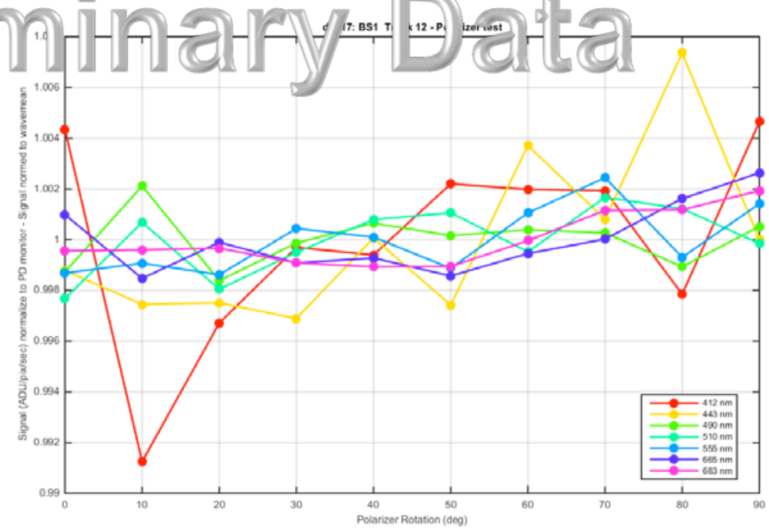

After, no polarization dependence evident signal within +- 0.2%, no cos(2*theta) dependence.

Refresh schedule

- The September deployment will have the new controller.
- We are working towards having the first deployment of the Blue spectroradiometer on the January deployment (along side the current system). We are aiming for at least a one year cross over experiment.
- We have been able to order the long lead time items for the red spectrometer.
- We expect that we will be able to start ordering the rest of the parts needed for complete refresh in late spring 2016.
- The goal is to be completely done with Refresh by Sept 2018.

Validation of VIIRS Ocean Color Products for the West Coast

Oregon State University
(C. Davis, N. Tufillaro and J. Nahorniak)

To evaluate VIIRS Ocean color products we compare them with *in situ* data and other satellite data. Examples using data from the Ocean Color AERONET site `Platform Eureka,' in the Southern California Bight, and cruises as part of the Hawaiian Ocean Time Series (HOT).

Data Sources:

VIIRS data sources:

- NASA VIIRS
- NOAA STAR VIIRS (MSL12)
- NOAA CLASS

In situ

- HyperPRO (Hawaii from OSU)
- SeaPRISM (Platform Eureka from NASA Ocean Color AERONET)
- HyperPRO and above water Rrs with Spectral Evolution PSR-1100

Satellite

- MODIS-AQUA (from NASA Ocean Color Website)
- Landsat-8

VIIRS and HOT data

Above and in-water light field measurements are routinely made at Station ALOHA, 100 km north of Oahu, Hawaii (22.75 ^{o}N, -158.00 ^{o}E) as part of the Hawaiian Ocean Time Series (HOT) program.
Spectral matches at Station ALOHA of VIIRS data with HyperPRO cruise data collected one minute apart (23:43 and 23:44 GMT).

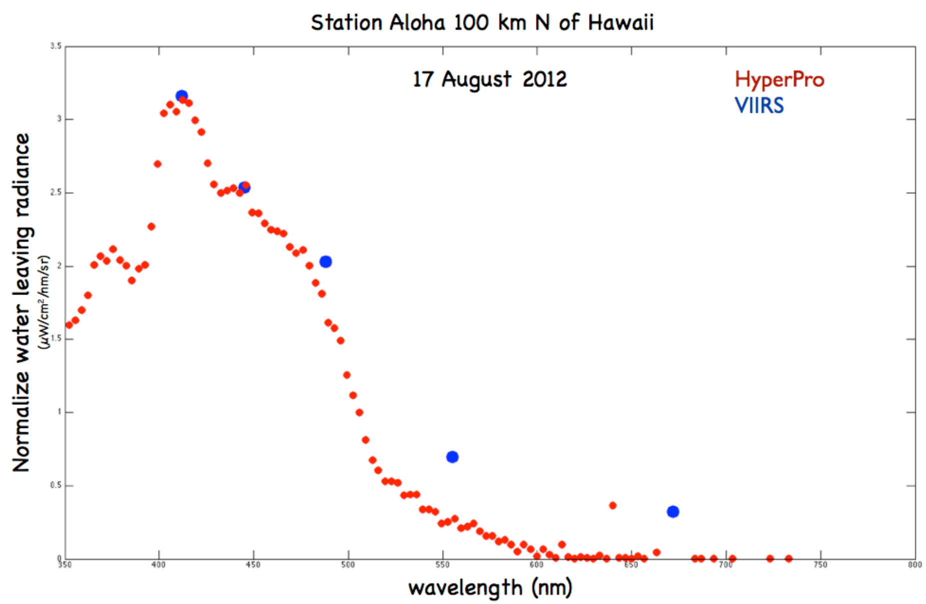

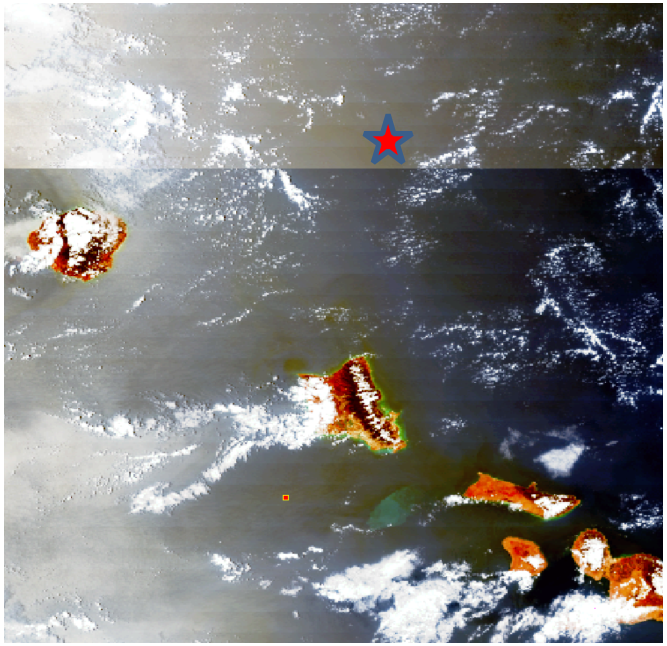

VIIRS image over Hawaii from 17 August 2012 (23:43 GMT). The star marks Station ALOHA.

Platform Eureka SeaPRISM

Use of the SeaPRISM hourly optical data at the Ocean Color AERONET site 'Platform Eureka' aboard an oil platform in the Southern California Bight.

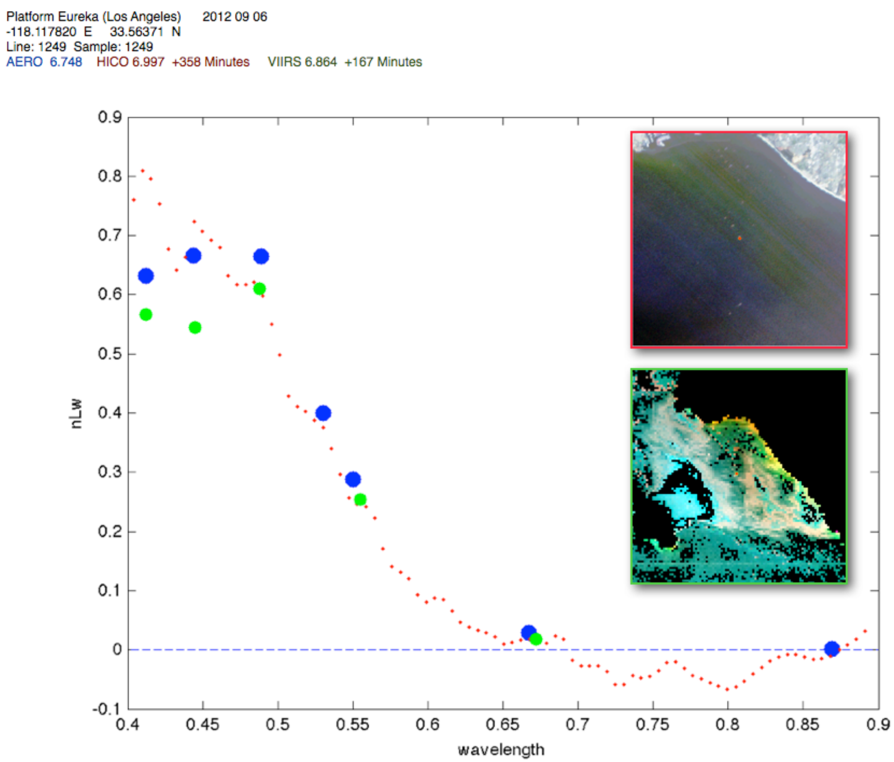

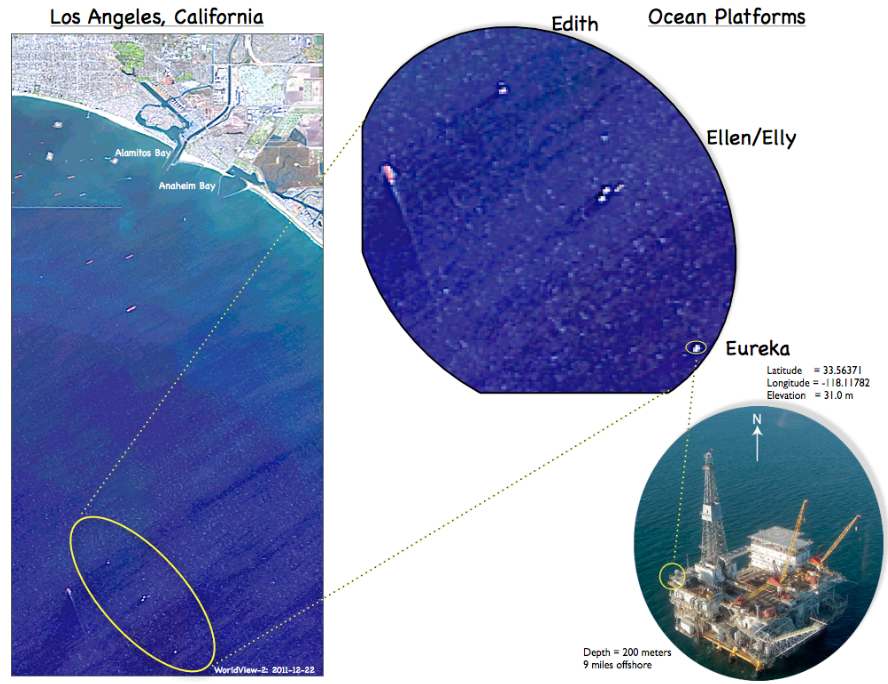

Spectral matchups at Platform Eureka between the in situ data (blue), HICO hyperspectral measurements (red), and VIIRS measurements (green). Data are from September 6, 2012.

Above and in water validations
Cruise October 2014

Satlantic HyperPRO in water Spectrometer

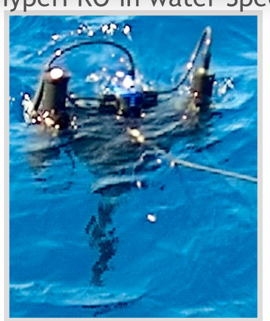

Spectral Evolution above water Spectral Reflectance with fiber optic.

SKY Measurement

WATER Measurement

Reflectance REFERENCE Measurement

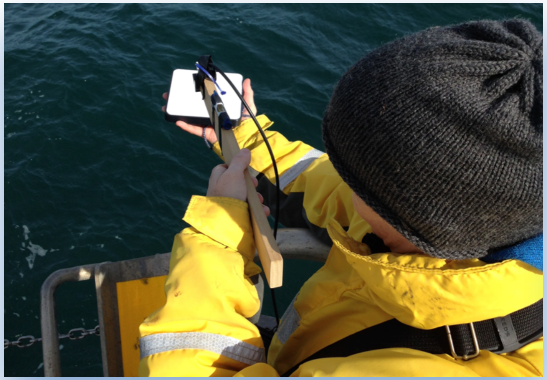

Example SPECTRA

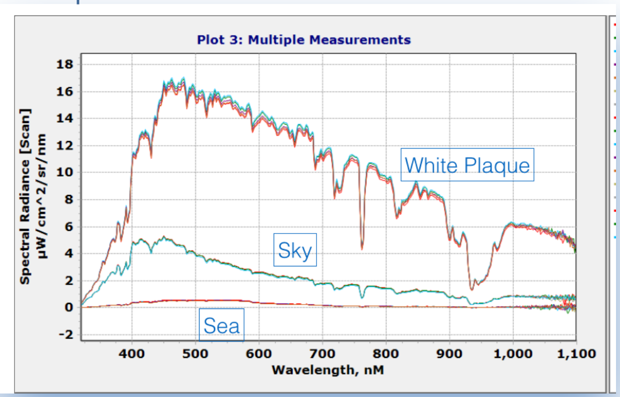

Platform Eureka: October-December 2014
October 7, 2014 Cruise Match Example

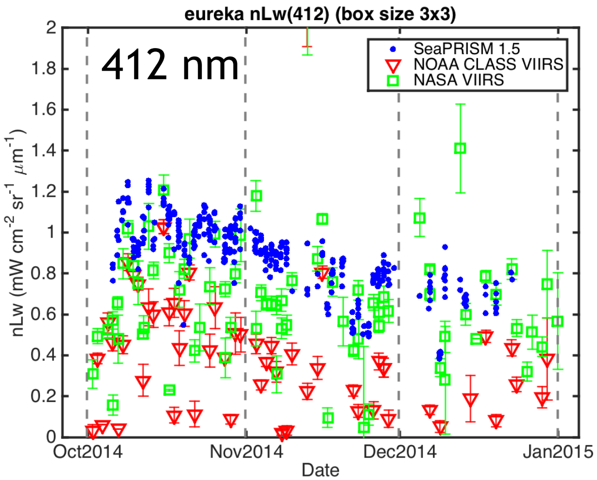

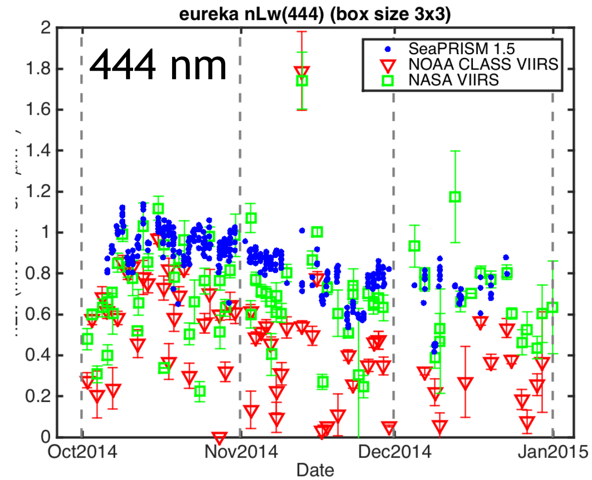

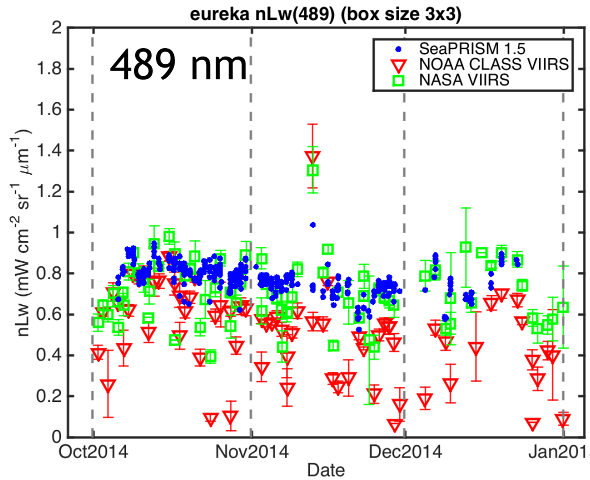

<u>Spectral Evolution PSR-1100</u>
Using 'empirical' correction (0.75) to get matches for new instrument

Current Processing with HyperPro showing good correlations.

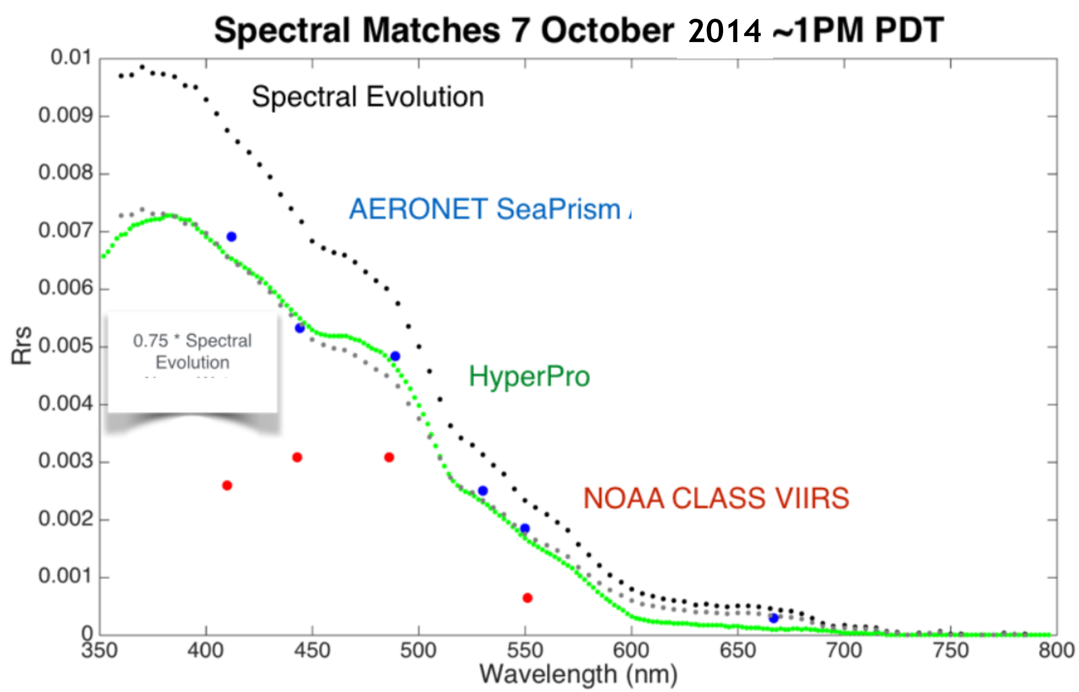

Landsat-8 OLI. Panchromatic Enhanced ~15 m.
7 November 2014, 18:28 GMT (11:28 PDT)

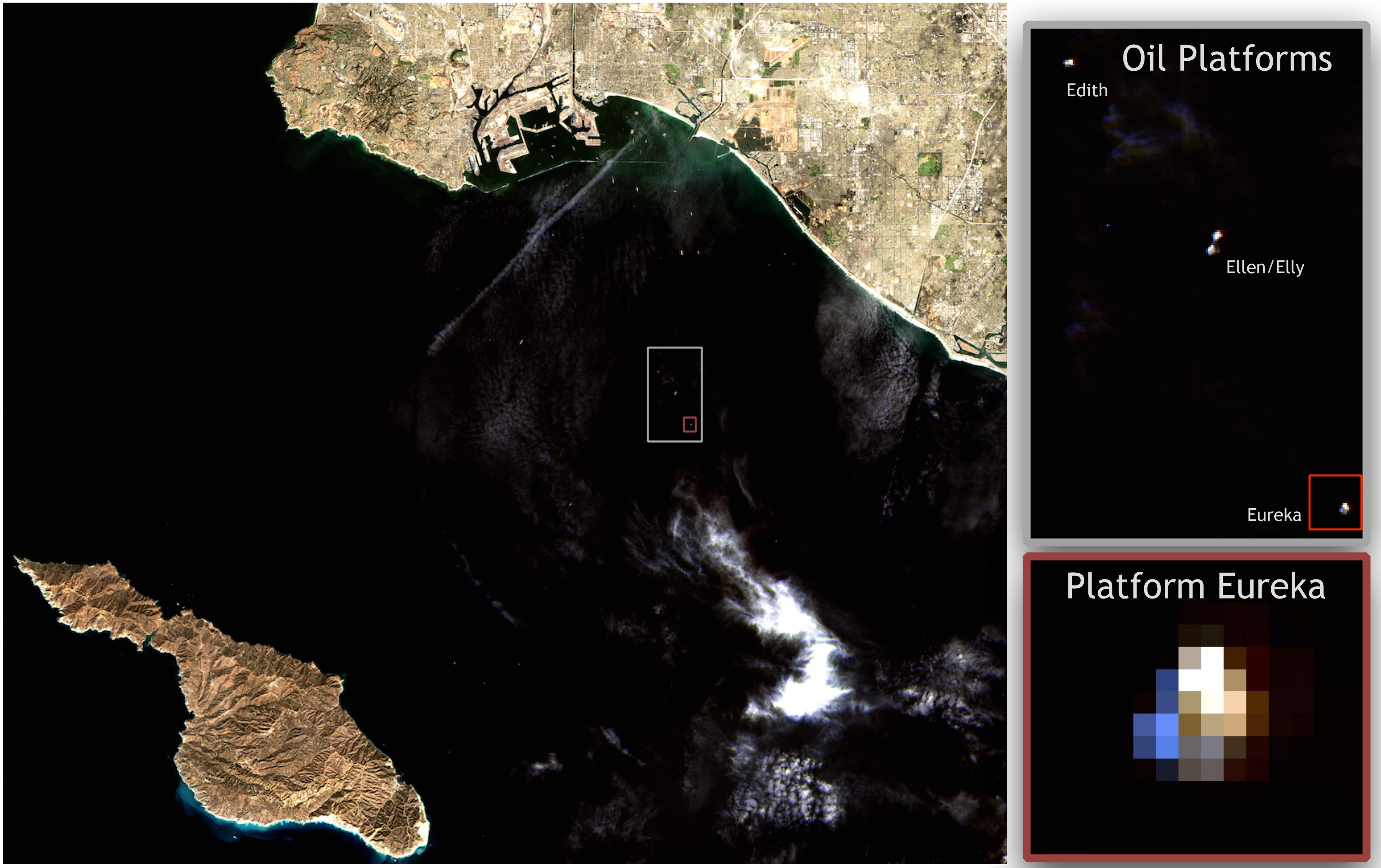

Landsat and VIIRS OC3 on 7 October 2014

Landsat OC3: 18:28 GMT (11:28 PDT)

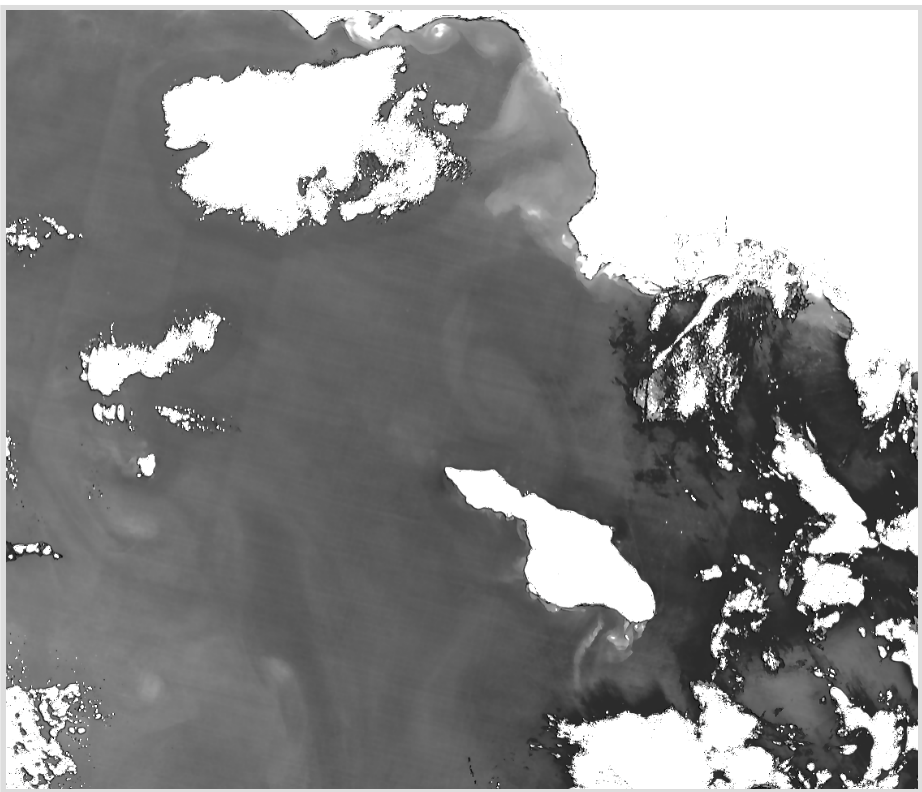

VIIRS OC3: 21:26 GMT (01:26 PDT); Landsat +2HRs

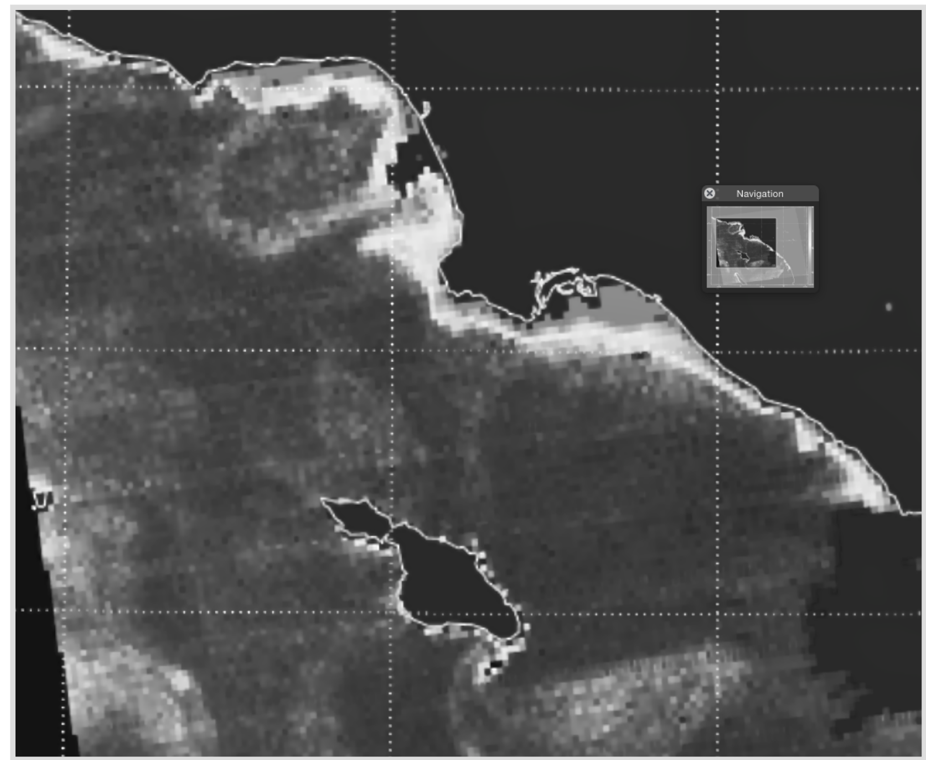

Linear Scale from 0 - 3 mg/L. Each image, though, has been individually contrasted adjusted to try to highlight features. Water was very clear this day.

Monitoring coastal 'Mesoscale' events

movie: click to play

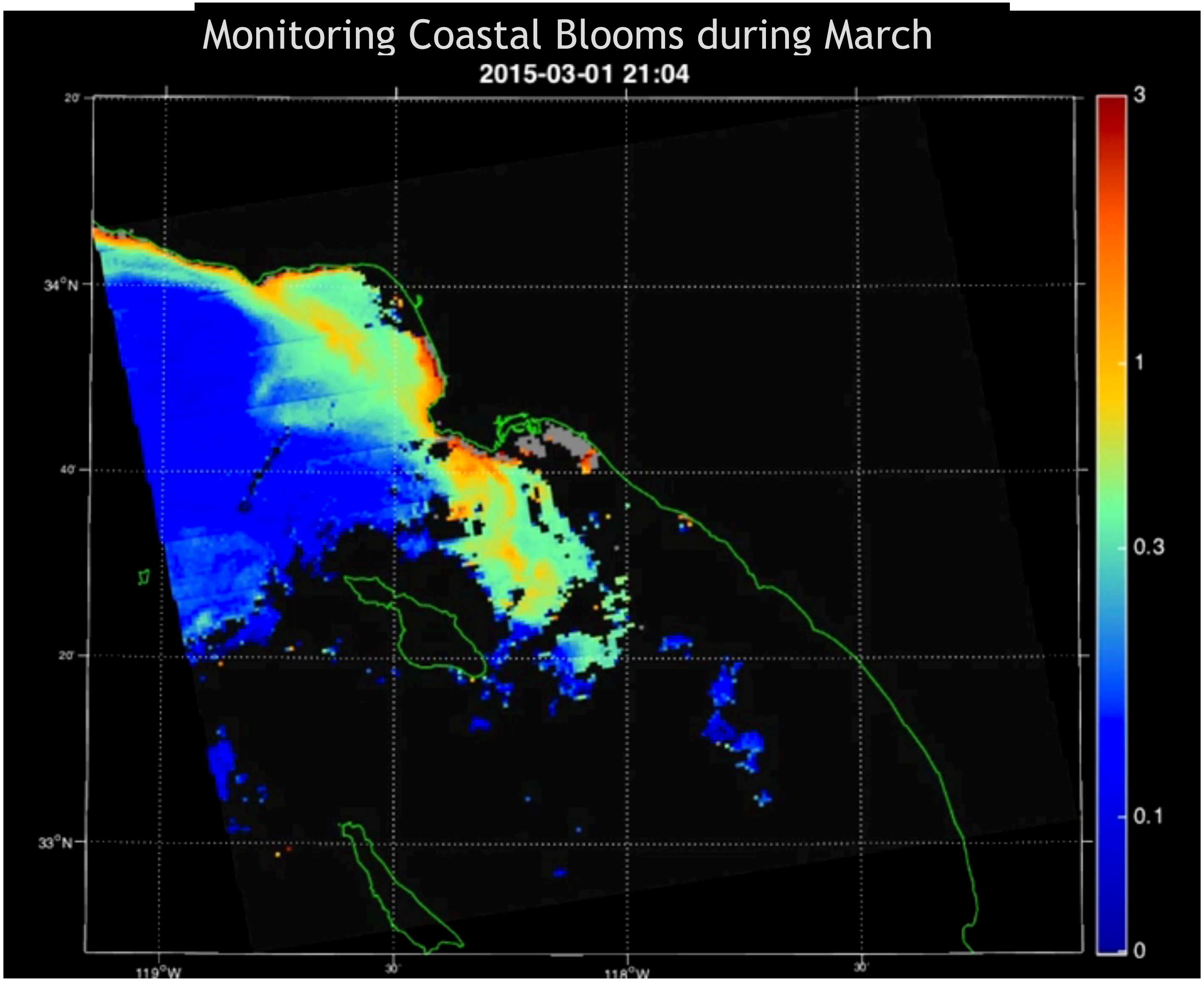

Platform Eureka time series

Time series of chlorophyll-a data from VIIRS shows Bloom/ Eddie passing by Platform Eureka during March 6-8, 2015.

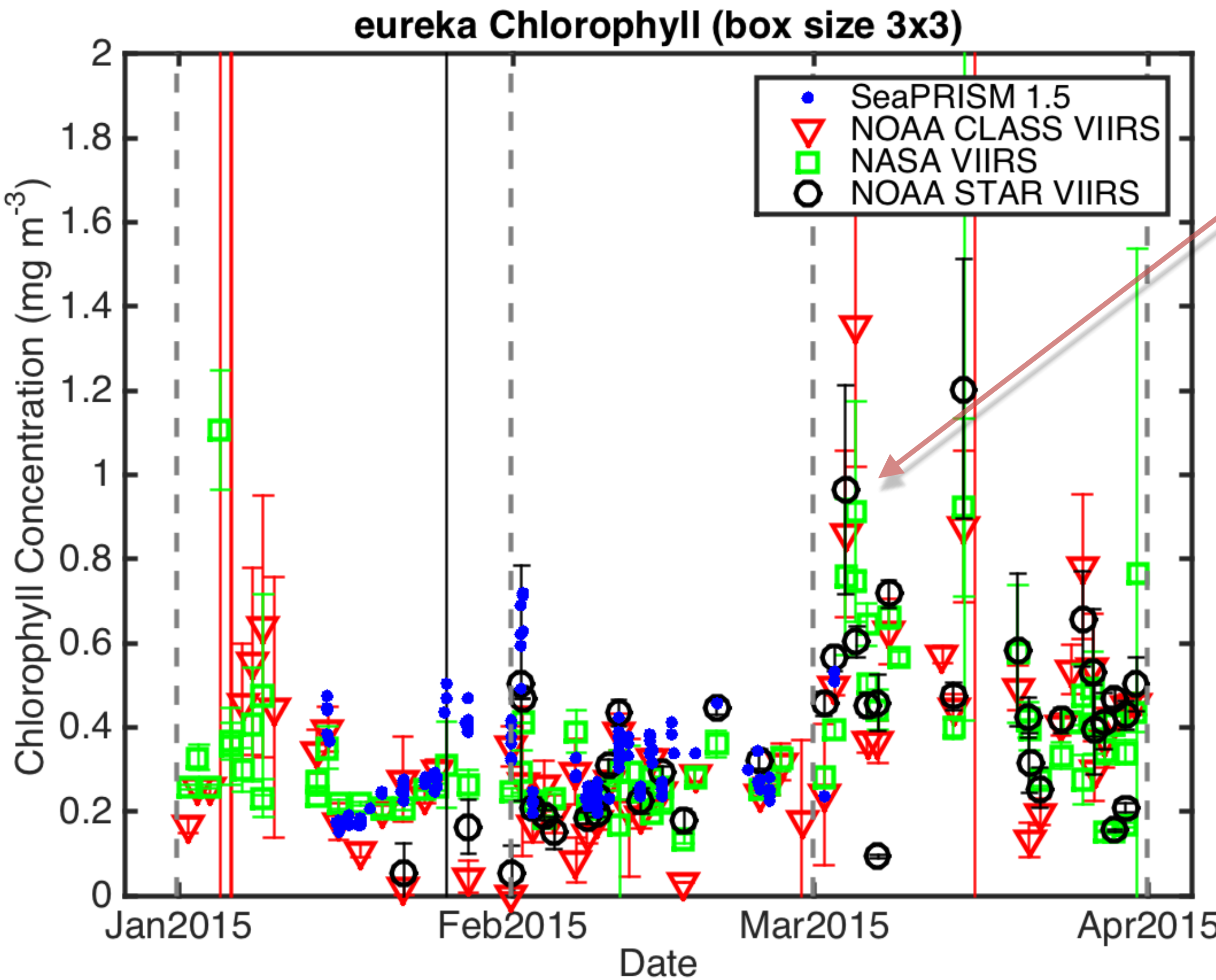

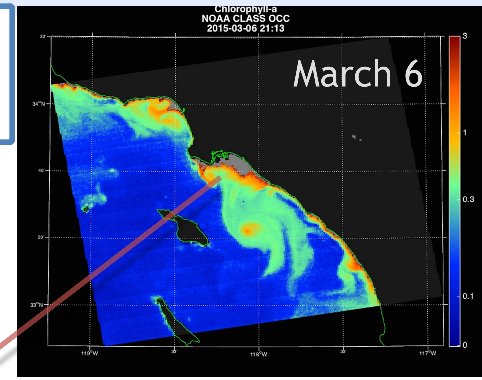

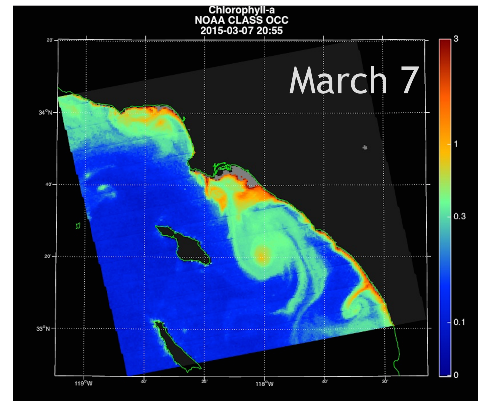

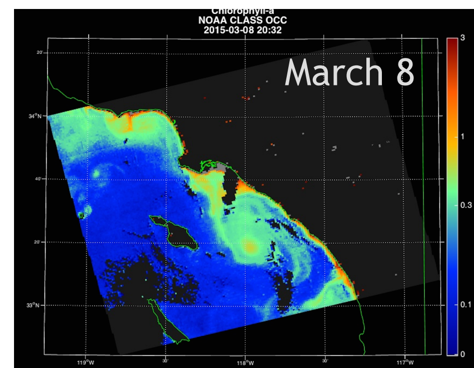

Example Time Series and Regressions: Jan-March 2015

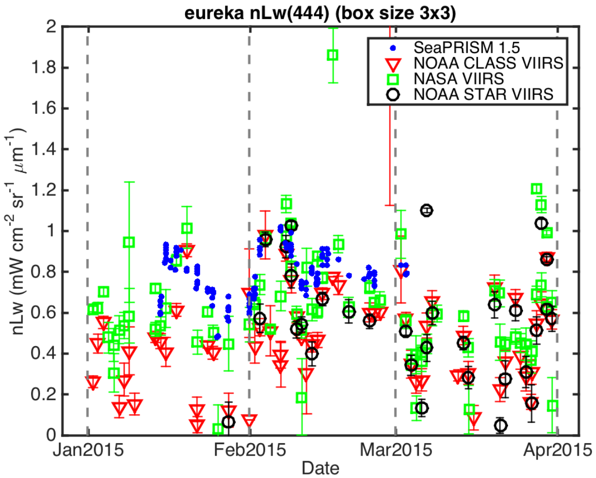

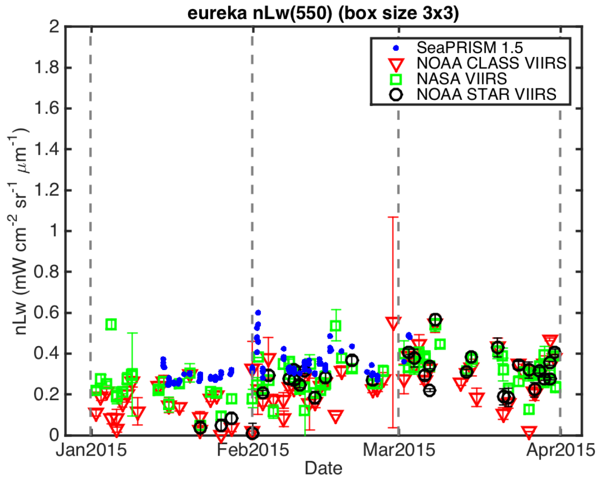

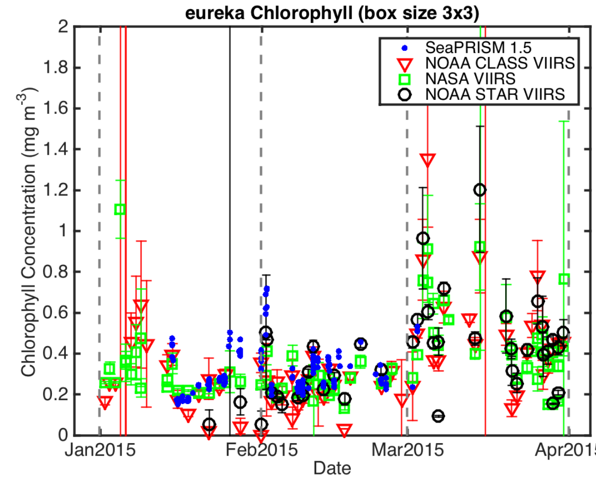

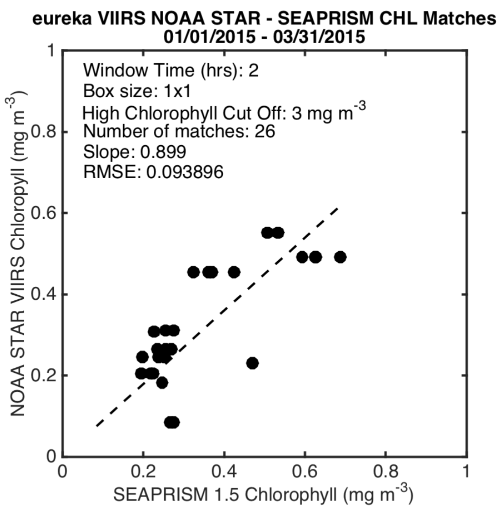

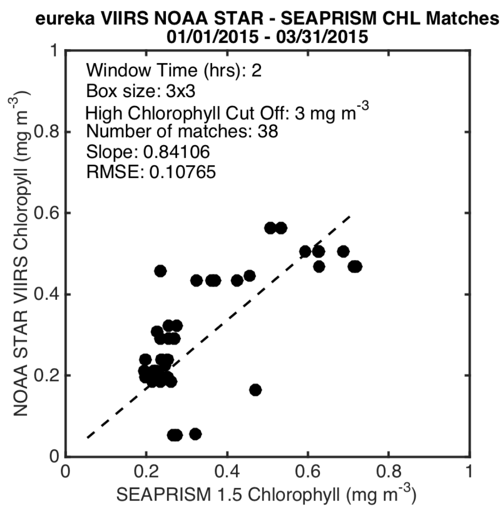

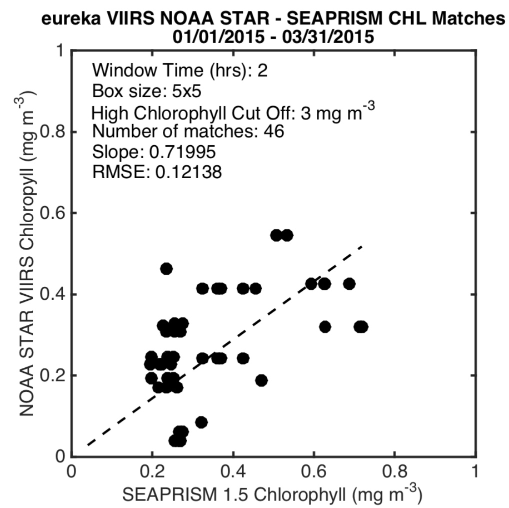

Chlorophyll Time Series 2015 at Platform Eureka

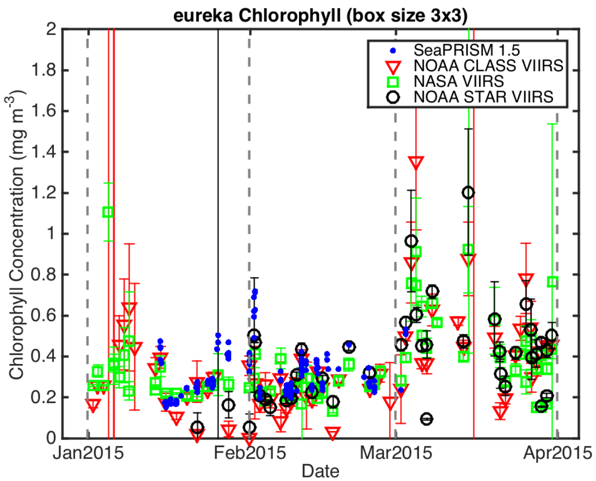

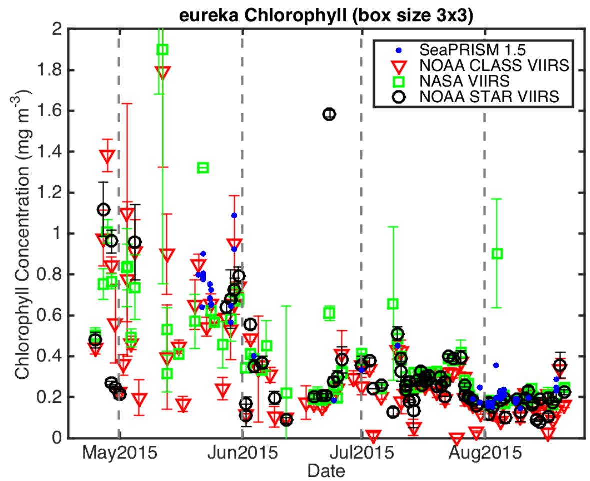

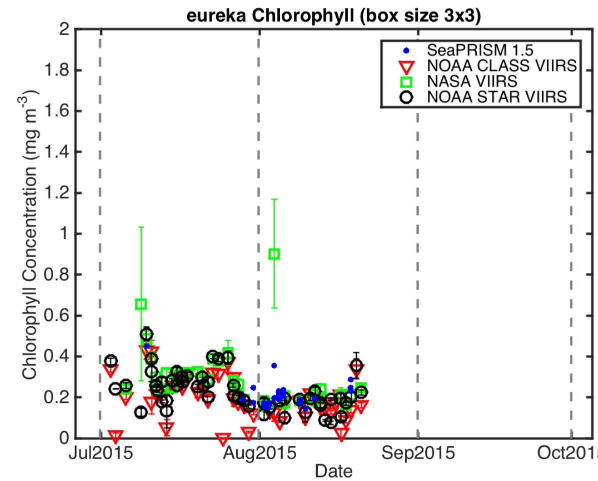

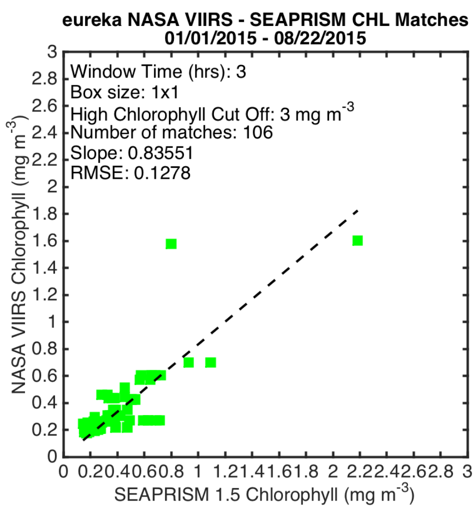

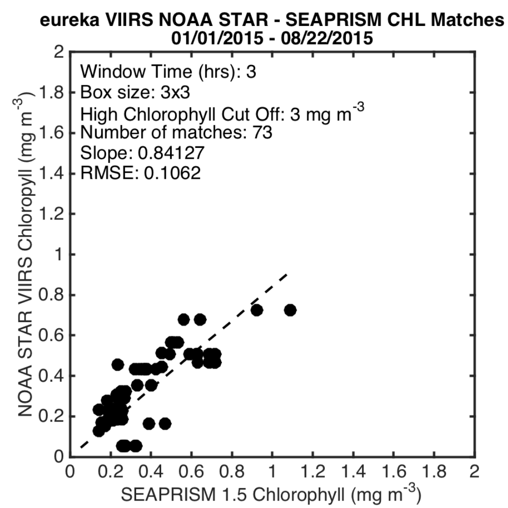

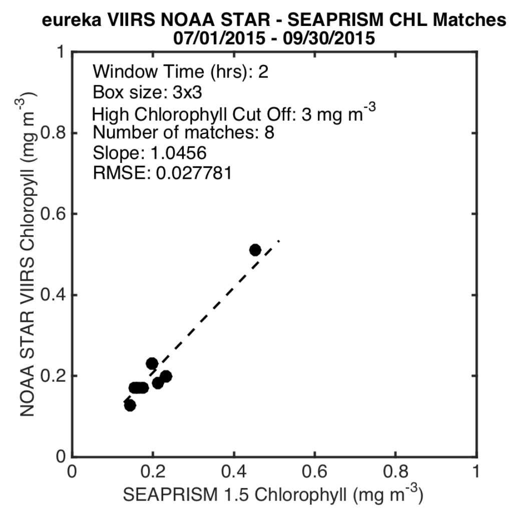

Platform Eureka Data Collection
Challenges

Platform Eureka SeaPRISM site is excellent and data is key for our work, however:

- Data flow has been intermittent; *New radio system installed.*
- Calibration issues: *Installed TWO SeaPRIMSs to cross-check.*
- Some NOAA STAR (MSL12) swaths not processed: *Will be picked up on reprocessing.*
- Protocols/Processing for New Spectrometer

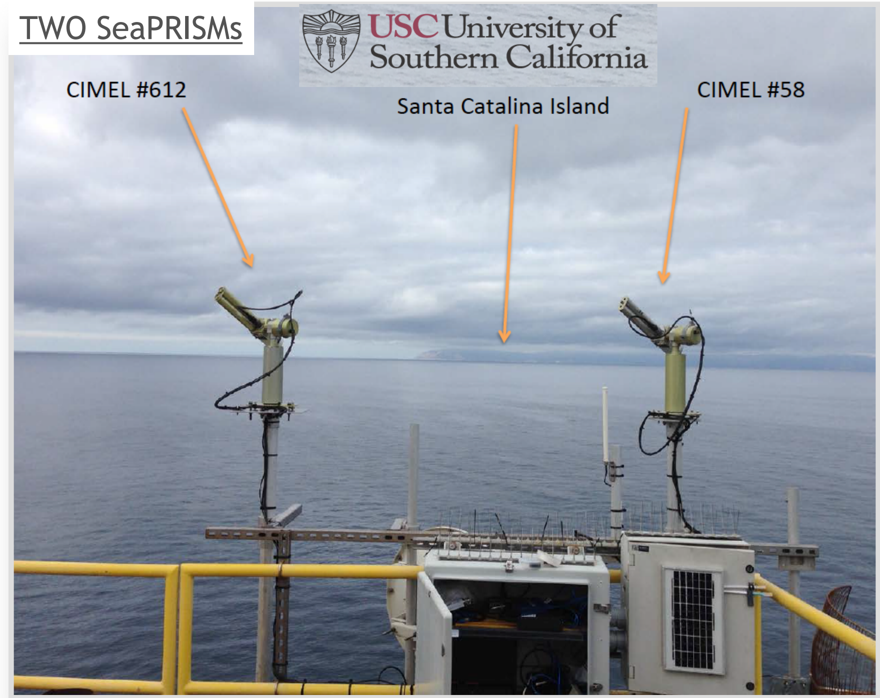

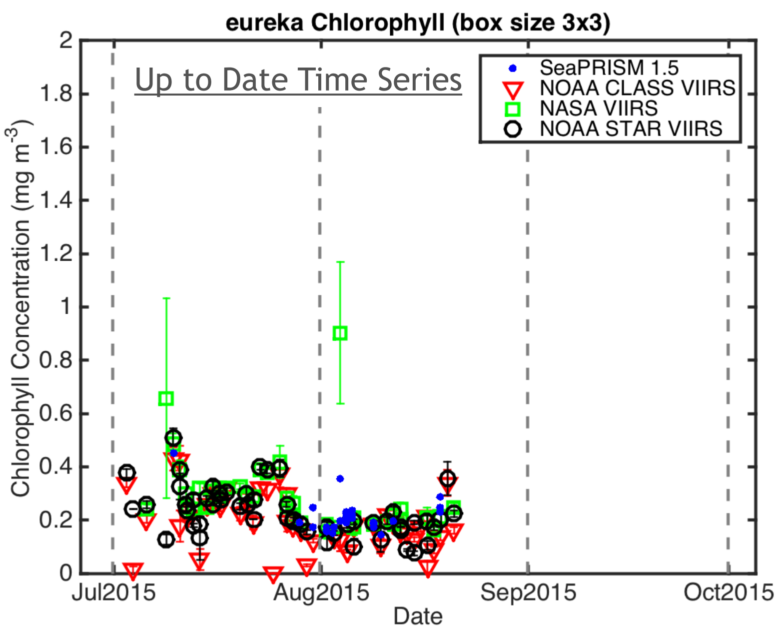

Example Data Gaps in MSL12: Year 2013

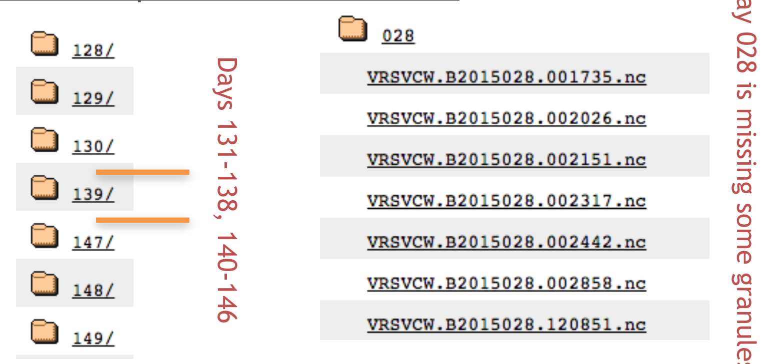

NOAA STAR (MSL12) Data Catalog

http://www.star.nesdis.noaa.gov/thredds/catalog/swathNPPVIIRSL2WW00/2015/catalog.html

Experimental Products

Research and development using 'optical flow' to interpolate and (short time) extrapolation of product fields — helps us to track 'mesoscale' events.

Steps:

1. *Destriping* building on NOAA's* variational methods
   - added optimization over spectra and time
   - automating optimization (does not require user to pick threshold)
   - 'in-painting' experiments to handle lost data due to cloud cover

2. Image sequence '*equalization*'
   - this is integrated into the destriping step

3. '*Optical flow*': variational functional is used to estimate vector fields between images
   - integration providing a dynamic model of the product fields evolution

Collaborators:

Erik Bollt and Ranil Basnayake, Clarkson University

Theory/numerics is part of NGA funded project to Clarkson University:

NGA 2013-15: *Impacts of Remote Multi-Attribute Spatiotemporal Dynamical Systems Analysis*, Erik Bollt, Clarkson University, PI.

***** Destriping References

Karlis Mikelsons, Alexander Ignatov, Marouan Bouali, and Yury Kihai. A fast and robust implementation of the adaptive destriping algorithm for snpp viirs and terra/aqua modis sst. volume 9459 of *Proc. SPIE*, pages 94590R–94590R–13, 2015.

Karlis Mikelsons, Menghua Wang, Lide Jiang, and Marouan Bouali. Destriping algorithm for improved satellite-derived ocean color product imagery. *Optics express*, 22(23):28058–28070, 2014.

Marouan Bouali and Alexander Ignatov. Adaptive reduction of striping for improved sea surface temperature imagery from suomi national polar-orbiting partnership (s-npp) visible infrared imaging radiometer suite (viirs). *Journal of Atmospheric and Oceanic Technology*, 31(1):150–163, 2015/06/25 2013.

Example of Striping in VIIRS Image

- Subsampled image near the Santa Monica region in Southern California on November 6th

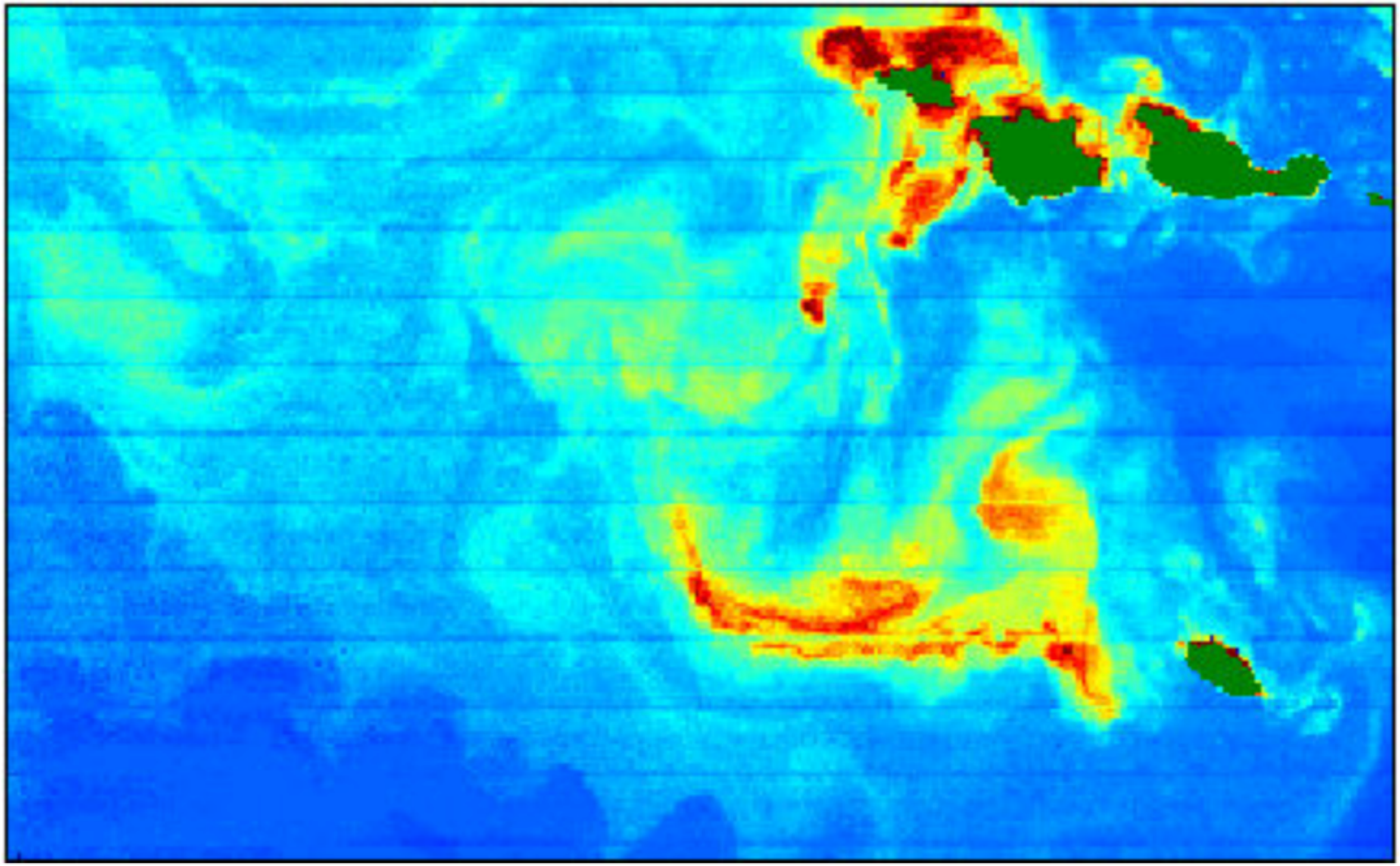

Example of destriping in VIIRS Image

- Subsampled image near the Santa Monica region in Southern California on November 6th

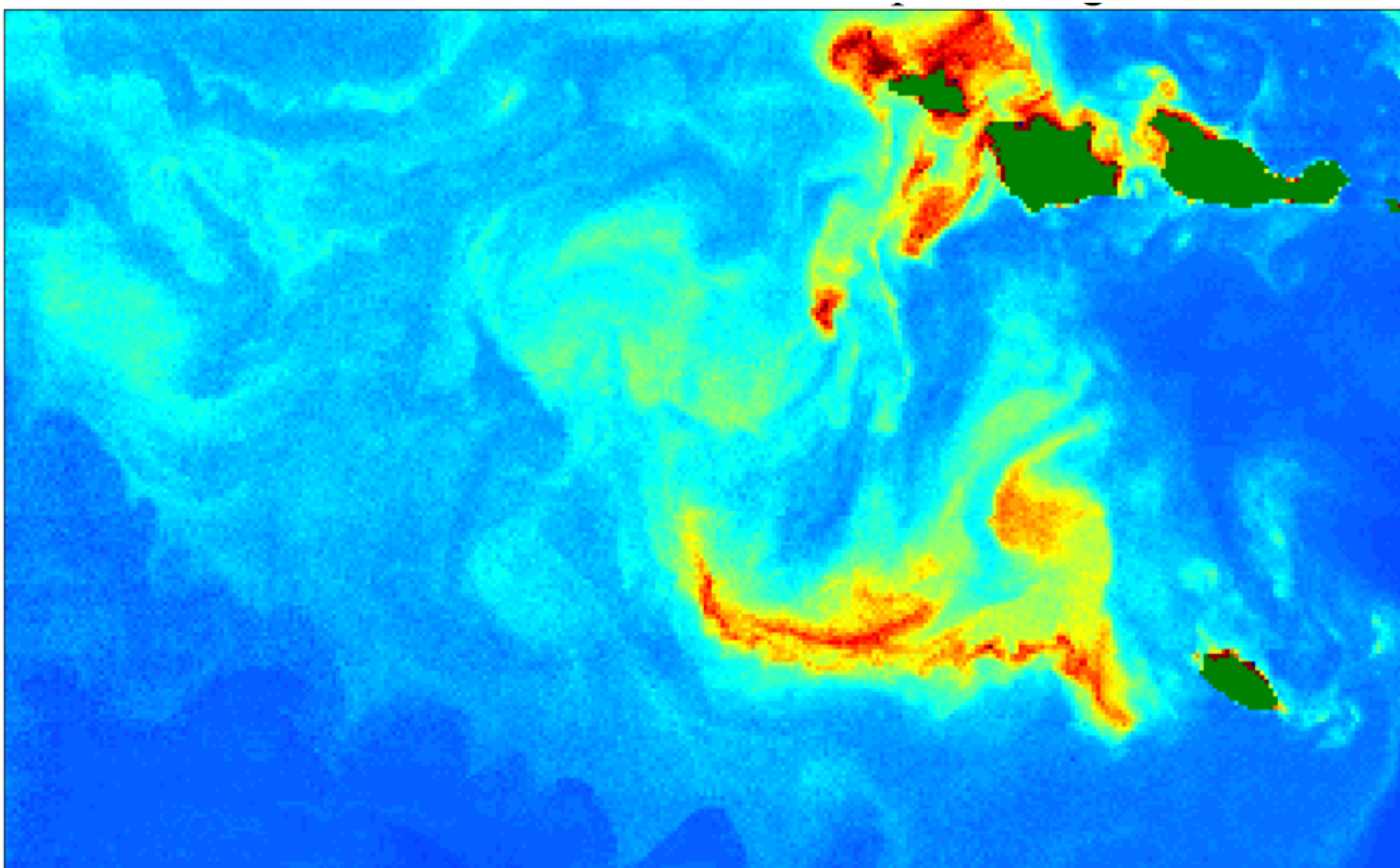

Example of a Destriped NASA image

(*.nc from NASA Ocean Color Site; NASA uses a vicarious destriping method based on a historic image and calibration database for VIIRS)

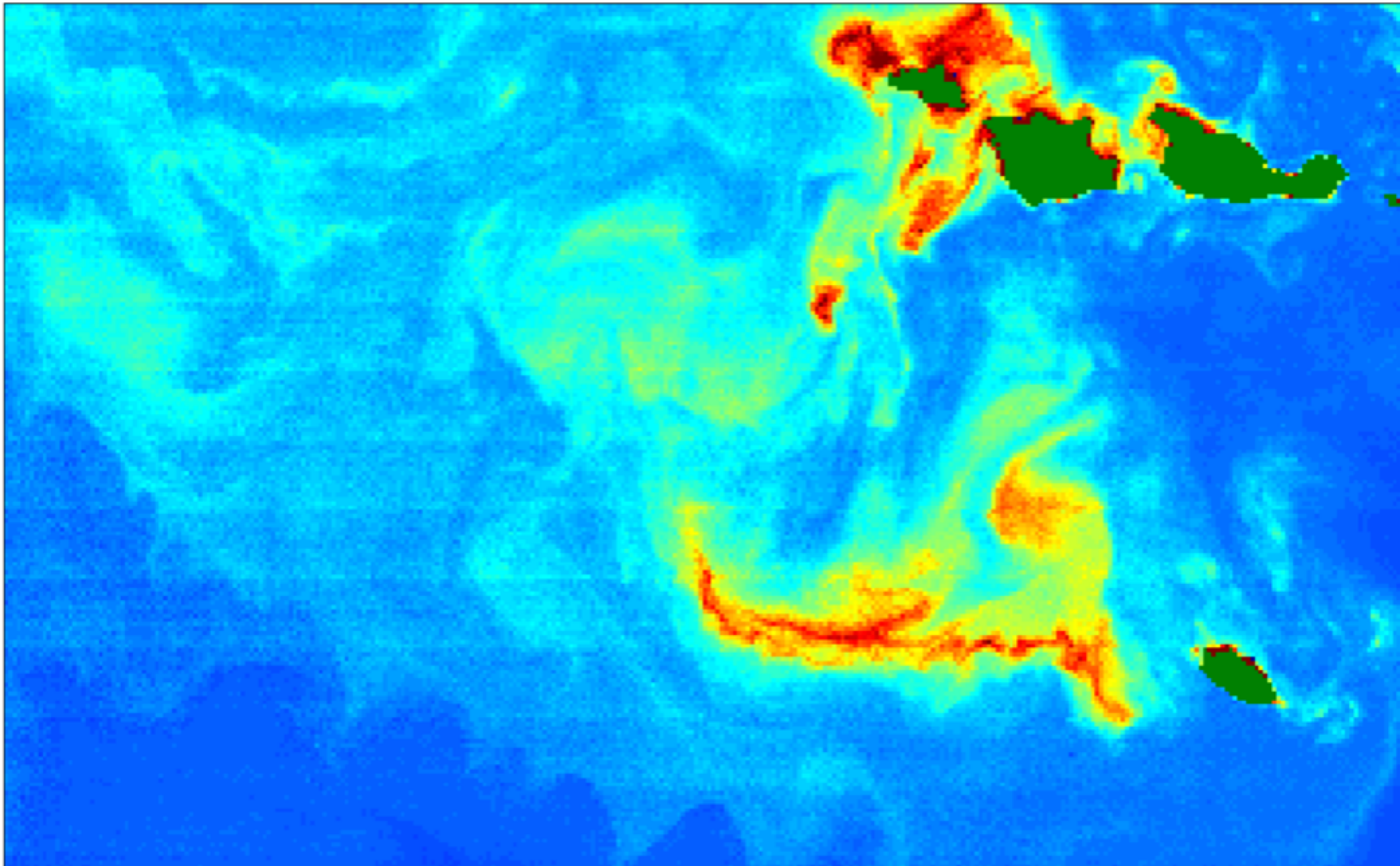

Example of a destriped image by applying two steps:
First, Vicarious destriping from NASA;
Second, a ‘Variational’ scene based destriping.

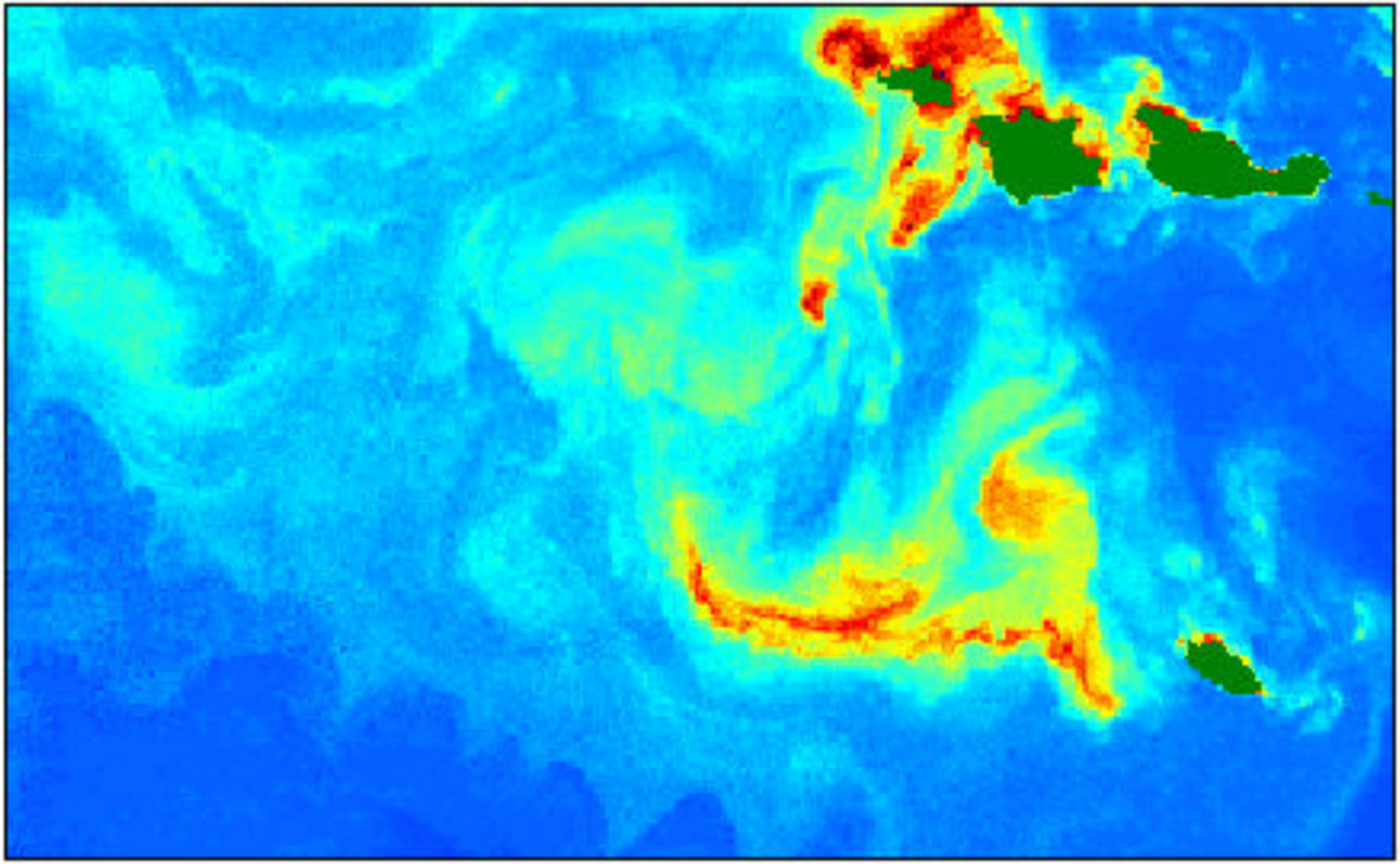

Optical Flow Example:
Chlorophyll flow map around Catalina and Platform Eureka, Work in progress

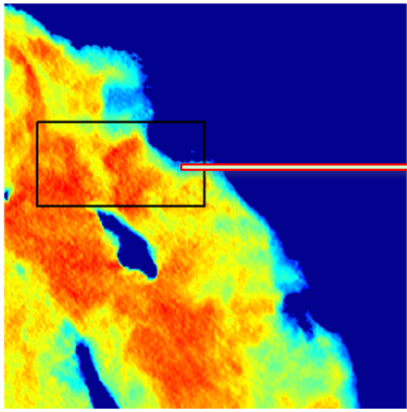

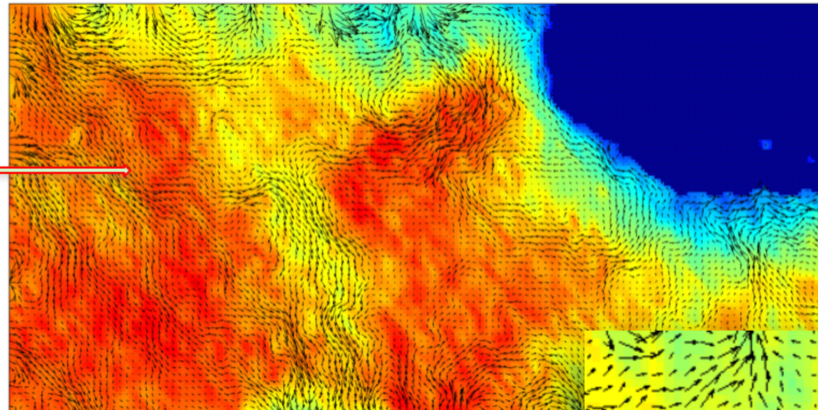

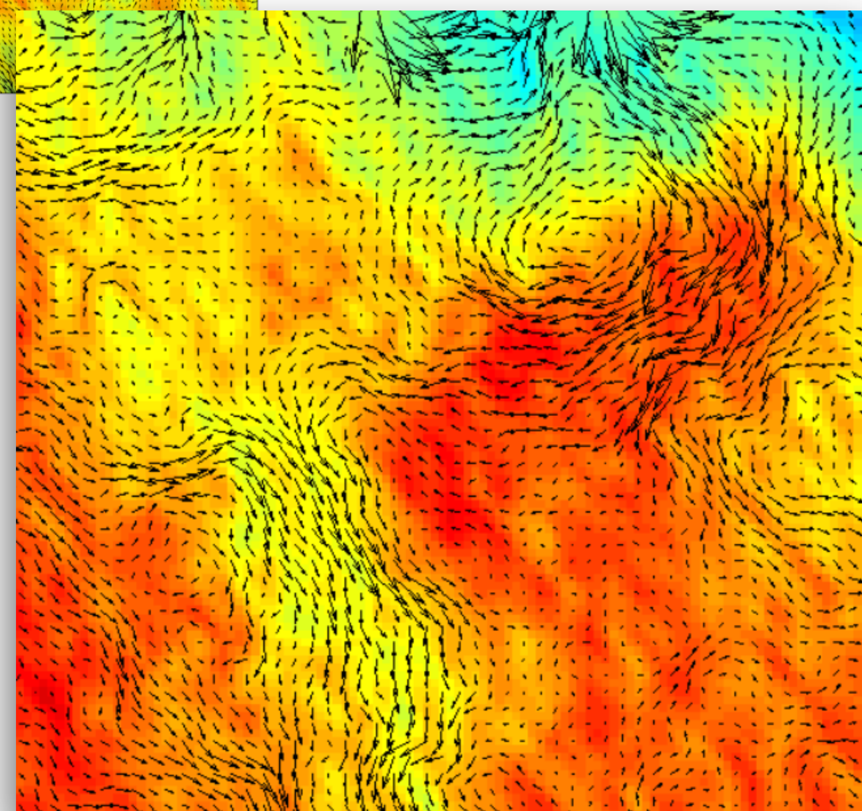

References:

E. Bollt, N. Tufillaro, R. Basnayake, J. Sin, and M. Gierach, Variational destriping on ocean color products with a simple numerical scheme, draft 2015.

A. Luttman, E. Bollt, R. Basnayake, S. Kramer, and N. Tufillaro, A framework for estimating Potential Fluid Flow form digital imagery, Chaos 23 (3), 2013.

Plans for July 2015-June 2016

- Participate in and present results at NOAA telecons and the NOAA STAR/JPSS Annual Meeting in August 2015.
- Participate in NOAA VIIRS science cruise for cross calibration of instruments and methods for:
  - Above Water Rrs
  - HyperPRO optical profiles
- Analysis of a two-year time series of NOAA STAR and NASA VIIRS data products at Platform Eureka.
- Publication on the Platform Eureka time series including comparisons with other SeaPRISM sites.
- Publication of statistical comparison of destriping methods on accuracy of final ocean color product fields.
- Research application of optical flow for dynamic ocean color product flow maps

University of Southern California

USC SeaPRISM

Burt Jones and Matthew Ragan

STAR/JPSS

27 August 2015

ACCOMLISHMENTS

- Performed CAL/VAL Cruise with OSU
- Updated Communications at Platform Eureka and Santa Catalina Island
- Installed Second CIMEL Sun Photometer for Data Comparison/Validation

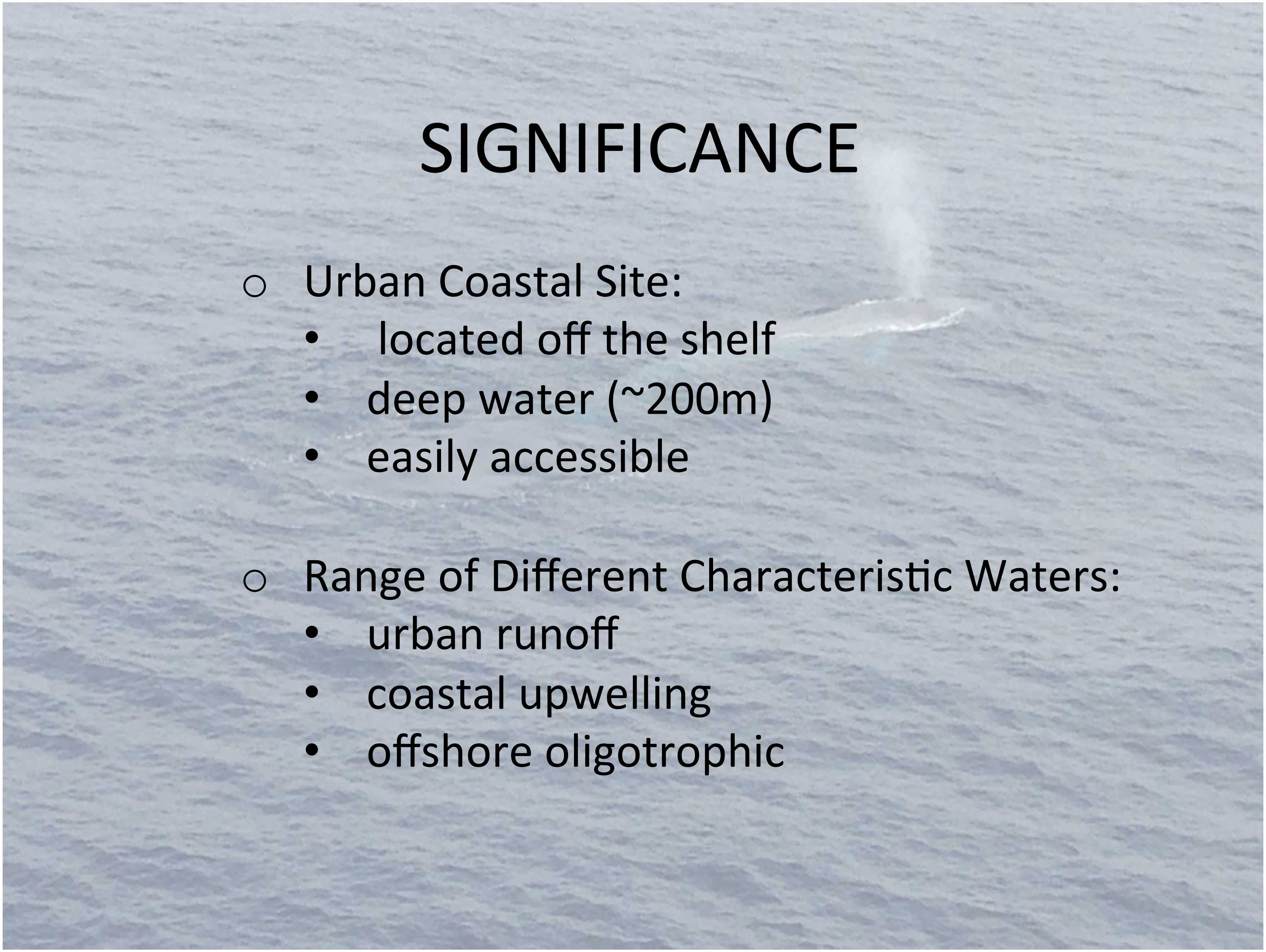

SIGNIFICANCE

- Urban Coastal Site:
  - located off the shelf
  - deep water (~200m)
  - easily accessible
- Range of Different Characteristic Waters:
  - urban runoff
  - coastal upwelling
  - offshore oligotrophic

SIGNIFICANCE

- Located in an Area of Important:
  - economic
  - societal
  - ecological

- Only Site in Eastern Pacific

RESULTS

- Fewer data interruptions with updated communications and new computer
- Collected in-situ measurements with OSU
- Analysis of data presented by OSU

Calibration Support for VIIRS Ocean Earth Data Records Products by NIST

Carol Johnson
Sensor Science Division, NIST

August 27, 2015

cjohnson@nist.gov

SeaPRISM080 is part of AERONET-OC

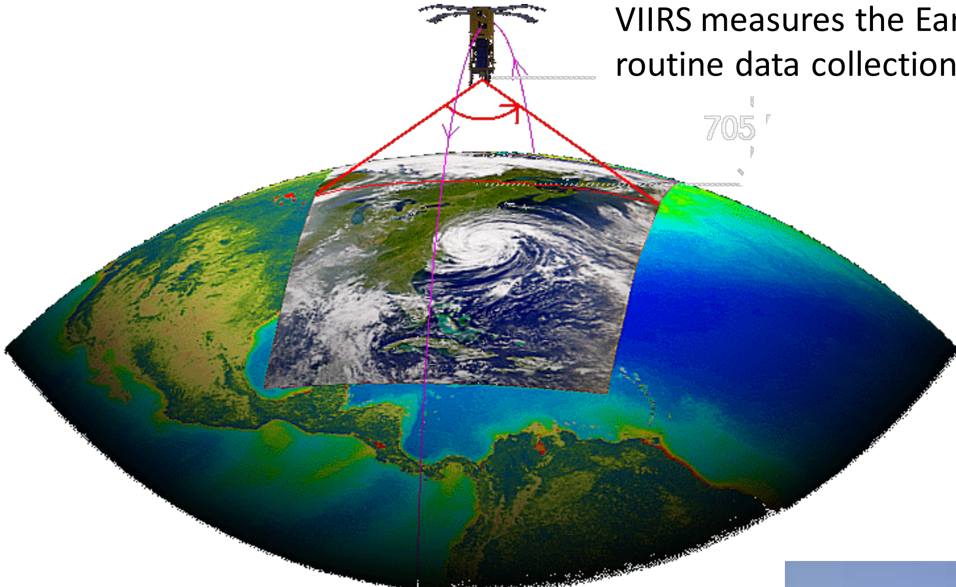

VIIRS measures the Earth for routine data collection

VIIRS measures the Moon – for mission drift corrections

Image Credit: SeaWiFS Project, NASA/GSFC, and GeoEye (oceancolor.gsfc.nasa.gov)

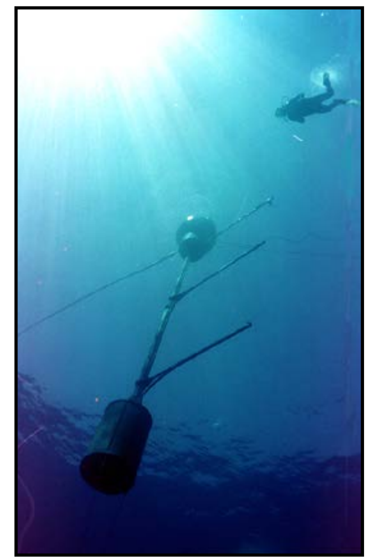

MOBY provides the in situ $L_w(\lambda)$ for vicarious calibration

https://moby.mlml.calstate.edu/

AERONET-OC: serves as a global validation network

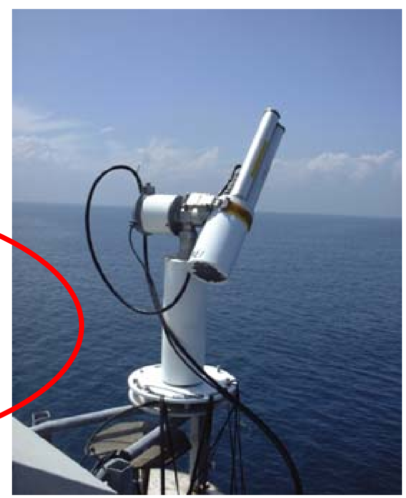

aeronet.gsfc.nasa.gov/new_web/ocean_levels_versions.html

SeaPRISM080 Calibration History

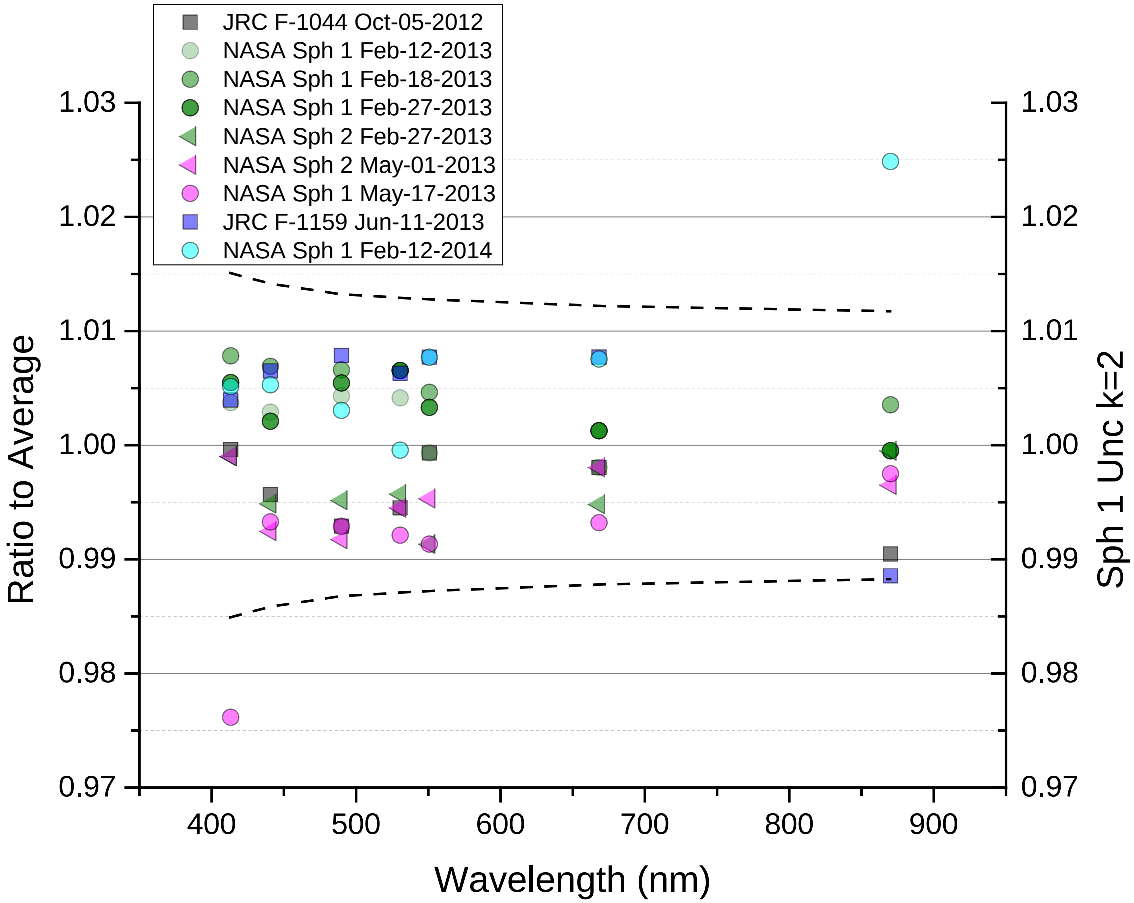

JRC's lamp/plaque (Credit: G. Zibordi, Joint Research Centre, Italy)

The agreement between GSFC and JRC for 080 for the radiance calibration is within +/- 1%.

We wanted to know how these source-based calibration coefficients compared to SIRCUS.

Spectral Responsivity

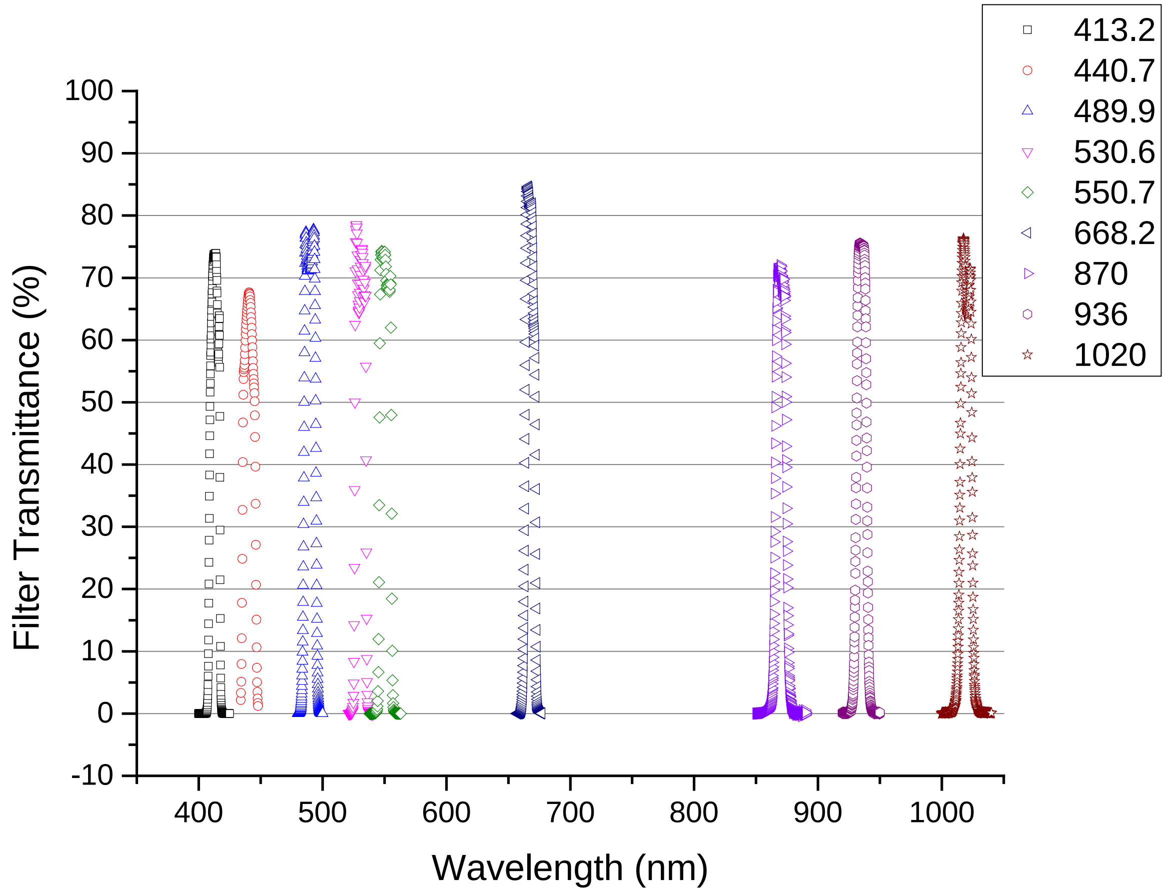

GSFC provided spectral responsivities derived from the vendor-supplied filter transmittance data. We wanted to compare these to the system level radiance responsivities measured on SIRCUS. Inaccuracies will impact the GSFC or JRC broadband calibration factors and the derived ocean color products.

SeaPRISM in AERONET-OC

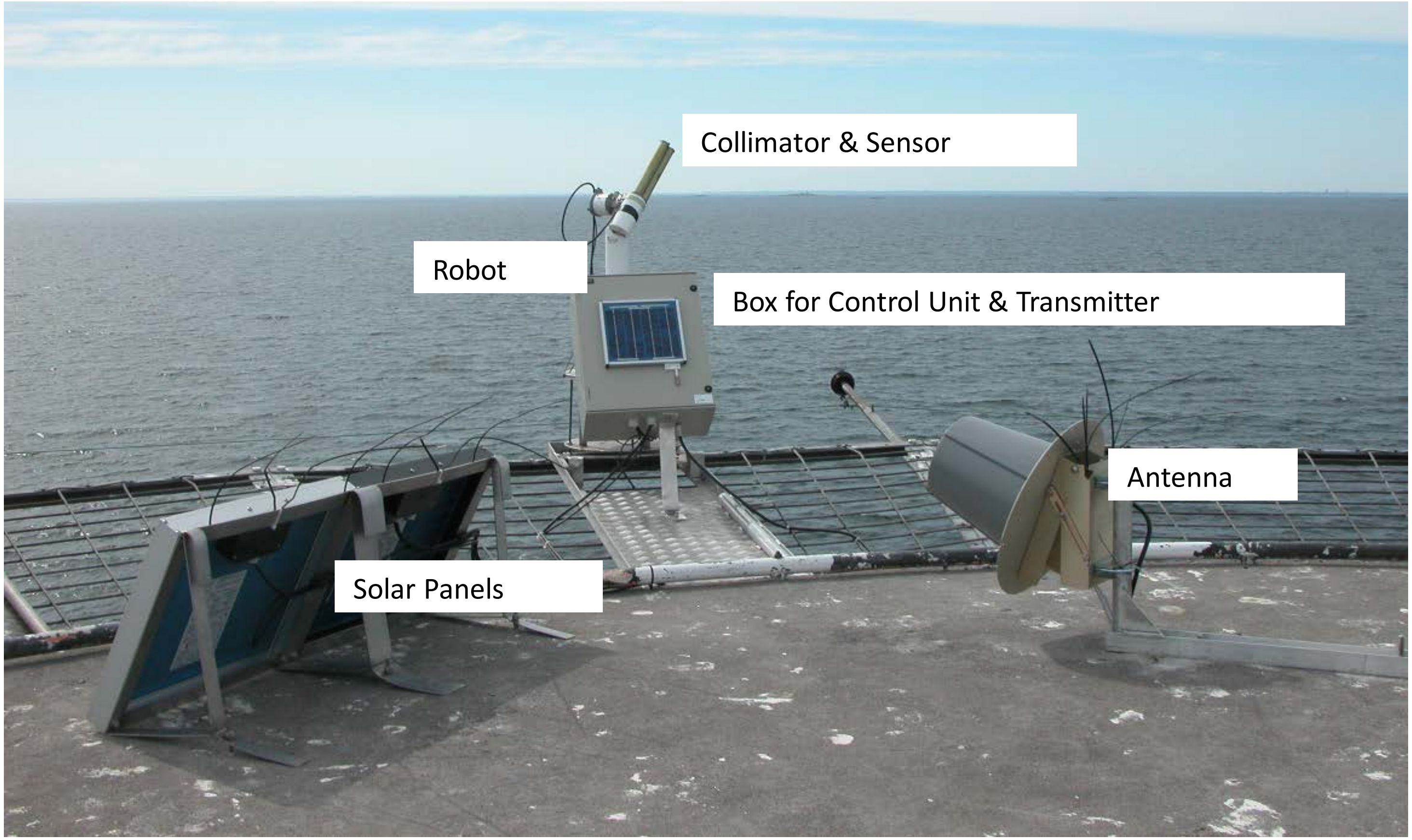

SeaPRISM at the Gustaf Dalen Lighthouse Tower in the northern Baltic. Credit: G. Zibordi, Joint Research Centre, Italy

SeaPRISMs operate autonomously. For SIRCUS, we needed to control the foreoptic selection, filter selection, and gain using RS232 interface and the instrument's command set.

SeaPRISM Program vs RS232 Commands

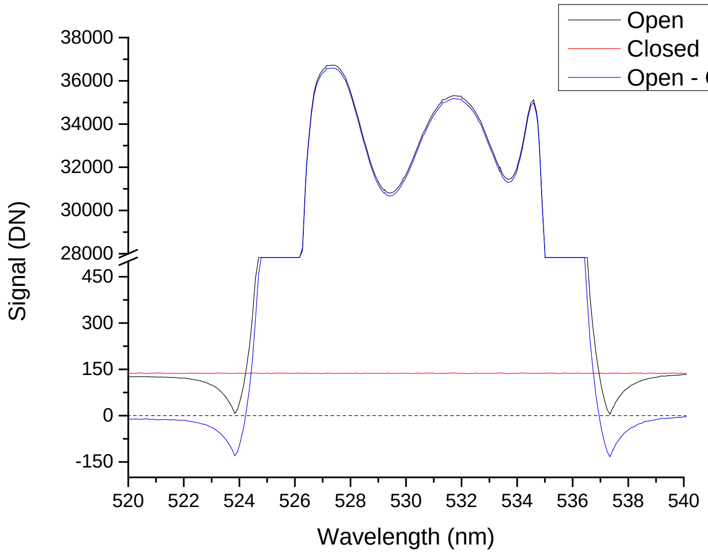

Normalized by the SIRCUS sphere monitor photodiode, SeaPRISM signals from 364k DN to 1.2k DN demonstrated a 20% nonlinearity – something never observed during GSFC or JRC characterizations.

SIRCUS laser blocked gave an offset; laser open gave signals that decreased to zero and then increased; hence nets were negative – not physical behavior. The PRS mode on a broadband source gave 0 DN with the source blocked.

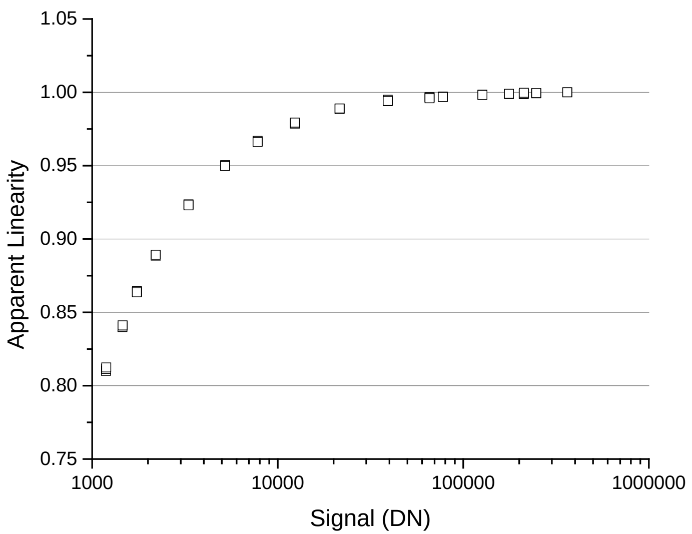

Measurement sequence: @, G, *i* then [Open, C, Close, C, step laser] x *N* times/band

Correction Model

- What if
  - *There is an internal offset B_{int}, a positive value in units of DN, that is always subtracted prior to outputting the measurement result; and*
  - *if the result of this internal subtraction is negative, the sign is reversed so that only positive values are output.*
- Identifying S_{closed} with B_{int} allowed us to correct the SIRCUS data

Ambiguity Exists for Low DN Output

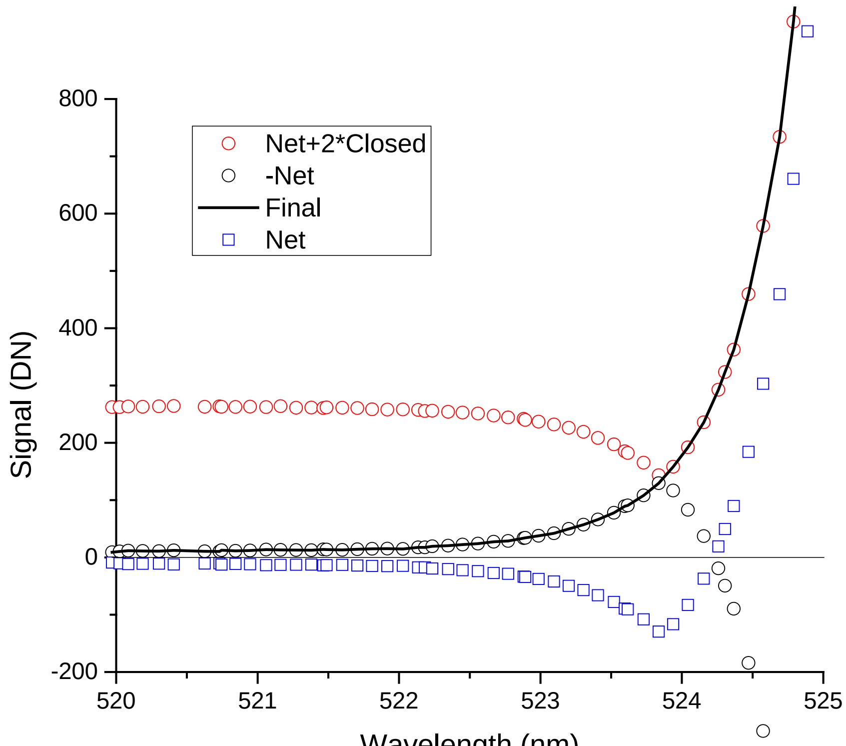

The ambiguity affects the spectral characterization: example: B_{int} = 138 DN, then an output of 2 DN means the signal was either 140 DN or 136 DN due to the internal subtraction and sign reversal. The relative error depends on the signal level – worse case is for zero or $2*B_{int}$. This limits the dynamic range, and measurements of the out-of-band at the system level are not possible.

Corrected Linearity

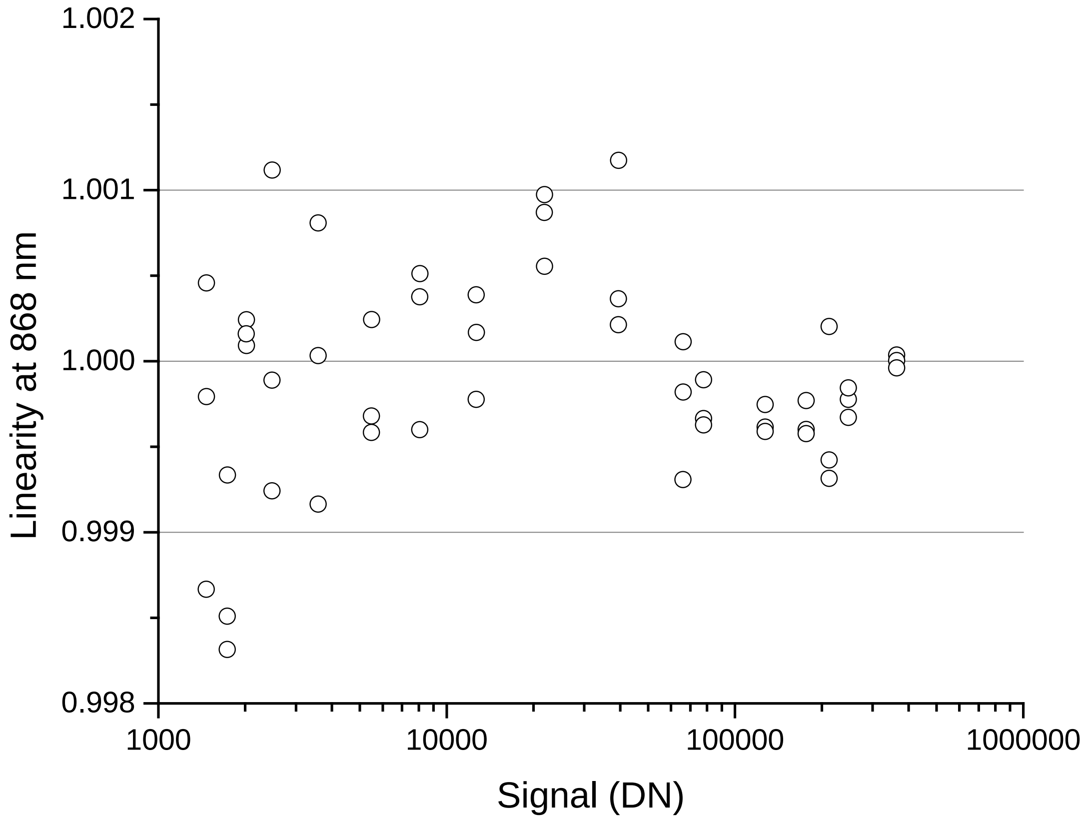

Apparent 20% at a laser wavelength of 868 nm for the 870 band is actually ±0.1%

Calibration Factor Comparison

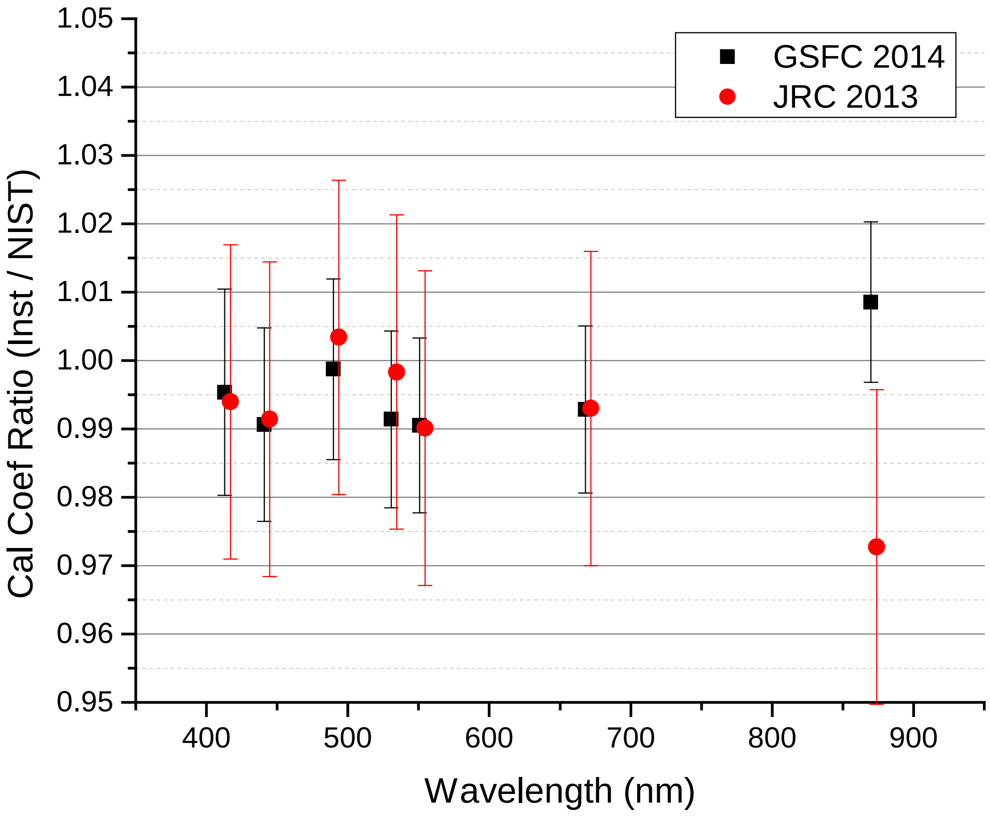

The uncertainties are estimates for the GSFC or JRC calibration factors.
A wavelength shift has been included for clarity. The agreement is excellent.

R_{rs} using Reflectance Standards

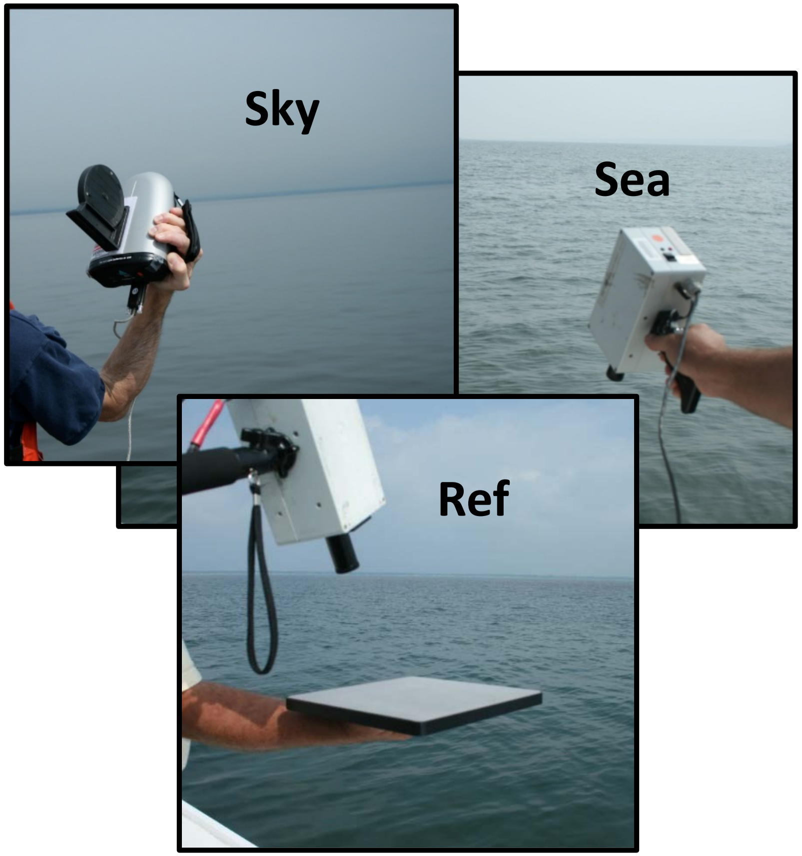

Question: Can we develop a faux reflectance target that mimics the water's spectral distribution, is Lambertian, and stable in time? Then, how well do all radiometers on a cruise agree with the faux target?

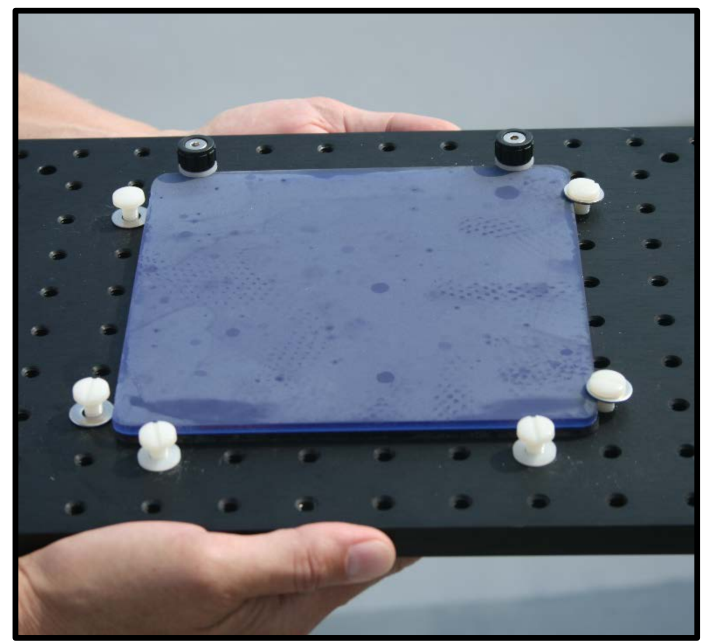

Prototype: ground blue glass, used in Long Island Workshop and Nov 2014 Nancy Foster cruise

Blue Tile 0/45 Reflectance Factor

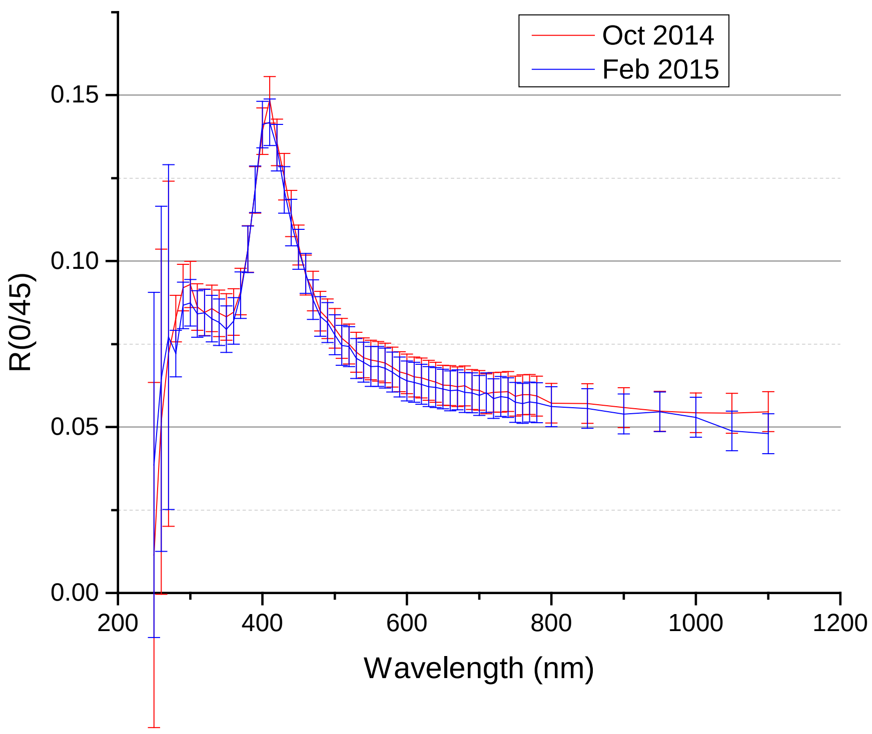

The NIST STARR facility measured the blue tile before and after the Nov 2014 cruise. The results agree within the uncertainties, so we can say the tile was stable.
The largest uncertainty component is from the lack of spatial uniformity.

Validation for NESDIS/STAR Lab

Is being modeled after the MOBY validation program (Jan 2015 most recent trip), except we will bring the sources to NIST's RSL facility

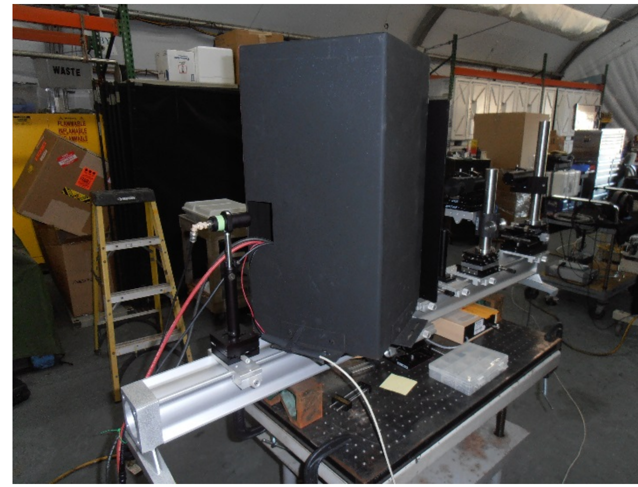

Cal Van, MOBY facility - radiance

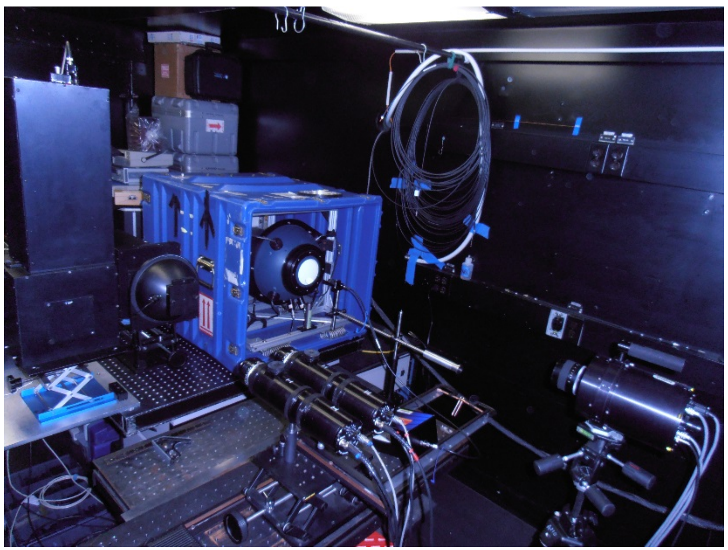

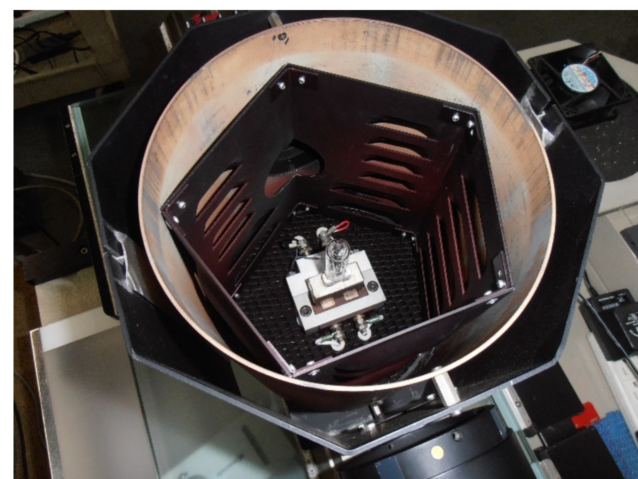

Tent, MOBY facility – irradiance NIST (top), MOBY (bottom)

Upcoming Work

- Measure SeaPRISM representative filters for out-of-band (component level test)
- Finish SeaPRISM080 archival paper (90% complete)
- Report on blue tile results for Nov cruise
- Continue investigation of best choice for colored “faux water” reflectance standards
- NESDIS/STAR irradiance and radiance source validation at NIST
- Colored radiance source for cruise validation at NESDIS

Community composition, biomass and photosynthetic competency of phytoplankton associated with microscale features and frontal zones of the Gulf Stream

Christy Jenkins, Joaquim I. Goes, Helga do R. Gomes, Alex Chekalyuk

Lamont-Doherty Earth Observatory
COLUMBIA UNIVERSITY | EARTH INSTITUTE

Robert A. Arnone

THE UNIVERSITY OF SOUTHERN MISSISSIPPI

BROAD OBJECTIVES

Examine the distribution and photo-physiology of phytoplankton functional types (PFTs) associated with microscale features and frontal zones in the Mid-Atlantic Bight shelf region using high resolution flow through measurements

Examine the potential of flow through measurements for enhancing the utility of satellite ocean color for PFT biomass and productivity estimates

FLOW-THROUGH SETUP

- ❑ Automated Laser Fluorometer (Chl *a*, CDOM, PE-1, PE-2, PE-3, Fv/Fm, NPQ, PQ)
- ❑ Satlantic FIRe (Chl *a*, Fv/Fm, sPSII)
- ❑ bbe-Moldaenke (Chl a - Diatoms, Cryptophytes, Green Algae, Cyanobacteria)
- ❑ FlowCAM (Phytoplankton imaging, taxonomy and size classification)

o WATER COLUMN MEASUREMENTS

- o Automated Laser Fluorometer (Chl *a*, CDOM, PE-1, PE-2, PE-3, Fv/Fm, sPSI)
- o Satlantic FIRe (Chl *a*, Fv/Fm, sPSII, Electron Transport Reactions)
- o FlowCAM (Phytoplankton imaging, taxonomy and size classification)
- o Phycobilipigment estimates in seawater

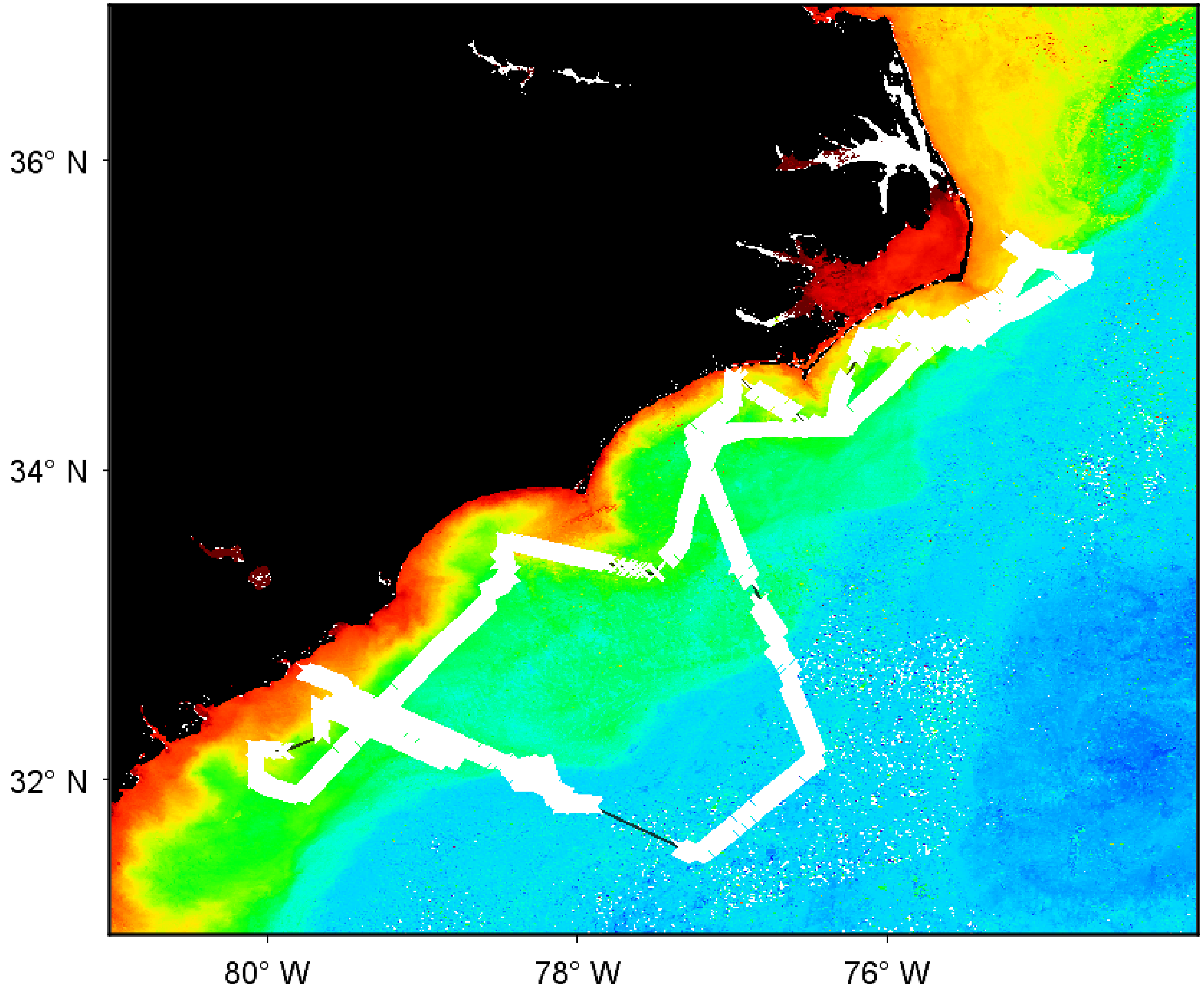

R/V Nancy Foster cruise track overlaid on VIIRS Chl data binned for the 1st week of Nov. 2014

Flow through set up

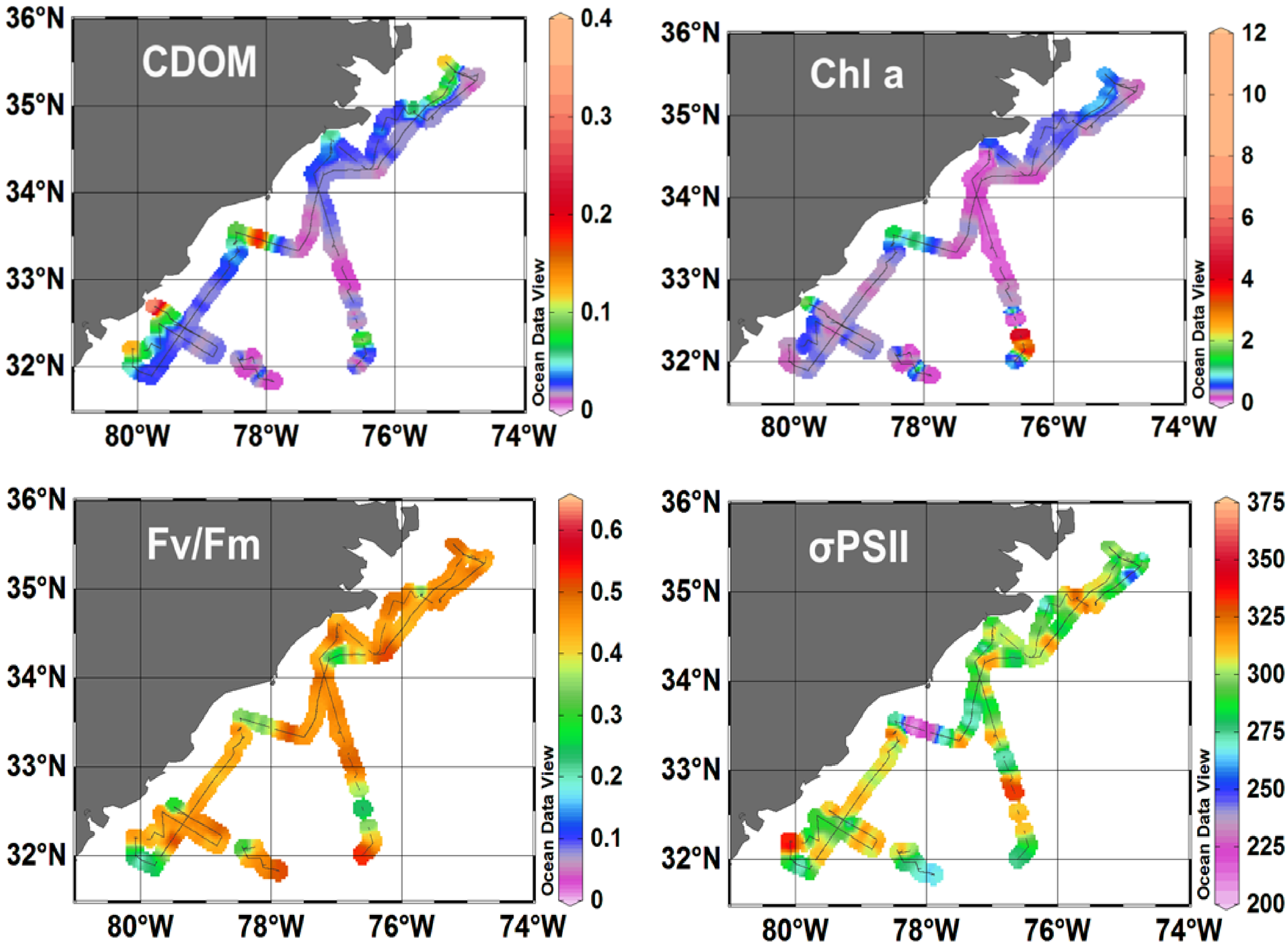

Distribution of CDOM, Chl *a*, variable fluorescence and σPSII along the cruise track as measured with the flow through system

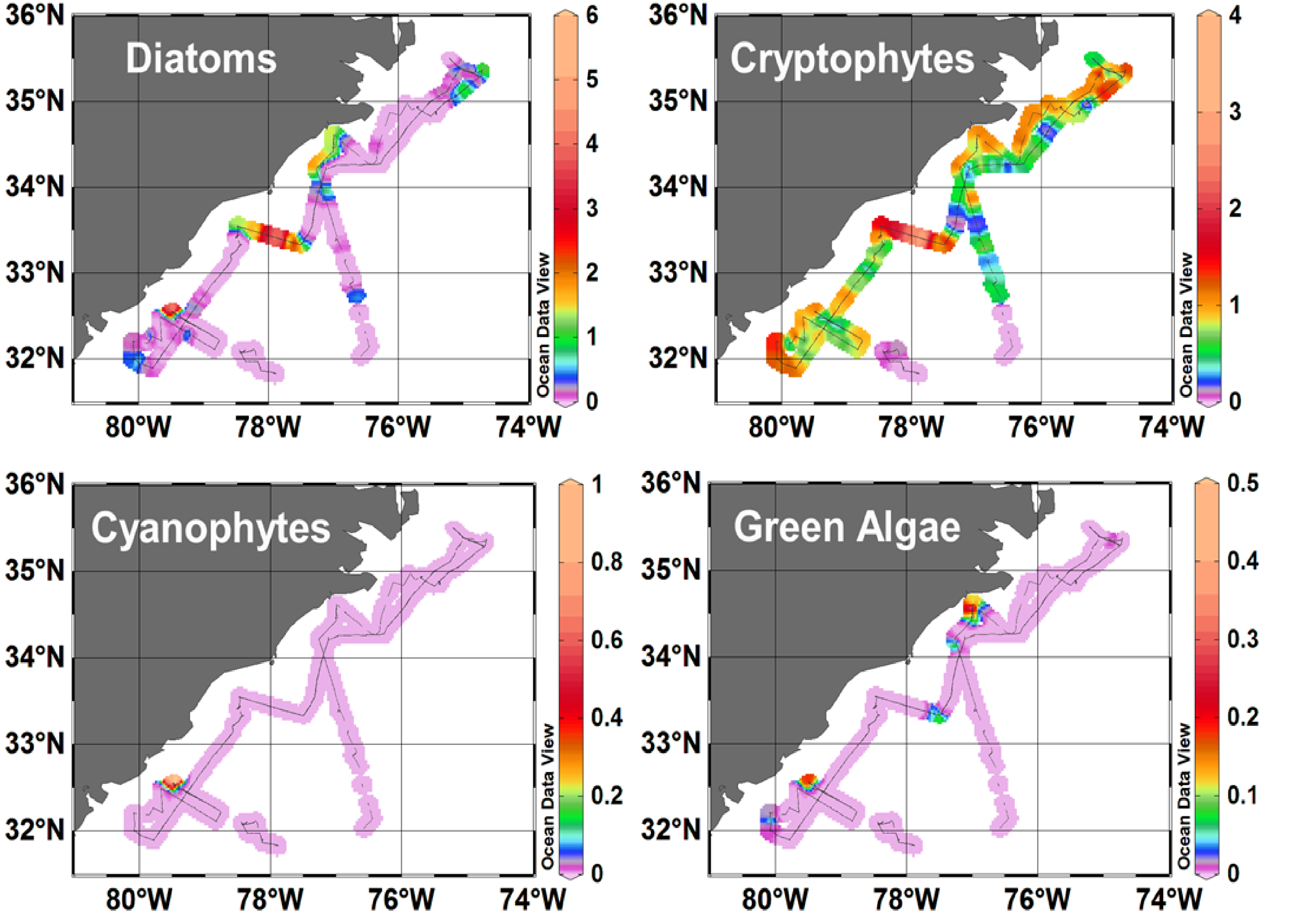

Distribution of biomass of PFTs along cruise track measured by bbe Molaedanke

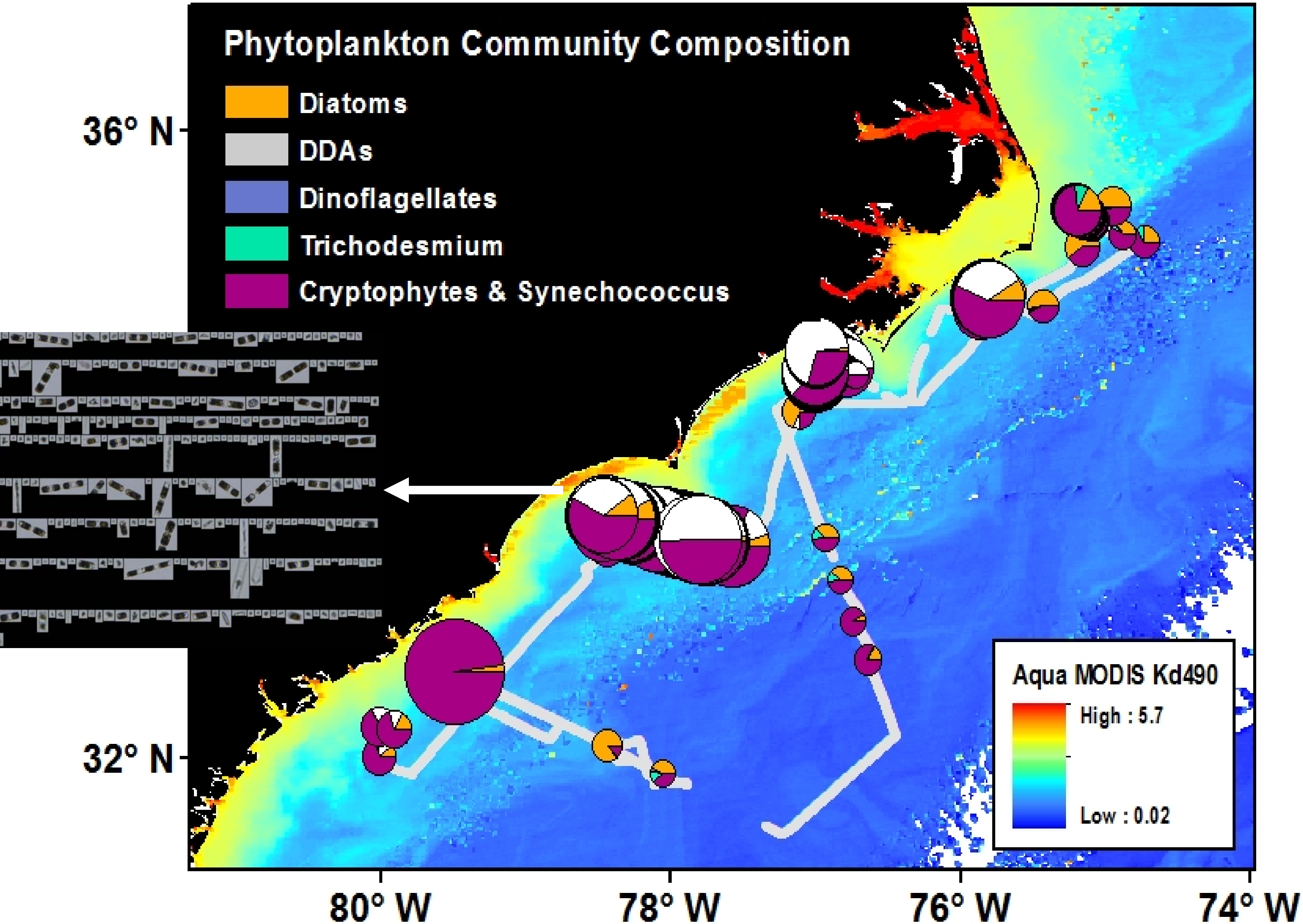

Distribution of major PFTs along the cruise track using FlowCAM

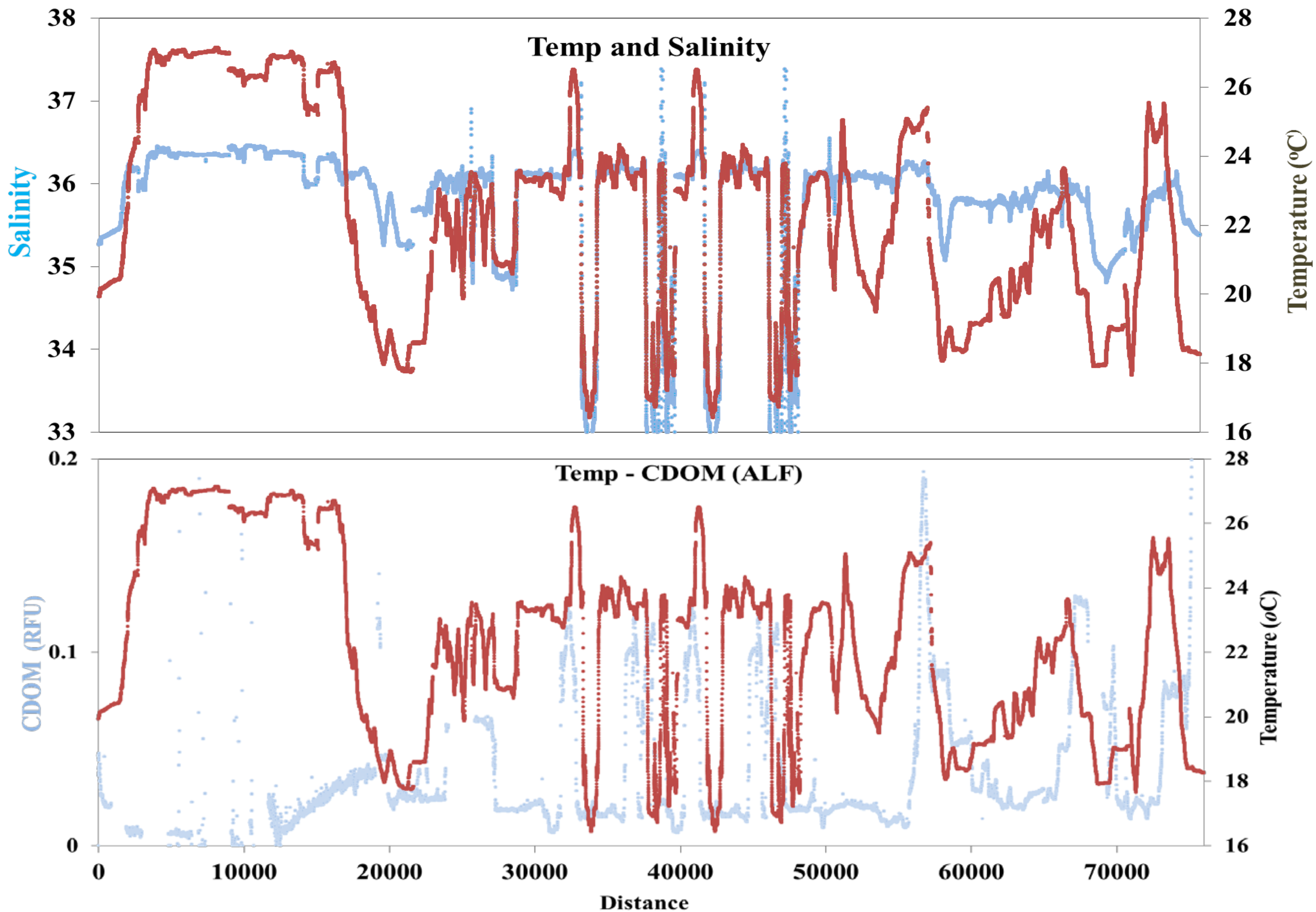

Distribution of CDOM, temperature and salinity along the cruise track

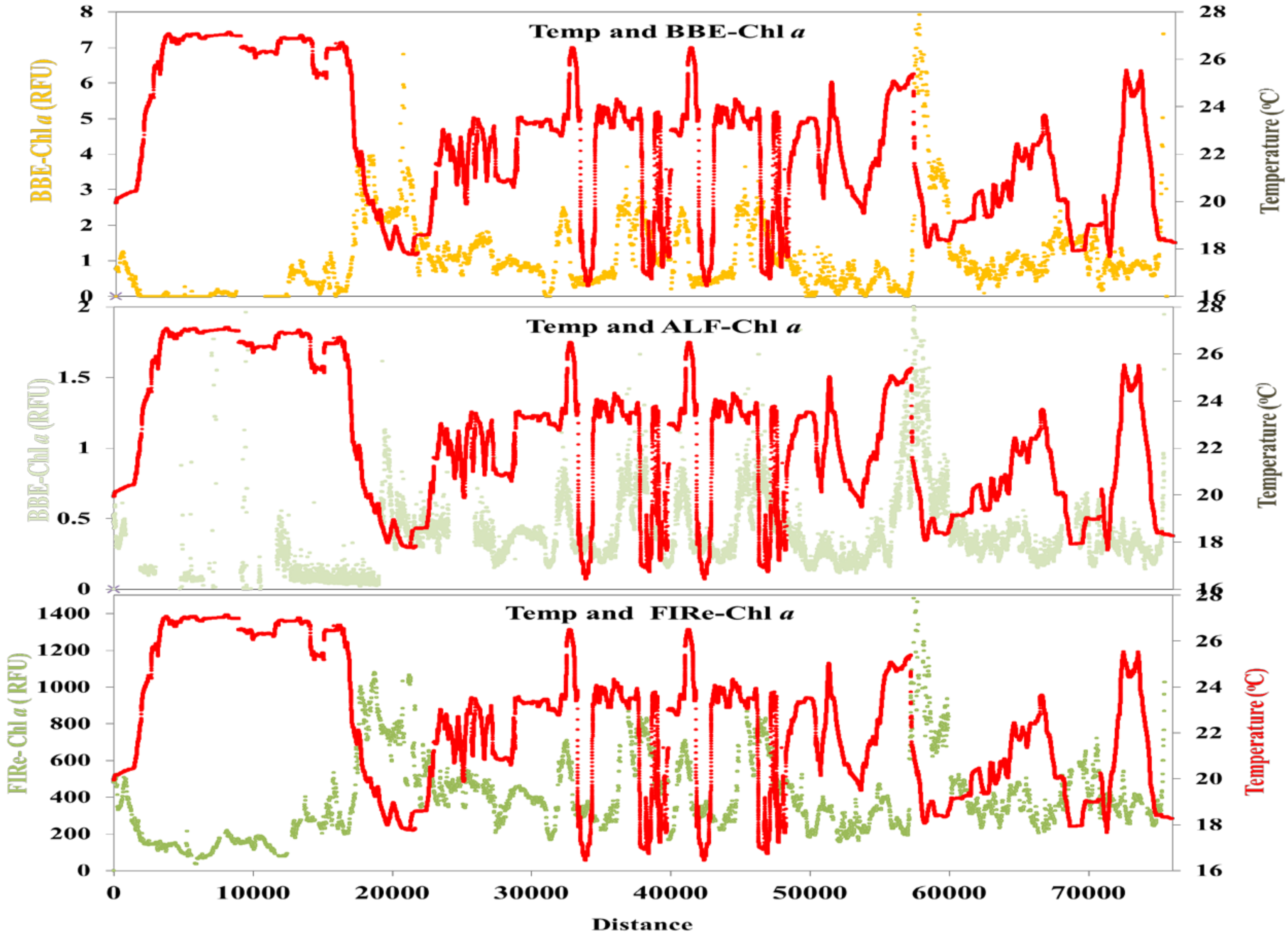

Distribution of Chl a (measured by three different instruments) temperature along the cruise track

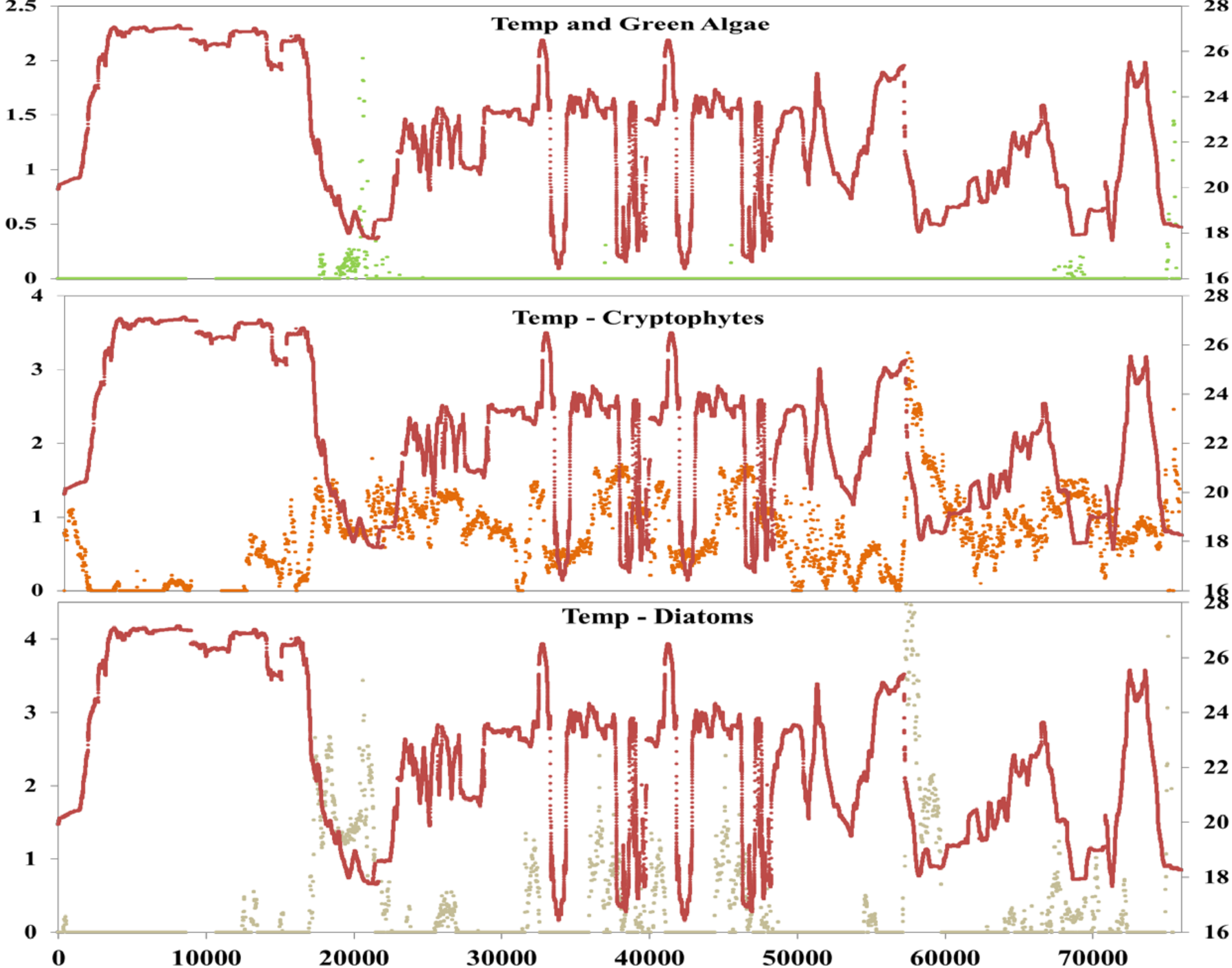

Variations in major PFTs with temperature along the cruise track (measured by bbe)

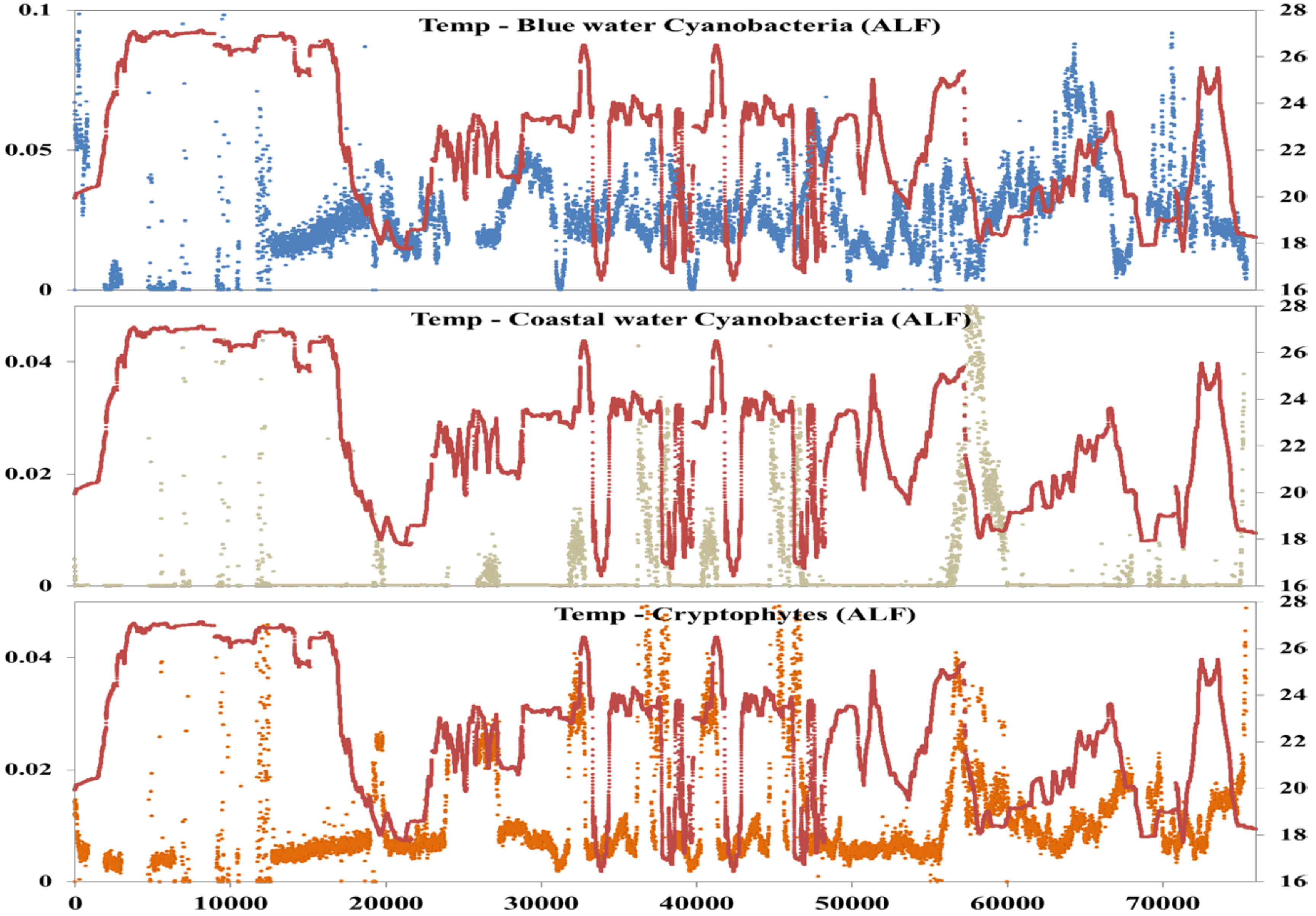

Variations in major phycobilipigment containing PFTs with temperature along the cruise track (measured by bbe)

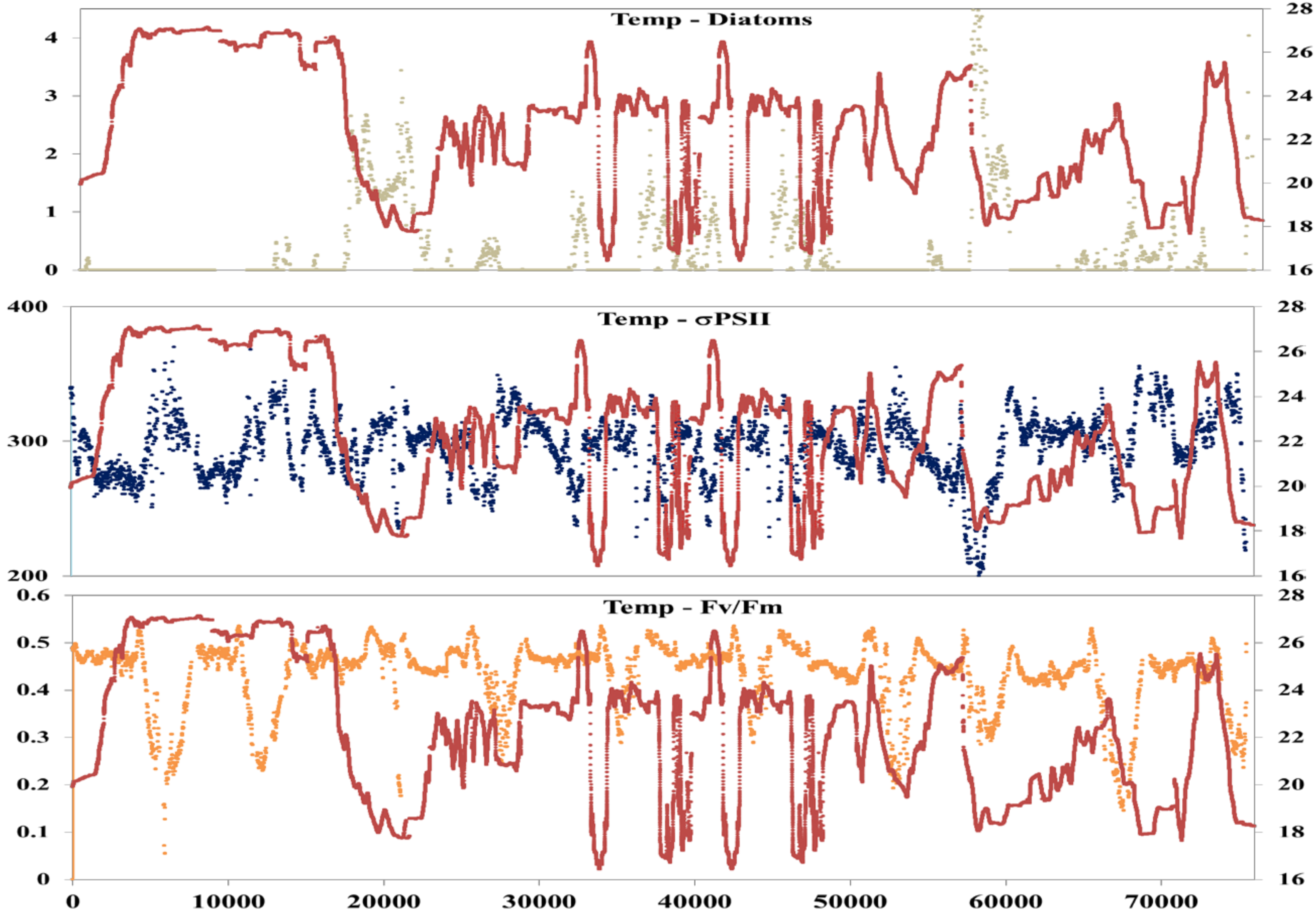

Variations in diatom biomass and photosynthetic competency of phytoplankton populations

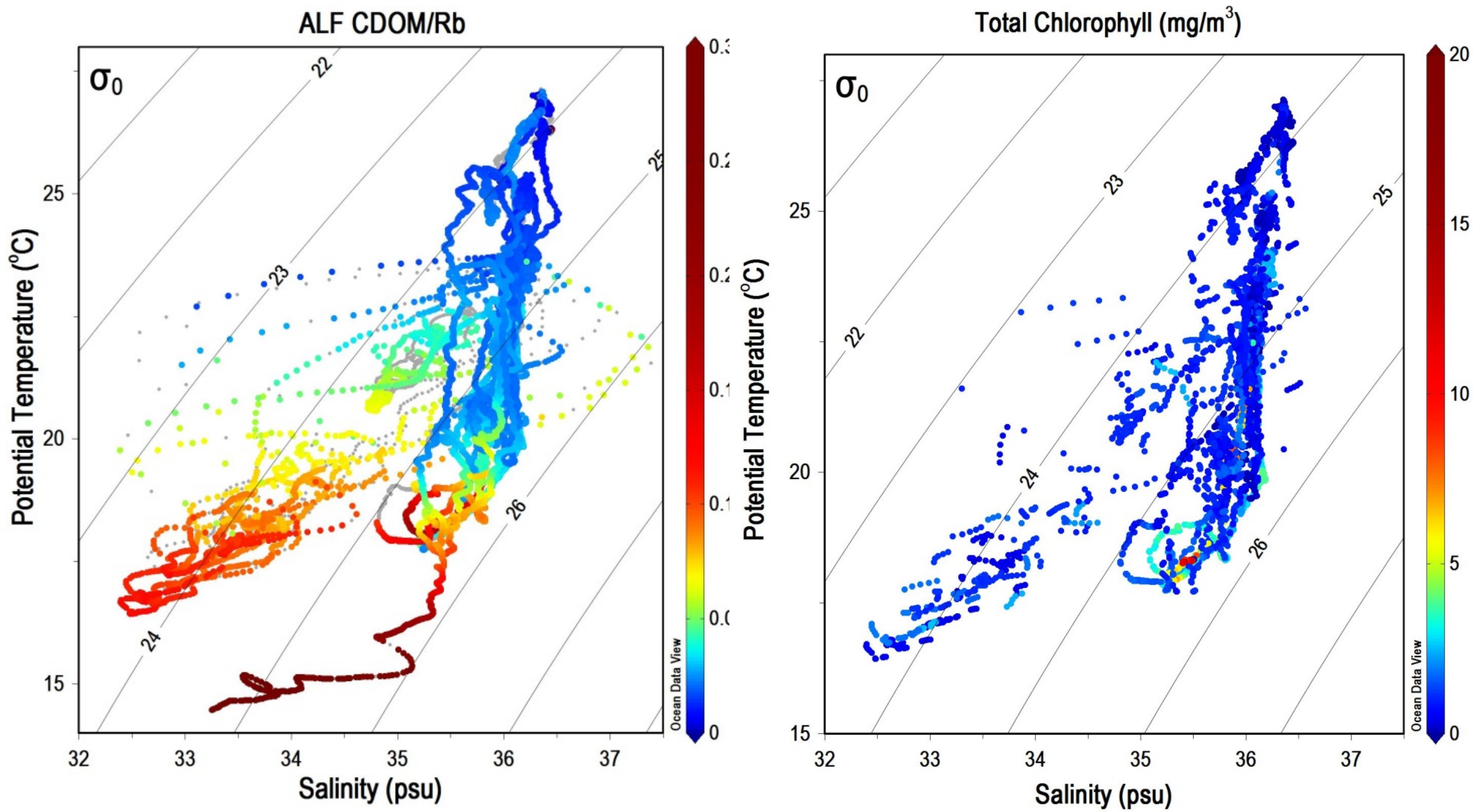

T-S plots showing CDOM concentrations and total Chl *a* associated with different water types

Blue water cyanobacteria **Coastal water cyanobacteria** **Cryptophytes**

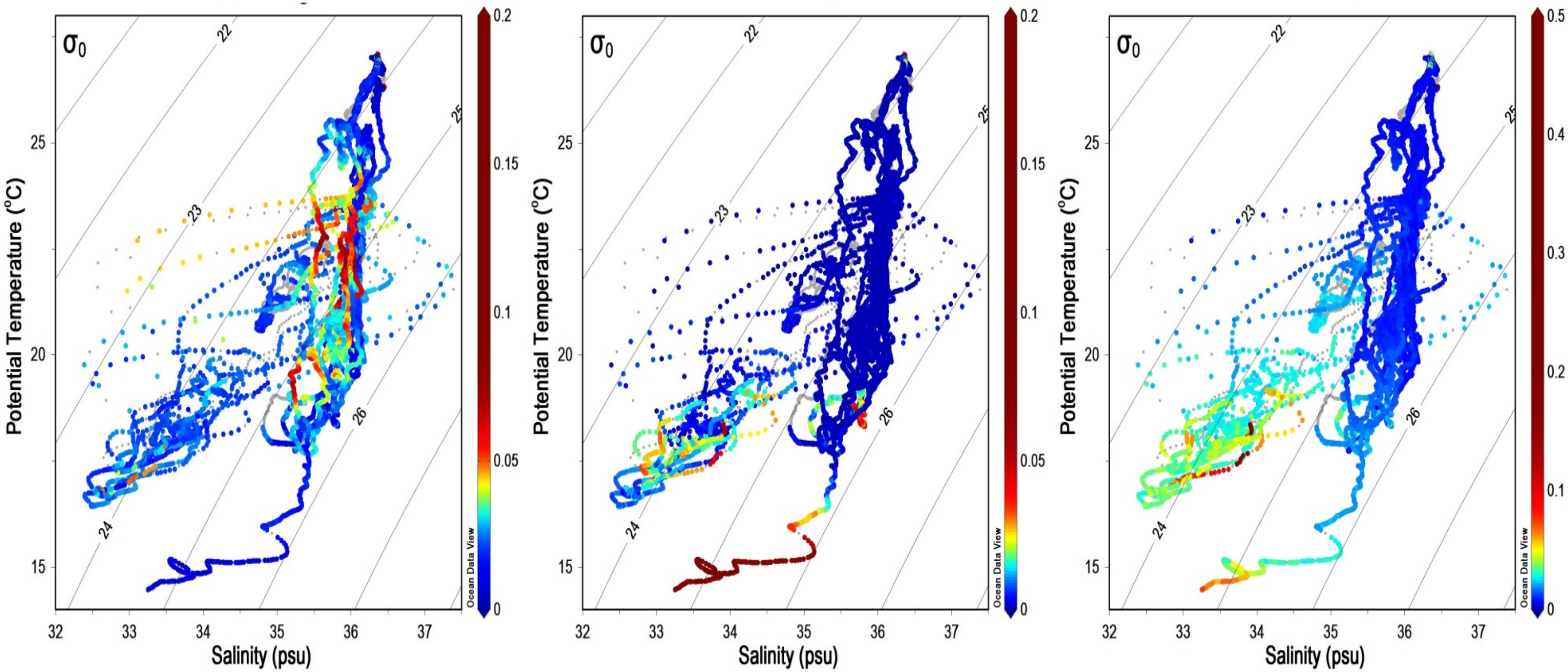

T-S plots showing PFTs associated with different water types

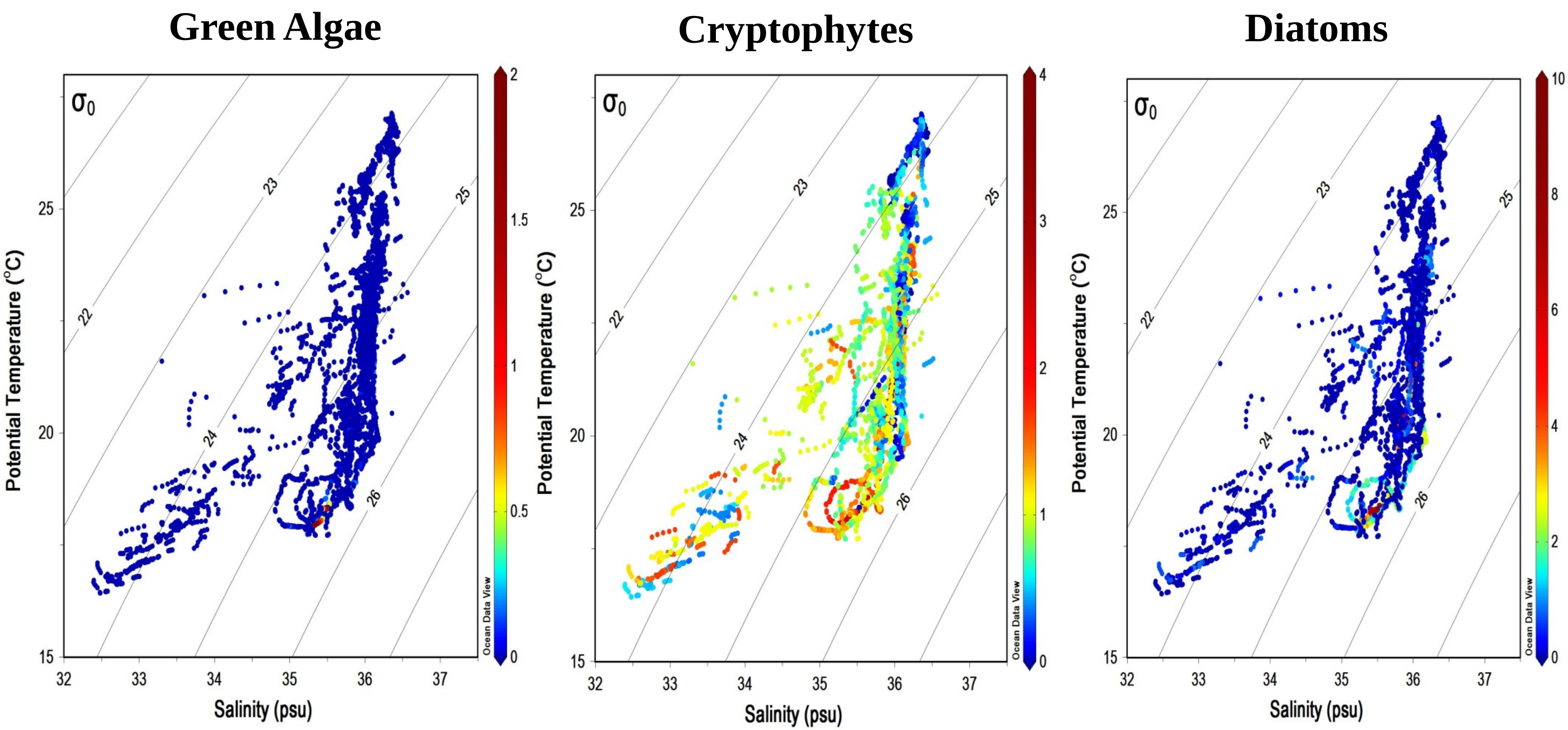

T-S plots showing PFTs associated with different water types

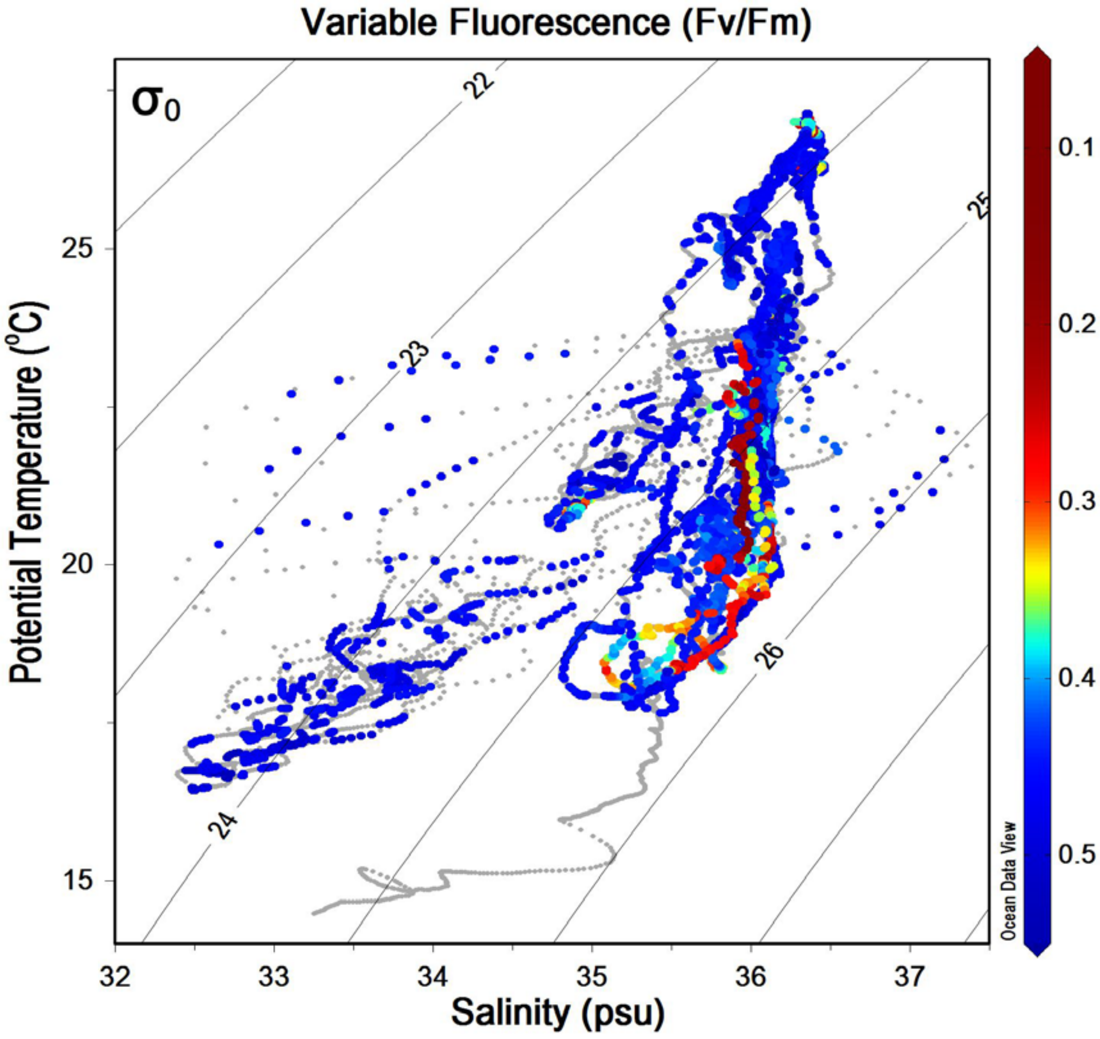

T-S plots showing photosynthetic performance of PFTs different water types

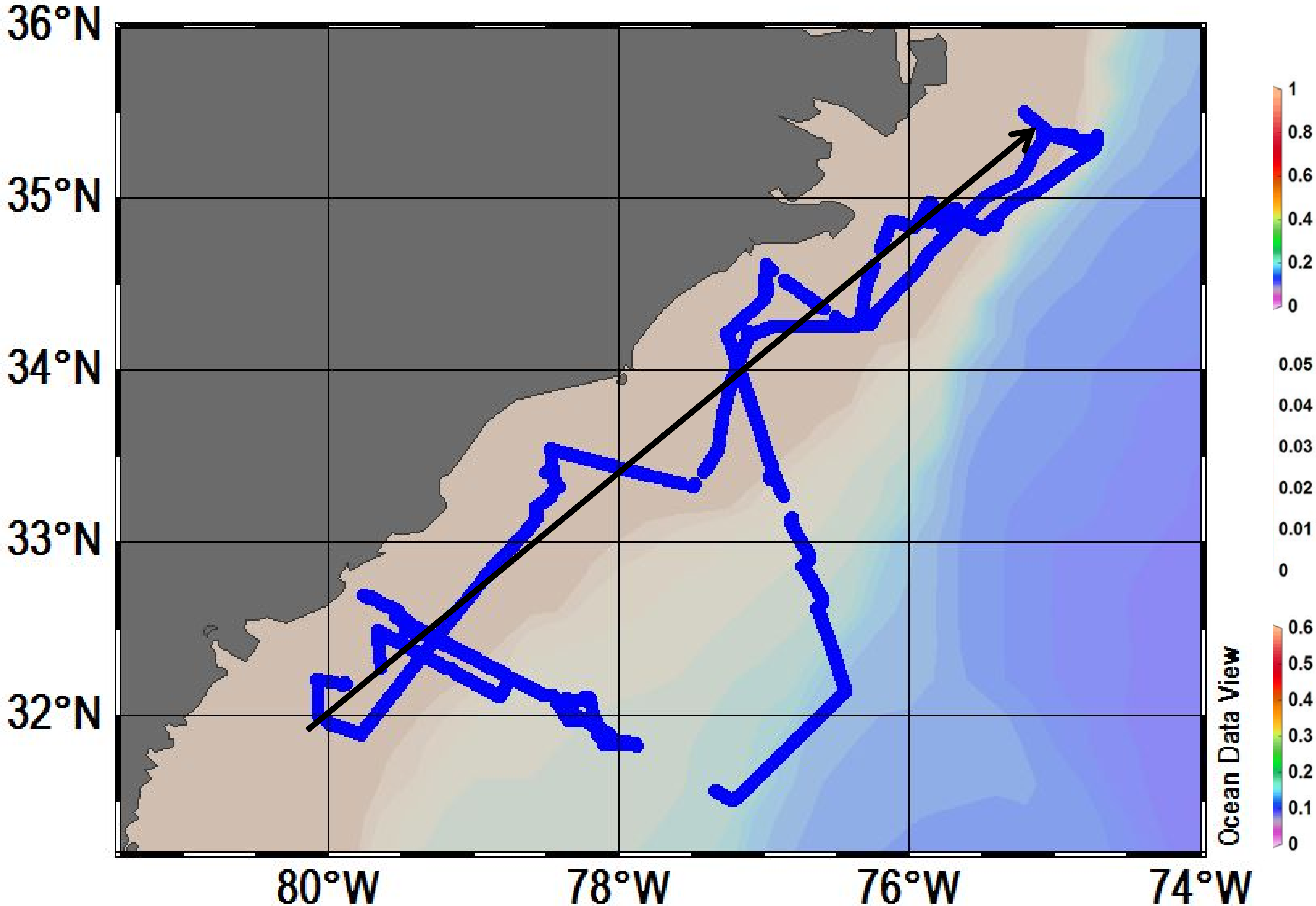

Cruise track showing N-S section from which seawater samples were drawn from different depths

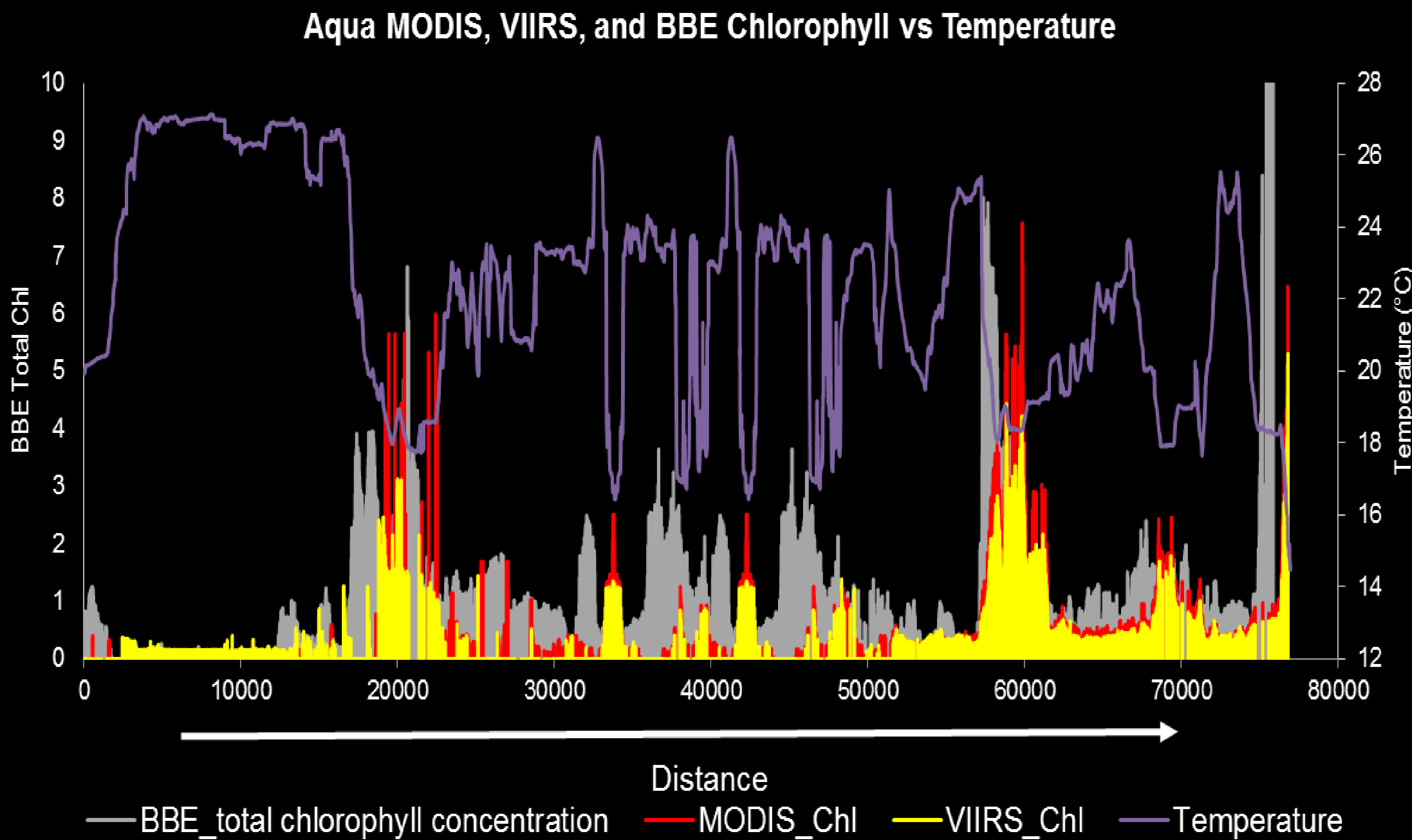

Comparison of MODIS-A and VIIRS derived Chl *a* with in-situ Chl *a* along the cruise track

FUTURE PLANS

- Development of PFT and phytoplankton size distribution algorithms using a combination of in-situ optical and hydrography measurements
- Distribution patterns of PFTs in relation to microscale features and frontal zones
- Estimation of primary productivity using measurements of phytoplankton biomass and photo-physiology

THANK YOU

An experimental evaluation of sea surface reflectance factors relevant to AERONET-OC above-water radiometry

Giuseppe Zibordi

Institute for Environment and Sustainability

Joint Research Centre

AERONET-OC sites

AERONET – Ocean Color is a sub-network of the Aerosol Robotic Network (AERONET), supporting ocean color validation activities with highly consistent time-series of $L_{WN}(\lambda)$ & $\tau_a(\lambda)$.

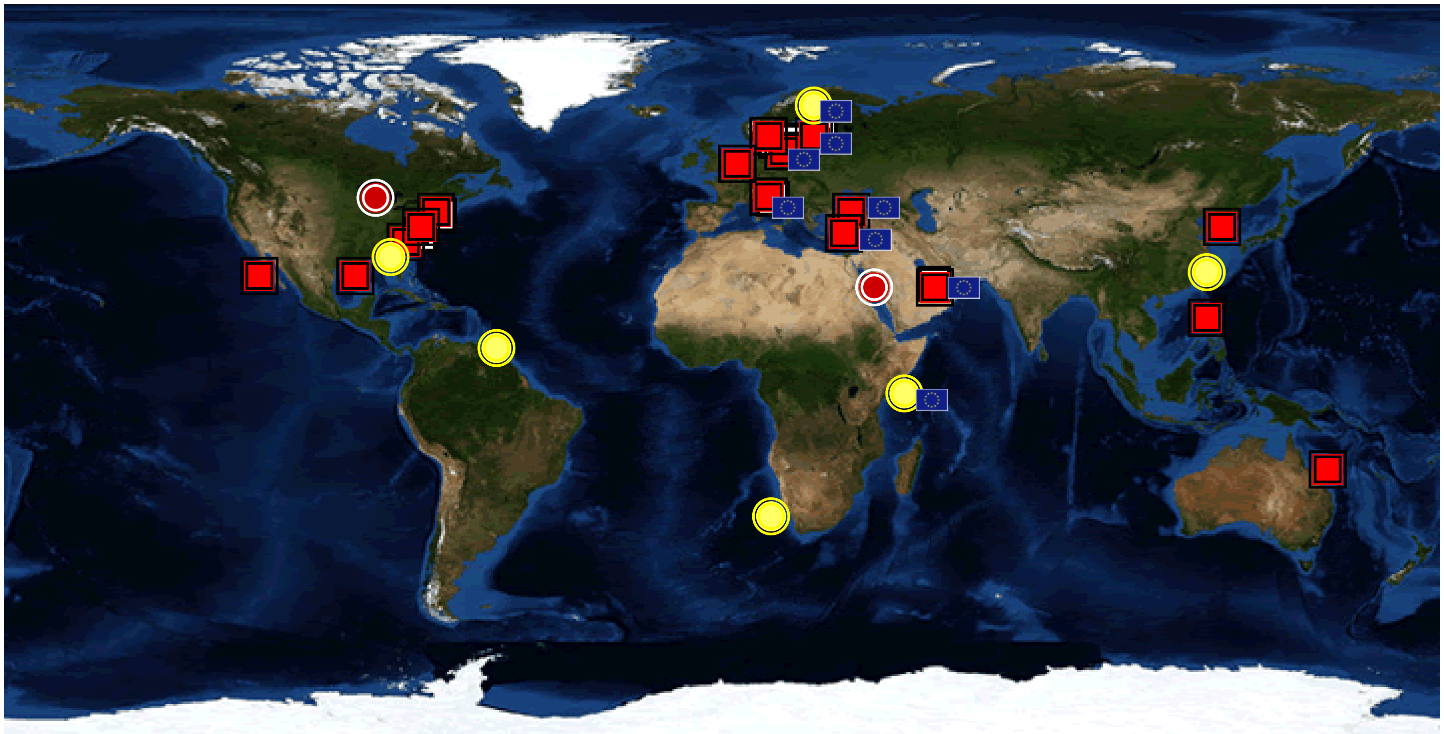

■ Current sites ● Planned sites ● Potential sites

- **NASA manages the network infrastructure (i.e., handles the instruments calibration and, data collection, processing and distribution within AERONET).**
- **JRC has the scientific responsibility of the processing algorithms and performs the quality assurance of data products (in addition to the management of 5 out of 15 sites).**
- **PIs establish and maintain individual AERONET-OC sites.**

G.Zibordi et al. A Network for Standardized Ocean Color Validation Measurements. Eos Transactions, 87: 293, 297, 2006.

Application of GLR AERONET-OC L_{WN} to VIIRS data products validation

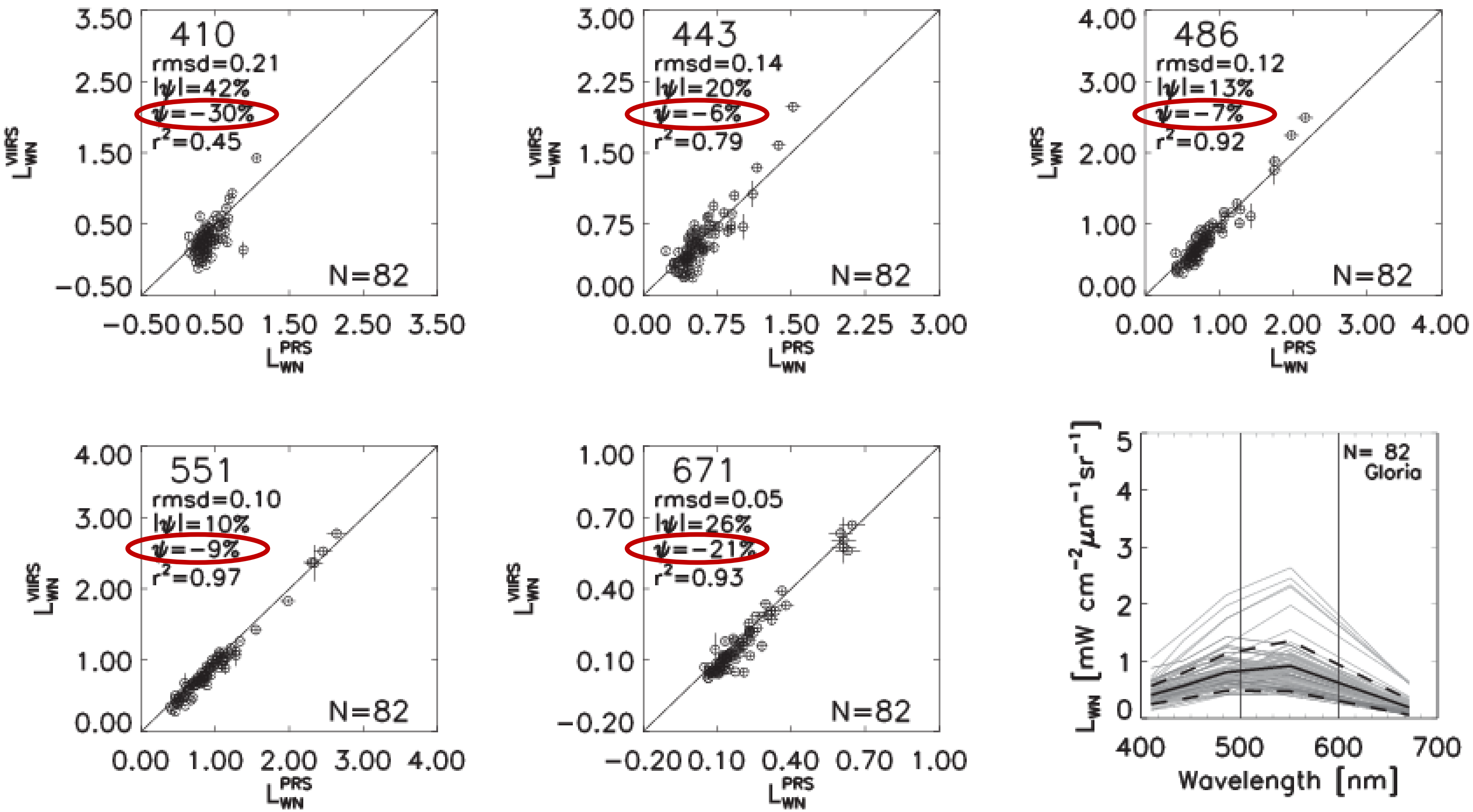

Zibordi, G., Mélin, F., Berthon, J.-F., and Talone, M.: In situ autonomous optical radiometry measurements for satellite ocean color validation in the Western Black Sea, Ocean Sci., 11, 275-286, doi:10.5194/os-11-275-2015, 2015.

Above-Water Radiometry

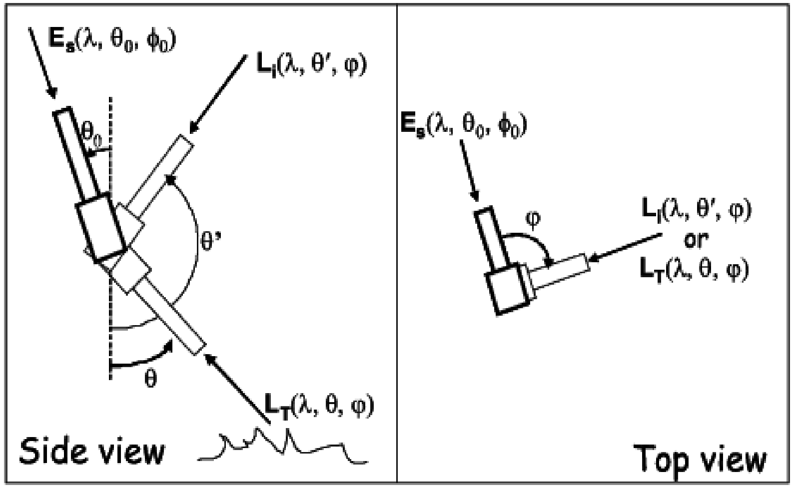

$$(\varphi = \varphi_0 + 90^0; \theta = 40^0; \theta' = 140^0)$$

Sky-radiance: L_i

Sea-radiance: L_T

Removal of sky-glint contribution

$$L_W(\varphi, \theta, \lambda) = L_T(\varphi, \theta, \lambda) - \rho(\varphi, \theta, \theta_0, W) L_i(\varphi, \theta', \lambda)$$

with L_T and L_i passing strict QA/QC tests, and L_T determined from the mean of relative minima

Correction for off-nadir view

$$L_W(\lambda) = L_W(\varphi, \theta, \lambda) C_{\Im Q}(\lambda, \theta, \varphi, \theta_0, \tau_a, IOP, W)$$

Transformation to exact normalized water-leaving radiance

$$L_{WN}(\lambda) = L_W(\lambda)\left(D^2 t_d(\lambda)\cos\theta_0\right)^{-1} C_{f/Q}(\lambda, \theta_0, \tau_a, IOP)$$

Zibordi, G. et al. (2009). AERONET-OC: a network for the validation of ocean color primary products. *Journal of Atmospheric and Oceanic Technology*, *26*(8), 1634-1651.

Values of ρ^U and ρ^P for the AERONET-OC measurement geometry

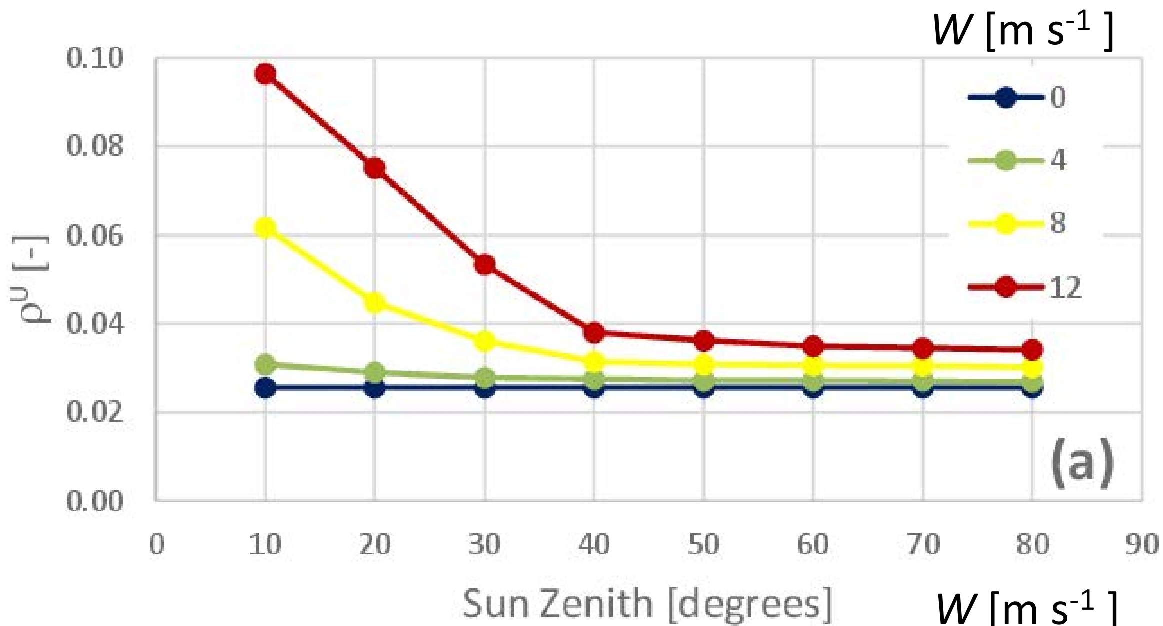

Unpolarized case

Rayleigh sky

Cox-Munk surfaces

Mobley, C. D. (1999). Estimation of the remote-sensing reflectance from above-surface measurements. Applied Optics, 38(36), 7442-7455.

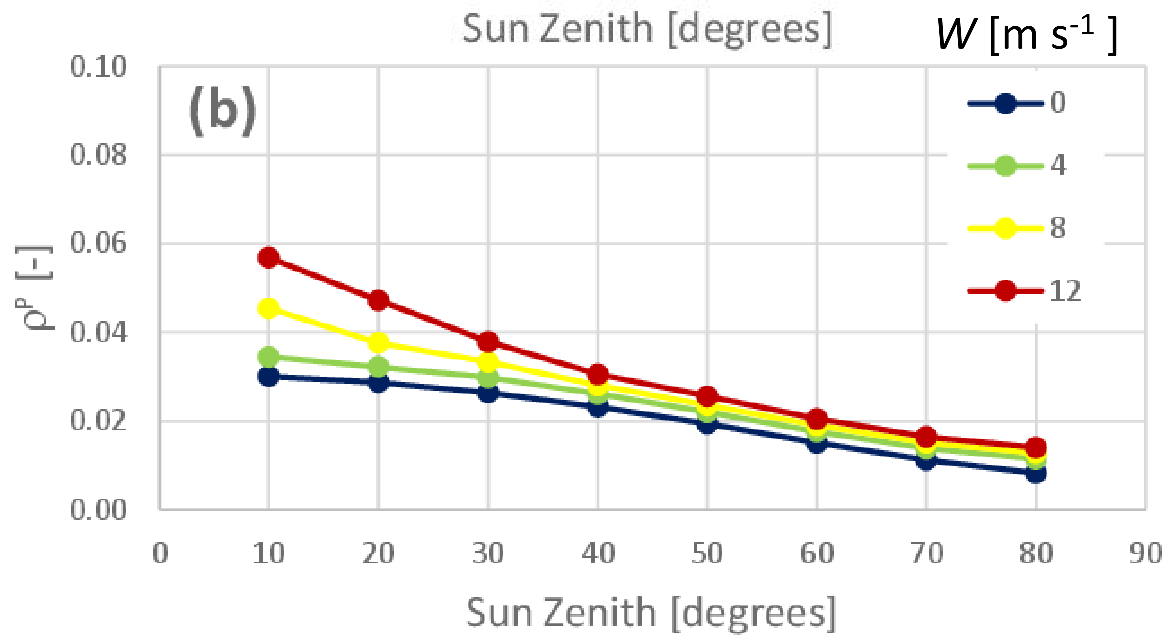

Polarized case

Rayleigh sky

FFT surfaces

Mobley, C. D. (2015). Polarized reflectance and transmittance properties of windblown sea surfaces. Applied Optics, 54(15), 4828-4849.

Matchup spectra and measurement conditions

Joint Research Centre

From above-water (AERONET-OC)

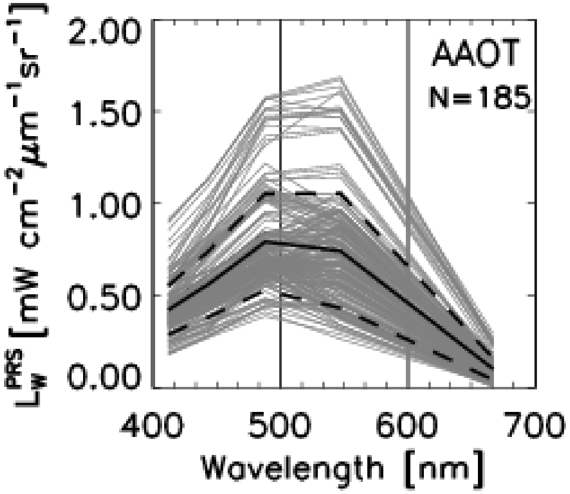

From in-water profiling

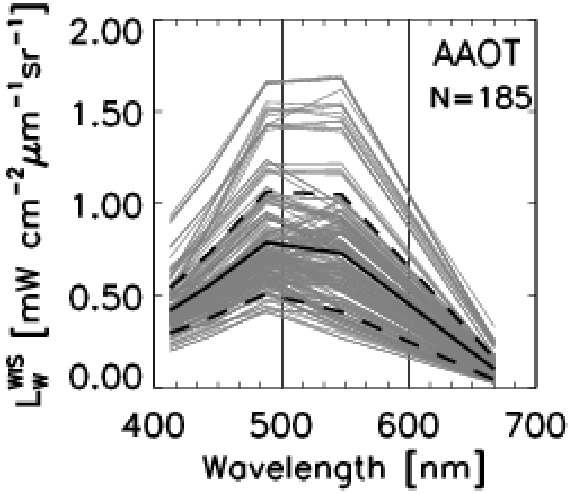

Acqua Alta Oceanographic Tower

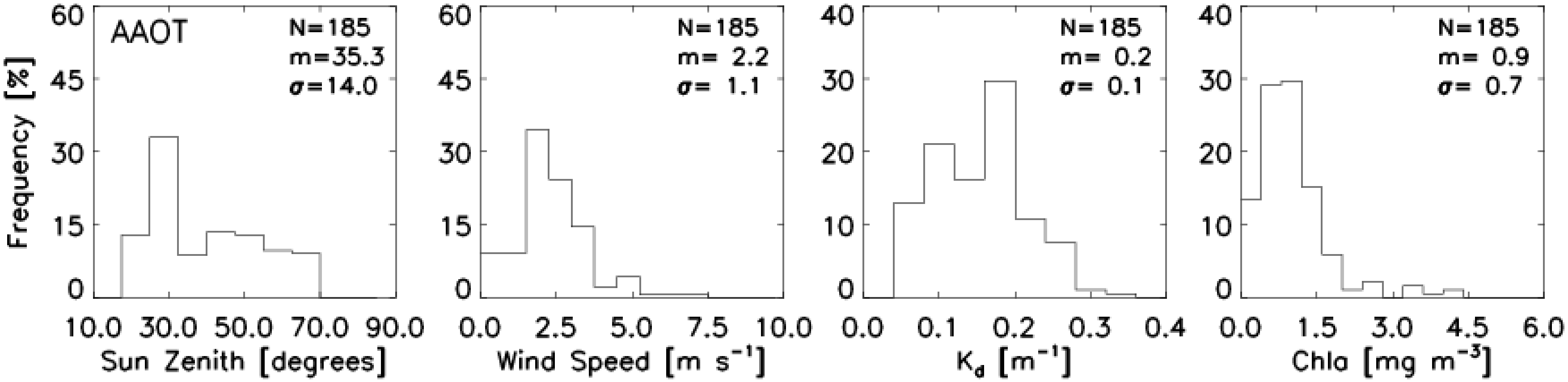

Distributions of ρ^U and ρ^P for matchups

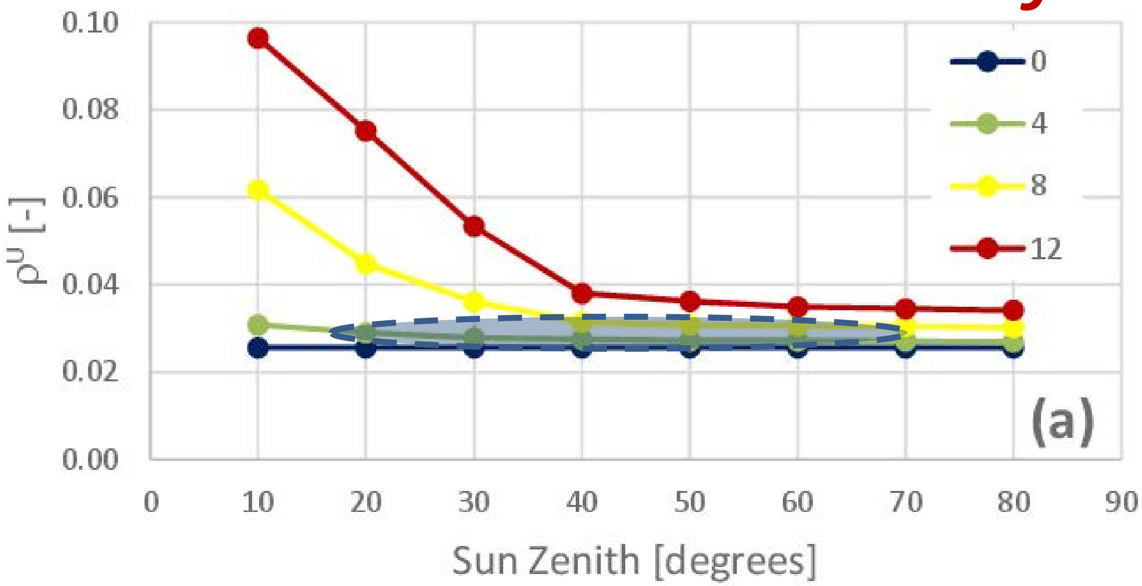

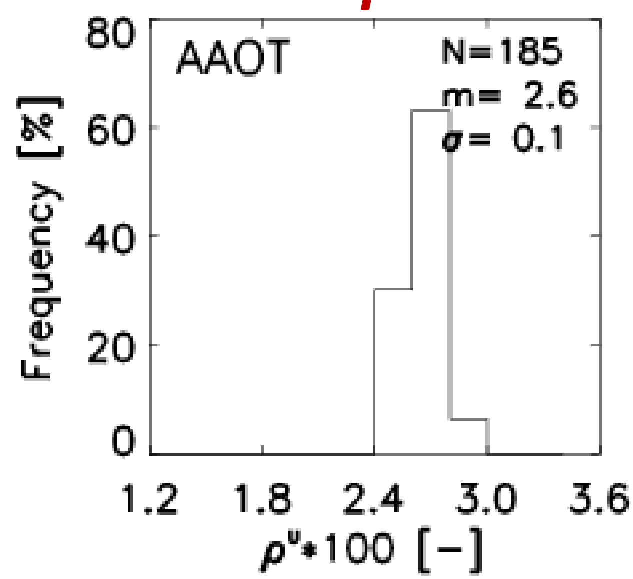

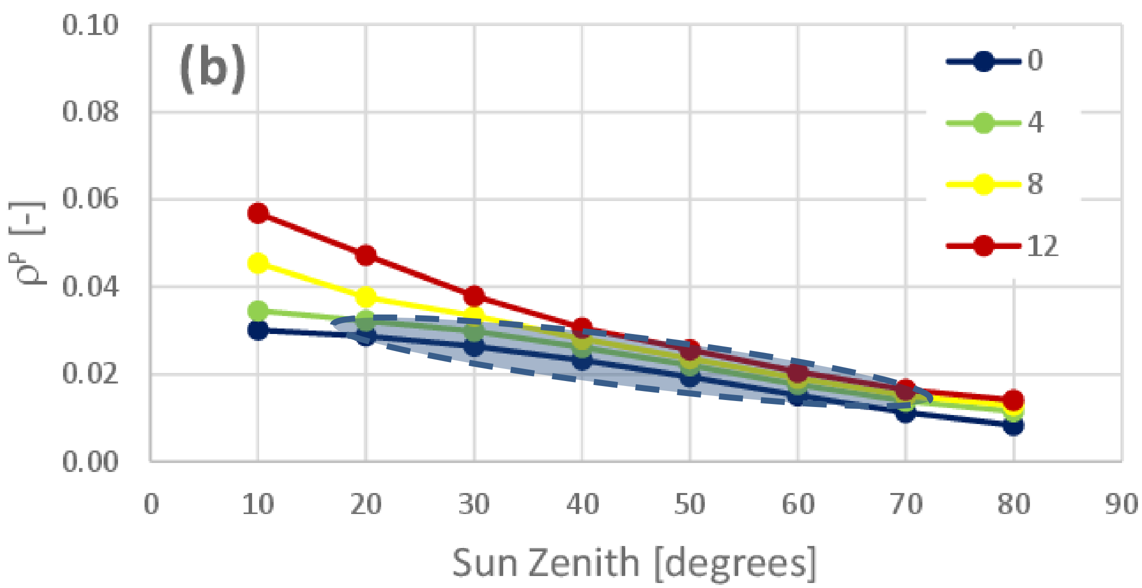

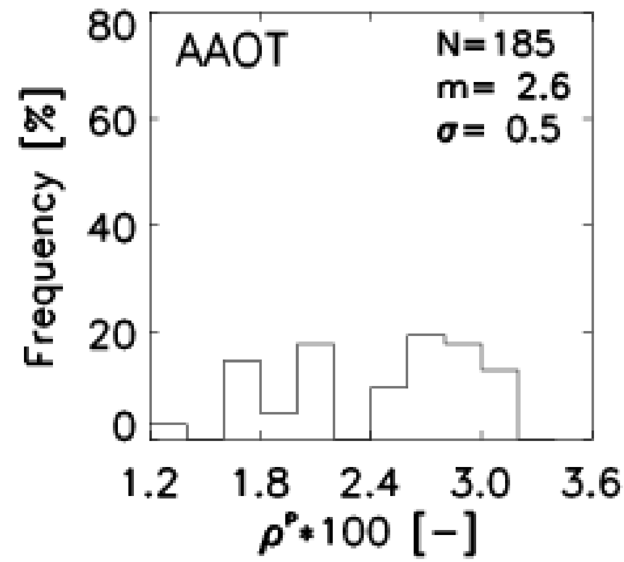

Joint Research Centre

Assessment AERONET-OC L_W from ρ^U

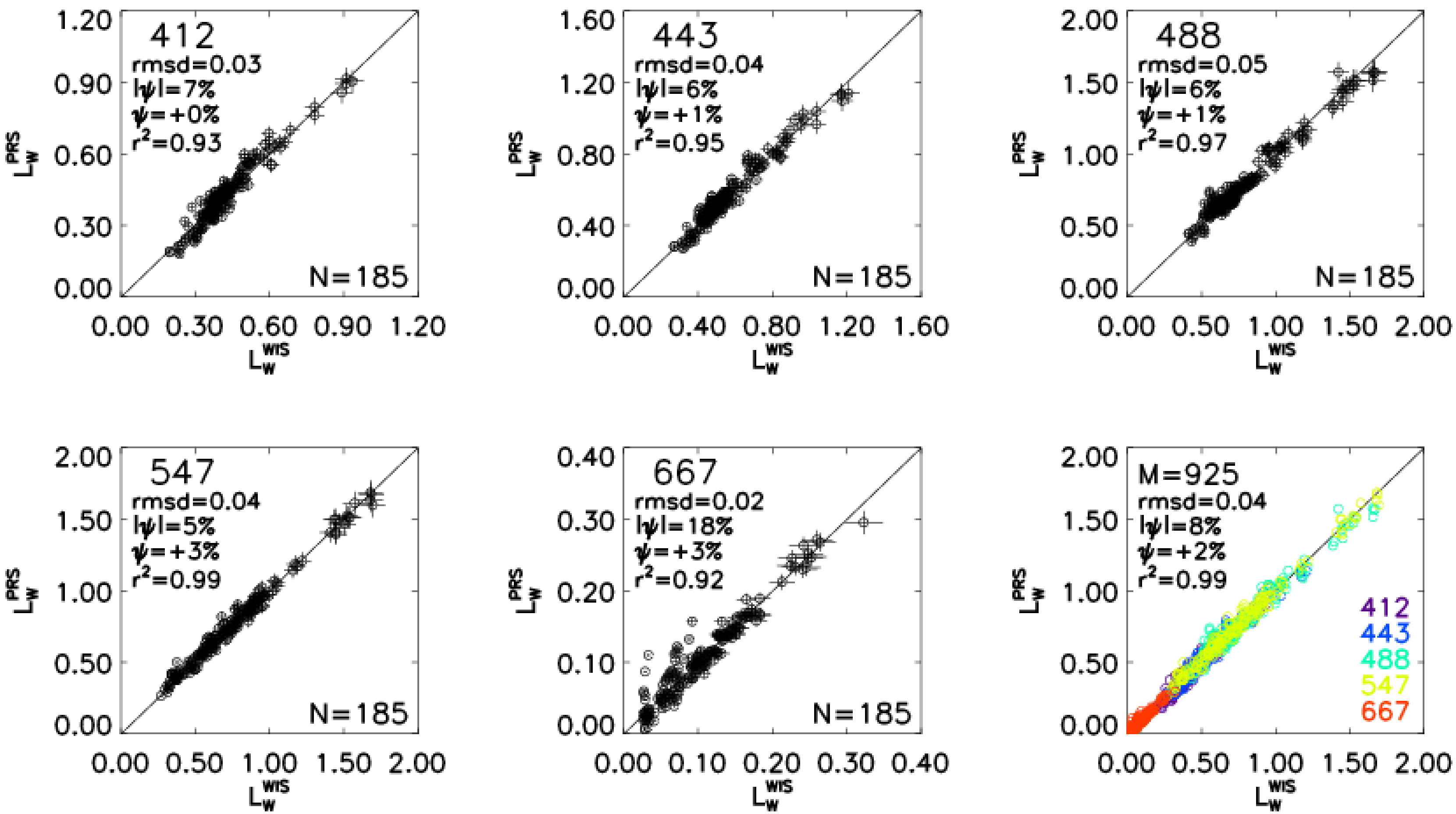

Assessment AERONET-OC L_W from ρ^P

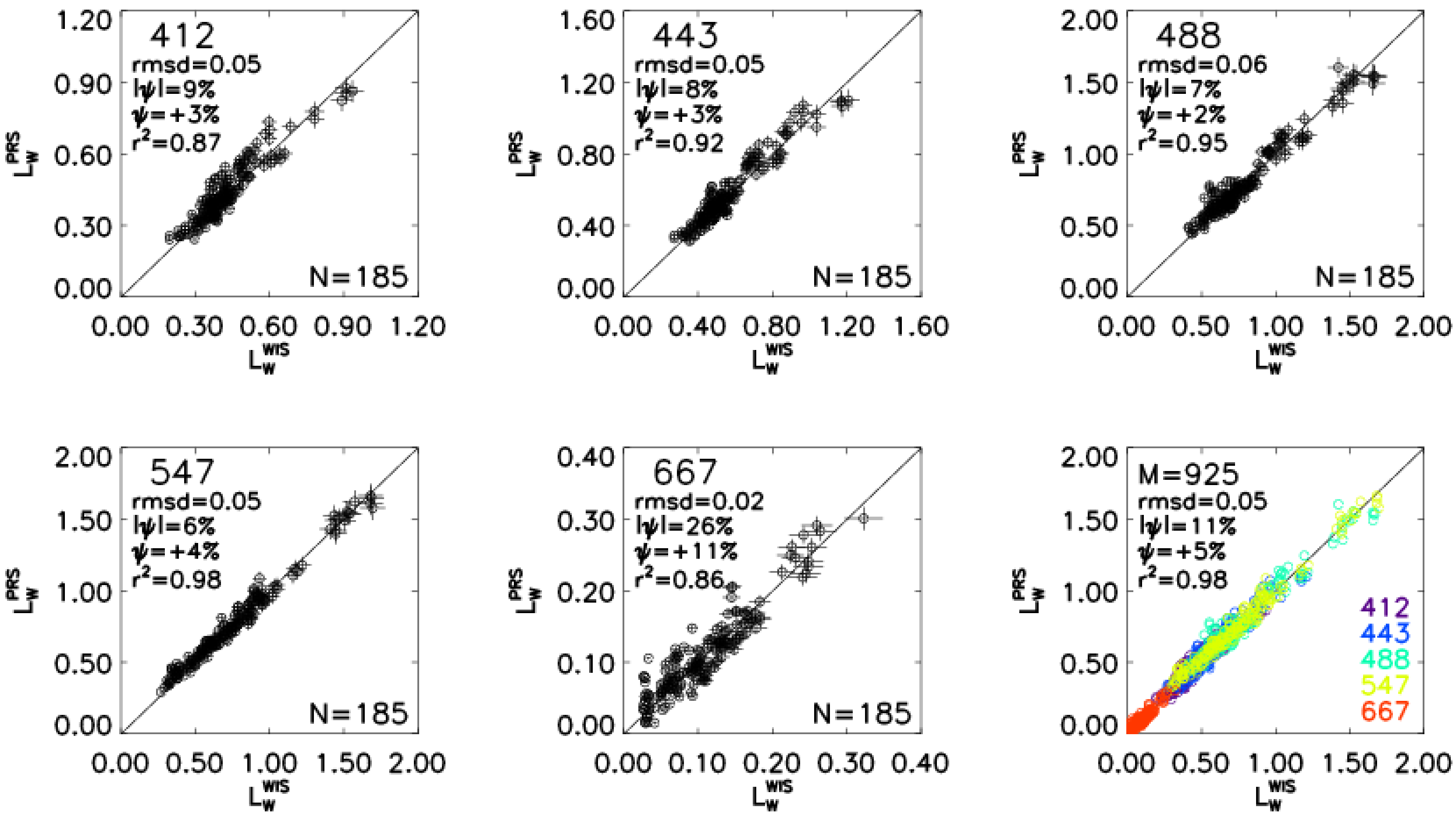

Joint Research Centre

Conclusions

The experimental assessment of the sea surface reflectance factors ρ^{U} and ρ^{P} (proposed by C. Mobley on 1999 and 2015, respectively) applied for the generation of AERONET-OC L_{W} data, beyond

a. limitations due to a restricted range of measurement conditions (e.g., low wind speeds which are however an intrinsic feature of AERONET-OC data products),

b. constrains (but also advantages) due to the applied technology and measurement methodology,

c. and the strict QA/QC criteria embedded in the AERONET-OC processing scheme designed to ensure the highest accuracy to data products at the expenses of their number:

1. indicates a generic better performance of ρ^{U} factors;
2. but it also indicates that most appropriate sea surface reflectance factors would vary between the ideal values of ρ^{U} and ρ^{P}, likely because of depolarization effects not accounted for in the computation of ρ^{P} (e.g., like those due to aerosols).

The previous findings do not presently suggest to revert the use of current ρ^{U} to ρ^{P} factors, nor any significant revision of the uncertainty budget for AERONET-OC data products determined with wind speed tentatively lower than 5 m s^{-1}.

Incorporating Ocean Color Remote Sensing in Ecosystem Based Fisheries Management

NOAA FISHERIES

Northeast Fisheries Science Center

Kimberly Hyde & Michael Fogarty

NOAA/NMFS/NEFSC

STAR JPSS Annual Science Team Meeting

Ecosystem Based Management

- Within NOAA there is a strong focus on Integrated Ecosystem Assessments and Ecosystem-Based Approaches to Management, with an increasing emphasis on ecological forecasting.

- There is also an emphasis to monitor changes in the oceans and how climate changes impact phytoplankton species composition and the marine food web.

- In this context, there is a need for accurate, timely, consistent and fit for purpose ocean color data/products to support NOAA (NMFS, NOS, OAR) and related users with ongoing coastal, ocean and inland water applications, especially fisheries and broader living marine resource management.

Ocean color remote sensing

- Documenting, monitoring and forecasting the response of marine ecosystems to environmental variability and climate change
- Assessing biodiversity
- Biogeochemical cycling
- Connections between seasonal blooms (phenology) and recruitment
- Examining variations in functional groups/size class abundance and distribution patterns (temporally and spatially)
- Food-web structure and secondary/tertiary production

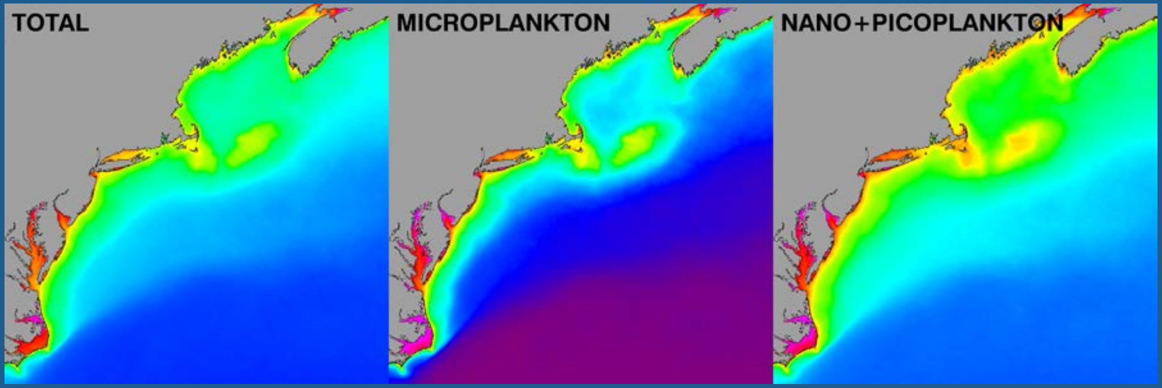

Ecosystem Production Potential

Goal: Use a bottom-up approach to determine fisheries production potential and exploitation for various ecosystem components.

- Benthos
- Benthivores
- Planktivores
- Piscivores

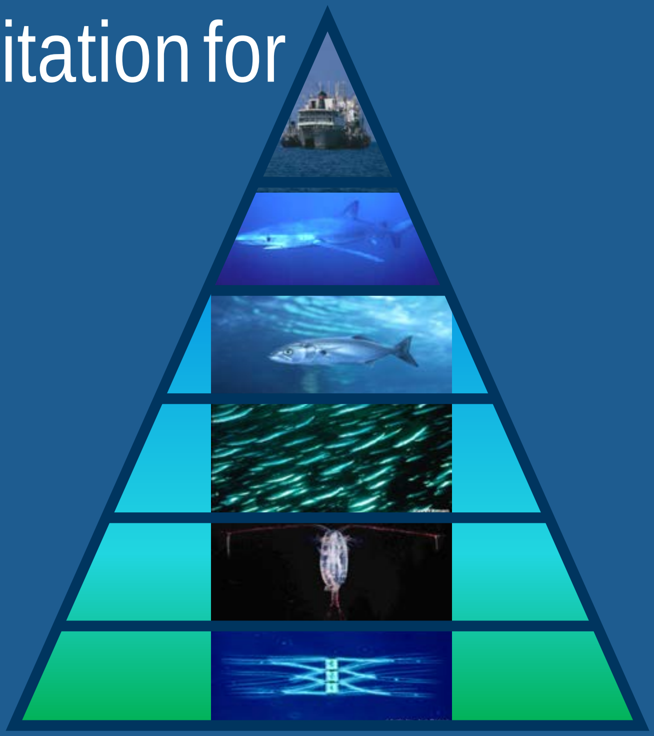

Question: How efficiently is primary production transferred to higher trophic levels?

Ecosystem Production Potential - Historical

$$EPP = PP \cdot T^{TL-1}$$

Where EPP is Ecosystem Production Potential,
T is the ecological transfer efficiency,
TL is the mean trophic level of the catch.

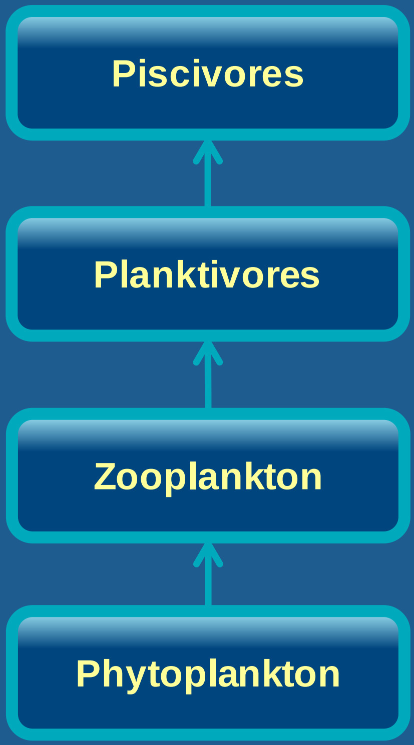

Historically, an exploitation rate of 50% was assumed to be sustainable.

(Pauly, 1995 – Fisheries Research)

Ecosystem Production Potential - Model

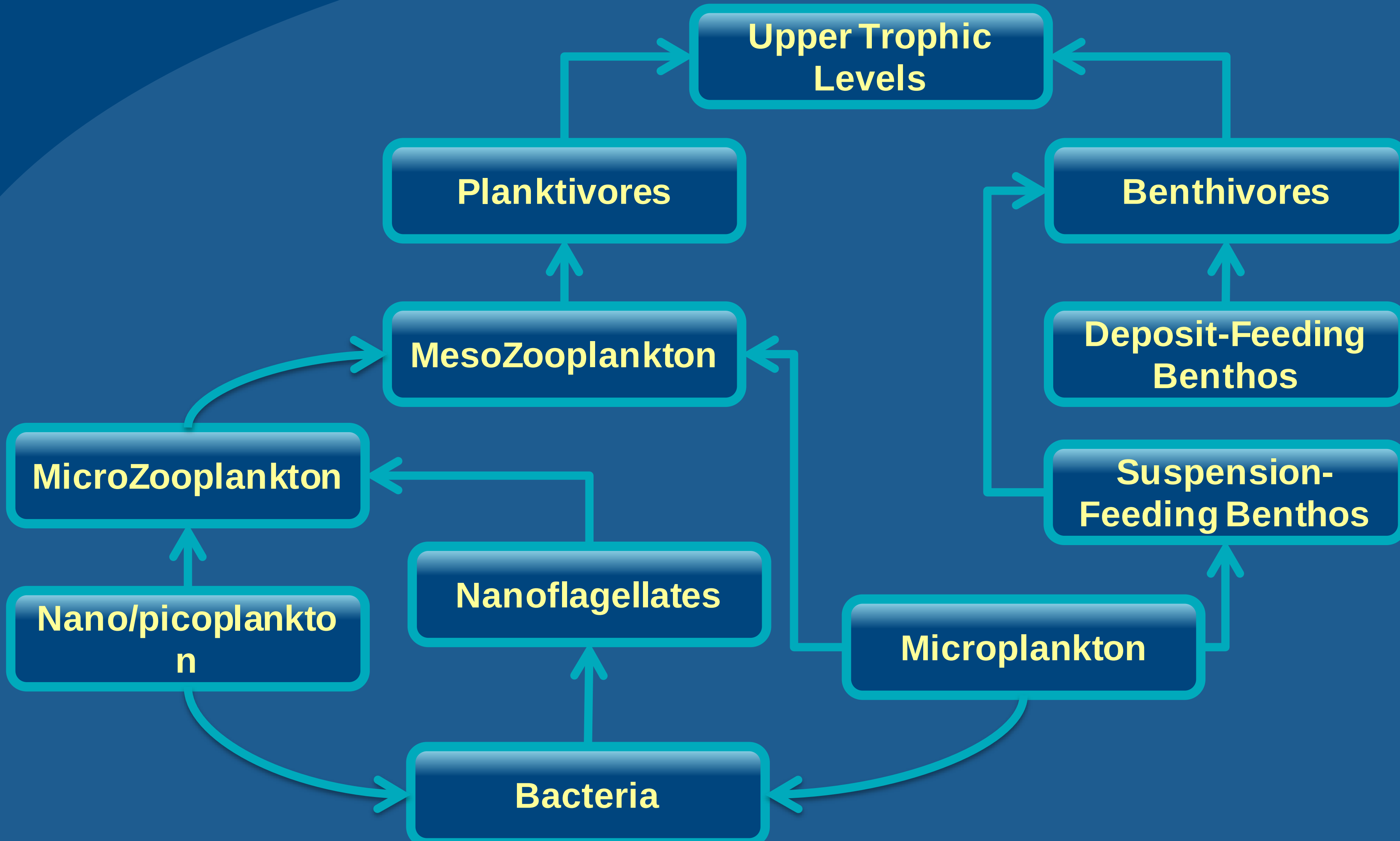

Ecosystem Production Potential - Model

$$P_i = T \cdot P_j + A_i - F_i$$

Where P_i is Production at the i^{th} node,

T is the matrix of ecological transfer efficiencies,

A_i is a vector of external inputs to the i^{th} node, and

F_i is a vector of losses from the i^{th} node.

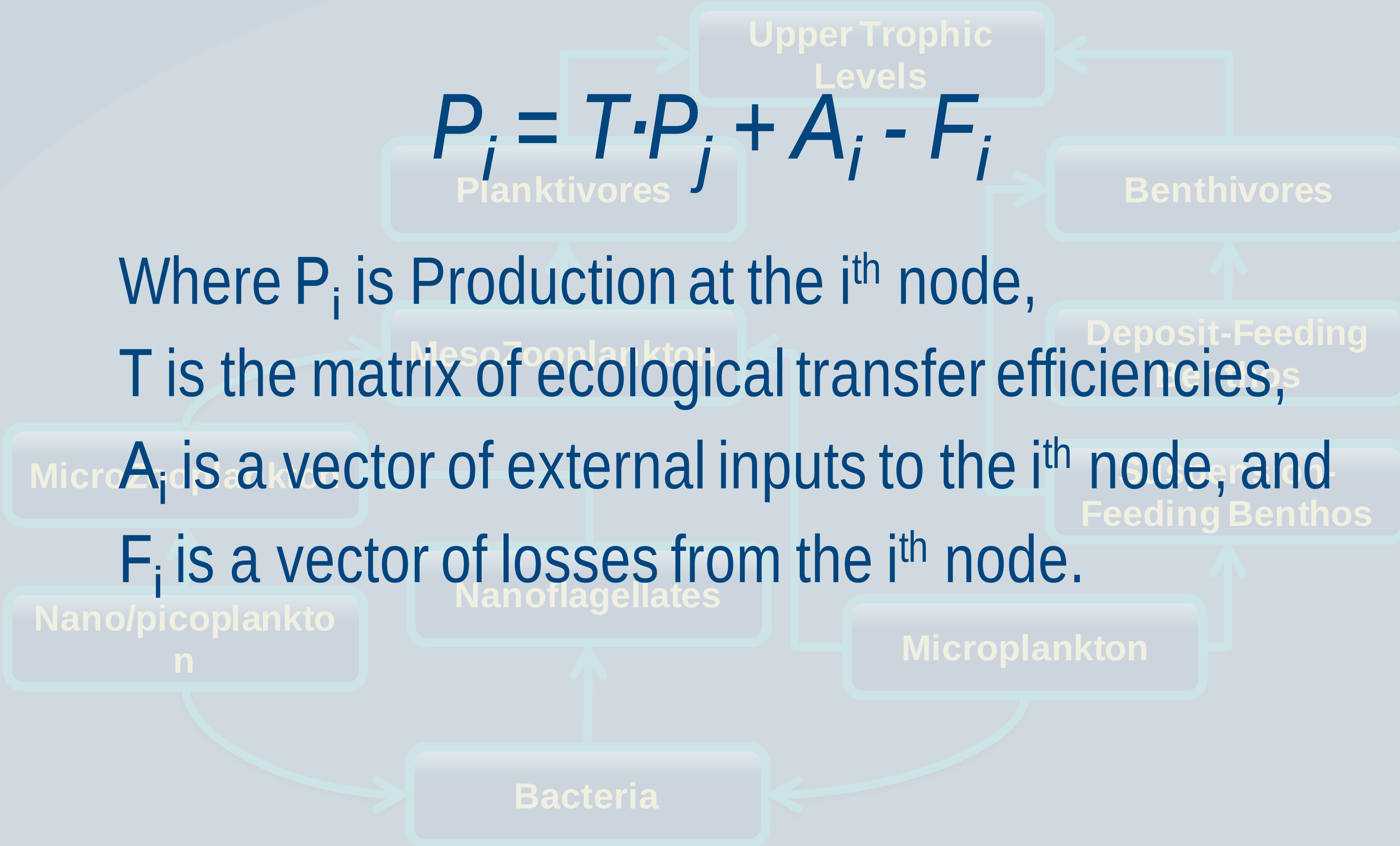

Ecosystem Production Potential - Model

Proposed Ecosystem Limit Reference Point:

The total Exploitation Rate should not to exceed the fraction of Microplankton Production in the System.

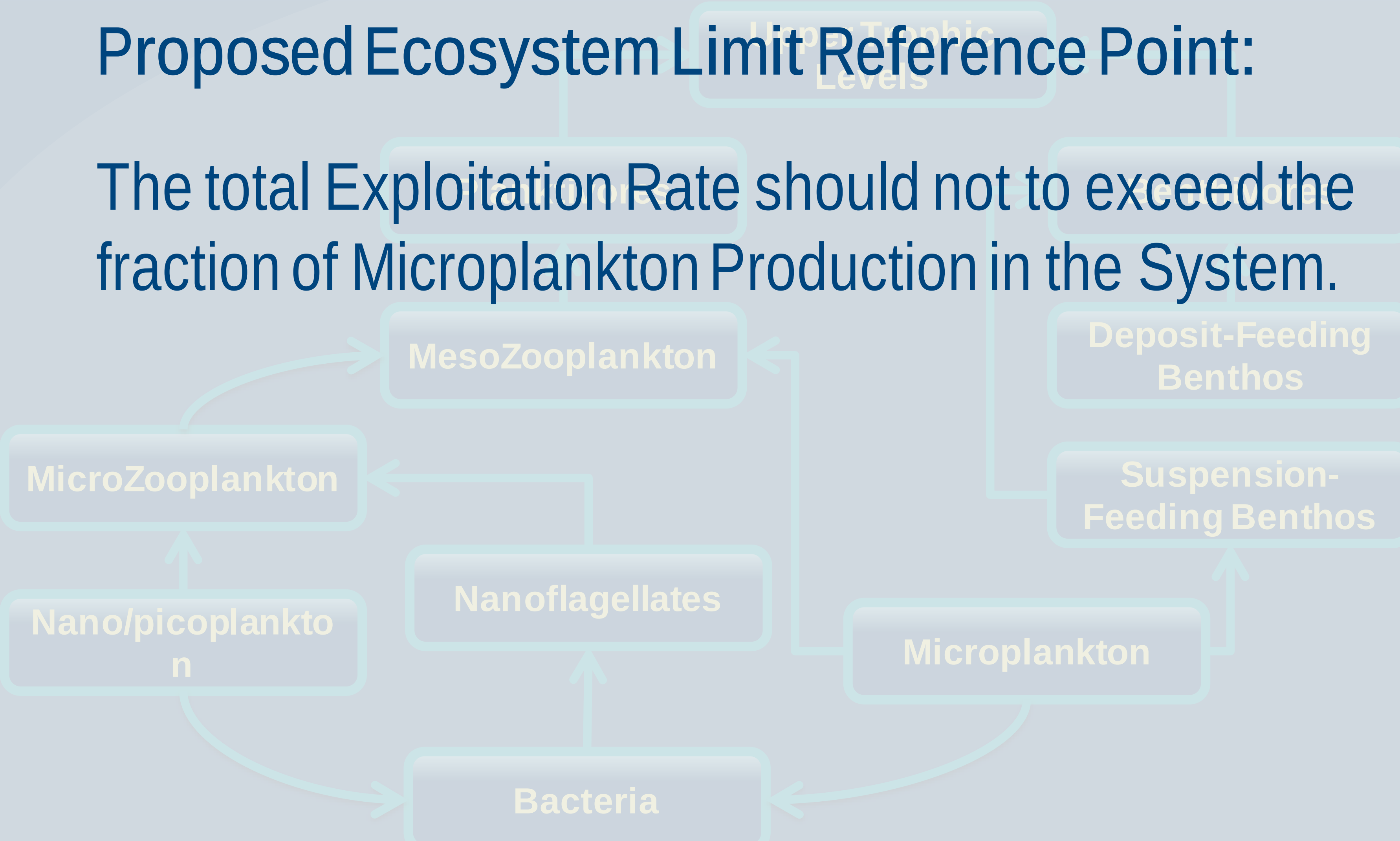

Ecosystem Production Potential - Model

Proposed Ecosystem Limit Reference Point:

The total Exploitation Rate should not to exceed the fraction of Microplankton Production in the System.

Use ocean color remote sensing to estimate the fraction of Microplankton Production.

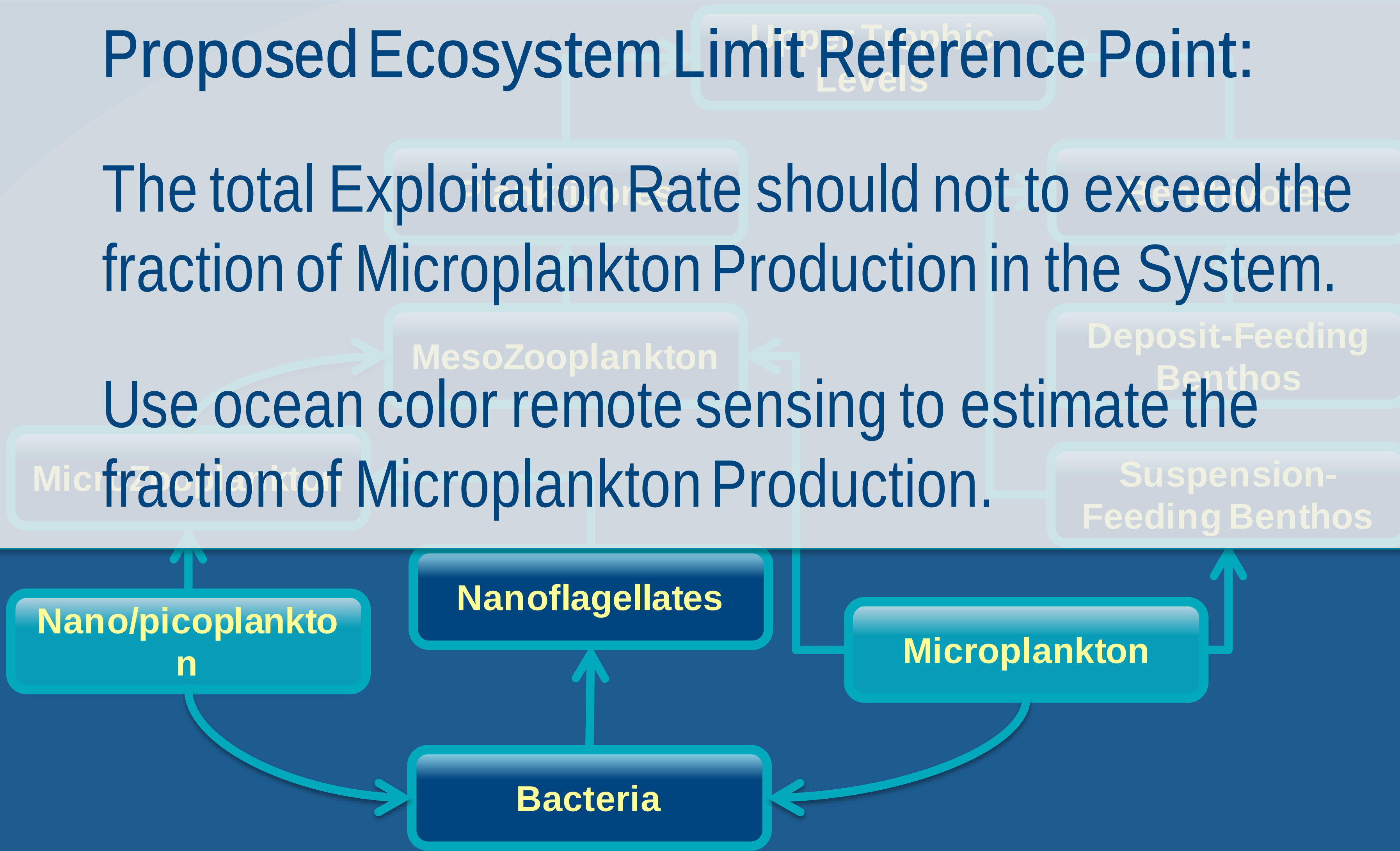

Phytoplankton size classes

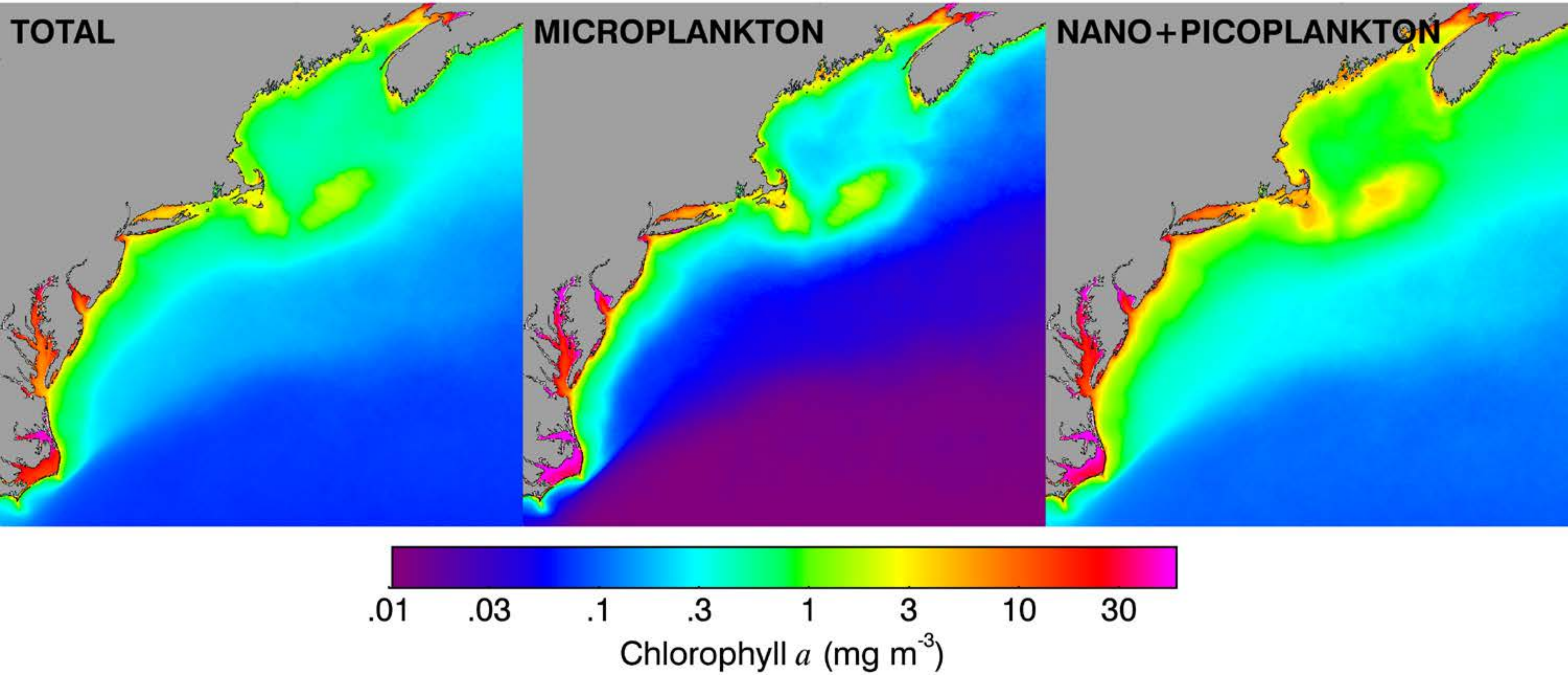

Pan et al. 2008 & 2010

Phytoplankton size classes

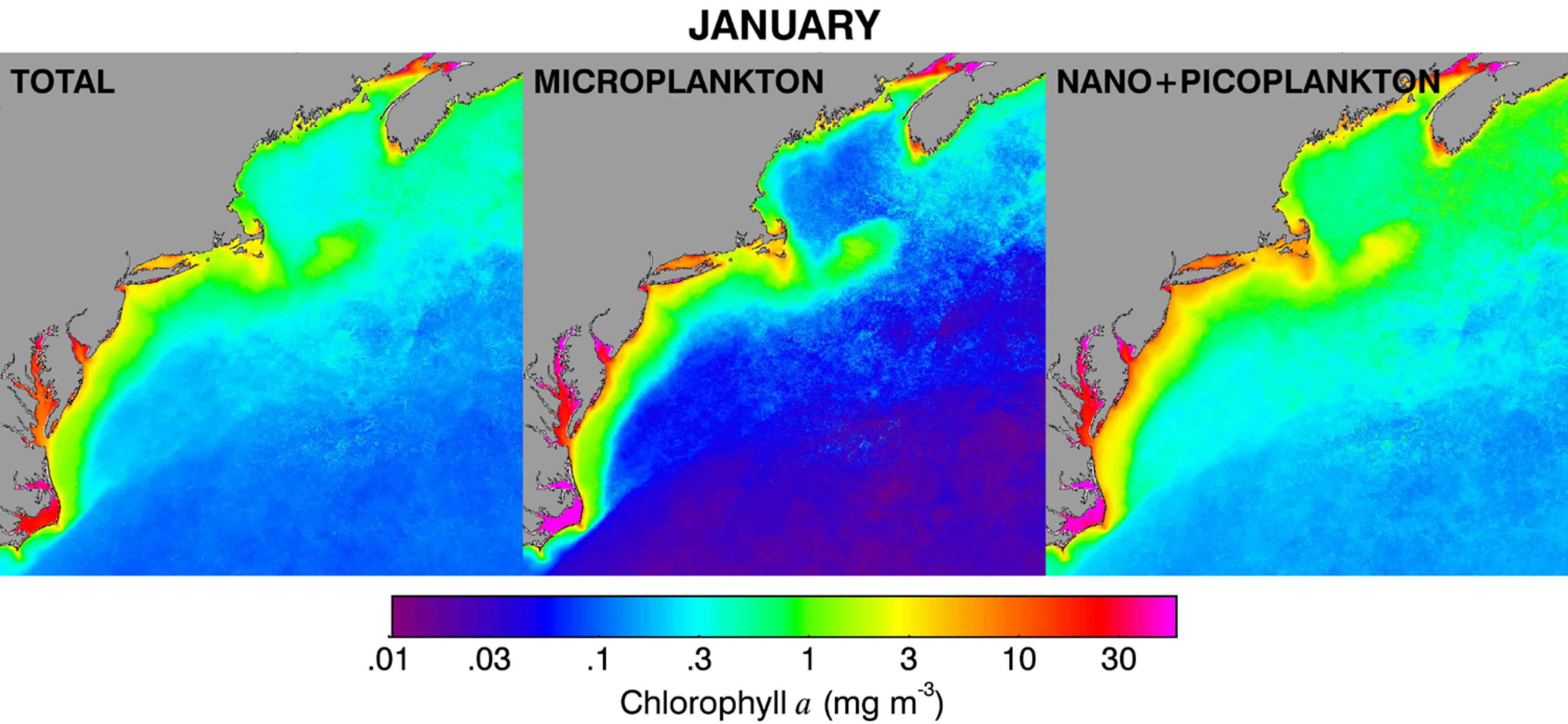

Pan et al. 2008 & 2010

Phytoplankton size classes

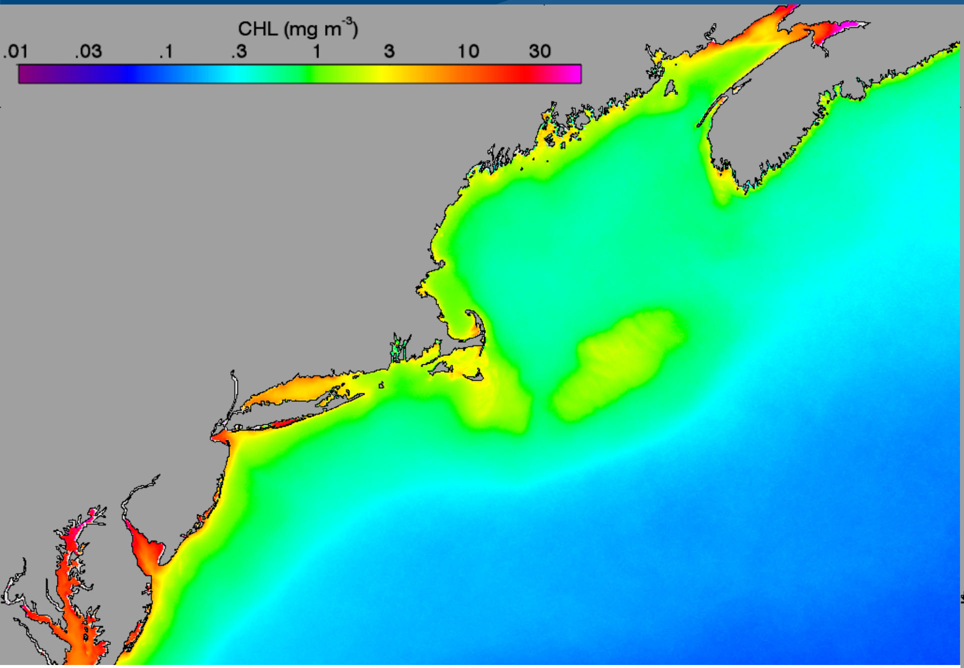

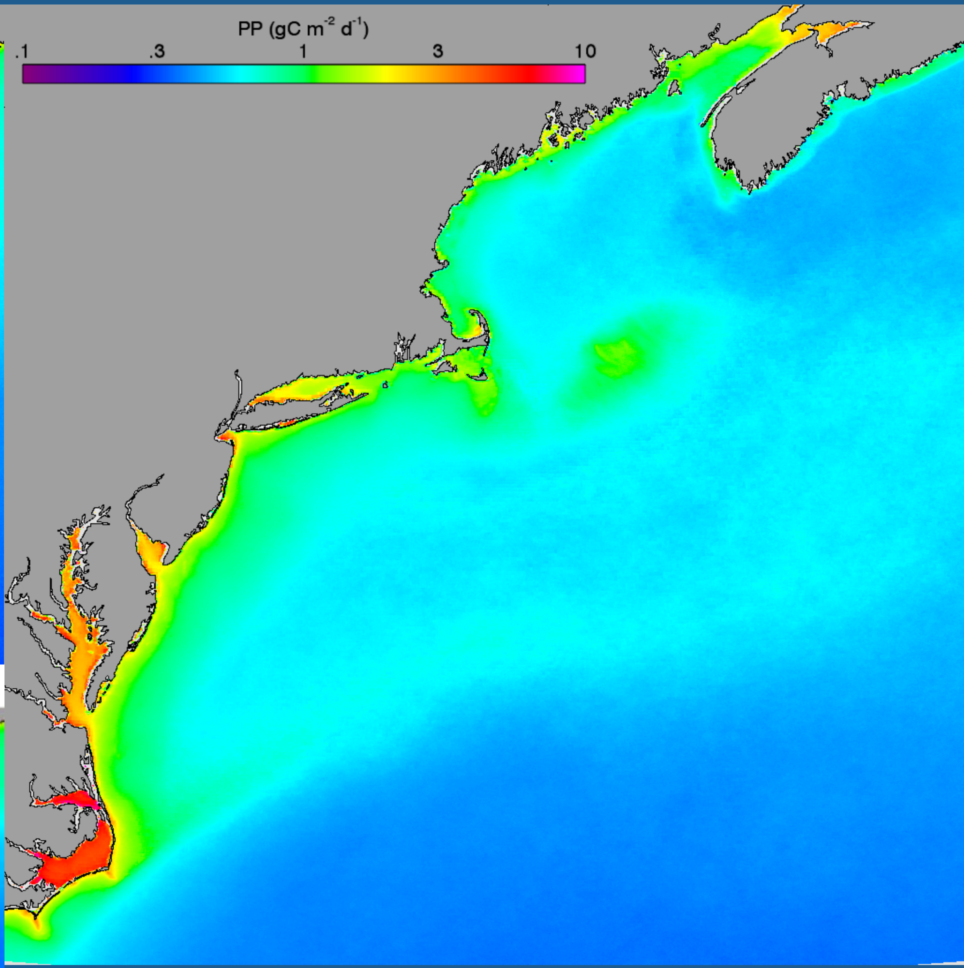

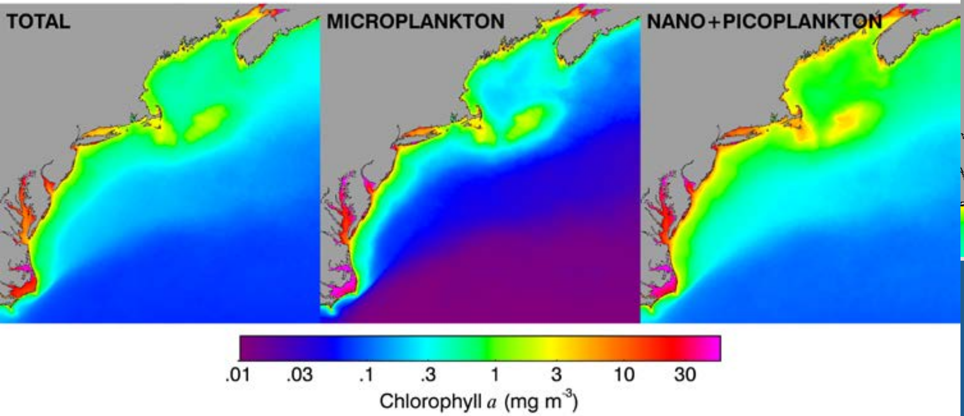

Size Fractionated Primary Production

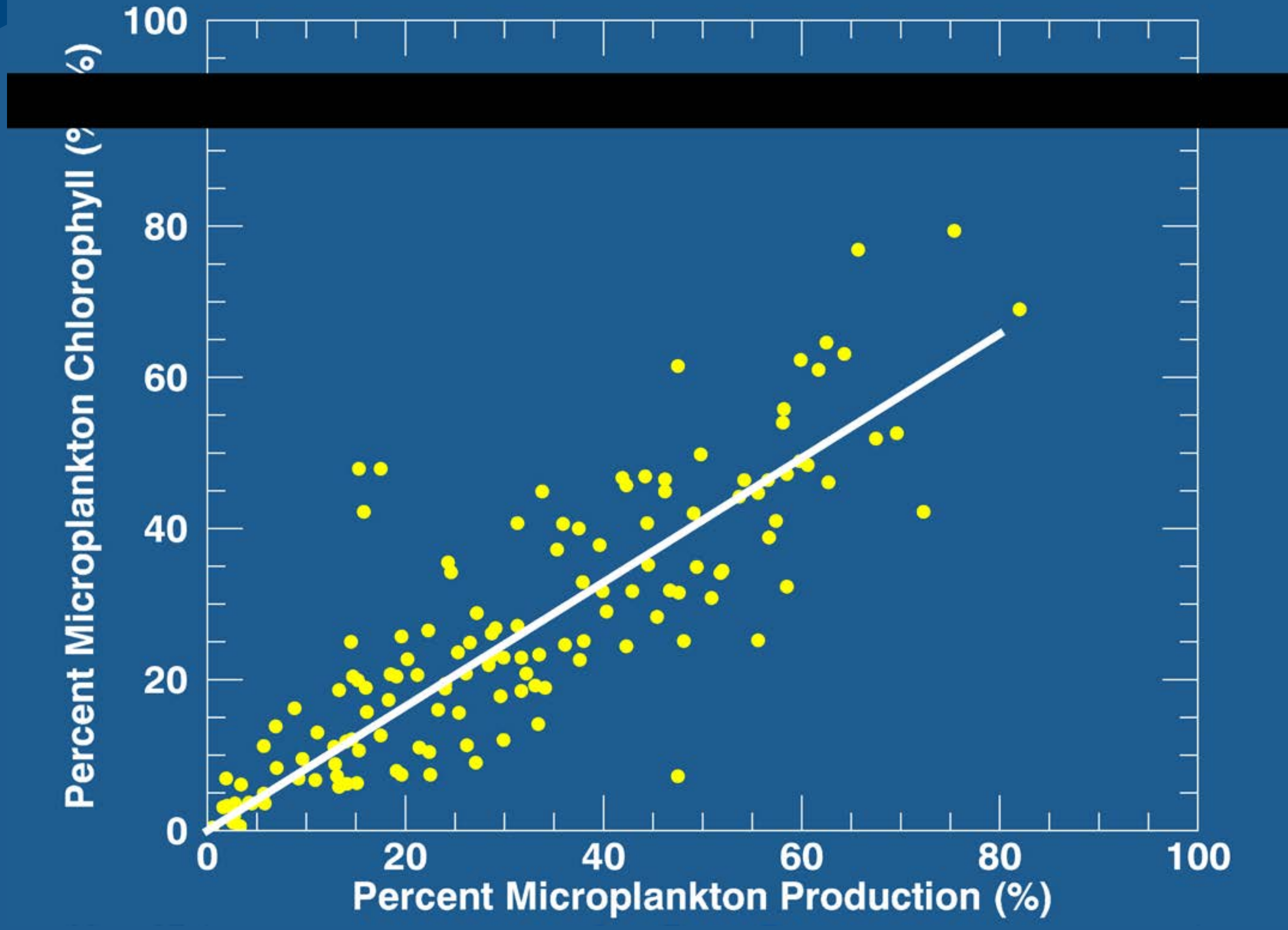

MARMAP - NEFSC

Size Fractionated Primary Production

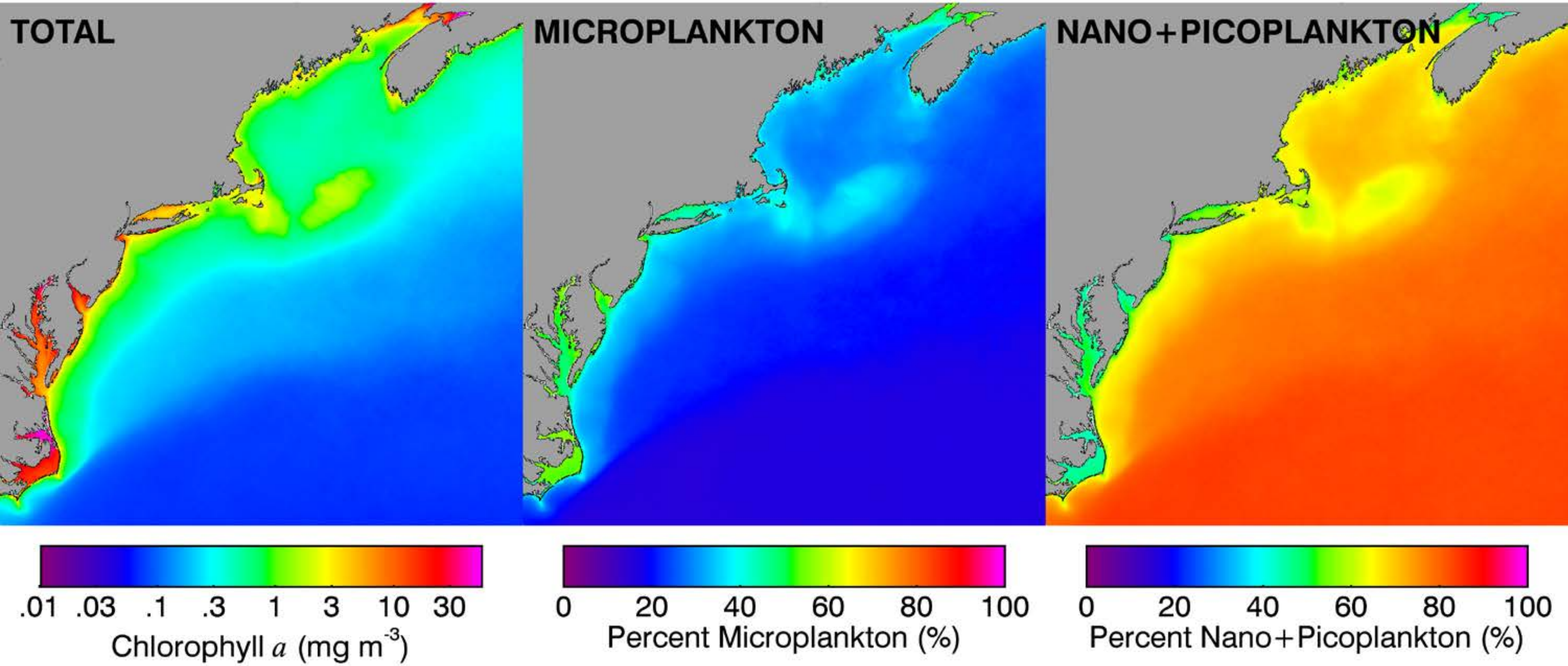

NOAA FISHERIES

Size Fractionated Primary Production

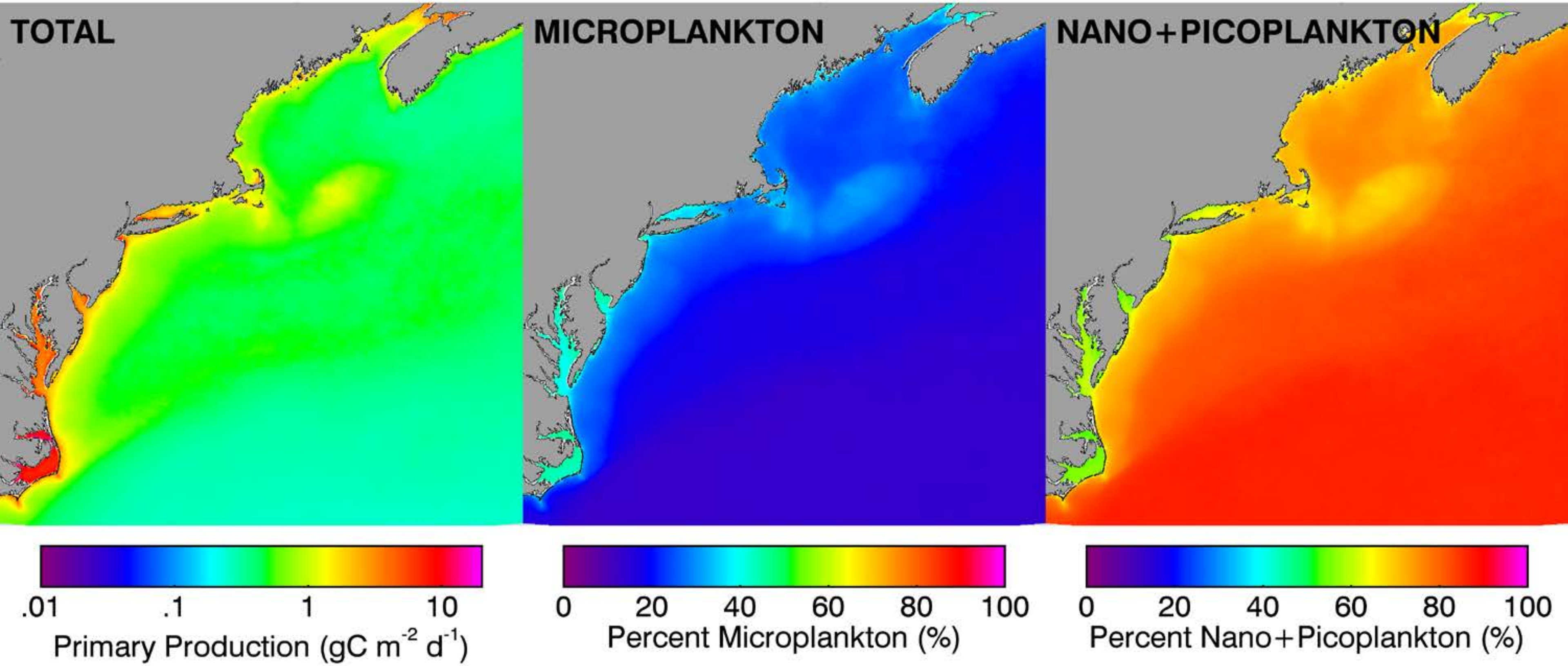

Size Fractionated Primary Production

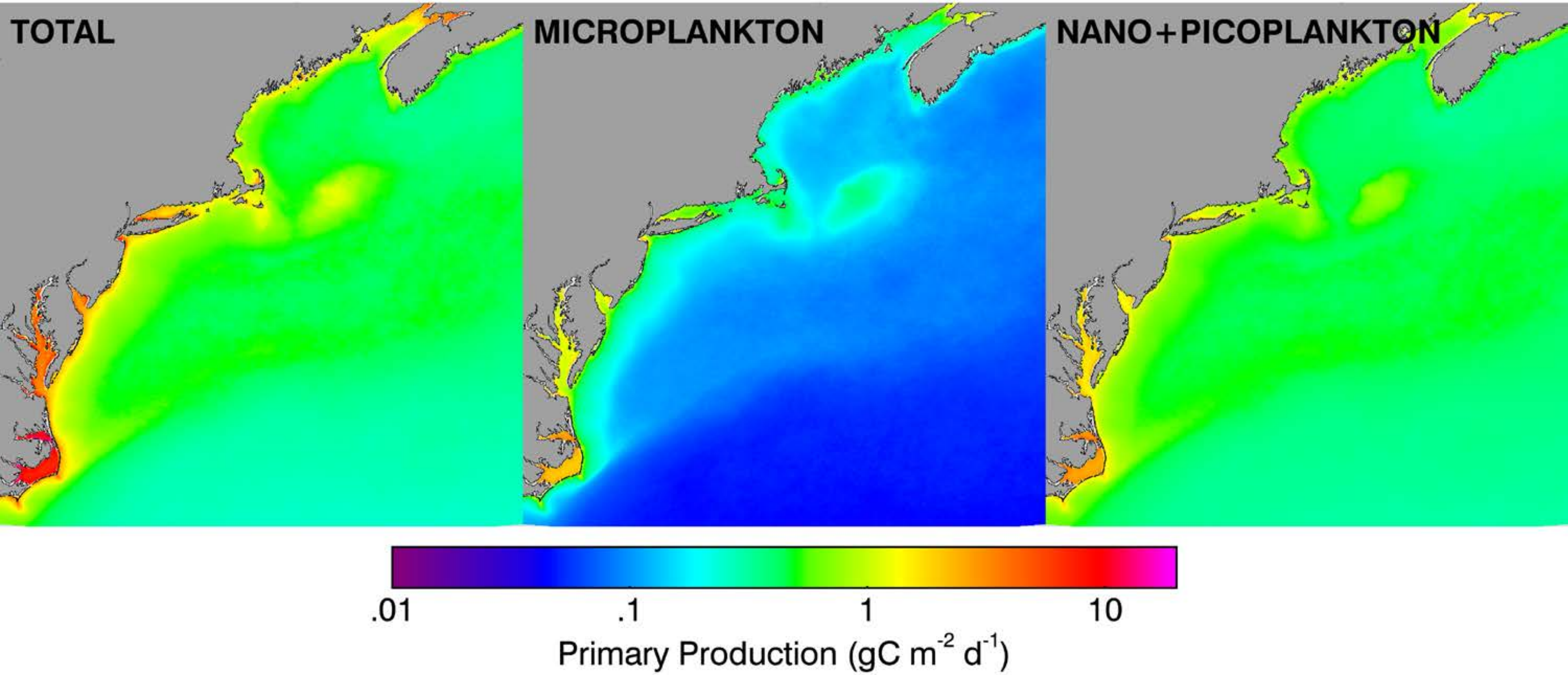

Size Fractionated Primary Production

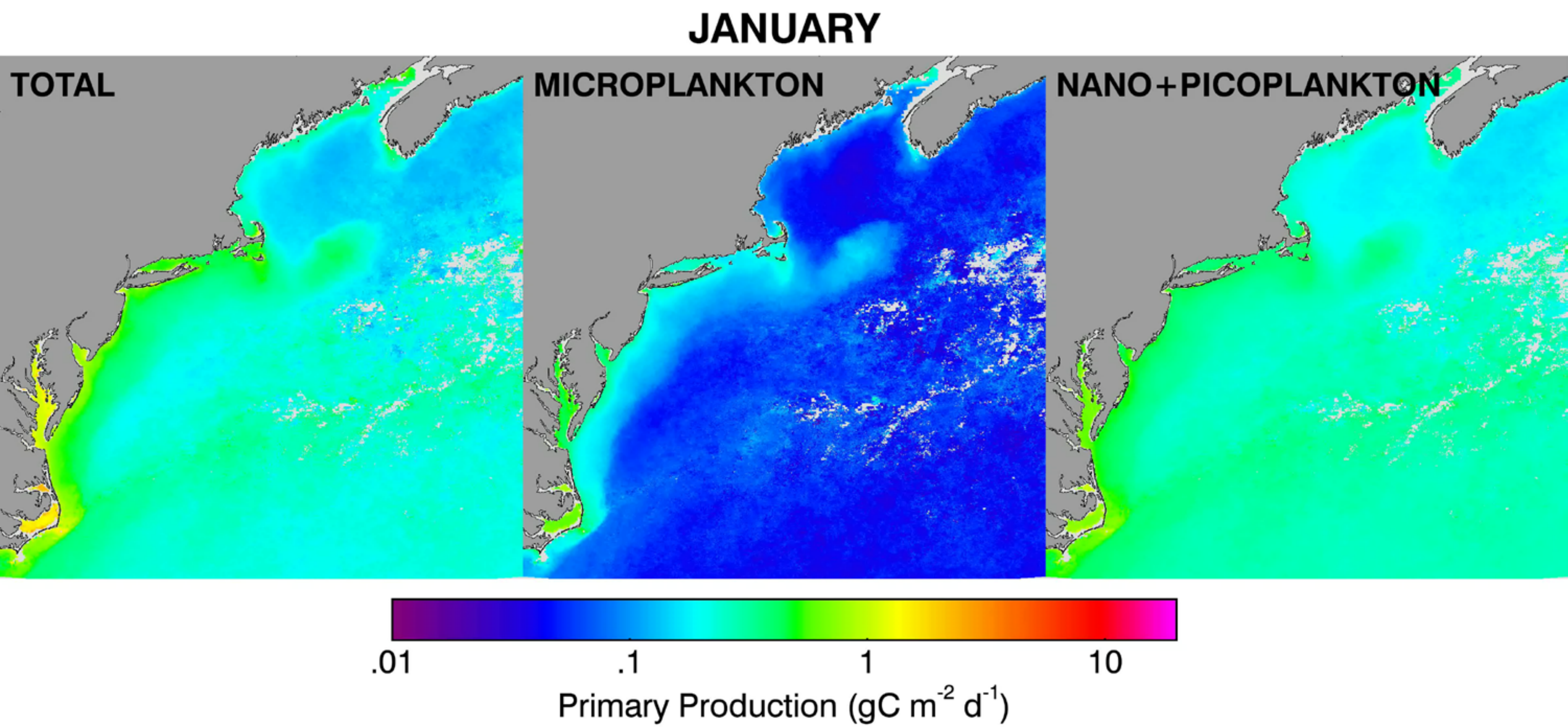

Size Fractionated Primary Production

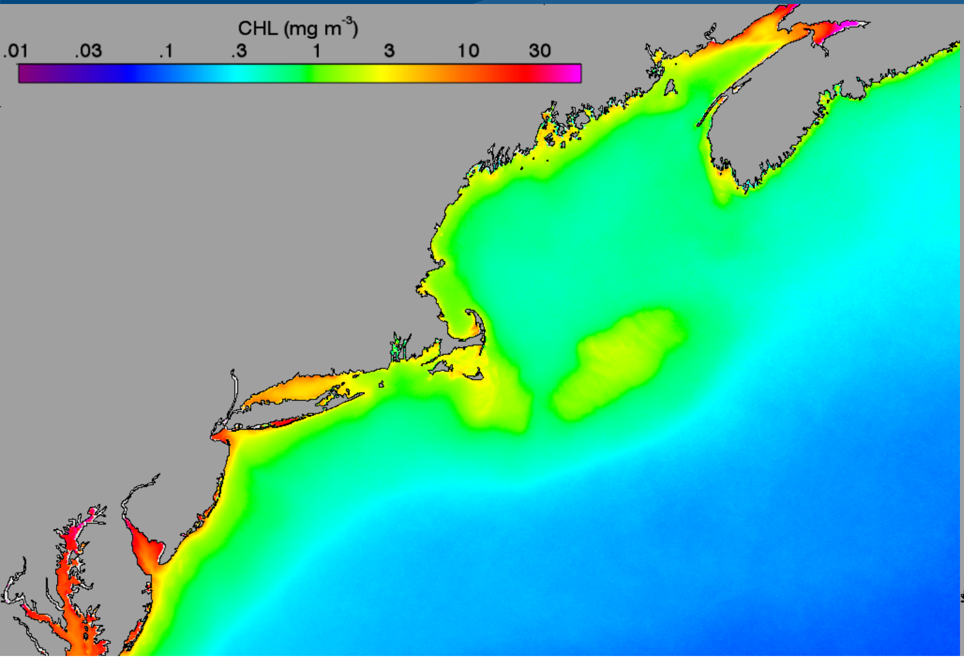

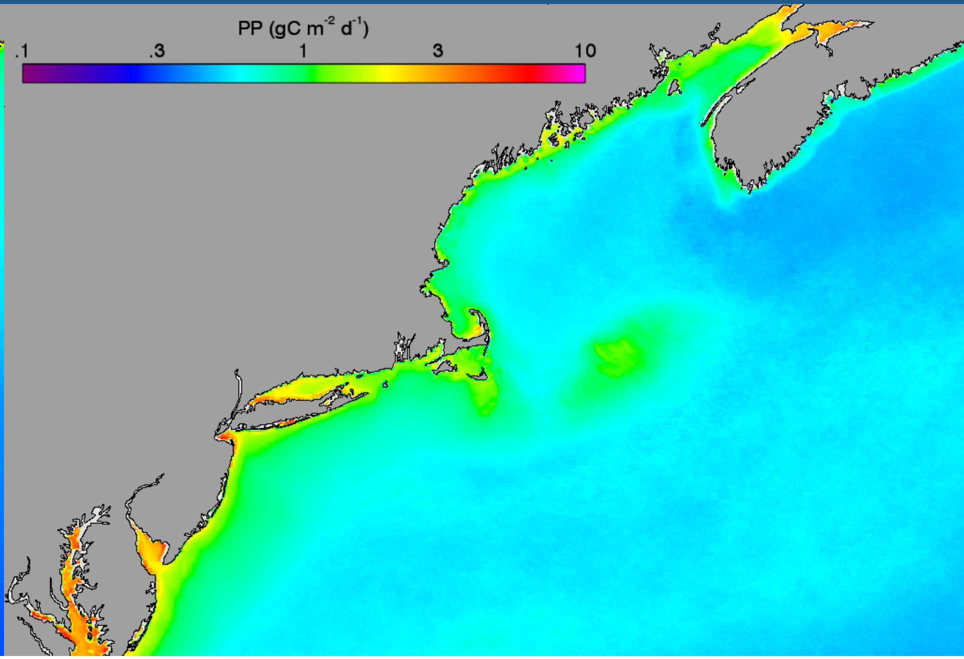

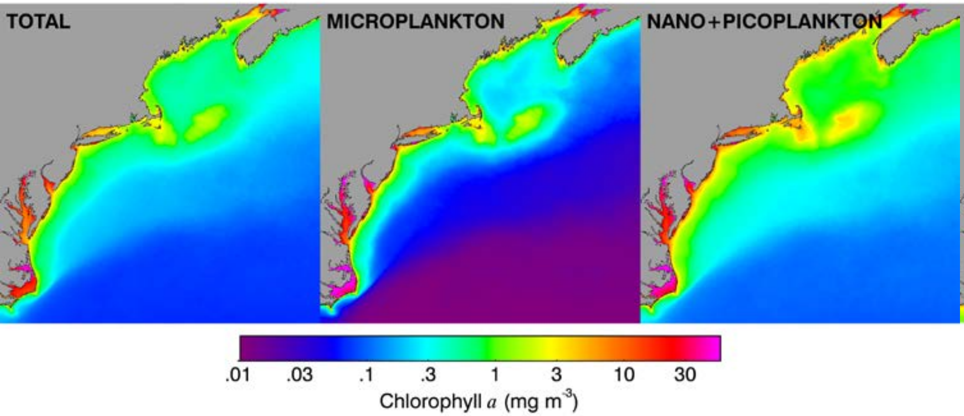

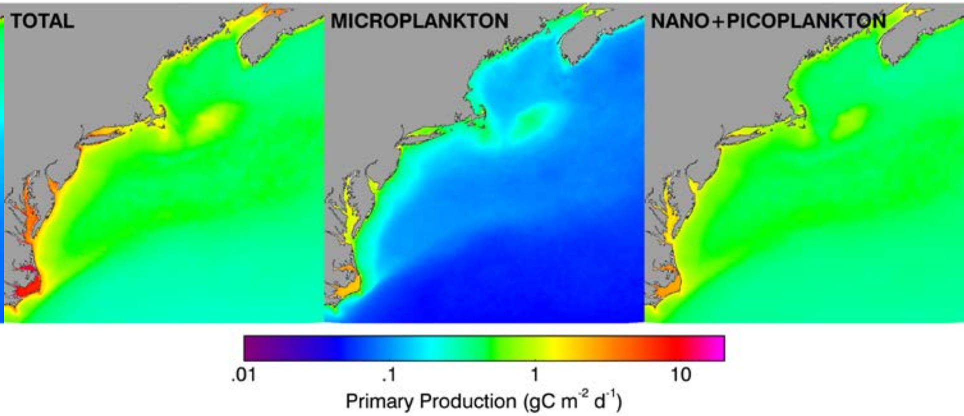

Ecosystem Production Potential - Model

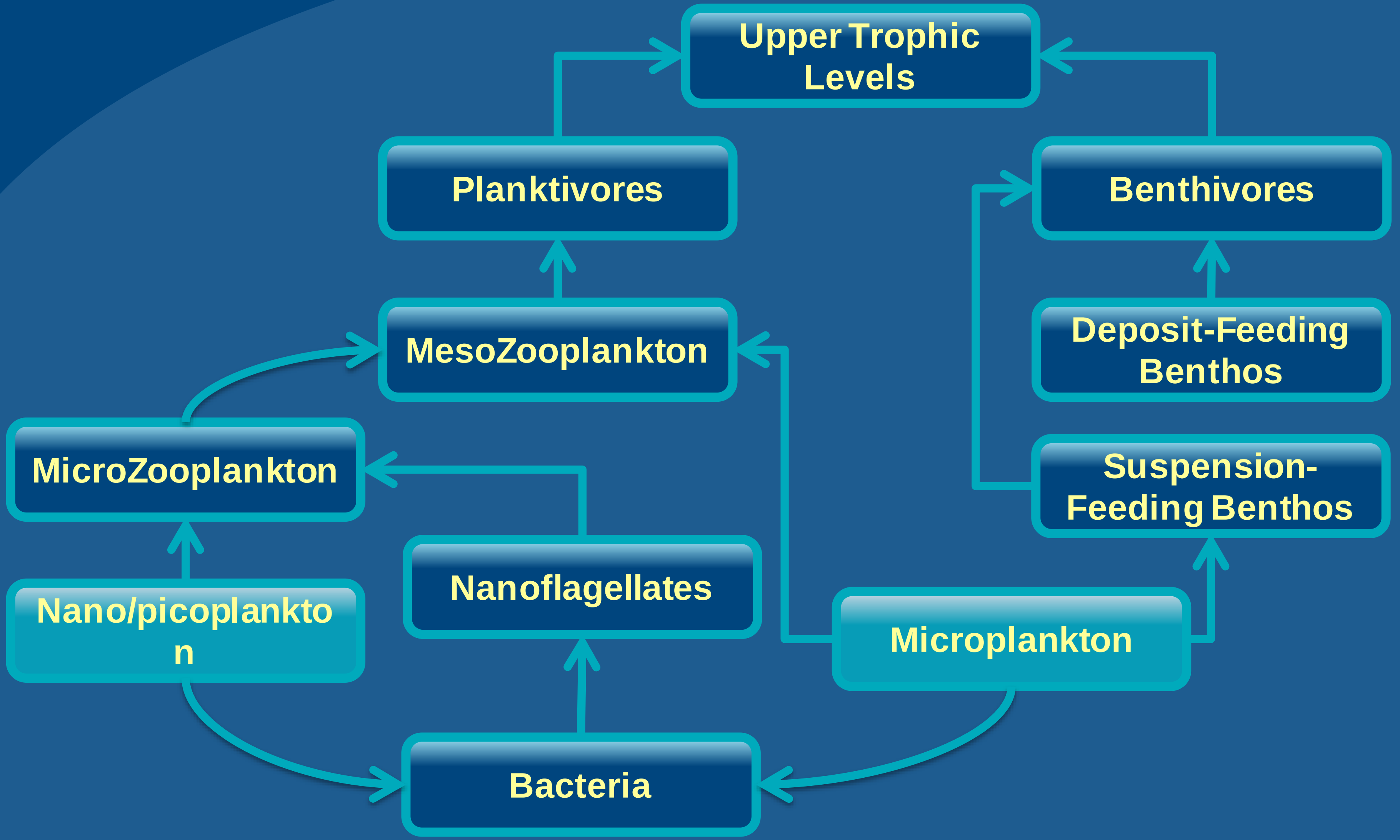

Summary

- The proposed ecosystem limit reference point is that the exploitation rate should not exceed the fraction of microplankton production in the system (~20-30%), which equates to ~825,000 t of harvestable production.

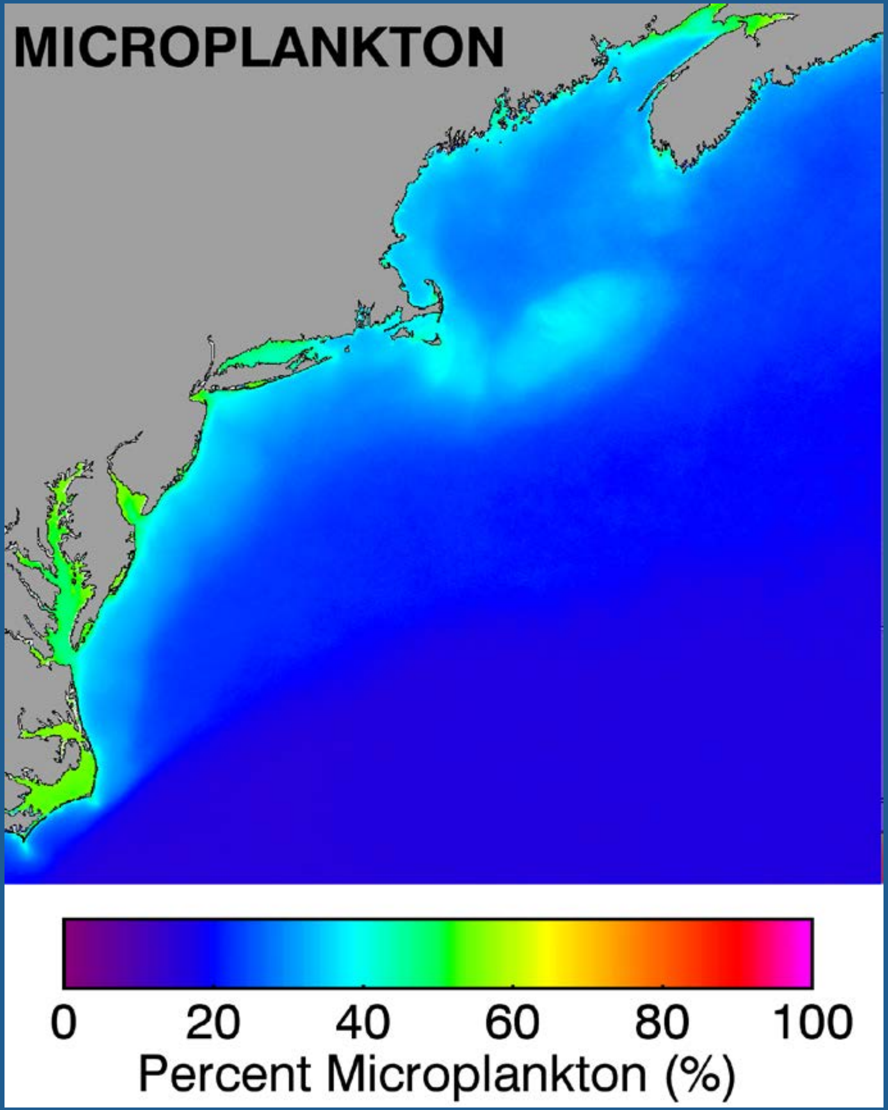

Summary

❑ Fishery removals exceeded recommended levels (~825,000 t) in the past, but are now close to estimates of sustainable extraction rates for the ecosystem as a whole.

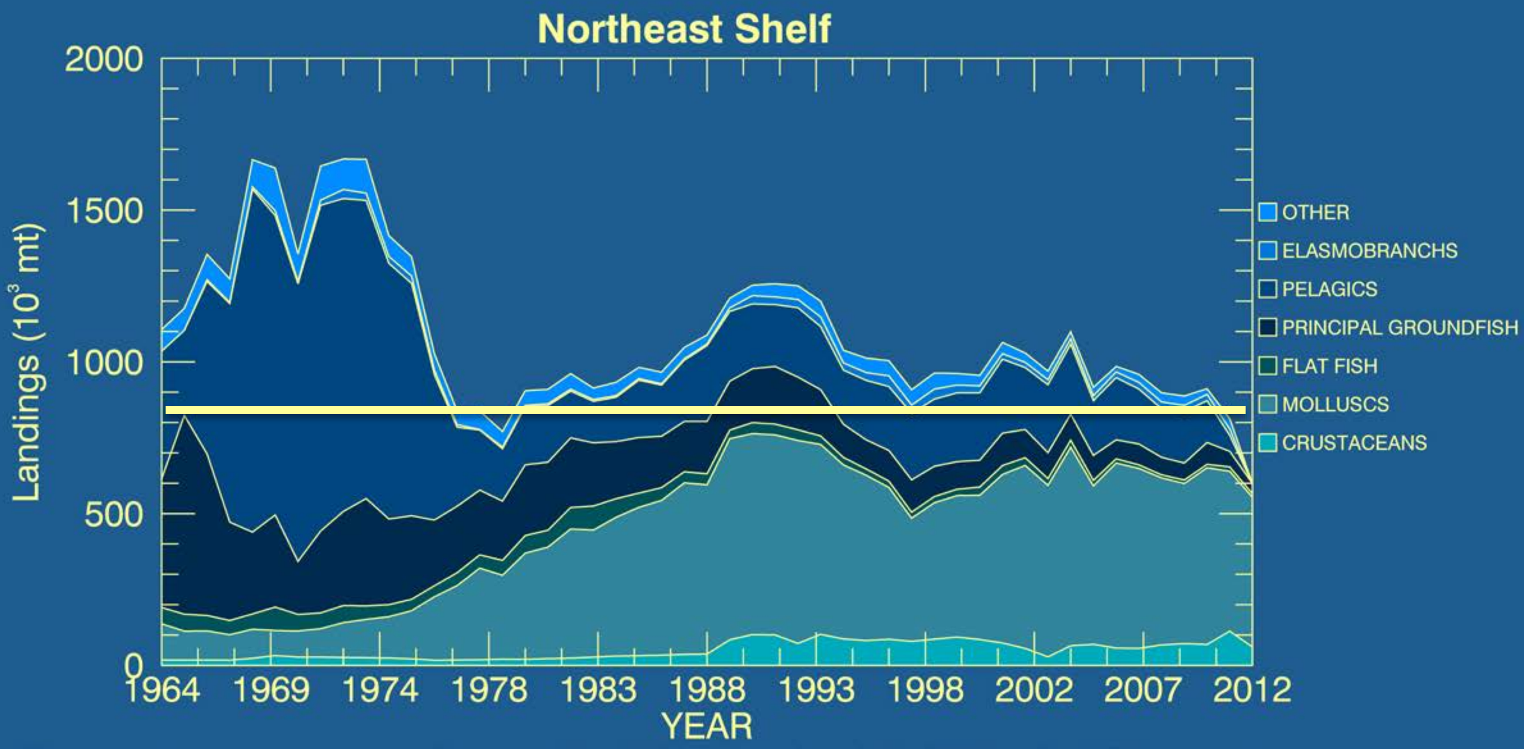

Summary

❑ Directed targeting of some species means that some functional groups are still at risk.

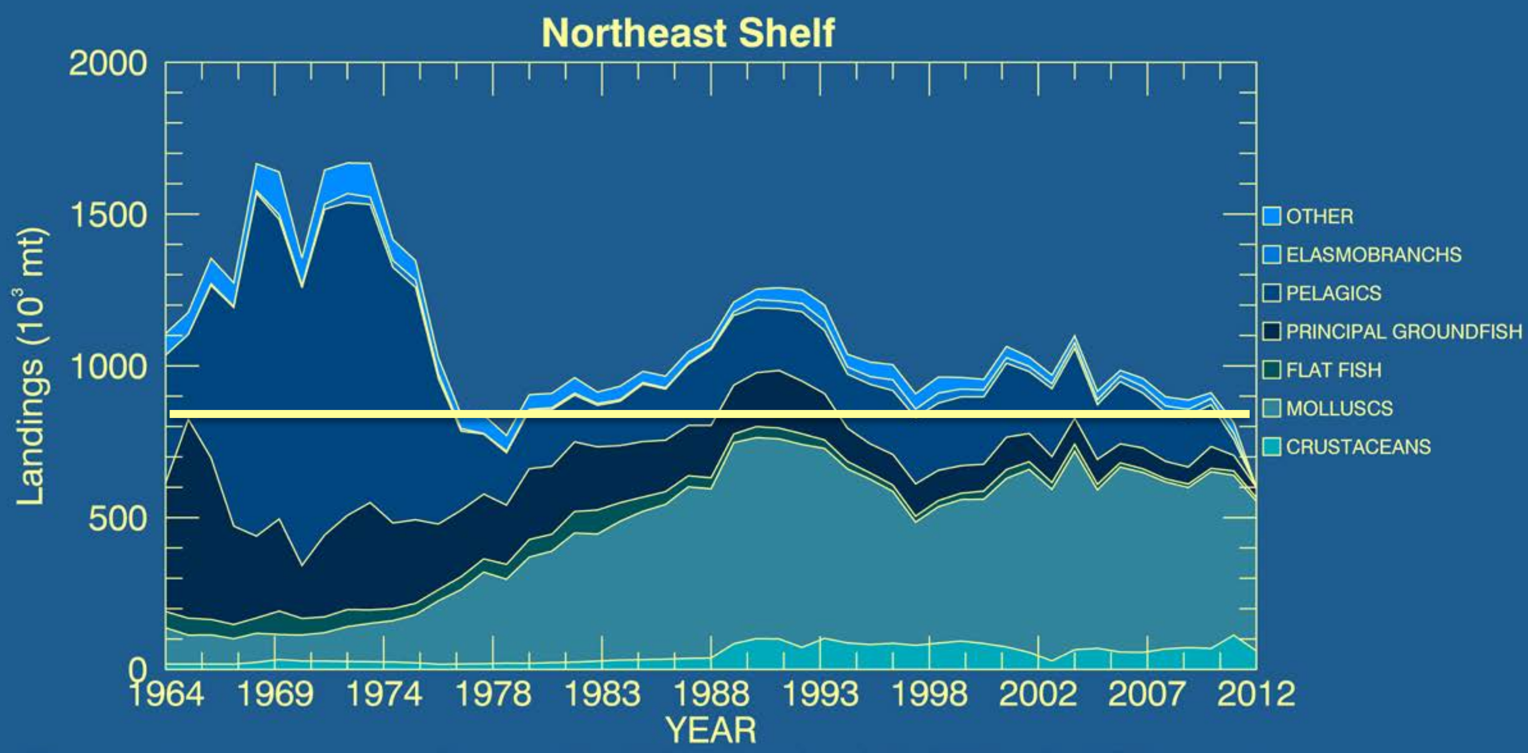

Summary

- A diversified catch will be necessary to create a more balanced harvesting policy.

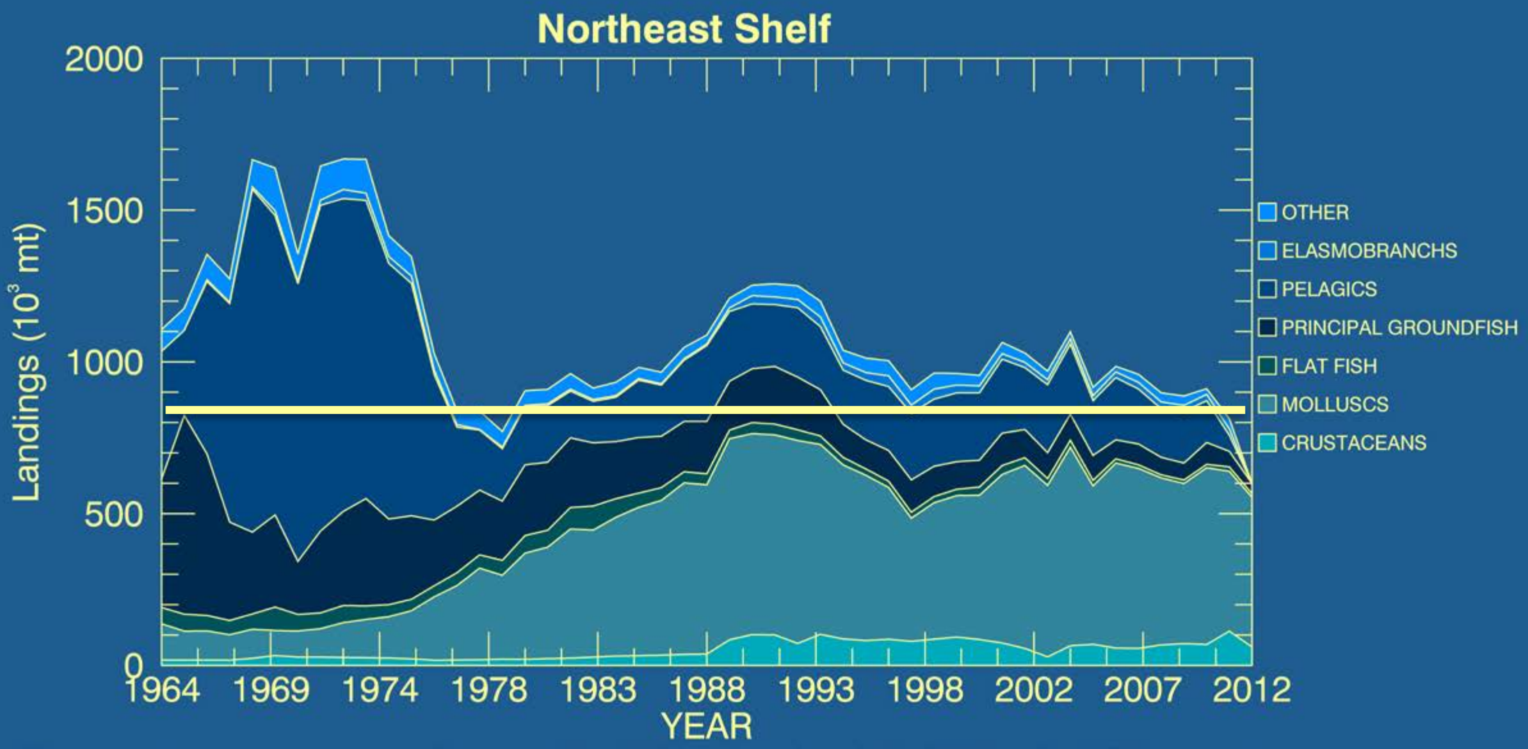

Summary

- Changes in the phytoplankton community composition and/or rates of primary production will affect the community production and the overall fisheries yield of the system. Thus, there is an ongoing need for:
  - Climatological quality (preferably hyper-spectral) ocean color remote sensing data (RRSs, PAR, CHL, IOPs, Kd) to monitor changes in the phytoplankton community.
  - Improved algorithms for measuring phytoplankton functional groups/size classes on the continental shelf.
  - *In situ* validation data of phytoplankton pigments, primary production, and other related parameters.

Predicting Phytoplankton Functional Types with Remote Sensing Data

Tim Moore
University of New Hampshire

Chris Brown
NESDIS STAR

8/27/15

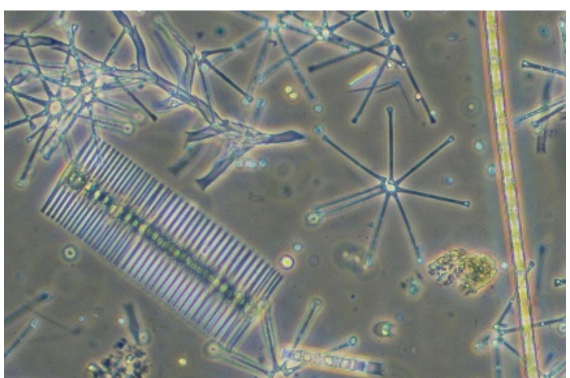

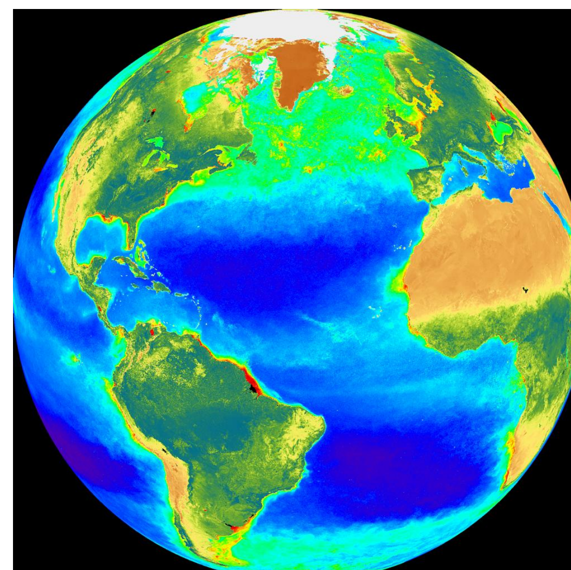

Ocean color approaches for discerning phytoplankton communities from remote sensing

- *Functional type* (biogeochemical function)
  - Spectral approach – PHYSAT, PhytoDOAS
- *Phytoplankton size* (governs many traits)
  - Spectral approaches (absorption, backscattering properties)
  - Chlorophyll approaches

Table 1. Summary of the algorithms, contact person, PFT represented.

Algorithm	Contact Person	PFTs	Methodology
Brewin et al. (2010)	R.J.W. Brewin	Micro, Nano, Pico	Abundance-based
Devred et al. (2006)	E. Devred	Micro, Nano+Pico	Abundance-based
OC-PFT	T.Hirata	Micro, Nano, Pico, Diatom, Haptophyte, Prokaryotes, Chlorophyte, Pico-Eukaryotes, Prochlorococcus	Abundance-based
Uitz et al. (2006)	J. Uitz	Micro, Nano, Pico	Abundance-based
PHYSAT	S. Alvain	Diatom, Nanoeukaryote, Prochlorococcus, Synechococcus-like, Phaeocystis	Optics-based
PhytoDOAS	A. Bracher	Diatom, Cocolithophore, Cyanobacteria	Optics-based
Ciotti and Bricaud (2002)	A. Bricaud	Micro, Pico	Optics-based
Fujiwara et al. (2011)	T. Hirawake	Micro, Nano, Pico	Optics-based
Kostadinov et al. (2009)	T. Kostadinov	Micro, Nano, Pico	Optics-based
Mouw et al. (2010)	C. Mouw	Micro, Pico	Optics-based
Roy et al (2012)	S. Roy	Micro, Nano, Pico	Optics-based

http://pft.ees.hokudai.ac.jp/satellite/index.shtml

Niche Concept

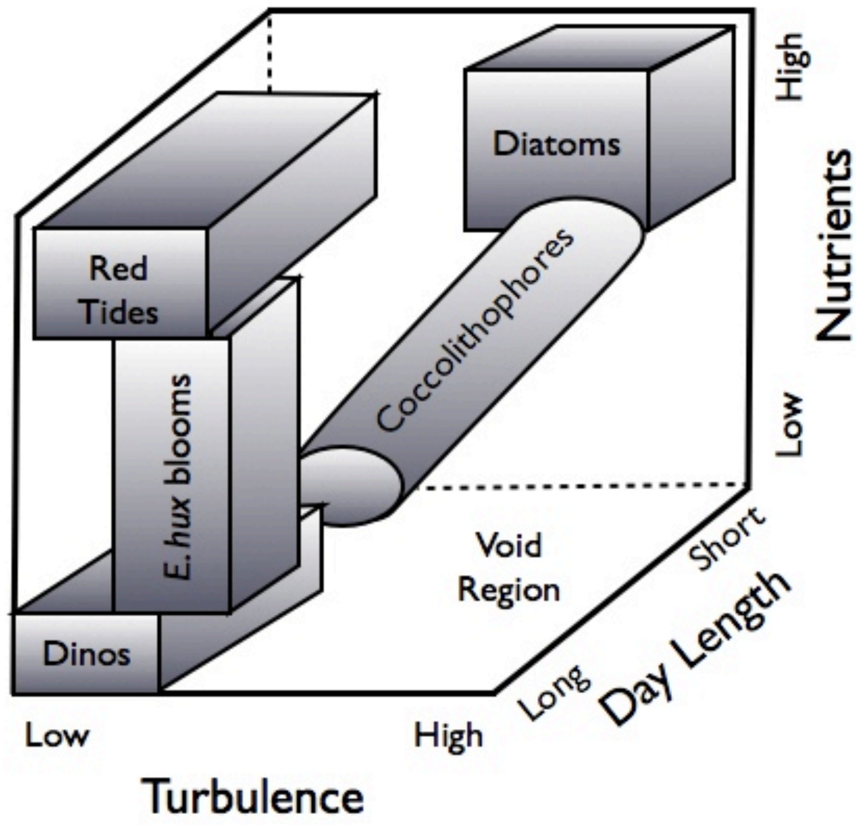

from Balch, 2004

- Widely accepted that PFT groups have distinct biogeography.
- Margalef Mandala is a useful construct to understand phytoplankton distributions across a varied environmental landscape.
- Niche models widely used in ecology to describe *species* distributions.
- Statistical in nature, and depends on assumptions regarding species presence/absence.

SeaWiFS coccolithophore bloom patterns

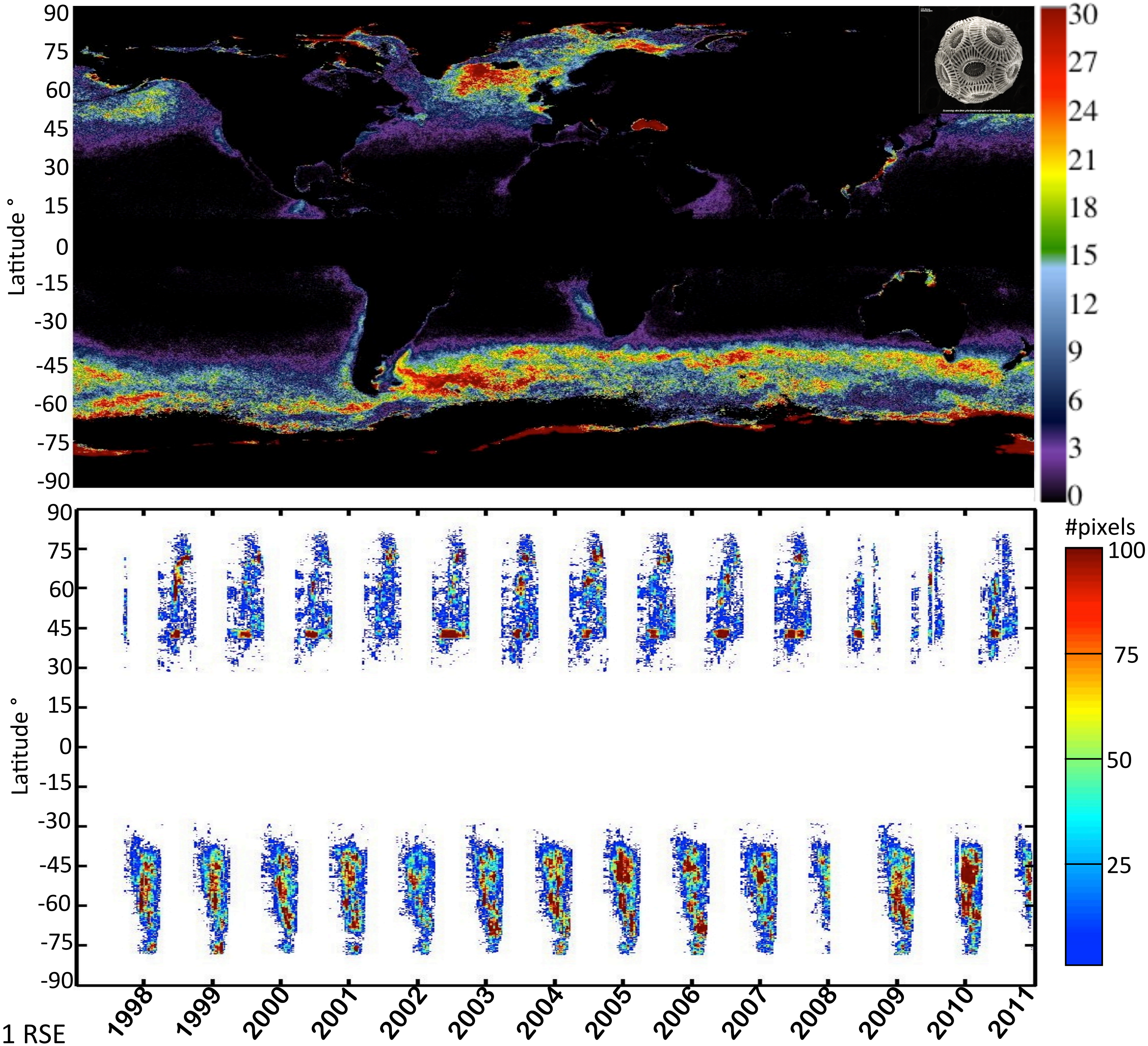

Moore et al, 2011 RSE

A Coccolithophore 'bloom' niche model

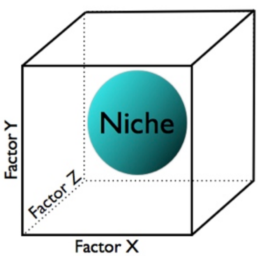

- Using OC data, bloom pixels used as mask to select co-located environmental data
- Niche was characterized by statistical distribution of environmental data (SST, MLD, PAR, Winds).

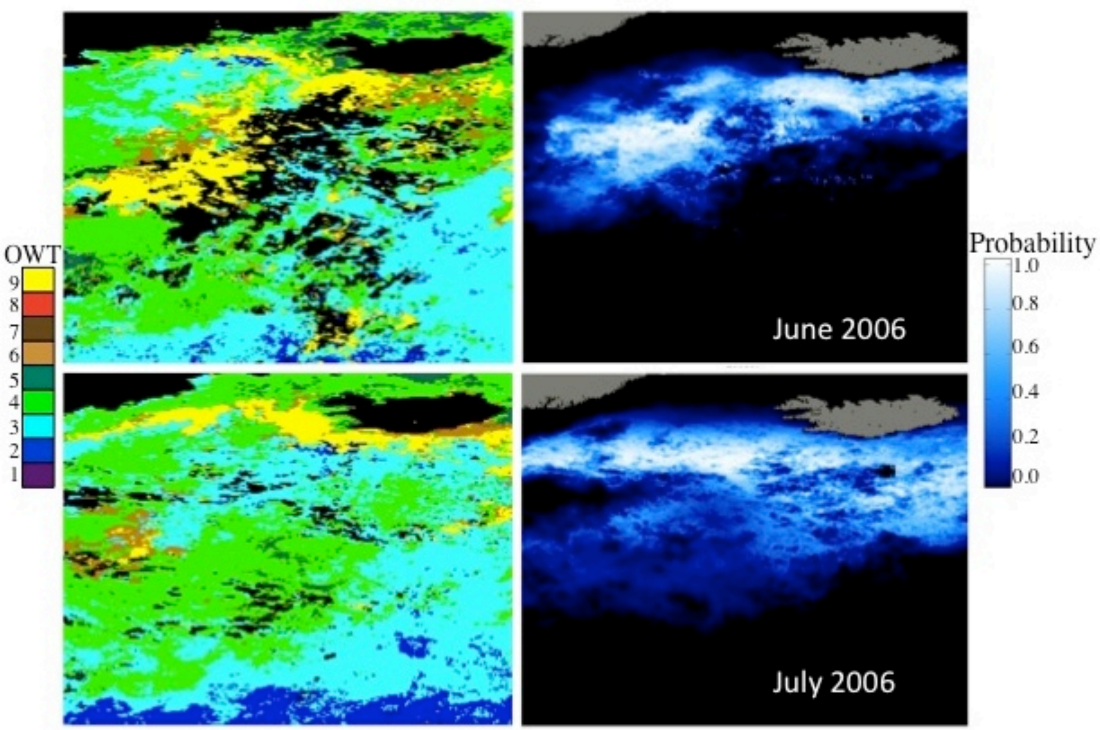

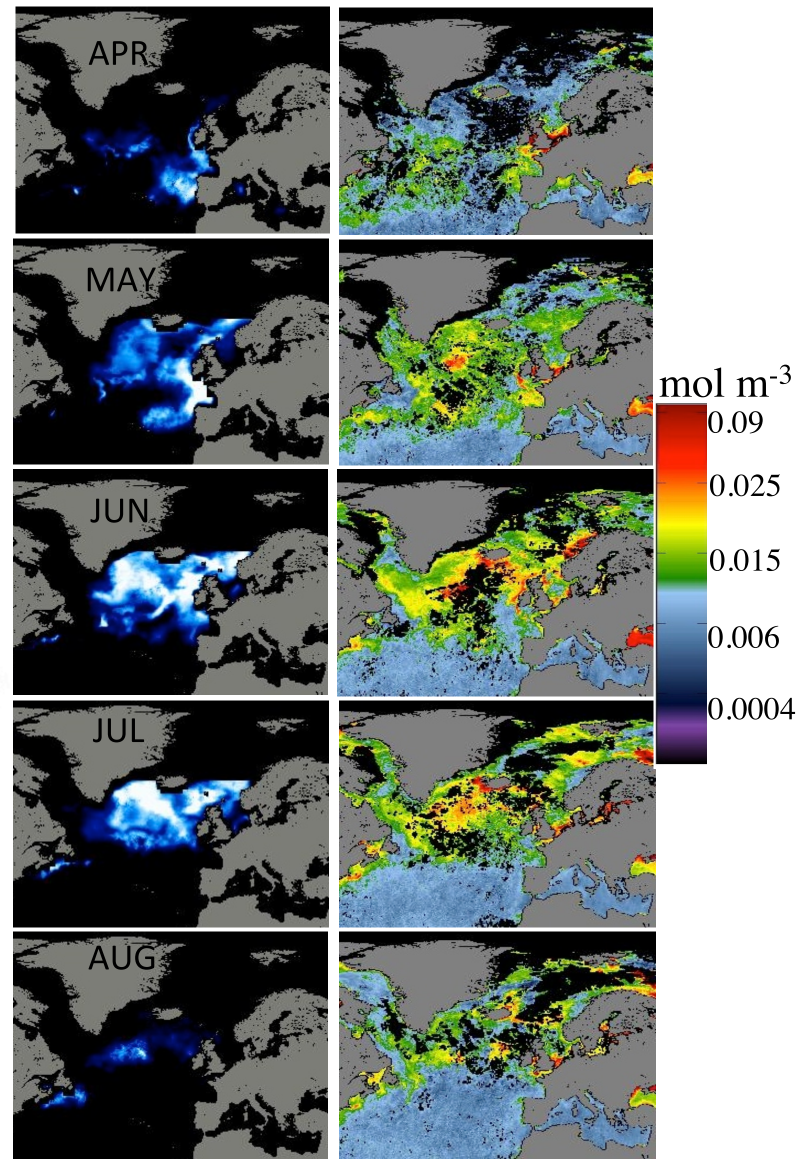

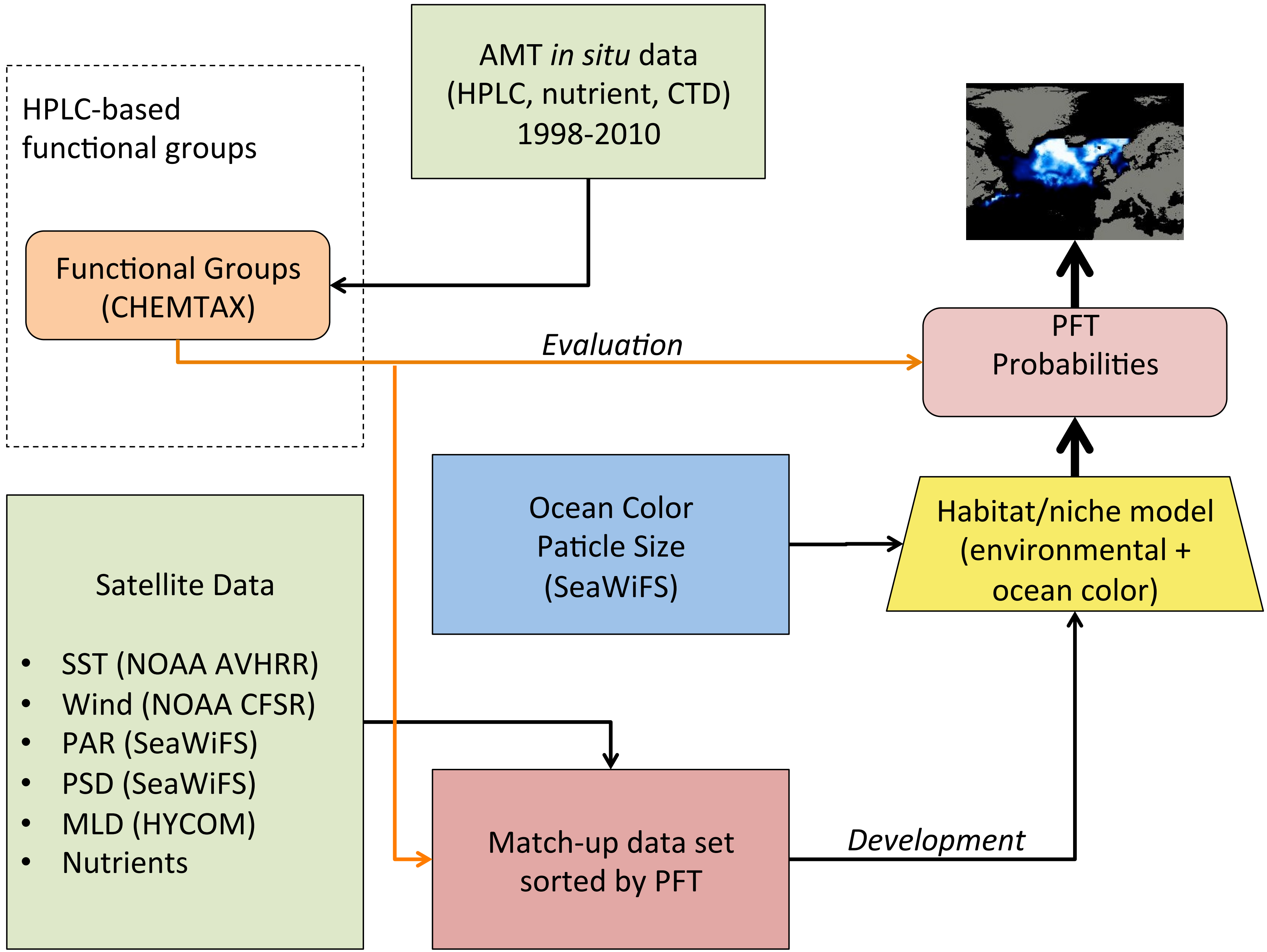
AMT *in situ* data
(HPLC, nutrient, CTD)
1998-2010
HPLC-based
functional groups
Functional Groups
(CHEMTAX)
Evaluation
PFT
Probabilities
Ocean Color
Paticle Size
(SeaWiFS)
Habitat/niche model
(environmental +
ocean color)
Satellite Data
SST (NOAA AVHRR)
Wind (NOAA CFSR)
PAR (SeaWiFS)
PSD (SeaWiFS)
MLD (HYCOM)
Nutrients
Match-up data set
sorted by PFT
Development

PFT Training Data Set

Atlantic Ocean
HPLC Data

AMT
SeaBASS
CLIVEC
Pangea

N ~ 2500

CHEMTAX
(based on ‘known’ pigment ratios)

% Phytoplankton of Chla

Diatoms
Dinoflagellates
Prochlorococcus
Prymensiophytes
Chlorophytes
Chrysophytes
Crytpophytes
Synechococcus
Prasinophytes

PFT groups

Diatoms
Synechococcus
Nano flagellates
Prochloro

- 4 PFT groups created
- Dominant PFT identified as fraction of biomass > 0.45
- Coccolithophores added from existing model

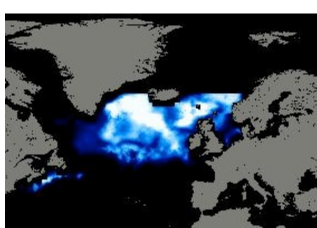

Atlantic matchup data set

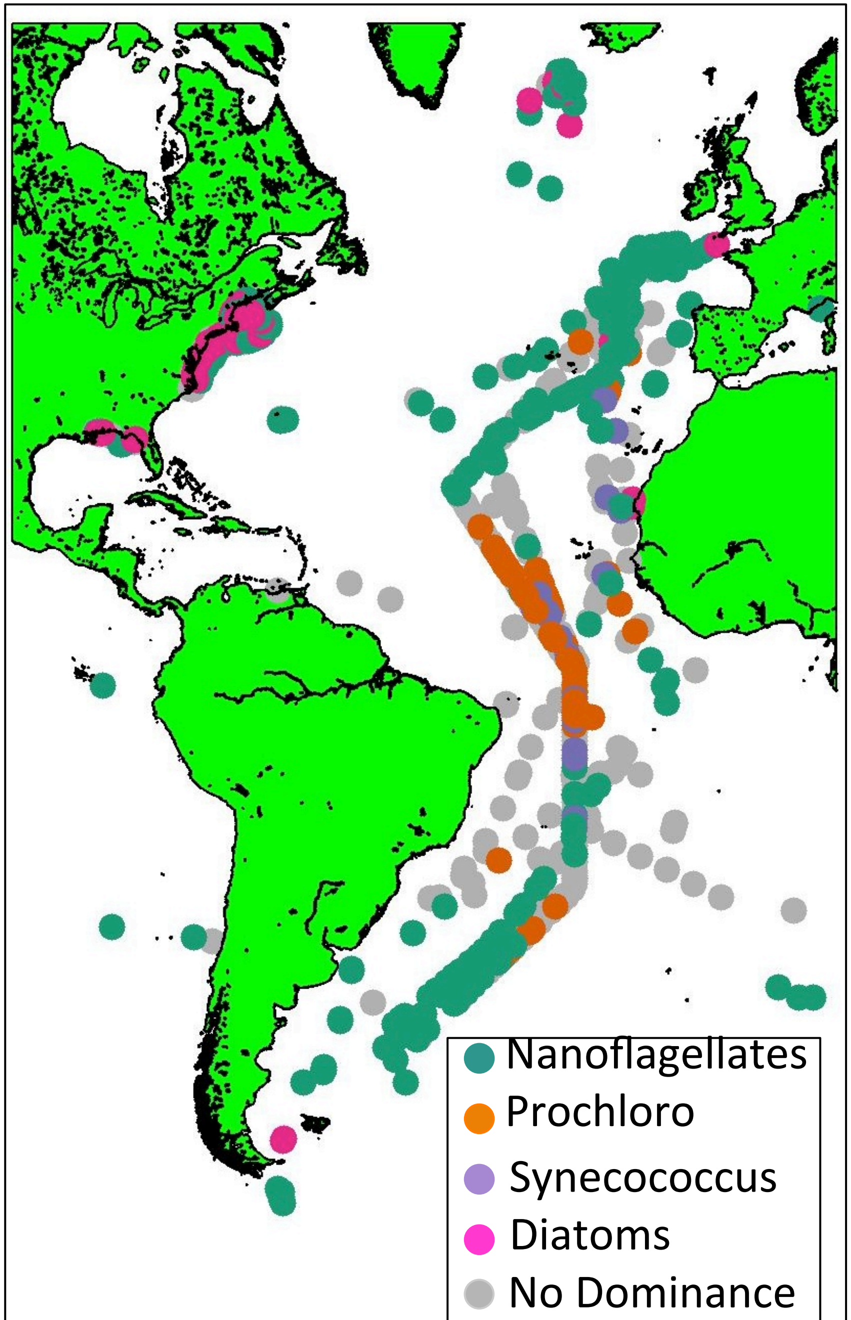

- ~800 matchup points between HPLC in situ and satellite variables.
- 340 points had a 'dominant' PFT present (~50%).
- Nanoflagellates dominated PFTs (~70%).
- Synechococcus dominant least abundant (5%).

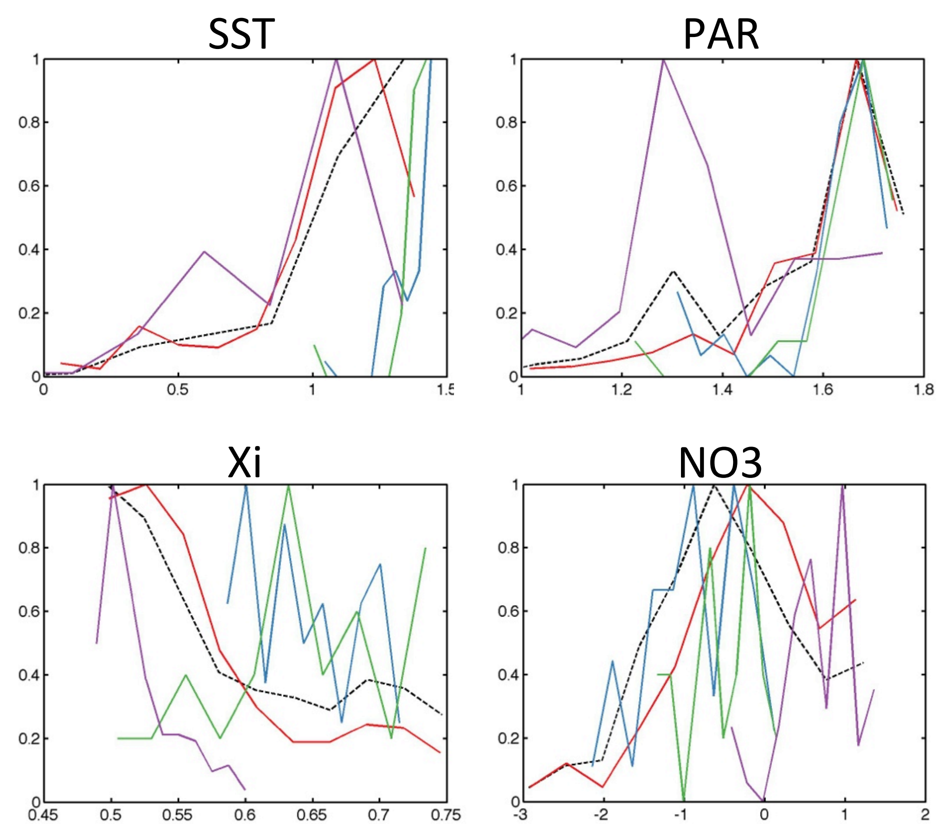

Statistical Model

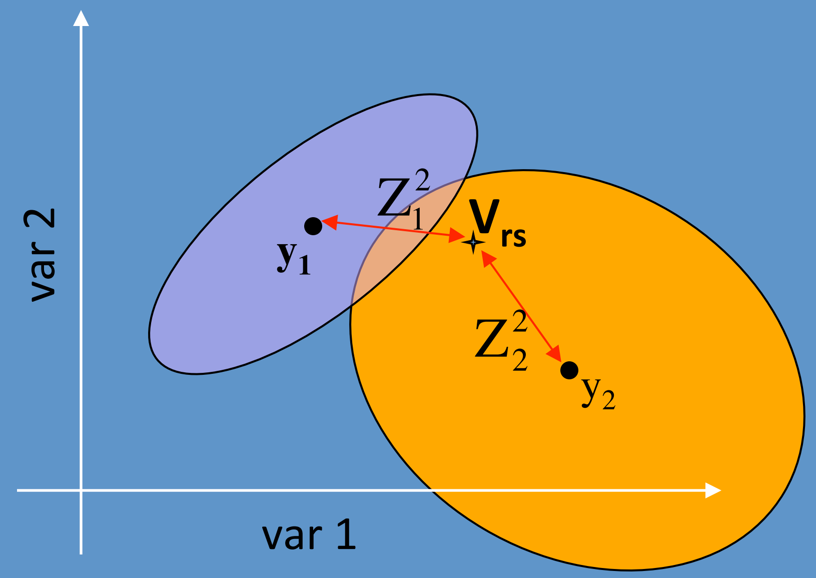

$$\boldsymbol{Z^2} = (\mathbf{V}_{\mathbf{rs}} - \mathbf{y}_j)^t \boldsymbol{\Sigma}_j^{-1} (\mathbf{V}_{\mathbf{rs}} - \mathbf{y}_j)$$ ⇒ Chi-square PDF

$\mathbf{V}_{\mathbf{rs}}$ – Environmental vector

$\mathbf{y}_j$ – jth PFT mean vector

$\boldsymbol{\Sigma}_j$ – jth PFT covariance matrix

Performance matrix – 5 PFT types

Scenario	Training* % correct	Eval** % correct
1	43.9	40.6
2	58.8	50.7
3	70.7	55.6
4	72.3	55.7
5	79.3	63.9
6	88.7	72.6

- Best performance with all variables combining OC & env data.
- Systematic additions of variables improved performance.

Scenario 1: PSD only
Scenario 2: Sc1 + SST
Scenario 3: Sc2 + PAR
Scenario 4: Sc3 + MLD
Scenario 5: Sc4 + wind
Scenario 6: Sc5 + nutrients

*Training Data used from 'dominant' points in pool of data (N=370)

**Data not used but 'not dominant' from remaining pool of data (N=421)

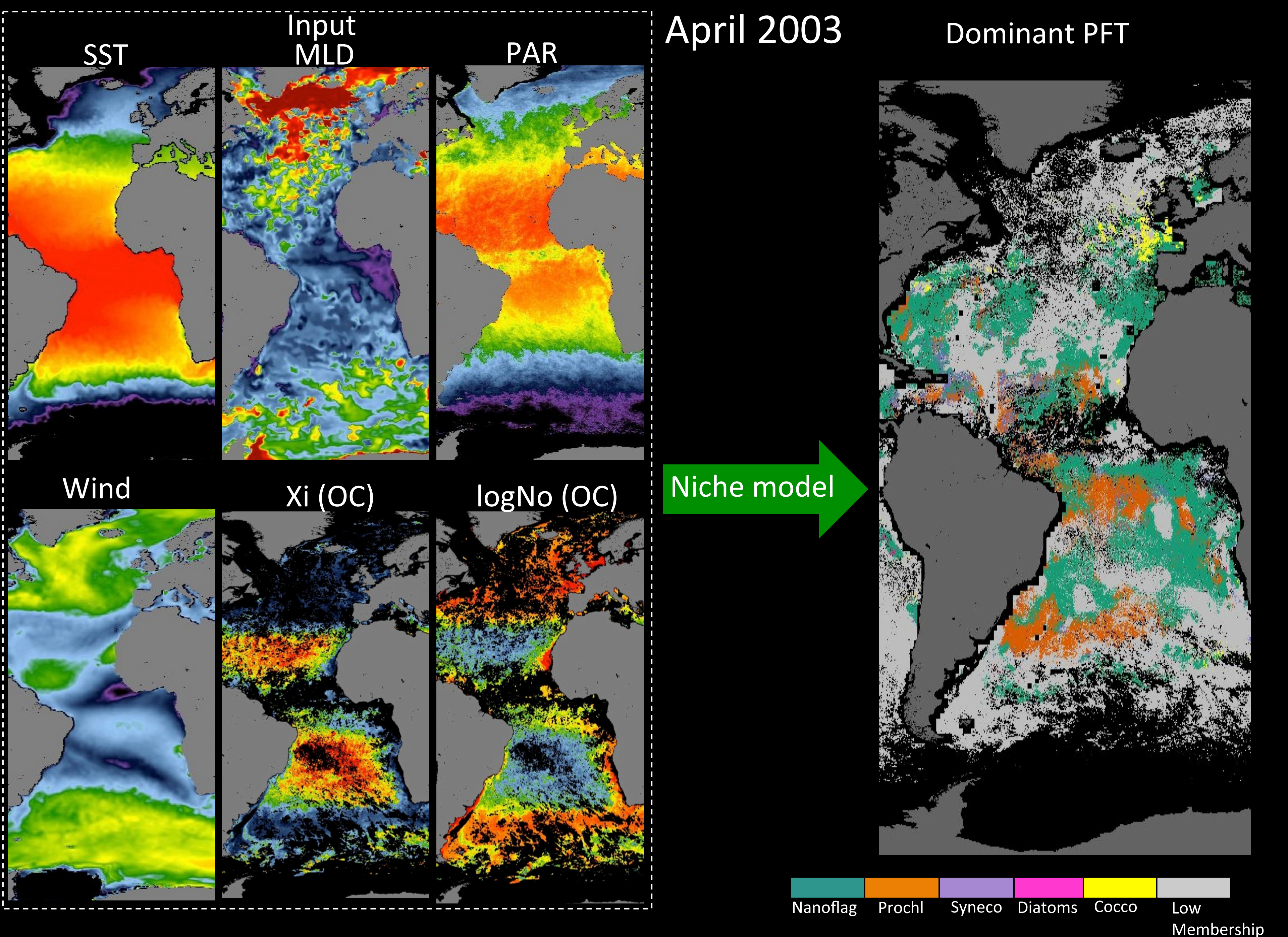

April 2003
Input
SST
MLD
PAR
Wind
Xi (OC)
logNo (OC)
Niche model
Dominant PFT
Nanoflag
Prochl
Syneco
Diatoms
Cocco
Low Membership

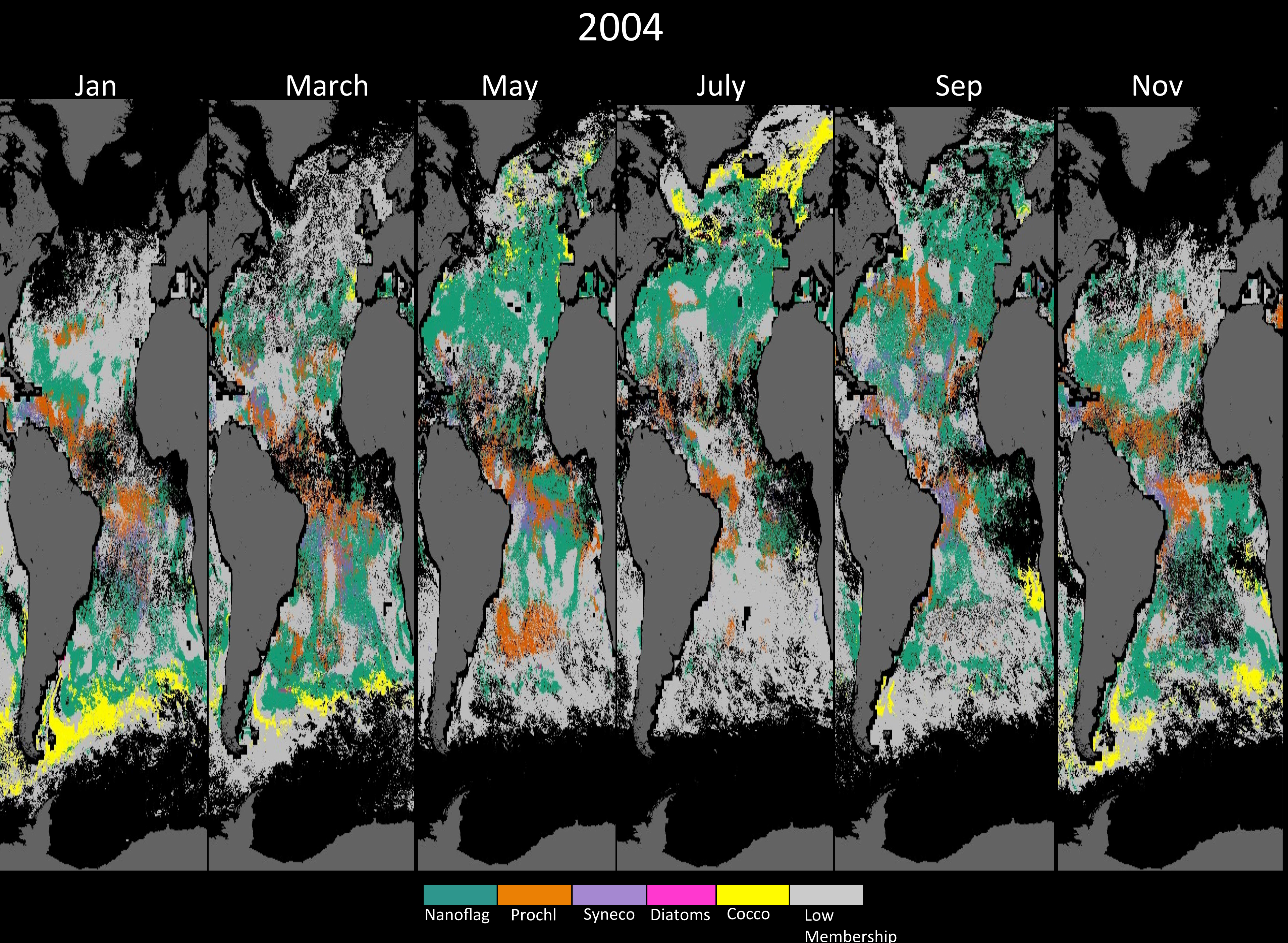
2004
Jan
March
May
July
Sep
Nov
Nanoflag
Prochl
Syneco
Diatoms
Cocco
Low Membership

Summary

- A model was developed to predict dominant PFT groups at the oceans *surface* using particle size information from ocean color imagery combined with environmental data.
- The model was based on a ‘habitat/niche’ concept formed by observed relationships between identified PFT groups (from in situ HPLC) and co-located satellite variables (e.g., PAR, MLD, wind, SST and nutrients).
- Model is driven by assumptions on 1) initial Chemtax-derived phytoplankton group accuracy, 2) partitioning of these groups into PFTs, and 3) niche concept applying to broad phytoplankton groups.
- 5 PFTs were characterized in this model: Nanoflagellates, Diatoms, Coccolithophores, Prochlorococcus and Synecococcus.

Summary (continued)

- The model currently works predicts correct PFT 86-90% based on training set, and about 70% accuracy with a separate data set that is not totally appropriate for the model since there are no 'Dominant' points in that data set.
- Despite the large matchup data set, only 1/3 of the points were 'dominant', and more data would be beneficial for both further training, and evaluation.
- The output maps look reasonable, but its difficult to assess without other metrics to validate.

Future Work

- Explore alternative PFT groupings.
- Utilize upcoming PSD imagery for Aqua and VIIRS (Kostadinov).
- Assess model with an appropriate validation data set.
- Utilize monthly nitrate product for Atlantic (J. Goes).

Backup Slides

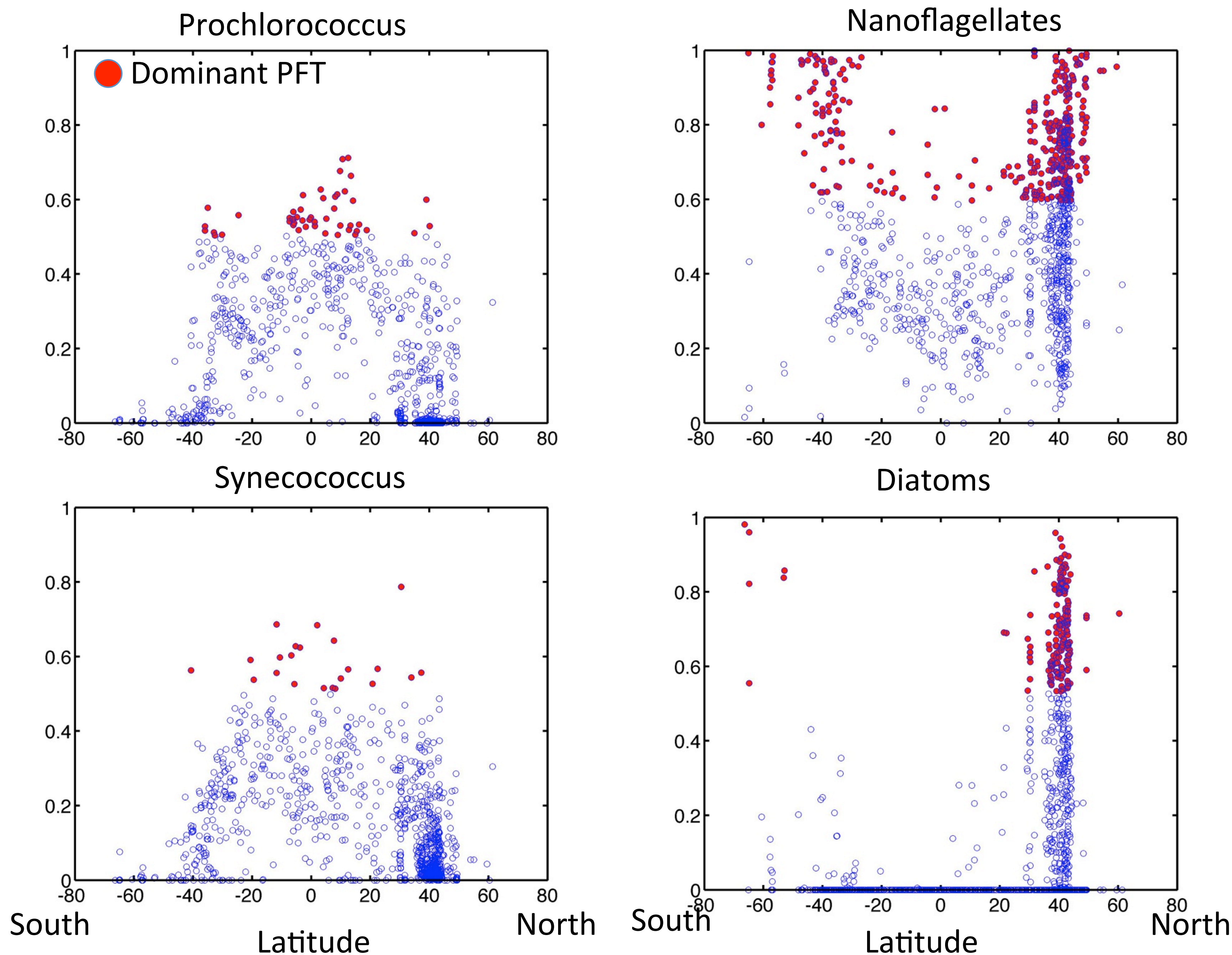

Prochlorococcus
Dominant PFT
Nanoflagellates
Synecococcus
Diatoms
0
0.2
0.4
0.6
0.8
1
-80
-60
-40
-20
0
20
40
60
80
South
Latitude
North

Building the capacity of monitoring water quality in coastal waters: Pilot studies in the Chesapeake Bay

Guangming Zheng[1,2], Paul M. DiGiacomo[1], Marilyn Y. Murphy[1]

[1]*NOAA/NESDIS/STAR*

[2]*Global Science & Technology, Inc.*

Water quality remote sensing in the Chesapeake Bay

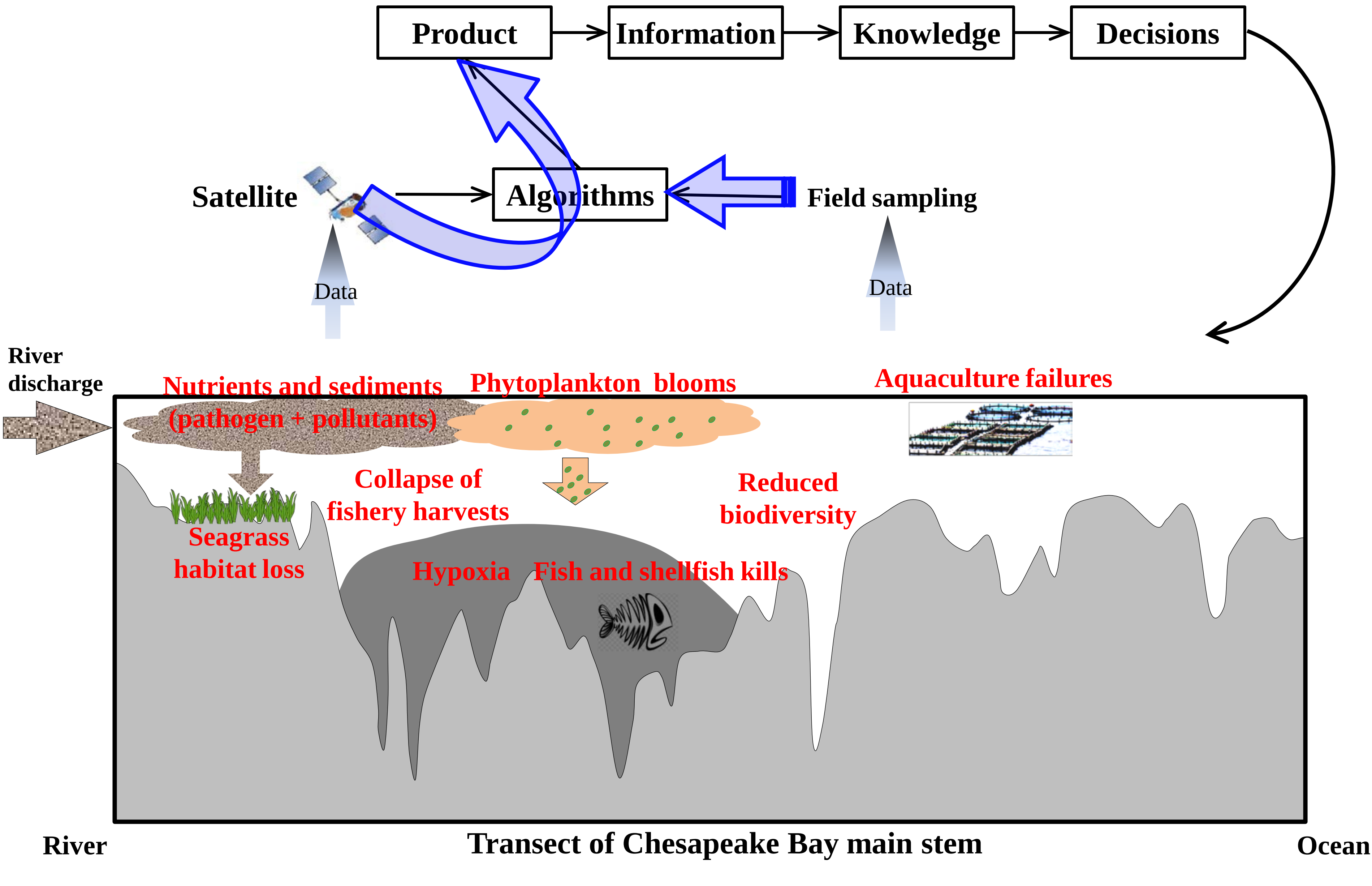

Evolution of sediment plumes in the Chesapeake Bay

[*Zheng et al.*, 2015a]

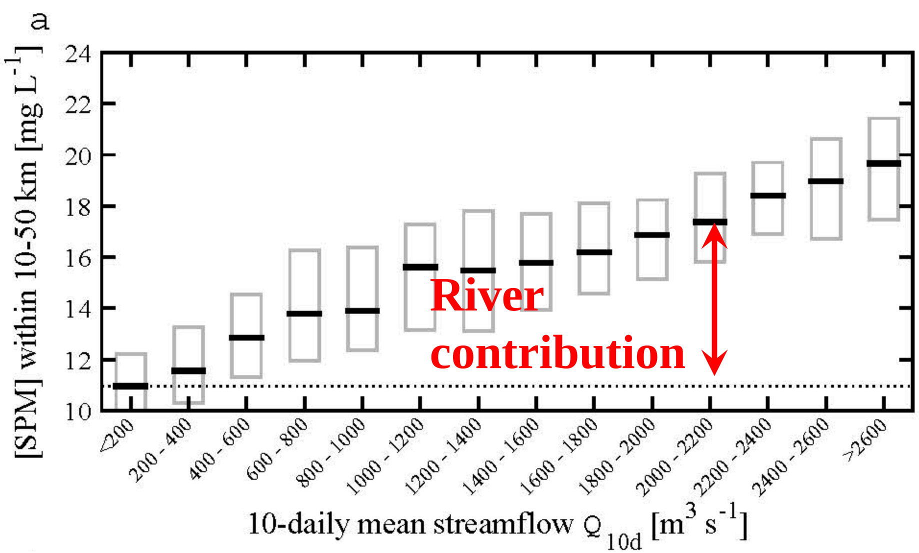

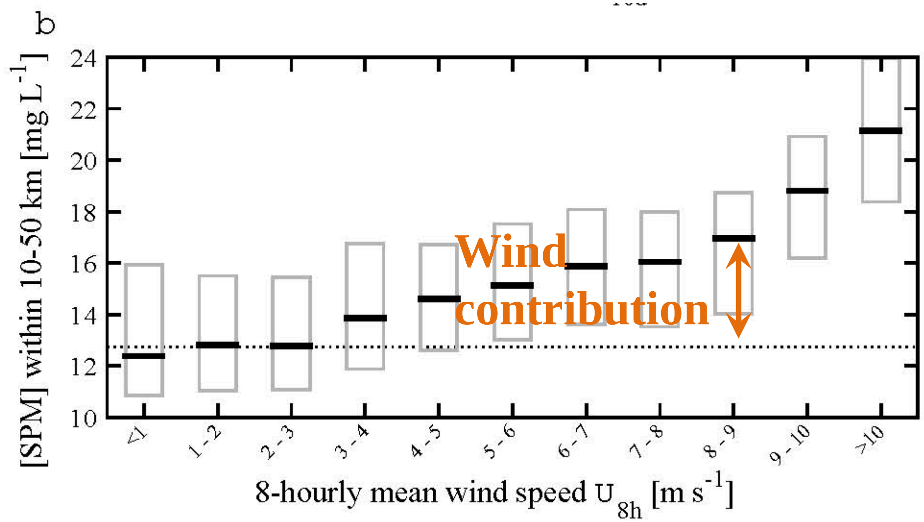

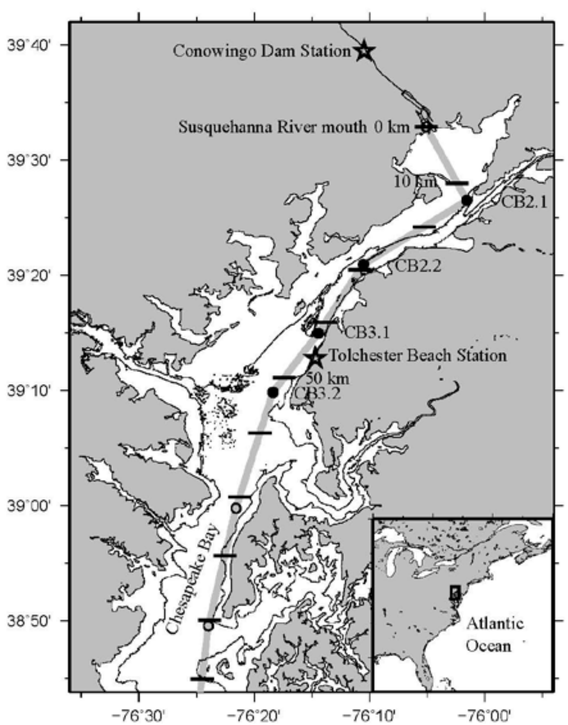

River > **Wind** **Wind** > **River**

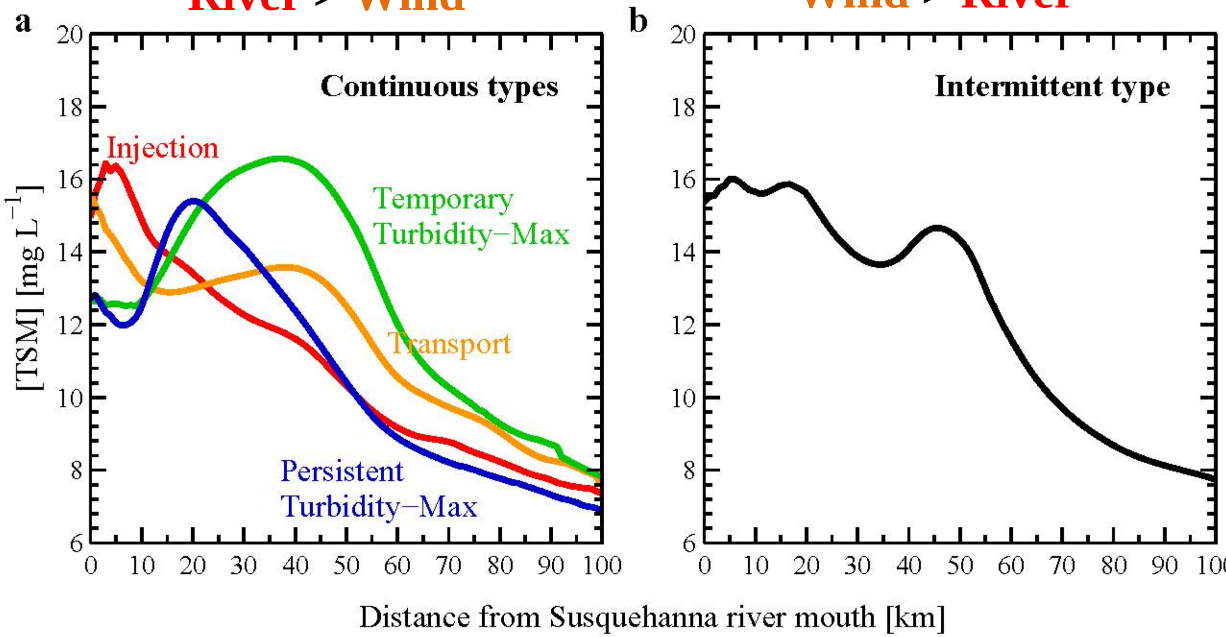

Short-term evolution of sediment plumes after discharge events

Types	Injection	Transport	Temporary Turbidity Max	Persistent Turbidity Max
Spatial shape of [SPM]	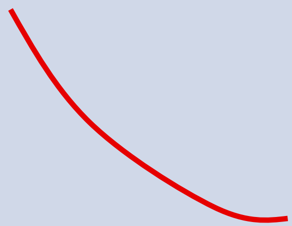	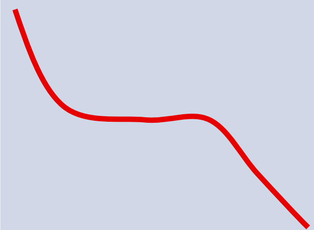	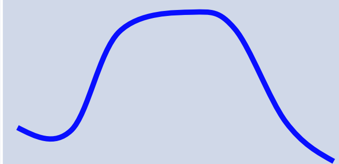	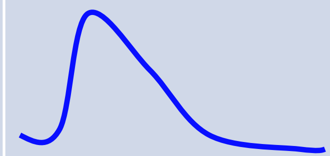
Timing (days)	0–5	3–10	5–30	>13

Long-term regime shift of typology

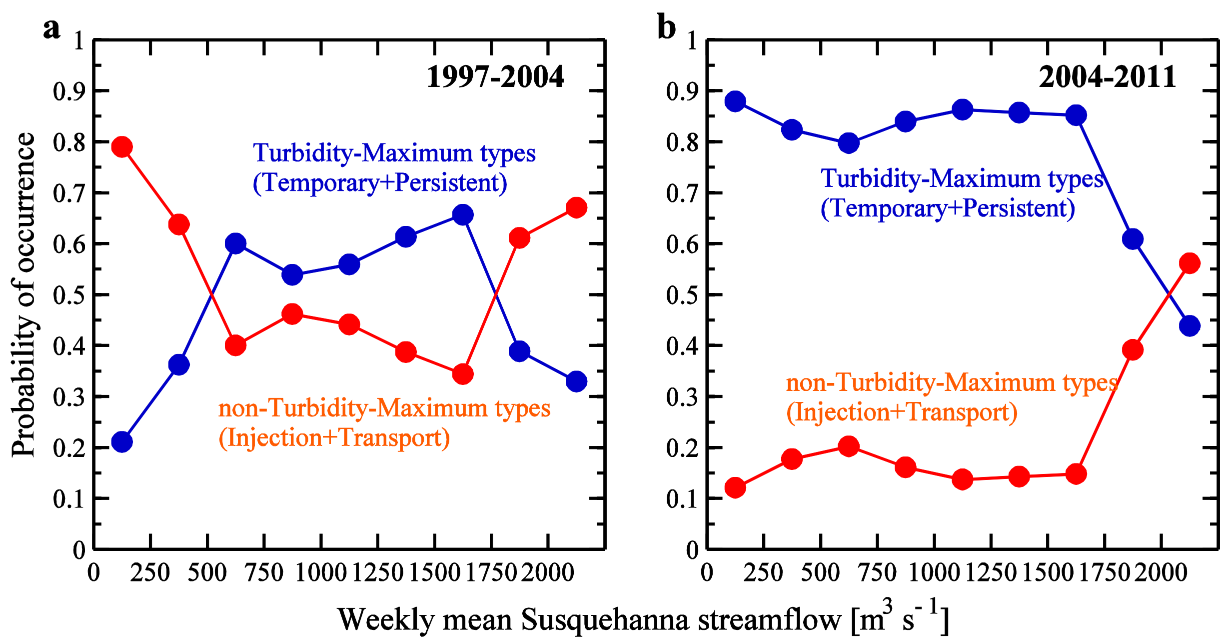

• The regime shift is likely associated with Hurricane Ivan (2004)

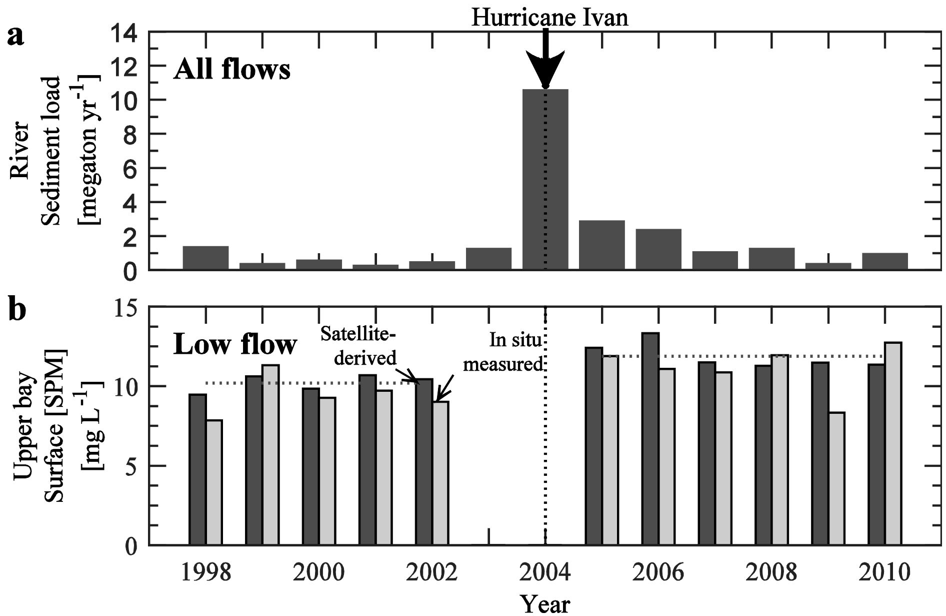

• Hurricane Ivan (2004) triggered a discharge of sediments equivalent to the total amount discharged over the preceding 10 years

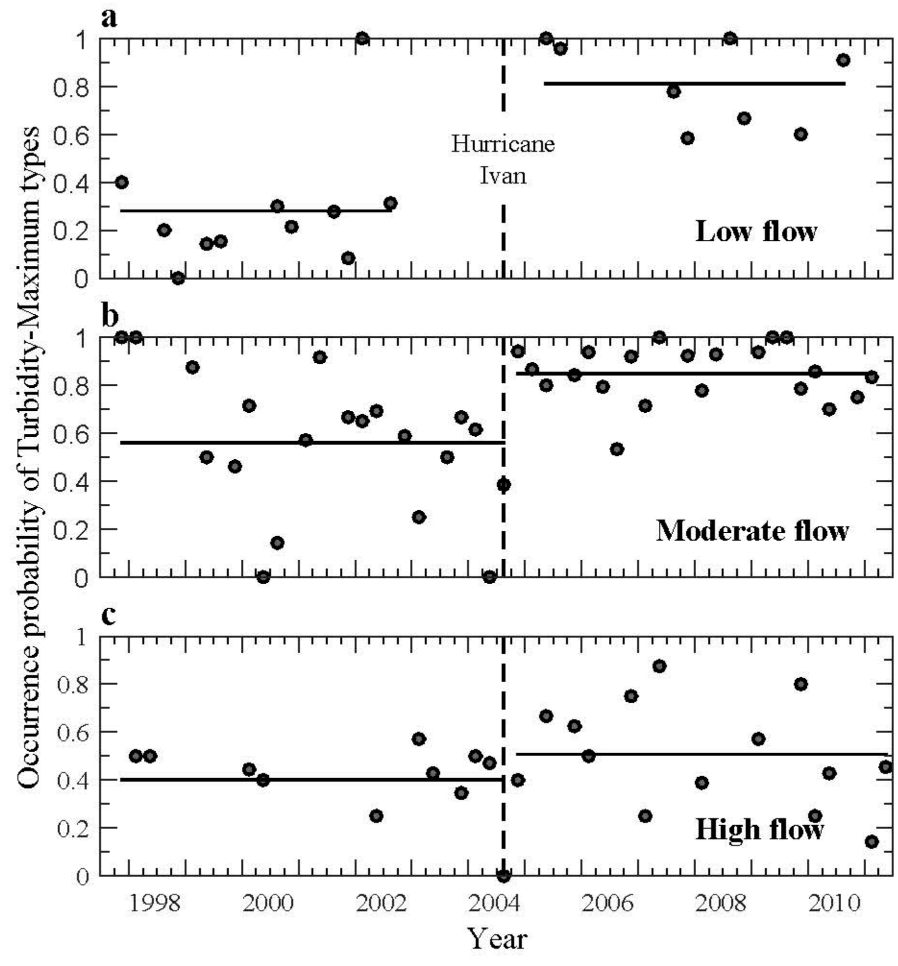

• The shift in typology occurred in an abrupt manner after Hurricane Ivan

Another important detail:

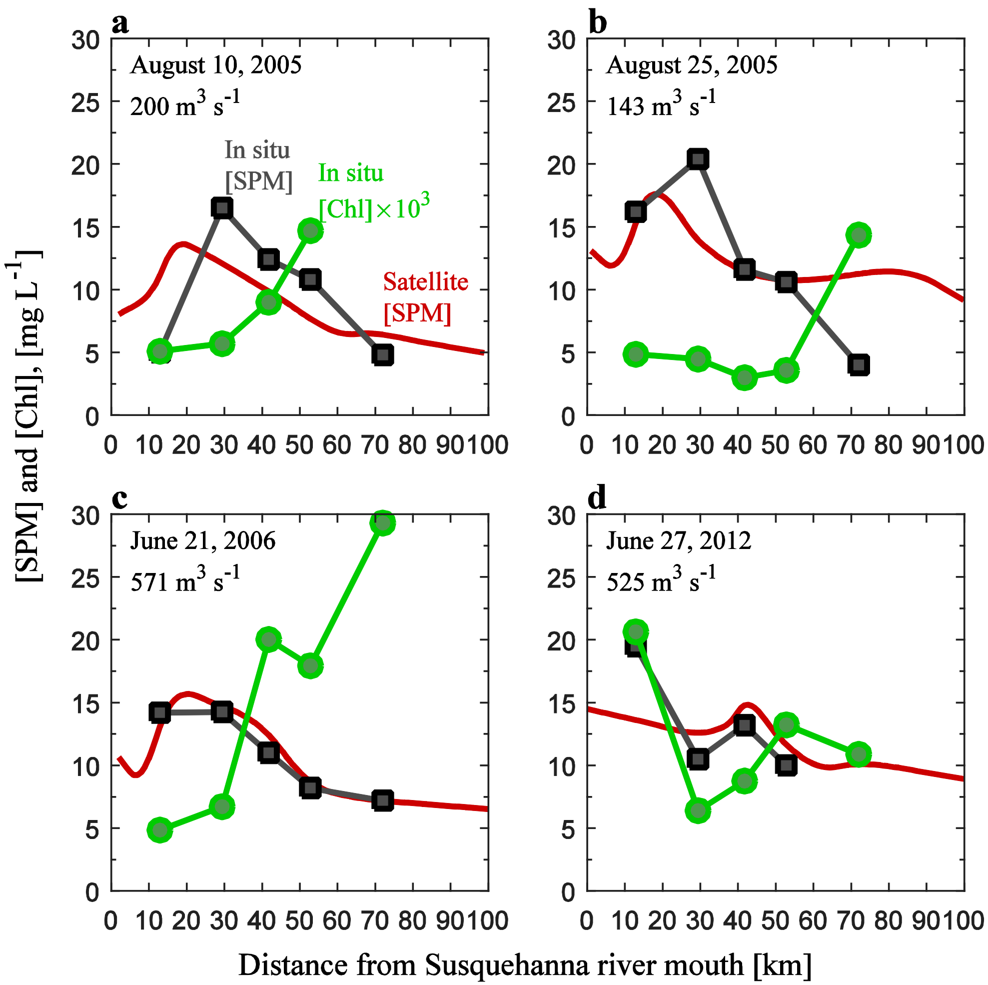

- Chlorophyll transect is decoupled from suspended sediment transect

- Higher algal biomass is located downstream of the Turbidity Max

Satellite Remote-sensing of water quality parameters: Current and future approaches

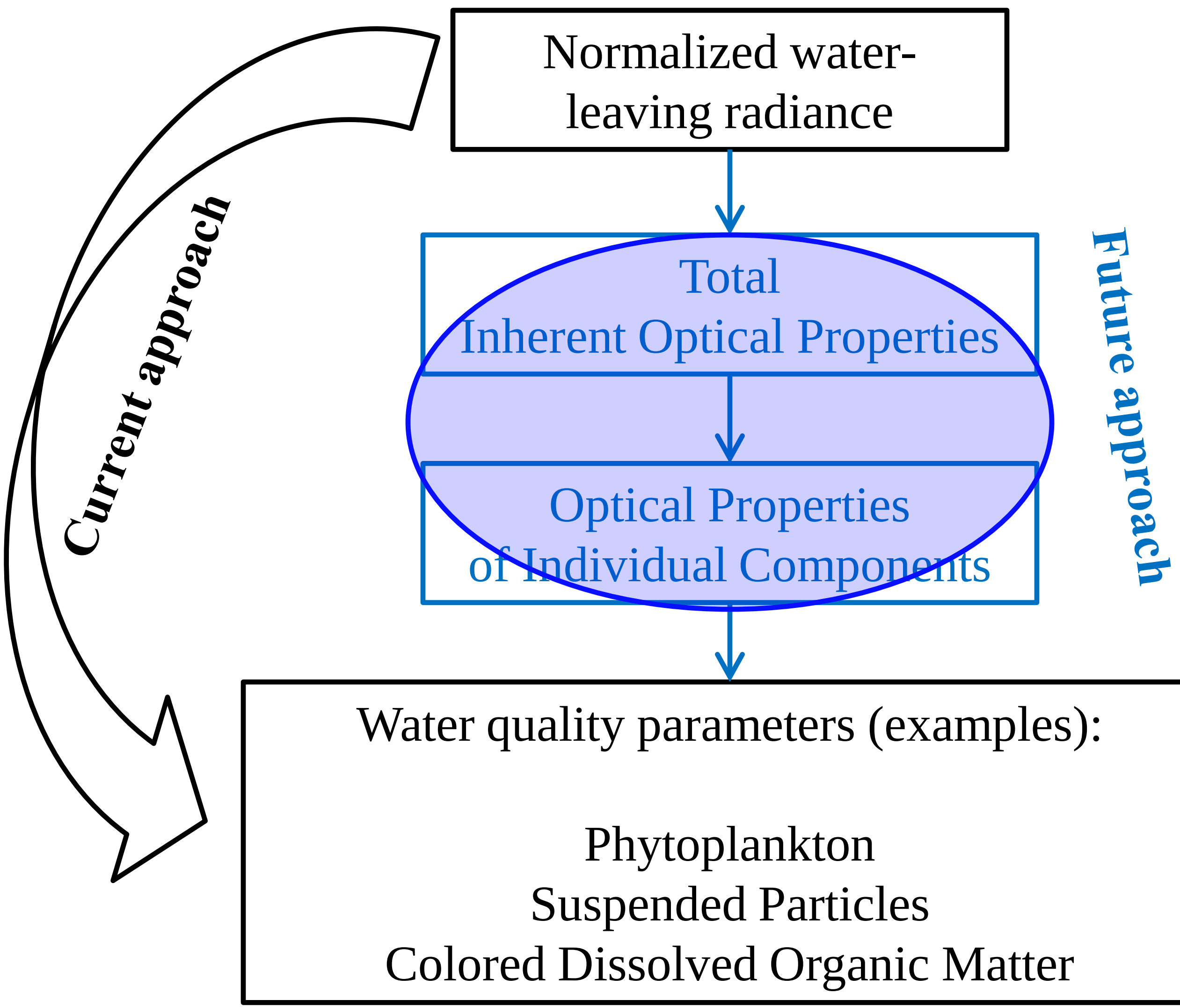

Generalized Stacked-Constraints Model (GSCM)

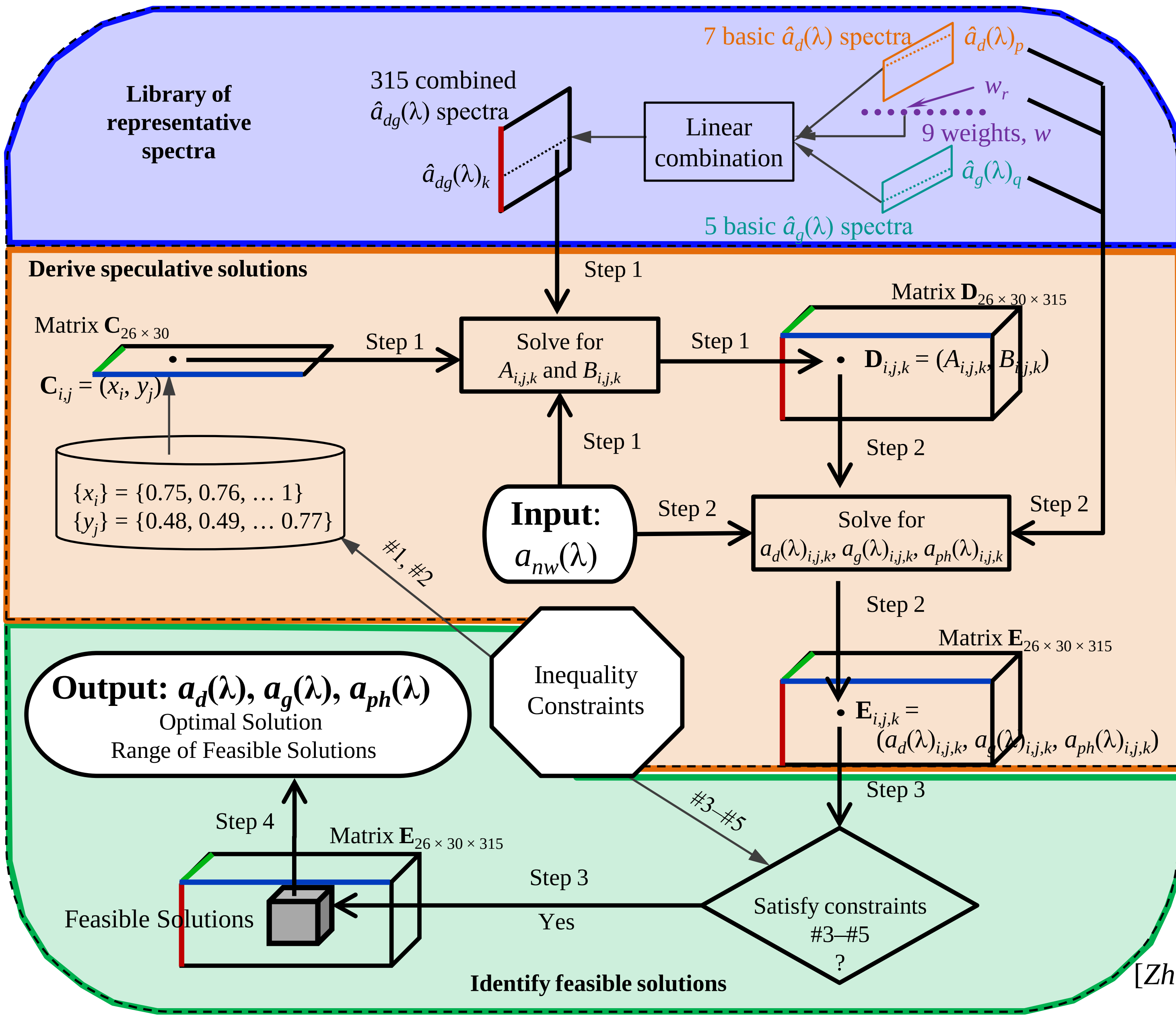

[*Zheng et al.*, 2015b]

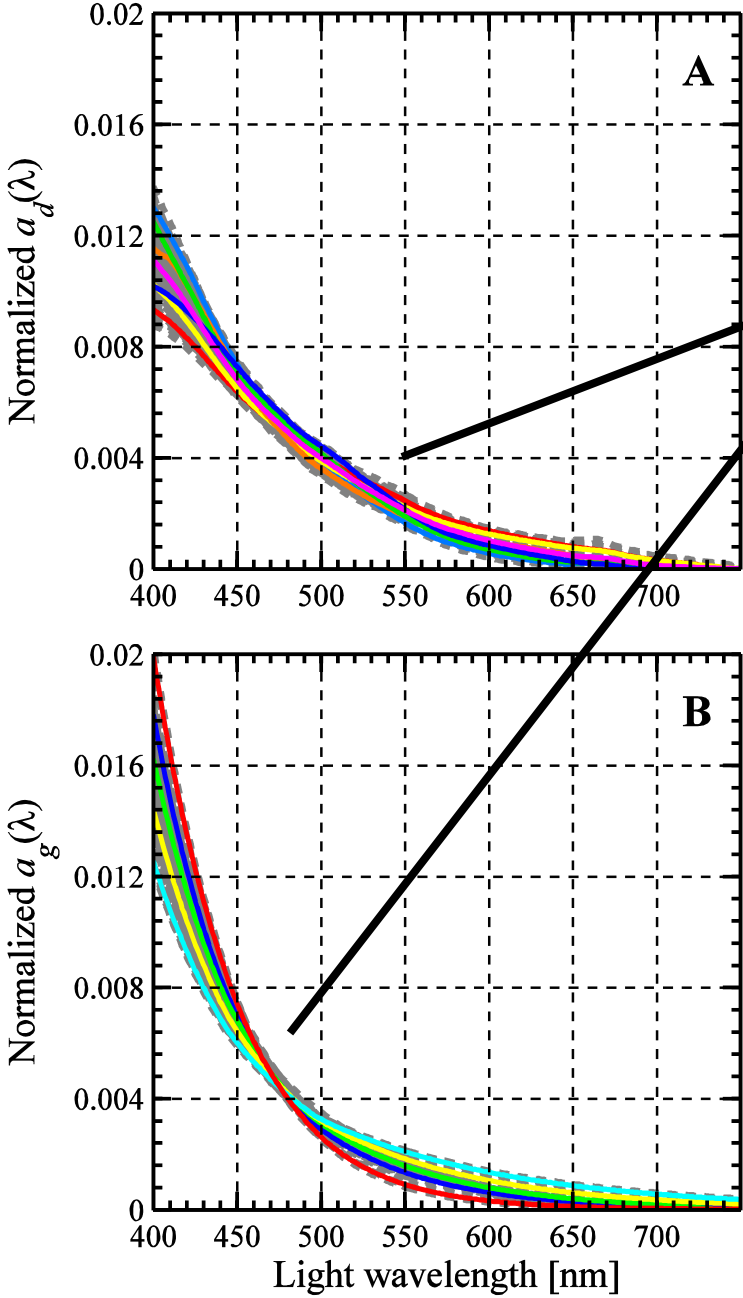

Advantages of GSCM

- Representative spectra determined from hierarchical cluster analysis using field data.

- The inequality constraints allows spectral shape of $a_{ph}(\lambda)$ to vary widely

Inequality Constraints	
#1	$0.75 < a_{ph}(412)/a_{ph}(443) < 1$
#2	$0.48 < a_{ph}(490)/a_{ph}(443) < 0.77$
#3	$0.76 < a_{ph}(469)/a_{ph}(412) < 1.13$
#4	$0.19 < a_{ph}(555)/a_{ph}(490) < 0.50$
#5	$0 < a_d(750)/a_d(443) < 0.3$

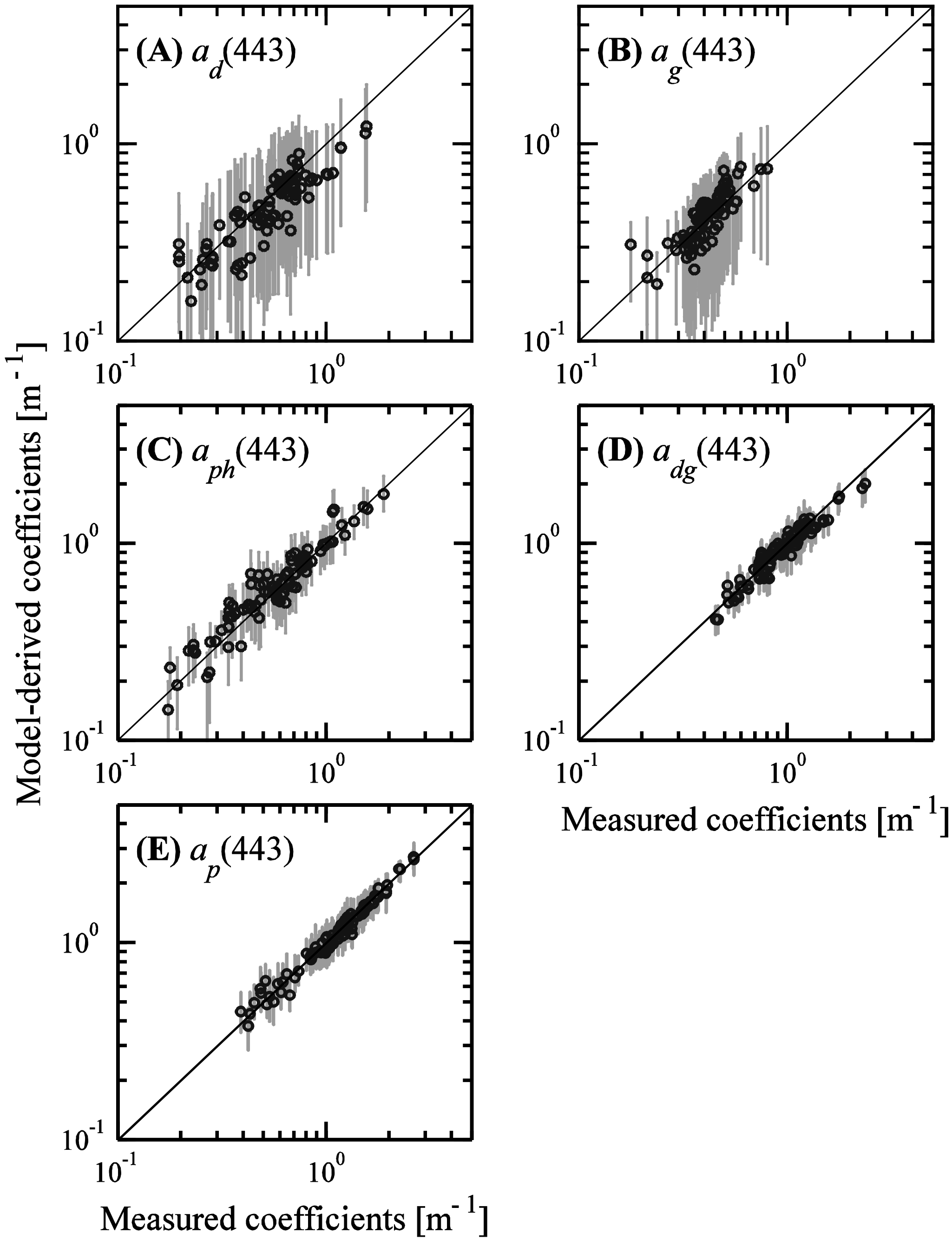

- The model-derived a_d, a_g, and a_{ph} agree reasonably well with measurements

- Small systematic error (e.g., *MR* differs within ±10% from 1 @443 nm)

- Small random error (e.g., *MPD* ranges between 11 and 17%, and *RMSD* between 0.07 and 0.14 m^{-1} @443 nm)

Application of GSCM to MODIS data

[*Zheng et al.*, in prep]

Input:

MODIS-Aqua $R_{rs}(\lambda)$
(SWIR atmospheric correction)

[*Wang*, 2007; *Wang & Shi*, 2007]

Raman-corrected $R_{rs}(\lambda)$

[*Lee et al.*, 2010]

Quasi-Analytical Algorithm (QAA), v5

[*Lee et al.*, 2009]

QAA Output:

- $a_{ph}(\lambda)$ Phytoplankton
- $a_{dg}(\lambda)$ NAP + CDOM
- $a_{nw}(\lambda)$
- $b_{bp}(\lambda)$ Total particulate matter

Generalized Stacked-Constraints Model (GSCM)

[*Zheng et al.*, 2015b]

QAA-GSCM Output:

- $a_d(\lambda)$ NAP
- $a_{ph}(\lambda)$ Phytoplankton
- $a_g(\lambda)$ CDOM

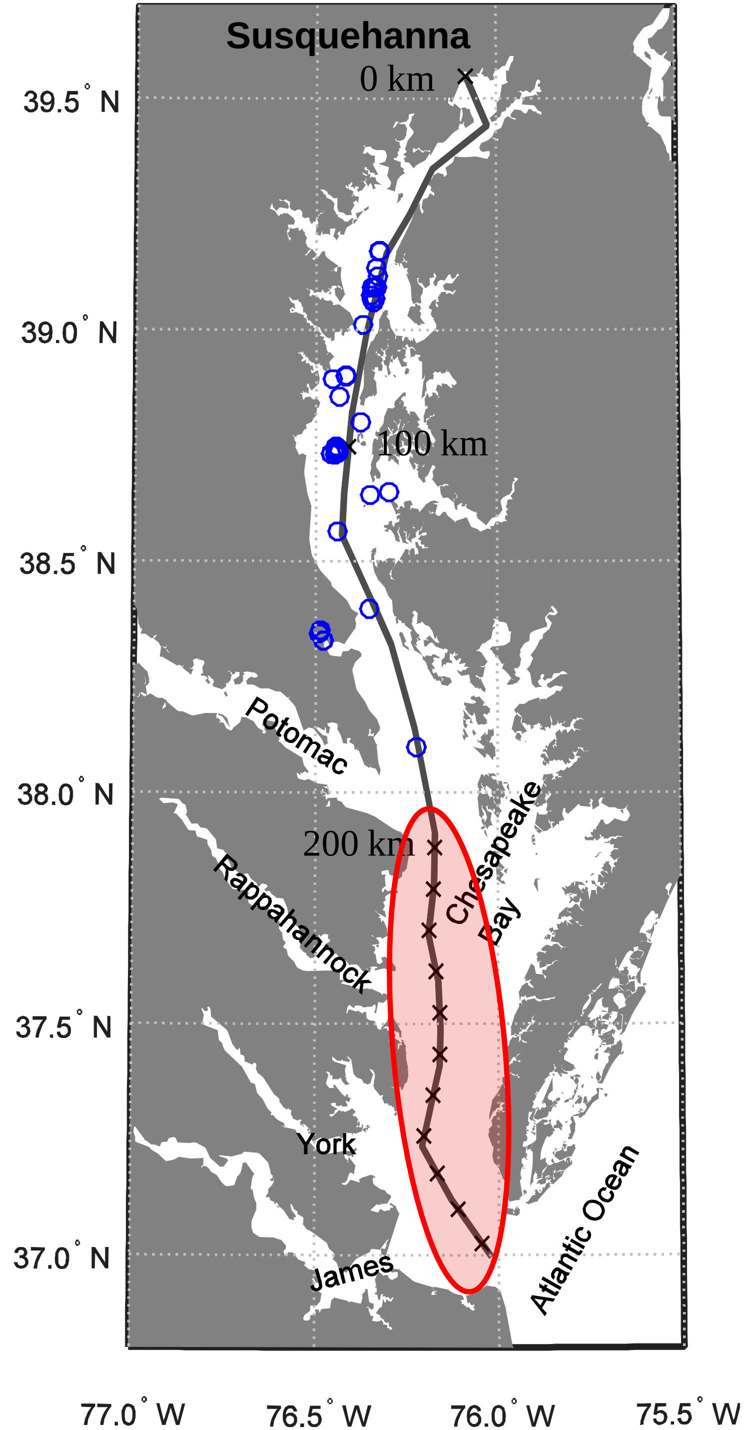

Optical identification of water mass

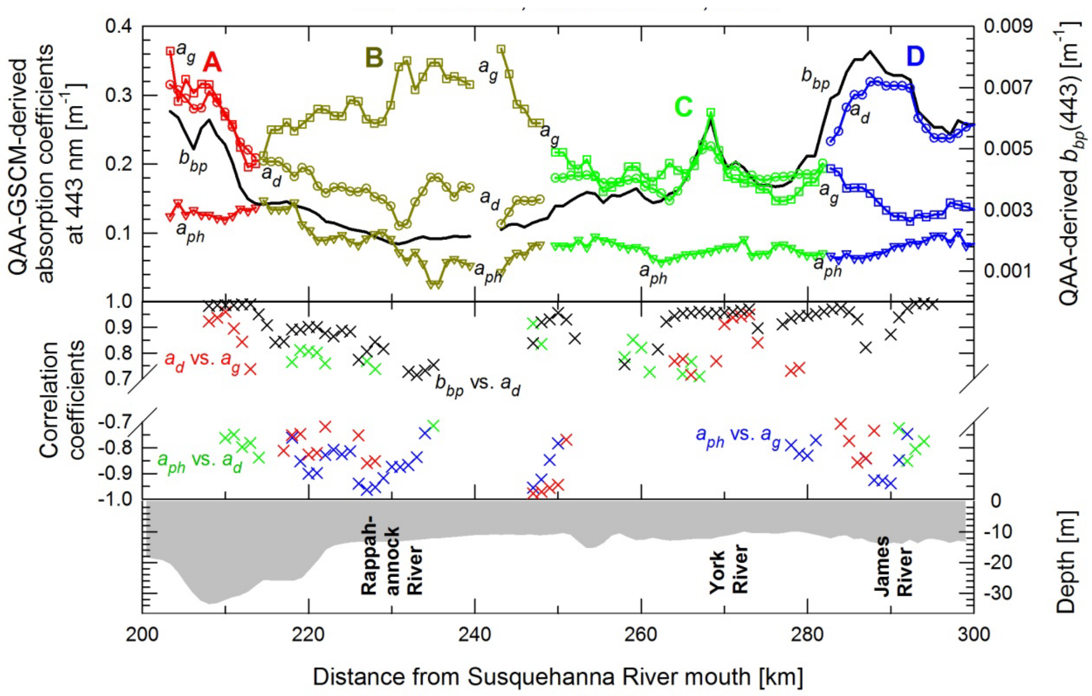

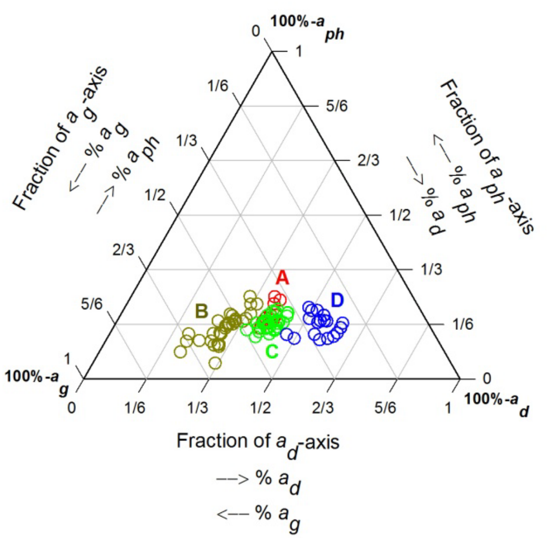

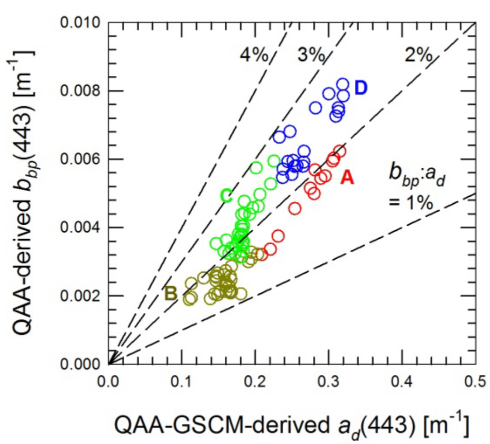

Fall 2002

- Water mass **A**:
  - o Potomac River plume
  - o CDOM and NAP dominated
  - o $b_{bp}(443):a_d(443) = 1.8 \pm 0.2$ %
  - o CDOM-NAP mixed plume
- Water mass **B**:
  - o Rappahannock River plume
  - o CDOM dominated
  - o $b_{bp}(443):a_d(443) = 1.5 \pm 0.2$ %
  - o “Tea-colored” plume
- Water mass **C**:
  - o York River plume
  - o CDOM and NAP dominated
  - o $b_{bp}(443):a_d(443) = 2.2 \pm 0.3$ %
  - o CDOM-NAP mixed plume
- Water mass **D**:
  - o James River plume
  - o NAP dominated
  - o $b_{bp}(443):a_d(443) = 2.5 \pm 0.2$ %
  - o “Turbid” plume

Conclusions

- Combining satellite-derived suspended sediments data and field-measured streamflow data allows us to elucidate short- and long-term trends of sediment distribution.

- The GSCM-type approach which allows the extraction of mathematically dissociated absorption coefficients of phytoplankton, nonalgal particles, and CDOM is a promising new tool for water quality research and applications.

Future research

- Improve the spectral shape of satellite-derived $R_{rs}(\lambda)$ in the blue spectral region
- Identify potential links between optical properties and water quality parameters such as toxins, harmful algal cell counts, dissolved oxygen, oxygen demands, priority pollutants, and etc.

Publications

- Zheng, G., P. M. DiGiacomo, S. S. Kaushal, M. A. Yuen-Murphy, and S. Duan (2015a), Evolution of sediment plumes in the Chesapeake Bay and implications of climate variability, *Environmental Science & Technology*, 49(11), 6494–6503, doi: 10.1021/es506361p.

- Zheng, G., D. Stramski, and P. M. DiGiacomo (2015b), A model for partitioning the light absorption coefficient of natural waters into phytoplankton, non-algal particulate, and colored dissolved organic components: A case study for the Chesapeake Bay, *Journal of Geophysical Research Oceans*, 120, 2601–2621, doi:10.1002/2014JC010604.

- Zheng, G., D. and P. M. DiGiacomo, and M. A. Yuen-Murphy, Dissociated absorption coefficients of phytoplankton, non-algal particles, and colored dissolved organic matter in the Chesapeake Bay from MODIS, *in prep*.

Acknowledgements

Projects presented here are funded by the NOAA Ocean Remote Sensing (ORS) Program.

We appreciate NOAA/NOS/CO-OPS, USGS, and NASA/GSFC/OBPG, for providing the wind, streamflow, and ocean color radiometric data. We thank Lide Jiang for providing the simulated tidal current data.

We thank all scientists and personnel who contributed to the collection and processing of field data of absorption coefficients used in this study. In particular, we thank L. W. Jr. Harding, C. Hu, and A. Mannino who made the data available through the NASA's SeaWiFS Bio-Optical Archive and Storage System (SeaBASS).

We are grateful to Menghua Wang and Seung-Hyun Son for providing MODIS Aqua reflectance data.

HOW SATELLITE OCEAN COLOR CAN AID OUR UNDERSTANDING OF OCEAN ACIDIFICATION

National Oceanic & Atmospheric Association (NOAA)

Ocean Acidification Program Office

Dwight Gledhill, NOAA OAP
Deputy Director

Presented for…
STAR JPSS 2015
Annual Science Team Meeting
'Session 7d.1: Ocean Color Breakout'
Users & New Applications
NOAA Center for Weather & Climate Prediction
27 August 2015

NOAA OCEAN ACIDIFICATION PROGRAM

http://www.oceanacidification.noaa.gov/

Ocean Acidification

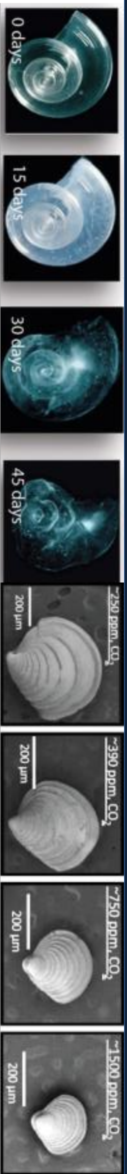

120 GT !

≈ 1/2 of fossil-fuel & cement-manufacturing emissions

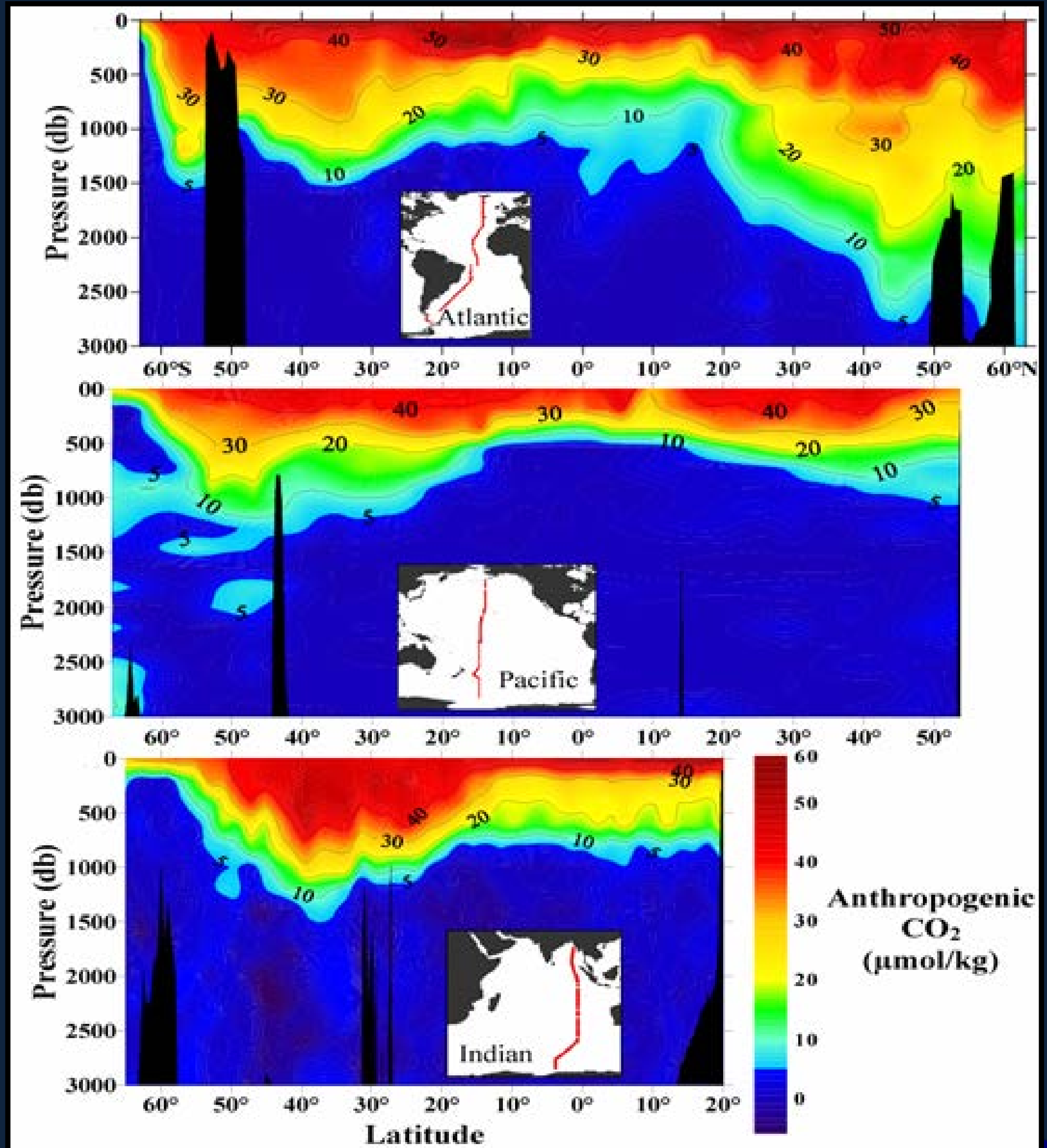

Sabine et al. Science (2004)

Ocean Acidification

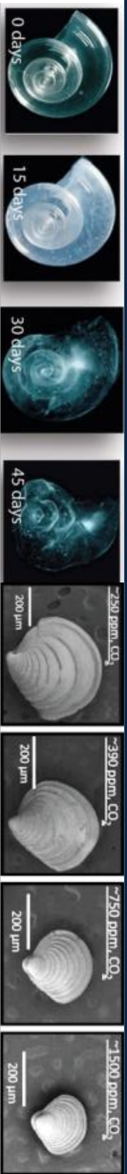

$$CO_{2,gas} + H_2O \rightarrow H^+ + HCO_3^-$$

$$H^+ + CO_3^{2-} \rightarrow HCO_3^-$$

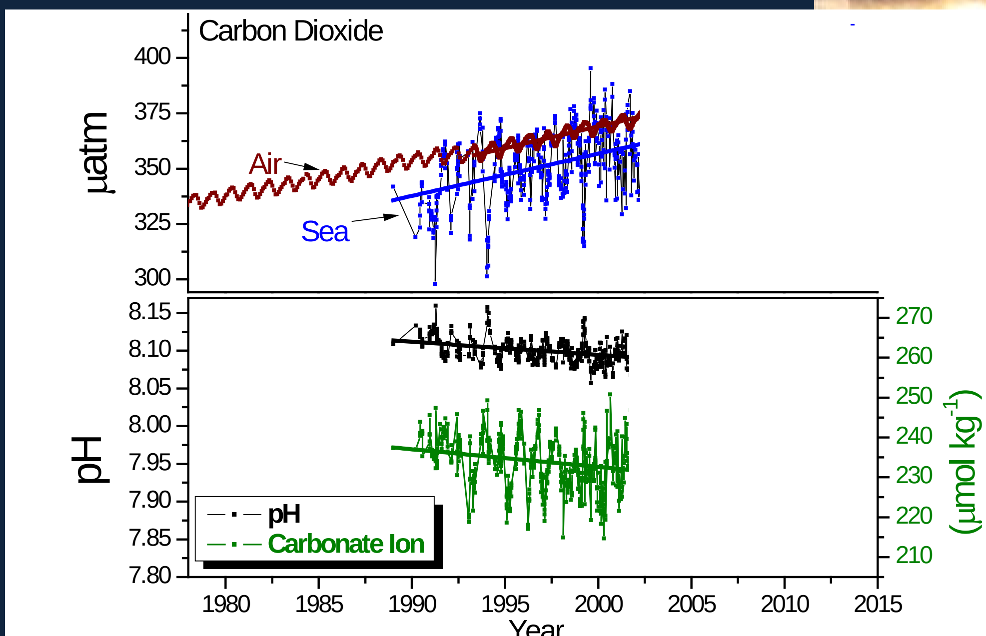

Hawaii Ocean Time-series (HOT)

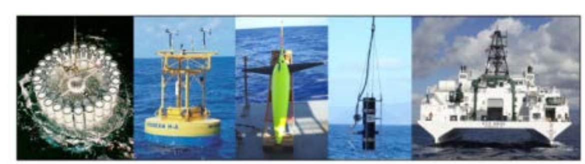

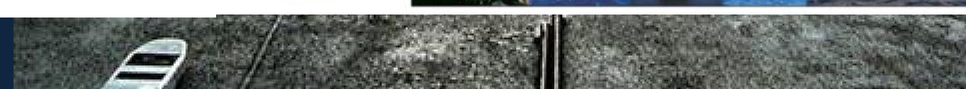

How significant are these changes?

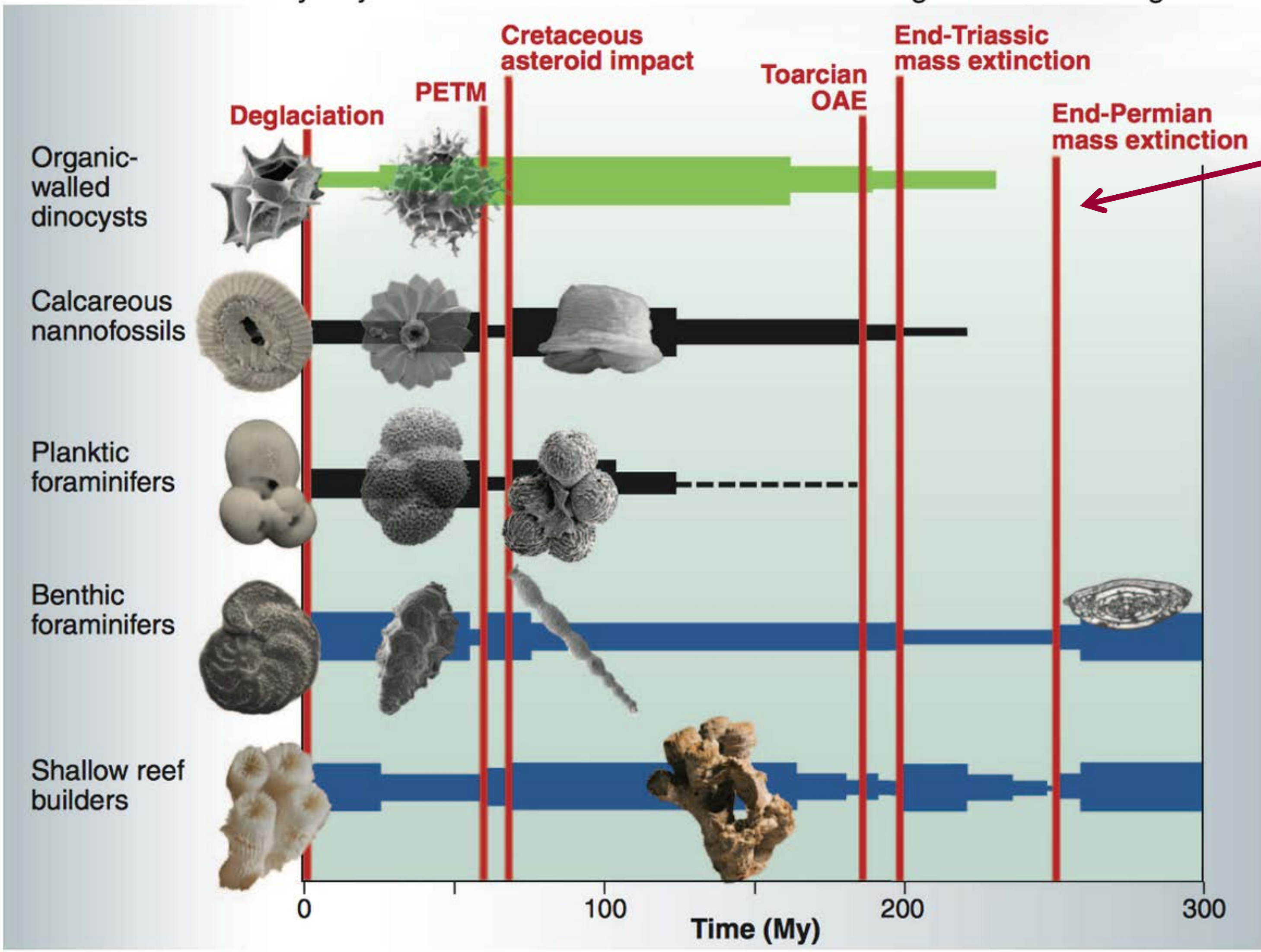

Source: Honisch et al 2012

2.4 PgC/year

Clarkson et al., 2015

Current fossil fuel emission rates
8.3 PgC/year

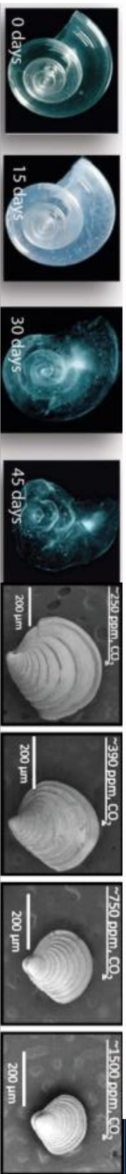

Federal Ocean Acidification Research and Monitoring (FOARAM) Act of 2009

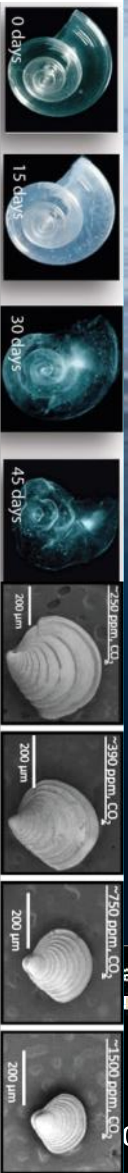

The **NOAA Ocean Acidification Program** (OAP) was established under SEC. 12406. of the Federal Ocean Acidification and Monitoring Act (FOARAM) to oversee and coordinate research, monitoring, and other activities consistent with the strategic research and implementation plan developed by the interagency working group on ocean acidification.

The program is to foster and direct …the establishment of a **long-term monitoring program of ocean acidification** utilizing existing global and national ocean observing assets, and adding instrumentation and sampling stations as appropriate to the aims of the research program…

agency Working
ip on Ocean Acidification

oceanacidification.noaa.gov/IWGOA.aspx

Species Response to Ocean Acidification

Ocean Acidification v2.0

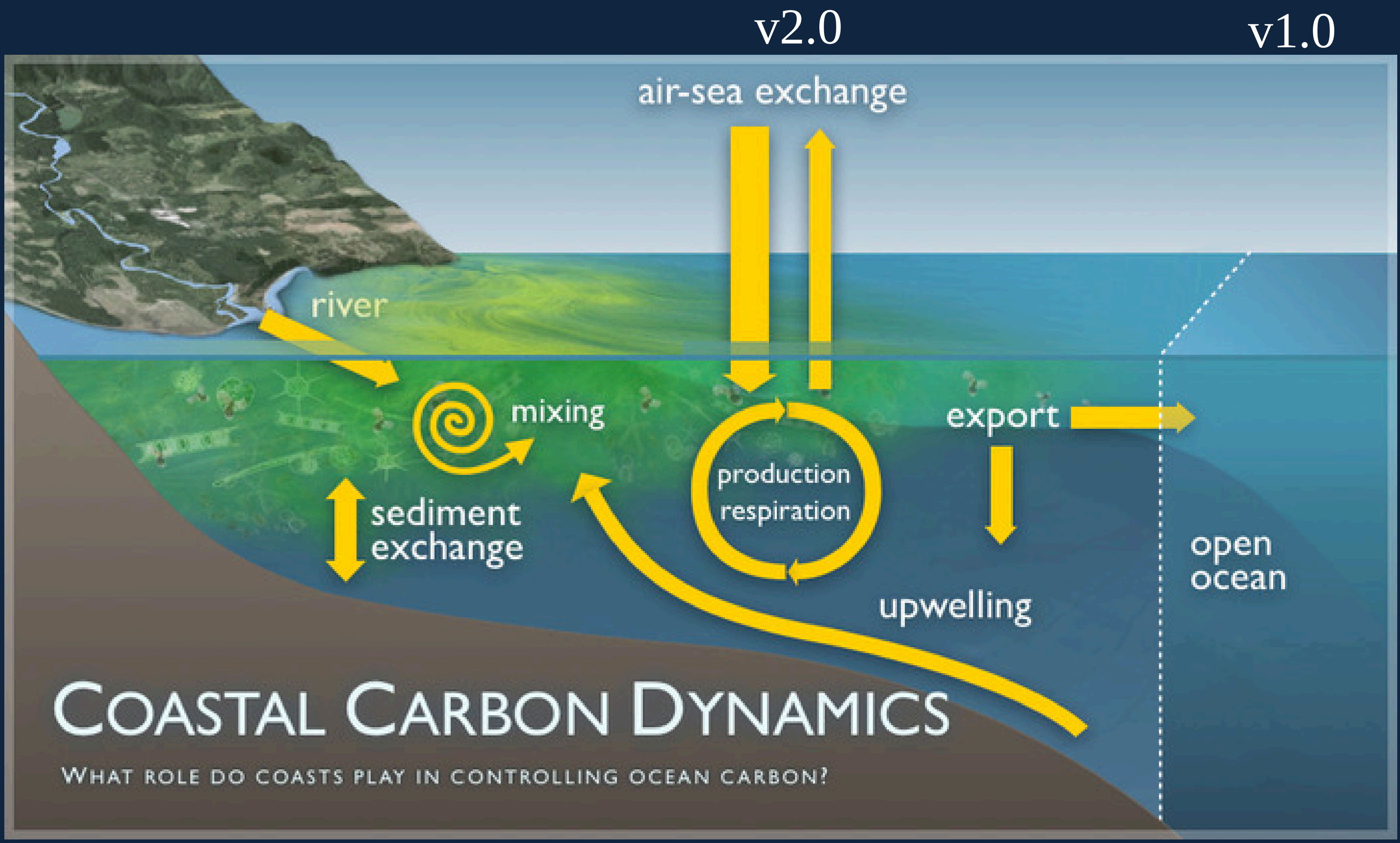

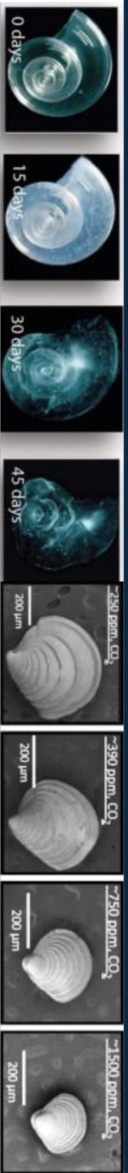

Ocean Acidification v2.0

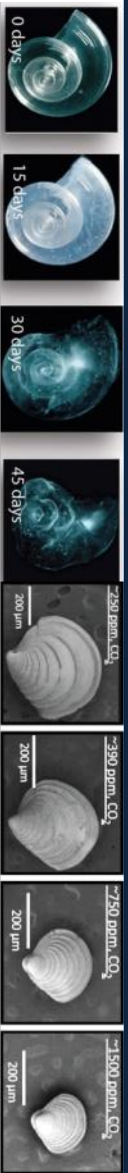

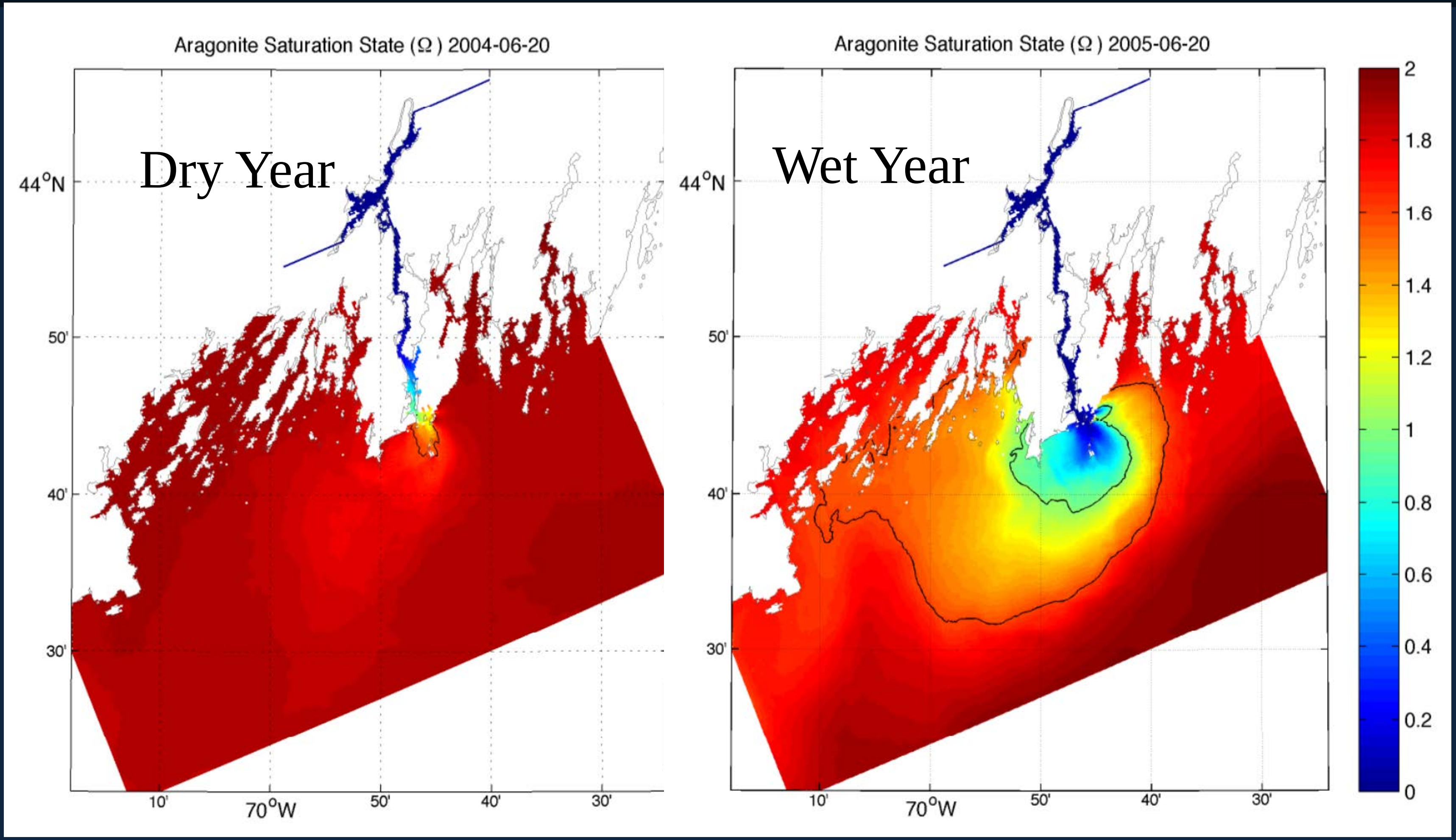

Corrosive plume off Casco Bay, Maine:

Salisbury et al., UHN

NOAA Ocean Acidification Monitoring

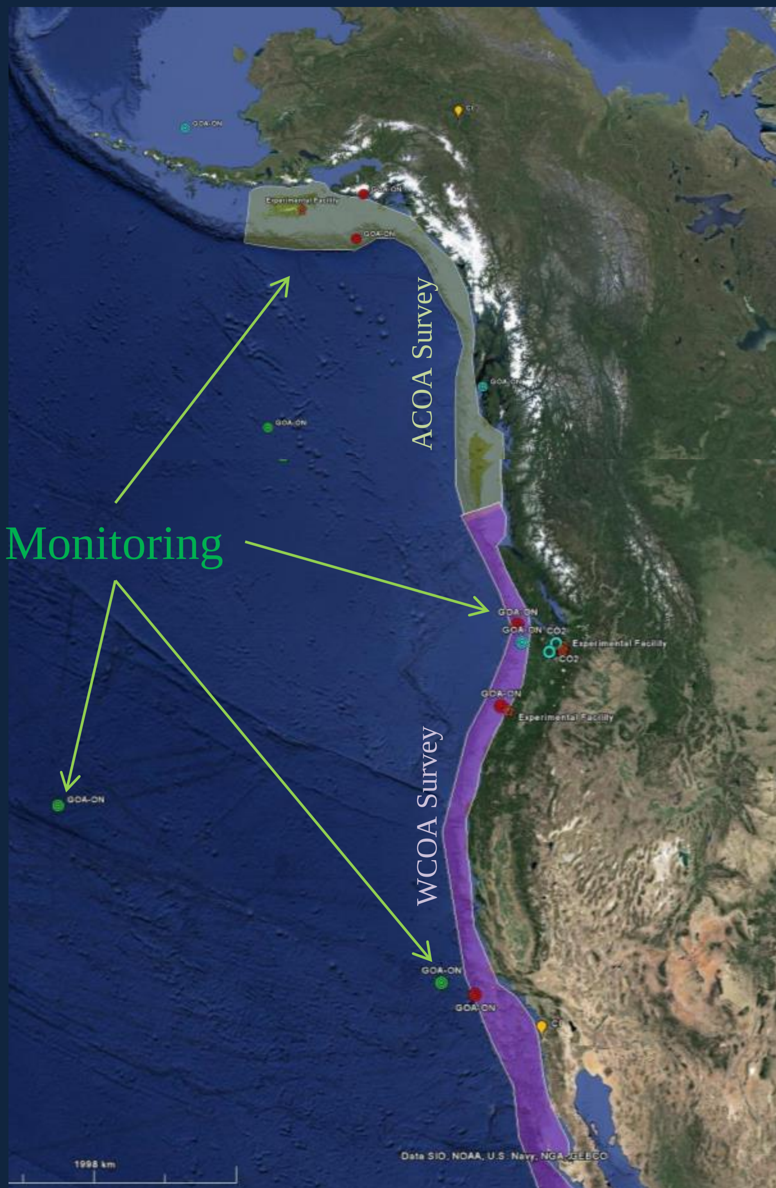

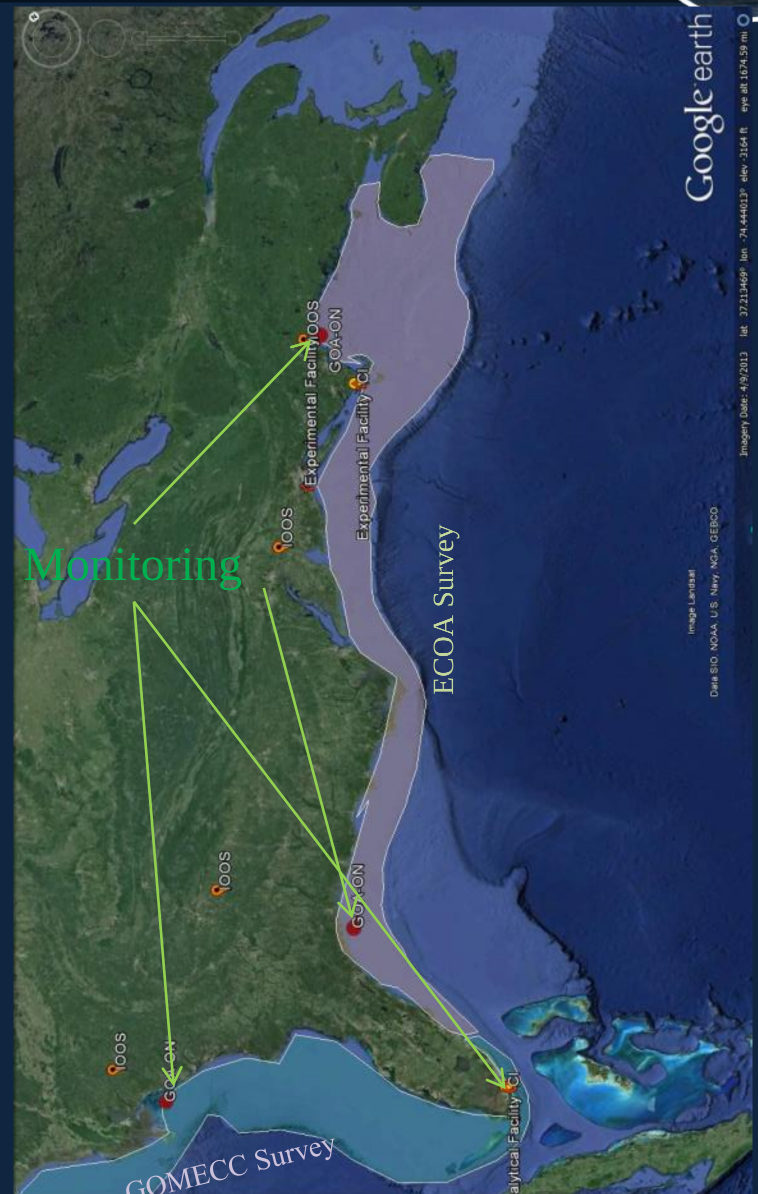

Remotely Sensing Ocean Acidification

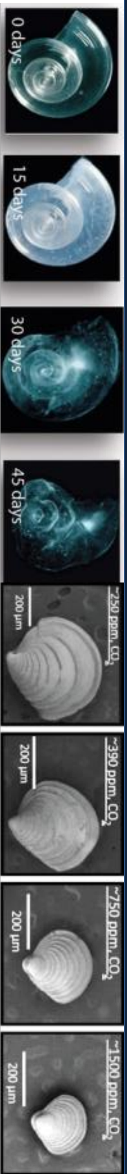

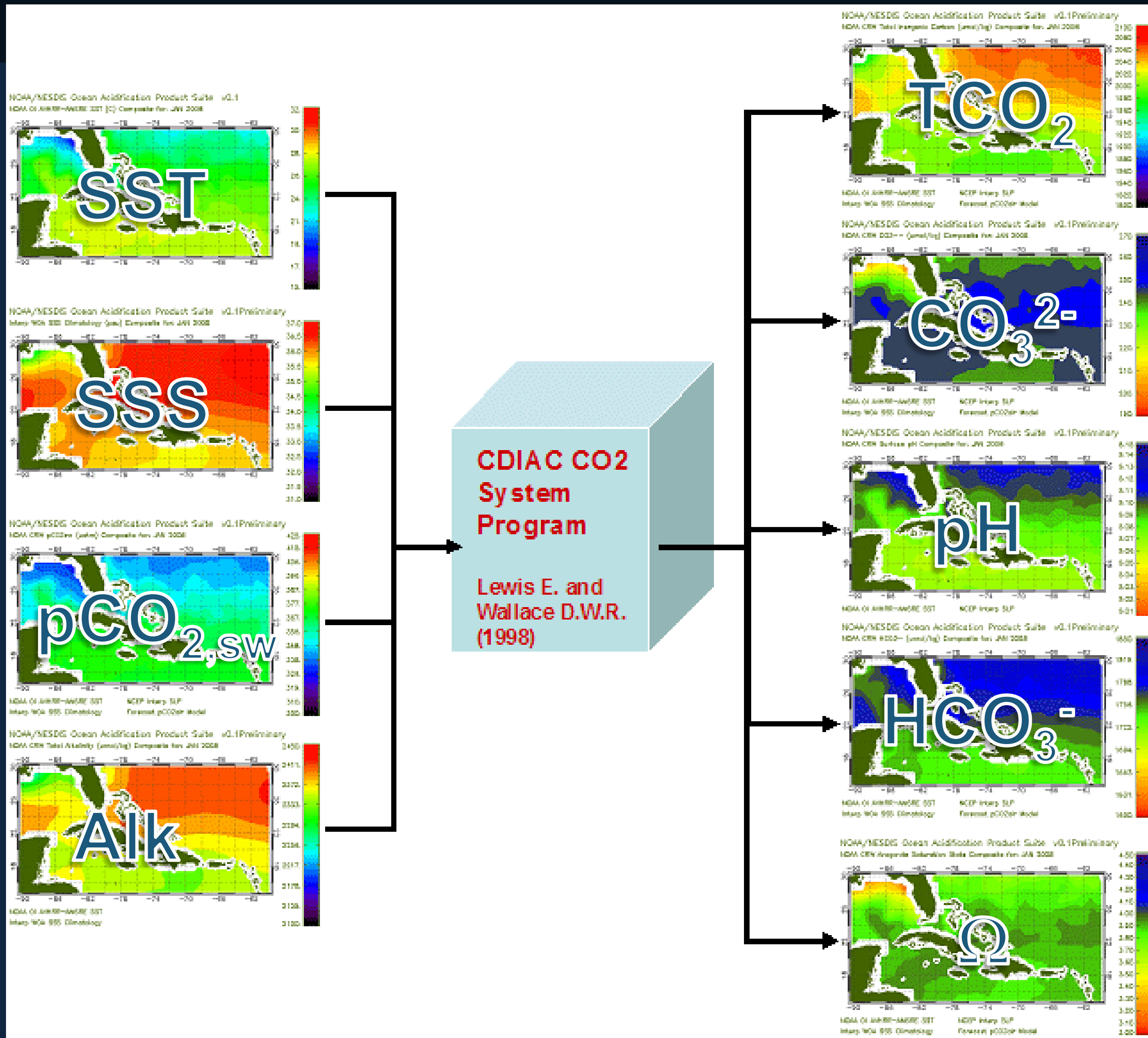

Remotely Sensing Ocean Acidification

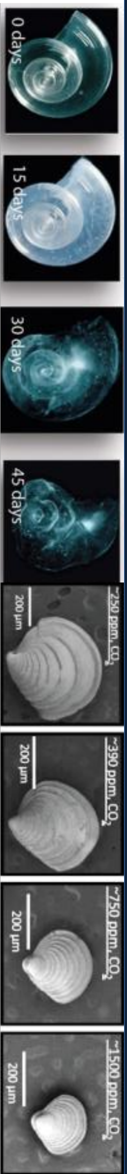

$$A_T = a + b(SSS - 35) + c(SSS - 35)^2 + d(SST - 20) + e(SST - 20)^2$$

Lee, K., L. T. Tong, et al. (2006). "Global relationships of total alkalinity with salinity and temperature in surface waters of the world's oceans." Geophysical Research Letters **33**.

$$pCO_{2,sw} = y_0 + A\,e^{(-K_0/B)} + pCO_{2,air}$$

Gledhill, D, R. Wanninkhof, et al. (2008). "Ocean Acidification of the Greater Caribbean 1996-2008." JGR **113**.

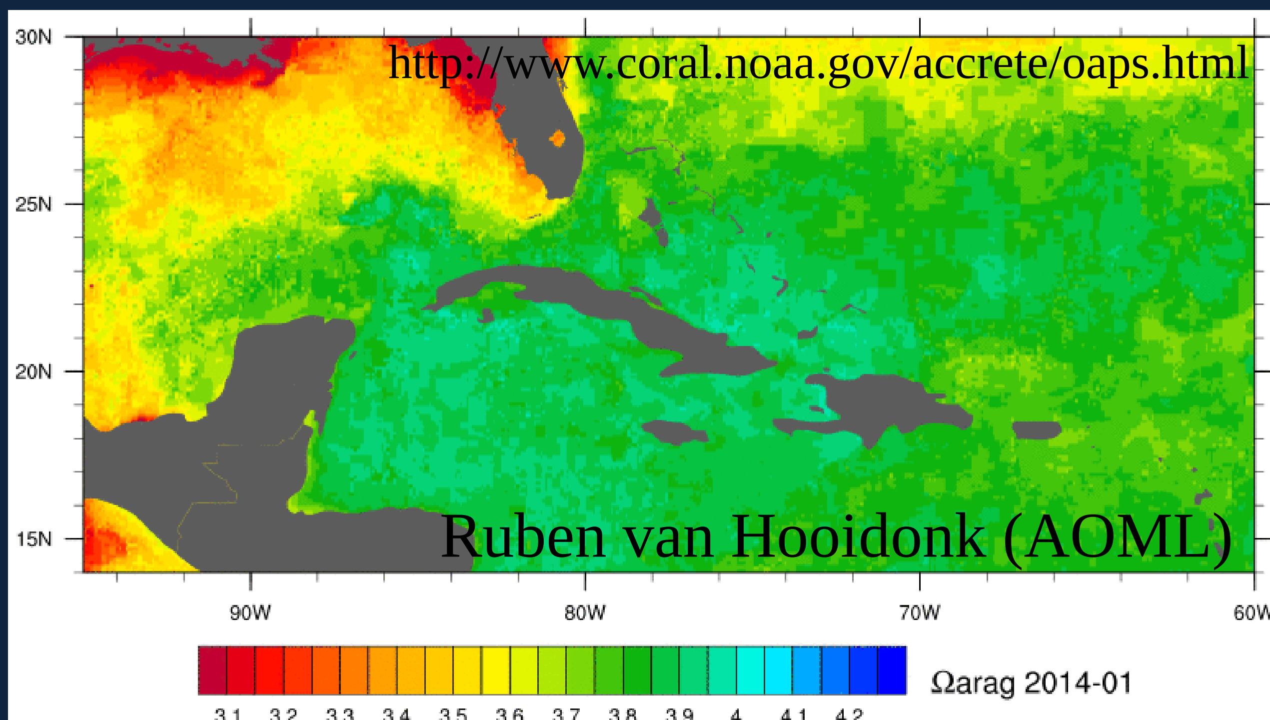

Remotely Sensing Ocean Acidification

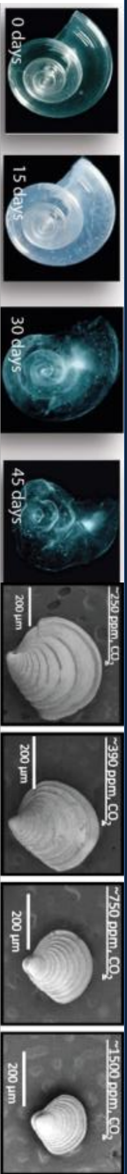

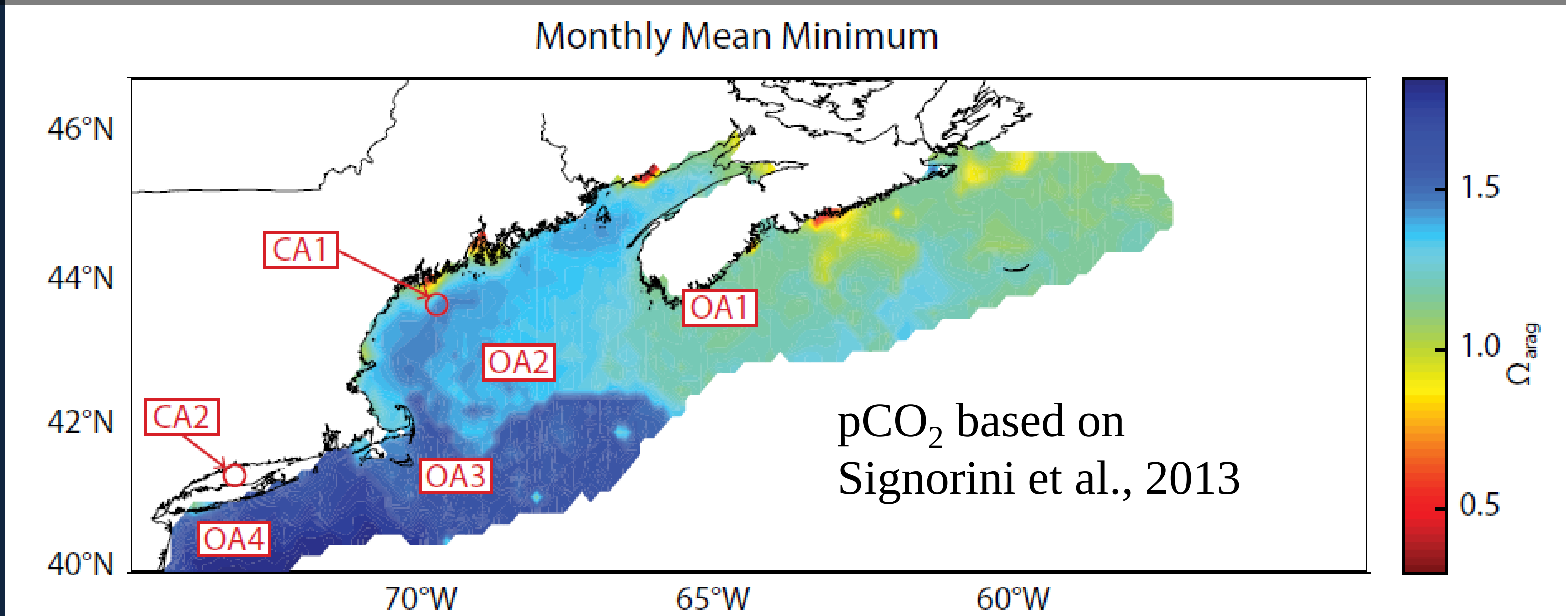

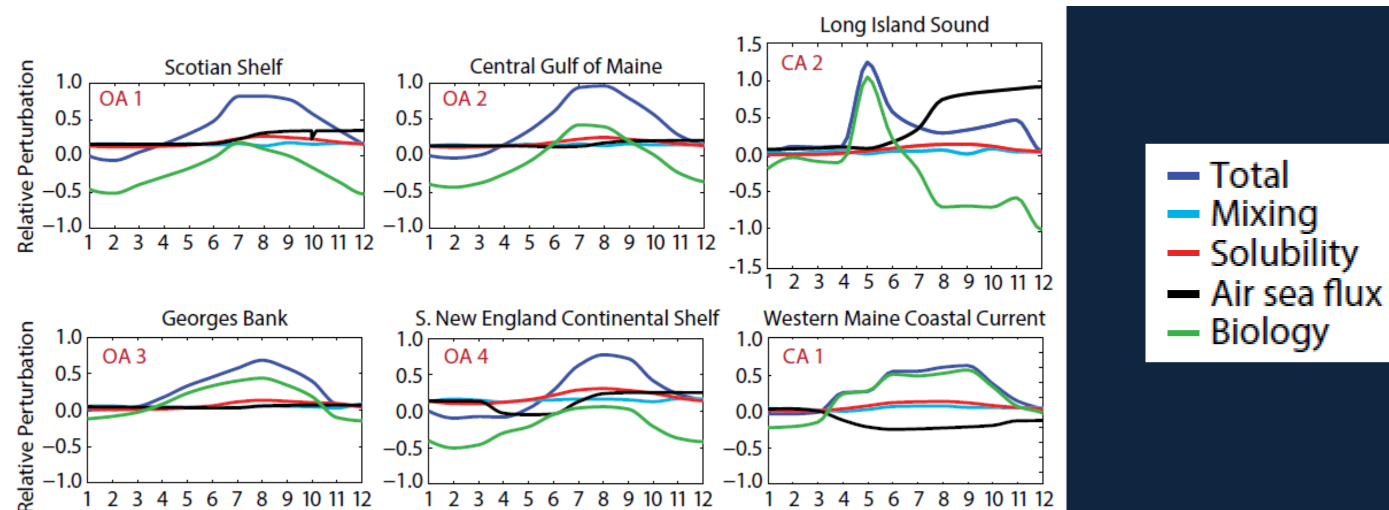

Gledhill et al., 2015. Ocean and Coastal Acidification off New England and Nova Scotia. *Oceanography* 28(2):182-197,http://dx.doi.org/10.5670/oceanog.2015.41.

Sea Surface Temperature Application to OA

Application: temperature, solubility of carbon dioxide, mineral solubility

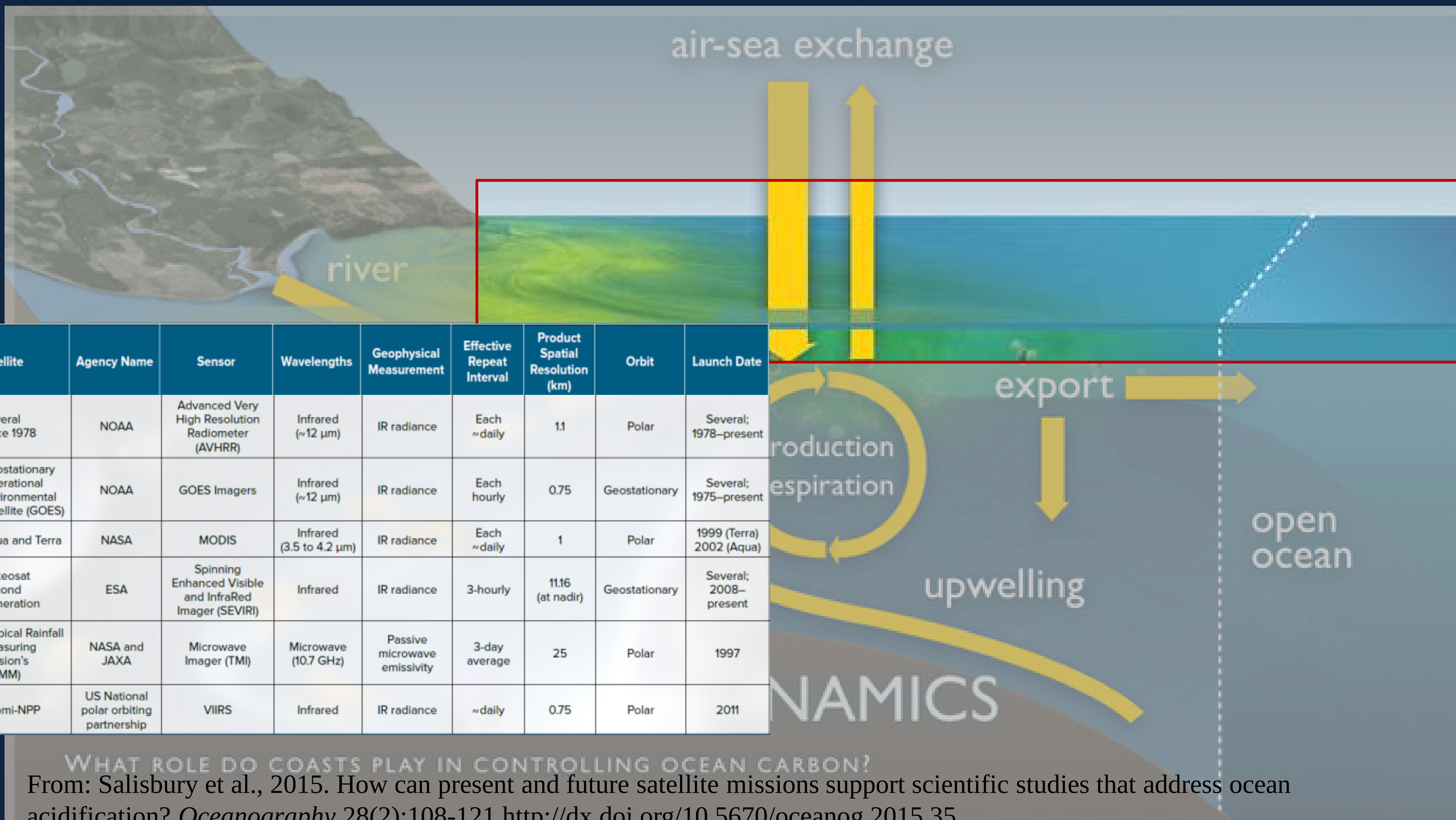

Satellite	Agency Name	Sensor	Wavelengths	Geophysical Measurement	Effective Repeat Interval	Product Spatial Resolution (km)	Orbit	Launch Date
Several since 1978	NOAA	Advanced Very High Resolution Radiometer (AVHRR)	Infrared (~12 µm)	IR radiance	Each ~daily	1.1	Polar	Several; 1978–present
Geostationary Operational Environmental Satellite (GOES)	NOAA	GOES Imagers	Infrared (~12 µm)	IR radiance	Each hourly	0.75	Geostationary	Several; 1975–present
Aqua and Terra	NASA	MODIS	Infrared (3.5 to 4.2 µm)	IR radiance	Each ~daily	1	Polar	1999 (Terra) 2002 (Aqua)
Meteosat Second Generation	ESA	Spinning Enhanced Visible and InfraRed Imager (SEVIRI)	Infrared	IR radiance	3-hourly	11.16 (at nadir)	Geostationary	Several; 2008–present
Tropical Rainfall Measuring Mission's (TRMM)	NASA and JAXA	Microwave Imager (TMI)	Microwave (10.7 GHz)	Passive microwave emissivity	3-day average	25	Polar	1997
Suomi-NPP	US National polar orbiting partnership	VIIRS	Infrared	IR radiance	~daily	0.75	Polar	2011

From: Salisbury et al., 2015. How can present and future satellite missions support scientific studies that address ocean acidification? *Oceanography* 28(2):108-121,http://dx.doi.org/10.5670/oceanog.2015.35.

Salinity Sensors Application to OA

Application: salinity, total alkalinity, solubility of carbon dioxide, mineral solubility, mixing

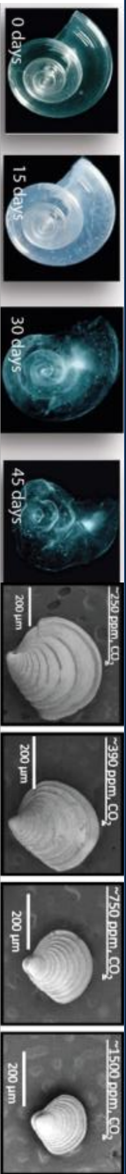

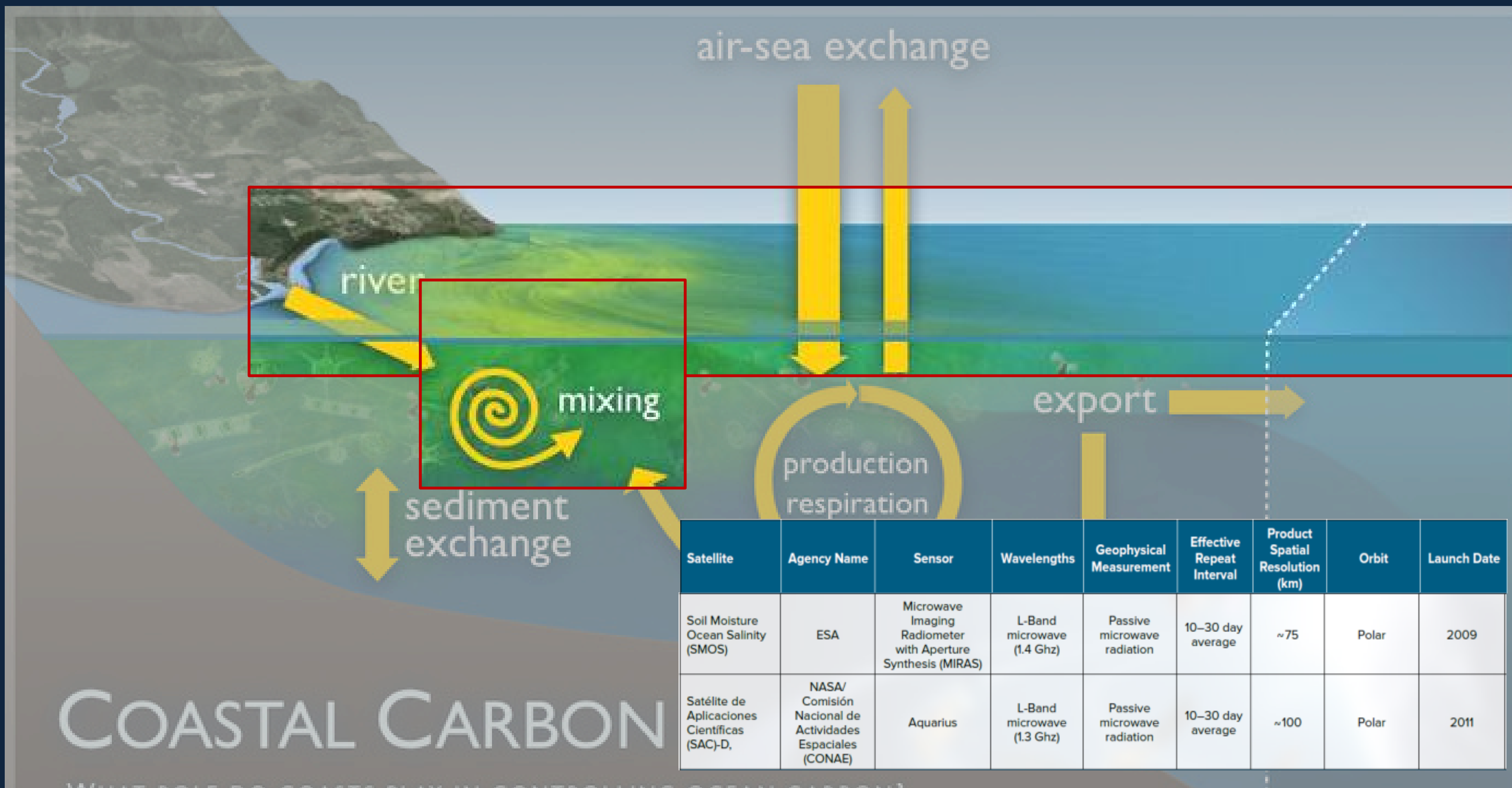

Satellite	Agency Name	Sensor	Wavelengths	Geophysical Measurement	Effective Repeat Interval	Product Spatial Resolution (km)	Orbit	Launch Date
Soil Moisture Ocean Salinity (SMOS)	ESA	Microwave Imaging Radiometer with Aperture Synthesis (MIRAS)	L-Band microwave (1.4 Ghz)	Passive microwave radiation	10–30 day average	~75	Polar	2009
Satélite de Aplicaciones Científicas (SAC)-D,	NASA/ Comisión Nacional de Actividades Espaciales (CONAE)	Aquarius	L-Band microwave (1.3 Ghz)	Passive microwave radiation	10–30 day average	~100	Polar	2011

From: Salisbury et al., 2015. How can present and future satellite missions support scientific studies that address ocean acidification? *Oceanography* 28(2):108-121,http://dx.doi.org/10.5670/oceanog.2015.35.

Atmospheric CO_2 Application to OA

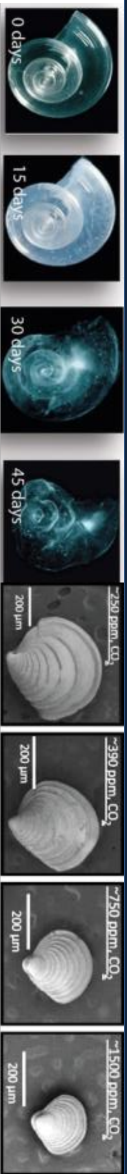

Application: air-sea gas disequilibrium, secular changes in OA

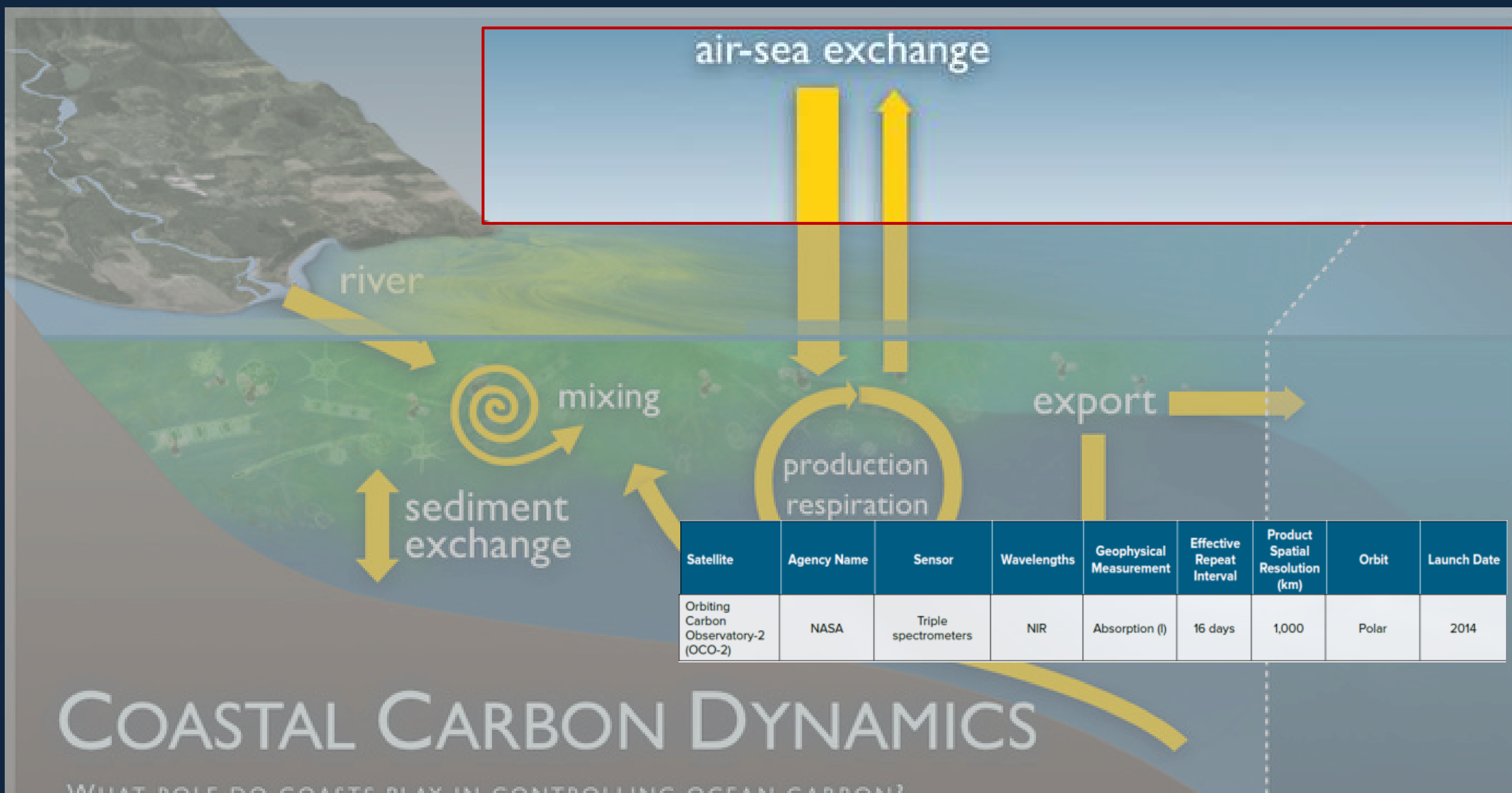

Satellite	Agency Name	Sensor	Wavelengths	Geophysical Measurement	Effective Repeat Interval	Product Spatial Resolution (km)	Orbit	Launch Date
Orbiting Carbon Observatory-2 (OCO-2)	NASA	Triple spectrometers	NIR	Absorption (l)	16 days	1,000	Polar	2014

From: Salisbury et al., 2015. How can present and future satellite missions support scientific studies that address ocean acidification? *Oceanography* 28(2):108-121,http://dx.doi.org/10.5670/oceanog.2015.35.

Scatterometretrs/Radiometers Application to OA

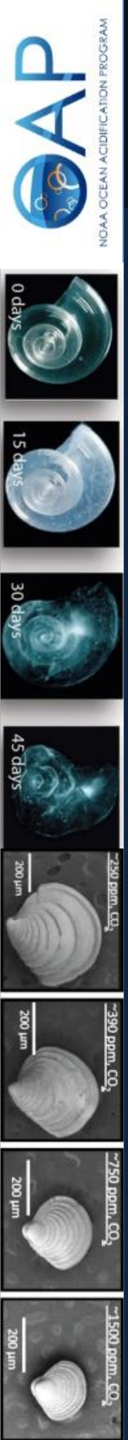

Application: air-sea gas exchange

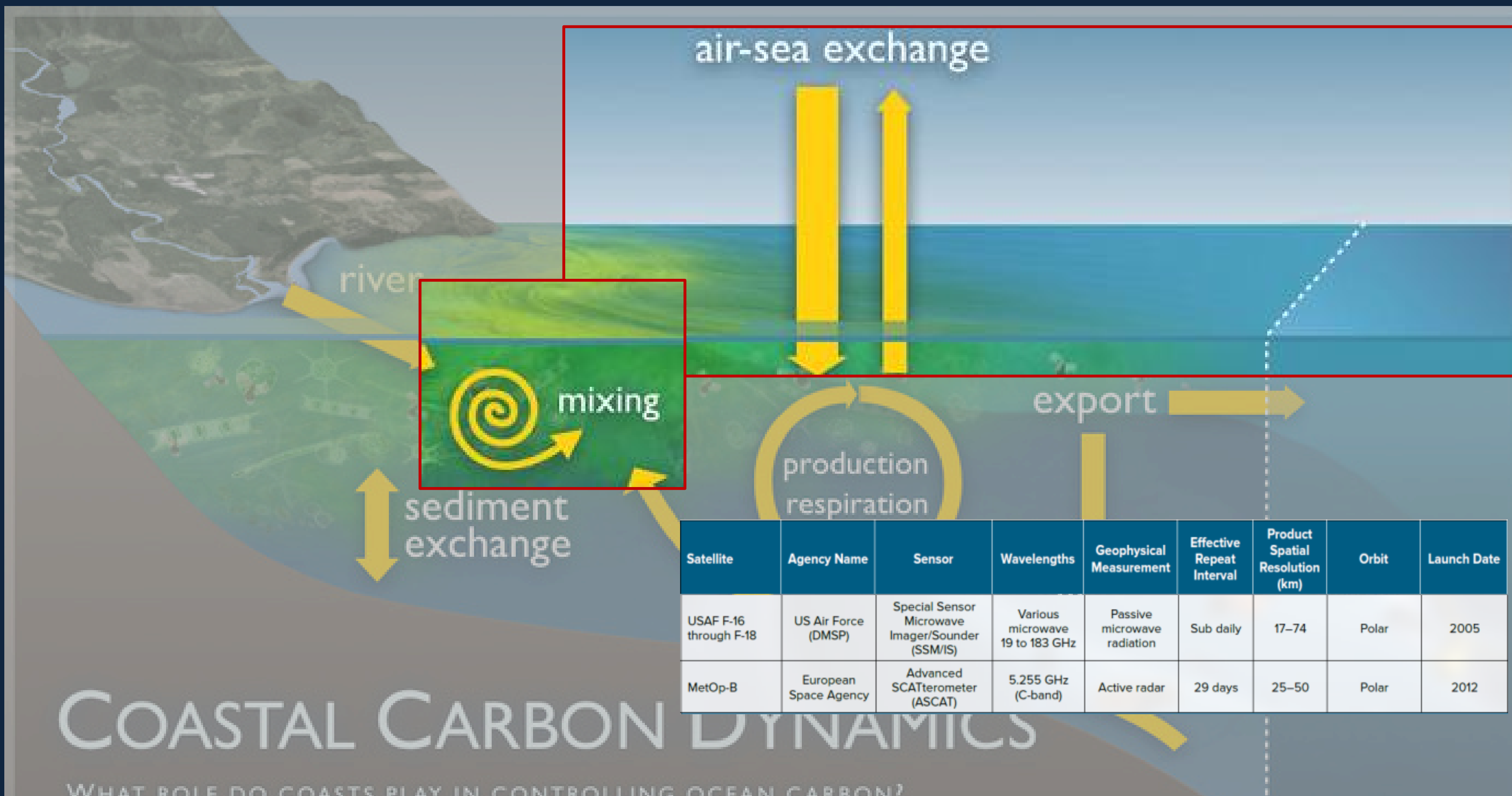

Satellite	Agency Name	Sensor	Wavelengths	Geophysical Measurement	Effective Repeat Interval	Product Spatial Resolution (km)	Orbit	Launch Date
USAF F-16 through F-18	US Air Force (DMSP)	Special Sensor Microwave Imager/Sounder (SSM/IS)	Various microwave 19 to 183 GHz	Passive microwave radiation	Sub daily	17–74	Polar	2005
MetOp-B	European Space Agency	Advanced SCATterometer (ASCAT)	5.255 GHz (C-band)	Active radar	29 days	25–50	Polar	2012

From: Salisbury et al., 2015. How can present and future satellite missions support scientific studies that address ocean acidification? *Oceanography* 28(2):108-121,http://dx.doi.org/10.5670/oceanog.2015.35.

Satellite Ocean Color Application to OA

Application: chlorophyll, particulate & dissolved colored carbon, particulate inorganic carbon, primary & net community productivity, classification

Satellite	Agency Name	Sensor	Wavelengths	Geophysical Measurement	Effective Repeat Interval	Product Spatial Resolution (km)	Orbit	Launch Date
Aqua and Terra	NASA	Moderate Resolution Imaging Spectroradiometer (MODIS)	Visible – near infrared	Water leaving radiance (λ)	~daily	0.25, 0.50, and 1.00	Polar	1999 (Terra) 2002 (Aqua)
Suomi-NPP	US National polar orbiting partnership	Visible Infrared Imaging Radiometer Suite (VIIRS)	Visible – near infrared	Water leaving radiance (λ)	~daily	0.75	Polar	2011
MERIS	European Space Agency	MEdium Resolution Imaging Spectrometer (MERIS)	Visible – near infrared	Water leaving radiance (λ)	~daily	0.3	Polar	2002
COMS	Korea Ocean Satellite Center	Geostationary Ocean Colour Imager (GOCI)	Visible – near infrared	Water leaving radiance (λ)	1 hour	0.5 (at nadir)	Geostationary	2009
OceanSat 2	Indian Space Research Organisation	Ocean Colour Monitor (OCM)	Visible – near infrared	Water leaving radiance (λ)	~daily	0.36	Polar	2009

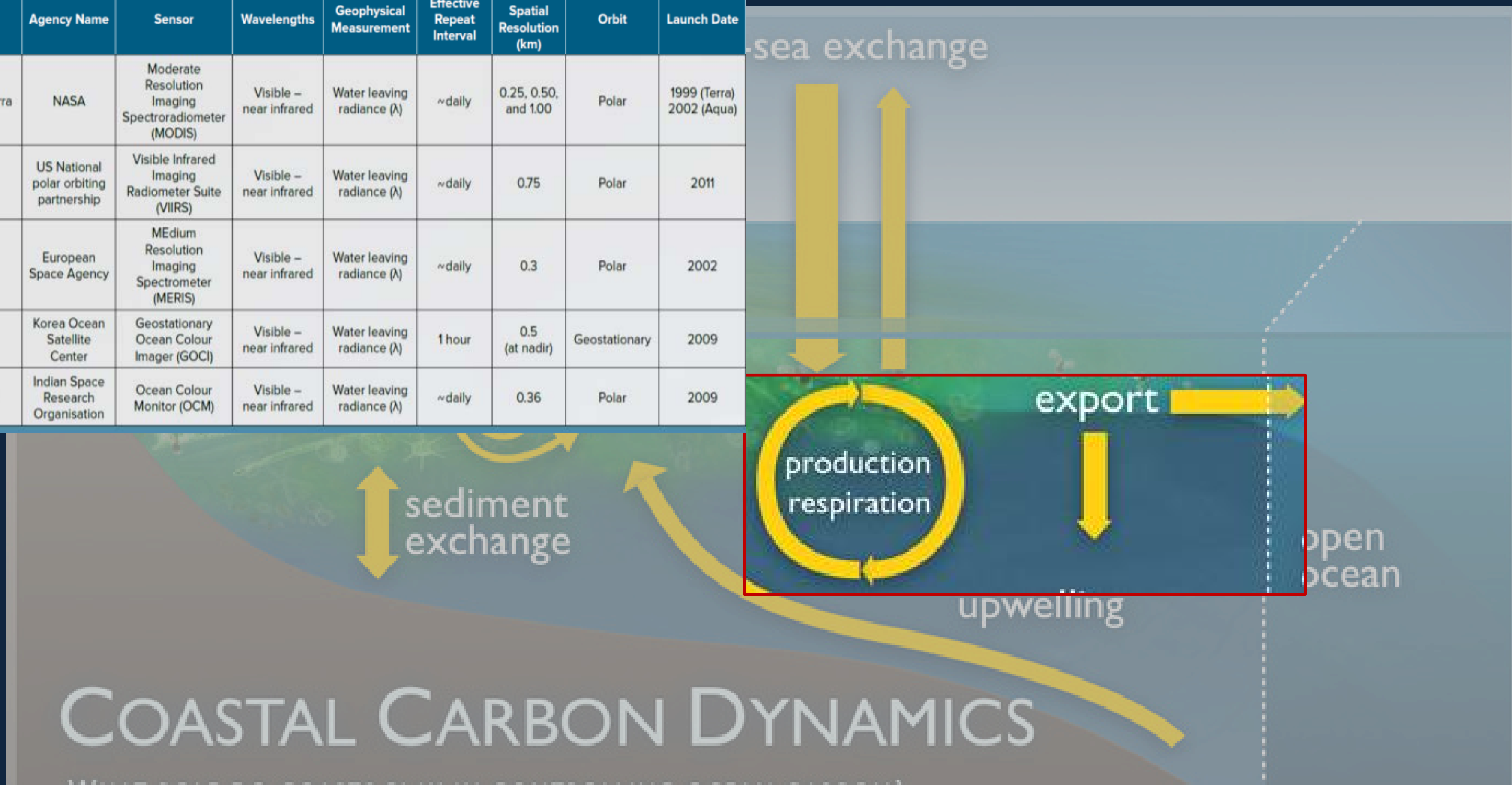

From: Salisbury et al., 2015. How can present and future satellite missions support scientific studies that address ocean acidification? *Oceanography* 28(2):108-121,http://dx.doi.org/10.5670/oceanog.2015.35.

Coastal Mapping Application to OA

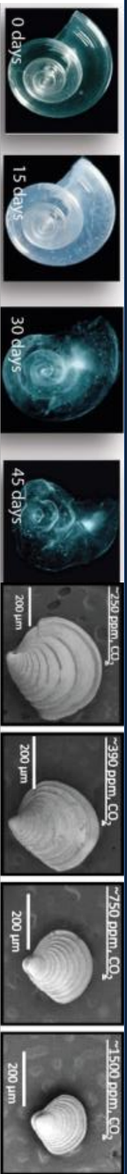

Application: coral reef area, coral reef health, shallow water resuspension, near coastal processes

Satellite	Agency Name	Sensor	Wavelengths	Geophysical Measurement	Effective Repeat Interval	Product Spatial Resolution (km)	Orbit	Launch Date	
Landsat-type; several since 1972	USGS	Operational Land Imager (OLI) on Landsat 8 is the latest	Visible – near infrared	Earth and water leaving radiance (l)		0.03	Polar	Several since 1972	Two presently commissioned
MERIS	European Space Agency	Medium Resolution Imaging Spectrometer	Visible – near infrared	Water leaving radiance (l)	~daily	0.3	Polar	2002	0.25 km product may be suitable for mapping
Aqua and Terra	NASA	MODIS	Visible – near infrared	Water leaving radiance (l)	~daily	0.25, 0.50, and 1.00	Polar	1999 (Terra) 2002 (Aqua)	0.30 km product may be suitable for mapping
Satellite Pour l'Observation de la Terre (SPOT)	CNES (Centre national d'études spatiales)	Spot XS	Visible – near infrared	Earth and water leaving radiance (l)	5–25 days	0.02	Polar	Several since 1986	
Quick Bird 2	Digital Globe (Commercial)	Digital Globe Constellation	1 visible, 1 near infrared	Earth and water leaving radiance (l)	3 days	0.005	Polar	2001	
RapidEye Earth Imaging System (REIS)	RapidEye (Commercial)	RapidEye Constellation	2 visible, 1 near infrared	Earth and water leaving radiance (l)	Several days	~0.010	Polar	2008	

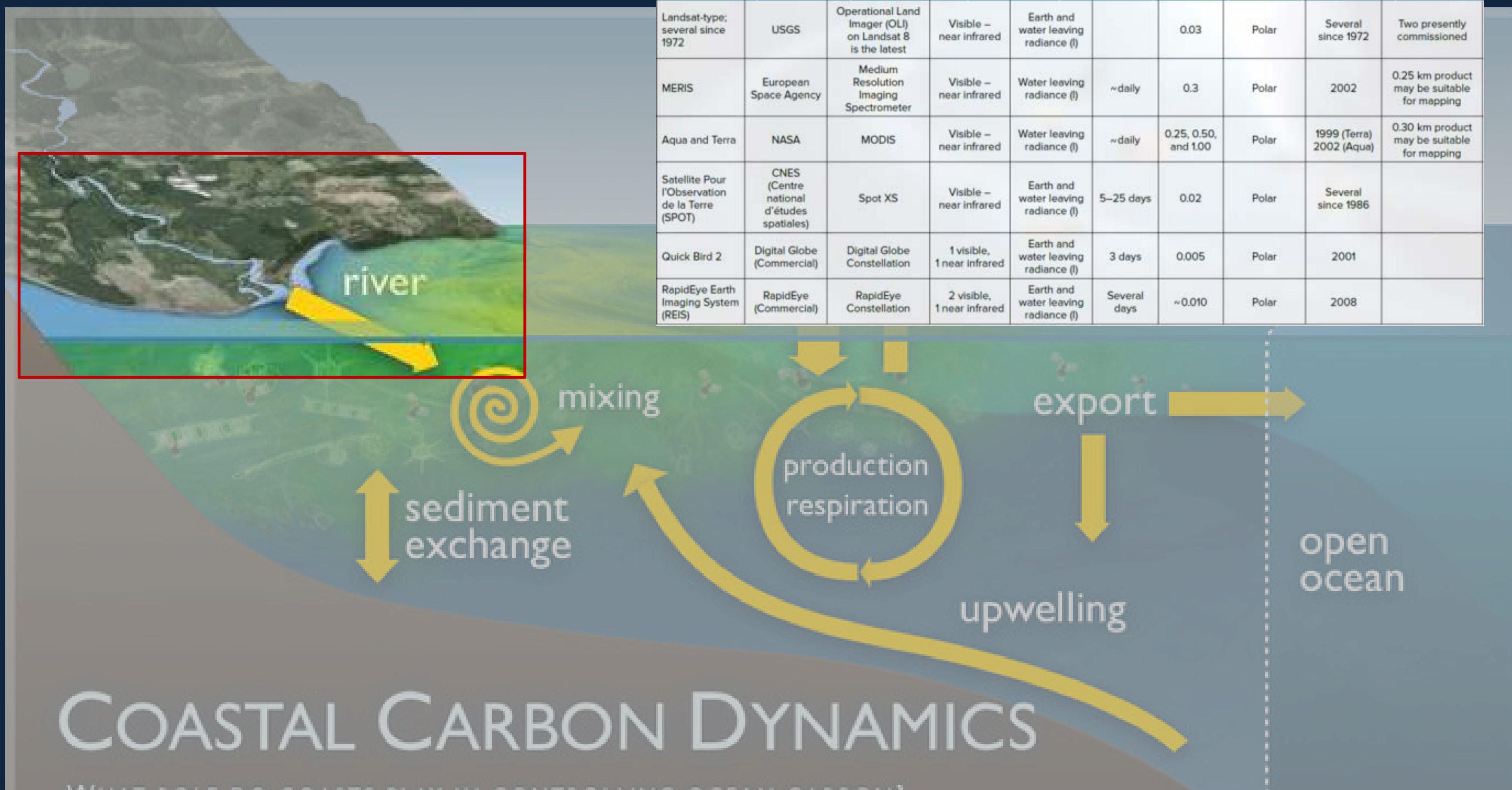

From: Salisbury et al., 2015. How can present and future satellite missions support scientific studies that address ocean acidification? *Oceanography* 28(2):108-121,http://dx.doi.org/10.5670/oceanog.2015.35.

Soil Moisture/Water Budgets Application to OA

Application: water cycle studies, freshwater flux to the ocean

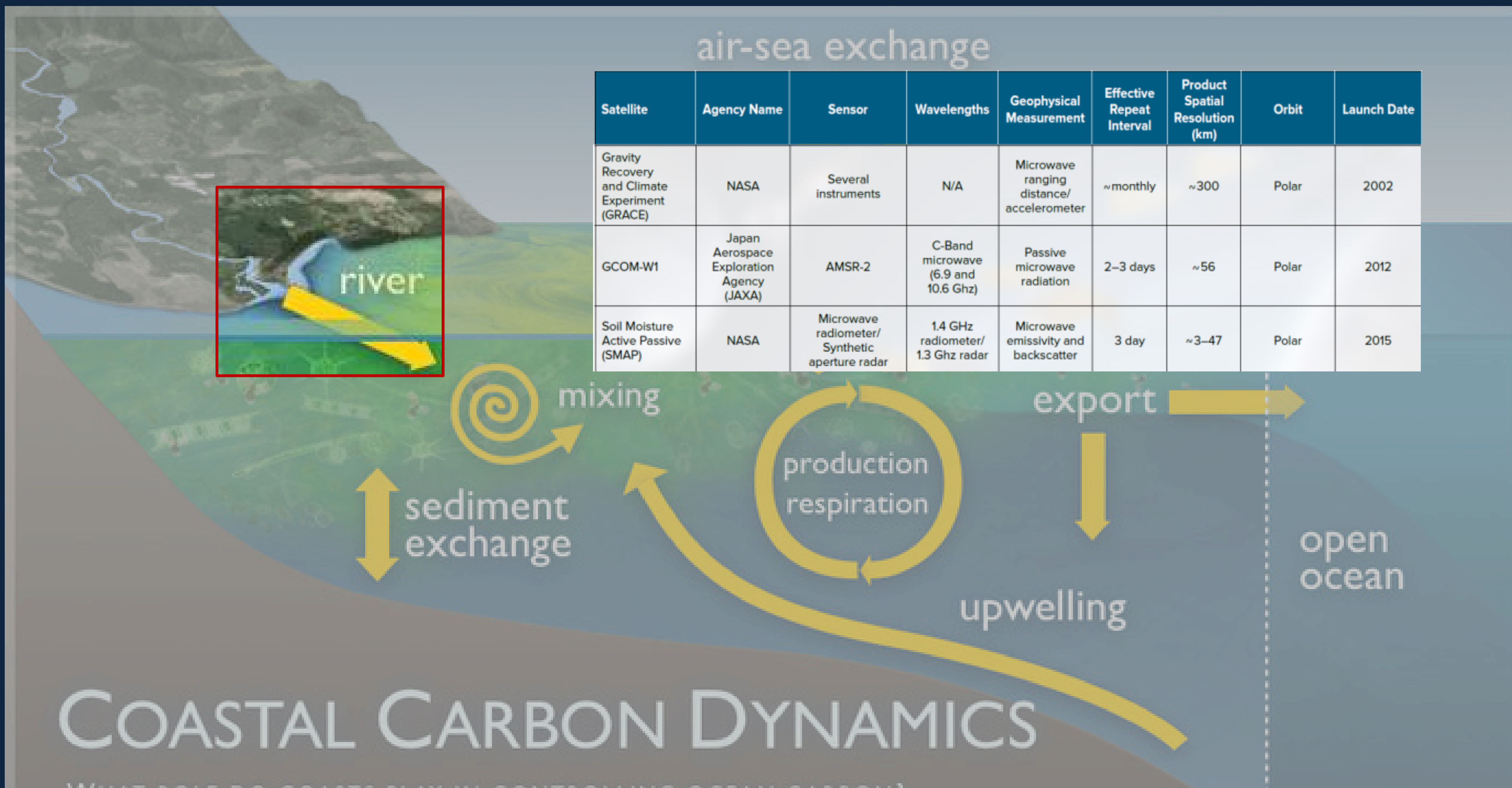

Satellite	Agency Name	Sensor	Wavelengths	Geophysical Measurement	Effective Repeat Interval	Product Spatial Resolution (km)	Orbit	Launch Date
Gravity Recovery and Climate Experiment (GRACE)	NASA	Several instruments	N/A	Microwave ranging distance/ accelerometer	~monthly	~300	Polar	2002
GCOM-W1	Japan Aerospace Exploration Agency (JAXA)	AMSR-2	C-Band microwave (6.9 and 10.6 Ghz)	Passive microwave radiation	2–3 days	~56	Polar	2012
Soil Moisture Active Passive (SMAP)	NASA	Microwave radiometer/ Synthetic aperture radar	1.4 GHz radiometer/ 1.3 Ghz radar	Microwave emissivity and backscatter	3 day	~3–47	Polar	2015

From: Salisbury et al., 2015. How can present and future satellite missions support scientific studies that address ocean acidification? *Oceanography* 28(2):108-121,http://dx.doi.org/10.5670/oceanog.2015.35.

Altimetry Application to OA

Application: ocean currents, mixing

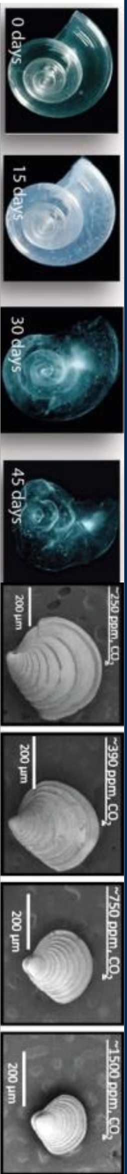

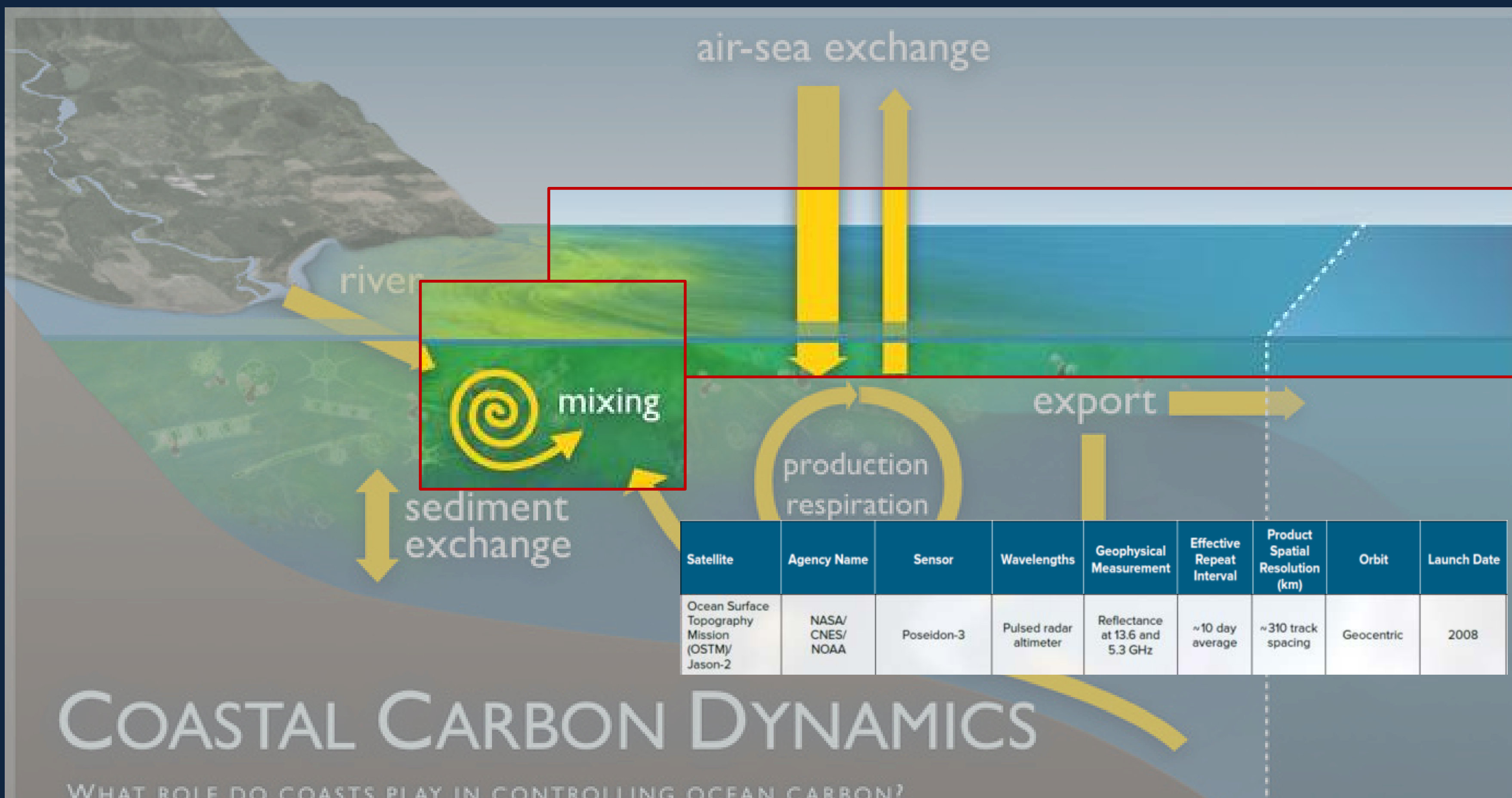

Satellite	Agency Name	Sensor	Wavelengths	Geophysical Measurement	Effective Repeat Interval	Product Spatial Resolution (km)	Orbit	Launch Date
Ocean Surface Topography Mission (OSTM)/ Jason-2	NASA/ CNES/ NOAA	Poseidon-3	Pulsed radar altimeter	Reflectance at 13.6 and 5.3 GHz	~10 day average	~310 track spacing	Geocentric	2008

From: Salisbury et al., 2015. How can present and future satellite missions support scientific studies that address ocean acidification? *Oceanography* 28(2):108-121,http://dx.doi.org/10.5670/oceanog.2015.35.

User Community and Stakeholders of OA Data

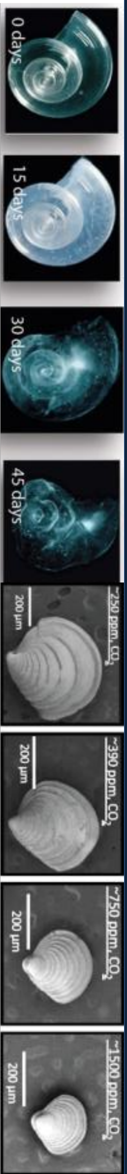

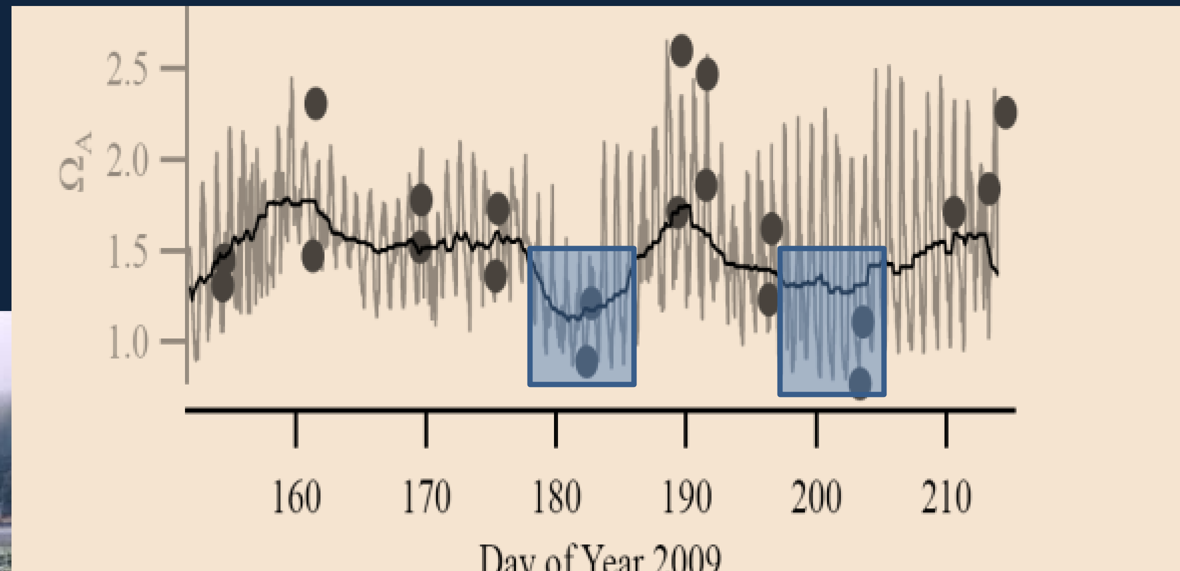

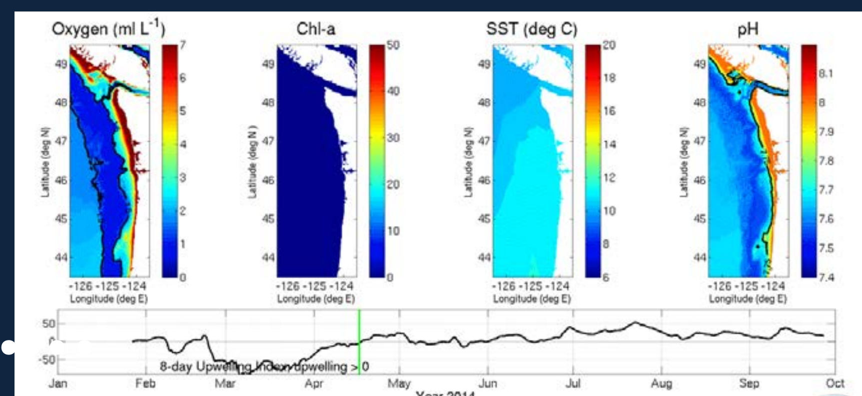

The J-SCOPE forecast system for Washington and Oregon coastal waters

User Community and Stakeholders of OA Data

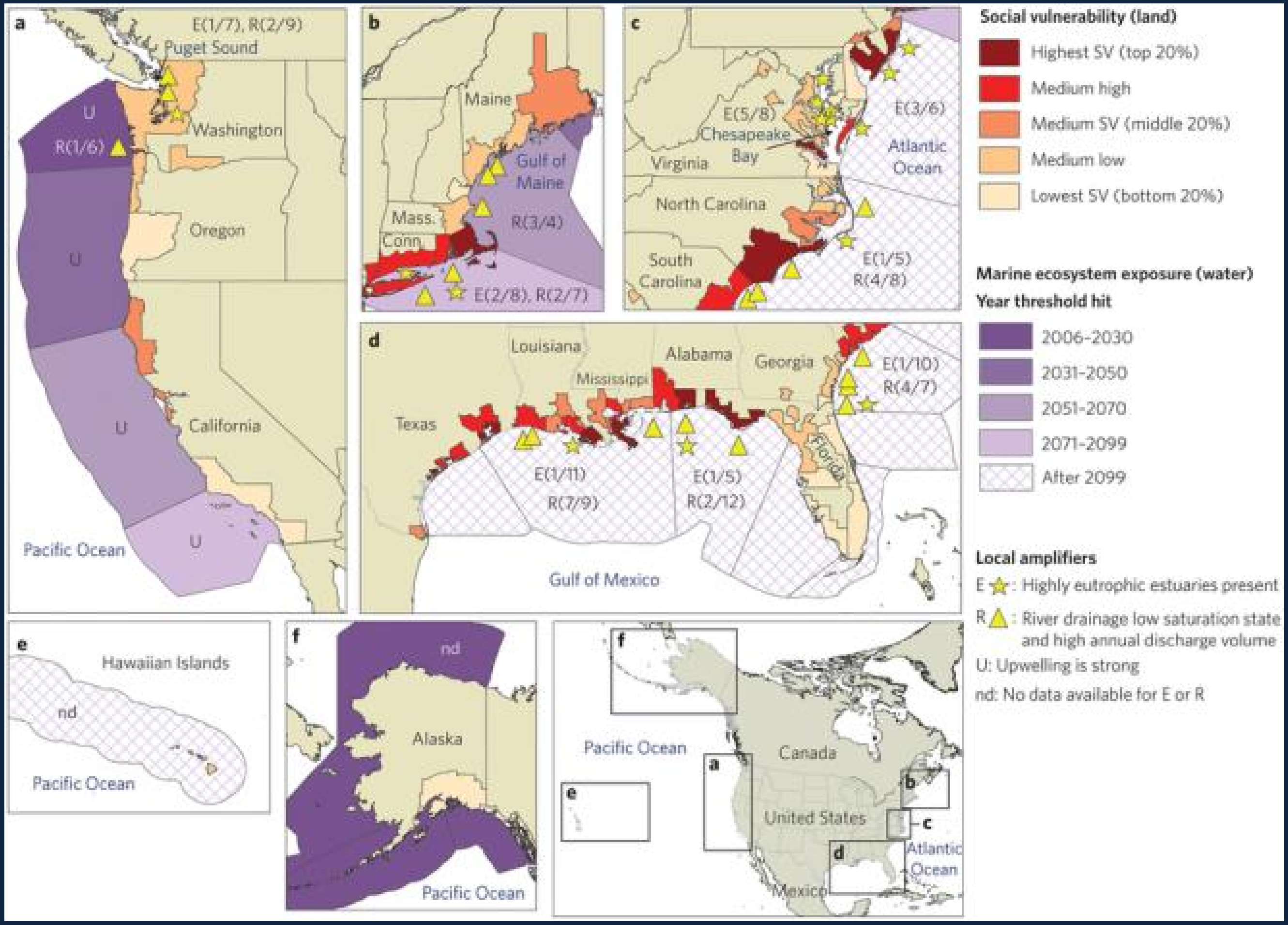

Vulnerability and adaptation of US shellfisheries to ocean acidification. Ekstrom et al., Nature Climate Change 5, 207–214 (2015) doi:10.1038/nclimate2508

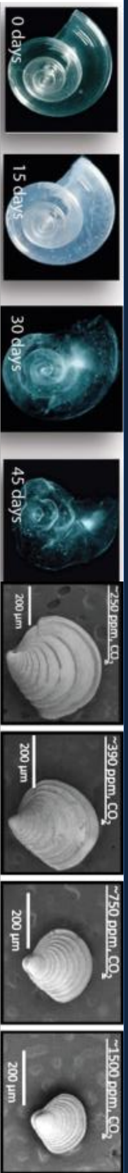

User Community and Stakeholders of OA Data

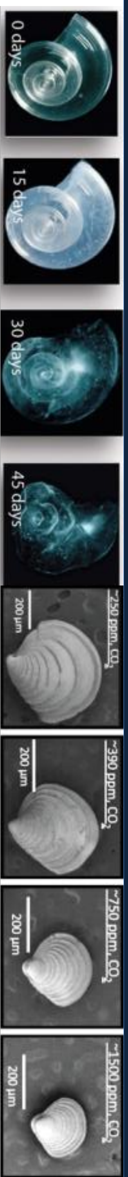

Applications, Tools, Products		
Name	Frequency	Users
LME 20xx Ecosystem Report Card	Annual	Alaska Fishery Management & Industries
Long-term bio-economic forecast	5-yr	Alaska Fishery Management & Industries
Regional Vulnerability Assessment	5-yr	Alaska Fishery Management & Industries
Regional OA Forecast & Scenario Projection	On-demand	New England and Mid-Atlantic Marine Fisheries Commission
Large Marine Ecosystem IEA	ND	Greater Atlantic Regional Fisheries Office
National Coral Reef Status & Trends Report Card	TBD	Regional Fishery Management Councils
Etc.		Coral Reef Management Community

Concluding Thoughts

- The vulnerability of society to the impacts of ocean acidification differs regionally due to local chemistry, biology, and economic dependence. This heterogeneity creates an opportunity for information product needs.
- Most of the user needs for OA data products emerge from the marine resource management and industry community in the form of synthesis assessments. Not necessarily nRT.
- Satellite Ocean Color products are particularly of aid in improving synoptic mapping of OA with the coastal domain where biological forcing imparts a first-order effect to carbonate system dynamics.
- Applications range from classification of water types for improved empirical relations to direct determination of relevant processes (e.g. NPP).
- Opportunities exist to further improve coastal/shelf algorithms by furthering joint OAR-NESDIS geochemical surveys (i.e. ECOA)

Thank you

http://oceanacidification.noaa.gov/

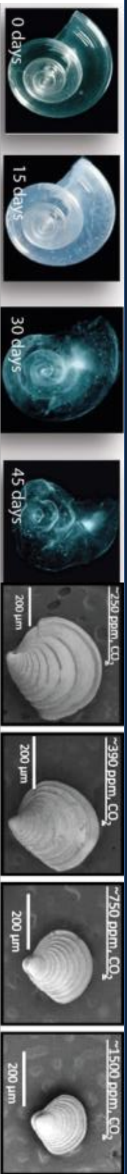

NOAA CoastWatch Ocean Color Data Dissemination

Paul M. DiGiacomo
NOAA/NESDIS/STAR
NOAA CoastWatch Program

STAR Center for Satellite Application and Research
National Environmental Satellite, Data, and Information Service (NESDIS)

NRT & Science Quality Data

Attribute	Near-Real Time	Delayed-Mode/Science-Quality
Latency:	Best effort, as soon as possible (~12-24h)	Best effort, ~1-2 weeks delay
Processing System:	MSL12	MSL12
SDR:	IDPS Operational SDR	OC-improved SDR
Ancillary Data:	Global Forecast System (GFS) Model	Science quality (assimilated; GDAS) from NCEP
Spatial Coverage:	May be gaps due to various issues	Complete global coverage
Processed by:	CoastWatch, transferring to OSPO (operational) FY16	NOAA/STAR
Disributed by:	CoastWatch	CoastWatch, NCEI
Archive Plans:	TBD (but not through STAR)	Yes, from CoastWatch to NCEI
Full Mission Reprocessing:	No	Yes, ~2-3 years or as needed

Suomi NPP VIIRS OC Data Products

- Near Real Time (Jan 21,2015 – Present; 2/2012 – Present in November)
    - Global
    - Regional

Suomi NPP VIIRS OC Data Products

- Near Real Time (Days 1-8)
  - Global
  - Regional

Available Now

- Science Quality (Days 8 – n)
  - Global
  - Regional
- Reprocessed (Mission)
  - Global

Available Early 2016

L3 Global 4km

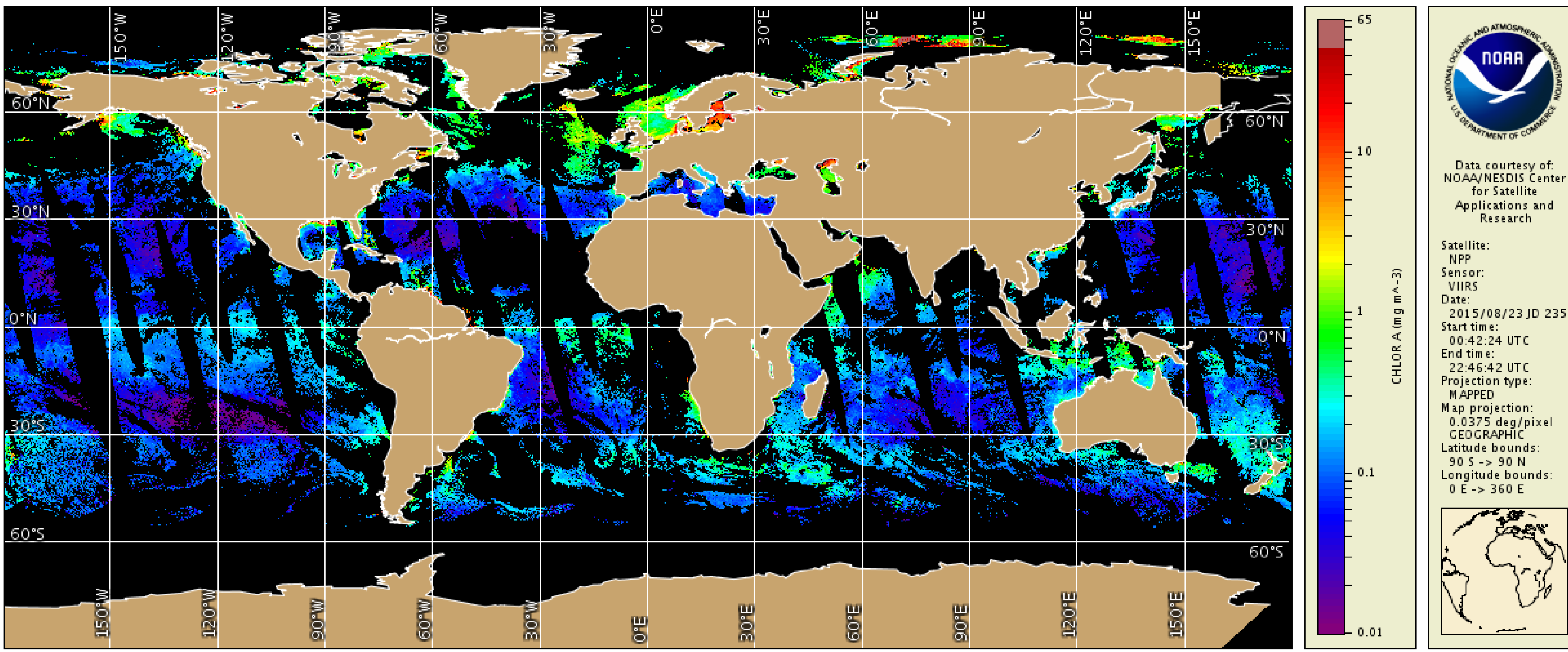

Daily Weekly Monthly

L3 Global 750m Sectors

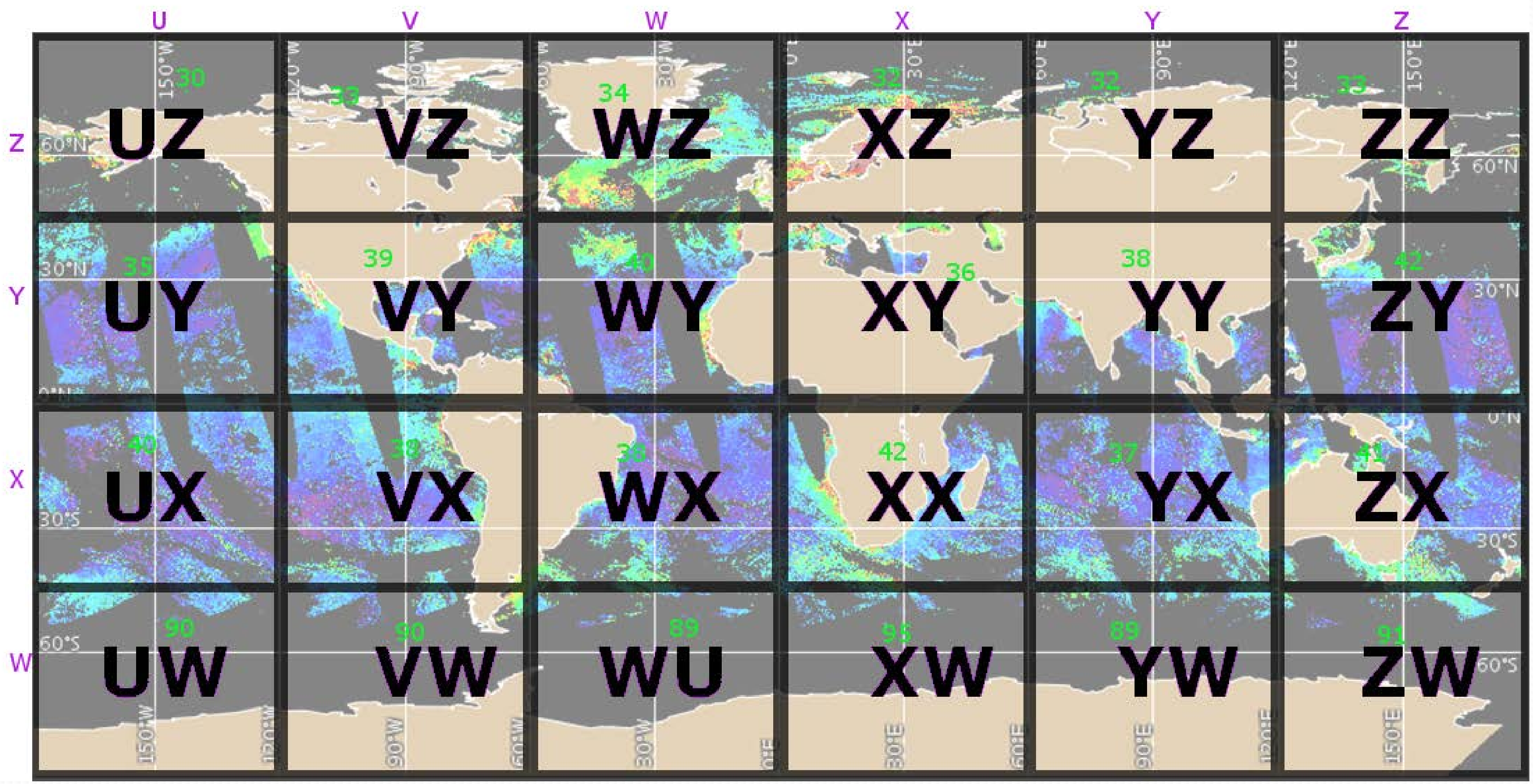

L3 Regional

- "CONUS" 750m regions: Hawaii, West Coast, Great Lakes, Northeast, Southeast, Gulf of Mexico, Caribbean

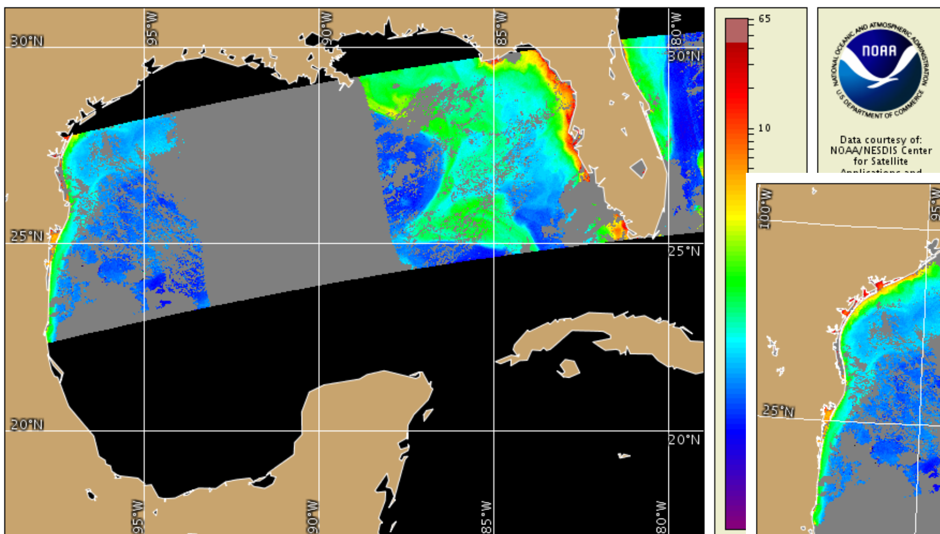

Granule

Daily Merge

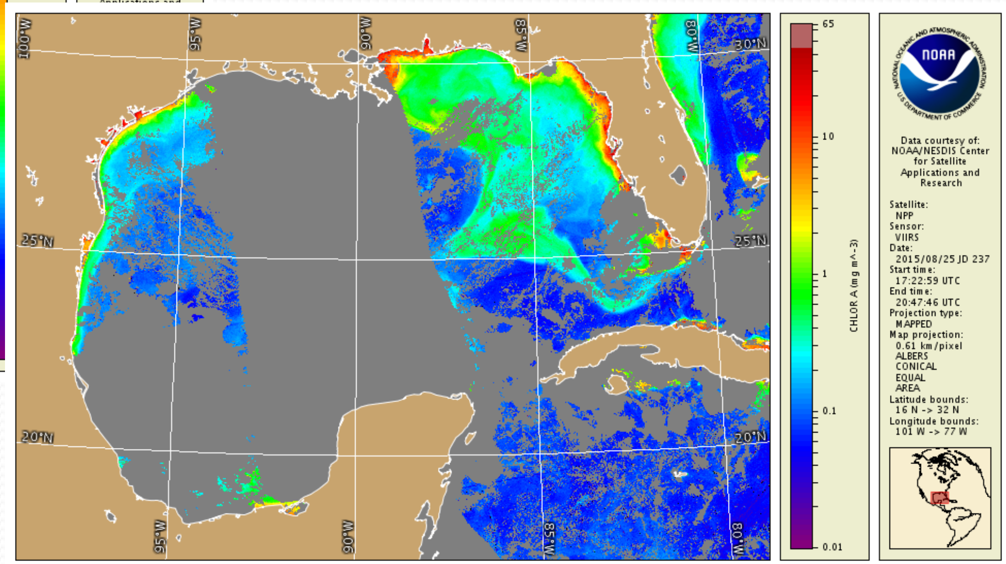

Regional Partners (1)

- EUMETSAT
  - Processing and staging of 750m Mediterranean datasets (L3 available through CoastWatch)
  - EUMETcast (Copernicus Service) broadcasts L2 VIIRS

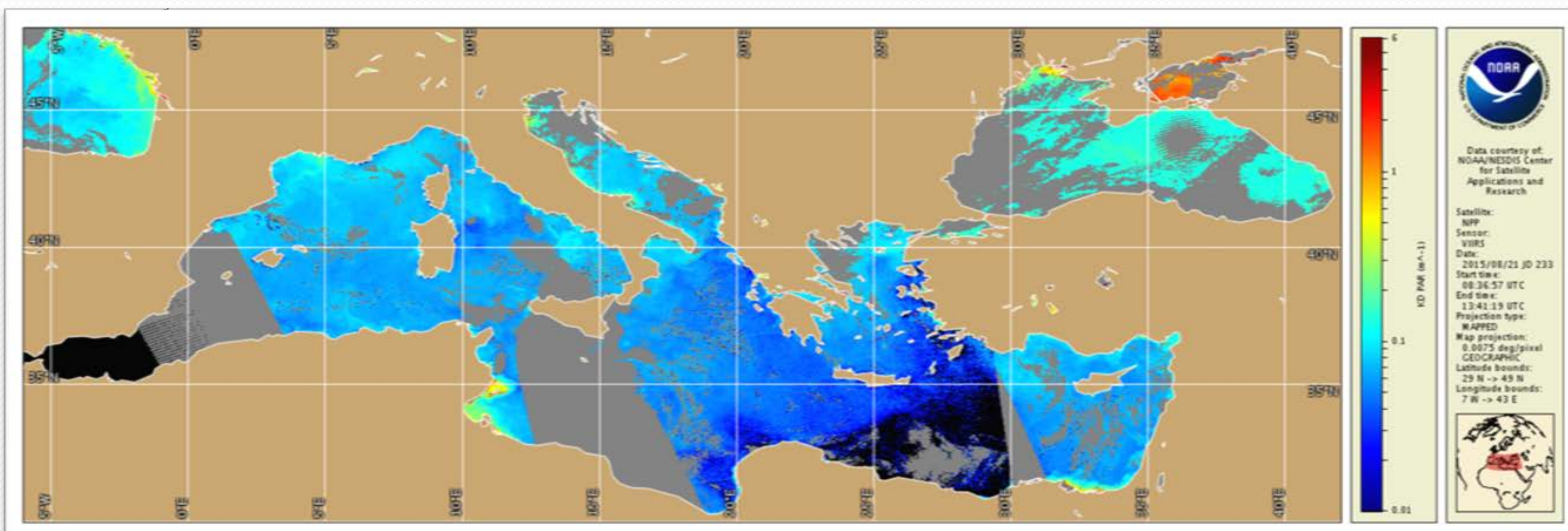

Shown: L3 Daily merge, kdPAR

Regional Partners (2)

- CSIRO
  - Processing and staging of L3 Australia 750m datasets

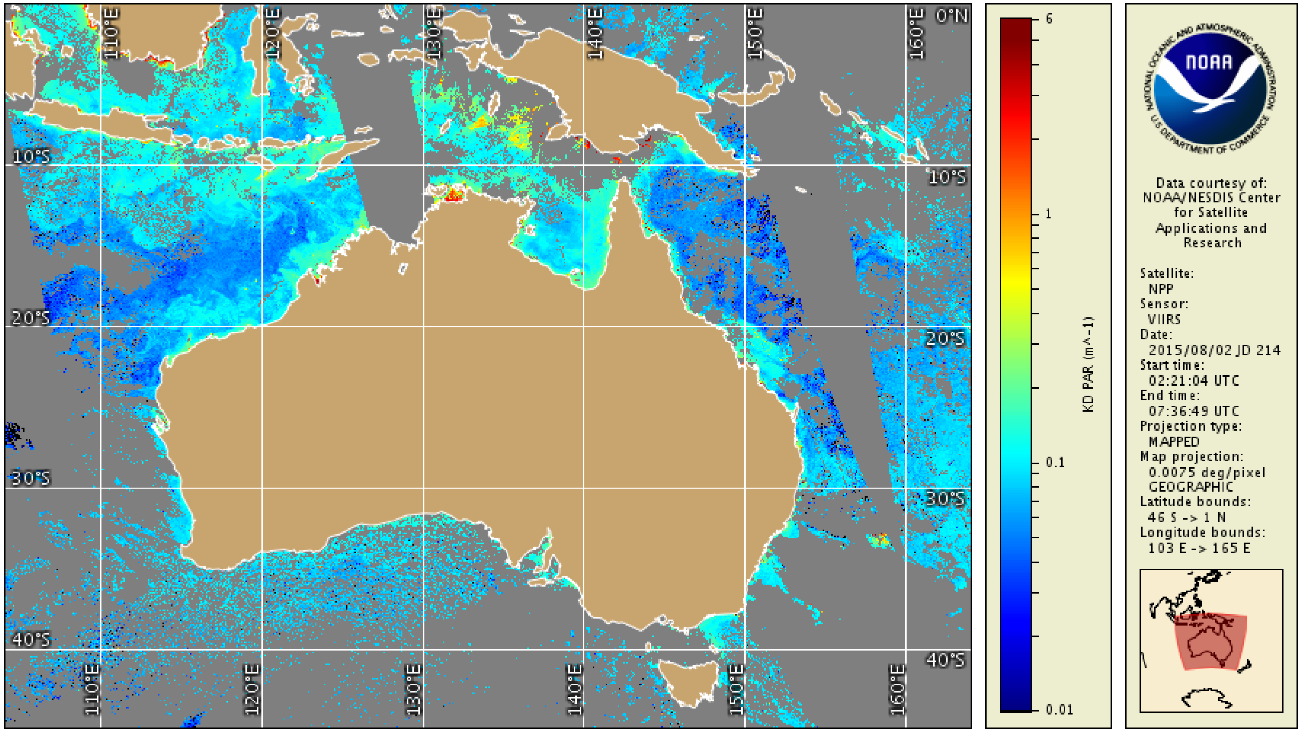

Daily Merge, kdPAR

L2 & L3 Global Products

- Standard:
  - Chlorophyll-a
  - Kd490
  - KdPAR
  - nLw_412
  - nLw_445
  - nLw_488
  - nLw_555
  - nLw_672
  - L2_flags
  - Latitude
  - Longitude

- Experimental:
  - IOPs
  - PAR

Future Inclusion

L2 & L3 Regional Products

- Standard:
  - Chlorophyll-a
  - Kd490
  - KdPAR
  - nLw_412
  - nLw_445
  - nLw_488
  - nLw_555
  - nLw_672
- Experimental:
  - IOPs
  - PAR

Future Inclusion

- L2 flags
- Latitude
- Longitude
- Edgemask

- User Driven:
  - HAB anomaly product
  - Rrs
  - Others TBD

Data Formats

- Global / Sector:
  - NetCDF (v4 CF)
  - GeoTIFF & PNG

- Regional:
  - NetCDF(v4 CF)
  - HDF (v4 with CoastWatch metadata)
  - GeoTIFF & PNG

Access & Protocols (1)

- HTTP
- FTP
- THREDDS
  - **OPENDAP**
  - **NetcdfSubset**
  - **WCS**
  - **WMS**
  - **NCML**
  - **ISO**
  - **UDDC**

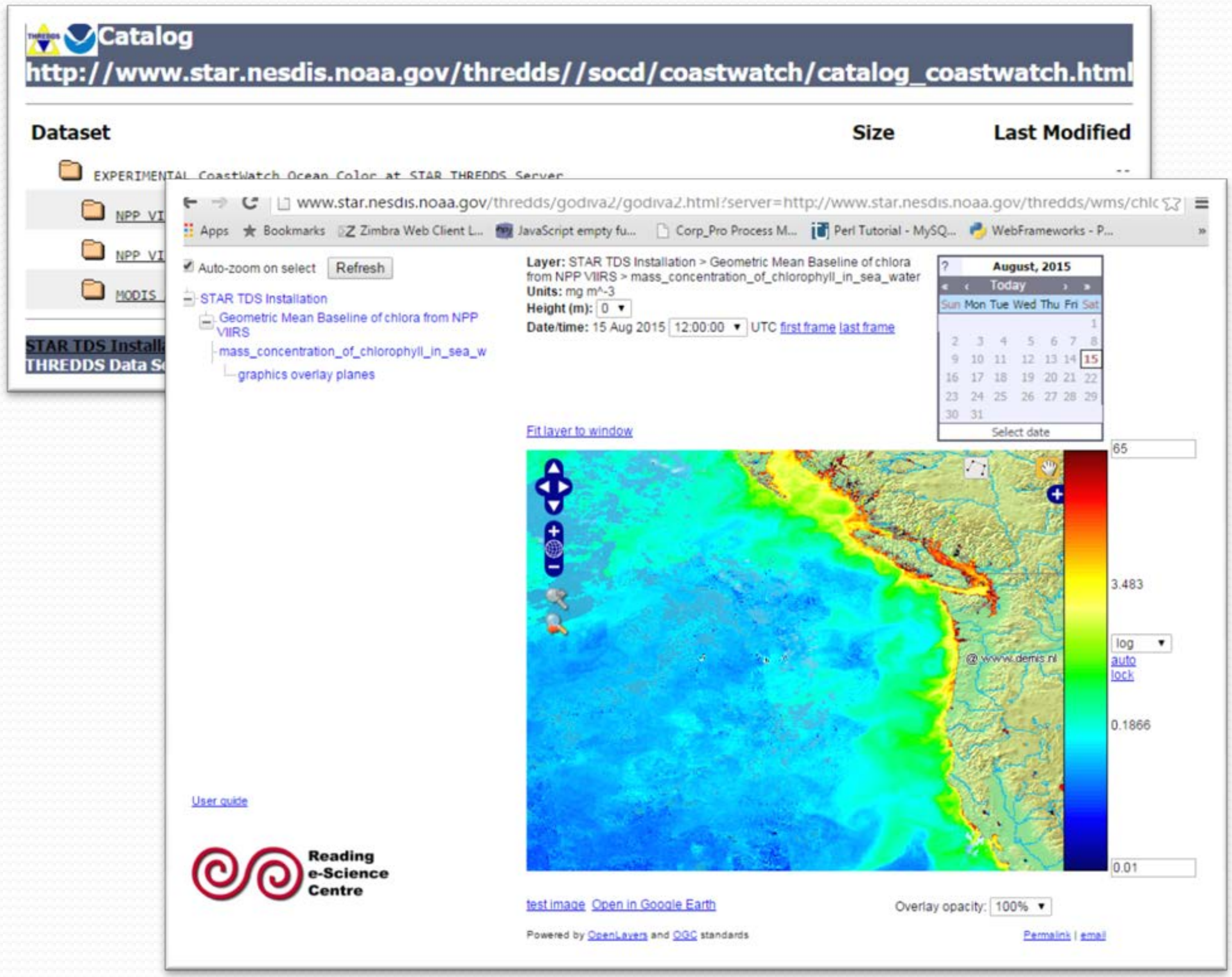

Access & Protocols (2)

- HTTP:
  - http://coastwatch.noaa.gov
- FTP:
  - ftp://star.nesdis.noaa.gov/pub/socd/mecb/coastwatch/viirs/
- THREDDS:
  - http://coastwatch.noaa.gov/thredds

L2 Granule Selector

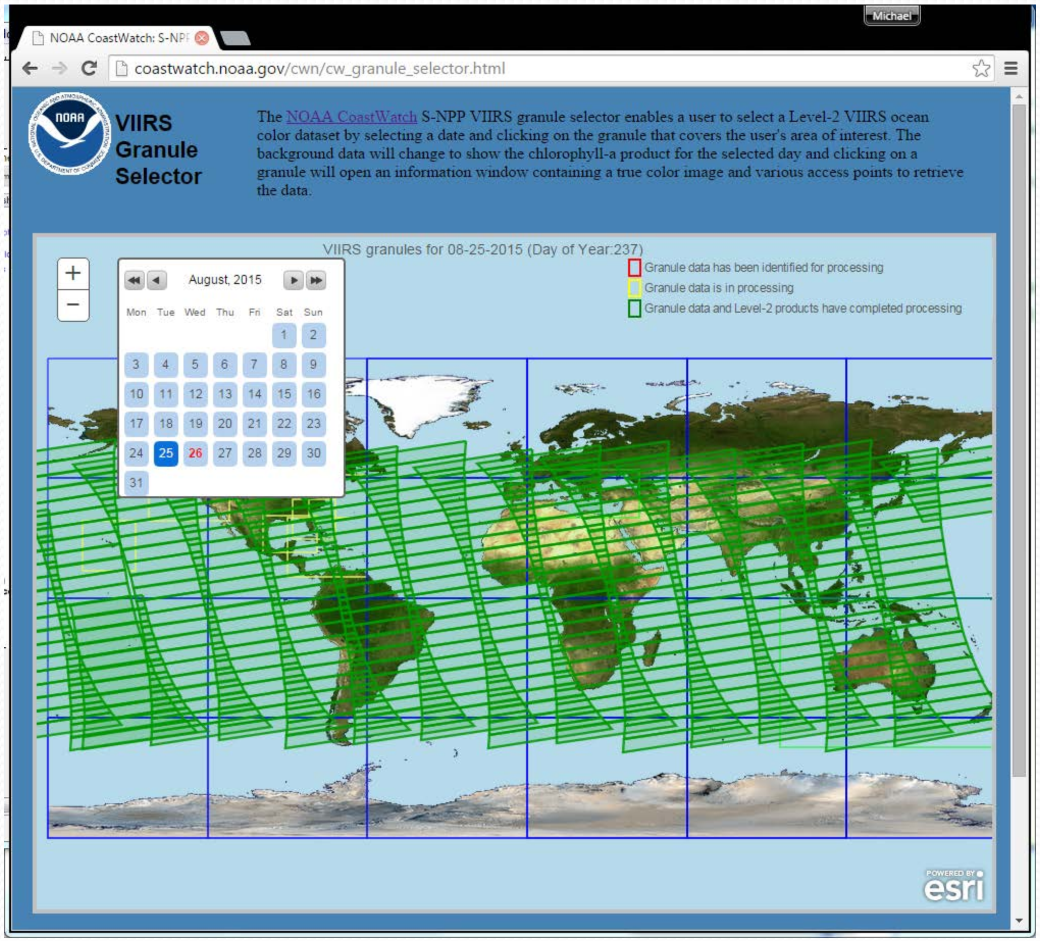

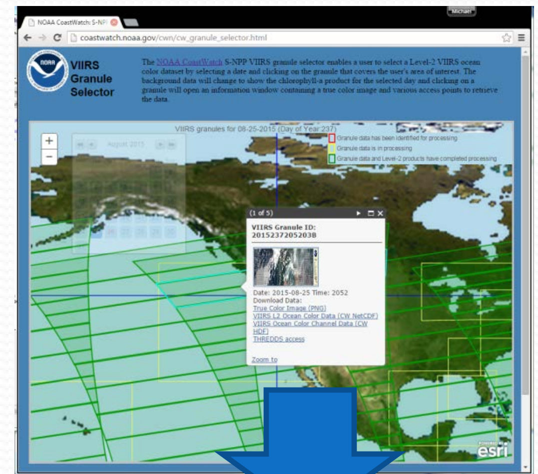

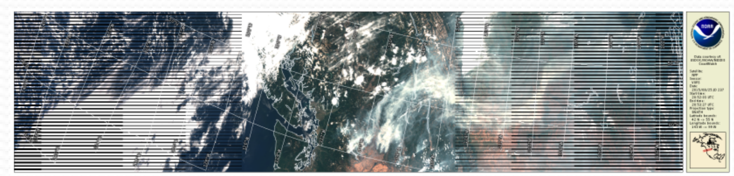

Date: 2015-08-25 Time: 2052
Download Data:
<u>True Color Image (PNG)</u>
<u>VIIRS L2 Ocean Color Data (CW NetCDF)</u>
<u>VIIRS Ocean Color Channel Data (CW HDF)</u>
<u>THREDDS access</u>

Planned Enhancements

- Data Portal
  - Facilitate the discovery and access to Ocean Data
  - Present a variety of search options
    - Locate the single or handful of datasets (Granule Selector/CW web search)
    - Locate a small to intermediate collection of data meeting user-driven criteria (in development)
    - Locate bulk collections of data (science data on FTP/THREDDS)

Sentinel-3A

- A Cooperative Arrangement between the United States and the European Commission is nearing ratification
- NOAA (NESDIS/)STAR plans to provide near real-time access to global OLCI and SLSTR data products from EUMETSAT
- EUMETSAT data transferred via terrestrial multicast to NOAA – initial tests promising
- OLCI data complements existing JPSS sensors:
  - 300m spatial resolution
  - Spectral bands meeting NOAA NOS HAB requirements
  - Relieves single point-of-failure for HAB forecasting

NOAA CoastWatch Ocean Color Data Dissemination

Paul M. DiGiacomo
NOAA/NESDIS/STAR
NOAA CoastWatch Program

STAR Center for Satellite Application and Research
National Environmental Satellite, Data, and Information Service (NESDIS)

Backup Slides

Example "Snapshot" 9/2016

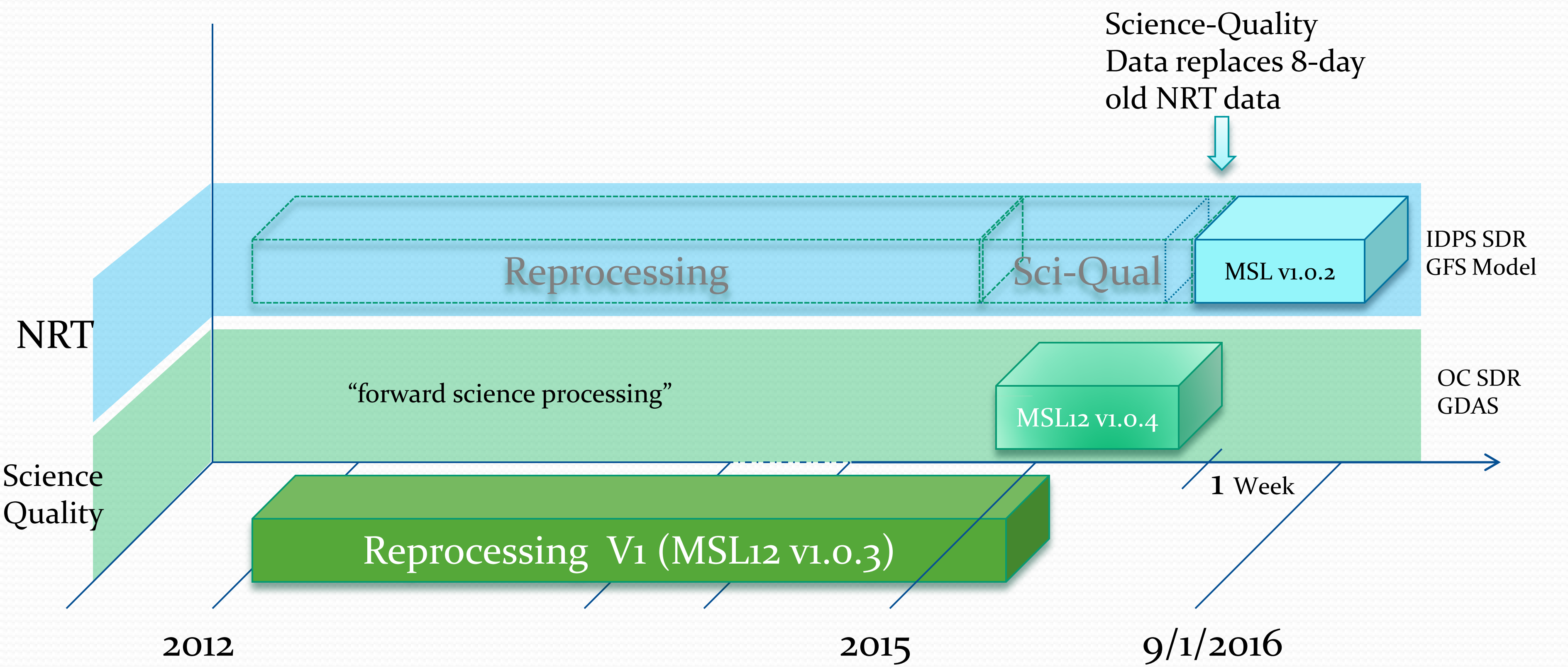

Example "Snapshot"